

# River Confluences, Tributaries and the Fluvial Network

Edited by

**Stephen P. Rice, Loughborough University, UK**

**André G. Roy, Université de Montréal, Canada**

**Bruce L. Rhoads, University of Illinois, USA**



John Wiley & Sons, Ltd



# **River Confluences, Tributaries and the Fluvial Network**



# River Confluences, Tributaries and the Fluvial Network

Edited by

**Stephen P. Rice, Loughborough University, UK**

**André G. Roy, Université de Montréal, Canada**

**Bruce L. Rhoads, University of Illinois, USA**



John Wiley & Sons, Ltd

Copyright © 2008 John Wiley & Sons Ltd, The Atrium, Southern Gate, Chichester,  
West Sussex PO19 8SQ, England  
Telephone (+44) 1243 779777

Chapters 9, 11 and 18 are the works of the US Government and are in the public domain in the United States of America.

Email (for orders and customer service enquiries): [cs-books@wiley.co.uk](mailto:cs-books@wiley.co.uk)  
Visit our Home Page on [www.wileyeurope.com](http://www.wileyeurope.com) or [www.wiley.com](http://www.wiley.com)

All Rights Reserved. No part of this publication may be reproduced, stored in a retrieval system or transmitted in any form or by any means, electronic, mechanical, photocopying, recording, scanning or otherwise, except under the terms of the Copyright, Designs and Patents Act 1988 or under the terms of a licence issued by the Copyright Licensing Agency Ltd, 90 Tottenham Court Road, London W1T 4LP, UK, without the permission in writing of the Publisher. Requests to the Publisher should be addressed to the Permissions Department, John Wiley & Sons Ltd, The Atrium, Southern Gate, Chichester, West Sussex PO19 8SQ, England, or emailed to [permreq@wiley.co.uk](mailto:permreq@wiley.co.uk), or faxed to (+44) 1243 770620.

Designations used by companies to distinguish their products are often claimed as trademarks. All brand names and product names used in this book are trade names, service marks, trademarks or registered trademarks of their respective owners. The Publisher is not associated with any product or vendor mentioned in this book.

This publication is designed to provide accurate and authoritative information in regard to the subject matter covered. It is sold on the understanding that the Publisher is not engaged in rendering professional services. If professional advice or other expert assistance is required, the services of a competent professional should be sought.

#### ***Other Wiley Editorial Offices***

John Wiley & Sons Inc., 111 River Street, Hoboken, NJ 07030, USA

Jossey-Bass, 989 Market Street, San Francisco, CA 94103-1741, USA

Wiley-VCH Verlag GmbH, Boschstr. 12, D-69469 Weinheim, Germany

John Wiley & Sons Australia Ltd, 33 Park Road, Milton, Queensland 4064, Australia

John Wiley & Sons (Asia) Pte Ltd, 2 Clementi Loop #02-01, Jin Xing Distripark, Singapore 129809

John Wiley & Sons Canada Ltd, 6045 Freemont Blvd, Mississauga, Ontario, L5R 4J3

Wiley also publishes its books in a variety of electronic formats. Some content that appears in print may not be available in electronic books.

#### ***Library of Congress Cataloging-in-Publication Data***

River confluences, tributaries, and the fluvial network / edited by Stephen P. Rice, André G. Roy, Bruce L. Rhoads.  
p. cm.

Includes bibliographical references and index.

ISBN 978-0-470-02672-4 (cloth)

1. Watersheds. 2. Geomorphology. 3. River engineering. I. Rice, Stephen P. II. Roy, André G.  
III. Rhoads, Bruce L.

GB562.R58 2008

551.48'3—dc22

2008016826

#### ***British Library Cataloguing in Publication Data***

A catalogue record for this book is available from the British Library

ISBN 978-0-470-02672-4

Typeset in 10.5/13pt Minion by Aptara Inc., New Delhi, India

Printed and bound in by Markono Printers, Singapore

This book is printed on acid-free paper

# Contents

<b>Preface</b>	<b>xi</b>
<b>List of contributors</b>	<b>xiii</b>
<b>1 Introduction: river confluences, tributaries and the fluvial network</b>	<b>1</b>
<i>Stephen P. Rice, Bruce L. Rhoads and André G. Roy</i>	
Introduction	1
Key aims of the book	4
Sections of the book	4
References	5
<b>I RIVER CHANNEL CONFLUENCES</b>	<b>11</b>
<b>2 Introduction to Part I: river channel confluences</b>	<b>13</b>
<i>André G. Roy</i>	
Introduction	13
Individual chapters	15
Reference	16
<b>3 Modelling hydraulics and sediment transport at river confluences</b>	<b>17</b>
<i>Pascale M. Biron and Stuart N. Lane</i>	
Introduction	17
Hydraulics	18
Bedload, suspended and solute transport	29
Conclusion	37
Acknowledgments	38
References	38
<b>4 Sediment transport, bed morphology and the sedimentology of river channel confluences</b>	<b>45</b>
<i>James L. Best and Bruce L. Rhoads</i>	
Context	45
Bed morphology	46

Sediment transport	56
Sedimentology	60
Conclusions	66
Acknowledgements	67
References	68
<b>5 Large river channel confluences</b>	<b>73</b>
<i>Daniel R. Parsons, James L. Best, Stuart N. Lane, Ray A. Kostachuk, Richard J. Hardy, Oscar Orfeo, Mario L. Amsler and Ricardo N. Szupiany</i>	
Introduction	73
Bed morphology	75
Flow structure at large river channel confluences	80
Flow mixing at large river confluences	85
Conclusions	87
Acknowledgements	88
References	88
<b>6 Management of confluences</b>	<b>93</b>
<i>Robert Ettema</i>	
Introduction	93
Unruly confluences	95
Management approaches	103
Managing confluences for sediment transport	104
Managing confluences for ice passage	111
Summary	116
References	116
<b>7 Unconfined confluences in braided rivers</b>	<b>119</b>
<i>Peter Ashmore and J. Tobi Gardner</i>	
Introduction	119
General characteristics and significance of confluences in braided channels	121
Confluence scour depth	125
Confluence kinetics and bar formation	128
Confluence spacing and the length-scale of braided morphology	130
Sediment transport and sediment budgets	132
Sediment sorting and alluvial deposits	135
Prospect	139
Acknowledgements	142
References	143
<b>II TRIBUTARY–MAIN-STEM INTERACTIONS</b>	<b>149</b>
<b>8 Introduction to Part II: tributary–main-stem interactions</b>	<b>151</b>
<i>Stephen P. Rice</i>	
Introduction	151
Individual chapters	153
References	155

<b>9</b>	<b>Spatial identification of tributary impacts in river networks</b>	<b>159</b>
	<i>Christian E. Torgersen, Robert E. Gresswell, Douglas S. Bateman and Kelly M. Burnett</i>	
	Introduction	159
	Data and measurement	160
	Analytical tools	167
	Future developments and challenges	175
	Acknowledgements	176
	References	176
<b>10</b>	<b>Effects of tributaries on main-channel geomorphology</b>	<b>183</b>
	<i>Rob Ferguson and Trevor Hoey</i>	
	Introduction	183
	Conceptual considerations	185
	Empirical evidence	187
	Theoretical models: (1) Regime analysis of confluences	191
	Theoretical models: (2) Numerical experiments with adjustable grain-size distributions	198
	Discussion	201
	Acknowledgments	206
	References	206
<b>11</b>	<b>The ecological importance of tributaries and confluences</b>	<b>209</b>
	<i>Stephen P. Rice, Peter Kiffney, Correigh Greene and George R. Pess</i>	
	Introduction	209
	Tributaries, confluences and river ecology	210
	Tributaries, ecosystem functions and river management	215
	Constraints on understanding and progress	217
	A case study	218
	Conclusion	235
	Acknowledgments	237
	References	237
<b>12</b>	<b>Tributaries and the management of main-stem geomorphology</b>	<b>243</b>
	<i>Frédéric Liébault, Hervé Piégay, Philippe Frey and Norbert Landon</i>	
	Introduction	243
	Conceptual framework for assessing the geomorphological impact of tributaries	245
	Managing the geomorphological impact of tributaries	251
	Conclusion	266
	Acknowledgments	267
	References	267
<b>13</b>	<b>Confluence environments at the scale of river networks</b>	<b>271</b>
	<i>Lee Benda</i>	
	Introduction	271
	River network structure and confluence environments	272

Symmetry ratios and confluence environments	273
Basin shape, network patterns and confluence environments	280
Local network geometry	284
Drainage and confluence density	284
River network scaling properties of confluence environments	285
The law of stream sizes and the spatial scale of morphological diversity related to confluences	289
Longitudinal extent and size of confluence environments	290
Stochastic watershed processes	291
The role of hierarchical branching networks	292
Discussion	295
River networks, resource management and river restoration	296
Acknowledgements	297
References	297
<b>III CHANNEL NETWORKS</b>	<b>301</b>
<b>14 Introduction to Part III: channel networks</b>	<b>303</b>
<i>Bruce L. Rhoads</i>	
Introduction	303
Individual chapters	304
References	305
<b>15 Hydrologic dispersion in fluvial networks</b>	<b>307</b>
<i>Patricia M. Saco and Praveen Kumar</i>	
Hydrologic dispersion effects on runoff response	307
Runoff response as travel-time distributions: the GIUH	309
Geomorphologic dispersion in stream networks	314
Non-linear effects and the use of hydraulic geometry relations	316
Kinematic dispersion in stream networks	318
The effect of scale and rainfall intensity on the dispersive mechanisms	320
Hillslope Dispersive effects	324
Kinematic dispersion effects using the meta-channel approach	329
Summary and future research directions	331
Acknowledgments	333
References	333
<b>16 Sediment delivery: new approaches to modelling an old problem</b>	<b>337</b>
<i>Hua Lu and Keith Richards</i>	
Introduction	337
The concept of sediment delivery	340
Difficulties in measuring and estimating sediment yield and SDR	341
Links between hydrology and sediment production and yield	347
Physical inferences of sediment delivery based on a simple lumped model	352
Practical large-scale application using a distributed model	358
Conclusions	361

Acknowledgements	362
References	362
<b>17 Numerical predictions of the sensitivity of grain size and channel slope to an increase in precipitation</b>	<b>367</b>
<i>Nicole M. Gasparini, Rafael L. Bras and Gregory E. Tucker</i>	
Introduction	367
Landscape-evolution models	370
Example simulation of network evolution	376
Discussion	386
Conclusions	388
Acknowledgements	389
References	389
<b>18 Solute transport along stream and river networks</b>	<b>395</b>
<i>Michael N. Gooseff, Kenneth E. Bencala and Steven M. Wondzell</i>	
Introduction	395
Review of current knowledge	396
Linking transport processes with the fluvial geomorphic template	404
Forward-looking perspective	410
Acknowledgements	413
References	413
<b>19 Fluvial valley networks on Mars</b>	<b>419</b>
<i>Rossmann P. Irwin III, Alan D. Howard and Robert A. Craddock</i>	
Introduction	419
Early observations	421
Distribution, age, origin and morphology of valley networks	422
Morphometry	432
Alluvial deposits	436
Hydrology	438
Summary	442
Acknowledgements	442
References	442
<b>Subject Index</b>	<b>453</b>
<b>Place Index</b>	<b>457</b>



# Preface

When the book proposal that led to this publication was reviewed, we were flattered, but mainly daunted, by the suggestion from a particularly generous referee that we should write this book ourselves. While grateful for the referee's support of the project, we persevered with our original intention of compiling an edited volume. The resulting collection of chapters draws on the research of an international group of scholars and practitioners who work in universities, government agencies, private consultancies and research establishments. Their expertise is in academic and applied geomorphology, hydrology, sedimentology, ecology and engineering. Their methods include numerical modelling, laboratory experimentation and detailed field investigations. Looking at the chapters that they have produced, it is clear to us that we were right to favour the great variety and depth of their expertise and experience over our own, inevitably inferior, knowledge of their areas of specialization. We are therefore grateful to our authors for embracing our project, for sharing their understanding and for helping us to, in a sense, avoid having to write this book ourselves.

And it is a book that needed to be written (in one way or another). River confluences are ubiquitous and critical nodes in river networks, and the branching pattern of tributaries and sub-networks is one of the most characteristic features of river systems on Earth and elsewhere. We find it somewhat remarkable, then, that this will be the first book to focus attention explicitly on confluence dynamics, tributary impacts and the links between processes at these scales and river network functions. We believe that understanding confluence processes and interactions between the tributary and main stem are keystones for scaling-up our understanding of river processes to the drainage network scale: without an understanding of the nodes in the network and the interactions between connected links, the development of basin-scale models and tools is restricted. We subscribe to the view that such network-scale understanding is central to the successful integration of Earth, environmental and biological sciences within riverine landscapes and thence the sustainable management of our riverscapes. We therefore hope that this book will be a helpful stepping-stone for the pursuit of an integrated, cross-scale river science.

To date, work in this area has been communicated almost exclusively via academic journals in geomorphology, ecology, geology and engineering. By bringing together the expertise represented here in one place, our aim is to provide a single benchmark reference that defines the current state of understanding as well as the leading edge of contemporary research. Each chapter is built around two central pillars: a critical review of work in the author's area of expertise and unpublished research that highlights the cutting edge of research in that area. In this way, the book is at once intended to fulfil the needs of students (of whatever age and standing) who require sound, thoughtful reviews of particular topics and also those who are actively involved in conducting and applying research on confluences, tributaries and networks. We therefore hope that the book will be useful both as a standard reference and as a source of new research questions and hypotheses.

To close, some thanks. First to the authors of these chapters for their time and effort: we are grateful and hope that the exercise has been rewarding. Each chapter was fully reviewed and we must thank the large number of colleagues who acted as independent referees; their input was consistently constructive and has substantially improved the quality of the end product. Natasha Todd-Burley's editorial assistance was invaluable during the final stages of production. Finally, the book has been a number of years in the making and we therefore want to thank family and friends for their continued support. In particular, SPR would like to thank Georgina for her support and encouragement throughout this process and dedicate his contribution to his brother Mike, who beat him to a publication with tributary associations. BLR thanks Kathy, Jamie and Steven for helping him to keep life in proper perspective at all times. AGR thanks his co-editors for their enthusiasm for this project, his research team for their constant support and Catherine for being there.

**Stephen Rice, Bruce Rhoads, André Roy**  
**October 2007**

# List of contributors

**Mario L. Amsler** (mamsler@fich1.unl.edu.ar) Facultad de Ingeniería y Ciencias Hídricas & Instituto Nacional de Limnología, Universidad Nacional de Litoral, Santa Fe 3000, Argentina

**Peter Ashmore** (pashmore@uwo.ca) Department of Geography, University of Western Ontario, London, Ontario, N6A 5C2, Canada

**Douglas S. Bateman** (doug.bateman@usgs.gov) Department of Forest Sciences, Oregon State University, Corvallis, OR 97331, USA

**Kenneth E. Bencala** (kbencala@usgs.gov) US Geological Survey, 345 Middlefield Road, Menlo Park, CA 94025, USA

**Lee Benda** (leebenda@earthsystems.net) Earth Systems Institute, 310 Mt Shasta Blvd, Mt Shasta, CA 96067, USA

**James L. Best** (jimbest@uiuc.edu) Departments of Geology and Geography and Ven Te Chow Hydrosystems Laboratory, University of Illinois at Urbana-Champaign, 1301 West Green Street, Urbana, IL 61801, USA

**Pascale M. Biron** (pascale.biron@concordia.ca) Department of Geography, Planning and Environment, Concordia University, 1455 de Maisonneuve Boulevard West, Montréal, Québec, H3G 1M8, Canada

**Rafael L. Bras** (rlbras@mit.edu) Department of Civil and Environmental Engineering, Massachusetts Institute of Technology, 77 Massachusetts Avenue, Cambridge, MA 02139, USA

**Kelly M. Burnett** (kmburnett@fs.fed.us) US Department of Agriculture, Forest Service, Pacific Northwest Research Station, 3200 Jefferson Way, Corvallis, OR 97331, USA

**Robert A. Craddock** (craddockb@si.edu) Center for Earth and Planetary Studies, National Air and Space Museum, Smithsonian Institution, 4th Street and Independence Avenue SW, WA 20013-7012, USA

**Robert Ettema** (rettema@uwyo.edu) Dean's Office, College of Engineering and Applied Science, University of Wyoming, 1000 E University Street, Laramie, WY 82071, USA

**Rob Ferguson** (r.i.ferguson@durham.ac.uk) Durham University, Department of Geography, Science Laboratories, South Road, Durham, DH1 3LE, UK

**Philippe Frey** (philippe.frey@cemagref.fr) Cemagref Groupement de Grenoble, Unité de Recherche ETNA (Erosion Torrentielle, Neige et Avalanches), Domaine universitaire, 2 rue de la Papeterie BP76, 38402 SAINT-MARTIN-D'HERES cedex, France

**J. Tobin Gardner** (jgardne7@uwo.ca) Department of Geography, University of Western Ontario, London, Ontario, N6A 5C2, Canada

**Nicole M. Gasparini** (nicoleg@alum.mit.edu) School of Earth and Space Exploration, Arizona State University, Tempe, AZ 85287-1404 USA

**Michael N. Gooseff** (mgooseff@engr.psu.edu) Department of Civil and Environmental Engineering, Pennsylvania State University, University Park, PA 16802, USA

**Correigh Greene** (Correigh.Greene@noaa.gov) NOAA NW Fisheries Science Center, 2725 Montlake Boulevard East, Seattle, WA 98112, USA

**Robert E. Gresswell** (bgresswell@usgs.gov) US Geological Survey, Northern Rocky Mountain Science Center, 1648 S. 7th Avenue, Bozeman, MT 59717, USA

**Richard J. Hardy** (r.j.hardy@durham.ac.uk) Durham University, Department of Geography, Science Laboratories, South Road, Durham, DH1 3LE, UK

**Trevor Hoey** (thoey@ges.gla.ac.uk) Department of Geographical and Earth Sciences, East Quadrangle, University Avenue, University of Glasgow, Glasgow, G12 8QQ, UK

**Alan D. Howard** (alanh@virginia.edu) Department of Environmental Sciences, University of Virginia, 291 McCormick Rd, PO Box 400123, Charlottesville, VA 22904-4123, USA

**Rossman P. Irwin III** (IrwinR@si.edu) Center for Earth and Planetary Studies, National Air and Space Museum, Smithsonian Institution, MRC 315, 6th Street and Independence Avenue SW, WA 20013-7012, USA

**Peter Kiffney** (Peter.Kiffney@noaa.gov) NOAA NW Fisheries Science Center, Mukilteo Field Station, Building B, Mukilteo, WA 98275, USA

**Ray A. Kostaschuk** (rkostasc@uoguelph.ca) Department of Geography, University of Guelph, Ontario, N1G 2W1, Canada

**Praveen Kumar** (kumar1@uiuc.edu) Department of Civil and Environmental Engineering, University of Illinois, 205 North Mathews Avenue, Urbana, IL 61801, USA

**Norbert Landon** (norbert.landon@univ-lyon2.fr) Université Lumière, Lyon 2, Faculté GHHAT, Institut de Recherche en Géographie, 5 avenue Pierre Mendès CP11, 69676 BRON cedex, France

**Stuart N. Lane** (s.n.lane@durham.ac.uk) Durham University, Department of Geography, Science Laboratories, South Road, Durham, DH1 3LE, UK

**Frédéric Liébault** (frederic.liebault@cemagef.fr) Cemagref Groupement de Grenoble, Unité de Recherche ETNA (Erosion Torrentielle, Neige et Avalanches), Domaine universitaire, 2 rue de la Papeterie BP76, 38402 SAINT-MARTIN-D'HERES cedex, France

**Hua Lu** (hlu@bas.ac.uk) British Antarctic Survey, High Cross, Madingley Road, Cambridge, CB3 0ET, UK

**Oscar Orfeo** (cecoal@arnet.com.ar) Centro de Ecología Aplicada del Litoral (CECOAL), Consejo Nacional de Investigaciones Científicas y Técnicas (CONICET), Corrientes City, Corrientes 3400, Argentina

**Daniel R. Parsons** (parsons@earth.leeds.ac.uk) School of Earth & Environment, University of Leeds, Leeds, LS2 9JT, UK

**George R. Pess** (george.pess@noaa.gov) NOAA – Northwest Fisheries Science Center, 2725 Montlake Boulevard East, Seattle, WA 98112, USA

**Hervé Piégay** (herve.piegay@ens-lsh.fr) Université de Lyon, UMR 5600 CNRS, Site ENS-LSH, Plateforme ISIG, 15 Parvis René Descartes, BP7000, 69342 Lyon cedex 07, France

**Bruce L. Rhoads** (brhoads@uiuc.edu) Department of Geography, University of Illinois at Urbana-Champaign, Room 220 Davenport Hall, 607 South Mathews Avenue, Urbana, IL 61801-3671, USA

**Stephen P. Rice** (s.rice@lboro.ac.uk) Department of Geography, Loughborough University, Loughborough, LE11 3TU, UK

**Keith Richards** (ksr10@cam.ac.uk) Department of Geography, University of Cambridge, Downing Place, Cambridge, CB2 3EN, UK

**André Roy** (andre.roy@umontreal.ca) Département de Géographie, Université de Montréal, CP 6128, succursale Centre-Ville, Montréal, Québec, H3C 3J7, Canada

**Patricia M. Saco** (patricia.saco@newcastle.edu.au) Civil and Environmental Engineering, University of Newcastle, Callaghan, New South Wales 2308, Australia

**Ricardo N. Szupiany** (rszupian@fich1.unl.edu.ar) Facultad de Ingeniería y Ciencias Hídricas, Universidad Nacional de Litoral en Santa Fe, Consejo Nacional de Investigaciones Científicas y Técnicas (CONICET), Santa Fe 3000, Argentina

**Christian E. Torgersen** (ctorgersen@usgs.gov) US Geological Survey, Forest and Rangeland Ecosystem Science Center, Cascadia Field Station, University of Washington, College of Forest Resources, Box 352100, Seattle, WA 98195, USA

**Gregory E. Tucker** (gtucker@cires.colorado.edu) Cooperative Institute for Research in Environmental Sciences (CIRES) and Department of Geological Sciences, University of Colorado at Boulder, 2200 Colorado Avenue, Boulder, CO 80309-0399, USA

**Steven M. Wondzell** (swondzell@fs.fed.us) USDA Forest Service, Pacific Northwest Research Station, Olympia Forestry Sciences Laboratory, 3625 93rd Avenue SW, Olympia, WA 98512, USA

# 1

## Introduction: river confluences, tributaries and the fluvial network

Stephen P. Rice<sup>1</sup>, Bruce L. Rhoads<sup>2</sup> and André G. Roy<sup>3</sup>

<sup>1</sup>*Department of Geography, Loughborough University, UK*

<sup>2</sup>*Department of Geography, University of Illinois, USA*

<sup>3</sup>*Canada Research Chair in Fluvial Dynamics, Département de Géographie, Université de Montréal, Canada*

### Introduction

That river systems are networks consisting of links and nodes is one of their most obvious characteristics. Despite the ubiquity of confluences and tributary networks, the first century of modern fluvial geomorphology paid little consistent attention to river junctions and the interactions between tributaries and the main stem (Kennedy, 1984). Important exceptions include classic contributions from Playfair (1802), Lyell (1830) and Sternberg (1875), works on tributary–main-stem interactions (e.g. Krumbein, 1942; Miller, 1958), considerations of junction hydraulics and mixing (e.g. Taylor, 1944; Mackay, 1970) and the seminal works on river network structure (e.g. Horton, 1945; Shreve, 1967). However, the 1980s marked the beginning of a period in which confluence, tributary and network studies developed rapidly. Key contributions were concerned with: confluence morphology, hydraulics and sedimentology (Mosley, 1976; Best, 1986, 1988; Roy *et al.*, 1988), tributary-induced changes in channel form (Richards, 1980; Roy

and Woldenberg, 1986; Rhoads, 1987) and bed sediments (Church and Kellerhals, 1978; Knighton, 1980), the ecological role of tributaries along unregulated (Bruns *et al.*, 1984) and regulated rivers (Petts, 1984; Petts and Greenwood, 1985), tributaries as repositories of paleoflood information (Kochel and Baker, 1982) and tributary network structure (Abrahams and Campbell, 1976; Flint, 1980; Abrahams and Updegraph, 1987).

Figure 1.1 indicates the rapid increase in the volume of published work on tributaries and confluences in the period since 1980 and illustrates how the initial impetus of the 1980s was consolidated in the 1990s. Ecological interest has lagged behind geomorphology and hydraulics, but it is clear that ecological interest is now growing at the fastest rate. This body of work has demonstrated that river confluences are critical nodes in river systems where tributary fluxes of water and sediment can elicit adjustments in the geomorphology, hydraulics, sedimentology and ecology of the recipient channel. At

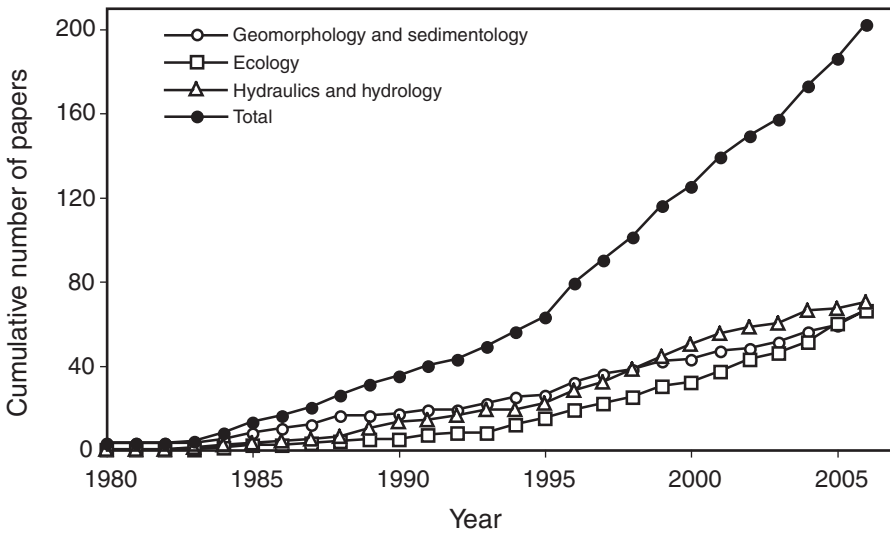


**Figure 1.1** The growth in research publications that deal with confluences and tributaries. Network research is not included. Because of the cross-disciplinary nature of many papers, the classification into sub-disciplines is imperfect. Searches were made for the period 1980–2007 using the ISI Web of Science, Science Citation Index – Expanded (<http://portal.isiknowledge.com/>). A primary search was made of titles, abstracts and keywords using the Boolean expression '(confluence\* OR tributar\*) AND (river\* OR channel\*)' and subsequent searches explored other likely terms. Results from these searches were then scrutinized and only those papers where tributaries or confluences were the primary subject matter or where they were used explicitly to explain observed phenomena were retained. Large numbers of papers that studied a particular river system including one or more of its tributaries or confluences but which did not focus on the properties or processes of confluences or tributaries were excluded. Because many papers on water chemistry across drainage basins fall into this category, the 'hydraulics and hydrology' classification does not include any water quality papers.

the smallest scales, research at river confluences examined the distinctive flows, morphologies, sedimentary assemblages and habitats that make confluence sites important local features. Most attention has been directed towards understanding flow mixing at junctions (Gaudet and Roy, 1995; Best and Ashworth, 1997; Biron *et al.*, 2004; Rhoads and Sukhodolov, 2004; Ding and Wang, 2006) and relations between sediment transport, morphology and stratigraphy (Biron *et al.*, 1993; Kenworthy and Rhoads, 1995; Ashworth, 1996; Leclair and Roy, 1997; Paola, 1997; Roy and Sinha, 2005; Boyer *et al.*, 2006). The biological attributes of confluences have received some attention (Cellot, 1996; Kupferberg, 1996; Franks *et al.*, 2002; Fernandes *et al.*, 2004; Krebs and Budiono, 2005; Kiffney *et al.*, 2006), as have the dynamics of ice jams at confluences (Prowse, 1986; Ettema *et al.*, 1997; Shen *et al.*, 2000; Ettema and Muste, 2001). At this scale, improved understanding informed, and was informed by, studies of confluences in braided rivers (Ashmore, 1991; Ashworth *et al.*, 1992; Best and Ashworth, 1997), which, arguably, has laid the foundation for recent investigations of the dynamics of river bifurcations (Dargahi, 2004; Federici and Paola, 2003; Khan *et al.*, 2000; Parsons *et al.*, 2007).

At a slightly larger scale, the confluence zone has been recognized as an important site of storage and staging for clastic and organic materials in fans and terraces (Albertson and Patrick, 1996; Brierley and Fryirs, 1999; Florsheim *et al.*, 2001; May and Gresswell, 2004; Gomez-Villar *et al.*, 2006). Ecological research at this scale suggests that tributary channels in the vicinity of confluences can provide important biological resources including, for example, refugia from high water temperatures (Bramblett *et al.*, 2002; Cairns *et al.*, 2005) and main-stem predators (e.g. Fraser *et al.*, 1995). It has been proposed that such factors, along with enhanced morphological heterogeneity in this confluence zone, may create hotspots of elevated biodiversity (Benda *et al.*, 2004a). At the larger, reach scale, main-stem adjustments to tributary fluxes of water, sediment and organic materials have been shown to structure the longitudinal operation of various abiotic and biotic processes leading to step-changes or gradient shifts in, for example, bed material grain size (Dawson, 1988; Rice and Church, 1998), longitudinal profile (Rice and Church, 2001; Hanks and Webb, 2006) and macroinvertebrate ecology (Perry and Schaeffer, 1987; Rice *et al.*, 2001). Earlier work on tributary influences has been extended to investigate what controls the magnitude of tributary impacts (Rice, 1998; Benda *et al.*, 2004b; Ferguson *et al.*, 2006; Rice *et al.*, 2006).

Understanding confluence dynamics and tributary impacts at these various scales is crucial for scaling-up knowledge of river processes to the drainage network scale: understanding the operation of the nodes in a network is necessary in order to develop network-scale models and tools. Indeed, there is increasing awareness that river system science requires a better integration of process knowledge across a range of spatial scales and particular emphasis is being placed on understanding network-scale functions (e.g. Paola *et al.*, 2006). Building on early work that focused on the topological properties of river networks (see Abrahams, 1984, for a review), a large body of research over the past 30 years has focused on the fractal properties and scaling relations of networks

and the way in which these properties and relations are connected to basin hydrological response (see Rodríguez-Iturbe and Rinaldo, 1997). This line of research has matured into the investigation and modelling of process dynamics at river network scales, for example in geomorphology (Gasparini *et al.*, 1999; Binnie *et al.*, 2006; Sklar *et al.*, 2006; Bigelow *et al.*, 2007) and lotic ecology (Poole, 2002; Power and Dietrich, 2002; Benda *et al.*, 2004a; Grant *et al.*, 2007; Thorp *et al.*, 2006; Bertuzzo *et al.*, 2007). Other emerging topics include the role of network structure in pollutant dispersion and the relation of channel networks on other planets to those on Earth – topics that are covered in the latter section of this volume.

## Key aims of the book

Work on confluence dynamics, tributary impacts and network-scale functions is, then, alive and well and involves experimental work in the field and laboratory, numerical modelling and large-scale empirical field investigations. This endeavour is frequently cross-disciplinary, challenging traditional boundaries between ecology, engineering, geomorphology, hydrology and sedimentology and emphasizing that river network form and functions control the spatio-temporal patterns of many physical, chemical and biotic processes at the Earth's surface (Paola *et al.*, 2006). At the onset of the second century of modern fluvial studies, our key aim in this book is to present a multidisciplinary, multiscale perspective on confluences, tributaries and river networks. Our intention is that by bringing together work on confluence dynamics and tributary–main stem interactions with network-scale perspectives, the reader will be better positioned to explore the links between processes across these scales. We have tried to draw out these linkages explicitly wherever possible. We hope that the book will provide a foundation upon which integrative effort can be built so that a truly network-scale understanding of river systems can be developed. A recurrent theme, raised by numerous authors, is the need for the continued collection of field and experimental data with which to develop and test our models of confluence, tributary and network processes, and we hope that the areas for further investigation highlighted herein will direct this effort. Also, by presenting the material here in book form, we hope to maximize the involvement of the wider community and facilitate the incorporation of new confluence, tributary and network understanding into the management of river processes and services.

## Sections of the book

The book is organized into three parts: (I) River Channel Confluences, (II) Tributary–Main-stem Interactions and (III) Channel Networks. Each section begins with a short

introductory essay that includes an overview of the papers in that section, so we refrain from providing such an overview here. Individual chapters focus on the core themes of research and knowledge as well as some topics that have received less attention (e.g. confluence and tributary management). Each chapter provides a review of current understanding, presents new research and considers where future efforts should be directed. We do not claim that the volume is comprehensive, and some topics, such as the structure and dynamics of distributary drainage networks, are not covered here. We do feel, however, that the book has sufficient scope to introduce the novice and scholar alike to many important issues at the forefront of research on river confluences, tributaries and networks. It is hoped that the book as a whole will provide a timely synthesis of a rapidly growing and important field of study but will also bring forward new and stimulating ideas that will shape a coherent and fruitful vision for future work.

## References

- Abrahams AD. 1984. Channel networks: a geomorphological perspective. *Water Resources Research* **20**: 161–188.
- Abrahams AD, Campbell RN. 1976. Source and tributary-source link lengths in natural channel networks. *Geological Society of America Bulletin* **87**: 1016–1020.
- Abrahams AD, Updegraph J. 1987. Some space-filling controls on the arrangement of tributaries in dendritic channel networks. *Water Resources Research* **23**: 489–495.
- Albertson PE, Patrick DM. 1996. Lower Mississippi River tributaries: Contributions to the collective science concerning the ‘Father of Waters’. *Engineering Geology* **45**: 383–413.
- Ashmore PE. 1991. How do gravel-bed rivers braid? *Canadian Journal of Earth Sciences* **28**: 326–341.
- Ashworth PJ. 1996. Mid-channel bar growth and its relationship to local flow strength and direction. *Earth Surface Processes and Landforms* **21**: 103–123.
- Ashworth PJ, Powell DM, Prestegard KL, Ferguson RI, Ashmore PE, Paola C. 1992. Measurements in a braided river chute and lobe. 2. Sorting of bedload during entrainment, transport, and deposition. *Water Resources Research* **28**: 1887–1896.
- Benda L, Andras K, Miller D, Bigelow P. 2004a. Confluence effects in rivers: Interactions of basin scale, network geometry, and disturbance regimes. *Water Resources Research* **40**: W05402.
- Benda L, Poff NL, Miller D, Dunne T, Reeves G, Pess G, Pollock M. 2004b. The Network Dynamics Hypothesis: How channel networks structure riverine habitats. *BioScience* **54**: 413–427.
- Bertuzzo E, Gatto M, Maritan A, Rodriguez-Iturbe I, Rinaldo A. 2007. River networks and ecological corridors: Reactive transport on fractals, migration fronts, hydrochory. *Water Resources Research* **43**: W04419. DOI: 10.1029/2006WR005533.
- Best JL. 1986. The morphology of river channel confluences. *Progress in Physical Geography* **10**: 157–174.
- Best JL. 1988. Sediment transport and bed morphology at river channel confluences. *Sedimentology* **35**: 481–498.
- Best JL, Ashworth PJ. 1997. Scour in large braided rivers, and the recognition of sequence stratigraphic boundaries. *Nature* **387**: 275–277.

- Bigelow PE, Benda LE, Miller DJ, Burnett KM. 2007. On debris flows, river networks, and the spatial structure of channel morphology. *Forest Science* **53**: 220–238.
- Binnie SA, Phillips WM, Summerfield MA, Fifield LK. 2006. Sediment mixing and basin-wide cosmogenic nuclide analysis in rapidly eroding mountainous environments. *Quaternary Geochronology* **1**: 4–14.
- Biron P, Roy AG, Best JL, Boyer CJ. 1993. Bed morphology and sedimentology at the confluence of unequal depth channels. *Geomorphology* **8**: 115–129.
- Biron PM, Ramamurthy AS, Han S. 2004. Three-dimensional numerical modeling of mixing at river confluences. *Journal of Hydraulic Engineering, ASCE* **130**: 243–253.
- Boyer C, Roy AG, Best JL. 2006. Dynamics of a river channel confluence with discordant beds: Flow turbulence bed load sediment transport and bed morphology. *Journal of Geophysical Research – Earth Surface* **111**: F04007. DOI: 10.1029/2005JF000458.
- Bramblett RG, Bryant MD, Wright BE, White RG. 2002. Seasonal use of small tributary and main-stem habitats by juvenile steelhead, coho salmon, and Dolly Varden in a southeastern Alaska drainage basin. *Transactions of the American Fisheries Society* **131**: 498–506.
- Brierley GJ, Fryirs K. 1999. Tributary-trunk stream relations in a cut-and-fill landscape: A case study from Wolumla catchment, New South Wales, Australia. *Geomorphology* **28**: 61–73.
- Bruns DA, Minshall GW, Cushing CE, Cummins KW, Brock JT, Vannote RL. 1984. Tributaries as modifiers of the river continuum concept: Analysis by polar ordination and regression models. *Archive Hydrobiologie* **99**: 208–220.
- Cairns MA, Ebersole JL, Baker JP, Wigington PJ, Lavigne HR, Davis JA. 2005. Influence of summer stream temperatures on black spot infestation of juvenile Coho salmon in the Oregon Coast Range. *Transactions of the American Fisheries Society* **134**: 1471–1479.
- Cellot B. 1996. Influence of side-arms on aquatic macroinvertebrate drift in the main channel of a large river. *Freshwater Biology* **35**: 149–164.
- Church M, Kellerhals R. 1978. On the statistics of grain size variation along a gravel river. *Canadian Journal of Earth Sciences* **15**: 1151–1160.
- Dargahi B. 2004. Three-dimensional flow modelling and sediment transport in the River Klaralven. *Earth Surface Processes and Landforms* **29**: 821–852.
- Dawson M. 1988. Sediment size variation in a braided reach of the Sunwapta River, Alberta, Canada. *Earth Surface Processes and Landforms* **13**: 599–618.
- Ding Y, Wang SSY. 2006. Optimal control of open-channel flow using adjoint sensitivity analysis. *Journal of Hydraulic Engineering, ASCE* **132**: 1215–1228.
- Ettema R, Muste M. 2001. Laboratory observations of ice jams in channel confluences. *Journal of Cold Regions Engineering* **15**: 34–58.
- Ettema R, Fujita I, Muste M, Kruger A. 1997. Particle-image velocimetry for whole-field measurement of ice velocities. *Cold Regions Science and Technology* **26**: 97–112.
- Federici B, Paola C. 2003. Dynamics of channel bifurcations in noncohesive sediments. *Water Resources Research* **39**: 1162.
- Ferguson RI, Cudden JR, Hoey TB, Rice SP. 2006. River system discontinuities due to lateral inputs: Generic styles and controls. *Earth Surface Processes and Landforms* **31**: 1149–1166.
- Fernandes CC, Podos J, Lundberg JG. 2004. Amazonian ecology: Tributaries enhance the diversity of electric fishes. *Science* **305**: 1960–1962.
- Flint JJ. 1980. Tributary Arrangements in Fluvial Systems. *American Journal of Science* **280**: 26–45.

- Florsheim JL, Mount JF, Rutten LT. 2001. Effect of base level change on floodplain and fan sediment storage and ephemeral tributary channel morphology, Navarro River, California. *Earth Surface Processes and Landforms* **26**: 219–232.
- Franks CA, Rice SP, Wood PJ. 2002. Hydraulic habitat in confluences: An ecological perspective on confluence hydraulics. In *The Structure, Function and Management Implications of Fluvial Sedimentary Systems*, Dyer FJ, Thoms MC, Olley JM (eds). International Association Hydrological Sciences Publications, Wallingford, UK: **276**, 61–67.
- Fraser DF, Gilliam JF, Yip-Hoi T. 1995. Predation as an agent of population fragmentation in a tropical watershed. *Ecology* **76**: 1461–1472.
- Gasparini NM, Tucker GE, Bras RL. 1999. Downstream fining through selective particle sorting in an equilibrium network. *Geology* **27**: 1079–1082.
- Gaudet JM, Roy AG. 1995. Effect of bed morphology on flow mixing length at river confluences. *Nature* **373**: 138–139.
- Gomez-Villar A, Alvarez-Martinez J, Garcia-Ruiz JM. 2006. Factors influencing the presence or absence of tributary-junction fans in the Iberian Range, Spain. *Geomorphology* **81**: 252–264.
- Grant EHC, Lowe WH, Fagan WF. 2007. Living in the branches: Population dynamics and ecological processes in dendritic networks. *Ecology Letters* **10**: 165–175.
- Hanks TC, Webb RH. 2006. Effects of tributary debris on the longitudinal profile of the Colorado River in Grand Canyon. *Journal of Geophysical Research-Earth Surface* **111**: F02020.
- Horton RE. 1945. Erosional development of streams and their drainage basins: Hydrophysical approach to quantitative morphology. *Geological Society of America Bulletin* **56**: 275–370.
- Kennedy BA. 1984. On Playfair's law of accordant junctions. *Earth Surface Processes and Landforms* **9**: 153–173.
- Kenworthy ST, Rhoads BL. 1995. Hydrologic control of spatial patterns of suspended sediment concentration at a stream confluence. *Journal of Hydrology* **168**: 251–263.
- Khan AA, Cadavid R, Wang SSY. 2000. Simulation of channel confluence and bifurcation using the CCHE2D model. *Proceedings of the Institution of Civil Engineers-Water Maritime and Energy* **142**: 97–102.
- Kiffney PM, Greene C, Hall J, Davies J. 2006. Gradients in habitat heterogeneity, productivity, and diversity at tributary junctions. *Canadian Journal of Fisheries and Aquatic Sciences* **63**: 2518–2530.
- Knighton AD. 1980. Longitudinal changes in size and sorting of stream bed material in four English Rivers. *Geological Society of America Bulletin* **91**: 55–62.
- Kochel RC, Baker VR. 1982. Palaeoflood hydrology. *Science* **215**: 353–361.
- Kreb D, Budiono YK. 2005. Conservation management of small core areas: Key to survival of a critically endangered population of irrawaddy river dolphins *Orcaella brevirostris* in Indonesia. *Oryx* **39**: 178–188.
- Krumbein WC. 1942. Flood deposits of the Arroyo Seco, Los Angeles County, California. *Geological Society of America Bulletin* **53**: 1355–1402.
- Kupferberg SJ. 1996. Hydrologic and geomorphic factors affecting conservation of a river-breeding frog (*Rana boylii*). *Ecological Applications* **6**: 1332–1344.
- Leclair SF, Roy AG. 1997. Variability of bed morphology and sedimentary structures at a discordant river confluence during low flows. *Geographie Physique et Quaternaire* **51**: 125–139.
- Lyell C. 1830. *Principles of Geology*. John Murray: London.

- Mackay JR. 1970. Lateral mixing of Liard and Mackenzie Rivers downstream from their confluence. *Canadian Journal of Earth Sciences* **7**: 111–124.
- May CL, Gresswell RE. 2004. Spatial and temporal patterns of debris-flow deposition in the Oregon Coast Range, USA. *Geomorphology* **57**: 135–149.
- Miller JP. 1958. *High Mountain Streams: Effects of Geology on Channel Characteristics and Bed Material*. Memoir 4, State Bureau of Mines and Mineral Resources, New Mexico Institute of Mines and Mining Technology, Socorro, New Mexico.
- Mosley MP. 1976. An experimental study of channel confluences. *Journal of Geology* **84**: 535–562.
- Paola C. 1997. When streams collide. *Nature* **387**: 232–233.
- Paola C, Foufoula-Georgiou E, Dietrich WE, Hondzo M, Mohrig D, Parker G, Power ME, Rodriguez-Iturbe I, Voller V, Wilcock P. 2006. Toward a unified science of the Earth's surface: Opportunities for synthesis among hydrology, geomorphology, geochemistry, and ecology. *Water Resources Research* **42**: 10.1029/2005WR004585.
- Parsons DR, Best JL, Lane SN, Orfeo O, Hardy RJ, Kostaschuk R. 2007. Form roughness and the absence of secondary flow in a large confluence–difffluence, Rio Parana, Argentina. *Earth Surface Processes and Landforms* **32**: 155–162.
- Perry JA, Schaeffer DJ. 1987. The longitudinal distribution of riverine benthos: A river discontinuum? *Hydrobiologia* **148**: 257–268.
- Petts GE. 1984. *Impounded Rivers: Perspectives for Ecological Management*. John Wiley and Sons: Chichester.
- Petts GE, Greenwood M. 1985. Channel changes and invertebrate faunas below Nant-y-Moch dam, River Rheidol, Wales, UK. *Hydrobiologia* **122**: 65–80.
- Playfair J. 1802. *Illustrations of the Huttonian Theory of the Earth*. Dover: London.
- Poole GC. 2002. Fluvial landscape ecology: Addressing uniqueness within the river discontinuum. *Freshwater Biology* **47**: 641–660.
- Power ME, Dietrich WE. 2002. Food webs in river networks. *Ecological Research* **17**: 451–471.
- Prowse TD. 1986. Ice jam characteristics, Liard-Mackenzie Rivers confluence. *Canadian Journal of Civil Engineering* **13**: 653–665.
- Rhoads BL. 1987. Changes in stream channel characteristics at tributary junctions. *Physical Geography* **8**: 346–361.
- Rhoads BL, Sukhodolov AN. 2004. Spatial and temporal structure of shear layer turbulence at a stream confluence. *Water Resources Research* **40**: W06304.
- Rice SP. 1998. Which tributaries disrupt downstream fining along gravel-bed rivers? *Geomorphology* **22**: 39–56.
- Rice SP, Church M. 1998. Grain size along two gravel-bed rivers: Statistical variation, spatial pattern and sedimentary links. *Earth Surface Processes and Landforms* **23**: 345–363.
- Rice SP, Church M. 2001. Longitudinal profiles in simple alluvial systems. *Water Resources Research* **37**: 417–426.
- Rice SP, Greenwood MT, Joyce CB. 2001. Tributaries, sediment sources and the longitudinal organisation of macroinvertebrate fauna along river systems. *Canadian Journal of Fisheries and Aquatic Sciences* **58**: 824–840.
- Rice SP, Ferguson RI, Hoey T. 2006. Tributary control of physical heterogeneity and biological diversity at river confluences. *Canadian Journal of Fisheries and Aquatic Sciences* **63**: 2553–2566.
- Richards KS. 1980. A note on changes in channel geometry at tributary junctions. *Water Resources Research* **16**: 241–244.

- Rodríguez-Iturbe I, Rinaldo A. 1997. *Fractal River Basins: Chance and Self-Organization*. Cambridge University Press: Cambridge.
- Roy AG, Woldenberg MJ. 1986. A model for changes in channel form at a river confluence. *Journal of Geology* **94**: 402–411.
- Roy NG, Sinha R. 2005. Alluvial geomorphology and confluence dynamics in the Gangetic plains, Farrukhabad-Kannauj area, Uttar Pradesh, India. *Current Science* **88**: 2000–2006.
- Roy AG, Roy R, Bergeron N. 1988. Hydraulic geometry and changes in flow velocity at a river confluence with coarse bed material. *Earth Surface Processes and Landforms* **13**: 583–598.
- Shen HT, Su JS, Liu LW. 2000. SPH simulation of river ice dynamics. *Journal of Computational Physics* **165**: 752–770.
- Shreve RL. 1967. Infinite topologically random channel networks. *Journal of Geology* **77**: 397–414.
- Sklar LS, Dietrich WE, Foufoula-Georgiou E, Lashermes B, Bellugi D. 2006. Do gravel-bed river size distributions record channel network structure? *Water Resources Research* **42**: DOI: 10.1029/2006wr005035.
- Sternberg H. 1875. Untersuchungen über längen- und Querprofil geschiebeführender Flüsse. *Zeitschrift für Bauwesen* **25**: 483–506.
- Taylor EH. 1944. Flow characteristics at rectangular open channel junctions *Transactions of the American Society of Civil Engineers* **109**: 893–912.
- Thorp JH, Thoms MC, Delong MD. 2006. The riverine ecosystem synthesis: Biocomplexity in river networks across space and time. *River Research and Applications* **22**: 123–147.



# I

## River Channel Confluences



# 2

## Introduction to Part I: river channel confluences

**André G. Roy**

*Canada Research Chair in Fluvial Dynamics, Département de Géographie, Université de Montréal, Canada*

### Introduction

River channel confluences are critical interfaces where intense changes in physical processes occur. These changes affect both the local and downstream characteristics of the river flow and of the bed. How and why these changes occur are fundamental questions for our understanding of the dynamics of the whole of the river system. In view of the importance of channel confluences, it is surprising to note that it has taken much time before confluences have become an object of scientific inquiry. This is partly explained by the complex character of river channel confluences. Considering the difficulties posed by the understanding of flow structure in single channels, how does one expect to grasp the behaviour of flows when two streams with different characteristics meet? Such complexity has defied researchers for years and, as a result, the interactions between flows, sediments and bed morphology at confluences have long been neglected.

With the development of advanced instrumentation and of novel experimental designs, research evolved quickly in the last two decades of the twentieth century. It is of great interest to see how the science of river confluences has evolved since the 1980s through an intricate and effective blend of laboratory work, field studies and numerical modelling. The acquisition of this new knowledge on confluences has also had major

implications for the management of river systems. Tremendous advances in knowledge have followed the seminal work of Mosley published in 1976. His laboratory experiments paved the way for the identification of major controls on the flow structure and on the associated bed morphology of river channel confluences. Two key variables, the junction angle and the ratio of discharges between the confluent channels, have been shown to affect the size and shape of the principal zones of the flow (e.g. flow separation downstream from the tributary entrance) and of the scour area that is characteristic of most confluences. The systematic investigation of confluence dynamics in the laboratory has produced a solid framework against which the results from field research can be gauged. For instance, the hydraulics of confluences involve a number of processes: flow separation, flow acceleration, flow stagnation and a shear layer with very high turbulence intensity. These processes all take place within the confluence volume and vary in space and time. Field studies have not only documented this variability but also allowed researchers to discover new controlling variables and to develop a more complete model of river confluence dynamics. For instance, the role of bed discordance has emerged as a critical variable. In turn, the effect of this variable on the flow structure was systematically tested in the laboratory. This interaction between laboratory and field studies has been extremely fruitful. This, however, has raised the persistent issue of how these results scale up. Researchers have recently tested the potential of applying results from small laboratory and field experiments to large rivers, including some of the largest confluences in the world. This has led to the identification of other critical variables, such as the channel width-to-depth ratio. Advances have also come from the substantial contributions of computational fluid dynamics (CFD). The systematic examination of the effects of various confluence geometries and planforms on the flow structure has been successfully conducted. The application of CFD has been an audacious venture. The complexity of the bed geometry as well as the high turbulence intensity generated by a range of processes presented enormous challenges to researchers. The applications have produced insightful results that both confirmed some of the empirical observations and provided new hypotheses to be tested. This knowledge has also important implications for the management and design of river channel confluences. Confluences are often preferential sites for flooding and ice jams and for bed instability. These features are of great concern because they threaten many infrastructures, like bridges and buildings.

This first section of this book aims at reviewing and expanding the current state of knowledge on river channel confluences. As a reflection of the complex interactions among processes at confluences, the material that composes this section is heavily interrelated. It has been a challenge to divide the knowledge already gained on river channel confluences into five individual chapters. Because we were hoping that the material could be read as separate, stand-alone, chapters as well as a coherent set of contributions, the amount of overlap between chapters had to be gauged carefully. This section will provide readers with an exhaustive overview of our current understanding

of the fundamental physical processes at confluences, of the potential to scale up these processes to unconfined and large river systems and of the application of this knowledge to the management of confluences. All chapters cover extensively the literature and present new results and ideas for future work.

## Individual chapters

In Chapter 3, Biron and Lane examine the flow and sediment-transport processes from a modelling point of view. The authors set the stage by documenting the debate that has emerged around the many (often conflicting) views on the flow structures at confluences. They highlight the critical role of planform geometry, of topographic forcing by the bed and of the shear layer that develops in between the confluent flows. They present the challenges that modellers face when attempting to represent numerically these flow processes and illustrate the effectiveness of three-dimensional models to represent confluence dynamics. They also discuss models used for the transport of matter through confluences, including solute, suspended and bedload sediment transport.

Following on this work, Best and Rhoads (Chapter 4) present the relations between flow processes and the morphology of river channel confluences. They describe in detail the typical morphological features found at river channel confluences (e.g. scour, tributary-mouth bars). These forms vary with planform geometry and with the discharges and depths of the confluent channels. They also describe bedload sediment-transport patterns and their consequences on channel changes and on the imprints of confluences in the sedimentological record.

Chapter 5 extends the work presented in the previous chapters as it is applied to very large confluences (more than a kilometre wide). Written by a group of researchers under the lead of Parsons, the chapter utilizes data collected in the first five years of the twenty-first century. This work has been possible through advances in instrumentation allowing for the measurement of flow and bed morphology over large bodies of water. The authors highlight both the similarities and differences between small- and large-scale confluences using selected examples. The fact that channel width increases faster than flow depth when rivers grow in size is shown to be a critical factor for explaining some of the features of the bed morphology and flow processes at large confluences.

In Chapter 6, Ettema discusses the management approaches used in the context of river channel confluences. He emphasizes two aspects of river channel confluences: sediment transport and ice passage. Through examples, the author illustrates the 'unruliness' of confluences and the main issues associated with channel (in)stability at confluences. Management strategies to alleviate the effects of bed instability and of ice jams are explored and discussed. The author also introduces a novel dimensional analysis of the problem of ice passage.

In the final chapter of the section, Ashmore and Gardner examine the morphology and dynamics of unconfined confluences especially in the context of braided river systems where confluences form a fundamental unit of the channel pattern. The authors distinguish the main characteristics of the confluence-bar-bifurcation unit and link the variable expression of this morphology with flow processes. The formation of deep scour zones and of extensive bars is discussed in relation to the more classical setting of confined channels. The authors describe the relations between bedforms and sediment transport and present new methods and ideas for the understanding of the sorting patterns of particles at confluences.

These chapters show how vital channel confluences are for the whole of the river system and they set the stage for the next sections as the scale of interest is shifted towards the role of tributaries and the properties of drainage networks.

## Reference

Mosley MP. 1976. An experimental study of channel confluences. *Journal of Geology* **84**: 535–562.

# 3

## Modelling hydraulics and sediment transport at river confluences

Pascale M. Biron<sup>1</sup> and Stuart. N. Lane<sup>2</sup>

<sup>1</sup>*Department of Geography, Planning and Environment, Concordia University, Canada*

<sup>2</sup>*Department of Geography, Durham University, Science Laboratories, UK*

### Introduction

River confluences are key features of drainage basins in terms of geomorphology, hydrology, the routing of water, sediments, pollutants, for geological records, as well as from a habitat point of view. Confluences are also sites of complex hydraulics with many controlling factors. The observation, measurement and modelling of the hydraulic behaviour of river confluences has proved to be a difficult enterprise. Earlier modelling attempts of open-channel junctions focused on hydraulics using 1D approaches based on momentum changes at confluences (Taylor, 1944; Webber and Greated, 1966; Ramamurthy *et al.*, 1988; Hager, 1989a; Hsu *et al.*, 1998; Shabayek *et al.*, 2002). However, these theoretical approaches are based on a series of over-simplified assumptions (e.g. constant width, negligible friction). Furthermore, they do not take into account mixing processes, and are thus not well suited to represent the highly three-dimensional flow at river confluences.

The advent of hydrodynamic modelling, particularly in three dimensions, has greatly improved our understanding of the dynamics of confluences (Weerakoon and Tamai,

1989; Weerakoon *et al.*, 1991; Bradbrook *et al.*, 1998, 2000a, 2000b, 2001; Huang *et al.*, 2002; Biron *et al.*, 2004a). Hydrodynamic models complement field and laboratory studies of confluences, as they allow the exploration of a greater number of scenarios (e.g. combinations of discharge or velocity ratio, junction angle, bed morphology, bed roughness etc.) than can commonly be measured in the field or the laboratory. However, their value in hypothesis testing is commonly challenged by two issues. First, confluences contain aspects of flow, mixing and sediment-transport processes, notably those associated with turbulence, that represent extreme challenges for numerical models. Second, the worth of hydrodynamic models in addressing some of the key unanswered questions regarding confluences remains to be established. This is notably the case for issues regarding large river junctions, where questions are emerging about the transferability of conclusions reached from small-scale field and laboratory studies (Parsons *et al.*, this volume, Chapter 5; Parsons *et al.*, 2007; Lane *et al.*, in press) where numerical modelling represents a particular challenge as a result of limits to effective computation over such large spatial scales. This chapter reviews the key findings that result from hydraulics and sediment-transport modelling of confluences and uses these to present new ideas on the generalization of observations from the laboratory scale to the very large scale.

## Hydraulics

### Key elements of confluence hydraulics

The first real attempt to develop a general model of confluence hydraulics followed from Mosley (1976) and was developed by Best (1987, 1988). The latter defined six distinct elements of confluence hydraulics: (1) a zone of flow stagnation at the upstream junction corner, (2) flow deflection where each tributary enters the confluence, (3) a flow-separation zone below the downstream junction corner (also described in detail in Best and Reid, 1984), (4) an area of maximum velocity, (5) a gradual flow recovery area downstream from the flow-separation zone and (6) several distinct shear layers associated with vortex generation (Figure 3.1(A)). The dominant controls on these zones were believed to be confluence angle and discharge ratio. For instance, Best and Reid (1984) show the effects of these two variables on the size of the separation zone (Figure 3.1(B)). As the confluence angle or the discharge ratio increases, the zone of separation widens and increasingly dominates the dynamics of the confluence. These variables are also associated with the bed morphology of the confluence (Best and Rhoads, this volume, Chapter 4). There are, however, other factors that intervene, and the presence of a shear layer is a dominant feature of the confluence. It is perhaps unfortunate that on the visual representation of this model, the shear layer between

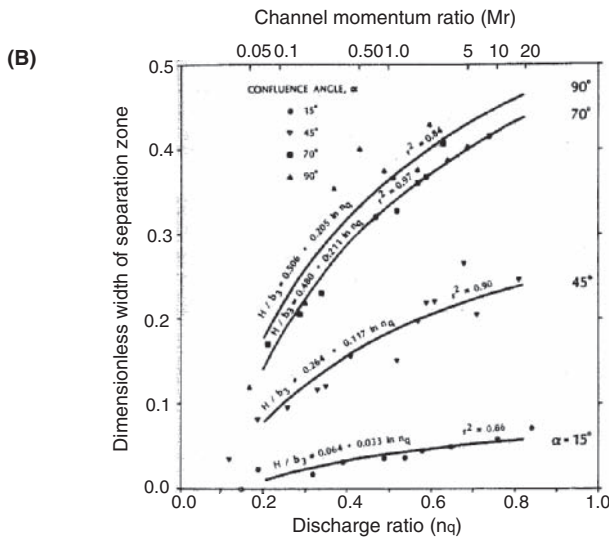
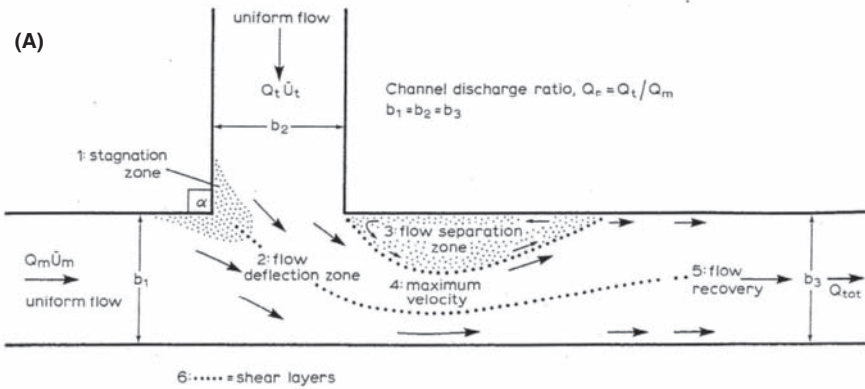


**Figure 3.1** (A) Best (1987) model of flow dynamics at river channel confluences; (B) relationship between maximum separation zone width and the ratio of the angled tributary to post-confluence total discharge ( $n_q$ ), and the channel momentum ratio ( $Mr$ ) defined as  $(\langle U_2 \rangle^2 / \langle U_1 \rangle^2) \times (b_2 / b_1)$ , where  $\langle U \rangle$  is mean flow velocity,  $b$  is channel width and subscript 1 and 2 correspond to the main channel upstream from the junction and the angled tributary respectively (from Best and Reid, 1984).

the two incoming streams appears as a simple dotted line (Figure 3.1(A)), as one does not readily see the importance of this zone which can occupy a significant area of the receiving channel (Biron *et al.*, 1993; De Serres *et al.*, 1999; Rhoads and Sukhodolov, 2001). However, Best (1987) explicitly reveals the importance of this element in the text: ‘A feature of great significance in this region is that a shear layer is created between the two convergent flows along which powerful, vertical vortices are generated. These are

responsible for increased bed shear stresses within the junction which, together with the increase in velocity as both flows enter the confluence, are responsible for considerable bed scour' (Best, 1987, p. 31).

There has been surprisingly little research done on shear-layer dynamics at natural confluences, at least for angled junctions. Indeed, most of our understanding on Kelvin–Helmholtz instabilities generated in mixing zones comes from laboratory studies at parallel junctions (Winant and Browand, 1974; Chu and Babarutsi, 1988; Babarutsi and Chu, 1998; Uijttewaals and Tukker, 1998; Uijttewaals and Booij, 2000; Van Proijen and Uijttewaals, 2002). At natural junctions, Leclair and Roy (1997) provide evidence of the shear layer expansion at low-flow and Roy *et al.* (1999) document the dynamics of eddies in the mixing zone with a combined use of visualization and velocity time series. However, to our knowledge, only the field studies of Biron *et al.* (1993) and Rhoads and Sukhodolov (2004) quantify in detail shear-layer dynamics at natural confluences, with the use of time series and spectral analyses of velocity measurements collected at relatively high sampling frequency (20 and 25 Hz respectively). Although the quantification of the coherent rotating mixing-layer vortices at natural confluences provides a useful tool to characterize these features, visualization remains particularly efficient to enhance our understanding of the complex processes occurring in mixing zones. The ideal situation is when a colour difference exists between the incoming streams (e.g. Bayonne–Berthier confluence, Roy *et al.*, 1999). Otherwise, dye can be injected, as was done in the Kaskaskia River–Copper Slough (KRCS) junction (Sukhodolov and Rhoads, 2001; Rhoads and Sukhodolov, 2004). Care is required, however, when using this method as the injection point may affect the interpretation of the results. For example, the same mixing zone appears differently with dye being injected from the stagnation zone (Figure 12, Sukhodolov and Rhoads, 2001) or spread across the entire width of the Kaskaskia River (Figure 13, Rhoads and Sukhodolov, 2004), where much larger coherent structures seem to prevail.

## Current debate on confluence hydraulics

A long-standing debate about the nature and cause of observed flow structures at the junction of two rivers has followed the work of Mosley (1976) and Best (1987, 1988). This debate has mostly grown in the Earth science literature, as engineers have looked at the merging of two channels from a different perspective, focusing on lateral momentum exchange (Ramamurthy *et al.*, 1988), the velocity field (Wang *et al.*, 1996; Weber *et al.*, 2001), water-surface variation (Wang *et al.*, 1996; Khan *et al.*, 2000; Weber *et al.*, 2001; Huang *et al.*, 2002) and subcritical versus supercritical differences (Hager, 1989a, 1989b; Gurram *et al.*, 1997).

A common view is that a major component of flow structure at confluences is the presence of two rotating cells which are converging at the surface in the centre of the channel, and diverging near the bed (Figure 3.2(A)) (Mosley, 1976; Ashmore, 1982; Ashmore and

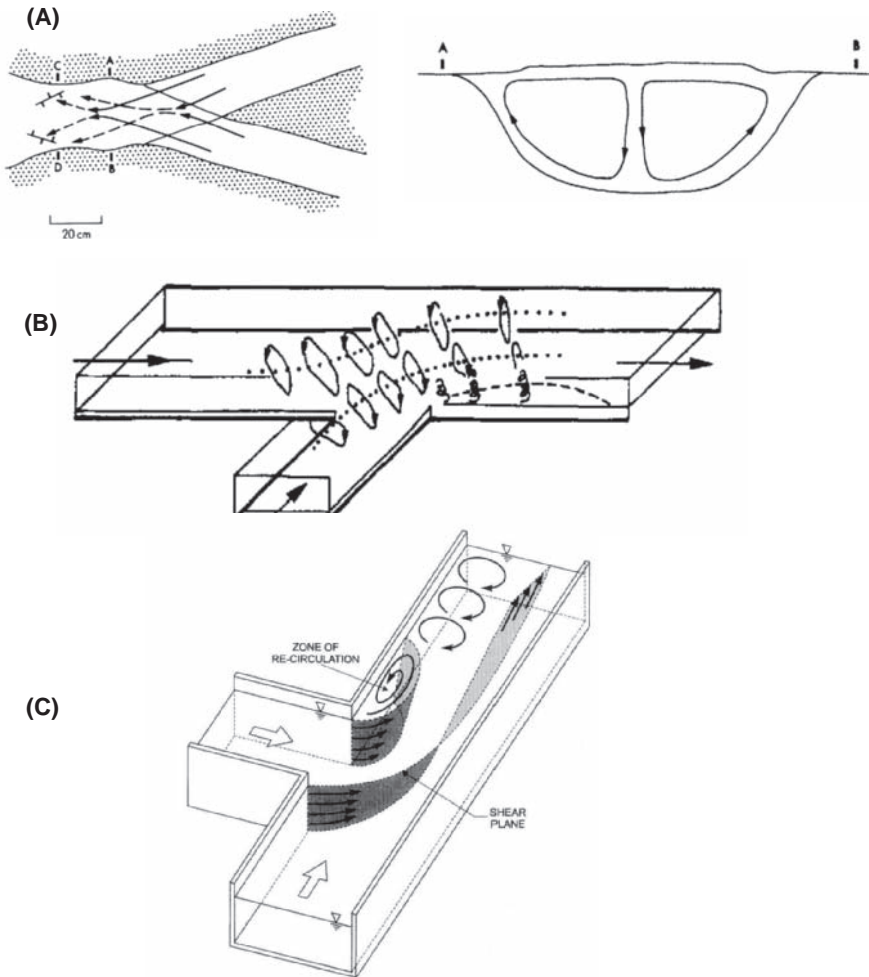


**Figure 3.2** Different perspectives on secondary flow circulation models at confluences: (A) dominating model in Earth science, with a back-to-back meander analogy implying two counter-rotating cells converging at the surface and diverging at the bed at a symmetrical junction (from Ashmore, 1982); (B) an engineering perspective on secondary flow showing the two cells rotating in opposite directions at an asymmetrical junction (from Gurram *et al.*, 1997, based on the study by Fujita and Komura, 1989); (C) another engineering perspective with only one clockwise cell downstream of the separation zone (from Weber *et al.*, 2001).

Parker, 1983; Ashmore *et al.*, 1992; Rhoads and Kenworthy, 1995, 1998; McLelland *et al.*, 1996; Rhoads, 1996; Richardson *et al.*, 1996; Richardson, 1997; Bradbrook *et al.*, 2000b, 2001; Rhoads and Sukhodolov, 2001). Field measurements (Rhoads and Kenworthy, 1995, 1998; Rhoads, 1996) and hydrodynamic modelling (Bradbrook *et al.*, 2000b) suggest that these can rapidly evolve into a single, channel-width circulation cell as a result of differences in the angular momentum of the two confluent tributaries.

It has been suggested that such cells are responsible for scour formation as a result of depression of the core of maximum velocity and/or intense shear towards the bed by downwelling flow (e.g. Ashmore, 1982; Ashmore *et al.*, 1992; Bridge, 1993). Studies also describe either twin helical cells rotating in the *opposite* direction (Figure 3.2(B)) or a single clockwise cell (Figure 3.2(C)). The latter is less surprising as hydrodynamic modelling of trapezoidal channels (Bradbrook *et al.*, 1998, 2001) has shown that there are situations when single rotating cells form as flows join. The case shown in Figure 3.2(B) does not match the current understanding of confluence hydrodynamics.

Part of the difficulty in producing a general model of flow structure formation at confluences is that, whilst the processes that drive flow structure formation will be the same, their manifestation in particular places may be very different as a result of differences in the associated boundary conditions. There are a number of reasons for this. The first, and one still overlooked in confluence studies, is the role played by upstream planform forcing. For example, Ashmore and Parker (1983) present a situation where both incoming streams are curved in an opposite way (one convex, the other concave) in a braided system (Figure 3.3(A)). In this case, the helical flow pattern inherited from the two upstream meanders would indeed produce downwelling in the centre of the channel at the junction as the cell motion is anticlockwise in the right tributary (looking downstream) and clockwise in the left tributary. However, if the same situation is viewed as part of a braid bar unit (e.g. Ashworth *et al.*, 1992; Bridge, 1993; Figure 3.3(B)), whether or not there is opposite curvature depends upon the rate at which helical circulation responds to upstream planform forcing. In Figure 3.3(B), downwelling should migrate towards the outer bank of each distributary channel alongside and immediately downstream of the maximum bar width. Downstream from here, the curvature in both distributaries reverses to mirror that in Figure 3.3(A), and the downwelling zone should migrate back across towards the downstream end of the bar. The rate of adjustment between planform forcing and helical circulation will then determine the nature of the helical circulation at the entrance to the confluence. Figure 3.3(C) shows a third scenario where the two upstream channels curve in the same direction as per the Bayonne–Berthier confluence studied by Biron *et al.* (1993, 2002), De Serres *et al.* (1999) and

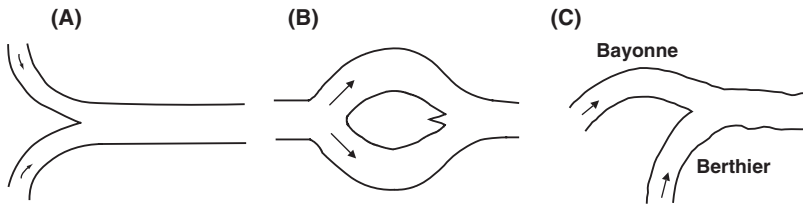


**Figure 3.3** Different planform geometries of channels upstream of junctions: (A) braided river upstream channels as depicted by Ashmore and Parker (1983); (B) braided river upstream channels as depicted by Ashworth *et al.* (1992) and Bridge (1993); (C) confined confluence planform geometry at the Bayonne–Berthier confluence (Québec) (De Serres *et al.*, 1999).

Boyer *et al.* (2006). In theory, this should produce two anticlockwise cells when looking downstream at the junction entrance. These observations are important because most laboratory studies use straight incoming channels (e.g. Mosley, 1976; Best, 1987, 1988), which effectively eliminates the possibility of there being planform curvature and so it is not surprising that such studies have tended to underestimate its importance.

The second challenge, and one related to the influence of upstream planform forcing, comes from the differences that emerge between laboratory studies which use rectangular channels (e.g. Ramamurthy *et al.*, 1988; Fujita and Komura, 1989; Best and Roy, 1991; Gurram *et al.*, 1997; Weber *et al.*, 2001) and laboratory and field studies of self-formed confluences (e.g. Mosley, 1976; Ashmore, 1982; Ashmore and Parker, 1983; Best, 1987, 1988). This difference is crucial because the latter introduce an additional set of forcing terms into the analysis associated with topography. As the width-to-depth ratio rises, such terms will become increasingly dominant in the momentum balance and cause deviation from models of confluence hydrodynamics that consider only bed pressure gradients caused by curvature-driven helical circulation. These processes will not only matter in relation to the confluence zone itself but will also condition the rate at which flow patterns adjust to upstream planform forcing. They will also be controlled by the relative submergence of bed roughness such that rivers with different bed sedimentologies should be associated with different magnitudes of the topographic forcing terms and potentially different flow structures. If flow structures are a critical determinant of sediment transfer and morphological changes in confluences, this may well contribute to differences in the morphology of confluences in sand and gravel-bed rivers.

The third issue represents a specific extreme of topographic forcing. Confluences commonly have a marked scour, and this may generate flow separation on both avalanche faces. As such faces commonly extend across the tributary entrance tangential to tributary flow direction, they may well cause helical circulation that has the same orientation as would be expected from curvature-induced helical circulation of the sort expected in Figure 3.3(A). Indeed, Best (1987, 1988) suggests that, in his experiments, the counter-rotating helical vortices were resulting from – not causing – scouring, and describes them as ‘leeside eddies’, that is flow-separation cells in the lee of each avalanche face which contribute to further segregate bedload transport on each side of the scour, thus maintaining a deep scour. Bed morphology, rather than planform curvature, could thus be the primary control for the development of these cells. The issue is still not resolved as numerical models suggest that planform curvature in the absence of any kind of topographic forcing does result in the formation of counter-rotating helical cells (Bradbrook *et al.*, 2000a), although there are no coupled laboratory or numerical studies of confluence evolution from the flat bed case. As we explain below, such a study is a critical requirement but not at all straightforward.

Fourth, distortion of the shear layer due to bed discordance and vertical separation may be more important than planform curvature in some situations (Best and Roy, 1991; Gaudet and Roy, 1995; Biron *et al.*, 1996a, 1996b; De Serres *et al.*, 1999; Boyer *et al.*, 2006). At many natural junctions, the tributary is shallower than the main channel,

leading to a depth difference which can be quantified by the depth ratio  $D_r$  (average depth of the tributary over that of the main channel). Values of depth ratio as low as 0.36 have been observed in an estuary channel confluence (Pierini *et al.*, 2005). Small depth ratios often occur in large confluences, such as the Negro and Solimões ( $D_r \sim 0.6$ , Laraque *et al.*, in press) and the Paraguay–Paraná ( $D_r = 0.5$ , Lane *et al.*, in review). At a smaller confluence (Bayonne–Berthier, about 10 m wide),  $D_r$  values ranged from 0.36 at low flow to 0.72 at high flow (De Serres *et al.*, 1999). At discordant bed confluences in small rivers, the role of vortices in the distorted mixing layer has been shown to be crucial for sediment transport and scour formation (Biron *et al.*, 1993; De Serres *et al.*, 1999; Roy *et al.*, 1999; Boyer *et al.*, 2006). However, Sukhodolov and Rhoads (2001) state that although the shear layer is in general located within the scour-hole area, it does not necessarily imply that shear-layer turbulence generates scouring. They believe that helical motions, despite not being systematically present at junctions (Rhoads and Sukhodolov, 2001), contribute to scour at confluences. Ashmore *et al.* (1992) also acknowledges that Best (1988) considers helical circulation in confluences as arising primarily from horizontal separation vortices in the lee of avalanche faces, but they state that ‘it is possible that when flow separation occurs at the entrance it reinforces, rather than replaces, the circulation due to streamline curvature’ (p. 300), and they conclude that secondary circulation is dominated by double helical cells back-to-back. The causal role of these cells is also highlighted by Bridge (1993), who states that ‘the location and relative depth of the confluence scour zone is clearly influenced by the curvature-induced spiral flow’ (p. 40), indicating that helical cells are not perceived as leeside separation cells but rather as meander-like cells.

It is interesting to note that most of the studies which have described twin-secondary cells as the dominating flow feature were carried out using relatively small width-to-depth ratios, with an average of around 6 (ranging from 3 to 8) (Mosley, 1976; Ashmore, 1982; Ashmore and Parker, 1983; Ashmore *et al.*, 1992; Rhoads and Kenworthy, 1995; McLelland *et al.*, 1996; Rhoads, 1996; Rhoads and Kenworthy, 1998). In most natural rivers, the width-to-depth ratio is much higher, particularly for large rivers as downstream hydraulic geometry dictates that the rate of increase of width with discharge should be greater than the rate of increase in depth (Leopold and Maddock, 1953). Whilst the width-to-depth ratio may at first glance seem to be the variable that matters, the magnitude of water surface super-elevation at a confluence associated with planform curvature alone should actually depend on the ratio of river width to radius of curvature (Bradbrook *et al.*, 2000b; Lane and Ferguson, 2005). The water-surface elevation difference across a section normal to the direction of streamline curvature ( $\Delta E_{ni}$ ) will depend upon the centrifugal acceleration, and for tributary  $i$  is given by:

$$\Delta E_{ni} = \frac{\overline{U_{si}}^2}{g} \cdot \frac{w_i}{R_i} \quad (3.1)$$

where:  $U_{si}$  is the streamwise section-averaged velocity in tributary  $i$ ,  $w_i$  is the width of tributary  $i$ ,  $g$  is the acceleration due to gravity and  $R_i$  is the radius of the curvature of tributary  $i$ . If we assume that there is a linear association between the radius of the curvature and width (Leopold and Wolman, 1960; but note this needs to be tested for large rivers) and because the rate of increase in section-averaged velocity with downstream changes in river discharge is commonly much smaller than in width (Leopold and Maddock, 1953), the magnitude of water surface super-elevation will not scale with width. Thus, the magnitude of the driving component of curvature-driven circulation is likely to be very small indeed, and it is not surprising that early results from large rivers do not find helical circulation (e.g. Parsons *et al.*, 2007). However, for the same river, Lane *et al.* (in press) show that there are situations in which channel-scale helical-like circulation can form. They do not associate this with curvature-induced effects but with the interaction of angular momentum and topographic discordance that created a particular scenario in which the deeper channel could penetrate fully underneath the shallower channel. What emerges from this discussion is that we need to make sure that studies of confluences explore the full range of width-to-curvature ratios, in the presence of variable degrees of topographic forcing, including the extreme case when scour or discordance can lead to flow separation.

## Hydrodynamic modelling of confluence hydraulics

From the previous section, it is clear that laboratory and fieldwork both suffer from limitations (e.g. site-specific, with varying upstream curvatures and bed roughness, low width-to-depth ratio) which often prevent any comparison of results between studies, and complicates the task of determining the dominant features and control variables of confluence hydraulics. Hydrodynamic modelling can help in solving many of these issues, although confluences represent an extreme challenge for hydrodynamic modelling due, for example, to complex bed geometry, high three-dimensionality in the flow field and the need for accurate turbulence representation of the mixing-layer zone. This is particularly the case for natural junctions.

Some attempts were made to use two-dimensional (Khan *et al.*, 2000; Weerakoon *et al.*, 2003; Zanichelli *et al.*, 2004) or pseudo three-dimensional models (Wang *et al.*, 1996) for confluence modelling. However, Lane *et al.* (1999) show that the predictive ability of a three-dimensional model is markedly increased over a two-dimensional model at confluences, particularly if the two-dimensional model is not corrected for the effect of secondary circulation. Furthermore, three-dimensional velocity data collected at confluences indicate large variations from the bed to the water surface in the flow field (De Serres *et al.*, 1999; Rhoads and Sukhodolov, 2001), which would not be adequately simulated in a two-dimensional model. However, for large confluences where, for example, the objective is to investigate flood-control measures rather than detailed mixing

processes (Weerakoon *et al.*, 2003), depth-averaged models still represent a reasonable compromise if secondary circulation corrections are available.

In all existing studies on three-dimensional numerical modelling at junctions, the full three-dimensional form of the Navier–Stokes equations, based on finite-volume discretization, has been used (Weerakoon and Tamai, 1989; Weerakoon *et al.*, 1991; Bradbrook *et al.*, 1998; 2000a, 2000b, 2001; Lane *et al.*, 1999, 2000; Huang *et al.*, 2002; Biron *et al.*, 2004a). For steady-flow conditions, the Reynolds-Averaged Navier–Stokes (RANS) equations are used, for which a turbulence model needs to be specified. The standard  $k-\varepsilon$  turbulence model (Huang *et al.*, 2002) or the modified renormalization group (RNG)  $k-\varepsilon$  model, which has been shown to perform better in situations where flow separation occurs (Yakhot *et al.*, 1992; Bradbrook *et al.*, 1998, 2000b, 2001; Richardson and Panchang, 1998; Lane *et al.*, 2000; Biron *et al.*, 2004a), are commonly adopted. It is interesting to note that many of these three-dimensional models were developed by Earth scientists, but that their work is not always acknowledged in the engineering literature despite publications in engineering journals (e.g. Bradbrook *et al.*, 2001; Biron *et al.*, 2004a). For example, Parsons (2003) notes that Huang *et al.* (2002) stress an urgent need to develop and to validate a three-dimensional numerical method that is suitable for simulating open-channel junction flow, even though this had already been successfully achieved a few years before by Bradbrook *et al.* (1998, 2000a, 2000b, 2001).

The complex geometry of confluences creates difficulties when developing a numerical mesh. First, a multiblock approach is typically required to represent the main and tributary channel (Bradbrook *et al.*, 2001; Huang *et al.*, 2002). Second, except for the special cases of parallel junction (Bradbrook *et al.*, 1998) or 90° junction (Huang *et al.*, 2002) where a Cartesian grid can be used, a boundary-fitted coordinate approach is required to limit abrupt changes in the aspect ratio of cells or in gridline direction (Weerakoon and Tamai, 1989; Weerakoon *et al.*, 1991; Bradbrook *et al.*, 2000b, 2001; Biron *et al.*, 2004a). Third, modelling of natural junctions requires either an innovative representation of the three-dimensional variability in bed topography in structured meshes (e.g. Lane *et al.*, 2004; Hardy *et al.*, 2005) or the use of unstructured meshes (see below).

Virtually all three-dimensional modelling studies at junctions have focused on time-averaged flow structures. However, the understanding of the effect of processes that are occurring at various timescales (from the fraction of a second to several minutes when looking at the mixing layer's turbulence dynamics) is very important (Bradbrook *et al.*, 2000b). A solution to this problem is unsteady turbulence modelling with large eddy simulation (LES), where direct numerical simulation is used for flow fluctuations greater than the local grid dimension, and a sub-grid-scale turbulence model is used only for fluctuations smaller than this dimension (Keylock *et al.*, 2005). Bradbrook *et al.* (2000a) have successfully used LES for both a laboratory and natural discordant-bed junction, and have captured large-scale turbulence associated with these sites.

Three-dimensional numerical modelling studies have provided very helpful insights to the flow structure control at river confluences. For example, Bradbrook *et al.* (1998)

demonstrate that secondary circulation can develop at a parallel junction, that is in the absence of planform curvature. They determine that the key control on the secondary circulation strength was the velocity ratio rather than the junction angle and that, in the presence of bed discordance, this effect was increased (Bradbrook *et al.*, 1998, 2001). Numerical modelling not only allows for a variety of scenarios to be tested but also provides physical explanations which would otherwise be difficult to obtain as they are related to a variable – pressure – that is complicated to quantify in both experimental or fieldwork. For example, two factors appear to greatly control flow dynamics at junctions: (i) the cross-stream pressure gradient, dependent upon the velocity ratio, and (ii) the vertical extent of this pressure gradient, related to depth ratio and determining the relative depth of flow for cross-stream mass transfer (Bradbrook *et al.*, 1998).

At the Kaskaskia River and Copper Slough (KRCS) confluence, where helical cells have been detected both from two-dimensional and three-dimensional velocity measurements (Rhoads and Kenworthy, 1995, 1998; Rhoads, 1996; Rhoads and Sukhodolov, 2001), downwelling has been observed upstream of the scour hole in a three-dimensional numerical simulation, and has been associated with the water surface super-elevation present at confluences (Bradbrook *et al.*, 2000b). However, Bradbrook *et al.* (2000b) also performed an interesting numerical simulation of the KRCS confluence by numerically filling the scour hole by 0.4 m (reducing the depth from 1.4 to 1 m). Their results show that the zone of downwelling into the scour was no longer present. This suggested that bed topography, that is scour hole and point bar at asymmetrical confluences, reinforces the flow structures associated with planform curvature and that topographic steering is playing a role similar to that observed in meanders.

Three-dimensional numerical modelling has also been used to compare secondary flow generated at a symmetrical confluence to that resulting from a single meander channel (Bradbrook *et al.*, 2000b). Although the symmetrical junction did produce two cells, there were still important differences compared to the meander case. For instance, the surface elevation at the outer bank of the meander was greater than at the centre of the symmetrical junction, and a much greater surface depression resulted on the opposite side of the meander. Therefore, the water surface slope of meanders provides a greater centrifugal force to turn the flow than what was observed at a junction. In other words, a fluid encountering a solid boundary (meander bank) does not behave the same way as a fluid encountering another fluid, where a mixing layer develops.

## Challenges for confluence hydraulics modelling

The numerical representation of confluence geometry remains a challenge for three-dimensional modelling. This is ‘the stage where the CFD modeller has the largest impact on solution quality. Ideally, meshes are composed of hexahedral (8-node) elements that are orthogonal (i.e. each element corner is  $90^\circ$ ), distributed in the physical domain in

such a way that all gradients are represented adequately, and oriented with the direction of flow. When complex geometries are involved, non-uniform meshes must be used. A high quality non-uniform mesh satisfies criteria in attributes such as element size, element-to-element size variation, aspect ratio, skewness, smoothness, and boundary resolution' (Weber *et al.*, 2006, p. 278). As will be seen in the section on sediment transport, an ideal mesh would not only minimize changes in direction or aspect ratio between cells but also allow the mesh to be recomputed based on scouring and deposition processes.

In many three-dimensional models, a rigid-lid approximation is used for the treatment of water surfaces (Weerakoon and Tamai, 1989; Weerakoon *et al.*, 1991). This, however, is not adequate for confluence junction flows where water surface super-elevation is known to occur in the centre of the receiving channel (Mosley, 1976; Bradbrook *et al.*, 1998, 2000b; Biron *et al.*, 2002). A porosity approach has been used in many confluence three-dimensional simulations (Bradbrook *et al.*, 1998, 2000b, 2001; Biron *et al.*, 2002; 2004a) to correct for the effects of using a rigid-lid treatment. This approach does not involve generating a new mesh. Instead, porosity is defined for each cell in the top layer of fluid, and the flux across any cell face is equal to the porosity multiplied by the area of the face and the velocity component perpendicular to it. Super-elevation is represented by porosity values greater than 1.0, whereas surface depression has a porosity value less than 1.0 (Bradbrook *et al.*, 1998). Using this free-surface approximation, an improved correlation in the downstream velocity component between the simulated and the experimental data of Biron *et al.* (1996a, 1996b) was obtained (Bradbrook, 1999; Han, 2002). Results also indicate that including water surface topography as a boundary condition may improve the correlation between simulated and measured data (Biron *et al.*, 2002). However, this method is limited to situations where the water surface depression or super-elevation is smaller than the height of the top cell. Other methods exist to deal with free-surface variation, such as the Volume of Fluid (VOF) method (Ma *et al.*, 2002), the two-dimensional Poisson equation (Wu *et al.*, 2000), the kinematic and dynamic free surface conditions, where the mesh is regenerated through stretch or compression (Huang *et al.*, 2002), and a direct approach based on pressure distribution at the surface, which also involves regenerating the mesh (Rameshwaran and Naden, 2004). For all these methods, one of the difficulties is that there are very few detailed datasets of water surface topography for comparing simulated output, particularly at natural confluences.

The free-surface porosity method described above is limited to small water fluctuations and is not adequate for examining the more complex case of unsteady flow conditions due, for example, to the passage of a flood. At confluences, this is further complicated by the fact that floods may not be synchronized in both incoming streams, giving rise to a varying discharge or momentum flux ratio, which in turn can affect the position of the mixing zone (De Serres *et al.*, 1999; Boyer *et al.*, 2006). In order to run these simulations, a wetting and drying algorithm would be needed. Most of

the wetting and drying models, either based on a moving-mesh or a fixed-mesh approach, were developed for two-dimensional models or three-dimensional models with Cartesian fixed grids in the vertical direction (Lin and Falconer, 1997; Jiang and Wai, 2005). When the vertical grid size is very small due to a three-dimensional model following the bed topography, it may prove difficult to reach a stable solution (Bates and Horritt, 2005; Jiang and Wai, 2005). Furthermore, stable algorithms need to be derived to accurately compute changes in the free water surface in three-dimensional models (Olsen, 2003). Thus, a wetting and drying approach is still difficult to implement in a three-dimensional confluence model using boundary-fitted coordinates.

The numerical modelling of mixing-layer dynamics requires the use of LES to examine the different temporal scales present in mixing zones (Bradbrook *et al.*, 2000a; Keylock *et al.*, 2005). Even though the ever-increasing power of computers will facilitate LES studies of these zones in the near future, it will remain difficult to determine the impact of these vortices on bed shear stress, and hence on bedload transport (Keylock *et al.*, 2005). Boyer *et al.* (2006) emphasize the inadequacy of the mean Reynolds shear stress ( $-\rho \langle u'w' \rangle$ , where  $\rho$  is water density,  $u'$  and  $w'$  represent longitudinal and vertical velocity fluctuations and  $\langle \rangle$  denotes a time average) to quantify the magnitude of the forces exerted on the river bed at a river confluence. They suggest including all turbulent stress fluctuations to explain instantaneous bedload transport rates. Obtaining accurate values of these quantities in three-dimensional modelling remains a challenge. Estimates of bed shear stress in mixing zones could perhaps be made using the turbulent kinetic energy approach, where shear stress is proportional to the fluctuations in velocity of the three velocity components (Biron *et al.*, 2004b; Tilston and Biron, 2006). However, not all scales of turbulence present in a mixing layer can be modelled using LES, and the marked increases in turbulent fluctuations, and hence in turbulent kinetic energy, which were observed in mixing zones (De Serres *et al.*, 1999; Roy *et al.*, 1999) remain to be adequately quantified by a three-dimensional model. In order to determine whether mixing-layer vortices can indeed generate bed shear stress values high enough to be responsible for scour formation at junctions, these modelling issues must be addressed at the same time as additional field measurements are collected in a wide variety of scales of confluences with different scour depths.

## **Bedload, suspended and solute transport**

### **Bedload sediment transport at confluences**

Very few studies have investigated sediment transport at confluences, with the exception of Best (1987, 1988), Roy and Bergeron (1990), Rhoads (1996) and Boyer *et al.* (2006). In his sand-bed experiments, Best (1988) shows clear segregation of bedload

transport on each side of the scour, with very little going through the scour in both a laboratory flume and a field study. A segregation around the scour zone was also observed by Rhoads (1996), although bedload sediments appeared to mix over a relatively short distance downstream of the scour. In a gravel-bed confluence, tracked marked particles revealed a very different pattern, with particles from both tributaries converging towards the scour zone, with no apparent segregation (Roy and Bergeron, 1990). Boyer *et al.* (2006) observe that the lateral distribution of bedload transport in a sand-bed confluence showed highest values generally close to the edges of the mixing layer. No clear correlation was established between mean Reynolds shear stress and bedload transport rates, but the pattern of horizontal–vertical cross stresses ( $\rho \langle Uw' \rangle$ , where  $U$  is the mean streamwise velocity) appeared related to bedload transport patterns. Corridors of high bedload transport were not associated with the existence of helical cells but the shear layer zone, which is characterized by high turbulence intensities, was believed to play an important role in the transport of sediment (Boyer *et al.*, 2006). Roy *et al.* (1999) also link high turbulence levels observed in the shear layer at the same field site to higher bedload transport rates, despite lower mean downstream velocity. A modelling approach using LES may help establish clearer links between instantaneous stresses and bedload transport (Zedler and Street, 2001), although this has seldom been attempted so far (Keylock *et al.*, 2005). Best and Rhoads (this volume, Chapter 4) provide an exhaustive review of the interactions between bed morphology and sediment transport.

## Suspended and solute transport at confluences

The suspended and dissolved load transport at confluences has rarely been quantified at confluences. This problem has been more often examined from a perspective of mixing rates downstream of junctions. The general belief is that mixing distances downstream of confluences are in the order of around 100 channel widths (Mackay, 1970; Smith and Daish, 1991; Rutherford, 1994). According to Jirka (2004): ‘Regardless of potential amplifications and complexities, the following rules of thumb apply for the mixing properties of point sources in rivers: (1) Complete vertical mixing is a rapid process with maximal dimensions of a few decades of the water depth. (2) Complete lateral mixing requires large distances. For typical river morphology ( $B/h = 10$  to  $100$ ) the complete mixing will require from 100 to 1000 river widths’ (p. 17, where  $B$  is channel width and  $h$  is flow depth). However, Gaudet and Roy (1995) observed much faster mixing (around 25 channel widths) downstream from discordant bed confluences of widths ranging from 5 to 15 m. This was attributed to the distortion of the mixing layer when water from the shallower tributary tends to flow above the water from the deeper main channel (Best and Roy, 1991; Gaudet and Roy, 1995). Dye injection experiments did not reveal any mixing-layer distortion at the KRCS concordant bed confluence (Rhoads and

Sukhodolov, 2004), which corresponds to the two-dimensional mixing layer observed in parallel junctions (Uijtewaal and Tukker, 1998; Uijtewaal and Booi, 2000).

As the width-to-depth ratio is believed to affect mixing rates (Chu and Babarutsi, 1988), an important question is whether processes such as those observed by Gaudet and Roy (1995) in small discordant confluences, usually characterized by a relatively small width-to-depth ratio, are comparable to processes occurring in much larger confluences, with larger width-to-depth ratios. Visualization provided by colour differences between the two incoming channels at many natural confluences is particularly useful to investigate this question. In the Amazonian basin, this situation arises where a white-water river (with a high suspended load coming from its Andean sources) encounters a blackwater river (with very limited suspended and nutrient load, and brown-coloured acidic waters due to a high content of humic compounds) (Maurice-Bourgoin *et al.*, 2003). Typically, white rivers are markedly deeper than black rivers (A. Laraque, personal communication). For example, the white Solimões River near Manaus (Brazil) is 55 m deep at its junction with the black Negro River, which is 35 m deep (Sternberg, 1995; Laraque *et al.*, 2000). Figure 3.4 illustrates remarkable similarities between mixing layers in two discordant junctions with two-order magnitude differences in scale, the Bayonne (turbid) and Berthier (clear) rivers in Québec (Figure 3.4(A)) and the Rios Mamoré (white) and Guaporé-Itenez (black) in Brazil (Figure 3.4(B)), suggesting that the suspended and dissolved load mixing processes at confluences are not scale-dependent.

There are unfortunately no data available yet to quantify the rate of mixing at the Mamoré and Guaporé-Itenez confluence, but it is very obvious from Figure 3.4(B) that a very rapid mixing of their suspended load is occurring downstream of the junction. At another large Amazonian confluence, between the Negro and Solimões rivers, an extensive field survey was conducted at the end of the 1990s. Suspended load distribution was measured at nine cross-sections along two to four verticals (Guyot *et al.*, 1998; Laraque *et al.*, in press). Not surprisingly, 96.5 per cent of the suspended load came from the Solimões River (with a total load of  $4910 \text{ kg s}^{-1}$  during the survey of September 1997). Mass balance showed that the mixing of waters at this confluence was achieved 25 km downstream of the confluence (Tao *et al.*, 1999; Maurice-Bourgoin *et al.*, 2003). This, considering the width of the Negro channel (approximately 4 km), is extremely rapid as it is equivalent to around six times the width. However, the explanations for this rapid mixing are not clear. Further, a visual survey of large river junctions (Lane *et al.*, in press) suggests that some large river junctions can require a very large distance downstream to mix completely. At present, we have no clear understanding of what drives mixing in large rivers.

The evidence produced by three field studies forms the basis of an embryonic model for large rivers. First, Lane *et al.* (in press) present evidence from a situation when mixing downstream of the confluence of the Paraná and Paraguay rivers (post mixing width of 2.8 km) takes over 400 km. They show that shear-related mixing processes

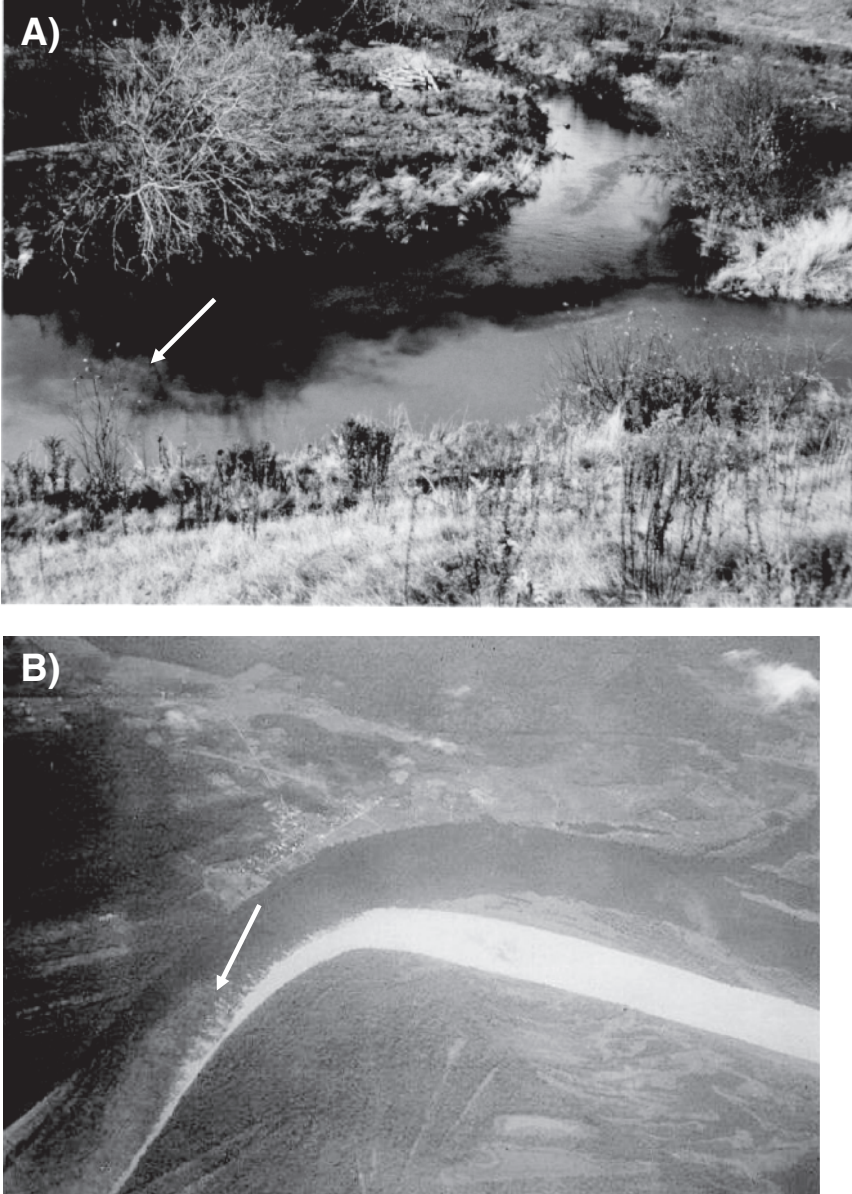


**Figure 3.4** The mixing-layer zone in two confluences of different scale with highly contrasted colours: (A) the Bayonne (turbid) and Berthier (clear) confluence (Québec), with a width of about 10 m; (B) the Rios Mamoré (white) and Guaporé-Itenez (black) at the border between Brazil and Bolivia, with a width of around 1 km (photograph J.-L. Guyot). Note the coherent vortices in the mixing layer and pockets of turbid water on the other side of the receiving channel indicating rapid mixing of the suspended load. In both cases, the turbid river is deeper than the clear-water one. Flow is from right to left.

resulted in some mixing but that this was largely confined to close to the upstream junction corner (less than 0.5 multiples of post-confluence width downstream). They could find no evidence of channel-scale helical circulation and they use this observation to conclude that near-field mixing processes were a necessary requirement for rapid mixing in large river junctions. Second, Laraque *et al.* (in press) in the Amazon have observed the sliding of the Solimões waters under those of the Negro and attribute this phenomenon to the larger speed, discharge and density in the Solimões River. The larger density of the Solimões River is due to its higher suspended load and slightly colder temperatures caused by a difference in albedo due to the dark-coloured Negro River, and it might contribute to explaining why this river would slide under the Negro River. Kelvin–Helmholtz instabilities in the shear layer may be amplified by the density difference, resulting in an upwelling of large boils of the denser Solimões water within the Negro River (see Figure 1 in Biron *et al.*, 1996b). The presence of large dunes (several metres high), as well as the depth difference between the two rivers, may also explain this particularly strong upwelling (A. Laraque, personal communication). Third, Lane *et al.* (in press) also report on a case where mixing takes place at the Paraguay–Paraná confluence in only 8 km downstream as compared with the more normal 400 km. They show that this was because the combination of bed discordance with tributary angular-momentum ratio resulted in the formation of channel-scale circulation that was sufficient to transfer the more turbid water from the Paraguay rivers across the full width of the post-confluence channel. This observation is interesting as it matches the results from numerical modelling of small laboratory-style channels that show that discordance at river junctions matters, although the effects of discordance are conditioned by momentum ratio (Bradbrook *et al.*, 1998, 2001).

### Three-dimensional numerical modelling of solute transport

Three-dimensional numerical modelling has been used successfully to investigate mixing patterns between water from two tributaries by simulating a numerical tracer subject to advection by the mean flow and turbulent diffusion (Bradbrook *et al.*, 1998, 2000a, 2001). These simulations confirmed field observations by Gaudet and Roy (1995) that mixing is greatly enhanced by the presence of bed discordance. However, to our knowledge, the role of a density difference between the two channels, as is typically the case at the large Amazonian confluences between a whitewater with a high suspended load and a blackwater river (e.g. Negro and Solimões Rivers, Laraque *et al.*, in press; Paraguay and Paraná Rivers, Lane *et al.*, in press), has never been investigated.

The three-dimensional model used by Bradbrook *et al.* (1998, 2000a, 2001), PHOENICS (from CHAM), is used here to investigate the density difference impact on mixing. The model uses a finite volume approach to solve the fully three-dimensional

form of the Reynolds-Averaged Navier–Stokes equations in each cell of the modelling domain. All simulations are performed using the RNG  $k$ - $\varepsilon$  turbulence model.

A simple  $90^\circ$  junction with rectangular channels is used to represent a confluence with features similar to the Negro and Solimões confluence, where the Solimões channel joins the Negro river at an angle close to  $90^\circ$ . The computational domain is 5 m in length, each tributary is 0.6 m wide, the receiving channel downstream from the junction is 0.65 m wide and the flow depth is 0.1 m. A Cartesian grid of  $140 \times 80 \times 12$  (in the longitudinal, lateral and vertical dimensions, respectively) is used with inlet velocities of 0.3 m/s for both tributaries. The standard law-of-the-wall is used at the bed and banks (Bradbrook *et al.*, 2001), with the roughness term defined as a median diameter of 1 mm. The porosity method is used for free-surface approximation (as described in detail in Bradbrook *et al.*, 1998). Four different scenarios are simulated: (A) concordant beds with equal density, (B) concordant beds where the density of the angled tributary is raised to  $998.32 \text{ kg m}^{-3}$ , to represent an increased density due to a high-suspended load such as that measured in the Paraguay River in 2004 by Lane *et al.* (in press), compared to a main channel density of  $996.57 \text{ kg m}^{-3}$  (as in the Paraná River, Lane *et al.*, in press), (C) discordant beds with a depth ratio of 0.7 with equal density and (D) discordant beds with a higher density in the tributary (same density ratio as in (B)). Mixing is visualized with the aid of a numerical tracer with a concentration of 1 in the main channel and 0 in the tributary.

Figure 3.5 shows that even a small density difference of  $1.75 \text{ kg m}^{-3}$  (density ratio of 1.0018) has a marked impact on the mixing layer between the two tributaries. When both streams are concordant and have the same water density, the mixing zone is vertical and the segregation in the concentration of each tributary remains very strong downstream (Figure 3.5(A)). However, when the tributary is denser, the heavier tributary pushes the other stream near the bed, whereas at the surface the lighter fluid is sliding above the tributary and is oriented towards the left bank (looking downstream), resulting in a distorted mixing layer (Figure 3.5(B)). Enhanced mixing is also observed due to bed discordance, where the mixing layer becomes distorted as its base is pulled towards the shallower tributary (Figure 3.5(C)). Interestingly, when the tributary is both shallower and denser, the initial mixing-layer distortion due to bed discordance is present close to the bed at the junction, but a reversed distortion occurs due to the density difference, which pushes the near-bed (denser) part of the mixing layer towards the right bank, despite the pressure difference due to discordance (Figure 3.5(D)).

The deviation from complete mixing (Figure 3.6) was calculated for the four downstream transects of Figure 3.5. This is defined as:

$$Dev = \frac{(C_s - C_p)}{C_p} \times 100 \quad (3.2)$$

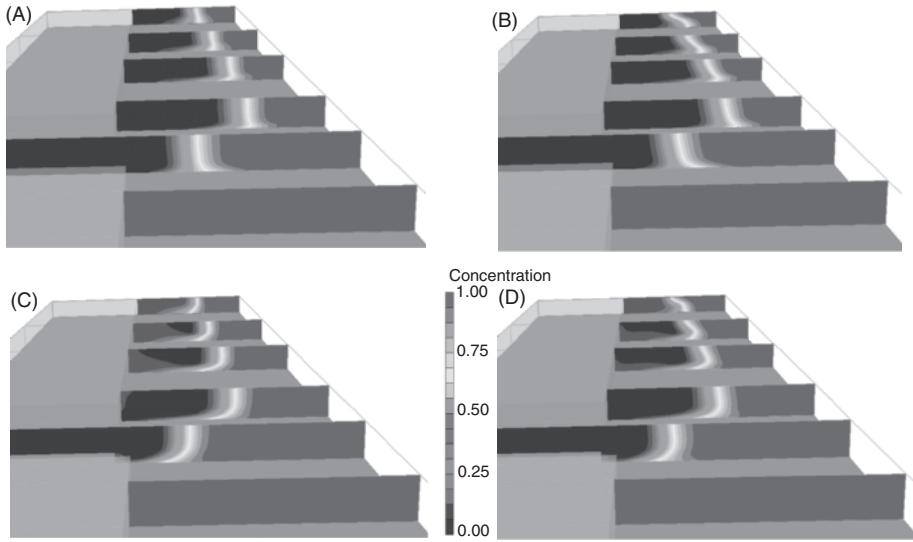


**Figure 3.5** Simulated numerical tracer downstream of the confluence where blue corresponds to a value of 0 and red to a value of 1 for (A) concordant beds with equal density, (B) concordant beds where the tributary density is increased to  $998.32 \text{ kg m}^{-3}$ , with the density of the main channel set at  $996.57 \text{ kg m}^{-3}$  (following the density difference of the Paraguay and Paraná Rivers, Lane *et al.*, in press), (C) discordant beds (shallower tributary) with equal density and (D) discordant beds with a higher density in the tributary (same as in B). Flow is towards the top. A colour reproduction of this figure can be seen in the colour section towards the centre of the book.

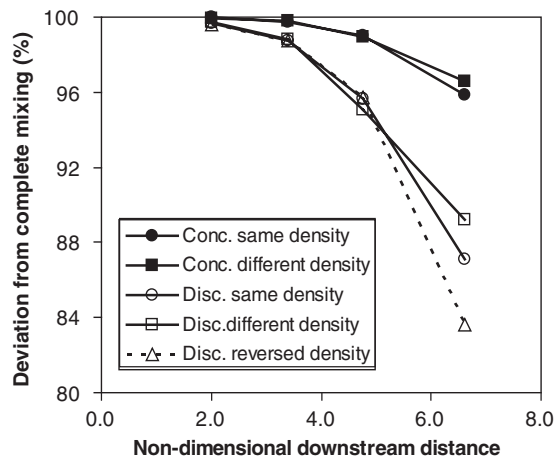


**Figure 3.6** Deviation from complete mixing for the minimum values of concentration at the four downstream cross-sections shown in Figure 3.5. Non-dimensional downstream distances are computed by dividing the distance from the upstream junction corner by the width of the parent channel. The discordant reversed density represents the case where the denser channel is the main channel instead of the tributary.

where  $C_s$  is the minimum simulated concentration of each transect and  $C_p$  is the predicted concentration (Gaudet and Roy, 1995). The predicted concentration is:

$$C_p = \frac{(C_1 Q_1 + C_2 Q_2)}{Q_3} \quad (3.3)$$

where  $C_1$  and  $C_2$  are the concentrations in the main and tributary channels,  $Q_1$  and  $Q_2$  are the discharge in the main and tributary channels and  $Q_3$  is the total discharge downstream of the junction. As expected, mixing is faster for discordant beds than for concordant beds (Figure 3.6). Because the tributary channel is denser, the density difference when beds are discordant appears to slightly decrease mixing due to bed discordance. To verify the impact of density on mixing rates, another simulation was performed using a denser fluid in the main channel instead of the tributary channel. This, for example, would represent the situation of the Negro and Solimões confluence. Figure 3.6 indicates that the combined effect of bed discordance and density difference when the deeper channel is denser is producing a faster mixing.

### Challenges for confluence sediment-transport modelling

Three-dimensional models have been used successfully to simulate bedload and suspended load transport (Wu *et al.*, 2000; Olsen, 2003; Nagata *et al.*, 2005). Both structured (Wu *et al.*, 2000; Nagata *et al.*, 2005) and unstructured grids (Olsen, 2003) have been employed. In some cases, a mass balance function is used to obtain the overall sediment transport (Wu *et al.*, 2000; Olsen, 2003). This can be further divided into a suspended load component, which uses the convection–diffusion equation (Wu *et al.*, 2000; Olsen, 2003), and a bedload component, where a van Rijn (1987) equation (Wu *et al.*, 2000; Olsen, 2003) or a momentum equation have been used (Nagata *et al.*, 2005). In all cases, the grid must be able to adjust to account for erosion and deposition occurring at the bed. To avoid creating a new grid at each time step, the bed porosity approach could be used, where each cell is given a porosity value of 0 if it is fully within the bed or the banks, 1 if it only consists of fluid and between 0 and 1 if it is partly in the bed or banks (Lane *et al.*, 2004; Hardy *et al.*, 2005). The value of porosity would then change according to erosion and deposition patterns, but the grid would remain constant. So far, this method has been used successfully to represent bed roughness, but it has not been tested with a coupled sediment-transport algorithm. Since our understanding of the role of spatially distributed bed roughness as a control on flow and sediment transport at confluences is limited at this stage, the porosity approach would allow for a further testing of this question in gravel-bed rivers. Nevertheless, at river confluences, adding a sediment-transport module remains a challenge considering the previously mentioned difficulties in designing a suitable numerical mesh.

Furthermore, all existing methods for coupling a three-dimensional hydrodynamic model with a sediment-transport module are based on determining shear velocity or shear stress – required in bedload transport equations – from the equilibrium or non-equilibrium logarithmic law in the boundary cells (e.g. Wu *et al.*, 2000; Nagata *et al.*, 2005). However, turbulence intensity in the mixing layer, which is important to initiate and sustain particle motion in the mixing zone (Boyer *et al.*, 2006), may not be adequately simulated by this approach. A bed shear stress approximation based on instantaneous fluctuations of velocity, such as Reynolds shear stress or turbulent kinetic energy (Biron *et al.*, 2004b) or horizontal–vertical cross-stresses (Boyer *et al.*, 2006), may be more directly related to sediment transport at confluences. The calculation of these parameters would require the use of non-steady simulations such as LES to adequately simulate the fluctuations in velocity associated with the passage of Kelvin–Helmholtz instabilities in the mixing zone. However, this could only be obtained by running the complete LES simulations before computing bed shear stress or cross stresses, which would then preclude a grid adjustment at each time step based on erosion and deposition patterns (Keylock *et al.*, 2005).

## Conclusion

Three-dimensional numerical modelling is a very powerful tool for improving our understanding of flow dynamics at complex sites such as river confluences as it allows the assessment of the role of controlling variables more efficiently than in experimental or field studies. It has also helped to clarify the debate surrounding the role of back-to-back helical cells at the junctions of two streams, although it has yet to resolve the question of whether or not helical circulation is a cause or a consequence of confluence scour. A second aspect that three-dimensional models have not fully clarified yet is the role of the mixing-layer zone, as it requires running LES simulations, which are computer-intensive. Considering the large number of studies which have emphasized the essential role of vortices in the mixing zone in confluence dynamics and sediment transport, it is important that future research examines this issue.

Most studies on river confluences so far, including numerical simulations, have examined small junctions where the width-to-depth ratio was small. More field data are needed in larger width-to-depth ratio environments. Recent studies in large Amazonian confluences suggest that factors which were not deemed important in small junctions, such as the presence of large dunes or a density difference between incoming channels, could play a fundamental role in large junctions (see Parsons *et al.*, this volume, Chapter 5). The three-dimensional simulations presented in this chapter clearly reveal the importance of density ratio on mixing rates, but field and laboratory data are required to validate these simulations.

More research is also required on the use of three-dimensional numerical models for large confluences, for example examining problems of numerical instability created by the aspect ratio of grid cells, where the horizontal scale of cells could be a few orders of magnitude larger than the vertical scale. The research agenda in confluence studies should target the development of hydrodynamic models applicable at all scales, including the large Amazonian confluences, with a coupled sediment-transport module. This will require major efforts from a numerical modelling perspective, as well as additional suspended and bedload transport data at small and large natural confluences to calibrate and validate these models.

## Acknowledgments

This paper is based upon research supported by the Natural Science and Engineering Research Council (Biron) and the Natural Environment Research Council (Lane). The paper has benefited greatly from the constructive suggestions of one anonymous reviewer and of the co-editor André Roy.

## References

- Ashmore PE. 1982. Laboratory modelling of gravel braided stream morphology. *Earth Surface Processes and Landforms* **7**: 201–255.
- Ashmore PE, Parker G. 1983. Confluence scour in coarse braided streams. *Water Resources Research* **19**: 392–402.
- Ashmore PE, Ferguson RI, Prestegard KL, Ashworth PJ, Paola C. 1992. Secondary flow in coarse-grained braided river confluences. *Earth Surface Processes and Landforms* **17**: 299–312.
- Ashworth PJ, Ferguson RI, Powell DM. 1992. Bedload transport and sorting in braided channels. In *Dynamics of Gravel-Bed Rivers*, Billi P, Hey RD, Thorne CR, Tacconi P (eds). John Wiley & Sons: Chichester; 497–513.
- Babarutsi S, Chu VH. 1998. Modeling transverse mixing layer in shallow open-channel flows. *Journal of Hydraulic Engineering* **124**: 718–727.
- Bates PD, Horritt MS. 2005. Modelling wetting and drying processes in hydraulic models. In *Computational Fluid Dynamics: Applications in Environmental Hydraulics*, Bates PD, Lane SN, Ferguson RI (eds). John Wiley & Sons: Chichester; 121–146.
- Best JL. 1987. Flow dynamics at river channel confluences: Implications for sediment transport and bed morphology. In *Recent Developments in Fluvial Sedimentology*, Ethridge FG, Flores RM, Harvey MD (eds). Society of Economic Palaeontologists and Mineralogists Special Publication 39; 27–35.
- Best JL. 1988. Sediment transport and bed morphology at river channel confluences. *Sedimentology* **35**: 481–498.
- Best JL, Reid I. 1984. Separation zone at open-channel junctions. *Journal of Hydraulic Engineering* **110**: 1588–1594.

- Best JL, Roy AG. 1991. Mixing-layer distortion at the confluence of channels of different depth. *Nature* **350**: 411–413.
- Biron P, De Serres B, Roy AG, Best JL. 1993. Shear layer turbulence at an unequal depth channel confluence. In *Turbulence: Perspectives on Flow and Sediment Transport*, Clifford NJ, French JR, Hardisty J (eds). John Wiley & Sons: Chichester; 197–213.
- Biron P, Best JL, Roy AG. 1996a. Effects of bed discordance on flow dynamics at open channel confluences. *Journal of Hydraulic Engineering* **122**: 676–682.
- Biron P, Roy AG, Best JL. 1996b. Turbulent flow structure at concordant and discordant open-channel confluences. *Experiments in Fluids* **21**: 437–446.
- Biron PM, Richer A, Kirkbride AK, Roy AG, Han S. 2002. Spatial patterns of water surface topography at a river confluence. *Earth Surface Processes and Landforms* **27**: 913–928.
- Biron PM, Ramamurthy AS, Han S. 2004a. Three-dimensional numerical modeling of mixing at river confluences. *Journal of Hydraulic Engineering* **130**: 243–253.
- Biron PM, Robson C, Lapointe MF, Gaskin SJ. 2004b. Comparing different methods of bed shear stress estimates in simple and complex flow fields. *Earth Surface Processes and Landforms* **29**: 1403–1415.
- Boyer C, Roy AG, Best JL. 2006. Dynamics of a river channel confluence with discordant beds: Flow turbulence bed load sediment transport and bed morphology. *Journal of Geophysical Research – Earth Surface* **111**: F04007. DOI: 10.1029/2005JF000458.
- Bradbrook KF. 1999. *Numerical field and laboratory studies of three-dimensional flow structures at river channel confluences*, Unpublished PhD thesis, Department of Geography University of Cambridge.
- Bradbrook KF, Biron PM, Lane SN, Richards KS, Roy AG. 1998. Investigation of controls on secondary circulation in a simple confluence geometry using a three-dimensional numerical model. *Hydrological Processes* **12**: 1371–1396.
- Bradbrook KF, Lane SN, Richards KS, Biron PM, Roy AG. 2000a. Large eddy simulation of periodic flow characteristics at river channel confluences. *Journal of Hydraulic Research* **38**: 207–215.
- Bradbrook KF, Lane SN, Richards KS. 2000b. Numerical simulation of three-dimensional time-averaged flow structure at river channel confluences. *Water Resources Research* **36**: 2731–2746.
- Bradbrook KF, Lane SN, Richards KS, Biron PM, Roy AG. 2001. Role of bed discordance at asymmetrical river confluences. *Journal of Hydraulic Engineering* **127**: 351–368.
- Bridge JS. 1993. The interaction between channel geometry water flow sediment transport and deposition in braided rivers. In *Braided Rivers*, Best JL, Bristow CS (eds). Geological Society Special Publication No 75. Geological Society: London; 13–72.
- Chu VH, Babarutsi S. 1988. Confinement and bed-friction effects in shallow turbulent shear layers. *Journal of Hydraulic Engineering* **114**: 1257–1274.
- De Serres B, Roy AG, Biron PM, Best JL. 1999. Three-dimensional structure of flow at a confluence of river channels with discordant beds. *Geomorphology* **26**: 313–335.
- Fujita I, Komura S. 1989. Visualization of the flow at a confluence. In *Proceedings of the 3rd International Symposium on Refined Flow Modelling and Turbulence Measurements, Tokyo, Japan*; 691–698.
- Gaudet JM, Roy AG. 1995. Effect of bed morphology on flow mixing length at river confluences. *Nature* **373**: 138–139.
- Gurram SK, Karki KS, Hager WH. 1997. Subcritical junction flow. *Journal of Hydraulic Engineering* **123**: 447–455.

- Guyot JL, Filizola N, Guimarães V. 1998. Amazon suspended yield measurements using an Acoustic Doppler Current Profiler (ADCP): First results. In *Hydrology in the Humid Tropic Environment, Kingston, November 1996*, Johnson AI, Fernandez-Jauregui CA (eds). IAHS Publication 253; 109–115.
- Hager WH. 1989a. Transitional flow in channel junctions. *Journal of Hydraulic Engineering*. **115**: 243–259.
- Hager WH. 1989b. Supercritical flow in channel junctions. *Journal of Hydraulic Engineering*. **115**: 595–616.
- Han S. 2002. Three-dimensional numerical modelling of mixing at river confluences, Unpublished MSc thesis, Department of Building Civil and Environmental Engineering, Concordia University.
- Hardy RJ, Lane SN, Lawless MR, Best JL, Elliott L, Ingham DB. 2005. Development and testing of a numerical code for treatment of complex river channel topography in three-dimensional CFD models with structured grids. *Journal of Hydraulic Research* **43**: 468–480.
- Hsu CC, Lee WJ, Chang CH. 1998. Subcritical open-channel junction flow. *Journal of Hydraulic Engineering* **124**: 847–855.
- Huang J, Weber LJ, Lai YG. 2002. Three-dimensional numerical study of flows in open-channel junctions. *Journal of Hydraulic Engineering* **128**: 268–280.
- Jiang YW, Wai OWH. 2005. Drying-wetting approach for 3D finite element sigma coordinate model for estuaries with large tidal flats. *Advanced in Water Resources* **28**:779–792.
- Jirka GH. 2004. Mixing and dispersion in rivers In *River Flow 2004*, Greco M, Carravetta A, Della Morte R (eds). Taylor & Francis Group: London; 13–27.
- Keylock CJ, Hardy RJ, Parsons DR, Ferguson RI, Lane SN, Richards KS. 2005. The theoretical foundations and potential for large-eddy simulation (LES) in fluvial geomorphic and sedimentological research. *Earth Science Reviews* **71**: 271–304.
- Khan AA, Cadavid R, Wang SS-Y. 2000. Simulation of channel confluence and bifurcation using the CCHE2D model. *Proceedings of the Institution of Civil Engineers – Water and Maritime Engineering* **142**: 97–102.
- Lane SN, Ferguson RI. 2005. Modelling reach-scale fluvial flows. In *Computational Fluid Dynamics: Applications in Environmental Hydraulics*, Bates PD, Lane SN, Ferguson RI (eds). John Wiley & Sons: Chichester; 217–269.
- Lane SN, Bradbrook KF, Richards KS, El-Hames A, Biron PM, Roy AG. 1999. The application of computational fluid dynamics to natural river channels: Three-dimensional versus two-dimensional approaches. *Geomorphology* **29**: 1–20.
- Lane SN, Bradbrook KF, Richards KS, Biron PM, Roy AG. 2000. Secondary circulation cells in river channel confluences: Measurement artefacts or coherent flow structures? *Hydrological Processes* **14**: 2047–2071.
- Lane SN, Hardy RJ, Elliott L, Ingham DB. 2004. Numerical modeling of flow processes over gravelly surfaces using structured grids and a numerical porosity treatment. *Water Resources Research* **40**: W01302. DOI: 10.1029/2002WR001934.
- Lane SN, Parsons DR, Best JL, Orfeo O, Kostachuk R, Hardy RJ. In press. The causes of rapid mixing at a junction of two large rivers the Rio Paraná and Rio Paraguay, Argentina, *Journal of Geophysical Research – Earth Surface*.
- Laraque A, Guyot JL, Seyler P, Filizola N. 2000. Hydrological and geochemical dynamics of the mixing waters zone of the Rios Negro and Solimões in the Amazone basin. In *Joint Conference on Water Resources Engineering and Water Resources Planning and Management*

- *Modern velocity and discharges measurement techniques and applications* – July 30–August 2, 2000. Minneapolis, Minnesota.
- Laraque A, Guyot JL, Filizola N. In press. The Amazon river mixing processes at the Negro and Solimões rivers confluence Encontro das Aguas, Manaus, Brazil. *Hydrological Processes*.
- Leclair SF, Roy AG. 1997. Variability of bed morphology and sedimentary structures at a discordant river confluence during low flows. *Géographie physique et Quaternaire* **51**: 125–139.
- Leopold LB, Maddock T. 1953. The Hydraulic Geometry of Stream Channels and Some Physiographic Implications. *US Geological Survey Professional Paper* 252.
- Leopold LB, Wolman MG. 1960 River Meanders. *Geological Society of America Bulletin* **71**: 769–794.
- Lin B, Falconer RA. 1997. Three-dimensional layer-integrated modelling of estuarine flows with flooding and drying. *Estuarine, Coastal and Shelf Science* **44**: 737–751.
- Ma L, Ashworth PJ, Best JL, Elliot L, Ingham DB, Whitcombe LJ. 2002. Computational fluid dynamics and the physical modelling of an upland urban river. *Geomorphology* **44**: 375–391.
- Mackay JR. 1970. Lateral mixing of the Liard and Mackenzie rivers downstream from their confluence. *Canadian Journal of Earth Sciences* **7**: 111–124.
- Maurice-Bourgoin L, Quemerais B, Moreira-Turcq P, Seyler P. 2003. Transport distribution and speciation of mercury in the Amazon River at the confluence of black and white waters of the Negro and Solimões Rivers. *Hydrological Processes* **17**: 1405–1417.
- McLelland SJ, Ashworth PJ, Best JL. 1996. The origin and downstream development of coherent flow structures at channel junctions. In *Coherent Flow Structures in Open Channels*, Ashworth PJ, Bennett SJ, Best JL, McLelland SJ (eds). John Wiley & Sons: Chichester; 459–490.
- Mosley MP. 1976. An experimental study of channel confluences. *Journal of Geology* **84**: 535–562.
- Nagata N, Hosoda T, Nakato T, Muramoto Y. 2005. Three-dimensional numerical model for flow and bed deformation around river hydraulic structures. *Journal of Hydraulic Engineering* **131**: 1074–1087.
- Olsen NRB. 2003. Three-dimensional CFD modelling of self-forming meandering channel. *Journal of Hydraulic Engineering* **129**: 366–372.
- Parsons DR. 2003. Discussion of “Three-dimensional numerical study of flows in open-channel junctions” by Huang J, Weber LJ, Lai YG. *Journal of Hydraulic Engineering* **129**: 822–823.
- Parsons DR, Best JL, Lane SN, Orfeo O, Hardy RJ. 2007. Form roughness and the absence of secondary flow in a large confluence-difffluence Rio Paraná Argentina. *Earth Surface Processes and Landforms* **32**: 155–162.
- Pierini JO, Perillo GME, Carbone ME, Marini FM. 2005. Residual flow structure at a scour-hole in Bahia Blanca estuary Argentina. *Journal of Coastal Research* **21**: 784–796.
- Ramamurthy AS, Carballada LB, Tran DM. 1988. Combining open channel flow at right-angled junctions. *Journal of Hydraulic Engineering* **114**: 1449–1460.
- Rameshwaran P, Naden PS. 2004. Three dimensional modelling of free surface variation in a meandering channel. *Journal of Hydraulic Research* **42**: 603–615.
- Rhoads BL. 1996. Mean structure of transport-effective flows at an asymmetrical confluence when the main stream is dominant. In *Coherent Flow Structures in Open Channels*, Ashworth PJ, Bennett SJ, Best JL, McLelland SJ (eds). John Wiley & Sons: Chichester; 491–517.
- Rhoads BL, Kenworthy ST. 1995. Field measurements of flow structure at a high-angle asymmetrical stream confluence. *Geomorphology* **11**: 273–293.
- Rhoads BL, Kenworthy ST. 1998. Time-averaged flow structure in the central region of a stream confluence. *Earth Surface Processes and Landforms* **23**: 171–191.

- Rhoads BL, Sukhodolov AN. 2001. Field investigation of three-dimensional flow structure at stream confluences: 1 Thermal mixing and time-averaged velocities. *Water Resources Research* **37**: 2393–2410.
- Rhoads BL, Sukhodolov AN. 2004. Spatial and temporal structure of shear layer turbulence at a stream confluence. *Water Resources Research* **40**: W06304. DOI: 10.1029/2003WR002811.
- Richardson JE, Panchang VG. 1998. Three-dimensional simulation of scour-inducing flow at bridge piers. *Journal of Hydraulic Engineering* **124**: 530–540.
- Richardson WR. 1997. Secondary Flow and Channel Change in Braided Rivers, Unpublished PhD thesis, University of Nottingham, UK.
- Richardson WR, Thorne CR, Mahmood S. 1996. Secondary currents and channel changes around a bar in the Brahmaputra River Bangladesh. In *Coherent Flow Structures in Open Channels*, Ashworth PJ, Best JL, Bennett SJ, McLelland SJ (eds). John Wiley & Sons: Chichester; 519–544.
- Roy AG, Bergeron N. 1990. Flow and particle paths at a natural river confluence with coarse bed material. *Geomorphology* **3**: 99–112.
- Roy AG, Biron PM, Buffin-Bélanger T, Levasseur M. 1999. Combined visual and quantitative techniques in the study of natural turbulent flows. *Water Resources Research* **35**: 871–877.
- Rutherford JC. 1994. *River Mixing*. John Wiley & Sons: Chichester.
- Shabayek S, Steffler P, Hicks F. 2002. Dynamic model for subcritical combining flows in channel junctions. *Journal of Hydraulic Engineering* **128**: 821–828.
- Smith R, Daish NC. 1991. Dispersion far downstream of a river junction. *Physics of Fluids A-Fluid Dynamics* **3**: 1102–1109.
- Sternberg HO'R. 1995. Waters and wetlands of Brazilian Amazonia: An uncertain future. In *The Fragile Tropics of Latin America: Sustainable Management of Changing Environments*, Nishizawa T, Uitto JI (eds). United Nations University Press: Tokyo; 113–179.
- Sukhodolov AN, Rhoads BL. 2001. Field investigation of three-dimensional flow structure at stream confluences: 2 Turbulence. *Water Resources Research* **37**: 2411–2424.
- Tao F, Aucour AM, Sheppard S, Benedetti M, Guyot JL. 1999. Mixing at the Negro/ Solimões rivers confluence: Isotopic constraints and major elements redistribution. In *International Symposium on Hydrological and Geochemical Processes in Large Scale River Basins, Manaus, 15–19 November*. IRD-HiBam Publications: Brasilia, Brazil (CDRom).
- Taylor EH. 1944. Flow characteristics at rectangular open channel junctions *Transactions of the American Society of Civil Engineers* **109**: 893–912.
- Tilston M, Biron PM. 2006. Three-dimensional flow structure turbulence and bed shear stress in a meander loop. *Géographie physique et Quaternaire* **60**: 225–240 (in French).
- Uijttewaal WSJ, Booij R. 2000. Effects of shallowness on the development of free-surface mixing layers. *Physics of Fluids* **12**: 392–402.
- Uijttewaal WSJ, Tukker J. 1998. Development of quasi two-dimensional structures in shallow free-surface mixing layer. *Experiments in Fluids* **24**: 192–200.
- Van Prooijen BC, Uijttewaal WSJ. 2002. A linear approach for the evolution of coherent structures in shallow mixing layers. *Physics of Fluids* **14**: 4105–4114.
- Van Rijn LC. 1987. Mathematical modeling of morphological processes in the case of suspended sediment transport. *Delft Hydraulic Communication No. 382*. Delft Hydraulics Laboratory: Delft, The Netherlands.
- Wang K-H, Cleveland TG, Fitzgerald S, Ren X. 1996. Hydrodynamic flow modeling at confluence of two streams. *Journal of Hydraulic Engineering* **122**: 994–1002.

- Webber NB, Greated CA. 1966. An investigation of flow behaviour at the junction of rectangular channels. *Proceedings of the Institution of Civil Engineers* **34**: 321–334.
- Weber LJ, Schumate ED, Mawer N. 2001. Experiments on flow at a 90° open-channel junction. *Journal of Hydraulic Engineering* **127**: 340–350.
- Weber LJ, Goodwin RA, Li S, Nestler JM, Anderson JJ. 2006. Application of an Eulerian-Lagrangia-Agent method (ELAM) to rank alternative designs of a juvenile fish passage facility. *Journal of Hydroinformatics* **8**: 271–295.
- Weerakoon SB, Tamai N. 1989. Three dimensional calculation of flow in river confluences using boundary fitted co-ordinates. *Journal of Hydroscience and Hydraulic Engineering* **7**: 51–62.
- Weerakoon SB, Kawahara Y, Tamai N. 1991. Three dimensional flow structure in channel confluence of rectangular section. In *Proceedings of the 25th International Association for Hydraulic Research Congress A*. International Association for Hydraulic Research: Madrid; 373–380.
- Weerakoon SB, Tamai N, Kawahara Y. 2003. Depth-averaged flow computation at a river confluence. *Proceedings of the Institution of Civil Engineers-Water and Maritime Engineering* **156**: 73–83.
- Winant CD, Browand FK. 1974. Vortex pairing: The mechanism of turbulent mixing layer growth at moderate Reynolds numbers. *Journal of Fluid Mechanics* **63**: 237–255.
- Wu WM, Rodi W, Wenka T. 2000. 3D numerical modeling of flow and sediment transport in open channels. *Journal of Hydraulic Engineering* **126**: 14–15.
- Yakhot V, Orzag SA, Thangam S, Gatshi TB, Speziale CG. 1992. Development of a turbulence model for shear flow by a double expansion technique. *Physics of Fluids A* **4**: 1510–1520.
- Zanichelli G, Caroni E, Fiorotto V. 2004. River bifurcation analysis by physical and numerical modelling. *Journal of Hydraulic Engineering* **130**: 237–242.
- Zedler EA, Street RL. 2001. Large-eddy simulation of sediment transport: Currents over ripples. *Journal of Hydraulic Engineering* **127**: 444–452.



# 4

## Sediment transport, bed morphology and the sedimentology of river channel confluences

**James L. Best<sup>1</sup> and Bruce L. Rhoads<sup>2</sup>**

<sup>1</sup>*Departments of Geology and Geography and Ven Te Chow Hydrosystems Laboratory, University of Illinois at Urbana-Champaign, USA*

<sup>2</sup>*Department of Geography, University of Illinois at Urbana-Champaign, USA*

### Context

River channel confluences are sites of significant hydraulic and morphological change within fluvial networks (Richards, 1980; Rhoads, 1987; Ferguson *et al.*, 2006; Biron and Lane, this volume, Chapter 3) and also occur within river channels where islands or bars are present. The local and downstream effects of confluences can have a profound influence on the geomorphology and ecology of river channels – see, for example, Rice *et al.* (2001) – as well as on strategies for effective channel management (Pinter *et al.*, 2004). For these reasons, the morphology of river channel confluences is of major importance within a range of considerations and disciplines. For example, scour-depth predictions at channel junctions are clearly needed in the design of engineering structures, whilst the recognition of confluence scour is important in reconstructions of ancient sedimentary environments (Bristow *et al.*, 1993; Siegenthaler and Huguenberger, 1993;

Miall and Jones, 2003). Within contemporary environments, considerations of channel and floodplain ecology may also be critically affected by confluence morphodynamics (Ezcurra de Drago *et al.*, 2007).

The morphodynamics of the confluence hydrodynamic zone (CHZ; Kenworthy and Rhoads, 1995) can be related to the complex fluid dynamics of confluences, which, in turn, are controlled by several principal factors, including: (i) the planform geometry of the confluence, including the confluence angle,  $\alpha$ , and the planform shape of the upstream and post-confluence channels, (ii) the ratio of discharges ( $Q_r = Q_t/Q_m$ , where subscripts t and m refer to the mainstream and tributary respectively) or momentum ( $M_r = \rho_t Q_t U_t / \rho_m Q_m U_m$ , where  $\rho$  and  $U$  are the flow density and mean velocity respectively) between the confluent rivers, (iii) the presence and nature of any bed height discordance between the levels of the incoming tributary beds and (iv) any differences in density between the incoming flows. Although these factors strongly influence the bed morphology at channel junctions through their imprint on the fluid dynamics, the feedback among flow, sediment transport and bedform must also be accounted for because flow within a fully formed mobile bed will be distinctly different from flow within sediment-free channels (Best, 1988). Thus, a full understanding of the morphodynamics of channel confluences requires an intimate knowledge of the dynamic interactions among flow, sediment transport and bed morphology over a range of spatio-temporal scales, ranging from flow in rill networks (Bryan and Kuhn, 2002) to the dynamics of junctions within the world's largest rivers (Best and Ashworth, 1997; Amsler *et al.*, 2007). Although measurements of bed morphology have been made at a range of junctions of different sizes, far less work has sought to quantify the nature of sediment transport at confluences. Furthermore, the temporal evolution of bed morphology in relation to changing flow and sediment dynamics has been extremely difficult to measure and has been tackled in even fewer studies: this topic represents an area of great future promise for field, laboratory and numerical experimentation.

This chapter will review the nature of bed morphology and sediment transport at open-channel confluences and examine the nature of the morphodynamic feedbacks between fluid and sediment movement at these sites and the development of bed morphology. It also explores the sedimentology of channel confluences and how such sites may be represented within the ancient sedimentary record. Herein, we largely restrict our attention to the confluence of smaller channels since the morphodynamics of large junctions are discussed in Parsons *et al.*, this volume, Chapter 5.

## Bed morphology

Our present knowledge of the morphology of channel confluences has come from a range of studies that have examined a variety of field junctions at differing scales, as well as physical experimentation that has detailed the nature of bed morphology within

fixed-wall channels and also within completely mobile beds (e.g. Ashmore and Parker, 1983). Based on these studies, five principal morphological features can be identified at channel confluences, although the presence/absence of these features and their exact nature are dependent on a range of controlling parameters that are examined below:

1. a scour hole whose orientation approximately bisects the junction angle and whose origin is linked to increased velocities and turbulence within the junction and the transport pathways of sediment (see below)
2. tributary-mouth bars, or topographic steps, that form at the mouth of one or both tributaries and often slope into the scour hole
3. a mid-channel bar or bars within the post-confluence channel
4. bank-attached lateral bars in the post-confluence channel that are associated with regions of flow deceleration and/or flow separation
5. a region of sediment accumulation near the upstream confluence corner, perhaps associated with flow stagnation.

Each of these morphologic units is examined below, within a range of differing scale confluences, and the controlling variables influencing each are identified and discussed.

### **Confluence scour**

Considerable work has been devoted to documenting the depth and form of scour at channel junctions, since such scour may have adverse effects on engineering structures within rivers and the maximum scour depth must be known for design purposes. In confluences with asymmetric or symmetric planforms, a zone of scour often exists with an axis of maximum depth that approximately bisects the junction angle (Mosley, 1975, 1976, 1982; Ashmore and Parker, 1983; Best, 1988). Such scour holes can be found at many junctions, ranging from small single-channel rivers to braided river junctions and anabranching rivers (Rodrigues *et al.*, 2006) to the world's largest channel confluences (Klaassen and Vermeer, 1988; Best and Ashworth, 1997; Sarker, 1996). Studies detailing scour depths at river channel confluences include those of Mosley (1975, 1976, 1982), Best (1988), Ashmore and Parker (1983), Rezaur *et al.* (1999), Bryan and Kuhn (2002) and Ghobadian and Bajestan (2007), whilst Kjerfve *et al.* (1979), Ginsberg and Perillo (1999) and Pierini *et al.* (2005) document the morphology and dynamics of similar channel confluence scours within estuarine channels.

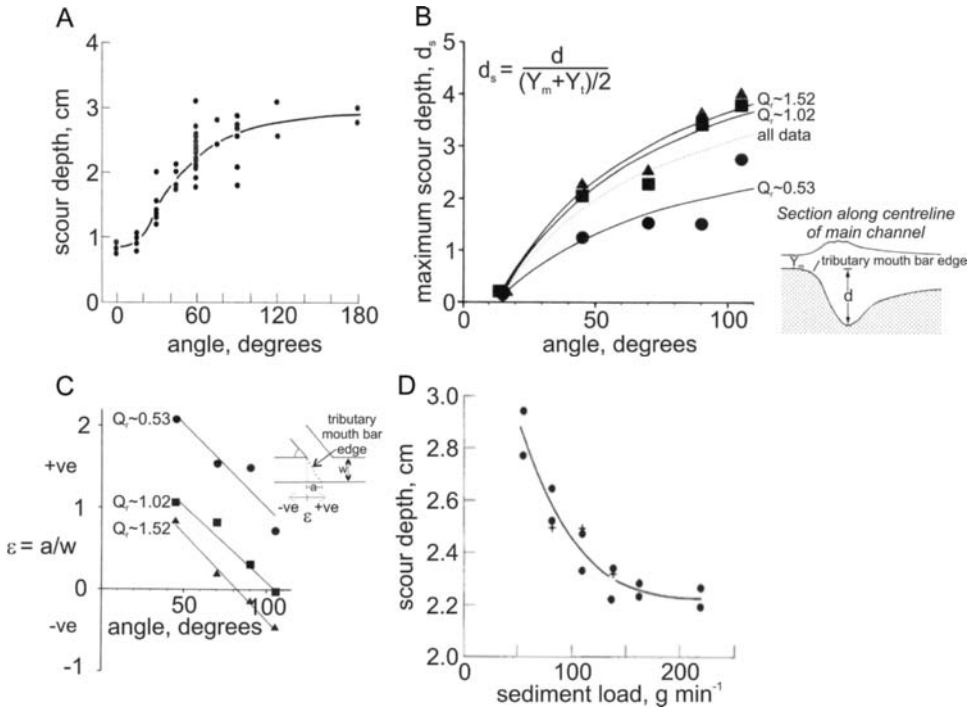


**Figure 4.1** Various controls on the morphology of channel confluences in laboratory experiments: (A) Scour depth (cm) as a function of junction angle (degrees; redrawn from Mosley, 1976); (B) Scour depth ( $d_s$ , see inset diagram for definition) as a function of junction angle and discharge ratio,  $Q_r$  (redrawn from Best, 1988); (C) Plot of the penetration of the tributary-mouth bar edge ( $\epsilon$ , see inset diagram for definition) into the junction as a function of confluence angle, and discharge ratio,  $Q_r$  (redrawn from Best, 1988); (D) Scour depth (cm) as a function of the total sediment load passing through the confluence ( $g \text{ min}^{-1}$ ; redrawn from Mosley, 1976).

Best (1988) found that the orientation of the maximum scour depth responded to the discharge ratio between the confluent streams, with the scour responding to the increased penetration of the tributary fluid into the junction at higher discharge ratios. Mosley (1975, 1976) documents the form of confluence scour in a series of mobile-bed physical experiments and found that the depth of scour became greater with an increasing junction angle (Figure 4.1(A)), although the relationship was non-linear and flattened off at junction angles higher than approximately  $100^\circ$ . Best (1988) also confirmed this relationship and found that, at a given junction angle, scour depth increased as the relative discharge of the tributary channel increased relative to that of the mainstream (Figure 4.1(B)). In a study of scour at the confluence of rills, Bryan and Kuhn (2002) found that the junction planform was a more important influence on bed scour than junction angle. In symmetrical (Y-shaped) confluences, the confluence

scour was symmetrical in planform shape. However, asymmetrical junctions tended to have more complex scours that eventually led to the evolution of a symmetrical junction planform through bank erosion opposite the tributary mouth, which eventually led to higher confluence angles than the original channels. Mosley (1975, 1976) also found some change in the alignment of the junction scour in asymmetrical junctions, largely forced by the growth of a bar within the separation zone (see below) and subsequent bank erosion, but he concludes that confluences exhibit little tendency to evolve towards any equilibrium angle based on the flow and sediment discharges in each confluent channel. Such differences between these studies may be linked to the very different hydraulic conditions present in many rill junctions, where supercritical flows, hydraulic jumps and flows that are shallow with respect to the bed roughness are frequently present.

Biron *et al.* (1993) document that in junctions where there is a discordance in bed height between the two tributaries (see below) the central confluence scour may be small or absent. The lack of substantial scour may be linked to the different nature of flow at these sites, especially the presence of upwelling in the leeside of the step at the mouth of the shallower channel (see Best and Roy, 1991; Biron *et al.*, 1996a, 1996b; Bradbrook *et al.*, 2000, 2001). Additionally, confluences with lower junction angles or bed material that imparts a high relative roughness (Roy *et al.*, 1988) also have smaller scour depths or beds that possess no scour. Additionally, most studies of channel junctions have assumed or imposed straight channels upstream of the junction whereas many confluences possess curved channels in one of both tributaries (see Biron and Lane, this volume, Chapter 3). Indeed, as long ago as 1902, Calloway noted that many river tributaries entered the mainstream on the concave outer bank of meander bends. In this case, curvature within the upstream confluent channels may also lead to differences in flow structure at the junction (Roberts, 2005) and promote smaller scour holes than would be expected for a given confluence angle and discharge ratio at the junction of straight channels. More work on confluent meander bends is needed to understand the morphodynamics of these types of confluences.

It is interesting to examine the nature of confluence scour over a range of channel sizes, since there are several studies that have documented confluence scour in large rivers (see Parsons *et al.*, this volume, Chapter 5) as well as those from smaller channel junctions. Sambrook Smith *et al.* (2005) present a plot that compiles data from a range of studies. These data are replotted and further examined in Figure 4.2. These data, consisting of 233 data points compiled from 20 studies, show that there is a broad relationship between scour depth and junction angle. The broad scatter is not surprising and can be attributed to variations in scour caused by other important controlling parameters, such as discharge ratio, junction planform type, bed discordance and sediment load. If the data are decimated on channel size (Figure 4.2 and see Sambrook Smith *et al.*, 2005), it appears that the larger junctions (here arbitrarily chosen as  $> 5$  m depth) are often characterized by smaller relative scour depths than shallow confluences with equivalent junction angles. This difference may reflect the increasing complexity of larger channels,

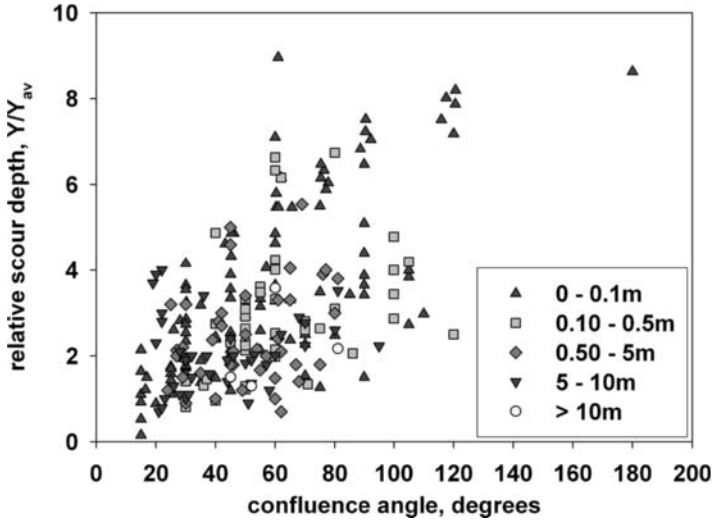


**Figure 4.2** A summary of scour depth data from channel confluences (see Sambrook Smith *et al.*, 2005). Data sources are from experimental studies of channel junctions and a range of field studies. Data from Mosley (1975, 1976, 1982), Ashmore and Parker (1983), Best (1985, 1988), Klaassen and Vermeer (1988), Roy and De Serres (1989), Orfeo (1995), Best and Ashworth (1997), Roy *et al.* (1988), McLelland *et al.* (1996), Rhoads and Sukhodolov (2001) and from research in Bangladesh (see Sarker, 1996; Delft Hydraulics and Danish Hydraulics Institute, 1996). A colour reproduction of this figure can be seen in the colour section towards the centre of the book.

their often greater width–depth ratios and the probable increased influence of both form roughness and width-scale variations in flow processes and sediment transport (see Parsons *et al.*, this volume, Chapter 5 and also Szupiany *et al.*, in review).

### Tributary-mouth bars

Many junctions possess accumulations of sediment at the mouth of one, or both, of the confluent channels that have widely been termed ‘tributary-mouth bars’ (Alam *et al.*, 1985; Best, 1988; Bristow *et al.*, 1993; Biron *et al.*, 1993; Rhoads and Kenworthy, 1995; Rodrigues *et al.*, 2006). These bars may possess steep avalanche faces that dip, at up to the angle of repose, into the central scour (see Mosley, 1976; Best, 1986, 1988; Petts and Thoms, 1987; Bristow *et al.*, 1993), although these slopes may be much lower in angle, particularly at large channel junctions (Parsons *et al.*, this volume, Chapter 5). The position of the edges of these bars responds to the ratio of discharges, or momentum, between the two confluent channels, with experimental work (Figure 4.1(C)) demonstrating the increased penetration of the bar edges into the junction at higher discharge ratios. The position of tributary-mouth bars is also a function of the junction angle, in that, at a given  $Q_r$ , a higher junction angle will result in greater flow deflection

between the confluent streams, changes in the sediment-transport paths (see **Sediment transport** below) and the consequent reduction of the penetration of the bar into the junction (Figure 4.1(C)). Spectacular field examples of this have been presented where one channel has been dominant during a flood (Jaeggi, 1986; Reid *et al.*, 1989) or as a result of dam impoundment in one of the tributaries that results in the other confluent channel becoming dominant in its sediment and fluid discharge contribution to the junction (e.g. Lodina and Chalov, 1971; Petts and Thoms, 1987; Mosher and Martini, 2002): both of these result in the tributary-mouth bar from one channel migrating into the junction. This migration clearly provides potential for infill of the scour and the preservation of the tributary-mouth bar (see **Sedimentology** below). Biron *et al.* (1993), Rhoads (1996) and Boyer *et al.* (2006) describe morphological change at small channel confluences and show how the position of the tributary-mouth bar from one channel, as well as the angle of the avalanche face, respond to a changing momentum ratio and the position of the shear layer between the two mixing flows. Such rapid morphological change at the junction of small rivers is also evident in the maps presented by Biron *et al.* (2002) that show changes in the position of the tributary-mouth bar as a function of a changing discharge ratio and flow stage (Figure 4.3).

The suppression of flooding through upstream damming can have particularly marked impacts at channel confluences through the enhanced progradation of tributary-mouth bars. Erskine *et al.* (1999), in a study of channels affected by the Snowy Mountains hydroelectric scheme in New South Wales, Australia, found that spatially variable channel shrinkage (5–95 per cent) is actively occurring due to the suppression of floods and the loss of high spring baseflows. Erskine *et al.* (1999) reason this regulation caused several effects linked to the tributary-mouth bars:

1. tributary-mouth bars were able to form and prograde into the confluence due to the tributary channels and gullies joining a reduced-flow mainstream
2. side bars and slackwater deposits subsequently formed due to the reworking of the tributary-mouth bar deposits
3. the confluence scour was infilled by the tributary-mouth bar progradation and biogenic sediment
4. native and exotic vegetation was then able to invade and establish itself, resulting in the stabilization of these deposits.

The net result of these changes due to mouth bar progradation was to lower the ecological diversity of the river, and suggests that maximum flows in impounded rivers must be kept sufficient to maintain the hydrogeomorphic diversity of the river, of which channel junctions and tributary-mouth bars are a key element.

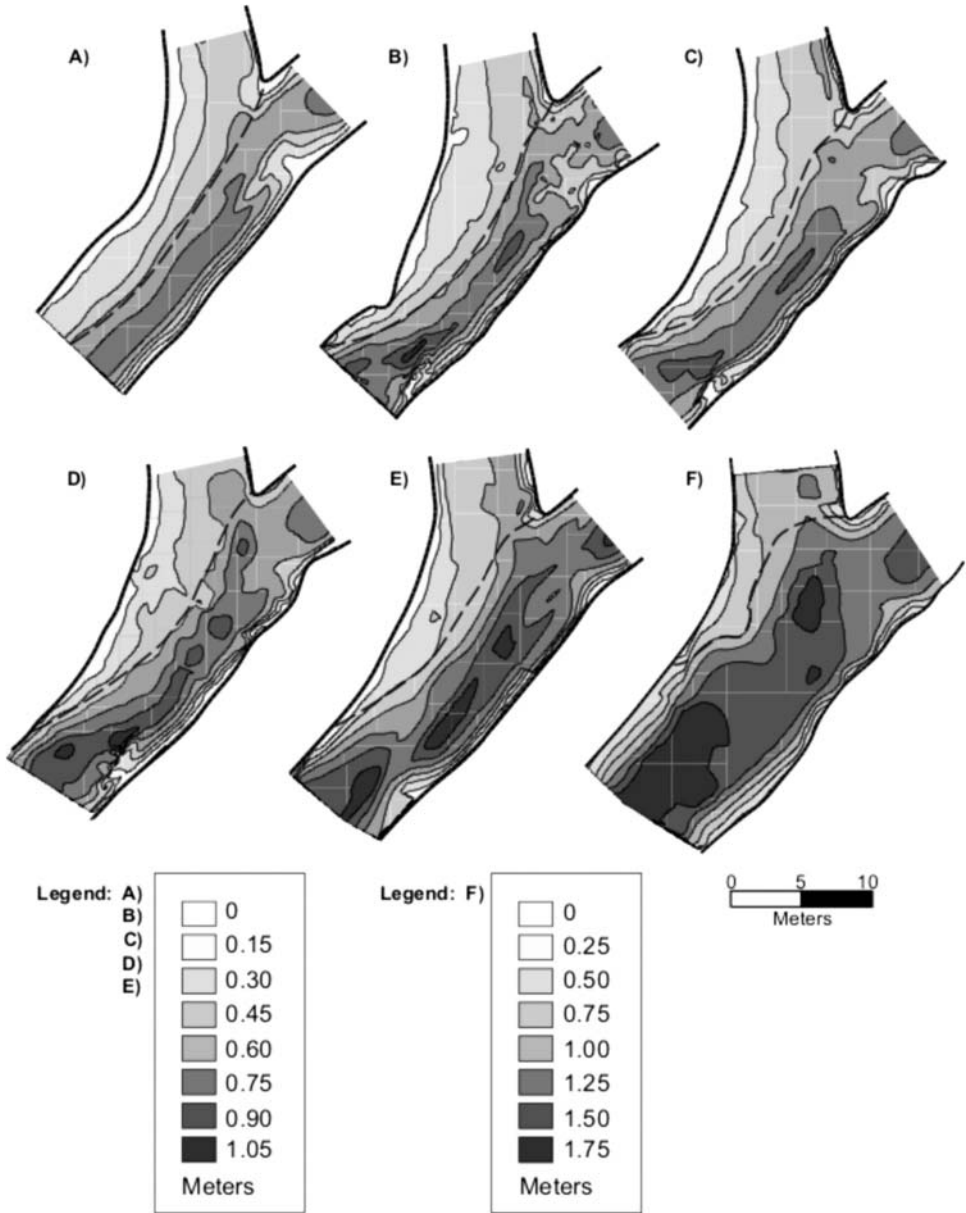


**Figure 4.3** Bed morphology of the confluence between the Berthier (top) and Bayonne (right) rivers, Quebec, and its variation as a function of flow stage and changing discharge ( $Q_r$ ) or momentum ( $M_r$ ) ratio between the rivers. A) Low Flow;  $Q_r = 0.85$ ;  $M_r = 0.91$ ; B) Low Flow;  $Q_r = 0.57$ ;  $M_r = 0.71$ ; C) Low Flow;  $Q_r = 1.20$ ;  $M_r = 2.22$ ; D) Low Flow;  $Q_r = 1.19$ ;  $M_r = 1.80$ ; E) Mid Flow;  $Q_r = 1.48$ ;  $M_r = 02.16$ ; F) High Flow;  $Q_r = 01.38$ ;  $M_r = 1.76$ . The dashed line represents the limit of the tributary-mouth bar from the Berthier and zero elevation is the water surface. Note the greater depth range in F). From Biron *et al.* (2002).

The beds of confluent rivers may be either equal or unequal in height at the junction, and these are termed ‘concordant and discordant bed confluences’ respectively. The presence of a bed height discordance can be a common feature of many junctions and has been shown to radically alter the flow dynamics within the confluence (Best and Roy, 1991; Biron *et al.*, 1993, 1996a, 1996b). Kennedy (1984) found that many confluences are distinctly discordant, and reasoned that discordance was more likely as the magnitude of the confluent rivers becomes increasingly disparate. Kennedy (1984) thus concludes that Playfair’s Law, which states that rivers largely adjust to become concordant at junctions, is largely incorrect. Concordance or discordance at the confluence will influence both the flow dynamics and sedimentology, and could vary from event to event as a tributary-mouth bar migrates into and out of a confluence. The importance of bed discordance for mixing processes at junctions is also demonstrated by Gaudet and Roy (1995) who show that the presence of bed discordance may increase the rapidity of flow mixing at confluences by a factor of 5–10.

### **Post-confluence mid-channel bars**

A bar is often present in the middle of the post-confluence channel (Mosley, 1976; Best, 1988), especially in junctions that have a Y-shaped planform. This feature sometimes forms the confluence–diffluence unit characteristic of braided rivers. Mosley (1975, 1976) records how this mid-channel bar deposition can cause bank erosion in each channel and lead to channel widening. The formation of this bar is linked by Mosley (1975) to the convergence of sediment-transport paths downstream of the junction scour (see **Sediment transport** below), where sediment may be routed around, rather than through, the scour (Mosley, 1975; Best, 1985). Additionally, if sediment is scoured in the upstream region, the declining flow velocities downstream from the region of maximum flow acceleration, as well as decreasing turbulence intensities as the shear layer dissipates (see Sukhodolov and Rhoads, 2001; Rhoads and Sukhodolov, 2004), will inevitably lead to sediment deposition. Ashmore (1993) shows that medial-bar deposition downstream of a junction in scaled braided river models can often be linked to the passage of a unit bar or gravel sheet through the junction. Passage of this sediment pulse through the junction and its emergence downstream as a mid-channel bar are principal mechanisms of braid initiation (Ashmore, 1993; Ashworth, 1996; Ashworth *et al.*, 2000) and will thus be controlled by the confluence dynamics and downstream development of the bifurcation (Parsons *et al.*, 2007).

### **Bank-attached bars**

Experimental studies in rectangular channels have shown that a bar may form in the region(s) of flow separation/expansion formed at the downstream junction corner(s) (Mosley, 1976; Best, 1987, 1988), and such accumulations have been found in several

field studies (e.g. Best, 1988; Biron *et al.*, 1993; Rhoads and Kenworthy, 1995; Rhoads, 1996; Mosher and Martini, 2002). These bars, which have been termed ‘separation zone bars’ (Best, 1988) and ‘bank-attached bars’ (Bristow *et al.*, 1993) may be characterized by finer bed sediments than in the adjacent channel (Best, 1988), and can become emergent at low flow stages (Rhoads, 2006). Best (1988) attributes the origin of these bars to flow separation at the downstream junction corner. However, it is evident that these bars may also form in regions of flow deceleration/expansion in this region but without flow separation, since separation may be impeded by both a rounded junction corner and the presence of appreciable roughness (large grains in tributaries, vegeta-

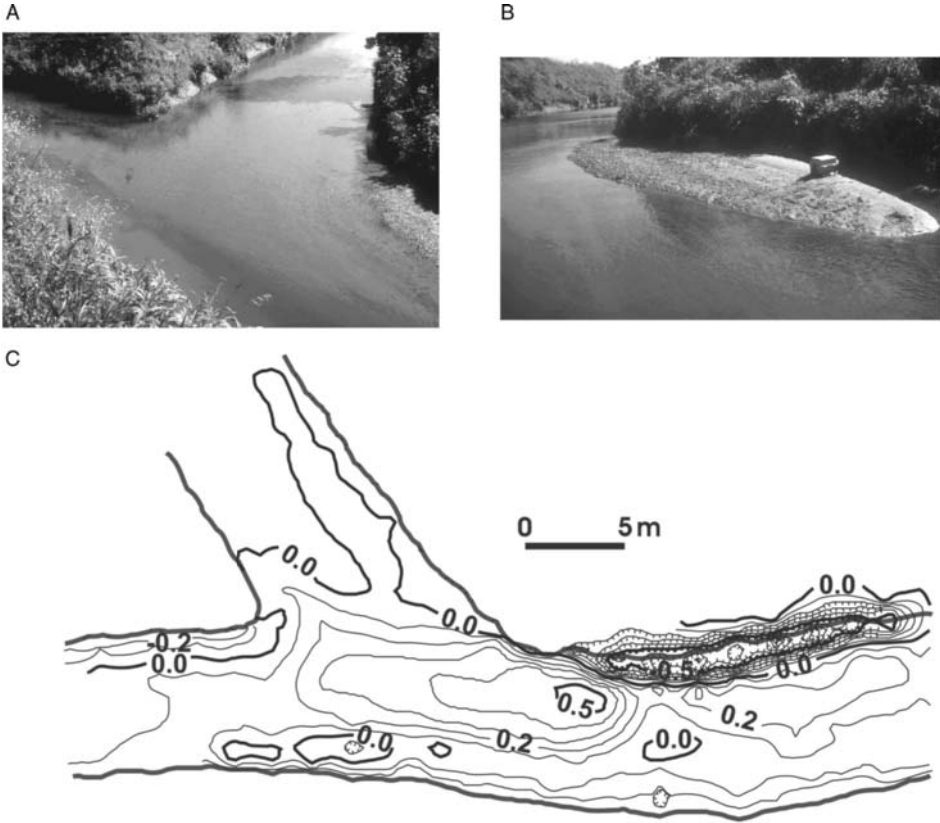


**Figure 4.4** Morphology of the Kaskaskia River – Copper Slough (KRCS) confluence, Illinois. (A) Progradation of tributary-mouth bar into KRCS after high momentum-ratio flow in July 1991 (Kaskaskia River to the left, Copper Slough towards the top); (B) bank-attached, junction-corner bar that is part of the prograding tributary-mouth bar, July 1991; (C) isopach map showing changes in bed morphology between May 1990, when bed morphology was dominated by  $M_r < 1.0$  flows, and July 1991, when bed morphology was dominated by  $M_r > 1.0$  flows. Note deposition in the center of the confluence and near the downstream junction corner. Erosion of the inner bank of the downstream channel was caused by flows with  $M_r < 1.0$  occurring between May 1990 and July 1991.

tion), and flow separation can be expected to lessen as the separation zone fills with sediment. Changes in bed morphology in response to individual hydrological events at the asymmetrical confluence of the Kaskaskia River Copper Slough (KRCS) suggest that the bank-attached bar that develops during high-momentum-ratio events may join with elevated regions of a tributary-mouth bar complex that progrades into the confluence (Rhoads and Kenworthy, 1995; Rhoads, 2006; Figure 4.4), a feature also noted in the study of Mosher and Martini (2002). The presence of coarse gravel on the surface of the junction-corner bar indicates that it is a zone of active downstream bedload transport during formative events (Rhoads, 2006). The downstream edge of this junction-corner bar at the KRCS site consists of an elevated ridge of fine sand that appears to mark the edge of an adjacent region of flow separation. Deflection of subsequent flows by the junction-corner bar can produce deposition of a fine-grained bar in the region of separated, recirculating flow in the lee of the main bar (Rhoads and Kenworthy, 1995). Sediment deposited on the separation-zone bar may come from both suspension, due to entrainment into the separation zone along the bounding shear layer, and also bedload, as evidenced by upstream migrating bedforms. Coarse deposits at the head of bank-attached confluence bars are noted by Petts and Thoms (1987) and Best (1988). Downstream coarsening of gravel-size material was documented on a bank-attached bar at a confluence on the North Tyne River, United Kingdom, with the coarsest material occurring in the middle of the bar (Petts and Thoms, 1987). Material also coarsened laterally towards the adjacent scour hole. In contrast, Best (1988) found that gravel-size material became finer towards the middle of a bar at the confluence of the River Ure and Widdale Beck, United Kingdom, but coarsened towards the bar tail. It is evident that the sedimentology of junction-corner bars is complex, and that flow patterns near the downstream junction corner and the supply of sediment to this region are critical in determining bar morphology and bed-material characteristics. These factors will be influenced, to a large extent, by upstream morphodynamics, which can feed coarse sediment into this region, and by the position and nature of the tributary-mouth bars.

### **Bed morphology at the upstream junction corner**

The region of flow near the upstream junction corner may be characterized by a zone of relatively slow-moving fluid, with slight water surface super-elevation, that is generated by the stagnation of flow in this region (Best, 1987; Biron *et al.*, 2002; Rhoads and Sukhodolov, 2001; Mosher and Martini, 2002). Flow within this stagnation zone can be recirculating, or exhibit reverse flow from one tributary into the other. Given the low velocities, bed surface sediment commonly is finer than in the adjacent channels (Best, 1988). Although no distinct bar forms are present in this region, bedforms can reflect flow patterns indicative of upstream flow.

## Sediment transport

Only a handful of studies have investigated bedload sediment transport within the confluence hydrodynamic zone, and this aspect of confluence dynamics is fertile ground for future research. Sediment transport, particularly bedload transport, serves as the link between confluence flow structure and bed morphology. The turbulent, three-dimensional flow at confluences produces patterns of bedload transport that are highly two-dimensional. Under steady flow conditions, such as those produced in laboratory experiments, flow and form evolve towards equilibrium conditions where a sediment-flux continuity is maintained throughout the junction, thereby maintaining a constancy of bed morphology. Conversely, during transient flow conditions, such as those that occur at natural confluences, the bed will dynamically evolve due to spatio-temporal variations in transport capacity.

Experimental studies have provided initial insight into patterns of bedload transport under equilibrium conditions in mobile-bed confluences with scour holes (Mosley, 1976; Best, 1988). Mosley (1976) observes that most sediment within symmetrical confluences moves along the flanks of the scour hole, rather than directly through it, and attributes this pattern to the presence of helical flow cells within the scour that sweep sediment laterally towards its margins. These zones of high sediment transport converge downstream of the scour to produce maximum transport rates in the centre of the channel (Mosley, 1976). Moreover, Mosley (1976) demonstrates that as total sediment load increases under conditions of constant flow and junction angle, the depth of the scour hole decreases. Mosley (1976) also reports that the scour depth decreases as the total sediment load passing through the junction becomes higher (Figure 4.1(D)), indicating an important feedback of transport rate on the depth of scour. The influence of total sediment load on scour depth was corroborated by the later work of Rezaur *et al.* (1999). Ashmore (1993) also highlights the important influence of pulses of bedload (that may be independent of discharge fluctuations, perhaps introduced by barform migration) that pass through confluences within braided rivers on the alignment of scour holes and the evolution of confluence morphology over time. The experimental work of Best (1988), which provides quantitative assessments of transport rates in asymmetrical confluences, confirms some aspects of the spatial patterns of sediment transport observed by Mosley (1976). In particular, the data of Best (1988) show that sediment loads from each stream are clearly segregated and that this effect becomes more pronounced as junction angle, mutual deflection of the incoming flows and scour-hole depth increase. In contrast to observations by Mosley (1976), a transport deficit occurred in the centre of the channel downstream of the scour hole at a high-angle ( $70^\circ$ ) asymmetrical junction. Transport rate increased in the centre of the downstream channel for a low-angle ( $15^\circ$ ) junction, but this confluence lacked a scour hole.

Particle-tracing experiments in natural confluences have been conducted to try to confirm the basic aspects of results derived from laboratory studies. At the confluence

of the River Ure and Widdale Beck in North Yorkshire, United Kingdom, gravel particles entering the junction from the mainstream River Ure move along a bar flanking the scour hole (Best, 1988). These particles remain along one side of the downstream channel and do not mix with sediment from the tributary Widdale Beck. In contrast, the movement of gravel particles through the scour hole and the mixing of particle paths within the confluence were noted in a study of a small junction in the Ruisseau de Sud watershed in Quebec, Canada (Roy and Bergeron, 1990). At both confluences, however, bedload particles travel more or less parallel to the channel banks and bed contours within the junction. An abrupt change in the alignment of migrating ripples was noted between the crest of a tributary-mouth bar and the bed of the main channel at the confluence of the Bayonne and Berthier rivers in Quebec, indicating that bed morphology at this discordant confluence has a substantial influence on patterns of bedload transport (Biron *et al.*, 1993). These studies suggest that patterns of particle movement at confluences are complex and require further study to better characterize sediment-transport paths.

Actual measurements of bedload-transport rates in asymmetrical confluences have been obtained by Rhoads (1996) and Boyer *et al.* (2006). At the concordant confluence of the KRCS in Illinois, United States of America, Rhoads (2006) found that, for a momentum ratio of less than 1.0, sandy bedload from the Kaskaskia River is clearly segregated from the gravel-dominated bedload of the Copper Slough within the scour hole. However, the highest transport rates also occurred within the scour hole, confirming that substantial amounts of material move through this feature. Within the downstream channel, the channel bed along the bank opposite the tributary mouth (outer bank) is swept free of sediment by inward-directed near-bed flow associated with large-scale helical motion. Here the bed consists of exposed glacial till. Along the channel bed on the tributary side of the confluence (inner bank), bedload from the tributary and main stem converge and mix. Here, size-selective sorting results in sandy bedload being confined to near-bank locations and gravel-dominated bedload moving along the inner flank of the scour hole.

The discordant confluence of the Bayonne–Berthier lacks a substantial scour hole but exhibits a dynamic prograding bar that influences patterns of sediment transport in relation to shear-layer-induced erosion within the confluence (Boyer *et al.*, 2006; Figure 4.5(A)). The highest bedload transport rates were found to occur near the edges of the shear layer (Boyer *et al.*, 2006; Figure 4.5(A)), and as the shear layer impinges on the tributary-mouth bar it was found to cause erosion of the bar, thereby resulting in high bedload transport rates. Thus, variations in the position of the shear layer produced by changing  $M_r$  can influence bedload transport rates through the interaction of the shear layer with the extant bed morphology, such as the tributary-mouth bar. No substantial segregation of sediment, such as that seen at the concordant KRCS, occurs at the discordant Bayonne–Berthier confluence, but instead bedload within the confluence is well mixed. However, at some flow stages, increased transport rates along the edges of the shear layer can lead to corridors of higher sediment-transport rates (Figure 4.5(A) and (B)).

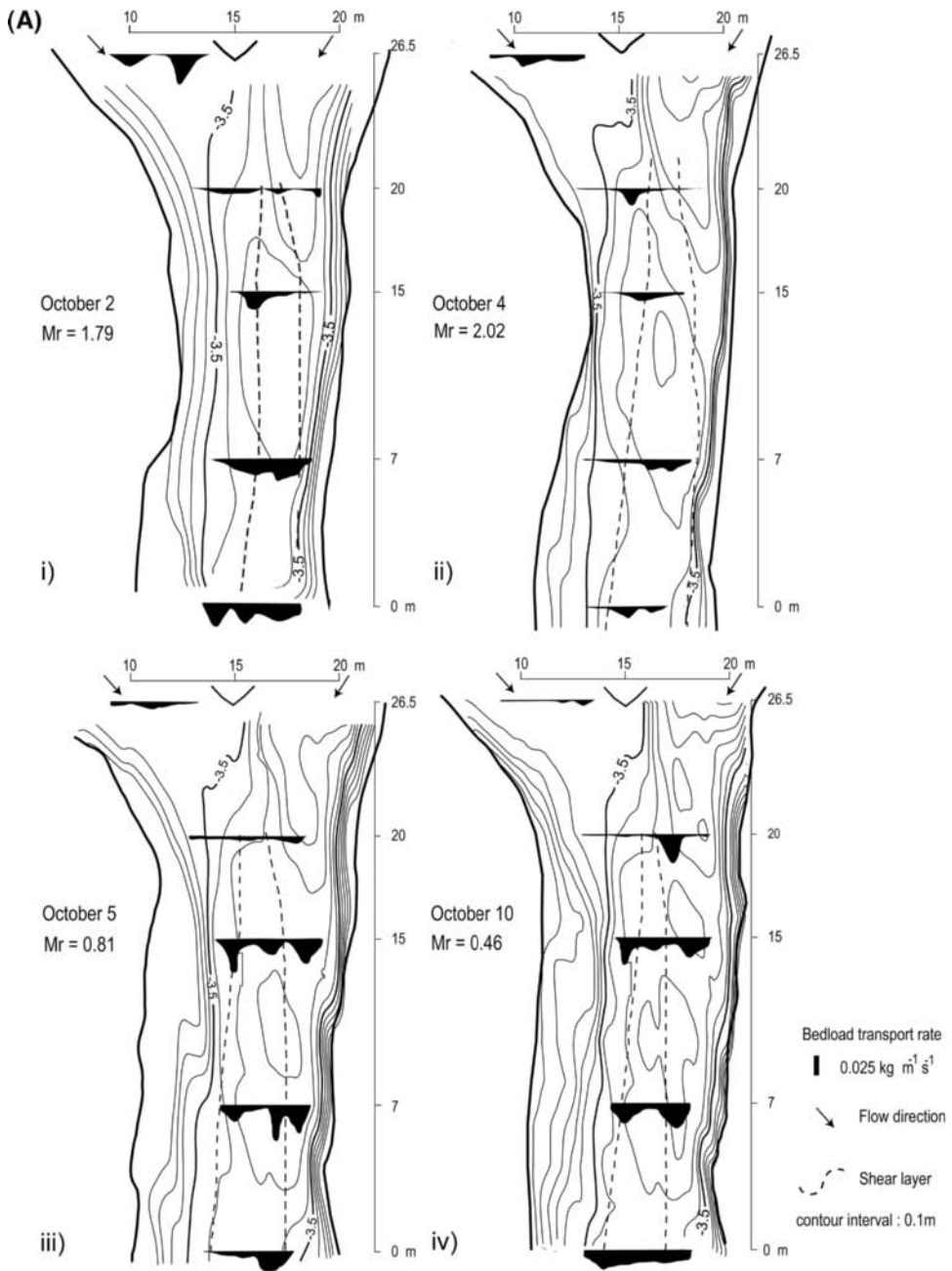


**Figure 4.5** (A) Spatial distributions of bedload transport rates at the Bayonne–Berthier discordant bed confluence, Quebec, for four different dates (i–iv) with differing values of momentum ratio. The background contours denote the bed morphology at these times (from Boyer *et al.*, 2006). (*continued*)

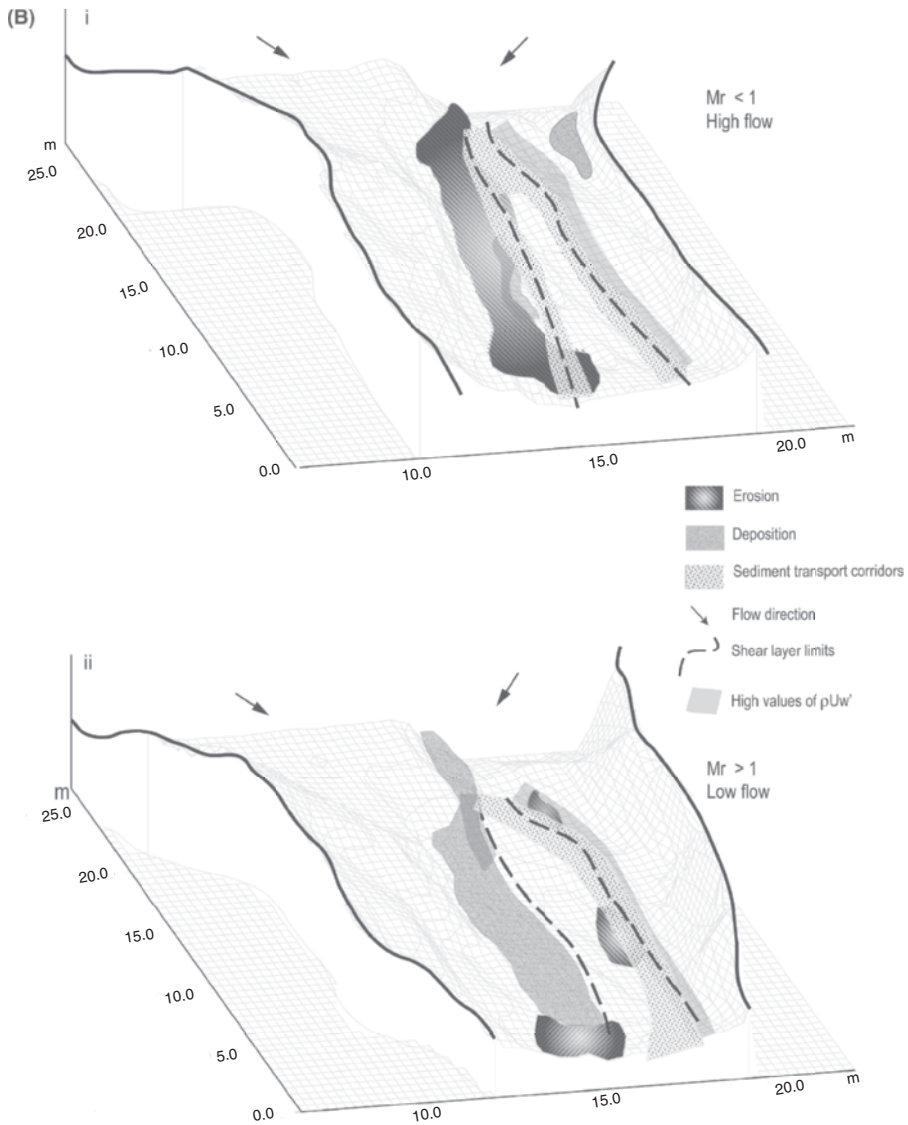


**Figure 4.5** (B) A conceptual model of sediment transport and morphological change at the Bayonne–Berthier bed confluence (from Boyer *et al.*, 2006), at different flow stages and momentum ratios: (i)  $M_r < 1$  and high flow; (ii)  $M_r > 1$  and low flow. The background grids show the bathymetry of the bed. In the confluence, high values of turbulent stresses ( $Uw'$ ; where  $U$  is the mean downstream velocity,  $w$  is the vertical component of flow and the prime denotes the deviatoric value) were observed along the edges of the shear layer, with the center of the shear layer being dominated by normal turbulent stress in  $w$  ( $w'^2$ ). Bedload transport measurements were used to define transport corridors, whilst regions of erosion and deposition were assessed from the measured changes in bed morphology and bedload transport patterns. A colour reproduction of this figure can be seen in the colour section towards the centre of the book.

The work by Boyer *et al.* (2006) highlights the connection between sediment transport and the dynamic change in bed morphology, but few studies, apart from this, have examined patterns of sediment transport in confluences when the bed is actively evolving. Such changes will be related to spatial variations in bedload transport capacities along or across the confluence, and in particular: (i) sediment-flux convergence, or decreasing transport capacity in the downstream or cross-stream direction, to generate deposition or (ii) sediment-flux divergence, or increasing transport capacity, to cause erosion. The dynamic change in bed morphology at the KRCS confluence (Figure 4.4) indicates that the alternation of high-momentum-ratio and low-momentum-ratio events results in scour within, and downstream of, the confluence when  $M_r < 1$ , but deposition within the confluence and along the downstream junction corner when  $M_r > 1$  (Rhoads and Kenworthy, 1995; Rhoads, 1996; Rhoads, 2006). In other words, sediment-flux convergence characterizes the dynamics of the confluence during the transition from  $M_r < 1$  to  $M_r > 1$ , whereas sediment-flux divergence occurs during the transitions from  $M_r > 1$  to  $M_r < 1$ . The net result of this change is the episodic storage and flushing of sediment from within the confluence during discrete transport-effective hydrologic events with different momentum ratios.

## Sedimentology

The depositional character of channel confluences has become a subject of great interest in the past decade, partly due to the fact that the sedimentary fill of confluences may be expected to be common in many rivers, such as rapidly migrating braided rivers, and partly due to the fact that confluences may represent some of the points of deepest incision into the underlying sediments. For instance, Ardies *et al.* (2002) show that in the Lower Cretaceous incised valleys of Western Canada, enhanced erosion at tributary junctions has produced regions, approximately 2–3 km in diameter, where the valley fill is up to five times thicker and much coarser grained than in the deposits of the adjacent valleys. This figure matches well with past studies examining the depth of scour within modern channels (Figure 4.2 and references therein). Ardies *et al.* (2002) highlight that these localized scour fills may be excellent targets for hydrocarbon exploration. The presence/absence of confluence scour and its depth may also be a considerable aid to deciphering the nature of autocyclic and allocyclic scour and identifying the controls on fluvial deposition (Salter, 1993; Best and Ashworth, 1997; Fielding, 2007); however, the scour zones need to migrate spatially through time to produce widespread erosion surfaces (see Roy and Sinha, 2005, for an account of migration of confluences of the Ganga–Ramganga–Garra rivers in India).

Based on the current understanding of the morphology of channel confluences, it can be expected that the sedimentology of these sites will be characterized by: (i) a scour hole, or erosion surface, that represents the confluence scour and its spatio-temporal

migration, (ii) sets of cross-strata, perhaps at a high angle-of-repose, that represent the migration of the tributary-mouth bars into the scour and (iii) sediments associated with other barforms within the junction. These depositional elements are used by Bristow *et al.* (1993) to propose a series of schematic facies models for confluence sedimentation that were based on junction angle and flow stage. The nature of sediment preservation at channel junctions will be largely a function of the evolution and migration of bars within the confluence, as is highlighted and discussed by Ashmore (1993) and Siegenthaler and Huggenberger (1993). Confluence sediments may also possess disparities in grain size, mineral composition and/or the type and abundance of sedimentary structures (see Frostick and Reid, 1977) that reflect differences in the sediment characteristics of the contributing drainage areas. For instance, in a study of sedimentation in an ephemeral river network, Frostick and Reid (1977) document that the number of planar laminae which can be found in sediments downstream of each junction increases downbasin in the main trunk channel. They reason that this phenomenon is due to the main channel capturing more and more tributary inputs in a downstream direction, with the asynchronous timing of water and sediment contributions from upstream ephemeral tributaries producing distinct laminae at each successive confluence. Heavy minerals may also concentrate along scour surfaces and within the sediments of channel junctions, and these sites can be areas of significant heavy-mineral accumulations (Mosley and Schumm, 1977; Best and Brayshaw, 1985; Carling and Breakspear, 2006).

In a historical context, Leeder (1998) presents a fascinating appraisal of the contribution of Charles Lyell to the study of sedimentology and highlights that some of the first descriptions of cross-stratification were those of Lyell (1830), who examined deposits at the confluence of the Arve and Rhône rivers in France (Figure 4.6), concerning a stratified sequence he observed in the incised flood deposits of the Arve within the Rhône. Leeder (1998) contends this is the first illustration and serious explanation of cross-bedding in the geological literature, with the sketch showing 'tangential thinning-downward foresets, truncated above by upper-phase plane beds, which are in turn succeeded by pebbly sand lenses' (p. 100). Leeder (1998) argues that these descriptions and the location of the outcrop show that Lyell was describing the avalanche-face cross-strata of a confluence tributary-mouth bar together with the overlying planar gravel strata. Lyell (1830) states that '[t]hese layers must have accumulated one on the other by lateral apposition, probably when one of the rivers was very gradually increasing or diminishing in velocity, so that the point of greatest retardation caused by their conflicting currents shifted slowly, allowing the sediment to be thrown down in successive layers on a sloping bank' (p. 255).

Siegenthaler and Huggenberger (1993) document pool deposits in the lowest depositional units of the Pleistocene Rhine gravels, which they argue are formed by sedimentation at channel confluences within a braided river. These pool fills (Figure 4.7(A)) are characterized by: (i) lateral dimensions of a few meters to more than a hundred meters, with thicknesses being approximately 0.5–0.6 m, (ii) in sections normal to paleoflow,

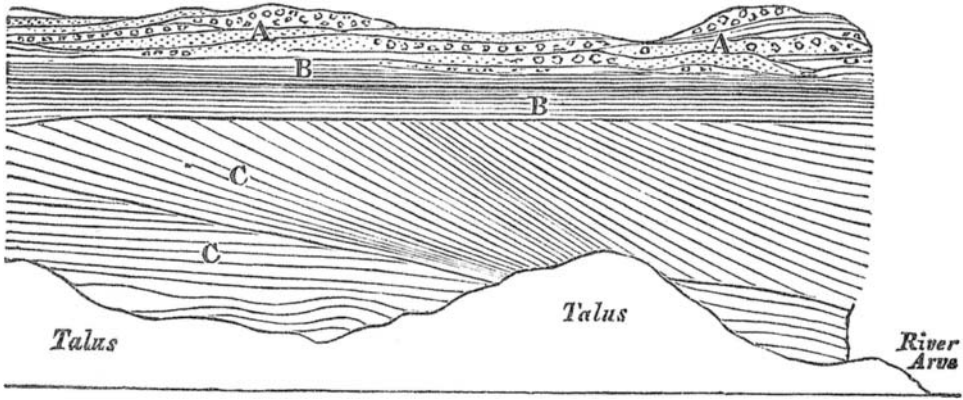


**Figure 4.6** A copy of the woodcut version (Lyell, 1830, p. 254, Figure 6) of Lyell's field sketch of cross-stratification taken at the confluence of the Rivers Rhône and Arve, as observed at low river stage by Charles Lyell in January 1829 (as given in Leeder, 1998; Lyell, 1830). The field of view is 3.66 m by 1.52 m, and illustrates cross-stratification from the tributary-mouth bar from the River Arve (labelled C), produced by the 1828 spring flood, that has been subsequently dissected by the River Rhône.

the erosional surface can be circular, (iii) the cross-sets that infill the scour are strongly curved and often tangential to the lower bounding surface and (iv) interfingering sets that infill the scour may show growth from two opposite directions, with there often being a textural/compositional variation between these sets. Siegenthaler and Huggenberger (1993) argue that this shows the sediments which form these sets were sourced from different input channels. Siegenthaler and Huggenberger (1993) also detail the nature of the sets that infill the pools, ranging from gravel dunes that form distinct gravel couplets formed on angle-of-repose avalanche faces (the faces of the tributary-mouth bars) through to lower-angle accretion surfaces lateral to the scour. Siegenthaler and Huggenberger (1993) also discuss how the mode of pool migration will influence what is preserved (Figure 4.7(B)) together with the orientation of the section within the deposits.

In describing trough-shaped depositional elements within the Quaternary deposits of a gravel-bed meandering river in the Neckar Valley, in north-west Germany, Kostic and Aigner (2007) detail concave-up erosion surfaces that are then filled by cross-sets that consist mainly of openwork and filled framework gravels (Figure 4.8). These scours were found to dominate the lowest parts of the channel fills, and are up to 1-m thick with widths often greater than 5 m and lengths of several tens of meters. The cross-sets that filled the scours are typically oblique to the lower bounding surface and may become tangential with the lower erosional surface (Figure 4.8(B)). Kostic and Aigner (2007) contend that these depositional structures, which represent confluence scour fills, are preferentially preserved as they constitute the lowest parts of formative braided channels,

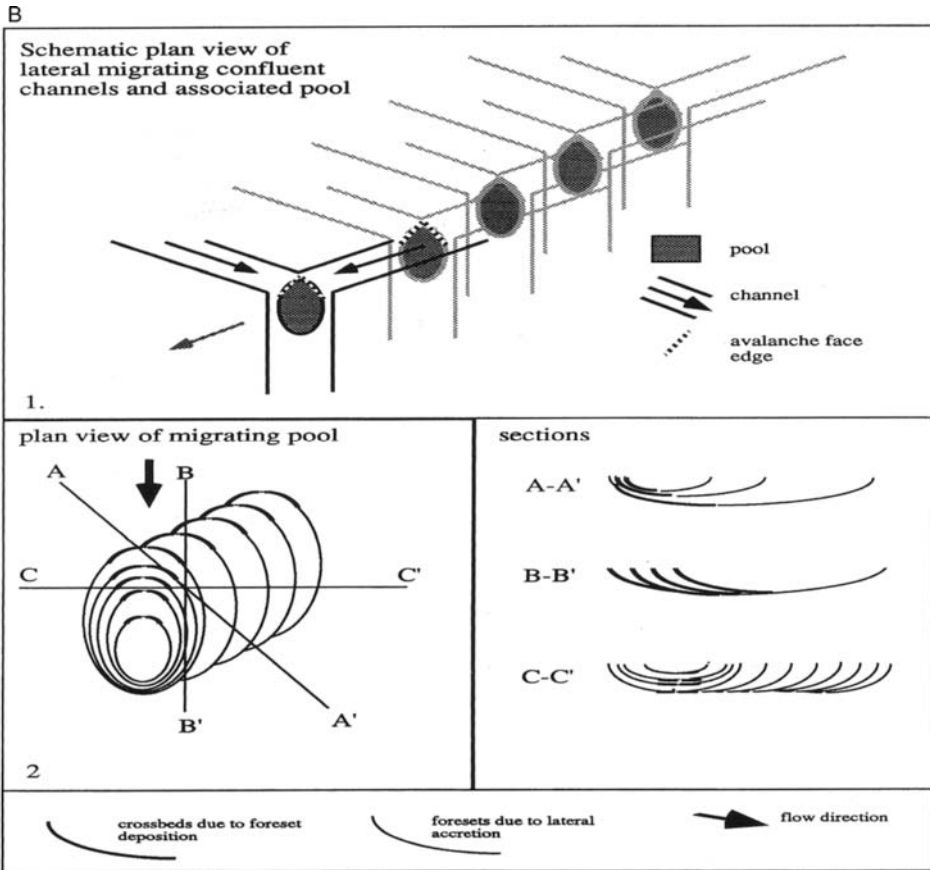


**Figure 4.7** (A) Photograph of the preserved 'pool' deposits of Siegenthaler and Hugenberg (1993) that were interpreted as caused by erosion and sedimentation at a channel junction. Note the concave-upwards, curved erosional base (labelled 'a') and infill with cross-stratification that becomes tangential to the lower bounding surface (labelled 'b'). (B) Schematic model of the migration of a braided river confluence and the nature of junction sedimentation as a function of outcrop orientation. From Siegenthaler and Hugenberg (1993), Geological Society of London Special Publication 75: 147–162.

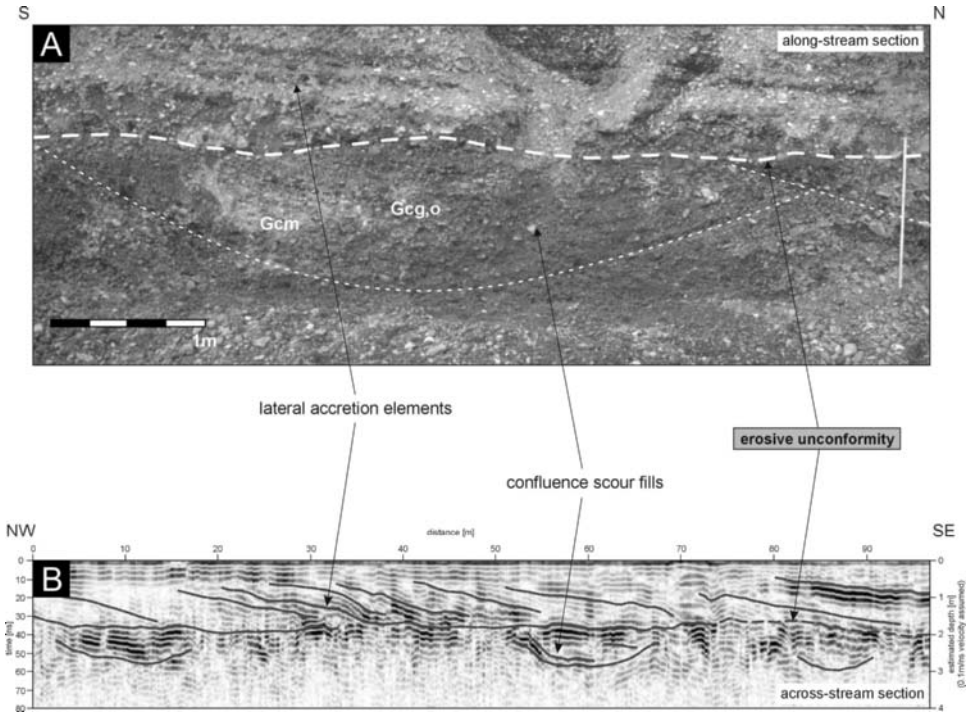


**Figure 4.8** Example of the confluence fills in the Neckar valley gravels as described by of Kostic and Aigner (2007): (A) trough-shaped fill that is composed mainly of cross-sets of openwork, filled or massive gravels (see Kostic and Aigner (2007) for facies descriptions and codes); (B) ground-penetrating radar plot of the Neckar valley gravels illustrating: (i) the scale of the confluence scours, (ii) their lower, concave-upwards erosional bases and (iii) dipping surfaces (cross-sets from tributary-mouth bars?) that infill the scours.

supporting the earlier contention of Bristow *et al.* (1993). The complex heterogeneity of such fills can be expected to form an extremely complicated hydrogeological suite with multilateral flowpaths (Kostic and Aigner, 2007; Whittaker and Teutsch, 1999). Heinz *et al.* (2003) also found the scours and fills of channel confluences to be dominant in the Quaternary glaciofluvial gravels of south-west Germany, and that the size, shape, orientation and migration directions of these scours are significant in controlling the flow of groundwater.

Similar scours have also been documented by Cowan (1991) in the Jurassic Morrison Formation of New Mexico as well as by Miall and Jones (2003) in the Triassic Hawkesbury sandstone of New South Wales, Australia. Miall and Jones (2003) describe their ‘hollow’ architectural facies elements (Figure 4.9) as being characterized by a scoop-shaped curved erosional base, lacking a flat floor, and a fill that is often composed of a single set of low-angle cross-bedding that dips obliquely to the margin of the hollow (Figure 4.9).



**Figure 4.9** Two examples of the 'hollow' architectural elements of Miall and Jones (2003) in the Triassic Hawkesbury Sandstone, New South Wales, Australia. These hollows were interpreted to represent the fill of channel confluences. Photographs courtesy of Andrew Miall. (A) Confluence scour and fill that is approximately 30 m wide, with the base of the confluence scour sharply truncating the cross-stratification in the underlying beds (arrowed); (B) a confluence scour that is 18 m wide, with faint, low-angle cross-stratification (tributary-mouth bar?; labelled 'a') dipping to the right. Again, note the sharply erosional lower contact (arrowed) and the steep right margin of the scour.

The hollows are up to 10 m deep and 60 m wide and in some cases show superimposition, illustrating the repeated occurrence of scour at the same site. Miall and Jones (2003) interpret these hollows as due to scour and infill at channel confluences and that they formed some of the largest scour surfaces within the sedimentary architecture of this deposit. Wooldridge and Hickin (2005), in a study of sedimentation in a stable 'wandering' gravel-bed river, note that confluence scours are not as common as found in earlier studies of braided rivers and attribute this to the relative stability of the islands, limited channel migration and hence a reduced probability of confluence migration. Salter (1993) and Best and Ashworth (1997) highlight the fact that channel confluences are

sites of some of the deepest scours within braided rivers and that, if they are mobile (see Siegenthaler and Huggenberger, 1993; Figure 4.7(B), this volume), scours may produce widespread erosion surfaces. In deciphering the impact of sea-level change (allocyclic control) versus intrinsic autocyclic channel scour within the ancient sedimentary record, it thus becomes important to be able to distinguish the effects of confluence erosion (Best and Ashworth, 1997; Fielding, 2007). Better recognition of the scale, infill and possible regional extent of these scour surfaces, and the junction fill, thus becomes important.

In a study of confluence sedimentation in an anastomosing river, Alam *et al.* (1985) record bidirectional current indicators on a tributary-mouth bar near the upstream junction corner of the Castlereagh River–Warrena Creek confluence, New South Wales, Australia. They record cross-sets of up to 0.40 m thickness and dip angles between 7 and 31° that extend upstream into the tributary Warrena Creek. Alam *et al.* (1985) outline three possible hypotheses for such cross-sets within the tributary channel at river junctions: (a) deposition on the upstream sides of antidunes (although the cross-stratification at their field site was clearly shown to be due to subcritical dunes and ripples), (ii) deposition by reverse flow in a separation zone (although the occurrence of reverse flow indicators across the whole tributary channel mouth, rather than just in an area near the upstream junction corner, negated this hypothesis) and (iii) deposition by flow reversal in the tributary channel due to local reversals in water-surface slope caused by backwater effects. Alam *et al.* (1985) thus argue that partial diversion of the mainstream flow was the cause of the bidirectional current indicators they recorded and that this effect is produced when the main channel flow is dominant. They further reason that such reversals in flow may be more common in low-gradient rivers where it may be easier to create favourable backwater conditions for such flows. Such conditions also may be more likely in catchments where there is a disparity in rainfall timing and quantity across the different tributary areas (see Frostick and Reid, 1977). Extreme cases of tributary sedimentation when the main channel is dominant come in the form of slackwater deposits within the tributary channel (e.g. Baker, 1984; Kochel and Baker, 1988; Leopold *et al.*, 2006): here, sediment is deposited within the stagnant backwater in the tributary when the main channel dominates the flow at a junction (i.e. very low  $Q_r$  values). Studies of such slackwater sites have shown the usefulness of these deposits for various paleoflood estimates, such as water depth and sediment load (Rudoy and Baker, 1993; Carling *et al.*, 2002).

## Conclusions

The morphology and sediment-transport characteristics of river channel confluences are highly complex and involve many interactions between flow structure, sediment transport (as both bed- and suspended load) and the development of bed morphology, which will change over differing spatial and temporal scales. Although the bed

morphology of a range of channel confluences has been found to have a number of common characteristics, namely a central scour, tributary-mouth bars and bars within the post-confluence channel, it is apparent that much work remains to be conducted in relation to a wide range of controlling boundary conditions. For instance, what effect is exerted on the bed morphology by differing curvature in the upstream confluent channels, by the presence and extent of bed discordance or by extreme discharge/momentum ratios?

Several broad areas appear ripe for research. First, most of our knowledge of the confluence hydrodynamic zone still stems from laboratory modelling and the study of relatively small field junctions. Although documentation of flow and morphology at larger junctions is now becoming a reality (see Parsons *et al.*, this volume, Chapter 5), it is evident that far more study is required into the nature of a range of differing size junctions, their controlling processes and the nature of any scale invariance in both form and process. Second, although progress has been made in quantifying the nature of sediment transport within channel confluences, much work remains to be done and we have a comparatively sparse knowledge of how sediments, of differing sizes, are routed through channel junctions. Field studies and numerical models that incorporate sediment transport would provide obvious approaches in which to gain key insights here and address this area, which is perhaps the most acute gap in our understanding of channel confluences. Thirdly, the role of confluences in relation to downstream sediment dispersal and bed morphology (for instance at bifurcations) appears an area for critical analysis and for informing ideas of how inherited flow structure affects large-scale channel morphology in these sites. Lastly, the depositional character of confluence sediments is becoming increasingly well known, and progress in our understanding of sediment routing within channel junctions will better inform depositional models that can be linked to hydrogeological predictions of the sub-surface behaviour of these elements of alluvial architecture.

## Acknowledgements

Our thanks go to our research colleagues, especially Stuart Lane, Dan Parsons, André Roy, Phil Ashworth, Pascale Biron, Claudine Boyer, Ian Reid, Lynne Frostick, Gary Parker, Mat Roberts, Stuart McLelland and Alex Sukhodolov, with whom we have been lucky enough to work on aspects of confluence flow and morphodynamics over the past 20 years. JLB is especially grateful to Ian Reid and Lynne Frostick for their original insight and vision in inspiring his interest in channel confluences and their study in both laboratory and field. Some of the ideas and data for this paper were also presented by JLB and BR in their talks at RCEM 2005, and we are grateful to Marcelo García and Gary Parker for their invitation to participate in this meeting and enabling us to think further about some of the issues discussed here. We would like to thank Tom Aigner,

Pascale Biron, Peter Huggenberger and Andrew Miall, who graciously provided us with top-copy photographs and images from their papers, and lastly we would like to thank André Roy for his editorial guidance and great patience.

## References

- Alam MM, Crook KAW, Taylor G. 1985. Fluvial herring-bone cross-stratification in a modern tributary mouth bar, Coonamble, New South Wales, Australia. *Sedimentology* **32**: 235–244.
- Amsler ML, Drago EC, Paira AR. 2007. Fluvial Sediments: Main Channel and Floodplain Interrelationships. In *The Middle Paraná River: Limnology of a Subtropical Wetland*, Iriondo MH, Paggi, JC, Parma MJ (eds). Springer-Verlag: Berlin-Heidelberg; 123–142.
- Ardies GW, Dalrymple RW, Zaitlin BA. 2002. Controls on the geometry of incised valleys in the basal quartz unit (Lower Cretaceous), Western Canada sedimentary basin. *Journal of Sedimentary Research* **72**: 602–618.
- Ashmore PE. 1993. Anabranch confluence kinetics and sedimentation processes in gravel-braided streams. In *Braided Rivers*, Best JL, Bristow CS (eds). *Geological Society of London Special Publication* **75**: 129–146.
- Ashmore PE, Parker G. 1983. Confluence scour in coarse braided streams. *Water Resources Research* **19**: 392–402.
- Ashworth PJ. 1996. Mid-channel bar growth and its relationship to local flow strength and direction. *Earth Surface Processes and Landforms* **21**: 103–123.
- Ashworth PJ, Best JL, Roden J, Bristow CS, Klaassen GJ. 2000. Morphological evolution and dynamics of a large, sand braid-bar, Jamuna River, Bangladesh. *Sedimentology* **47**: 533–555.
- Baker VR. 1984. Flood sedimentation in bedrock fluvial systems. In *Sedimentology of Gravels and Conglomerates*, Koster EH, Steel RJ (eds). Memoir of the Canadian Society of Petroleum Geologists **10**: 87–98.
- Best JL. 1985. *Flow and sediment transport at river channel confluences*, Unpublished Ph.D. Thesis, Birkbeck College, University of London.
- Best JL. 1986. The morphology of river channel confluences. *Progress in Physical Geography* **10**: 157–174.
- Best JL. 1987. Flow dynamics at river channel confluences: Implications for sediment transport and bed morphology. In *Recent Developments in Fluvial Sedimentology*, Etheridge FG, Flores RM, Harve MD (eds). Society of Economic Paleontologists and Mineralogists, Special Publication 39, SEPM: Tulsa; 27–35.
- Best JL. 1988. Sediment transport and bed morphology at river channel confluences. *Sedimentology* **35**: 481–498.
- Best JL, Ashworth PJ. 1997. Scour in large braided rivers and the recognition of sequence stratigraphic boundaries. *Nature* **387**: 275–277.
- Best JL, Brayshaw AC. 1985. Flow separation: A physical process for the concentration of heavy minerals within alluvial channels. *Journal of the Geological Society of London* **142**: 747–755.
- Best JL, Roy AG. 1991. Mixing layer distortion at the confluence of channels of different depth. *Nature* **350**: 411–413.
- Biron P, Roy AG, Best JL, Boyer CJ. 1993. Bed morphology and sedimentology at the confluence of unequal depth channels. *Geomorphology* **8**: 115–129.

- Biron P, Best JL, Roy AG. 1996a. Effects of bed discordance on flow dynamics at river channel confluences. *Journal of Hydraulic Engineering* **122**: 676–682.
- Biron P, Roy AG, Best JL. 1996b. Turbulent flow structure at concordant and discordant open-channel confluences. *Experiments in Fluids* **21**: 437–446.
- Biron PM, Richer A, Kirkbride AD, Roy AG, Han S. 2002. Spatial patterns of water surface topography at a river confluence. *Earth Surface Processes and Landforms* **27**: 913–928.
- Boyer C, Roy AG, Best JL. 2006. Dynamics of a river channel confluence with discordant beds: Flow turbulence, bed load sediment transport, and bed morphology. *Journal of Geophysical Research* **111**: F04007. DOI: 10.1029/2005jf000458.
- Bradbrook KF, Lane SN, Richards KS. 2000. Numerical simulation of three-dimensional, time-averaged flow structure at river channel confluences. *Water Resources Research* **36**: 2731–2746.
- Bradbrook KF, Lane SN, Richards KS, Biron PM, Roy AG. 2001. Role of bed discordance at asymmetrical river confluences. *Journal of Hydraulic Engineering* **127**: 351–368.
- Bristow CS, Best JL, Roy AG. 1993. Morphology and facies models of channel confluences. In *Alluvial Sedimentation*, Marzo M, Puigdefabregas C (eds). International Association of Sedimentologists Special Publication 17. Blackwells: Oxford; 91–100.
- Bryan RB, Kuhn NJ. 2002. Hydraulic conditions in experimental rill confluences and scour in erodible soils. *Water Resources Research* **38**: DOI: 10.1029/2000WR000140.
- Calloway C. 1902. On a cause of river curves, *The Geological Magazine*, New Series, Decade IV, **9**: 450–455.
- Carling PA, Breakspear RMD. 2006. Placer formation in gravel-bedded rivers: A review, *Ore Geology Reviews* **28**: 377–401.
- Carling PA, Kirkbride AD, Parnachov SV, Borodavko PS, Berger GW. 2002. Late-Quaternary catastrophic flooding in the Altai Mountains of south-central Siberia: A synoptic overview and an introduction to flood deposits sedimentology. In *Flood and Megaflood Processes and Deposits: Recent and Ancient Examples*, Martini PI, Baker VR, Garzon G (eds). International Association of Sedimentologists, Special Publication 32. Blackwells: Oxford; 17–35.
- Cowan EJ. 1991. The large-scale architecture of the fluvial Westwater Canyon Member, Morrison Formation (Jurassic), San Juan Basin, New Mexico. In *The Three-Dimensional Facies Architecture of Terrigenous Clastic Sediments, and Its Implications for Hydrocarbon Discovery and Recovery*, Miall, AD, Tyler N (eds). Society of Economic Paleontologists and Mineralogists, Concepts in Sedimentology and Palaeontology 3, SEPM: Tulsa; 80–93.
- Delft Hydraulics and Danish Hydraulics Institute (1996). *FAP24 River Survey Project, Final Report, Main Volume*. Prepared for Flood Plan Coordination Organisation, Dhaka, Bangladesh.
- Erskine WD, Terrazzolo N, Warner RF. 1999. River rehabilitation from the hydrogeomorphic impacts of a large hydro-electric power project: Snowy River, Australia. *Regulated Rivers: Research and Management* **15**: 3–24.
- Ezcurra de Drago I, Marchese M, Montalto L. 2007. Benthic Invertebrates. In *The Middle Paraná River: Limnology of a Subtropical Wetland*, Iriondo MH, Paggi JC, Parma MJ (eds). Springer-Verlag: Berlin Heidelberg; 251–275.
- Ferguson RI, Cudden JR, Hoey TB, Rice SP. 2006. River system discontinuities due to lateral inputs: Generic styles and controls. *Earth Surface Processes and Landforms* **31**: 1149–1166.
- Fielding CR. 2007. Sedimentology and stratigraphy of large river deposits: Recognition in the ancient record, and distinction from “incised valley fills”. In *Large Rivers: Geomorphology and Management*, Gupta A (ed.). John Wiley & Sons: Chichester; 97–113.

- Frostick LE, Reid I. 1977. The origin of horizontal laminae in ephemeral channel-fill. *Sedimentology* **24**: 1–9.
- Gaudet JM, Roy AG. 1995. Effect of bed morphology on flow mixing length at river confluences. *Nature* **373**: 138–139.
- Ghobadian R, Bajestan MS. 2007. Investigation of sediment patterns at river confluence. *Journal of Applied Sciences* **7**: 1372–1380.
- Ginsberg S, Perillo GME. 1999. Deep-scour holes at tidal channel junctions, Bahía Blanca Estuary, Argentina. *Marine Geology* **160**: 171–182.
- Heinz J, Kleinedam S, Teutsch G, Aigner T. 2003. Heterogeneity patterns of Quaternary glaciofluvial gravel bodies (SW-Germany): Application to hydrogeology. *Sedimentary Geology* **158**: 1–23.
- Jaeggi MNR. 1986. Non distorted models for research on river morphology. In *Proceedings of the Symposium on Scale Effects in Modelling Sediment Transport Phenomena, August 1986*. International Association of Hydrological Sciences: Toronto; 70–84.
- Kennedy BA. 1984. On Playfair's law of accordant junctions. *Earth Surface Processes and Landforms* **9**: 153–173.
- Kenworthy ST, Rhoads BL. 1995. Hydrologic control of spatial patterns of suspended sediment concentration at a small stream confluence. *Journal of Hydrology* **168**: 251–63.
- Kjerfve B, Shao CH, Stapor F. 1979. Formation of deep scour holes at the junction of tidal creeks: An hypothesis. *Marine Geology* **33**: 9–14.
- Klaassen GJ, Vermeer K. 1988. Confluence scour in a large braided river with fine bed material. In *Proceedings of the International Conference on Fluvial Hydraulics*. International Association of Hydraulic Research: Budapest, Hungary; 395–408.
- Kochel RC, Baker VR. 1988. Paleoflood Analysis Using Slackwater Deposits. In *Flood Geomorphology*, Baker VR, Kochel RC, Patton PC (eds). John Wiley & Sons: Chichester; 357–391.
- Kostic B, Aigner T. 2007. Sedimentary architecture and 3D ground-penetrating radar analysis of gravelly meandering river deposits (Neckar Valley, SW Germany). *Sedimentology* **54**: 789–808. DOI: 10.1111/j.1365–3091.2007.00860.x.
- Leeder MR. 1998. Lyell's Principles of Geology: Foundations of Sedimentology. *Geological Society of London, Special Publication* **143**: 95–110. DOI: 10.1144/GSL.SP.1998.143.01.09.
- Leopold M, Völkel J, Heine K. 2006. A ground-penetrating radar survey of late Holocene fluvial sediments in NW Namibian river valleys: Characterization and comparison. *Journal of the Geological Society of London* **163**: 923–936. DOI: 10.1144/0016-76492005-092.
- Lodina RV, Chalov RS. 1971. Effect of tributaries on the composition of river sediments and on deformations of the main river channel. *Soviet Hydrology: Selected Papers* **4**: 65–70.
- Lyell C. 1830. *Principles of Geology*, Vol. 1, Murray, London. (Facsimile reprint, University of Chicago Press, Chicago, 1991).
- McLelland SJ, Ashworth PJ, Best JL. 1996. The origin and downstream development of coherent flow structures at channel junctions. In *Coherent Flow Structures in Open Channels*, Ashworth PJ, Bennett SJ, Best JL, McLelland SJ (eds). John Wiley & Sons: Chichester; 491–519.
- Miall A., Jones BG. 2003. Fluvial architecture of the Hawkesbury Sandstone (Triassic), near Sydney, Australia. *Journal of Sedimentary Research* **73**: 531–545.
- Mosher S-J, Martini IP. 2002. Coarse grained flood bars formed at the confluence of two subartic rivers affected by hydroelectric dams, Ontario, Canada, In *Flood and Megaflood Processes and Deposits: Recent and Ancient Examples*, Martini PI, Baker VR, Garzon G (eds). International Association of Sedimentologists, Special Publication 32. Blackwells: Oxford; 213–231.

- Mosley MP. 1975. *An experimental study of channel confluences*, Unpublished Ph.D. thesis, Colorado State University.
- Mosley MP. 1976. An experimental study of channel confluences. *Journal of Geology* **84**: 535–562.
- Mosley MP. 1982. Scour depths in branch channel confluences: Ohau River, Otago, New Zealand. *Proceedings of New Zealand Institute of Professional Engineers* **9**: 17–24.
- Mosley MP, Schumm SA. 1977. Stream junctions: A probable location for bedrock placers. *Economic Geology* **72**: 691–697.
- Orfeo O. 1995. *Sedimentología del río Paraná en el área de confluencia con el río Paraguay*, Unpublished Ph.D. thesis, Facultad de Ciencias Naturales y Museo, Universidad Nacional de La Plata.
- Parsons DR, Best JL, Lane SN, Orfeo O, Hardy RJ, Kostaschuk R. 2007. Form roughness and the absence of secondary flow in a large confluence-diffuence, Río Paraná, Argentina. *Earth Surface Processes and Landforms* **32**: 155–162. DOI: 10.1002/esp.1457.
- Petts GE, Thoms MC. 1987. Morphology and sedimentology of a tributary confluence bar in a regulated river: North Tyne, UK. *Earth Surface Processes and Landforms* **12**: 433–440.
- Pierini JO, Perillo GME, Carbone ME, Marini FM. 2005. Residual flow structure at a scour-hole in Bahía Blanca Estuary, Argentina. *Journal of Coastal Research* **21**: 784–796.
- Pinter N, Miller K, Wolosinski JH, van der Ploeg RR. 2004. Recurrent shoaling and channel dredging, Middle and Upper Mississippi River, USA. *Journal of Hydrology* **290**: 275–296.
- Reid I, Best JL, Frostick LE. 1989. Floods and flood sediments at river confluences. In *Floods: Hydrological, Sedimentological and Geomorphological Implications*, Beven K, Carling PA (eds). John Wiley & Sons: Chichester; 135–150.
- Rezaur RB, Jayawardena AW, Hossain MM. 1999. Factors affecting confluence scour. In *River Sedimentation: Theory and Applications*, Jayawardena AW, Lee JHW, Wang ZY (eds). Balkema: Rotterdam; 187–192.
- Rhoads BL. 1987. Changes in stream characteristics at tributary junctions. *Physical Geography* **8**: 346–361.
- Rhoads BL. 1996. Mean structure of transport-effective flows at an asymmetrical confluence when the main stream is dominant. In *Coherent Flow Structures in Open Channels*, Ashworth PJ, Bennett SJ, Best JL, McLelland SJ (eds). John Wiley & Sons: Chichester; 491–517.
- Rhoads BL. 2006. Scaling of confluence dynamics in river systems: Some general considerations. In *River, Coastal and Estuarine Morphodynamics 2005*, Parker G, García MH (eds). Taylor and Francis: London; 379–387.
- Rhoads BL, Kenworthy ST. 1995. Flow structure in asymmetrical stream confluence. *Geomorphology* **11**: 273–293.
- Rhoads BL, Sukhodolov AN. 2001. Field investigation of three-dimensional flow structure at stream confluences: 1. Thermal mixing and time-averaged velocities. *Water Resources Research* **37**: 2393–2410.
- Rhoads BL, Sukhodolov AN. 2004. Spatial and temporal structure of shear-layer turbulence at a stream confluence. *Water Resources Research* **40**: 1–13.
- Rice SP, Greenwood MT, Joyce CB. 2001. Tributaries, sediment sources and the longitudinal organisation of macroinvertebrate fauna along river systems. *Canadian Journal of Fisheries and Aquatic Sciences* **58**: 824–840.
- Richards KS. 1980. A note on change in geometry at tributary junctions. *Water Resources Research* **16**: 241–244.

- Roberts M. 2005. *Flow dynamics at open channel confluent-meander bends*, Unpublished Ph.D. thesis, University of Leeds, UK.
- Rodrigues S, Bréhéret JG, Macaire JJ, Moatar F, Nistoran D, Juge P. 2006. Flow and sediment dynamics in the vegetated secondary channels of an anabranching river: The Loire River (France). *Sedimentary Geology* **186**: 89–109.
- Roy AG, Bergeron N. 1990. Flow and particle paths at a natural river confluence with coarse bed material. *Geomorphology* **3**: 99–112.
- Roy AG, De Serres B. 1989. Morphologie du lit et dynamique des confluent de cours d'eau. *Bulletin de la Societe Geographique de Liege* **25**: 113–127.
- Roy NG, Sinha R. 2005. Alluvial geomorphology and confluence dynamics in the Gangetic plains, Farrukhabad–Kannauj area, Uttar Pradesh, India. *Current Science* **88**: 2000–2006.
- Roy AG, Roy R, Bergeron N. 1988. Hydraulic geometry and changes in flow velocity at a river confluence with coarse bed material. *Earth Surface Processes and Landforms* **13**: 583–598.
- Rudoy AN, Baker VR. 1993. Sedimentary effects of cataclysmic late Pleistocene glacial outburst flooding, Altay Mountains, Siberia. *Sedimentary Geology* **85**: 53–62.
- Salter T. 1993. Fluvial scour and incision; models for their influence on the development of realistic reservoir geometries. In *Characterization of Fluvial and Aeolian Reservoirs*, North CP, Prosser DJ (eds). The Geological Society of London, Special Publication **73**: 33–51.
- Sambrook Smith GH, Ashworth PJ, Best JL, Woodward J, Simpson CJ. 2005. The morphology and facies of sandy braided rivers: Some considerations of scale invariance. In *Fluvial Sedimentology: VII*. Blum MD, Marriott SB, Leclair SF (eds). Special Publication of the International Association of Sedimentologists **35**. Blackwells: London; 145–158.
- Sarker MH. 1996. *Morphological processes in the Jamuna River*. Unpublished M.Sc. thesis, International Institute for Hydraulic and Environmental Engineering, Delft.
- Siegenthaler C, Huggenberger P. 1993. Pleistocene Rhine gravel: Deposits of a braided river system with dominant pool preservation. In *Braided Rivers*, Best JL, Bristow CS (eds). Geological Society of London Special Publication **75**: 147–162.
- Sukhodolov AN, Rhoads BL. 2001. Field investigation of three-dimensional flow structure at stream confluences: 2. Turbulence. *Water Resources Research* **37**: 2411–2424.
- Szupiany RN, Amsler ML, Best JL, Parsons DR, Haydel R. (in review). The morphodynamics of two braid-bar confluences, Río Paraná, Argentina.
- Whittaker J, Teutsch G. 1999. Numerical simulation of subsurface characterization methods: Application to a natural aquifer analogue. *Advances Water Resources* **22**: 819–829.
- Wooldrige CL, Hickin EJ. 2005. Radar architecture and evolution of channel bars in wandering gravel-bed rivers: Fraser and Squamish rivers, British Columbia, Canada. *Journal Sedimentary Research* **75**: 844–860.

# 5

## Large river channel confluences

**Daniel R. Parsons<sup>1</sup>, James L. Best<sup>2</sup>, Stuart N. Lane<sup>3</sup>,  
Ray A. Kostaschuk<sup>4</sup>, Richard J. Hardy<sup>3</sup>, Oscar Orfeo<sup>5</sup>,  
Mario L. Amsler<sup>6</sup> and Ricardo N. Szupiany<sup>6</sup>**

<sup>1</sup>*School of Earth and Environment, University of Leeds, UK*

<sup>2</sup>*Departments of Geology and Geography and Ven Te Chow Hydrosystems Laboratory,  
University of Illinois at Urbana-Champaign, USA*

<sup>3</sup>*Department of Geography, Durham University, UK*

<sup>4</sup>*Department of Geography, University of Guelph, Canada*

<sup>5</sup>*Centro de Ecología Aplicada del Litoral (CECOAL), Consejo Nacional de Investigaciones  
Científicas y Técnicas (CONICET), Argentina*

<sup>6</sup>*Facultad de Ingeniería y Ciencias Hídricas, Universidad Nacional de Litoral en Santa Fe,  
Consejo Nacional de Investigaciones Científicas y Técnicas (CONICET), Argentina*

### Introduction

River channel confluences are a fundamental component of fluvial systems and are ubiquitous within both dendritic drainage networks and most channel planforms. Despite the clear importance of fully understanding the processes and dynamics of river channel confluences, our current understanding is based largely on laboratory experiments (e.g. Mosley, 1976; Best, 1988; Best and Roy, 1991) and on the observations, measurements and numerical modelling of small-scale natural junctions, which are often less than tens of metres wide (Rhoads and Kenworthy, 1998; Bradbrook *et al.*,

1998; Lane *et al.*, 2000; Rhoads and Sukhodolov, 2004). Although investigations of channel junctions have become increasingly sophisticated, allowing identification of some of the key variables that control confluence morphodynamics, this advance has largely focused on small-scale confluences. Until recently, there have been almost no detailed studies of flow, sediment transport and bed morphology at larger scales, and it is reasonable to question whether or not current conceptual models of confluence dynamics are valid for larger rivers (channels  $\sim > 100$  m wide). This question is significant as the junctions of smaller channels can be expected to differ considerably from the junctions of channels several orders of magnitude larger. For example, smaller channels are usually characterized by relatively low channel width–depth ratios, whilst larger channels are usually wider and shallower. Moreover, the junction of two larger channels may drain significantly different areas in terms of geology and climate, and can thus have a greater range of inflow conditions at the confluence as compared to smaller junctions, which more frequently drain areas with similar catchment characteristics. Understanding the influence of such scale effects on the process dynamics of large river confluences is vital since they adopt a pivotal role in controlling, and regulating, the passage of colossal volumes of water and sediment, and determine the delivery and timing of fluid and sediment discharge to downstream coastal zones and oceans. Such influences can thus have a wide range of impacts at both the regional and global scale.

Recent developments in technology, and in particular advances in global positioning systems and the advent of acoustic Doppler current profiling and multibeam echo sounding, have begun to facilitate investigations of large river morphodynamics (e.g. Richardson and Thorne, 2001; McLelland *et al.*, 1999; Ashworth *et al.*, 2000; Parsons *et al.*, 2004, 2005, 2007; Szupiany *et al.*, 2005; Lane *et al.*, in press). These new instruments enable the rapid and precise mapping of flow fields and bed morphology from such large channels, and the initial results from these investigations (e.g. McLelland *et al.*, 1999; Parsons *et al.*, 2007) question whether large-scale secondary flows are present at large river channel confluences and suggest that boundary-layer effects at higher width–depth ratios and the impacts of high form roughness might suppress the development of such flow structures.

This chapter will examine the influence of scale on junction morphodynamics and highlight the similarities and differences between large and small confluences. The flow structure present at larger river confluences will be compared with models developed for smaller junctions, allowing discussion and speculation on the influence of these processes on the dynamics of fluid mixing at large river channel confluences. This chapter presents details from relatively new material, as data on large-scale confluences are only now becoming available, and highlights some of the challenges that such new information is raising.

## Bed morphology

A detailed review of bed morphology at smaller channel confluences is presented by Best and Rhoads (this volume, Chapter 4) and only a brief summary of this previous work is presented herein to provide the context for the present chapter. Confluences are often dominated by junction scour (Ashmore and Parker, 1983; Best, 1986, 1988; Bristow *et al.*, 1993; Rhoads and Kenworthy, 1998; Bradbrook *et al.*, 2000; Rhoads and Sukhodolov, 2001; Best and Rhoads, this volume, Chapter 4), with scour depth often being between three and five times the depth of the confluent channels. A range of small-scale laboratory experiments have shown scour depth to increase at both higher junction angles and discharge ratios (the ratio of discharges from the two tributary channels) between the confluent channels (Mosley, 1976; Ashmore and Parker, 1983; Best, 1988). Bedload transport rates through the confluence are also found to have an influence on scour depth, with less scour being observed as sediment flux increases through the junction. Despite some variability in these relationships, significant trends between junction angle, momentum ratio (the ratio of flow momentum between the two tributary channels) and scour depth have also been reported from a range of small-scale field investigations (e.g. Ashmore and Parker, 1983; see Sambrook Smith *et al.*, 2005; Best and Rhoads, this volume, Chapter 4). The presence of avalanche faces associated with tributary-mouth bars that dip into the scour has also been identified as a common morphological feature in numerous confluence studies (e.g. Best, 1986; Best and Roy, 1991; Bristow *et al.*, 1993; Gaudet and Roy, 1995; McLelland *et al.*, 1996; De Serres *et al.*, 1999; Biron *et al.*, 2004). Such features can be produced by relatively deep central scour (McLelland *et al.*, 1996) or by bed discordance (Kennedy, 1984; Biron *et al.*, 1993), where one tributary channel enters the confluence at a higher elevation to the other, thus forming a negative step. The presence of such morphological steps within channel confluences has also been found to significantly alter the flow structure and hence overall confluence dynamics (Best and Roy, 1991; Gaudet and Roy, 1995; Biron *et al.*, 1996; DeSerres *et al.*, 1999; Bradbrook *et al.*, 2001), with less deep scours often found at these sites with a bed discordance.

Downstream of the junction, as the flow recovers and shallows out of the scour hole, barforms often develop. The scale and location of these bars vary as a function of both planform geometry and discharge (momentum) ratio (Best, 1986; Bristow *et al.*, 1993). At symmetrical, roughly equal discharge channels, mid-channel bars often form in the centre of the post-confluence channel (Ashworth, 1996). However, below the downstream junction corner of asymmetrical junctions, bars often develop that are primarily produced by flow deceleration and flow separation as the tributary channel turns into the downstream channel alignment (Best and Reid, 1984; Rhoads and Kenworthy, 1995; Best and Rhoads, this volume, Chapter 4).

The influence of channel scale on these general features of confluence bed morphology and their controlling variables is not fully understood. Best and Ashworth (1997) present morphological data from one of the largest river confluences in the world, that of the Jamuna and Ganges rivers in Bangladesh (Figure 5.1), which indicate several features of bed morphology that are similar to smaller junctions: a central scour, the edges of mouth bars that dip into the scour and an accumulation of sediment below the downstream junction corner. Best and Ashworth (1997) present data from five bathymetric surveys taken at different times that show scour depth approaches 30 m at the junction, which equates to five times the mean depth of the confluent channels. A plot of scour-depth data from several junctions within the braided Jamuna River (Figure 5.2) also displays a similar range of relative scour depths (often around three times channel depth). A comparison of these dimensionless scour depths with data from smaller confluence sites ( $< 100$  m width) and previous laboratory investigations (see Sambrook Smith *et al.*, 2005, Best and Rhoads, this volume, Chapter 4) suggests some scale invariance in junction morphology, with scour depths typically ranging from two to four times the incoming tributary channel depths. However, despite the large scour depths, steep (angle-of-repose) avalanche faces were not found in the surveys reported by Best and Ashworth (1997), and the slopes of the bed dipping into the scour hole at the junction of the Jamuna–Ganges were typically less than  $5^\circ$  (Figures 5.1 and 5.3). Indeed, the depositional slopes of these tributary-mouth bars at the Jamuna–Ganges confluence are often  $2\text{--}3^\circ$ , with smaller dunes migrating down their faces (Figure 5.3), demonstrating the lack of large-scale sediment avalanching on these bar fronts. This is in marked contrast to data reported for smaller confluences, where avalanche faces typically approach the angle-of-repose (e.g. Best, 1988; McLelland *et al.*, 1996). Hence, although the relative scour depths at these larger confluences may be similar to smaller junctions, the morphology of the avalanche faces is not. This is significant as it points to the role of the junction flow dynamics, and specifically flow acceleration and shear-layer dynamics, in generating the scour, rather than flow over a steep morphological step or tributary-mouth bar front.

Other research (Parsons *et al.*, 2007; Szupiany *et al.*, 2007, submitted) has also identified similar scours at braid bar confluences on the Río Paraná, Argentina. The relative scour depths recorded at these relatively low-angle junctions (Figure 5.4) again fall within the range identified from laboratory investigations and smaller-scale confluences. In these junctions on the Río Paraná (Figure 5.4; Szupiany *et al.*, 2007), the scour depth is approximately two to three times the pre-confluence average channel depth, with scour depth reaching over 22 m at confluence B (Figure 5.4) and extending approximately 1000 m in length. At confluence A (Figure 5.4), although the central scour is not as well defined, there is a noteworthy discordance in the bed height between the confluent channels, with the true left channel being shallower ( $\sim 7$  m) than the true right channel ( $\sim 12$  m). However, once again and similar to the Jamuna–Ganges junction, the slopes dipping into the scours are very low-angle, being less than  $6^\circ$ .

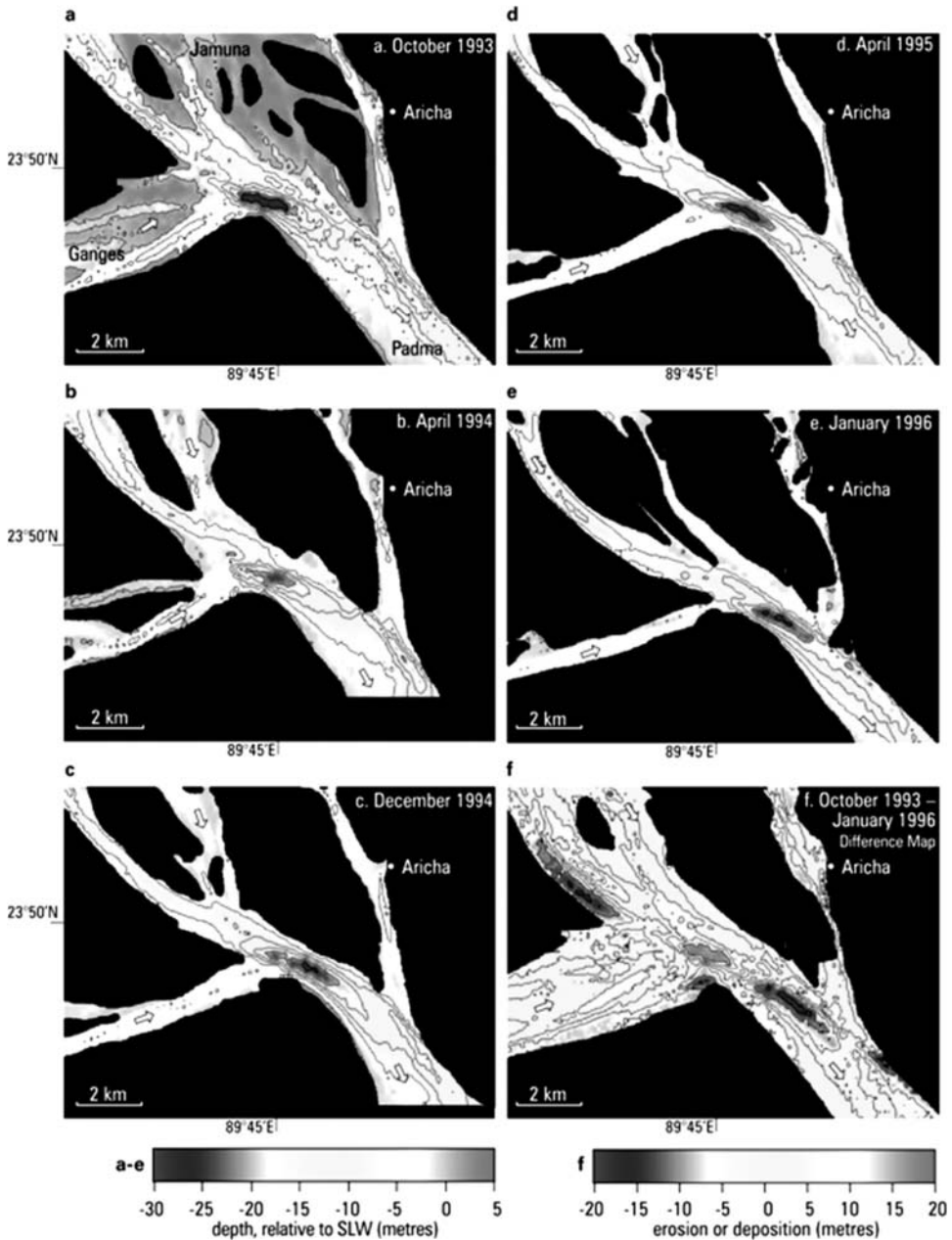


**Figure 5.1** Bed morphology at the confluence of the Jamuna and Ganges rivers, Bangladesh. Plots show morphology of confluence at various times (a–e) and a difference map of bed elevation (f). Reproduced from *Nature*, **387**: 275–277 (1997). A colour reproduction of this figure can be seen in the colour section towards the centre of the book.

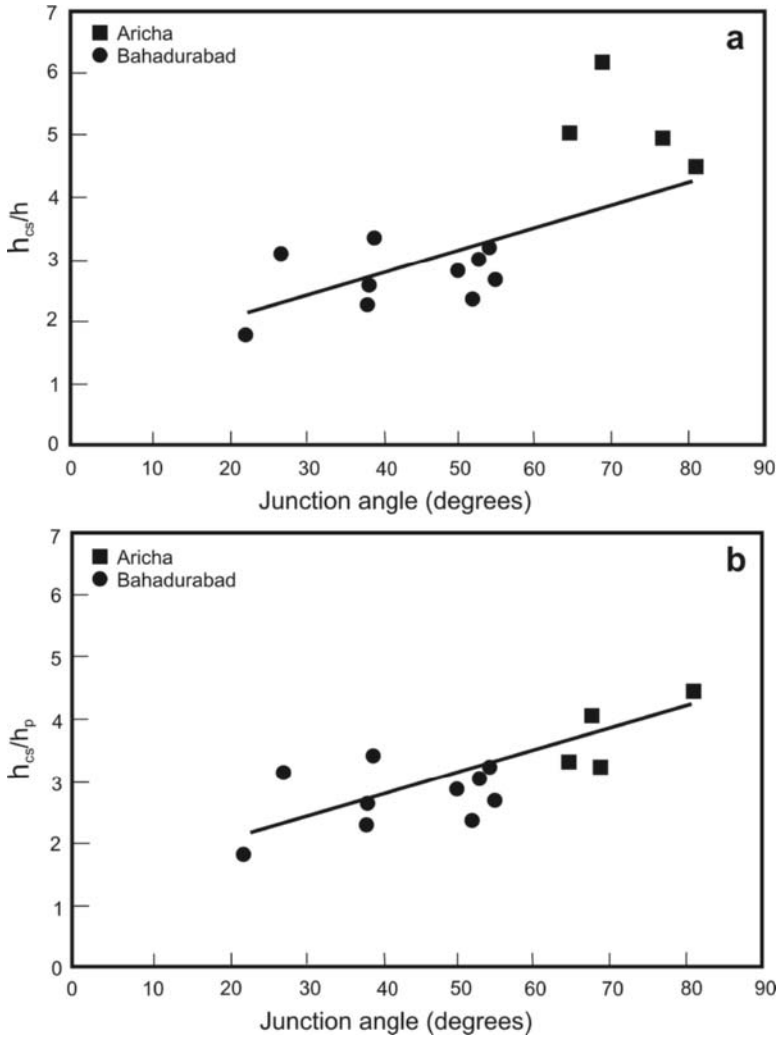


**Figure 5.2** Plots of dimensionless confluence scour depth from the braided Jamuna River, Bangladesh. From Sarker (1996) and Best *et al.* (2007).

These results thus suggest that steep avalanche faces may be rare features in these larger river channels, even though appreciable scour depths are not.

The plots of bed morphology presented in Figures 5.1 and 5.4 show that accumulations of sediment exist as bars in the post-confluence channel at all these sites. The formation of such bars in the downstream channel, and in particular at the downstream junction corner, mirror similar morphologies found in smaller junctions (see Best and Rhoads, this volume, Chapter 4) and point to possible similarities in sediment routing

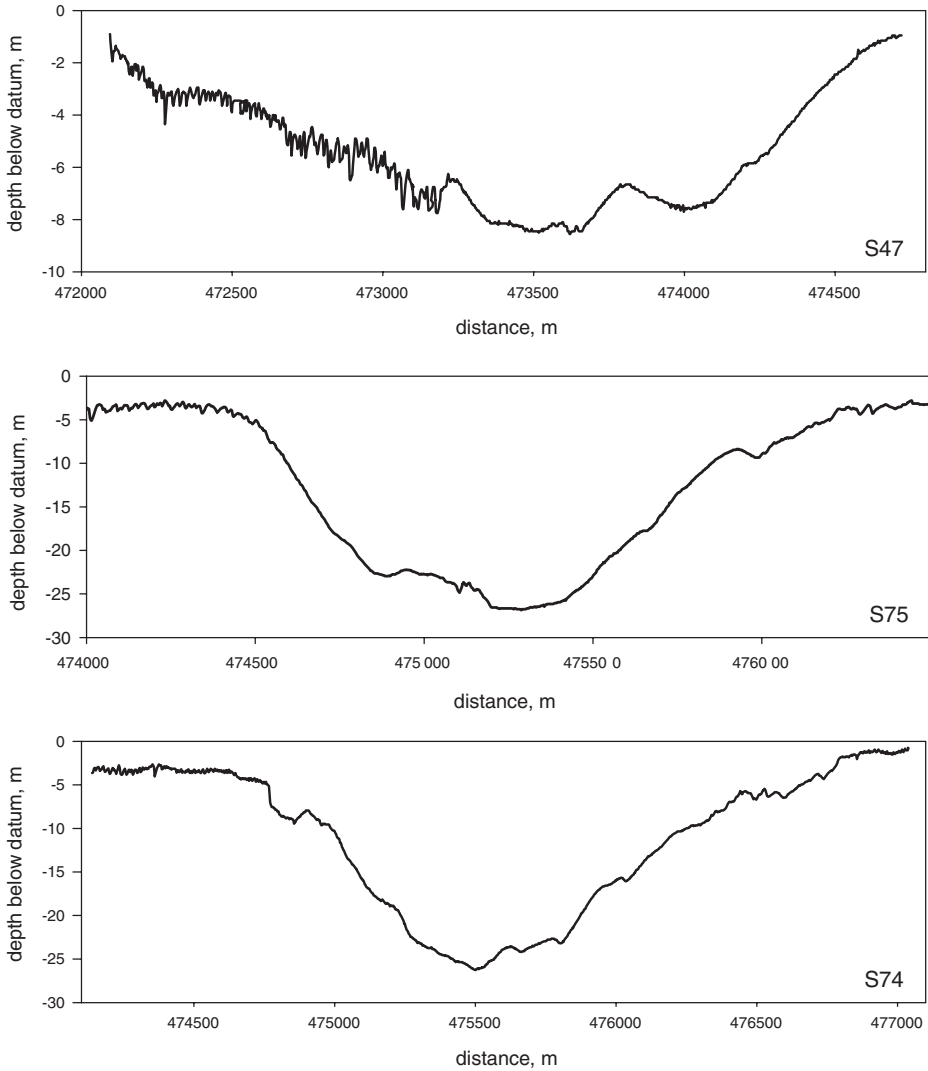


**Figure 5.3** Bed morphology at three cross-sections across the scour at the Jamuna–Ganges confluence (see Figure 5.1), illustrating the low angle of the slopes that dip into the scour and the superimposition of dunes upon those slopes.

at such sites. Finally, the presence of dune and bar forms in large sand-bed rivers may have a significant impact on flow and morphodynamics. For example, Figure 5.3 indicates the prevalence of dune forms migrating down the tributary-mouth bar face into the confluence scour, and these may have some role in modifying the flow structure, as speculated by Parsons *et al.* (2007), who highlight the role of form roughness in suppressing channel-scale secondary flows.

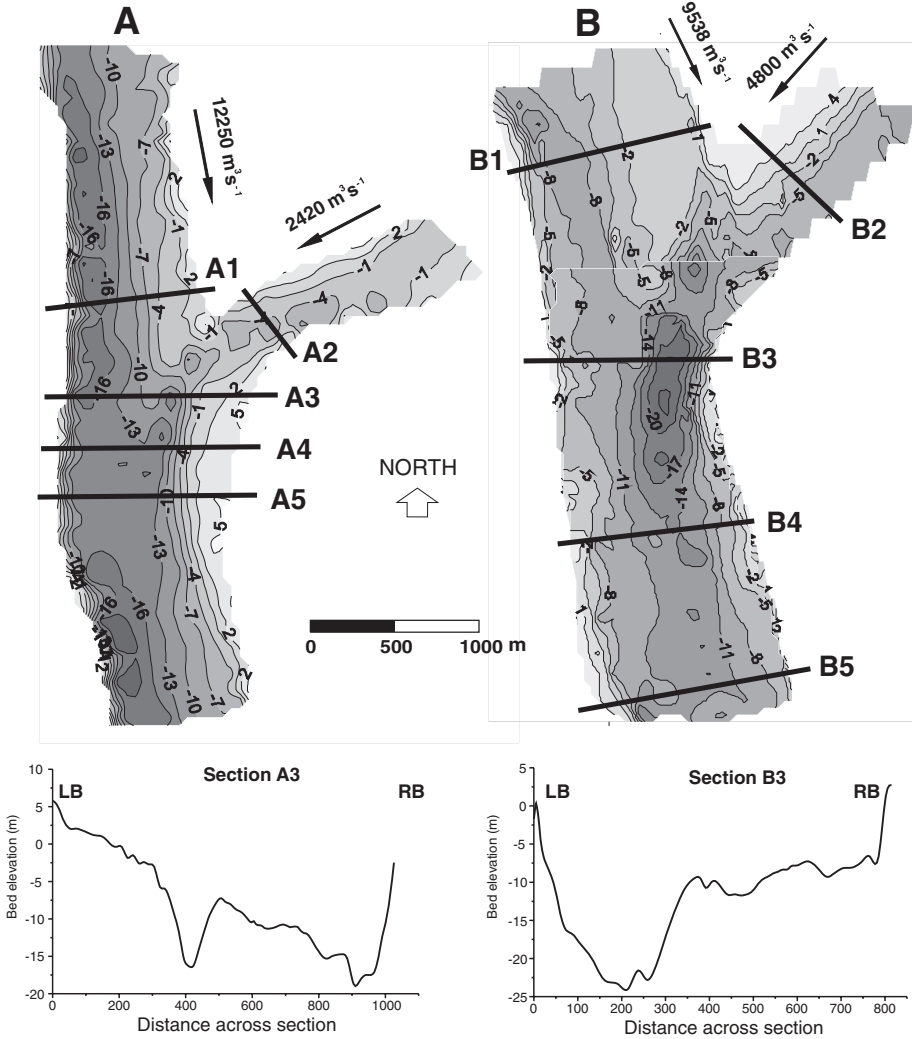


**Figure 5.4** Bed morphology of two braid bar confluences in the Río Paraná, Argentina (depths refer to the 0-m level in the Rosario Port gage in Argentina). Survey dates: 13/06/06 (A) and 07/06/06 (B). Reproduced from proceedings of the 5th International Conference on River, Coastal and Estuarine Morphodynamics, Twente, The Netherlands (2007).

### Flow structure at large river channel confluences

Research during the last quarter of the twentieth and the beginning of the twenty-first century has contributed greatly to our identification and understanding of the characteristic flow structures commonly found in confluences. Much of this work is summarized by Biron and Lane (this volume, Chapter 3). Key flow features reported

from past work include: (1) a region of stagnated, super-elevated flow at the upstream junction corner, (2) a shear or mixing layer between the two flows, (3) a zone of flow acceleration as the flows combine within the junction, (4) a region of separated flow below the downstream junction corner, (5) the possible presence of twin back-to-back helical flow cells that converge at the water surface over the region of maximum scour depth and diverge at the bed back towards the channel banks and (6) a region of flow recovery downstream from the confluence where the flows mix. The distance over which this mixing takes place in large rivers may appear, at first, to be very long. For instance, the distance required for complete mixing may be greater than 400 km at the junction of the Río Paraguay and Río Paraná, and upwards of 200 km in many other larger river channels (see Table 1 from Lane *et al.*, in press). Lane *et al.* (in press) show from semi-theoretical analysis that such long distances should be expected in the absence of the significant near-field mixing often observed in smaller junctions, and can be extremely rapid in cases with bed discordance (e.g. Gaudet and Roy, 1995). Below, we examine which aspects of this broad fluid dynamic pattern have been detected at the confluences of large channels and discuss the apparent differences in process dynamics between small- and large-river confluences.

## Flow acceleration

Fluid acceleration, as tributary flows combine at a confluence and pass into the downstream channel, is perhaps the most common feature of junction-flow dynamics (e.g. Roy *et al.*, 1988). Acceleration is produced by the reduction in cross-sectional area that often occurs (despite the presence of scour) and is linked to both non-linear changes in downstream hydraulic geometry, where width tends to increase more quickly than depth, and the local influence of the confluence bed morphology, particularly the development of junction bars. Research has identified flow acceleration in the very largest confluences in the world. Both Parsons *et al.* (2007) and Szupiany *et al.* (2007) identify the acceleration of flow at braid bar confluences on the Río Paraná. Figure 5.5 shows the post-confluence fluid acceleration from the data of Szupiany *et al.* (2007) from the Río Paraná, where accelerations of over 30 per cent are present in the downstream channel. Flow acceleration is thought to be one of the key drivers in the formation of scour at junctions and is likely to be of particular importance in large confluences given that the tributary-mouth bar faces appear to be significantly lower-angle or absent, suggesting that flow separation over these barforms may not be influential or even present. Although data are still limited, such flow acceleration appears to be a ubiquitous feature of confluence dynamics. However, Szupiany *et al.* (2007) do identify a possible significant difference with channel scale and suggest that, as the width–depth ratio of the confluent channels increases, then the distribution of the velocity across the tributary inflow may have a greater potential for variability as compared with smaller channels, particularly in the presence of larger bar forms. Such cross-sectional spatial variability

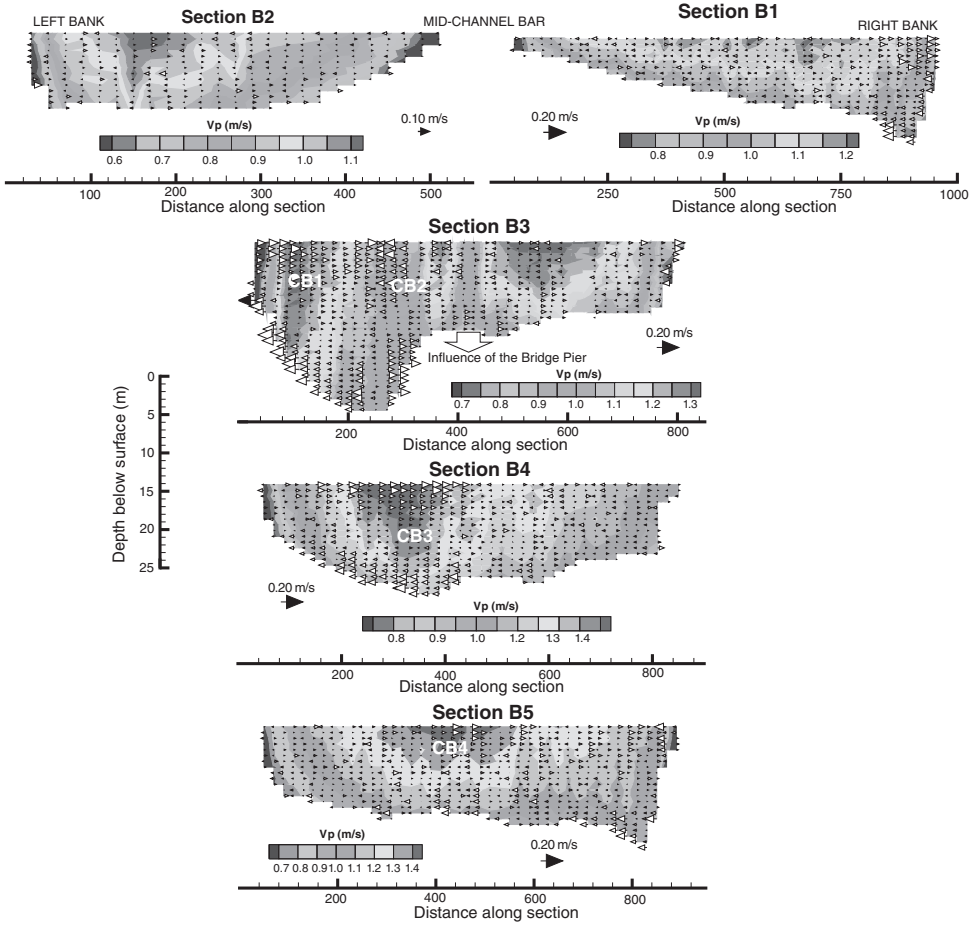


**Figure 5.5** Primary and secondary flow velocity fields at sections through a braid bar confluence on the Río Paraná (Confluence B in Figure 5.4). Reproduced from proceedings of the 5th International Conference on River, Coastal and Estuarine Morphodynamics, Twente, The Netherlands (2007). A colour reproduction of this figure can be seen in the colour section towards the centre of the book.

can be expected to alter the local momentum ratios as the channels combine, and thus influence flow acceleration and resultant scour within the junction. For example, at the Confluence B site of Szupiany *et al.* (2007), two areas of distinct flow acceleration and scour are present in the confluence (Figure 5.5). It can thus be speculated that such cross-sectional variability could have a significant and increasing control on the dynamics of larger confluences, particularly at lower flow stages where stronger topographic forcing may result in more variable flow fields through the section. This effect would significantly alter the dynamics of the combining flows, resulting in the generation of more complex patterns of flow at the confluence.

## Secondary flow

Flow through channel confluences is characterized not only by a general flow acceleration but also, in many cases, by two streamwise, counter-rotating helical flow cells (Mosley, 1976; Ashmore *et al.*, 1992; Rhoads and Kenworthy, 1995) that are convergent at the surface, downwell over the centre of the channel (scour region), diverge at the bed and upwell at the channel boundaries. Such secondary flow cells have been identified in a number of field cases, particularly where the tributary channels are concordant at their confluence (e.g. Ashmore *et al.*, 1992; Rhoads and Kenworthy, 1995, 1998; Rhoads and Sukhodolov, 2001), and have often been found to occupy the entire width of the channel. Such channel-scale flow features have also been identified in confluences with significant bed discordance, where the shear generated at the mixing interface occupies a large portion of the central channel and generates upwelling within the deeper channel near the downstream junction corner (e.g. De Serres *et al.*, 1999).

Although previous investigations of secondary flows in large rivers indicated that they can occupy large portions of the channel width (Richardson *et al.*, 1996), later research (Parsons *et al.*, 2007; Szupiany *et al.*, 2007), has questioned the validity of a scale invariant model for secondary flows at confluences. Indeed, Parsons *et al.* (2007) report results from a confluence–diffluence unit on the Río Paraná and found no evidence of the classic back-to-back helical circulation. Similarly, Parsons *et al.* (2007) also found no clear impact of the slight bed discordance ( $\sim 4$  m depth differential) at their field site upon the generation of secondary flows within the confluence. Szupiany *et al.* (2007), reporting on two braid bar confluences further downstream on the Río Paraná, did identify counter-rotating, surface-convergent, helical flow cells in their measurements (Figure 5.5). However, the spatial extent of these secondary cells was limited to only small proportions of the total channel width ( $<25$  per cent), compared with cells that often occupy over 80 per cent of the width in smaller confluences (e.g. Rhoads and Kenworthy, 1998). This again highlights the potential importance of the spatial non-uniformity of flow within a cross-section as the scale of the channels increases, and suggests that both flow acceleration and the presence of helical secondary flow cells at large junctions might be different from that which has been observed at small confluences.

The absence, or limited spatial extent, of helical circulation cells at large confluences is interesting. In the cases described above, the confluent channels are curved with flow convergence through the confluence zone, and it may be expected that the flow direction at the surface would differ from that at the bed. However, the fact that there is a near-uniform flow direction throughout the flow depth (Parsons *et al.*, 2007, their Figure 4) suggests that the steering of flow at the bed is readily transmitted throughout the entire flow depth, preventing channel-scale differences between near-bed and near-surface flow directions as found at smaller river confluences. Parsons *et al.* (2007) suggest that in the wide, relatively shallow, flows typical of larger river channels (Nezu and Nakagawa, 1993; Yalin, 1992) form roughness may assist this process, whereby

near-bed local steering of flow over bedforms is transmitted throughout the flow depth, thereby negating or lessening the production of channel-scale secondary flows. Szupiany *et al.* (2007) present data showing that cross-sectional variations in the incoming flows might also play an increased local role in the dynamics of confluences as channel scale increases, resulting in a localization of coherent secondary flows into smaller portions of the channel width. Such localization may also be reflected in local levels of water surface superelevation and pressure gradients across a section at large confluences, as it is unlikely that superelevation produced by curvature will scale with river width and be consistent across wider channels, but these variations might exist at the sub-section scale.

The influence of bed height discordance on the generation of any helical flow cells may also tend to diminish with increasing channel scale. As highlighted above, avalanche faces and morphological steps due to bed discordance are typically very low-angle in larger channels, preventing the formation of permanent flow separation that is often found over this morphological step at smaller confluences. Therefore, secondary flows generated through this mechanism (e.g. Best, 1987, 1988; McLelland *et al.*, 1996), and the three-dimensional distortion of the shear layer interface often caused by discordance (Best and Roy, 1991), may be significantly less likely to occur in larger channel confluences.

## Shear-layer dynamics

The development of shear at the interface of the combining flows can generate substantial levels of turbulence and may be a significant influence on confluence scour (Best, 1987) and mixing rates. Biron *et al.* (1993), Sukhodolov and Rhoads (2001) and Rhoads and Sukhodolov (2004) identify a number of scales of variability in velocity signals from within confluence shear zones: (i) longer-term fluctuations, possibly related to backwater effects, flow within the stagnation zone at the upper junction corner and larger-scale shifts in the shear-layer position, (ii) large-scale Kelvin–Helmholtz vortices generated by a velocity differential across the shear layer, and (iii) shorter period events nested within the larger structures. Bed discordance also appears to influence the form and nature of the shear layer between the two flows. For example, in the concordant bed junction examined by Rhoads and Sukhodolov (2004), the larger coherent flow structures they identify are quasi two-dimensional with little vertical motion. In contrast, Biron *et al.* (1993) and De Serres *et al.* (1999) identify significant vertical upwelling and three-dimensional turbulence generation in a junction with appreciable bed discordance, where flow over the discordant step interacted with the shear layer to produce large zones of upwelling near the downstream junction corner.

There is currently a paucity of data concerning the dynamics of shear layers at large confluences. Lane *et al.* (in press) identify, using at-a-point three-dimensional velocity

surveys, turbulent shear associated with a near-vertical shear layer at the confluence of the Río Paraná and Río Paraguay, Argentina. However, they note that this zone of turbulent shear was restricted to very close to the junction ( $<0.3$  post-confluence widths downstream). Lane *et al.* (in press) discuss how turbulence along the shear layer at the Paraná–Paraguay junction was manifested in the formation of three-dimensional instabilities that are associated with the intermittent upwelling of turbid Paraguay water into the clearer Paraná water. However, these features were not to be sustained for a great distance downstream and the flow became largely two-dimensional in less than  $\sim 0.3$  multiples of the post-confluence width downstream (Lane *et al.*, in press, their Figure 3). This resulted in a very rapid reduction in the lateral mixing between the two flows in only a short distance downstream from the confluence, with a significant reduction in shear and shear-layer expansion.

Given that large-scale bed discordance and significant morphological steps seem to be lower in magnitude at higher width–depth ratios ( $>100$ ), the possible distortion of the mixing-layer interface often found in small junctions may be less likely to form. The corollary of this speculation is twofold: first, the junction scour is likely to be concentrated along the vertical axis of the shear layer and, secondly, mixing rates at larger junctions are likely to be less rapid, as discussed in the following section.

## Flow mixing at large river confluences

Research on small channel junctions in the field and in the laboratory has shown that the three primary flow mechanisms that contribute to mixing at river confluences are: (i) shear between the confluent flows, (ii) helical motions associated with streamline curvature and (iii) the influence of bed discordance between the two confluent channels, which can drive the upwelling of fluid from one channel into the waters of the other confluent channel. Shear-generated vortices may lead to substantial lateral transfers of fluid between the two combining flows, although field observations in small channels suggest that this only results in mixing as long as the shear between the two flows is maintained (e.g. Sukhodolov and Rhoads, 2001; Rhoads and Sukhodolov, 2001). Channel-scale secondary circulation results in substantial flow mixing if the circulation is strong and may transform into a single, channel-scale, helical cell (e.g. Bradbrook *et al.*, 2000; Rhoads and Sukhodolov, 2001). Finally, the upwelling of water at discordant-bed junctions has been shown to reduce the downstream distance required for complete mixing, from approximately 100 multiples of the channel width ( $W$ ) to as little as 10 to 25  $W$  in small rivers (Gaudet and Roy, 1995).

Field measurements and remotely-sensed data show that the complete mixing of flows where two large rivers join commonly requires a significant river length (Mackay, 1970; Krouse and Mackay, 1971; Stallard, 1987), which can often extend to tens or even hundreds of kilometres. Fischer *et al.* (1979), applying a semi-theoretical analysis,

suggest that mixing distances should increase significantly in very large rivers because the rate of transverse diffusion is a function of the square of channel width. Moreover, as discussed above, channel-scale secondary flows are often absent (Parsons *et al.*, 2007) or restricted (Szupiany *et al.*, 2007) in larger channels, thus preventing the channel-scale overturning and mixing of flows. Furthermore, significant morphological steps or avalanche faces at larger confluences are also absent, and thus mixing driven by channel-scale shear-layer distortion may also be absent or weak. The absence of these factors should mean that mixing lengths downstream of confluences should retain a strong dependence on the square of channel width, and so be expected to be very long in large rivers.

Lane *et al.* (in press) present information on mixing processes from the Río Paraná–Paraguay confluence (Figure 5.6). Semi-theoretical analysis suggested that the mixing length should be greater than 400 km, and they documented one time period when this was the case. However, Lane *et al.* (in press) also obtained measurements on an occasion when the mixing length was only 8 km. For the slower mixing case, as mentioned above, three-dimensional flow structures were identified along the mixing interface, resulting in local mixing close to the upstream junction corner, well within one channel width downstream. However, after this distance, shear was minimal and the flows mixed very



**Figure 5.6** Oblique aerial photograph of the junction of the Río Paraná and Río Paraguay. Note the contrast produced by the higher suspended sediment concentrations of the Río Paraguay and the vorticity present along the mixing interface. A colour reproduction of this figure can be seen in the colour section towards the centre of the book.

slowly. Lane *et al.* (in press) found no channel-scale secondary flow in the slow mixing case and suggest that this, combined with reverse topographic forcing on the mainstream Río Paraná side of the river, effectively prevented substantial mixing at the confluence zone.

For the case of rapid mixing, Lane *et al.* (in press) identified significant channel-scale flow circulation, which was associated with penetration of the more turbid Río Paraguay water further across the channel width at depth, leading to much more rapid mixing. Research conducted in 1998, performed at the junction of the Negro and Solimões rivers in Brazil, also identified rapid mixing, complete within 25 km of the junction (Maurice-Bourgoin *et al.*, 2003), and thus in around six channel widths. The results presented by Lane *et al.* (in press) caution against the possibility of turbulence-driven mixing playing a significant role in very wide channels and instead highlight the importance of the interaction between the momentum ratio of the confluent channels and the channel-bed morphology in producing channel-scale circulation. Lane *et al.* (in press) suggest that mixing between two large rivers may be critically dependent upon the time-varying, basin-scale, hydrological response, and highlight that a differential hydrological response from each tributary is more likely as the scale of the confluent channels increases due to the different climatic zones each river may capture. Finally, because large rivers have a greater probability of draining different geological terrains, the potential for significant differences in suspended sediment concentrations between confluent channels increases. The influence that such density differences could have on confluence flow and mixing dynamics is currently unknown, although their role in enhancing shear-layer distortion may act to increase mixing rates at such sites. Further research is clearly required in this area of confluence-mixing dynamics in order to explore the variability of these mechanisms and identify the dominant controls at different spatio-temporal scales.

## Conclusions

Although river channel confluences are key nodes within fluvial systems, our knowledge and understanding is skewed significantly to investigations based upon small river channels and laboratory models. These small channels usually have small width–depth ratios. This is significant as a large number of variables do not scale linearly and in proportion to the observed processes occurring at these sites, and we therefore currently have a limited ability to assess the extent to which small-scale studies can be extrapolated to larger junctions.

This chapter has briefly reviewed the current state of knowledge with respect to the influence of scale on confluence morphodynamics and has highlighted some significant similarities and differences between small and large confluences (> 100 m wide). Significantly, large channel confluences appear to have a similar overall bed morphology to junctions several orders of magnitude smaller, with the presence of prominent scour

holes being the most distinctive feature. However, the morphological step and tributary-mouth bar face, which creates any bed discordance, have generally a low angle in large junctions and thus may have a far more limited impact on flow than within smaller junctions. Moreover, recent research has highlighted that channel-scale secondary flows can be absent or restricted to small spatial areas of channel cross-sections at large river junctions. The absence of such helical flows may be attributable to: (1) the fact that the rate of increase in channel width is greater than depth as river scale is increased, leading to relatively low depths for the channel widths being considered, (2) the role of form roughness, which effectively suppresses the development of such channel-scale flow structures, (3) the lesser importance of secondary flows driven by gradients in water-surface elevation at larger junctions and (4) the increased likelihood of spatial differences in bed morphology (bars and dunes), and thus the topographic forcing of flow fields, within large junctions. These significant differences have major impacts on confluence morphodynamics.

Despite the progress highlighted above, there remains a significant paucity of data on large river confluences. However, we are now far better equipped to measure and monitor large rivers than ever before. Future work clearly calls for quantification of bed morphology, flow and sediment transport at a wider range of confluence morphologies, and for this to be allied with developments in numerical modelling. Such an approach will yield a methodology for addressing a range of controls on confluence morphodynamics and how these vary with channel scale and at what scales such changes are manifest.

## Acknowledgements

DP, JLB and SNL are grateful to the UK Natural Environment Research Council for funding through various grants to research large channel confluences, including NER/A/S/2001/00445 and NER/B/S/2003/00243, and the Royal Society of London for a Joint International Project. DP also thanks NERC for his Fellowship funding in grant NE/C002636/1. RNS thanks the Earth and Biosphere Institute at the University of Leeds for funding a three-month research fellowship, which facilitated the data analysis that formed part of this paper. Finally, MLA and RNS thank to the Universidad Nacional del Litoral for funding the measurements performed in the Paraná River near Rosario city.

## References

- Ashmore P, Parker G. 1983. Confluence scour in coarse braided streams. *Water Resources Research* **19**: 392–402.
- Ashmore PE, Ferguson RI, Prestegard KL, Ashworth PJ, Paola C. 1992. Secondary flow in anabranch confluences of a braided, gravel-bed stream. *Earth Surface Processes and Landforms* **17**: 299–311.

- Ashworth PE, Best JL, Roden J, Bristow C, Klaassen G. 2000. Morphological evolution and dynamics of a large, sand braid-bar, Jamuna River, Bangladesh. *Sedimentology* **47**: 533–555.
- Ashworth PJ. 1996. Mid-channel bar growth and its relationship to local flow strength and direction. *Earth Surface Processes and Landforms* **21**: 103–123.
- Best JL. 1986. The morphology of river channel confluences. *Progress in Physical Geography* **10**: 157–174.
- Best JL. 1987. Flow dynamics at river channel confluences: Implications for sediment transport and bed morphology. In *Recent Developments in Fluvial Sedimentology*, Etheridge FG, Flores RM, Harvey MD (eds). Society of Economic Paleontologists and Mineralogists Special Publication 39, SEPM: Tulsa; 27–35.
- Best JL. 1988. Sediment transport and bed morphology at river channel confluences. *Sedimentology* **35**: 481–498.
- Best JL, Ashworth P. 1997. Scour in large braided rivers and the recognition of sequence stratigraphic boundaries. *Nature* **387**: 275–277.
- Best JL, Reid I. 1984. Separation zone at open-channel junctions. *Journal of Hydraulic Engineering* **110**: 1588–1594.
- Best JL, Roy AG. 1991. Mixing-layer distortion at the confluence of channels of different depth. *Nature* **350**: 411–413.
- Best J, Ashworth P, Sarker MH, Roden R. 2007. The Brahmaputra-Jamuna River, Bangladesh. In *Large Rivers: Geomorphology and Management*, Gupta A (ed.). John Wiley & Sons: Chichester; 395–433.
- Biron P, Roy AG, Best JL, Boyer CJ. 1993. Bed Morphology and Sedimentology at the Confluence of Unequal Depth Channels. *Geomorphology* **8**: 115–129.
- Biron P, Best JL, Roy AG. 1996. Effects of bed discordance on flow dynamics at open channel confluences. *Journal of Hydraulic Engineering* **122**: 676–682.
- Biron PM, Ramamurthy AS, Han S. 2004. Three-dimensional numerical modeling of mixing at river confluences. *Journal of Hydraulic Engineering* **130**: 243–253.
- Bradbrook KF, Biron PM, Lane SN, Richards KS, Roy AG. 1998. Investigation of controls on secondary circulation in a simple confluence geometry using a three-dimensional numerical model. *Hydrological Processes* **12**: 1371–1396.
- Bradbrook KF, Lane SN, Richards KS. 2000. Numerical simulation of three-dimensional, time-averaged flow structure at river channel confluences. *Water Resources Research* **36**: 2731–2746.
- Bradbrook KF, Lane SN, Richards KS, Biron PM, Roy AG. 2001. Role of bed discordance at asymmetrical river confluences. *Journal of Hydraulic Engineering* **127**: 351–368.
- Bristow CS, Best JL, Roy AG. 1993. Morphology and facies models of channel confluences. In *Alluvial Sedimentation*, Marzo M, Puigdefabregas C (eds). International Association of Sedimentologists Special Publication 17; 91–100.
- De Serres B, Roy AG, Biron PM, Best JL. 1999. Three-dimensional structure of flow at a confluence of river channels with discordant beds. *Geomorphology* **26**: 313–335.
- Fischer HB, List EJ, Koh RCY, Imberger J, Brooks NH. 1979. *Mixing in inland and coastal waters*. Academic Press: New York.
- Gaudet JM, Roy AG. 1995. Effect of Bed Morphology on Flow Mixing Length at River Confluences. *Nature* **373**: 138–139.
- Kennedy BA. 1984. On Playfair's law of accordant junctions. *Earth Surface Processes and Landforms* **9**: 153–173.

- Krouse HR, Mackay JR. 1971. Application of H<sub>2</sub>O-18/H<sub>2</sub>O-16 abundances to problem of lateral mixing in Liard–Mackenzie river system. *Canadian Journal of Earth Sciences* **8**: 1107–14.
- Lane SN, Bradbrook KF, Richards KS, Biron PM, Roy AG. 2000. Secondary circulation cells in river channel confluences: Measurement artefacts or coherent flow structures? *Hydrological Processes* **14**: 2047–2071.
- Lane SN, Parsons DR, Best JL, Orfeo O, Kostachuk R, Hardy RJ. In press. Why can large rivers take so long to mix downstream of tributary inflows? *Journal of Geophysical Research – Earth Surface*.
- Mackay JR. 1970. Lateral mixing of the Liard and Mackenzie rivers downstream from their confluence. *Canadian Journal of Earth Sciences* **7**: 11–124.
- Maurice-Bourgoin L, Quémenerais B, Moreira-Turcq P, Seyler P. 2003. Transport, distribution and speciation of mercury in the Amazon River at the confluence of black and white waters of the Negro and Solimões Rivers. *Hydrological Processes* **17**: 1405–1417.
- McLelland SJ, Ashworth PJ, Best JL. 1996. The origin and downstream development of coherent flow structures at channel junctions. In *Coherent Flow Structures in Open Channels*, Ashworth PJ, Bennett SJ, Best JL, McLelland SJ (eds). John Wiley & Sons: Chichester; 459–491.
- McLelland SJ, Ashworth PJ, Best JL. 1999. Flow structure and transport of sand-grade suspended sediment around an evolving braid bar, Jamuna River, Bangladesh. In *Fluvial Sedimentology VI*, Smith ND, Rogers J. (eds). International Association of Sedimentologists Special Publication 28. Blackwell: Oxford; 43–57.
- Mosley MP. 1976. An experimental study of channel confluences. *Journal of Geology* **84**: 535–562.
- Nezu I, Nakagawa H. 1993. *Turbulence in Open-Channel Flows*. Balkema: Rotterdam.
- Parsons DR, Best JL, Lane SN, Hardy RJ, Orfeo O, Kostaschuk R. 2004. The Morphology, 3D flow structure and sediment dynamics of a large river confluence: The Río Paraná and Río Paraguay, NE Argentina. In *River Flow 2004*, Greco M, Carravetta A, Della Morte R (eds). Proceedings of the Second International Conference on Fluvial Hydraulics, Napoli, Italy, Volume 1. Balkema: Leiden, The Netherlands.
- Parsons DR, Best JL, Orfeo O, Hardy RJ, Kostaschuk R, Lane SN. 2005. Morphology and flow fields of three-dimensional dunes, Río Paraná, Argentina: Results from simultaneous multibeam echo sounding and acoustic Doppler current profiling. *Journal of Geophysical Research* **110**: F04S03. DOI: 10.1029/2004JF000231.
- Parsons DR, Best JL, Lane SN, Orfeo O, Hardy RJ, Kostaschuk R. 2007. Form roughness and the absence of secondary flow in a large confluence–diffuence, Río Paraná, Argentina. *Earth Surface Processes and Landforms* **32**: 155–162.
- Rhoads BL, Kenworthy ST. 1995. Flow structure at an asymmetrical stream confluence. *Geomorphology* **11**: 273–293.
- Rhoads BL, Kenworthy ST. 1998. Time-averaged flow structure in the central region of a stream confluence. *Earth Surface Processes and Landforms* **23**: 171–191.
- Rhoads BL, Sukhodolov AN. 2001. Field investigation of three-dimensional flow structure at stream confluences: 1. Thermal mixing and time-averaged velocities. *Water Resources Research* **37**: 2393–2410.
- Rhoads BL, Sukhodolov AN. 2004. Spatial and temporal structure of shear layer turbulence at a stream confluence. *Water Resources Research* **40**: W06304. DOI: 10.1029/2003WR002811.
- Richardson WR, Thorne CR. 2001. Multiple thread flow and channel bifurcation in a braided river: Brahmaputra–Jamuna River, Bangladesh. *Geomorphology* **38**: 185–196.
- Richardson WRR, Thorne CR, Mahmood S. 1996. Secondary flow and channel changes around a bar in the Brahmaputra River, Bangladesh. In *Coherent Flow Structures in Open*

- Channels*, Ashworth PJ, Bennett SJ, Best JL, McLelland SJ (eds). John Wiley & Sons: Chichester; 459–490.
- Roy AG, Roy R, Bergeron N. 1988. Hydraulic geometry and changes in flow velocity at a river confluence with coarse bed material. *Earth Surface Processes and Landforms* **13**: 583–98.
- Sambrook Smith GH, Ashworth PJ, Best JL *et al.* 2005. The morphology and facies of sandy braided rivers: Some considerations of scale invariance. In *Fluvial Sedimentology: VII*, Blum MD, Marriott SB, Leclair SF (eds). Special Publication of the International Association of Sedimentologists 35. Blackwells: London; 145–158.
- Sarker MH. 1996. *Morphological Processes in the Jamuna River*, Unpublished M.Sc. thesis, International Institute for Hydraulic and Environmental Engineering, Delft, Netherlands.
- Stallard RF. 1987. Cross-Channel Mixing and Its Effect on Sedimentation in the Orinoco River. *Water Resources Research* **23**: 1977–1986.
- Sukhodolov AN, Rhoads BL. 2001. Field investigation of three-dimensional flow structure at stream confluences: 2. Turbulence. *Water Resources Research* **37**: 2411–2424.
- Szupiany RN, Amsler ML, Fedele JJ. 2005. Secondary flow at a scour hole downstream a bar-confluence Paraná River, Argentina. In *Proceedings of the 4<sup>th</sup> IAHR Symposium on River, Coastal, and Estuarine Morphodynamics, 4–7 Oct 2005, Urbana, IL*, Parker G, Garcia M (eds). Taylor and Francis: Philadelphia, PA, USA.
- Szupiany RN, Amsler ML, Parsons DR, Best JL, Haydel R. 2007. Comparisons of morphology and flow structure at two braid-bar confluences in a large river. *Proceedings of the 5<sup>th</sup> International Conference on River Coastal and Estuarine Morphodynamics, Twente, the Netherlands*.
- Szupiany RN, Amsler ML, Parsons DR, Best JL, Haydel R. (submitted). Flow structure and morphodynamics of two braid-bar confluences, Río Paraná, Argentina. *Earth Surface Processes and Landforms*.
- Yalin MS. 1992. *River Mechanics*. Pergamon: Oxford.



# 6

## Management of confluences

**Robert Ettema**

*College of Engineering and Applied Science, University of Wyoming, USA*

### Introduction

Left to nature, confluence morphologies adjust in response to variations of water flow and sediment transport. Further, for fluvial networks subject to frigid winters, confluence morphologies must also adjust to ice formation and passage. The combined impact of the adjustments can be substantial and dynamic, and thus may create difficulties for land use and infrastructure operation in the vicinity of confluences. Numerous case-study examples document such difficulties. Figure 6.1, for example, illustrates the substantial difficulties faced in maintaining flow conditions at the confluence of the Missouri and the Mississippi Rivers, especially during winter when ice adds complications.

Confluence management, the primary subject of this chapter, entails controlling confluence morphologies so as to mitigate or minimize the difficulties that they may pose for land use and infrastructure operation. The chapter discusses confluence management in terms of two issues:

1. sediment transport and channel stability
2. ice passage and channel stability.

The issues sometimes conflate. For fluvial networks in cold regions, sediment and ice jointly affect confluence morphology. Spatial distributions of sediment deposition and

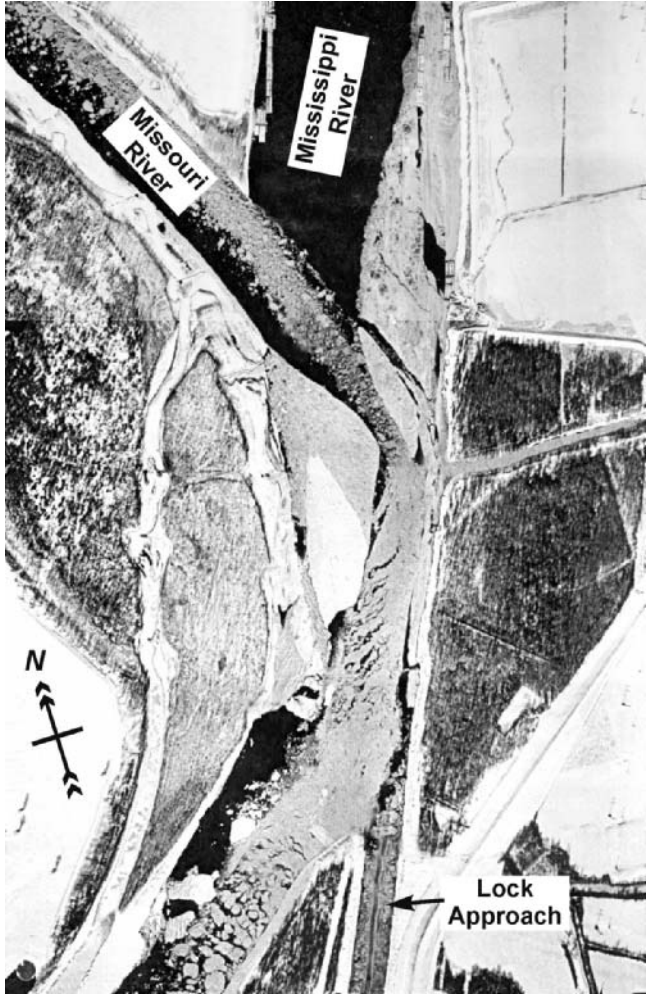


**Figure 6.1** Confluence adjustments in response to inflow variations of water, sediment and ice may hamper infrastructure activities, including navigation, as depicted here for the confluence of the Missouri and the Mississippi Rivers, January 1978.

scour within a confluence may limit its capacity to pass drifting ice. In turn, spatial distributions of ice growth and accumulation may alter channel alignment and hamper the confluence’s capacity to pass water and sediment. This chapter briefly recaps elements of the chapter by Best and Rhoads (this volume) regarding confluence morphology, outlines the ways whereby ice may affect confluence morphology and discusses approaches to managing confluences that seek to mitigate concerns regarding sediment transport and ice passage.

## Unruly confluences

Channel confluences may not readily lend themselves to the fixed alignments required for land use and infrastructure purposes. Consequently, confluences can seem unruly places, their morphologies complex, even untidy, frequently unstable and shifting. Moreover, confluences commonly are sites where drifting material, such as ice or woody debris, may choke a fluvial network.

### Morphological instabilities

Effective confluence management entails understanding the main aspects of confluent morphologies as well as the possible destabilizing impacts of variations in flow and sediment transport, and of ice formation and ice passage. As described in the preceding chapters of this book, confluence morphologies vary in accordance with relative magnitudes of confluent water and sediment flows, channel slopes and sediment characteristics. All manner of alluvial channel instability may occur at confluences. As with practically any alluvial channel, variations in water and sediment inflows may cause changes in channel grade, movement of the thalweg, bank erosion and formation or adjustment of various depositional forms.

Quite radical shifts of confluent channels can occur when a flow thalweg swings around the alternate sides of the various bar forms occurring in confluences, or when bank erosion triggers a lateral shift of a channel. Sometimes, the bars include remnants of adjoining land cut-off by a shift in a channel. Depositional bars typically form where flow capacity to move bed sediment locally diminishes. In particular, point bars may form within flow-separation zones that develop when confluent flows merge within the curved planform of a confluence. Deltaic bars may exist at the mouth of a channel confluent with a larger and more sluggish channel. As outlined in the ensuing section, ice formation can amplify the effective size of bars and, thereby, further induce changes in thalweg alignment.

### Ice effects on morphological stability

The annual cycle of ice formation and break-up is a prominent phenomenon of fluvial networks exposed to frigid winters. The extent to which ice affects channel morphology depends on a combination of factors, in addition to water flow rate. Particularly important are factors determining the amount of ice formed and the ways in which ice forms and then eventually breaks up. These factors assume great significance at confluences, where water, sediment and ice merge, and where channel morphology

becomes complicated. Prowse (2001), Ettema and Zabilansky (2004) and USACE (2006) summarize the extant knowledge regarding ice effects on channel stability. Ashton (1986) and Beltaos (1995), among others, are useful books on general aspects of river ice.

The total amount of ice formed along a channel usually is governed by the cumulative period of temperature degrees below the freezing temperature of water. Under conditions of unregulated flow, the annual cycle of ice formation is accompanied by a decline in water runoff and channel flow. Rates of sediment supply and channel transport diminish commensurately. Runoff and channel flow subsequently increase during spring thaws, and it is then that ice-cover effects on channel behaviour can become especially significant.

Ice may dampen or amplify erosion processes along channels. Additionally, its effects act over varying scales of time and channel length. Dampening effects include reduced rates of water runoff from the channel's watershed (snowfall instead of rain, freezing of overland flow), cementing of bank material by frozen water and armouring of bars and shorelines by ice-cover set-down when flow rates reduce as winter progresses. Ice, though, may amplify erosion and sediment-transport rates locally by concentrating flow within channels or under ice jams. Freeze-thaw weakening of banks greatly increases the amount of bank sediment entering a channel. During spring thaws and ice-cover break-up, the effects of ice coupled with high flows can be especially dramatic. The surge of water and ice consequent to the dynamic break-up of an ice cover or collapse of an ice jam can severely erode a channel's bed and banks.

Over a timescale of several months and length scale of miles of channel, ice alters the relationships between flow rate, flow depth and sediment-transport rates. As it forms, an ice cover usually increases and redistributes a channel's resistance to flow and reduces the capacity of flow to move water and sediment. In a sense, because the channel's bed roughness does not actually increase, ice-cover effect on channel morphology may be likened to the effect produced by a reduction in energy gradient associated with flow along the channel. More precisely, it may be likened to a change in thalweg sinuosity (Ettema and Zabilansky, 2004); the additional flow energy consumed overcoming the resistance created by the cover offsets a portion of the flow's energy that the channel dissipates by thalweg lengthening or bifurcation.

Locally, an ice cover may redistribute flow laterally across a channel reach, altering coherent flow structures, such as eddies, and accentuating erosion in one place and deposition in another. Such local changes of the bed may develop during the entire cycle of ice formation, presence and release. They may develop briefly, lasting slightly longer than the ice cover to then disappear shortly after the cover breaks up. Or, they may persist for some time, for example when they precipitate bank erosion. For confluences, whose morphologies already reflect quite delicate balances imposed by merging sets of water and sediment inflow, ice increases the complexity and seeming unruliness of confluence morphologies.

## Ice jams in confluences

The threat of ice jamming is a major concern for confluences in cold regions. Because confluences concentrate ice and water from upstream reaches, and confluence morphology can be complicated, confluences are prone to ice-jam formation. Ice quantities entering a confluence may exceed the capacity of the confluence to pass ice. In turn, by virtue of their influence on flow distribution and scour, jams may affect confluence stability. Therefore, it is no surprise that ice-jam literature often mentions confluences (e.g. Michel, 1972; Wuebben and Gagnon, 1995; Andres, 1996; Tuthill and Mamone, 1997; Ettema *et al.*, 1999; Ettema and Muste, 2001). Accordingly, confluence management often must include efforts to mitigate the formation and consequences of ice jams.

Ice moves through, and possibly jams, fluvial networks on two annual occasions. One is during winter when ice initially forms during frigid weather. Jams of newly formed ice are called 'freeze-up jams', and typically comprise accumulations of relatively small ice pieces. The other occasion is when an ice cover breaks up during warming weather, such as in spring. These jams are called 'break-up jams', and usually are formed of relatively large ice pieces.

The extents to which ice jams develop in confluences depend on the structure and orientation (north–south) of the fluvial network, the way ice forms and moves through the network, the location of the confluence in the network, the local morphologic features of the confluence itself and the characteristics of ice and water flow at a confluence. A general consideration associated with ice jams is the deceleration of the inflow that occurs once ice movement slows. Slowing and accumulating ice increases flow depth, and thereby decreases average velocity. Flow drag exerted against the accumulating ice decreases and ice motion may come to a halt. Increased flow depth, though, increases the hydrodynamic force of water exerted against the jam. Then, as ice warms and weakens, the jam eventually may collapse, releasing a surge of water and ice. Jam formation is an inherently unsteady process.

Field observations (e.g. Andres, 1996; Tuthill and Mamone, 1997) and laboratory experiments (Ettema *et al.*, 1999; Ettema and Muste, 2001) indicate that ice jams can result from the following sets of processes for confluences of rectangular channels (Figure 6.2):

1. An ice run in one channel is blocked by stationary or slow-moving ice in the outflow channel (Figure 6.2(a)).
2. A run of relatively large ice pieces (compared with channel width) lodge as an arch across the confluence (Figure 6.2(b)).
3. Merging ice runs congest the confluence (Figure 6.2(c)).
4. Cross-flow impact of flow from the other channel congests and blocks ice discharging from the other channel (Figure 6.2(d)).

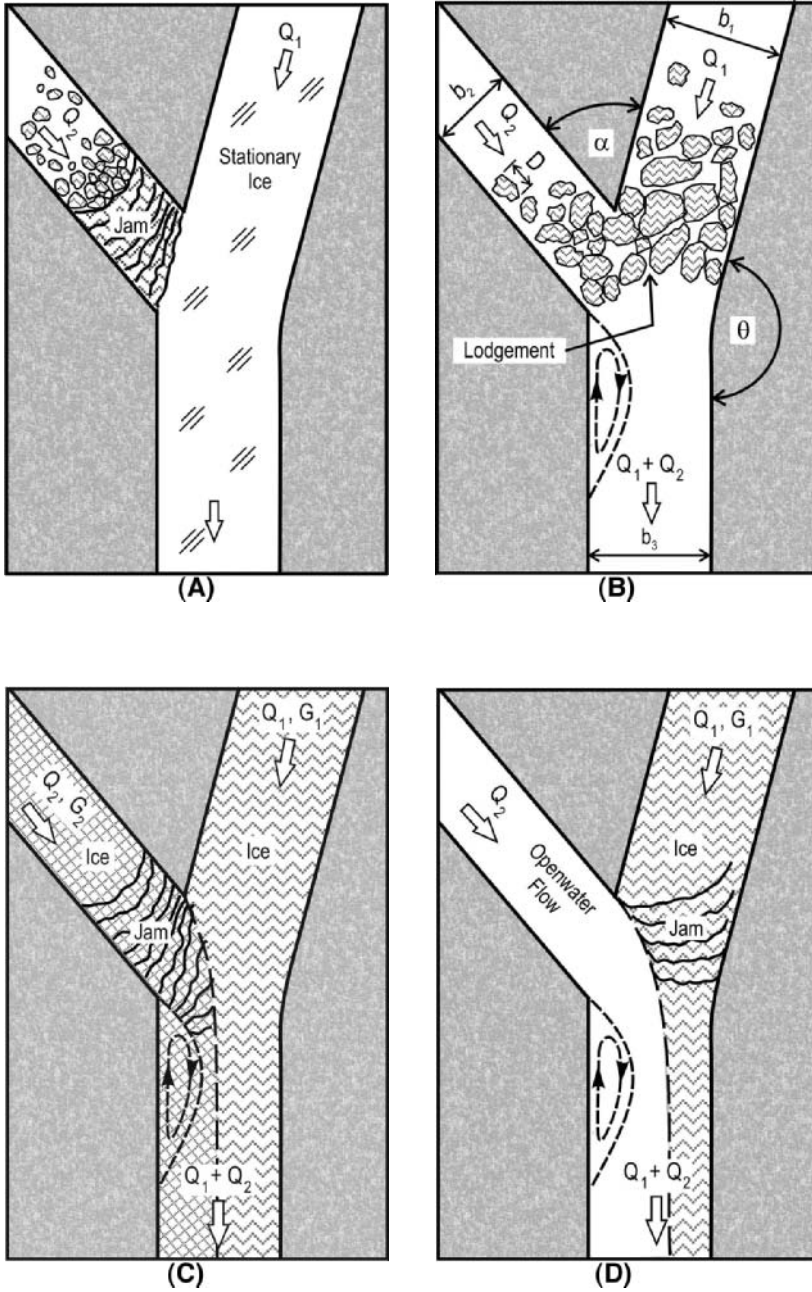


**Figure 6.2** Ice-jam processes in confluences: (a) drifting ice arrested by a stationary ice cover in the major channel; (b) lodgment arching of large ice pieces; (c) congestion of merging ice runs; (d) high cross velocities pressing ice against channel bank. Note: Q and G are water and ice discharges respectively.

Non-uniform flow depths and the morphological convolutions of alluvial bars within alluvial confluences slow ice passage and contribute to jamming. As Figure 6.3 illustrates, additional jamming mechanisms arise:

1. Congestion of a single ice at a confluence point bar (Figure 6.3(a)). During low flows, the bar increasingly constricts the surface of the outflow channel. Flow around the bar produces centrifugal forces compressing drifting ice towards one side of the outflow channel. Ice congestion adjacent to the confluence bar may occur whether ice enters the confluence from one inflow channel or from both. Ice passage is made more difficult by ice growth or accumulation at the point bar (Figure 6.3(b)).
2. Two ice runs congest the narrowed space adjacent to a point bar (Figure 6.3(c)).
3. Ice accumulation and bridging at deltaic bars or dunes (Figure 6.3(d)). During relatively shallow flow conditions in both confluent channels, ice from the smaller channel may ground on exposed alluvial bars and dunes. Grounded ice may cause other ice to arch between the bars or dunes and thereby initiate a jam.

Jamming implies congestion of ice and water flow. Two ice runs merging in the confluence may cause the ice run in one channel to congest and jam at a location near the channel's exit (Figure 6.2(c)), or congestion may form at the narrowed region adjoining a point bar (Figure 6.3(c)). The former congestion occurs if the upstream component of the lateral pressure exerted by ice discharging from one channel equals or exceeds the net force driving the ice in the second channel. This jamming mechanism arises when an ice run in a smaller channel tries to merge with an ice run in a channel that is larger or conveys more ice; jamming typically will occur in the smaller river, immediately upstream of the confluence. Jamming in the vicinity of the point bar arises when ice flows of about the same order of magnitude from the two channels squeeze past the separation bar. In short, the following four factors influence the jamming of merging ice runs:

1. the proximity to incipient jamming in each inflow channel
2. the relative location of the dividing streamline between the merging flows (see Figure 6.2(c))
3. the relative magnitude of the flow-separation zone (Figure 6.2(c)) or point bar (Figure 6.3(a) and (b)), which depends on relative magnitudes of the two inflows, and confluence geometry
4. the magnitude of the backwater effect in each channel that results from ice congestion in the confluence.

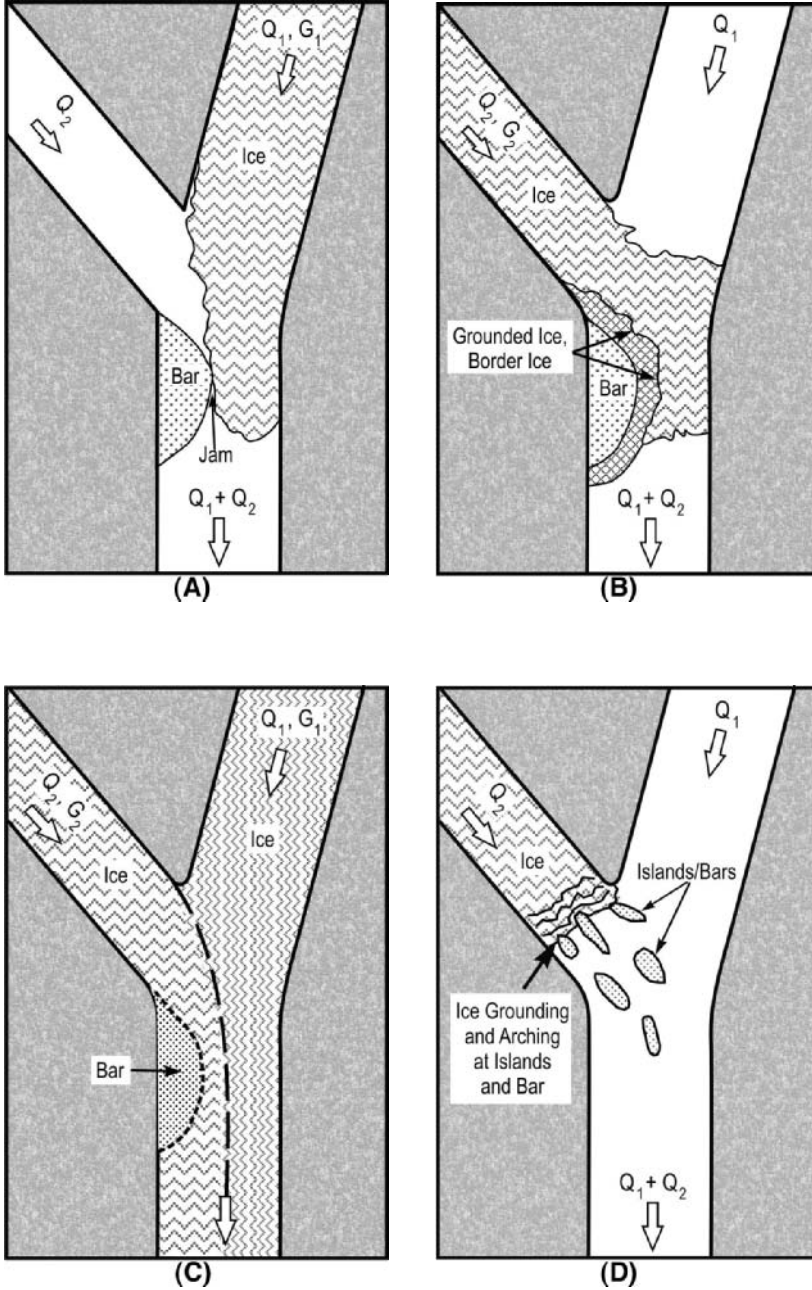


**Figure 6.3** Ice congestion at alluvial bars: (a) one ice run congested at a point bar; (b) one ice run at a point bar narrowed by border-ice formation; (c) two ice runs at a point bar; (d) one ice run congested at deltaic bars and islands.

Ice-jam literature elaborates how ice breaks up, moves and possibly jams in fluvial networks. Michel (1972), for instance, outlines a process typical of many fluvial networks. Ice-cover break-up begins in tributary channels, then progresses downstream to main-stem channels. He suggests that daytime fluctuations in springtime runoff flows have a greater destabilizing impact on ice covers in the steeper tributary channels of a network than on ice covers in the flatter-sloped main-stem channel of a network. In many networks, therefore, the break-up of tributary ice covers precedes break-up of the ice cover on a main-stem channel. Broken tributary ice accumulates at ice-covered reaches downstream, doing so in a sequential staggered manner. Further warming of weather, weakening of the downstream ice cover and increased runoff flow eventually cause the ice cover to collapse and the enlarged mass of broken ice to drift downstream or to move more dynamically as a surging ice run. In turn, an ice run may be impeded by the next ice-covered reach downstream, and form an ice jam of still greater size. With still further warming and flow increase, the ice reach and jam collapse, and another run ensues, possibly resulting in yet another jam downstream. It may take several runs for a fluvial network to release its ice or for ice to disintegrate and melt within the network. The manner and sequence of ice break-up, passage and disintegration along a fluvial network are strongly influenced by weather patterns, sources of runoff flow throughout the network, the north–south direction of flow and local channel morphology. Accordingly, jam configurations and channel impacts can vary widely.

Field observations indicate that the processes sketched in Figures 6.2(a–d) and 6.3(a–d) are common. Many illustrative case studies of ice-jam formation in confluences are documented. For example, USACE (1962, 1977), Wuebben and Gagnon (1995) and Tuthill and Mamone (1997) describe confluence jams in the United States. It is well known that problematic ice jams often use to form at the confluence of the Mississippi and Missouri Rivers (Figure 6.1). The jams blocked navigation through the confluence and would damage and disrupt towboat-fleeting activities in the vicinity of the confluence. Also, they would damage shoreline structures and threaten to laterally shift the confluence. The problem of ice-jam formation in the confluence of the Mississippi and Missouri Rivers was extensively investigated by USACE (1962, 1977), Stevens (1978), Ettema *et al.* (1999) and Ettema and Muste (2001). The two USACE studies document field conditions attendant to jam events. A review of ice-jam events shows that the jams typically are freeze-up jams that occur during a period of low flow in the Missouri and Mississippi Rivers and frigid weather conditions. For these flows, the confluence bar greatly constricts flow through the confluence. Additionally, during frigid weather, border ice growth and the accumulation of grounded ice amplify the constrictive effect of the bar. As described below, management methods were able to mitigate the problem, at least for typical winter conditions. Ettema *et al.* (1999) and Ettema and Muste (2001) describe laboratory studies aimed at confirming the efficacy of confluence-management methods to mitigate jamming.

The occurrence of confluence jams increases with latitude. Andres (1996, 1997, 1998) describes three situations in western Canada where jams result in recurrent flooding problems for towns located near confluences. Each case involved an ice run in the tributary channel blocked by a stationary ice-cover break-up on the main-stem channel. One case occurs at the confluence of the Smoky River and the Peace River, which is larger and has a more northern watershed (Andres, 1996). The ice cover on the Smoky River breaks up first during spring, but is blocked by the intact cover on the Peace River in British Columbia. If break-up flows are sufficiently large in the Smoky River, ice jammed at the confluence may thrust through ice on the Peace River and produce a subsequent jam a short distance downstream in the Peace River. Ice on the McLeod River typically breaks up before ice on the Athabasca River does, and it jams in the confluence of the two rivers (Andres, 1998). In some years, the jam develops in the Athabasca River at a short distance downstream of the confluence. A freeze-up ice jam commonly occurs at the confluence of the Nechako and Fraser Rivers in British Columbia (Andres, 1997). The Fraser River, the larger river, and of flatter slope, typically freezes over first.

Prowse (1986) presents the findings of an extensive investigation of ice jams formed in the Liard River at the confluence of the Liard and Mackenzie Rivers in the Northwest Territories, Canada. His study, conducted over a six-year period, 1978 through 1984, indicates that two factors led to jam formation in the Liard River at its confluence with the Mackenzie River. One factor was the presence of an ice cover in the Mackenzie River. Ice cannot pass out of the Liard River when the Mackenzie is ice-covered at the confluence. The other factor is the confluence morphology of the Liard and Mackenzie Rivers. The mouth of the Liard River opens relatively widely at the confluence and is marked by the presence of deltaic sand bars and islands, the latter having formed from the vegetated, more permanent, bars. Large ice pieces have difficulty moving through the mouth of the Liard River without arching or grounding. Arching of ice pieces at the mouth of the Liard may cause ice to jam in the Liard when openwater conditions exist in the Mackenzie River. In general terms, the confluent sub-channels of braided-meandering channels and sinuous-braided channels are potential sites within a channel where localized jams may form.

A comparatively unusual case associated with shallow flows in braided channels is worth mentioning. It concerns an ice jam formed at the confluence of the Porcupine River and its tributary the Bluefish River in the Yukon Territory (Jasek, 1997). The case is unusual because the jam was attributable to the formation of aufeis at the confluence. Aufeis is ice that forms in very shallow flows, extends up from the channel bed and thickens as shallow flow oozes and freezes over the aufeis (Schohl and Ettema, 1986). Aufeis formed in the Bluestone River encroached over and enveloped the ice cover formed over the Porcupine River. The aufeis thickened substantially and virtually dammed the Porcupine River, blocking the downstream passage of drifting ice.

For many large networks, the joint probability of ice discharging simultaneously from two channels into a confluence depends on the similarity of the two watersheds

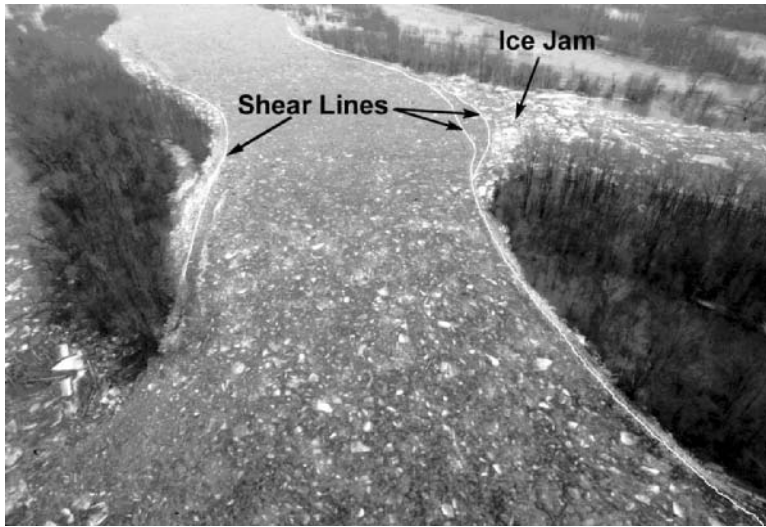


**Figure 6.4** Ice jamming, and consequent flooding, at the confluence of the Iowa and Cedar Rivers. The shear zones and lines form as an ice layer that pushes past stationary boundaries.

drained. The frequency of confluence jamming is less for rivers draining watersheds in significantly different hydrologic regions, though early break-up in one watershed and late break-up in the other can result in ice running from one watershed being blocked by an intact ice cover at the confluence (as sketched in Figure 6.2(a)). Rivers draining adjoining hydrologic regions are more likely to experience ice runs at about the same time. The confluence illustrated in Figure 6.4 frequently experiences ice jams, because an ice break-up occurs practically simultaneously for the watersheds of the merging, Midwest rivers.

## Management approaches

Two general conceptual approaches have been used to manage confluences in order to mitigate concerns about channel instability, and thus facilitate sediment transport and ice passage through confluences:

1. **Zoning:** limit land use and infrastructure development within a buffer region circumscribed around a confluence. This approach leaves a confluence more or less free to adjust its morphology, within the bounds of the buffer region. It is feasible when the land around a confluence is not entirely developed.

2. **Channel control:** employ channel-control methods to constrain confluence channels along, more or less, fixed alignments and channel widths, and protect channel banks. This approach is commonly used in locations where land and river use are well developed and it is necessary to intervene with channel-control methods.

Each approach entails the application of scientific and engineering principles, even if at times each also had a certain metaphysical or religious overtone. In ancient times, confluences were commonly viewed as sacred places best left alone whose management was tacitly accomplished by paying homage to the resident river deity or god. Celtic peoples, for instance, had a god devoted to confluence management: Condati, a god of water and its perceived magical properties (Ross, 1967). During more recent times, when population centres began growing along rivers in Europe (often near their confluences), fluvial channel behaviour was customarily regarded in biblical terms. River channels that shifted, eroded, flooded or turned land into swamp did not conform to biblical ideals of how a river should look and behave. To hard-working, devout people struggling to make land fruitful, such deviant behaviour was practically sinful and needed correction. Unruly channels also did not sit well with the land-use notions of ‘manifest destiny’, a belief strongly held in nineteenth-century North America.

A prominent early river engineer, or ‘river Korректор’ (as then called), Johan Tulla, set the tone in 1815 with his dictum: ‘As a rule, no stream or river needs more than one bed’ (Cioc, 2002, p. 3). His dictum practically became a law in the minds of engineers, whose education during the 1800s and 1900s emphasized orderliness and the application of the principles of engineering mechanics. Since Tulla’s early work along the Rhine and its tributaries, numerous channel confluences in developed locations throughout Europe and other places have been channelized. This work is mentioned in several books (e.g. Freeman, 1929; Schoklitsch, 1937). River-engineering literature, though, contains no general design guidelines, overall summary of experience or hindsight review of channel control at confluences. Much of the experience resides in reports on hydraulic laboratory studies of confluence control at specific sites (e.g. Franco and McKellar, 1973; McVan, 1997).

Starting in the later decades of the twentieth century and motivated substantially by environmental concerns, there has been a definite trend to lessen the use of channel-control methods for fluvial channels, including confluences, and where possible to rely more on the zoning approach. However, when certain infrastructure facilities must be protected, the zoning approach is not always feasible.

## Managing confluences for sediment transport

Confluences formed of stable channels having the capacity to convey water and transport sediment are required for many circumstances where channels flow through areas of developed land and infrastructure. Concerns about confluence stability and

sediment-transport often arise for the following infrastructure situations: protection of land, maintenance of river navigation, operation of water intakes and outfall structures, and the safety and performance of bridges and drainage structures.

The protection of land adjoining confluence channels is common to all of these situations, as it entails fixing the overall boundaries of the channels at a confluence.

## Protection of land

Confluence management for land protection entails the use of several channel-control methods, and sometimes bank-protection methods. Where originally the mouth of the tributary channel could shift from one to another main outlet (Figure 6.5(a)), channel control constrains the tributary channel to a constant width and alignment smoothly faired into the confluence (Figure 6.5(b)). The other channel also would be faired into the confluence in a manner whereby the inner banks of the confluence converge to an acute point. The inner banks forming the confluence point are protected by means of riprap stone, rock-filled gabions or sometimes sheet-piling. It is usual for the left bank (looking downstream) of the main channel to form a smoothly faired curve similarly protected.

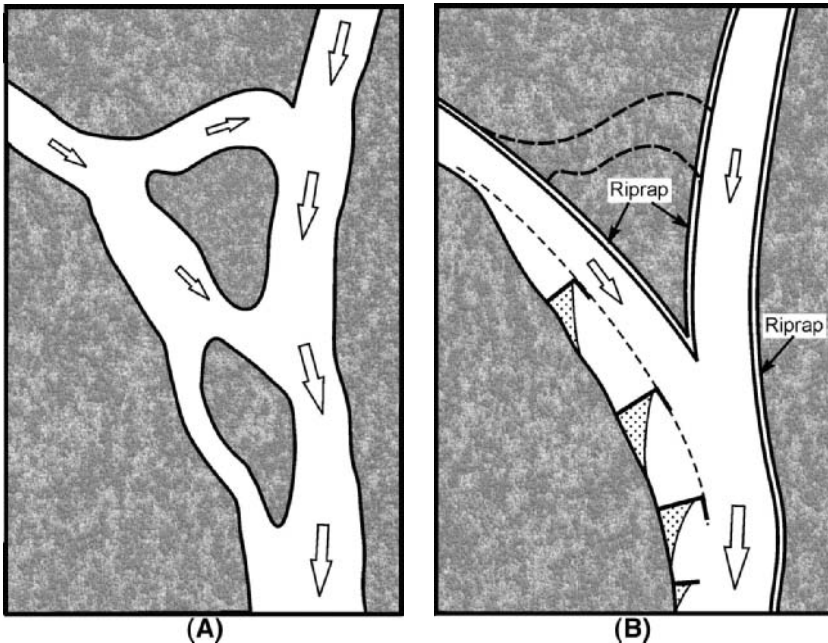


**Figure 6.5** Channel and bank control for land protection at a confluence: (a) natural condition; (b) channelized condition. The structural methods shown (riprap banks, spur dikes) are widely used, though they may vary in combination.

Information from laboratory experiments on flow behaviour at confluences is often used in checking that the channel-control concepts will not result in adverse scour or deposition conditions (e.g. Taylor, 1944; Fujita and Komura, 1986, 1989; Ramamurthy *et al.*, 1988; Hager, 1989; Gurram *et al.*, 1997; Hsu *et al.*, 1998).

The alignment of the right bank (looking downstream) of the lesser channel is typically maintained by means of a set of spur dikes, which sometimes may extend along the entire right bank of the confluence. The spur dikes fend flow away from the bank and delineate the channel's edge. Often, the flow-separation region developed within a confluence may cause sediment to deposit as a separation bar (see Best and Rhoads, this volume, Chapter 4) so that this portion of the right bank may not need protection. However, as discussed in *River navigation* below, it is sometimes necessary to limit the extent to which the bar encroaches into a confluence.

Figure 6.6 illustrates the confluence-management methods applied to protect land adjoining two scales of confluence. Figure 6.6(a) shows the riprap-protected inner banks of the confluence point between the Missouri and Mississippi Rivers. Figure 6.6(b) illustrates the same management method for the confluence of two much smaller rivers.

## Maintenance of river navigation

Maintenance of commercial navigation through a river confluence may require the use of additional methods of channel control besides those used for land protection. The navigation (sailing) path through a confluence usually coincides with the thalweg of the main channel, and sometimes the thalwegs of both channels. However, the sailing path may deviate from a thalweg at certain instances, such as the approach to a lock or a mooring area. Typically, the confluence is managed so that minimum flow depth and curvature of the sailing path meet the requirements for the commercial vessels passing through the confluence.

The additional channel-control methods comprise channel-control structures and, frequently, dredging. These methods seek to keep the alignment and depth of the sailing path steady so that river navigation vessels (towboats in rivers like the Mississippi River) can proceed safely along well-marked paths and can approach locks or mooring areas. The protection of land flanking the sailing path helps prevent any major lateral shifting of the channel. Also, channel-control structures may narrow the confluence channel and increase flow velocities, but only to within limits associated with the channel conditions needed for navigation. Sediment conveyed into a confluence may accumulate as bars or large dunes along the channel, causing the thalweg and sailing path to shift and possibly shoal. Dredging is conducted to remove sediment deposits along the sailing path and thereby maintain a minimum navigation depth through the confluence.



(A)



(B)

**Figure 6.6** Examples of channel control at confluences: (a) Missouri and Mississippi Rivers; (b) two small streams. Confluence boundaries lined with riprap or rock gabions, with spur dikes also used for outer banks

The scouring action of low-profile structures like bendway weirs (submerged, low, spur dikes, Davinroy, 1994), which can fit beneath over-passing vessels, further help to delineate thalweg and sailing path alignments, and thereby reduce the need for dredging. The flow of water and transport of sediment from the Missouri River show that bendway weirs deployed in the confluence of the Missouri and Mississippi Rivers force the thalweg to a reasonably central alignment in the confluence, while also enabling vessels to approach a lock at one side of the confluence. Figure 6.7(a) and (b) shows the deployment of bendway weirs, and bank armouring, at the confluence of the Mississippi and Missouri Rivers. The bendway weirs the weirs push the thalweg and sailing path to a more central alignment through the confluence.



**Figure 6.7** Water and sediment flow from the Missouri River into the Mississippi River, 1998 (a); and (b) detail of bathymetry showing use of bendway weirs, riprap-armoured banks, and dredging to maintain the sailing path through the confluence

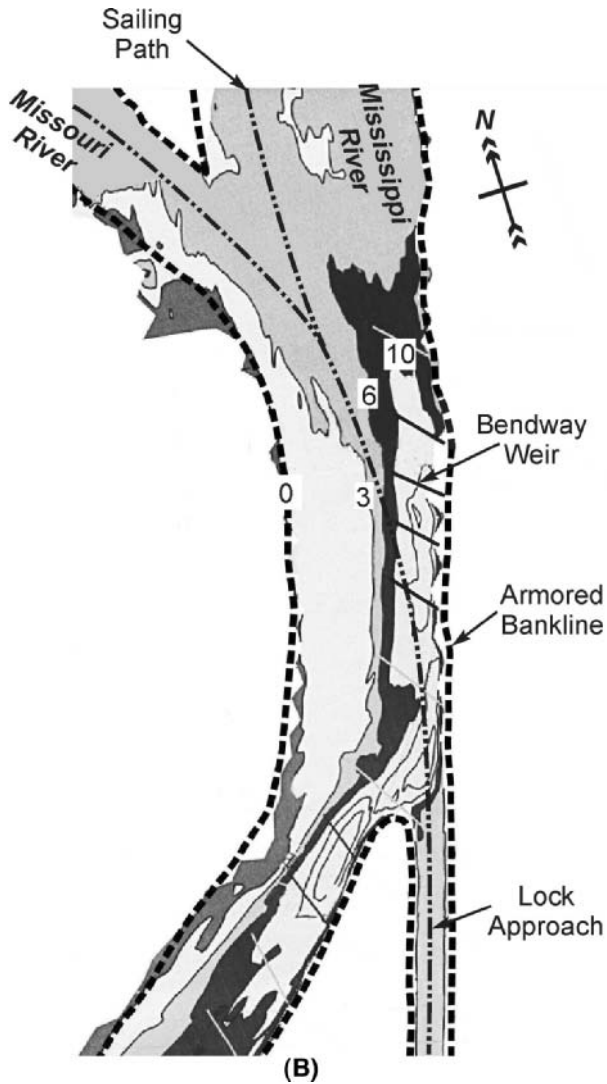


Figure 6.7 (Continued)

### Operation of water intakes and outfall structures

The function of concentrating water draining from two watersheds makes the channel immediately downstream of a confluence attractive for locating water intakes and wastewater outlets. However, thalweg shifting and sediment deposition, as well as scour, in the confluence along with channel shifting can cause problems for intakes. The main management concern is to ensure that adequate flow gets to the intake. An intake

sited near a point bar may encounter excessive sediment deposition and even become partially enveloped by the bar, while an intake sited on the bank opposite a point bar will have a scour concern if this bank erodes. Additional structures, such as spur dikes and vanes, placed within a confluence can be used to guide adequate flow to an intake.

## The safety and performance of bridges and drainage structures

The channel instabilities associated with many confluences pose problems for bridges at or near confluences and for culverts collecting water from confluent channels. The main problem for bridges concerns the possible shifting of a channel as it approaches the bridge to an orientation that causes a severe scour problem. This problem usually is addressed by means of guide banks extending upstream of the bridge so as to direct the flow suitably through the bridge waterway. It is a problem that also arises for culverts near the confluences of small streams and drainage channels.

A further confluence concern for bridges and culverts is getting the flow through their entrance opening. The capacity of a bridge or a culvert to pass flow may be reduced if the approach flows merge at their entrance, because the merged flow would not be well aligned with the opening. If the confluent approach flows convey sediment, they may deposit it at the entrance of a bridge or culvert, thereby partially blocking the entrance; this is a particularly severe problem for multibarrel culverts draining agricultural land subject to substantial soil erosion. Effective confluence management for bridges and culverts requires that confluent flows merge well upstream of the bridge or culvert, and the merged flow then be acceptably aligned towards the bridge or culvert. A pair of guide banks is commonly used for this purpose.

Finally, an interesting situation arises where a spill-through bridge abutment forces flow over the floodplain such that it subsequently merges with the flow in the main channel downstream. This is analogous to conditions at a confluence with discordant channel beds where particular patterns of flow and scour can develop (e.g. Biron *et al.*, 1996). In this compound-channel case, the angle between the two channels (now the main channel and the floodplain) is essentially zero degrees. The bathymetry of the scour hole formed near the abutment is then very similar to that for scour at a discordant bed confluence. In this case, the angle between the two channels (now the main channel and the floodplain) is essentially zero degrees. The bathymetry of the scour hole formed near the abutment is very similar to that for scour at a discordant-bed confluence. Indeed, the same formulation may be followed in estimating the scour depth. Any management of this confluence condition primarily entails ensuring that the approach flow can pass through the bridge waterway without causing unacceptable scour. This can be achieved by suitably armouring the sides of the abutment and the main channel in similar ways to armouring the banks of a confluence.

## Managing confluences for ice passage

Stabilizing confluence channels with regard to the consequences of ice formation and transport entails essentially the same activities as described above for land protection and navigation at a confluence. The overall aim of confluence management is to encourage water and ice to pass smoothly through a confluence while maintaining channel stability. The channel-control works illustrated in Figures 6.5 through 6.7 for the confluence of the Mississippi and Missouri Rivers have proven effective in reducing the incidence of ice jams as well as enhancing navigation through the confluence. Otherwise, not much work has been done regarding the enhancement of ice passage at confluences. The extant fieldwork is summarized by Tuthill and Mamone (1987), and laboratory work by Ettema *et al.* (1999) and Ettema and Muste (2001).

### Ice effects on channel control

Several ice-related considerations should be kept in mind regarding the selection and performance of channel-control structures in channels subject to frigid winters:

1. The length of such structures should not exceed the normal width of border ice at the bank they are required to protect. Compared to openwater conditions, shorter and closer-spaced structures are preferable for use in ice-covered flow. Structures longer than the normal width of border ice attached to a bank move the ice crack along the shoreline outwards into the channel, thereby widening border ice and increasing the ice load exerted on a bank. Border ice between and near groins or spur dikes form significantly wider than along an unprotected bank. When the river is ice covered, border ice forms a floating membrane attached to the groins and the bank. However, when the ice breaks up and flow stage subsides, large slabs of border ice collapse, possibly damaging the banks and vegetation along them.
2. Ice formation may alter the flow field around long groins, spur dikes and bendway weirs so as to negate their intended action. Ice formation may locally concentrate flow towards the bank rather than away from the bank.
3. Riprap stone must be sized, and riprap slope configured, for border-ice conditions. At some locations along the protected bank, riprap stones might be plucked from the bank by collapsed bank ice. The upper elevation of riprap stone placement should take into account the probable elevation of the ice cover.

Experience with control structures placed along the Missouri River, and several other rivers in the greater basin of the Mississippi River, substantiate these considerations (Zabilansky *et al.*, 2002).

As with confluence management for sediment transport, management for ice passage entails estimating ice-passage capacity and identifying locations where ice may accumulate. In this regard, it is useful to categorize the general conditions of ice passage through confluences and to identify useful non-dimensional parameters for describing them. The two conditions are:

1. a drifting individual ice pieces whose velocity is about that of the water surface; this condition may result in ice stoppage for channels of relatively mild slope conveying ice pieces that are relatively large compared to channel width
2. a moving layer of accumulated ice pieces extending approximately the full width of the channel and moving with a velocity significantly less than the bulk velocity of water flow in the channel. This condition may occur for larger channels of steeper slope, as larger forces normally are needed to convey a complete layer of ice pieces.

Figures 6.2 and 6.3 are simplified illustrations of variations of these two conditions and show where the congestion and jamming occur.

Differences occur in the way ice passes through confluences in these two conditions. For example, any significant shoving and thickening of the confluent accumulations would accompany the merging of two moving particulate layers. Shoving and thickening are much less likely to accompany the merging of free-drifting ice pieces. Instead, the aerial packing of pieces may be a characteristic feature. The forces propelling the ice into the confluence commensurately differ between the two conditions, and therefore differences arise between the sets of parameters needed to describe the two categories. Whereas flow drag and impact forces on individual ice pieces, and the inertia of individual ice pieces, drive free-drifting ice pieces into a confluence, boundary shear stress along the underside of an extensive accumulation of ice, together with a streamwise component of accumulation weight, drives a moving accumulation of ice. For the free drift of ice, the size of individual ice pieces is important. It is less important in describing the behaviour of an accumulation of ice, for which accumulation thickness and width are more important.

Ice passage through confluences is conveniently described in terms of non-dimensional parameters, though a potentially large number of parameters could be identified. A useful simplification is to consider the confluence as the intersection of two prismatic (rectangular) channels whose width greatly exceeds their depth. The influences of confluence morphology (bars, islands, large dunes, rock outcrops etc.) are not considered here. Also not considered are the influences of engineered features, such as bridges and channel-control structures. Additionally, hydrologic influences, such as air temperature, snow fall and wind, are neglected. While these physical, structural and hydrologic factors are important, arguably they do not play key roles in ice movement

through the confluence of prismatic channels, which is considered in the ensuing dimensional analysis. The approximations reduce the number of non-dimensional parameters needed to estimate the ice-passage capacity of a confluence.

### Passage of drifting ice pieces

Figure 2(b) indicates, in simplified format, the variables associated with ice pieces drifting through a confluence of two, fixed-bed channels of rectangular cross-section. The same size of ice piece is taken to be moving through both channels. The confluent inflow channels are designated with subscripts 1 and 2. The confluence outflow channel is designated with subscript 3. The confluence location of primary concern for ice passage is the constricted section where the flow-separation zone has maximum width. The variables associated with this section depend on the variables associated with confluence-channel elements 1, 2 and 3.

The discharge,  $Q$ , or a representative bulk velocity,  $V$ , of flow in one of the channels shown in Figure 6.2(b) can be described using the variables  $Y$ ,  $k$ ,  $S$  and  $b$ , for example by means of the Darcy–Weisbach equation for flow resistance. The present analysis uses  $Q$ , as the relative magnitudes of confluent channels usually are described in terms of flow discharge. The fluid properties of concern are kinematic viscosity,  $\nu$ , density,  $\rho$ , and surface-tension strength,  $\sigma$ . The ice pieces, are taken here to be of uniform size and are describable using a characteristic plan dimension,  $D$ , thickness,  $h$ , density,  $\rho_i$ , and friction coefficient for contact among ice pieces and with the channel banks,  $\mu$ . The flow is driven by specific weight:  $\gamma = \rho g$ , with  $g =$  gravity acceleration. The discharge of free-drifting ice pieces moving at nearly the surface water velocity in a single channel can be described in terms of aerial concentration,  $C$ . Ice discharge can then be calculated as  $G \approx C(hb)(Q/bY) = C(h/Y)Q$ .

A total of 13 variables are needed to describe the discharge of free-drifting ice in a channel:  $Q_1$ ,  $Y_1$ ,  $b_1$ ,  $k_1$ ,  $\nu$ ,  $\rho$ ,  $\sigma$ ,  $D$ ,  $h$ ,  $\rho_i$ ,  $\mu_i$ ,  $g$  and  $C_1$ . To describe ice discharge in two channels that differ only in geometry and discharges of water and ice the number of variables increases to 20; added for the second channel are  $Q_2$ ,  $Y_2$ ,  $b_2$ ,  $k_2$ ,  $C_2$ ,  $D_2$  and  $h_2$ . The material properties of water and ice are taken to be the same for all channels. To describe the merging of ice flow from two channels confluent into a single outflow channel, additional variables are needed to describe the orientation of the outflow channel relative to the confluent channels,  $\alpha$  and  $\theta$ , and the hydraulic characteristics of the outflow channel ( $b_3$ ,  $Y_3$  and  $k_3$ ). The total number of variables is now 25.

The present brief analysis considers incipient ice jamming at a confluence of rivers and at a river discharging into a reservoir or lake. Under the assumption that ice-piece dimensions,  $D$  and  $h$ , are the same for all channels, and that the channels have about

the same hydraulic roughness,  $k$ , the number of variables reduces to 21 ( $25 - 4$ ). For ice drifting in actual rivers, it can be assumed further that the influences of water viscosity,  $\nu$ , and surface tension,  $\sigma$ , are negligible (not so for most laboratory experiments, though). The number of variables finally reduces to 19 ( $21 - 2$ ).

If the ice pieces move through the confluence as a single layer of ice pieces of a given size, the following functional relationship may be written for the congesting aerial concentration of ice discharge at the narrowest cross-section of flow in the confluence outflow channel,  $C_3$ , as the dependent variable of interest:

$$C_3 = f_d(Q_1, Q_2, b_1, b_2, b_3, Y_1, Y_2, Y_3, k, D, h, C_1, C_2, \alpha, \theta, \mu, \rho, \rho_i, g) \quad (6.1)$$

The 19 variables in Equation 6.1 reduce to 16 non-dimensional parameters, given the three basic dimensions (length, mass and time) involved in the volumetric discharge of ice through a confluence. If a dimensional analysis is carried out using  $h$ ,  $Q_2$ , and  $\rho$  as the repeating variables (expressing length, time and mass units), the following functional relationship emerges for the limiting condition of a single layer of free-drifting ice discharging through a confluence:

$$C_3 = \varphi_{d2} \left( \frac{Q_1}{Q_2}, \frac{Q_2}{hb_2\sqrt{(\rho - \rho_i)gh/\rho}}, \frac{D}{h}, \alpha, \theta, C_1, C_2, \frac{b_1}{b_2}, \frac{b_2}{b_3}, \frac{b_3}{h}, \frac{k}{h}, \frac{Y_1}{h}, \frac{Y_2}{h}, \frac{Y_3}{h}, \frac{\rho}{\rho_i}, \mu \right) \quad (6.2)$$

These parameters are useful for describing how the basic confluence flow conditions illustrated in Figure 6.2(b) influence ice movement and jamming in a simple confluence of rectangular channels. Note that the second independent parameter essentially expresses a densimetric Froude number, which, together with  $D/h$ , characterizes criteria for the possible submergence of a drifting ice piece resting against a stationary ice cover and then the under-ice transport of ice pieces beneath a stationary ice cover (Beltaos, 1995):  $Q_2/hb \approx U_2$ , the bulk flow velocity in channel 2. The parameters in Equation 6.2 delineate conditions of thickened jamming in any channel of a confluence.

Ettema *et al.* (1999) report series of laboratory experiments to illuminate the influences on  $C_3$  (i.e. jam initiation at the flow-separation region within channel 3) of the first eight parameters in Equation 6.2. In their experiments,  $b_3 = b_2$ . The experiments showed that jamming would occur for a narrow range of values for the concentrations  $C_1$  and  $C_2$  (i.e. both values need to be close to the critical value of ice concentration for the flow in each inflow channel). The lateral pressure exerted by ice in one channel provides the additional resistance force needed to cause jamming in the other channel. A merging ice run exerts a force component upstream along the axis of the ice run

with which it merges. Values of ice-piece size relative to channel width,  $D/b_3$ , need to be sufficiently large such that the arching of ice pieces occurs in a confluence. Usually,  $D/b_3 > 1/7$  in order for arching to occur.

### Passage of moving ice layers

Water flow may convey moving layers of accumulated ice pieces, as sketched in Figures 6.2(c) and (d) and 6.3, and illustrated in Figure 6.4. This condition is common for steeper channels that mobilize a larger hydrodynamic force for given flow depth relative to ice-piece thickness. A simplified analysis, similar to that leading to Equation 6.2, provides a functional relationship for ice-layer thickness in channel 3,  $H_3$ . This is appropriate for layers merging in confluent rectangular channels and is especially appropriate in the vicinity of the point bar,

$$\frac{H_3}{Y_3} = \varphi_{d2} \left( \frac{Q_1}{Q_2}, \frac{(Q_2/H_2 b_2)^2}{(1 - \rho_i/\rho) g H_2 \tan \phi}, \frac{k_b}{b_2}, \frac{k_i}{b_2}, p_1, p_2, \frac{H_2}{b_2}, \frac{H_2}{H_1}, \frac{\rho_i}{\rho}, \phi, \mu, \alpha, \theta, \right. \\ \left. \frac{b_1}{b_2}, \frac{b_2}{b_3}, \frac{H_2}{Y_2}, \frac{Y_1}{Y_2}, \frac{Y_3}{Y_2} \right) \quad (6.3)$$

in which the material behaviour of each inflow layer can be defined using its thickness,  $H$ , angle of internal resistance,  $\phi$ , layer porosity,  $p$ , and friction between ice and banks,  $\mu$ . The volumetric rate of ice-layer discharge (a contiguous layer of accumulated ice pieces extending across the full width of the channel and moving at a speed less than the surface water speed in a single channel),  $G$ , can be written approximately as a volumetric proportion,  $\eta$ , of the water discharge, that is  $G = \eta Q(1-p)^{-1}$ . The hydraulic roughness of ice underside and channel bed are  $k_i$  and  $k_b$  respectively. The second parameter in Equation 6.3 expresses the relative magnitudes of the driving drag force and resisting internal strength of an ice layer.

Observations of model-ice movement and jamming in the confluences simulated with hydraulic models (Ettema *et al.*, 1999) reveal that an important factor associated with ice jams at confluences, and ice jams generally, is the deceleration of the inflow that occurs once ice movement slows. As an ice layer congests and thickens in a confluence, it retards the inflow, creating a backwater condition. As inflow depths increase and flow velocity decreases, flow drag force against the ice decreases and ice motion is more readily halted. Channel-control methods aimed at mitigating jamming, such as the deployment of bendway weirs shown in Figure 6.7, accelerate ice movement through a confluence. Figure 6.8 illustrates this effect in model of ice movement through a hydraulic model of the confluence of the Missouri and Mississippi Rivers.

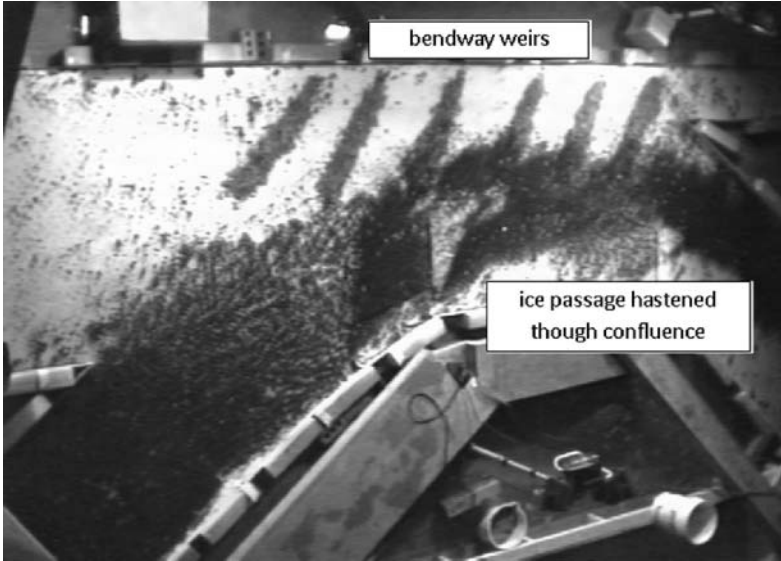


**Figure 6.8** A hydraulic model shows how the use of bendway weirs for channel control (as in Figure 6.7) hastens the passage of Missouri River ice through the Mississippi–Missouri confluence.

## Summary

The main purpose of this chapter is to outline methods used for managing alluvial-channel confluences with respect to channel stability and concerns regarding sediment and ice passage. As explained herein, difficulties associated with sediment and ice passage create concerns for human infrastructure activities in the vicinity of confluences. The concerns often are linked, insofar as sediment and ice processes may affect one another. For example, sediment bars hamper ice passage and often trigger ice jams. In turn, ice growth, ice passage and jams may alter flow distribution and modify channel morphology. The management methods essentially seek to facilitate unimpeded sediment and ice passage through confluences. Nature being what it is, though, the methods require constant monitoring.

## References

- Andres D. 1996. *Ice Formation and Breakup at the Town of Peace River: A Study of Regulated Conditions, 1969–94*. Report prepared for Town of Peace River, BC Hydro, and Alberta Environmental Protection. Trillium Engineering and Hydrographics Inc.: Edmonton, Canada.
- Andres D. 1997. *Freeze-up Ice Jams on the Nechako River at Prince George: Analysis of the 1996 Event*. Report prepared for Alcan Smelters and Chemicals Ltd., Kitimat, British Columbia. Trillium Engineering and Hydrographics Inc.: Edmonton, Canada.

- Andres D. 1998. *Analysis of Ice Jams and Associated Flood Levels and Ice Forces on the McLeod River at Whitecourt*. A letter report to Alberta Transportation and Utilities, Edmonton, Alberta. Trillium Engineering and Hydrographics Inc.: Edmonton, Canada.
- Ashton G. 1986. *River and Lake Ice Engineering*. Water Resource Publications: Littleton, Colorado.
- Beltaos S. 1995. *River Ice Jams*. Water Resources Publications: Littleton, Colorado.
- Biron P, Best JL, Roy AG. 1996. Effect of Bed Discordance on Flow Dynamics at Open Channel Confluences. *Journal of Hydraulic Engineering, ASCE* **122**: 676–682.
- Cioc M. 2002. *The Rhine: An Ecological Biography, 1815–200*. Weyerhaeuser Environmental Books, University of Washington Press, Seattle and London.
- Davinroy RD. 1994. The Bendway Weir Concept in the Mississippi River. *Proceedings of the International Navigation Congress, Seville, Spain*.
- Ettema R, Muste M. 2001. Ice Jams in River Confluences. *Journal of Cold Regions Engineering, ASCE* **15**: 41–51.
- Ettema R, Zabilansky L. 2004. Ice Influences on Channel Stability: Insights from Missouri's Fort Peck Reach. *Journal of Hydraulic Engineering, ASCE* **130**: 279–292.
- Ettema R, Muste M, Kruger A. 1999. Factors Influencing Ice Conveyance at River Confluences, Report No. 99–154. US Army Cold Regions Research and Engineering Laboratory: Hanover, NH.
- Franco J, McKellar C. 1973. *Navigation Conditions at Confluence of Arkansas, Verdigris, and Grand Rivers: Hydraulic Model Investigation*. Technical Report, US Army Corps of Engineers, Waterways Experiment Station: Vicksburg, MS.
- Freeman JR. 1929. *Hydraulic Laboratory Practice*. ASME: New York.
- Fujita I, Komura S. 1986. Application of the Free Streamline Theory to the Flow at a Confluence. *Proceedings of the 5th Asian and Pacific Regional Division Congress, IAHR, Seoul, Korea*; 103–120.
- Fujita I, Komura S. 1989. Visualization of the Flow at a Confluence. *Proceedings of the International Symposium on Refined Flow Modelling and Turbulence Measurements, Tokyo, Japan*; 517–524.
- Gurram SK, Karki KS, Hager WH. 1997. Subcritical Junction Flow. *Journal of Hydraulic Engineering* **123**: 447–455.
- Hager WH. 1989. Transition Flow in Channel Junctions. *Journal of Hydraulic Engineering, ASCE* **115**: 243–259.
- Hsu C-C, Wu F-S, Lee W-L. 1998. Flow at 90° Equal-Width open-Channel Junction. *Journal of Hydraulic Engineering, ASCE* **124**: 186–191.
- Jasek M. 1997. Ice Jam Flood Mechanisms on the Porcupine River at Old Crow, Yukon Territory. *Proceedings of 9th Workshop on River Ice, Fredericton, New Brunswick*; 351–370.
- McVan DC. 1997. *Model Study of the Confluence of San Juan Creek and Trabuco Creek, Orange County, California; Hydraulic Model Investigation*. Report A403133, US Army Corps of Engineers Waterways Experiment Station: Vicksburg, MS.
- Michel B. 1972. Properties and Processes of River and Lake Ice. *Proceedings of the IAHS Symposium on The Role of Snow and Ice in Hydrology, Banff, Alberta*; 454–481.
- Prowse TD. 1986. Ice Jam Characteristics, Liard–Mackenzie Rivers Confluence. *Canadian Journal of Civil Engineering* **13**: 653–665.
- Prowse TD. 2001. River-ice ecology I: Hydrologic Geomorphic and water-quality aspects. *Journal of Cold Regions Engineering* **15**: 1–16.
- Ramamurthy AS, Carballada LB, Tran MD. 1988. Combining Open Channel Flow at Right Angled Confluences. *Journal of Hydraulic Engineering, ASCE* **114**: 1449–1460.
- Ross A. 1967. *Pagan Celtic Britain*. Routledge and Kegan Paul: London.

- Schohl GA, Ettema R. 1986. Theory and Laboratory Observations of Naled Growth. *Journal of Glaciology* **32**: 168–177.
- Schoklitsch A. 1937. *Hydraulic Structures; a text and handbook*. Translated by Shulits S. American Society of Mechanical Engineers: New York.
- Stevens GT. 1978. *St Louis District Potomology Study (LL-1)*. Report submitted to the St Louis District, Army Corps of Engineers: St Louis, MO.
- Taylor EH. 1944. Flow characteristics at rectangular open channel junctions *Transactions of the American Society of Civil Engineers* **109**: 893–912.
- Tuthill A, Mamone AC. 1997. *Selection of Confluence Sites with Ice Problems for Structural Solutions*. US Army Cold Regions Research and Engineering Laboratory, Special Report 97–4: US Army Cold Regions Research and Engineering Laboratory, Hanover, NH.
- USACE. 1962. Report on 1962 Ice Gorge in the Mississippi River, St Louis District. Army Corps of Engineers: St Louis, MO.
- USACE. 1977. Report on Mississippi River Ice 1976–1977. St Louis District, Army Corps of Engineers: St Louis, MO.
- USACE. 2006. *Engineering and Design – Ice Engineering*. Engineering Manual 1110-2-1612, US Army Corps of Engineers, Dept of the Army: Washington, DC.
- Wuebben JL, Gagnon JJ. 1995. *Ice Jam Flooding on the Missouri River Near Williston, North Dakota*. CRREL Special Report 95-19, US Army Cold Regions Research and Engineering Laboratory: Hanover, NH.
- Zabilansky LJ, Ettema RJ, Wuebben J, Yankielun NE. 2002. *Survey of River-Ice Influences on Channel Bathymetry along the Fort Peck Reach of the Missouri River, Winter 1998–1999*. CRREL Technical Report 02-14, US Army Corps of Engineers, Cold Regions Research and Engineering Laboratory: Hanover NH.

# 7

## Unconfined confluences in braided rivers

**P. Ashmore and J.T. Gardner**

*Department of Geography, University of Western Ontario, Canada*

### Introduction

Confluences are basic building blocks of dendritic stream networks and also of anabranching or braided rivers with successive bifurcations and confluences of two or more channels. Simple confluences in these multichannel systems may have local morphology and flow structure similar to confluences at tributary junctions in dendritic stream networks, but they also differ from stream network confluences in some important respects. Tributary junctions in branching networks are confined in position, morphology and influence by local valley topography and network geometry, topology and size (Benda *et al.*, 2004). These network confluences experience essentially constant average discharge and sediment delivery regimes to which confluence morphology is adjusted, and the confluences themselves have little, even local, effect on downstream channel morphology, except in some steep basins (Benda *et al.*, 2004).

In contrast, confluences in multichannel rivers are unconfined in the sense that they migrate laterally and longitudinally, and come and go, as the river morphology changes and the local distribution of flow and sediment-transport shift, unconstrained by the basin-scale topography. Confluences in multichannel rivers are an integral part of the entire channel morphology, channel-pattern dynamics, sediment-transport rate and routing, and formation of alluvial deposits. Their influence is at the scale of the channel planform morphology rather than the stream network structure and they develop and

change at the spatial and temporal scales of channel-reach morphology. These attributes make confluences in multichannel rivers a key element of river morphodynamics in a way that tributary confluences in branching networks typically are not. However, the fact that both network confluences and unconfined confluences in multichannel rivers share similar local morphology and flow structure, at least in well-defined, two-channel confluences, means that the rapid adjustment between flow structure, sediment transport and confluence morphology in unconfined braided-river confluences provides an opportunity to observe these interactions over short timescales and to gain insights into some of the dynamics and morphology of more-stable river network confluences. There are exceptions to this distinction between dendritic stream network (confined) and multichannel anabranch (unconfined) confluences that blur the boundaries. An obvious example is confluences of large, alluvial, floodplain rivers (Best and Ashworth, 1997; Roy and Sinha, 2005), which look much like unconfined confluences in an anabranching or braided river, migrate in response to upstream channel migration and variation in discharge and sediment delivery and affect downstream patterns of sedimentation and channel development.

Multichannel rivers cover a wide spectrum of morphological types, including truly braided rivers and a wide range of anabranching (Nanson and Knighton, 1996; Makaske, 2001; Amsler *et al.*, 2005) morphologies. By definition, anabranching channels have vegetated, stable alluvial islands (Nanson and Knighton, 1996) in contrast to braided rivers, in which the vegetation of bars is limited, channels are very unstable and confluence–bifurcation dynamics are a dominant component of the channel morphology (Makaske, 2001; Ashmore, 2003). Studies of the morphology, dynamics and sedimentation processes in anabranching systems have not generally emphasized the role of channel confluences, but a recent example is work on the morphology and flow characteristics at a relatively stable confluence–bifurcation formed around islands in the anabranching Río Paraná (Parsons *et al.*, 2007). In many cases, multichannel formation and maintenance is dominated by other processes (e.g. ridge and channel systems; Nanson and Knighton, 1996) or by fine-sediment transport and deposition, and avulsion, in which case confluence dynamics may be less important to channel morphology. In channels with significant sand or gravel bedload and vegetated banks and islands (e.g. ‘wandering’ rivers), lateral migration may be restricted by cohesive and/or vegetated banks. These channels may have some of the characteristics of confluence–bifurcation dynamics found in braided rivers but morphological change is slower and channel-pattern change is dominated by avulsion (Burge, 2005; Burge and Lapointe, 2005). The effect of vegetation in slowing lateral migration and changing channel complexity has now been demonstrated for braided rivers using field observations, physical experiments and numerical models (Gran and Paola, 2001; Murray and Paola, 2003; Tal *et al.*, 2003). Thus, while confluences may be significant in the morphology and dynamics of a number of multiple-channel river types with a range of channel stability, it is in braided rivers that the morphodynamics and function of unconfined confluences is best exemplified.

Much of the research on confluence dynamics and braided-river morphology has been done in gravel-bed rivers, and it is on this river type that this chapter focuses. The overall goal is to review, and add new observations and ideas to, current understanding of confluence morphodynamics and sedimentology primarily in gravel braided rivers and thus (indirectly) to illustrate ways in which unconfined confluences in this setting may differ in characteristics and function from those at tributary junctions in river networks.

## General characteristics and significance of confluences in braided channels

Active confluences are significant elements of braided-river morphology because they are funnels for bedload transfer along the river and affect rates of transport, the downstream distribution and redeposition of transported sediment and, therefore, channel morphology and dynamics. They are zones of distinctive flow structure and dynamics, leading to local bed scour and fill as well as significant bar deposition and spatial sorting of grain sizes in gravel-bed rivers. The local scour associated with confluences, and the related flow structure, have drawn much of the attention of researchers (Best and Rhoads, this volume, Chapter 4; Biron and Lane, this volume, Chapter 3), but the influence of confluence zones extends beyond this immediately obvious feature, affecting downstream patterns of channel migration, bifurcation and avulsion and the channel-pattern dynamics in general (Smith, 1973; Mosley, 1976; Hein and Walker, 1977; Ashmore, 1982, 1991; Southard *et al.*, 1984; Davoren and Mosley, 1986; Ferguson *et al.*, 1992).

Many researchers have identified confluences and their associated bed scour and bar deposition as a building block of braided-river morphology with distinctive 'unit processes' (Ferguson, 1993). The confluence-bar-bifurcation unit is seen as a basic morphological component of braided channels (especially in gravel), which is equivalent to the pool-riffle or pool-bar unit of single-channel streams. However, not all anabranch confluences have distinctive and well-developed flow structure, bed scour and associated deposition. Figure 7.1(a) shows a reach of a gravel braided river with several confluences, illustrating the variety and complexity of confluence planform (and hence topography and dynamics) in a typical braided river. There are few confluences with two well-defined channels of similar size, and many have multiple confluent channels that converge progressively over some distance. Pronounced bed scour is a feature of many confluences (Figure 7.1(b)), although the size and depth of scour also varies, depending on confluence planform geometry and other factors (see below). Single anabranches of braided rivers also contain simple pool-riffle units, with significant local scour and deposition

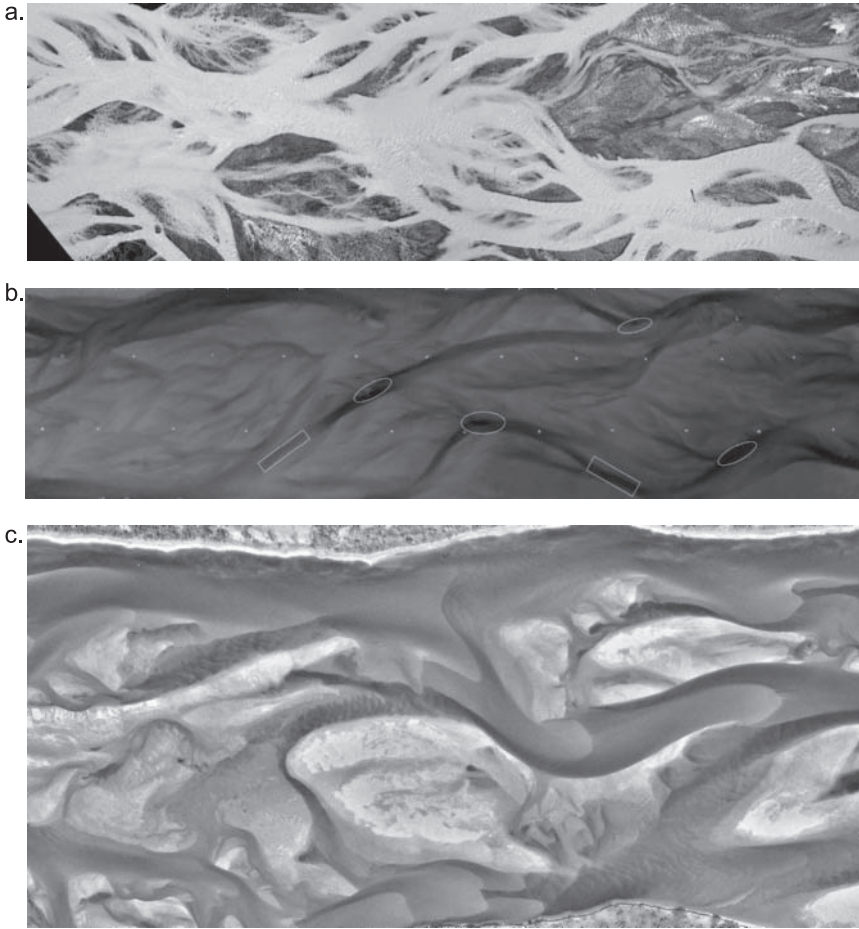


**Figure 7.1** Examples of confluence zones in braided rivers: (a) ortho-photo of a reach of the Sunwapta River, Canada, highlighting complex planform morphology of most confluences. Flow is from left to right; (b) DEM of a physical model (approximately 1:30 scale) of a gravel-bed braided river in a laboratory flume. The image covers an area in the model approximately 12 m x 3 m. Darker shades indicate lower elevation. Note deep scour associated with confluences (ovals) and bend scours (rectangles) in several locations. Flow was left to right; (c) aerial photograph of the sand-bed, braided South Saskatchewan River, Canada. Flow is left to right and darker areas in the channels are areas of deeper flow (scour).

that are also important in braided-river morphology, and some of these features can be seen in the digital elevation model (DEM) in Figure 7.1(b).

There are few measurements of flow structure in braided-river confluences, but the main elements of the structure, at least in symmetrical, Y-shaped confluences, are similar to those found in confined confluences with similar planform configuration and channel geometry (Ashmore *et al.*, 1992; McLelland *et al.*, 1996). There is a strong shear layer

in the centre of the confluence, and secondary flow is dominated by a double-helical circulation with a downward component in the shear zone and flow obliquely outward at the bed (Biron and Lane, this volume, Chapter 3). This structure will inevitably be different in less-symmetrical confluences with more-complex morphology (Ashmore *et al.*, 1992), but this has never been documented.

While anabranch confluences do occur in sand-bed braided rivers (Klaassen and Vermeer, 1988; Bristow *et al.*, 1993; Best and Ashworth, 1997; Sambrook Smith, *et al.*, 2005), their characteristics have not often been analysed beyond simple descriptions of morphology and/or sediments, and descriptions of sandy braided-river morphology focus much more on the bars, dunes and other bedforms (e.g. Collinson, 1970; Smith, 1971; Cant and Walker, 1978; Sambrook Smith *et al.*, 2005, 2006). Scour in sand-bed braided rivers occurs at confluences (Figure 7.1(c)) and also as local deep troughs alongside individual bars that evolve rapidly in shape in response to the evolution of bar morphology. In general, channels in sandy rivers are also less well defined than in gravel-bed channels, resulting in an impression that confluences and confluence scour are similarly much less well defined in sand-bed rivers, except when forced around, for example, vegetated islands. The major distinction presumably arises from differences in bed-material mobility and dominant channel-scale bedforms between the two cases, as well as the effects of sand dunes that affect local flow and bedload transport patterns in larger sand-bed rivers (Parsons *et al.*, 2007).

Bed morphology at well-defined, two-channel, symmetrical confluences is characteristically a spoon (at high confluence angles) or trough (at low angles) shape (Figure 7.2) (see Best and Rhoads, this volume, Chapter 4, for more detail on confluence morphology). The upstream entrance to the confluence may have high-angle avalanche faces, although this varies with the depth of the scour relative to confluent-channel depth and bed-material grain size. These features are more pronounced in higher-angle confluences (where scour depth is greater) and when the confluent channels are of a similar size. When confluent channels are of unequal size, an avalanche-face bar may prograde into the confluence from the larger channel (Figure 7.2(b)) (Best, 1986, 1988; Ashmore, 1993) or may be entirely absent (Figure 7.2(e)). In high-angle confluences, it is common to find submerged 'wings' of finer sediment deposited on either side of the downstream part of the scour pool, apparently related to bed-flow vectors diverging strongly at the centre of the confluence and pushing sediment out towards the channel margin (Figure 7.2(a–c)). Typically, there is bar deposition along the margins of the confluence and often in the centre of the channel downstream of the confluence (Smith, 1973; Ashmore, 1982, 1993; Davoren and Mosley, 1986; Best, 1986), although this may be restricted to confluences at higher angles (Mosley, 1976) (Figures 7.1 and 7.2(a) and (c)). Lateral deposition is more pronounced when the confluent channels are unequal and the confluence migrates towards the smaller confluent channel. In these cases, the overall morphology becomes very similar to that of bend scour and deposition in a single, low-sinuosity channel.

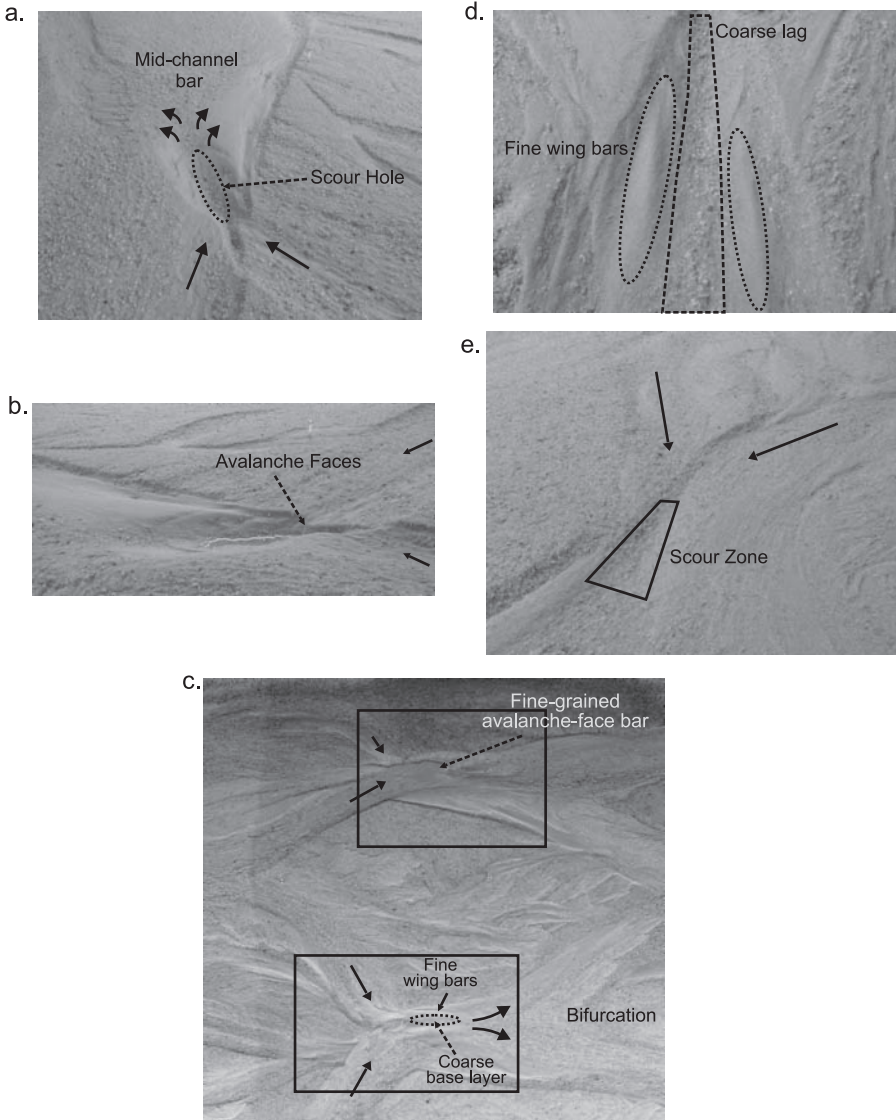


**Figure 7.2** Examples of confluence-zone morphology in a small-scale physical model of a gravel-bed braided river with the water drained: (a) oblique view looking downstream of a symmetrical confluence showing avalanche faces, scour hole, downstream divergence and bar formation, and lateral sorting of particle size; (b) side view (flow was right to left) of scour hole and avalanche faces at a confluence; (c) ortho-photo of an area of the river showing both symmetrical (lower box) and asymmetrical (upper box) confluences and associated features and sorting patterns. Image area is approximately 3 m x 3 m and flow is left to right; (d) oblique, close-up view of symmetrical scour hole looking upstream and illustrating the low relief 'wings' of fine deposition on either side of the scour hole with area of coarse particles in between; (e) oblique, upstream view of an asymmetrical confluence with minimal scour and sediment sorting.

## Confluence scour depth

Analyses of scour depth at confluences have been approached either by controlled experiments on small-scale, single confluences using fixed (or partially constrained) morphology (Mosley, 1976; Best, 1988) or by measurements of freely developed confluences in braided rivers or physical models (Ashmore and Parker, 1983). While the experiments on single confluences can be used to isolate the effects of particular variables, they do not allow the full range of adjustment of natural, unconfined confluences. Mosley (1976) supposes that his single-confluence measurements represent unconfined confluences in a braided river, but presents only informal descriptions from the field as supporting evidence. Measurements in natural confluences may identify the range of variability in morphology but, even so, measurements tend to focus on simple morphologies similar to the controlled, single-confluence experiments. There has been no systematic study of the morphological variation or range and frequency of scour depth within a reach of a braided river in relation to the range of confluence morphology.

The data from single, fixed-configuration confluences (e.g. Mosley, 1976; Best, 1988) show that maximum (absolute) scour depth, or scour depth relative to the depth of incoming channels, increases with increasing confluence angle (up to about  $90^\circ$ ) (Mosley, 1976; Best, 1986, 1988) and with increasing equality in the flow characteristics (discharge or momentum) of the confluent channels for a given total discharge. Confluence depth is typically two to four times the mean depth of the confluent channels (Mosley, 1976; Best 1986) but is lower in more-cohesive material (Mosley, 1976). There is no significant increase in depth at the confluence when confluence angle is less than about  $15^\circ$  (Best, 1986). There is also a significant effect (reduction in depth) due to increased sediment delivery to the confluence (Mosley, 1976).

These effects of angle, discharge ratio and sediment delivery are also observed in natural anabranch confluences and in physical models of braided rivers, confirming that the fixed-geometry laboratory confluences represent some of the major features of simple configurations in unconfined confluences (Ashmore and Parker, 1983) and showing that these relationships are consistent over a wide range of physical scales (see Best and Rhoads, this volume, Chapter 4, Figure 4.2 and Sambrook Smith *et al.*, 2005, Figure 2). Typical maximum flow depth at well-defined natural confluences is three to five times the mean confluent-channel depth for confluence angles from  $30^\circ$  to  $100^\circ$  (Ashmore and Parker, 1983; Klaassen and Vermeer, 1988) in both sand- and gravel-bed rivers. In the sand-bed Jamuna River, Klaassen and Vermeer (1988) observed lower relative scour depths, for given discharge ratio and confluence angle, than in gravel-bed rivers (Ashmore and Parker, 1983) and speculate that this is related to the large suspended sand load of the Jamuna River at high flow, but there may also be an effect due to channel size alone.

Relationships between scour depth and confluence angle and discharge ratio have greater scatter in natural confluences than in fixed-geometry laboratory experiments

(Ashmore and Parker, 1983; Ashmore, 1985). There may also be an effect on scour depth due to bed-material size, sorting or mobility (Ashmore and Parker, 1983), but this has not been clearly established. The greater scatter in relationships between scour depth and confluence geometry in natural confluences is presumably the consequence of greater variation in morphology (seldom are they the neat, Y-shaped planform of fixed-geometry experiments), temporary effects of flow or bedload variation at the time of measurement and the possibility (especially in the field) that measurements are made under non-equilibrium or evolving flow field, morphology and confluence geometry. Flow stage may also affect scour depth directly and the relative flow depth in the confluent channels and confluence. Observations of gravel-bed rivers indicate that confluences do not fill with sediment during the falling stage except for some reworking of steep, avalanche faces in some cases. Further details on these aspects of confluence morphology are in Best and Rhoads (this volume, Chapter 4).

Much of the focus of the analysis of confluence scour depth has been on maximum confluence depth relative to the mean depth of the confluent channels. Data show self-similarity in relative flow depth over a range of confluence scales and in particular show the effect of confluence geometry and discharge ratio on confluence depth in a gravel-bed river. While the focus has been on relative depth, little attention has been paid to absolute depth at confluences, which has been shown to have a clear relationship with total discharge at confluences in gravel braided rivers (Mosley, 1981; Ashmore, 1985). Further analysis of data from the Sunwapta River and from physical model experiments (Ashmore, 1985) suggests that maximum confluence flow depth follows a relationship much like the mean- or maximum-depth relationships in standard hydraulic-geometry equations for stable gravel channels. Figure 7.3 illustrates this using maximum flow depth at confluences compared with mean and maximum depths of anabranches immediately upstream of confluences in the Sunwapta River and in physical models of a braided river. The depth–discharge relationships and ratio of maximum to mean depth (1.3–1.5) for the anabranch confluences are very similar to those for stable, single, gravel-bed channels (Hey and Thorne, 1986), which confirms the reliability of the data. Presumably, the exact discharge–depth scaling relationship will vary with confluence geometry, but existing data are insufficient to confirm this.

For a given total discharge, typical scour depth at confluences is greater than the maximum and mean depth of the confluent anabranches by a factor of about two for maximum depth and a factor of three for mean anabranch depth. This is consistent with the relative depth data discussed above. Maximum anabranch depth (rather than mean) is used here because confluence depth is also a maximum, not a cross-section, mean. Note also that the increase in discharge alone at a confluence is expected to cause an increase in mean depth by a factor of 1.2–1.3 in symmetrical confluences. In asymmetrical confluences, the increase in confluence discharge is smaller relative to the discharge of the larger confluent channel, and this may partially account for the lower

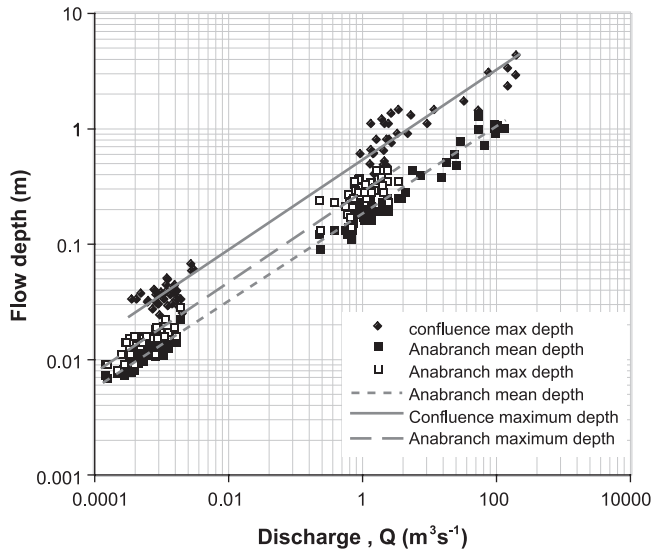


**Figure 7.3** Flow depth versus discharge in confluences and upstream anabranches (single channels) for confluences on Sunwapta and Ohau Rivers (from Mosley, 1981) and unconfined confluences in a physical model of a braided river (data from Ashmore, 1985) showing almost identical depth scaling with discharge for confluences and single channels.

relative scour depth at asymmetrical confluences. The analysis also demonstrates that maximum confluence depth follows a hydraulic geometry relation with an exponent almost identical to those for mean and maximum anabranch depth (all three regressions yield exponents of 0.38–0.39) and very similar to those typically found for the mean and maximum depth of gravel-bed channels (Hey and Thorne, 1986). The differences in absolute scour depth are expected to be smaller at lower confluence angles and in asymmetrical confluences, but it is likely that the overall discharge scaling relationship is preserved.

The analysis of confluence morphology in terms of scour depth and easily measured variables, such as confluence angle and relative discharge of the confluent channels, is clearly a simplification of the physics and morphology of the confluence. These may be viewed as surrogates for more direct physical controls (Roy and Lane, 2003) but also miss important complexities and differences in confluence geometry. Measurement and computational flow modelling of flow structure at confluences has led to considerable insight into the effects of specific aspects of morphology on flow structure, but little progress on the feedback of between flow and spatio-temporal variation in bed-material transport at the timescale of the significant morphological development of confluences (Ashmore, 1993; Roy and Lane, 2003). Although there are descriptions of key features of unconfined and developing confluences, there has

been no analysis of the complete three-dimensional geometry of confluence scour that takes our understanding beyond the prediction of maximum scour depth. There are very few data on even simple aspects of confluence shape and limited descriptions of major morphological features of confluences. In the case of unconfined confluences, such as those in braided rivers, this is clearly an important area for future research that may be led by new developments in computational flow modelling and also by advances in the measurement of complex geometry and sediment-sorting patterns discussed below.

## Confluence kinetics and bar formation

It is apparent from the earliest experiments that confluence geometry adjusts to changes in the confluent flow and sediment supply (see Best and Rhoads, this volume, Chapter 4). Mosley (1976) argues that the geometry of the upstream channels could be regarded as independent of the confluence geometry and that the confluence responded largely to conditions upstream. For example, the orientation of the confluence channel tends to rotate to reflect the balance of flow and sediment input from the confluent channels (Mosley, 1976; Ashmore, 1982, 1993; Best 1988). Mosley (1976) developed a simple total-momentum relationship for the confluent channels that predicts the orientation of the channel exiting the confluence relative to the confluent-channel angles. This appears to be different from the predictions developed for branching networks (Horton, 1945; Howard, 1971) in which the slope ratio is the primary predictor of exit angle, although Howard's (1971) modified equation based on discharge ratio gives a reliable prediction of exit angle in some cases (Mosley, 1976). A modification of Howard's (1971) optimization approach (Roy, 1985), based on analogy with locational analysis using stream power or total flow resistance, predicts that junction-angle asymmetry is controlled by the relative discharges of the confluent channels and by the downstream hydraulic geometry with respect to average flow velocity. The importance of discharge asymmetry is consistent with other models and with observations in braided rivers and laboratory experiments, but the model has not been tested on unconfined confluences in braided rivers.

When the confluence is formed by two channels of equal momentum (or discharge), the longitudinal axis of the confluence tends to bisect the confluence angle. When the confluent channels have unequal discharge, the confluence axis rotates to align more closely with the larger channel and the scour shifts laterally within the confluence towards the smaller of the confluent channels. This is often associated with the progradation of a sediment lobe or bar into the confluence from the larger channel (Ashmore, 1982; Best 1986). These shifts of confluence position have also been observed in large sand-bed rivers (Klaassen and Vermeer, 1988; Best and Ashworth, 1997).

Bar deposition and the development of new bifurcations is common downstream of pronounced confluences. In some cases, this can be seen to originate with the passage of a pulse of bedload through the confluence from upstream, re-forming downstream of the confluence as a prograding sediment lobe (Ashmore, 1993). This lobe, accompanied by channel widening, then forms the core of a new lateral or mid-channel bar and subsequent bifurcation or cut-off leading to renewed braiding. The deposit at the bifurcation is often built subsequently by gravel sheets migrating through, and directed by, the upstream confluence. It is possible that in some cases the material scoured at the confluence initiates the downstream bar formation but this has never been directly tested. Observations in single channel pool-bar sequences (e.g. Pyrcz and Ashmore, 2005) indicate that most of the particles eroded from the pool are deposited on the next bar downstream and it is likely that the same is true in the case of confluences. Recent radio-tracing observations (Obermoser, 2004) have shown that grains introduced upstream of the confluence pass through the confluence and are deposited in the downstream bifurcation, as are particles introduced directly into the confluence. This is consistent with earlier suppositions (Carson and Griffiths, 1987) that the confluence operates mainly as a transfer zone between upstream lateral-erosion sites and downstream bar deposition, and that particle transfer occurs in short steps commensurate with the bar-pool-bar spacing.

Confluences may also cause bar incision and erosion if expansion (associated with an increased flow in the confluent channels), reorientation or downstream migration (caused by migration of the confluent channels) brings the confluence closer to the downstream bar or changes the geometry of the channel network downstream (Ashmore, 1993). Lateral migration of a confluence, away from the larger of the confluent channels, can produce extensive bar deposits similar to point bars in low-sinuosity, single-channel rivers (Bluck, 1971, 1974; Ashmore, 1982, 1993). Distinctive lateral accretion deposits of overlapping gravel sheets can be seen alongside laterally migrating confluences. The adjustability and response of confluences to the number and geometry of confluent channels and to changes in the balance of discharge and sediment supply cause a wide range of responses. Confluences can migrate laterally or downstream, expand or contract in extent, and rotate into new orientations. The long-term development of single, long-lasting confluences can therefore affect the pattern of sedimentation and braiding morphology for much of the river width and can propagate downstream through successive confluences (Ashmore, 1993). Ultimately, all confluences have a defined lifespan, at the end of which they are abandoned, become single channels or are filled by migration of the nearby channels (Ashmore, 1993). However, there has been no analysis of the life history of confluences from which the length and direction of typical migration pathways, along with variation in dimensions, might be developed. The processes of migration, the way in which they are abandoned and filled, and their morphology, may all be a significant influence on the geometry of braided river deposits (see below).

## Confluence spacing and the length-scale of braided morphology

The confluence and bifurcation of anabranches are defining features of braided river morphology. The downstream spacing of these features is controlled by channel processes locally within the river channel and by the overall size of the river. Thus, indirectly, drainage basin properties may influence confluence spacing but not in the direct way in which tributary-junction nodes in a branching channel network are controlled by basin-scale processes and structure.

The spacing of confluences and bifurcations arises because they are part of the basic pool-bar morphological unit apparent in many coarse-bed channels (Ferguson, 1987, 1993). While in single-channel streams the pool-bar unit is fundamental to the geomorphological functioning of the river and the length scale of the morphology (bend wavelength), in braided channels the equivalent morphological unit is the confluence–diffluence. This can be seen directly by observing that braiding in laboratory models often develops by the chute cut-off of alternating bars in an initial sinuous, single channel, or multiple-row bars in a wide channel (Fujita, 1989), and that the downstream spacing of the resulting confluences or diffluences is similar to the wavelength of the initial bars (Ashmore, 1985). The initial cut-off produces two channels, both with bends, that diverge upstream of the bend apexes and converge downstream. The converging segments merge close to the apex of the second bend in the initial single channel. In this way, the downstream spacing of confluences is controlled by the wavelength of the initial single channels and by the wavelength of the individual anabranches, both of which are related to the fundamental bar-pool spacing (Bertoldi, 2005). Presumably, as with pool-bar length in single channels, confluence–diffluence spacing in braided rivers is controlled by the size (width or discharge) of the confluence channel: larger confluences would have greater distances to the downstream bifurcation.

This effect of channel size or discharge on morphological length scale can be seen in relation to the total discharge of the river (Ashmore, 2001, Figure 1) in which the average spacing of nodes (confluences or bifurcations) in the braided network increases approximately as the square root of total river discharge. This may be expected on the basis that the total discharge of the stream is likely to be a strong control on the width of individual channels within the braided system. A larger total discharge will result in larger average anabranch widths, given that the proportional allocation of flow between channels is similar in streams of different discharge (Mosley, 1983, Figure 23). The overall trend parallels that of the well-known meander wavelength–discharge relationship but the braid wavelength is shorter for a given discharge, presumably because the braided-river discharge is divided among several channels. Dividing the flow into more than one channel reduces the characteristic wavelength for each channel and therefore for the river as a whole. One implication of this is that, for a given discharge, rivers with higher

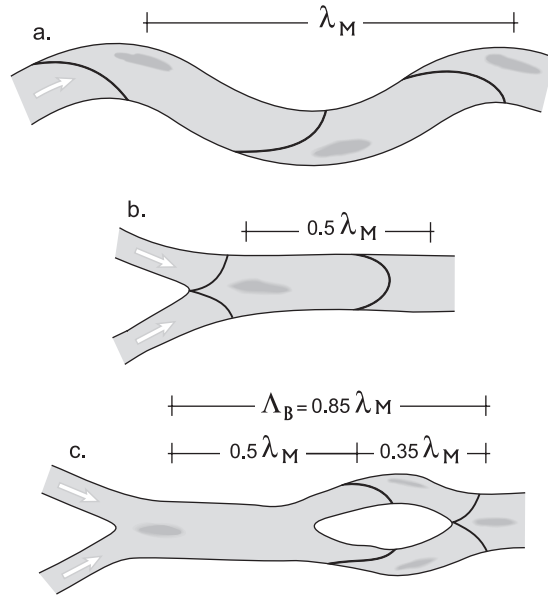


**Figure 7.4** A possible relationship between meander wavelength and braid wavelength (confluence spacing) of a simple braided channel for identical total channel-forming discharge.

braiding intensity will have a smaller average anabranch width and therefore shorter confluence–bifurcation spacing.

Braid wavelength, as defined in the previous paragraph, is shorter than meander wavelength for a given total discharge by a factor of about 0.88, based on data in Ashmore (2001) and standard relationships for meander wavelength. Assuming the simplest scenario of a flow combining and dividing equally in a single confluence–bar sequence, and based on the square-root relationship between discharge and wavelength, it is possible to see how this relationship might arise (Figure 7.4). The combined flow downstream of the confluence would have a wavelength equivalent to the pool–bar spacing (half the wavelength) in a single channel with the same discharge. The channels downstream of the bifurcation tend to form pool and bar topography at a scale commensurate with their discharge, which is half of the total discharge. This produces a pool–bar spacing 0.7 times shorter than in the channel upstream of the bifurcation, in other words 0.35 times the pool–bar spacing of a single channel with the same discharge. This results in spacing between successive confluences (or bifurcations) 0.85 times the meander wavelength of the equivalent single channel. This is clearly a simplified scenario but it may provide the basis for a theoretical analysis of the distribution of length scales of braided–river confluence–bar sequences and for the river morphology as a whole.

## Sediment transport and sediment budgets

The overall flow structure and pattern of flow velocity, shear stress and bedload associated with confluence zones is important in understanding confluence development and downstream effects on the stream network. Experimental and theoretical studies of the stability and morphology of bifurcations in braided rivers have emphasized the potential effect of migrating bars and transverse flow on the evolution of bifurcations (Bolla Pittaluga *et al.*, 2003). The few synoptic studies of the rate and patterns of bedload transport in confluences (e.g. Thompson, 1985; Davoren and Mosley, 1986; Ferguson *et al.*, 1992; Goff and Ashmore, 1994; Luce, 1994; Varkaris, 1999) show that the confluence is a zone of generally higher bedload transport rate that peaks near the downstream end of the scour pool at the transition into the downstream depositional area. An overall decrease in average shear stress then accompanies downstream deposition, but this depends on the details of the morphology in particular cases. This fits with Carson and Griffiths' (1987) concept of the confluence as bedload conduit between upstream bar erosion and downstream deposition and implies that, in a developed confluence, vertical scour contributes little to the total transport.

The pattern of flow, bedload and morphological change varies as the confluence zone develops and the confluence fluctuates between erosional and depositional states (Ferguson *et al.*, 1992; Luce, 1994; Varkaris, 1999). For example, repeated mapping of the morphology of a developing confluence and downstream bar in the Sunwapta River (Luce, 1994) revealed daily changes in the spatial pattern of morphological change and erosion, deposition and bed-material transport within the confluence zone as the confluence morphology evolved. Often, the confluence zone did not have the expected pattern of erosion in the centre of the confluence and sedimentation downstream but was either largely erosional or depositional over its length before becoming abandoned, and partially filled, as a consequence of channel migration. The downstream pattern of inferred bedload-transport rates varied accordingly. Because the confluence was eventually abandoned and partially filled, the whole confluence zone showed net deposition during the observation period, and deposition volumes were greatest in the scour zone.

A similar analysis of sediment budgets from an evolving confluence zone in a physical model of a braided river (Varkaris, 1999) showed that, during development and periods of morphological stability, the cross-section averaged transport rate (back-calculated from DEMs of topographic change) generally increased through the confluence, peaking at the scour hole or at the downstream end of the confluence, and migrating with the scour hole (Figure 7.5). Often, the peak in transport rate was related to the lateral erosion and migration of the confluence, rather than scour enlargement. However, as the confluence became less active, the locus of maximum transport rate became less tied to confluence morphology and shifted upstream of the confluence during net deposition at the confluence or the onset of local scour in the upstream anabranches.

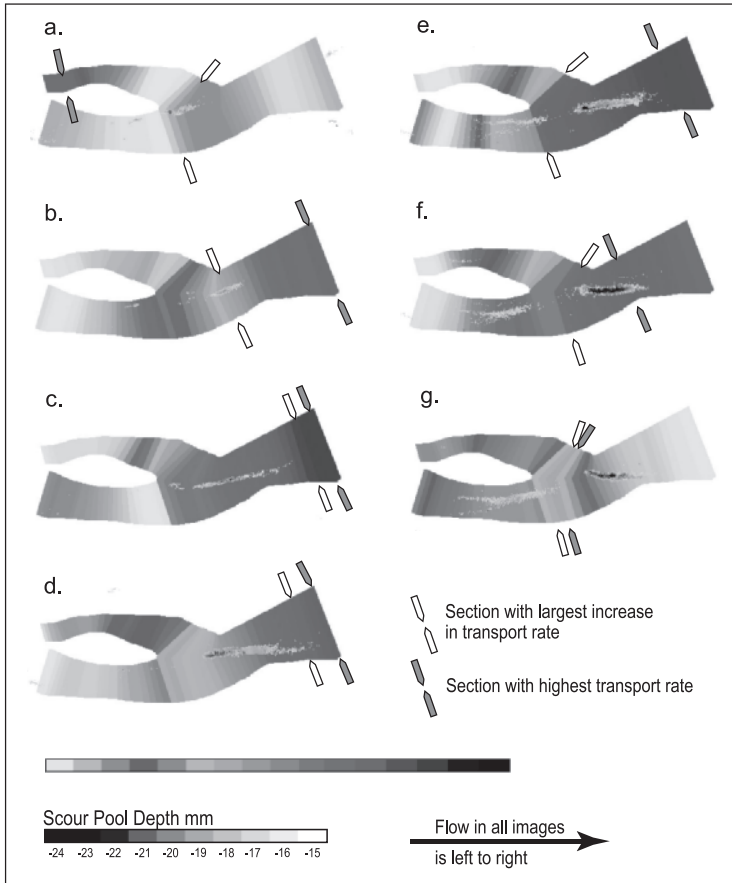


**Figure 7.5** Maps of a sequence (a–g) of changes in the downstream pattern of bedload transport rate in two confluent anabranches and the downstream confluence in a physical model of a braided river over a period of approximately one hour. The plots are approximately 10 minutes apart in time. Colour transition from blue to red indicates increasing transport rate and the location and bed elevation in the scour hole is shown in grey tones superimposed on the transport pattern. Cross-section average transport rates were calculated by morphological methods (Ashmore and Church, 1998) at a series of closely spaced cross-sections based on high-resolution, photogrammetric DEMs (Stojic *et al.*, 1998). Flow is left to right. A colour reproduction of this figure can be seen in the colour section towards the centre of the book.

Particular modes of confluence adjustment and change are therefore expected to have associated patterns of erosion/deposition and therefore distinctive downstream trends in bedload transport through a confluence zone, tied to the particular morphological changes (Ashmore, 1993; Luce, 1994; Varkaris, 1999). The confluence itself is by no means always, or even mainly, a zone of erosion and maximum bedload-transport rate. Thus, confluences have a life history during which the flow structure, spatial

pattern of bed-material transport and associated morphological change (sediment-flux convergence or divergence) undergo constant change along the time line from initial development and scour, through phases of development and migration to abandonment or infilling, during which the confluence is a net source, a transfer zone or a net sink for bed material. In this respect, confluence-zone dynamics is an important element of the spatial and temporal variation of the bedload-transport rate in braided rivers, driven by the inherent instability of braided-river morphology.

There is a very clear link between confluence-zone morphodynamics and the spatial and temporal pattern of bedload flux locally along the river. It is well known from physical model studies that the bedload-transport rate, integrated across the river, fluctuates over a range of frequency and amplitude even at constant river discharge (Ashmore, 1988; Young and Davies, 1991; Hoey and Sutherland, 1991; Hoey *et al.*, 2001; Bertoldi *et al.*, 2006). One approach to explaining these fluctuations is to envisage a spatial pattern of variation in shear stress along the braided network associated with major morphological features of braided morphology, such as confluences, that cause downstream changes in the transport rate related to the changes in shear stress (Davoren and Mosley, 1986; Hoey *et al.*, 2001). An alternative is to view this variation in transport rate as being related to the processes of morphological change, such as bar migration, avulsions, cut-offs and the formation/filling of scour holes (Ashmore, 2001). These may not be explicitly predictable and tied to channel hydraulics in a system that is intrinsically unstable and typically in disequilibrium (Ashmore, 2001; Paola, 2001).

Confluence formation is one of a set of processes that may generate pulses and fluctuations in the bedload transport rate as they pass through cycles of formation, migration, stability and abandonment. However, they represent one of several sets of such processes, which include scour in other locations such as bar margins or bends in single anabranches. Analyses of physical model data on braiding and sediment transport (Ashmore, 1988; Hoey and Sutherland, 1991; Bertoldi *et al.*, 2006) suggest that a variety of scales of morphological processes can be associated with bedload fluctuations. The longer-period fluctuations (one to eight hours in a typical model) can be related to the temporal development of confluences and bifurcations and to the period of overall shift or avulsion of the channel network that induces a phase of increased transport rate as the network adjusts to the new configuration (Bertoldi *et al.*, 2006). In all cases, the development and morphodynamics at nodes in the network are implicated, directly or indirectly, in the fluctuations of transport rate. The spatial patterns of bedload associated with confluences, along with their length scale and rate of migration, may be a significant control on the amplitude and frequency of bedload variation along a braided river and over time at a given cross-section. Direct measurements of these patterns using, for example, inverse methods based on mapping volumes of erosion and deposition (Ashmore and Church, 1998) are needed to provide the direct connection between confluence morphodynamics and the characteristics of the bedload time series and spatial patterns of variation of bedload in braided rivers. This will also help to address

the possibility (Carson and Griffiths, 1987) that the funnelling of bedload through active confluence zones may facilitate bedload transport in braided rivers to the extent that they do so more efficiently than single-thread channels.

## Sediment sorting and alluvial deposits

Much of the channel migration, bar deposition and development of bed topography in braided rivers can be related in some way to confluences and associated features and dynamics. One implication of this is that confluences may be a significant component of braided-river deposits. While this has been recognized by a number of sedimentologists (e.g. Bridge, 1993; Siegenthaler and Huggenberger, 1993, and see Best and Rhoads, this volume, Chapter 4), the evidence remains poor, the criteria for recognizing confluence deposits are unclear and there is no conceptual or quantitative model of the way in which confluence processes and features are preserved in sandy or gravely braided-river deposits.

The combining flows, abrupt changes in bed elevation and rapid erosion and sedimentation at confluences create the potential for distinct patterns of particle size sorting, especially in a gravel-bed river. Two primary effects are the oblique and diverging flows at the bed in the downstream parts of the confluence zone and steep avalanche faces at the upstream end of the confluence. In symmetrical, high-angle confluences, these sorting patterns may be very distinct and have pronounced, bilateral fining outwards from the thalweg in the scour pool (Figure 7.2(a–c)) driven by obliquely outward flow at the bed (Ashworth *et al.*, 1992; Bridge, 1993; Powell, 1998). This often evolves downstream into distinct coarse-grained deposits in the centre of the channel and on the downstream bar head (Figure 7.2(a)). At the same time, there may be vertical sorting by avalanching at the entrance to the scour pool, which tends to cause larger particles to fall to the base of the avalanche face, near the centre of the scour pool (Ashmore, 1982). In symmetrical confluences, this bilateral fining tends to dominate but is not ubiquitous (Jackson, 1994). In asymmetrical confluences, in which the outward-directed (at the bed) flow structure is less developed and in which the scour hole is smaller and occupies less of the channel width, sorting patterns are more variable and many have unilateral fining (fining towards the larger channel) as well as bilateral fining (Jackson, 1994) (Figure 7.2(c) and (e)). In more complicated confluences, the sorting patterns may be completely disrupted. Observations (Ashmore, 1985; Jackson, 1994) also show that sorting patterns are disrupted by gravel sheets and bedload pulses passing through the confluence. Under these conditions, sorting may be dominated by the internal sorting in sediment lobes emerging from the confluence, and by the normal flow structure in the confluence being disrupted. The overall consequence is that sorting patterns in many confluences constantly adjust to the prevailing geometry and sediment supply and are very sensitive to changes in any of these conditions.

Whether, and which, sorting patterns are preserved in the deposits depends on the manner in which the filling occurs and the development of the confluence itself. Examples of confluence deposits to date have tended to focus on static, symmetrical confluences with little analysis of if, and how, the sorting patterns evolve or are preserved during migration, morphological development and infilling. Focusing on symmetrical confluence morphology ignores the fact that most confluences in braided rivers have complex morphology and are seldom symmetrical. In terms of the preservation of associated deposits, it seems more likely that asymmetrical confluences, which migrate and infill much like low-sinuosity meanders, are more likely to have extensive preserved deposits (Bridge, 1993).

Within both sand and gravel braided rivers, confluences have the potential to migrate across a braid-plain and to erode to the greatest depth (Ashmore and Parker, 1983; Klaassen and Vermeer, 1988; Best and Ashworth, 1997; Sambrook Smith *et al.*, 2005), resulting in a significant preservation potential (Bridge, 1993; Siegenthaler and Huggenberger, 1993). Confluences must therefore have a significant influence on overall and maximum bed thickness. In the context of braided-river alluvium, confluence scour zones may constitute a large proportion of the preserved sediments (Cowan, 1991). If so, then the structure of braided-river alluvium may be largely explained by the migration and filling of confluences. However, there are relatively few examples of confluence scour deposits in the literature, and a number of these are essentially snapshots of a single scour feature (Williams and Rust, 1969; Cowan, 1991; Siegenthaler and Huggenberger, 1993; Heinz *et al.*, 2003). There is an apparent paradox that confluence zones are morphologically and sedimentologically significant but yet seldom feature in analyses and models of braided-river alluvium. Indeed, Miall and Jones (2003) wonder why more examples of confluence deposits were not found in the Hawksbury formation (an analogue for the Brahmaputra River's deposits). The answer may be that there is insufficient understanding of the geometry and internal structure of confluence deposits and that existing ideas of the likely characteristics of confluence deposits are incomplete. To date, there has been no systematic, process-based analysis of the morphological and sedimentological development of confluence zones to encourage the development of diagnostic features of confluence deposits.

While there are examples in the literature identified as preserved confluence deposits (Williams and Rust, 1969; Cowan, 1991; Siegenthaler and Huggenberger, 1993; Heinz *et al.*, 2003), it is apparent that deposits of static and migrating confluences will differ in sorting and geometry. An asymmetrical, migrating confluence may move across a braid-plain maintaining approximately the same geometry and flow structure as it migrates. In this way, the confluence erodes older adjacent deposits and is filled in, leaving an erosion surface at its base distinguished by a coarse, open-framework, layer. A possible example of this was provided by Heinz *et al.* (2003), who interpreted large sections of the ancient Rhine deposits to be confluence fills. An analysis of their data shows the aspect ratios of these confluence fills are similar to documented cases of gravel-bed

sheets (aspect ratio =  $\sim 15+$ ) rather than scours (aspect ratio =  $\sim 5$ ) (e.g. Sheets *et al.*, 2002). The migration of the confluences may explain these larger aspect ratios and thus the wide fills. This contrasts with the 'onion' structure of confluence deposits, identified by Siegenthaler and Huggenberger (1993), that may be indicative of a more stable confluence scour migrating only a small (less than the confluence dimensions) distance laterally and downstream. An intermediate example may be that of Wooldridge and Hickin (2005, Figure 12, p. 855), who document a possible example of a stalled and reactivated confluence scour zone. The depositional form resulting from confluence migration may therefore be a thick horizontal bed of massive or graded material – the type of geometry usually associated with bar deposits in previous studies.

Sedimentological analysis of braided and wandering rivers is becoming more quantitative and based on complete three-dimensional data and histories of deposit development in contemporary rivers from direct observation and shallow geophysical methods (e.g. Lunt *et al.*, 2004; Wooldridge and Hickin, 2005). The possibility of acquiring quantitative data on a wide range of morphological and sedimentological processes and characteristics now exists. These might include the length scale of bars and scours associated with confluences, the frequency distribution of scour depth, amplitude and spatial pattern of topography and topographic change and the typical distance and pathways of scour-zone migration. Quantitative analysis of relationships such as the distribution of bed thickness based on the amplitude of scour-bar topography, similar to that proposed for dune deposits (Paola and Borgman, 1991), are now possible. The technology for achieving this in the field has developed rapidly in the past decade (e.g. Chandler *et al.*, 2002; Westaway *et al.*, 2003), although turbid water still presents a problem for remote sensing and laser-based measurement of topography. In laboratory models, with reduced timescale, high-resolution DEMs may be acquired from laser scanning or photogrammetry (e.g. Stojic *et al.*, 1998, and see Figures 7.1(b) and 7.6(b), this chapter) at high frequency and over timescales commensurate with a complete reworking of the river bed and for channel length covering several confluence zones. At the same time, automated image analysis (e.g. Carbonneau *et al.*, 2005) can provide complete high-resolution mapping of grain size. The differencing of successive DEMs enables the measurement of the shapes of erosion and deposition volumes (e.g. Ashmore, 2001; Westaway *et al.*, 2003) that can be related to channel morphology and sedimentary processes. These data will also provide a source of verification information for numerical models (Doeschl and Ashmore, 2005).

As an example of the development and utility of this new type of data, Figure 7.6 shows a vertical image, derived DEM and grain-size map of a confluence zone in a physical model of a gravel braided river. DEMs (Figure 7.6(b)), with a resolution and precision of about 1 mm, were generated using Leica Photogrammetry Suite, and the images used in the photogrammetry were also used to produce calibrated grain-size maps based on textural analysis (Figure 7.6(c)) (Carbonneau *et al.*, 2005). The three images combined can be used to see morphological detail, measure topography and elevation distribution

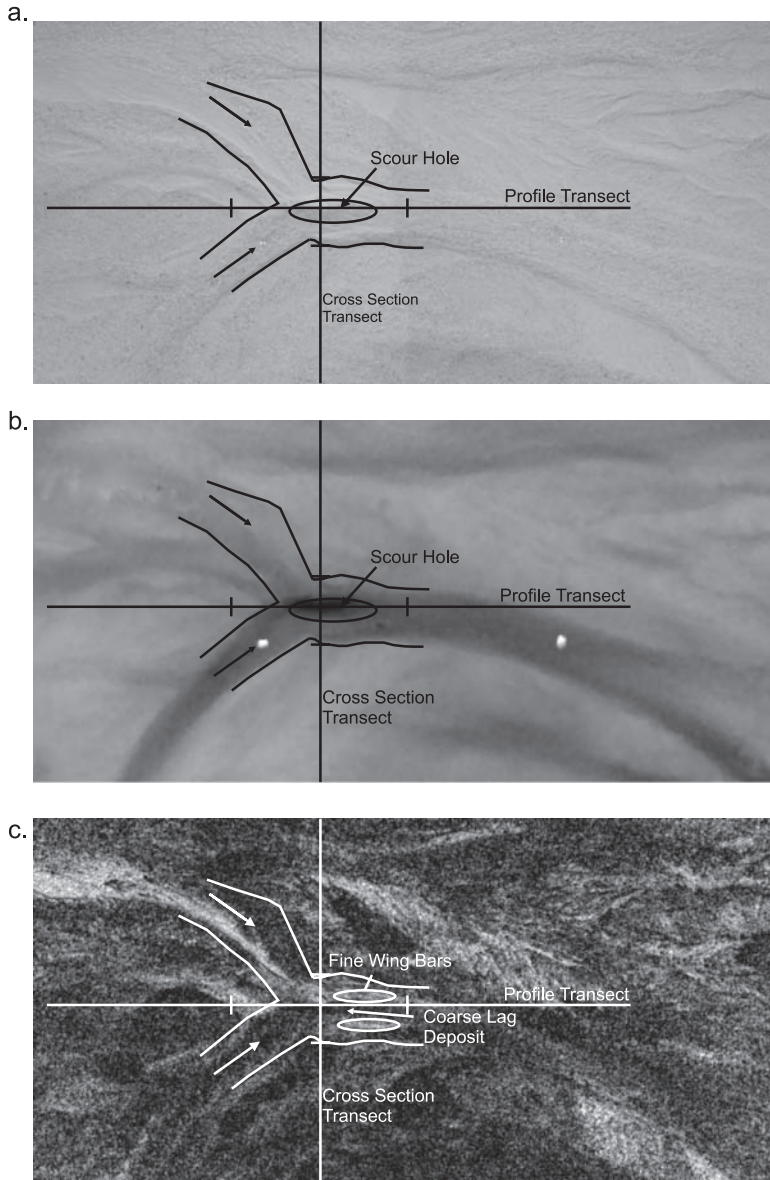


**Figure 7.6** Confluence scour zone in a braided-river model: (a) ortho-photo mosaic of the river bed at the confluence (drained of water) with approximate channel boundary outlined. Flow direction was left to right. The positions of the cross-sections in Figure 7.7(b) and (c) are shown, along with the position of the bounding boxes in those diagrams; (b) DEM of river bed at confluence. Darker areas represent lower elevations, lighter areas are higher elevations; (c) grain-size map of the river bed showing sorting patterns at the confluence. Lighter areas are fine-grained pixels and darker areas are coarse-grained pixels.

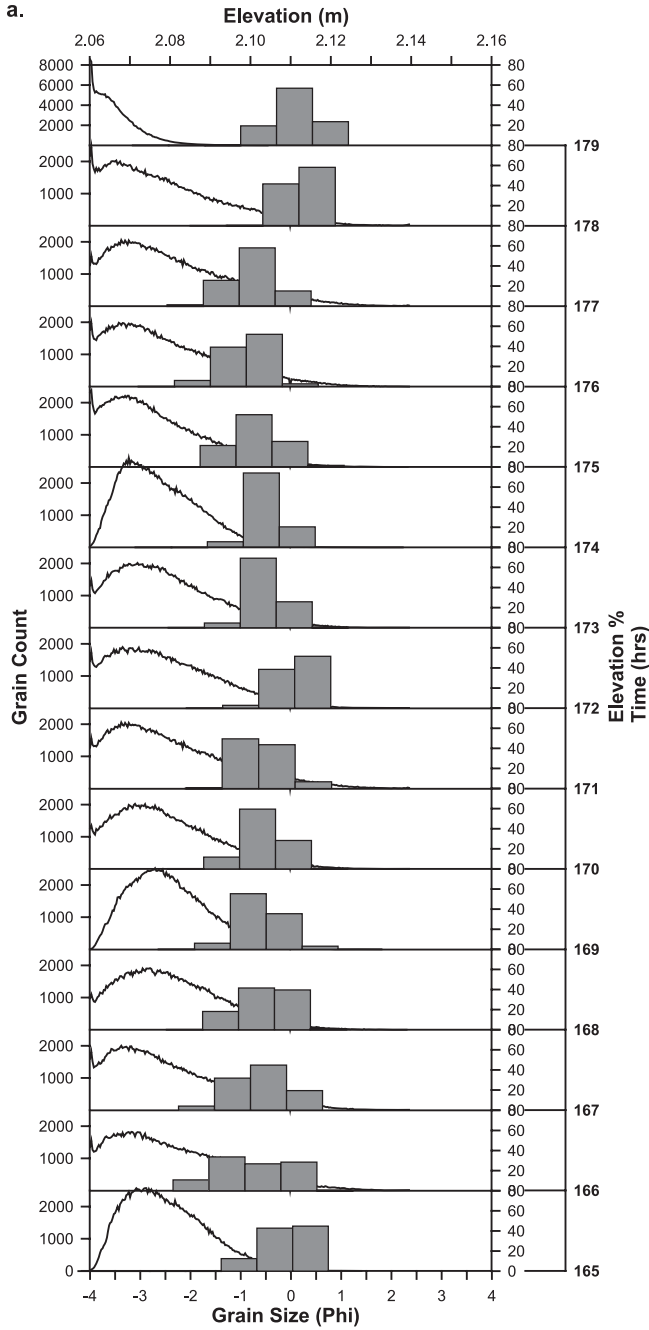
and correlate these with spatial and topographic grain-sorting patterns. For example, local areas of fine and coarse grains are readily seen in the area of the confluence scour. A sequence of such data through time enables the analysis of the changes in topography, elevation and grain-size distribution within a developing confluence zone and could be used to develop high-resolution, three-dimensional information on deposit geometry and grain size.

Figure 7.7 shows the overall pattern of elevation and grain size change within the confluence over a period of 15 hours. After initial scour and coarsening (Figure 7.7(a) (165–169 hr), there are further phases of filling and grain-size change before a final fill with coarse sediment from the true left confluence anabranch (179 hr). Further detail of sorting patterns can be obtained from single transects across the river in any orientation and a time series of transects can be used to visualize changes in these patterns. Transverse and longitudinal profiles (Figure 7.7(b) and (c)) show a complex relationship between grain size and bed elevation in general but also clear lateral sorting (fines input from left anabranch, coarser near the centre and at right anabranch) in the confluence scour hole and a coarsening at lower elevations, that may represent a basal scour layer, along the longitudinal profile. Temporal sequences such as these can be used to develop relationships between elevation and grain size and between elevation change and vertical fining or coarsening. These can then be used to construct a quantitative model of the braided-river deposit geometry in association with particular features and events and to evaluate the nature of the contribution from confluence morphology, kinetics and size sorting.

## Prospect

There is enormous scope and a need for analyses that build on the existing descriptions of the morphodynamics of unconfined confluences in braided rivers (see also conclusions of Best and Rhoads, this volume, Chapter 4). This will contribute insight into the comparative significance of confluences in the functioning of a range of multichannel river types, differences between sand-bed and gravel-bed rivers and the role of lateral (in)stability (e.g. through bank-vegetation effects) on confluence and river dynamics. In addition, there is the potential to increase our understanding of the morphology and dynamics of alluvial junctions in branching networks and their influence on sediment transport and river morphology.

A variety of new techniques make it possible to develop a more sophisticated and quantitative understanding of confluence behaviour in relation to a variety of problems. Locally at confluences there has been little analysis of the mutual interaction of flow, sediment transport, morphology and sediment-size sorting. Developments in numerical modelling (e.g. Bradbrook *et al.*, 2000; Biron and Lane, this volume, Chapter 3) hold great promise in this respect but at the same time techniques for synoptic



**Figure 7.7** Changes in topography, elevation and grain size within a developing confluence zone: (a) frequency distributions of bed elevation and grain sizes in the confluence through 15 hours of experiment time; (continued)

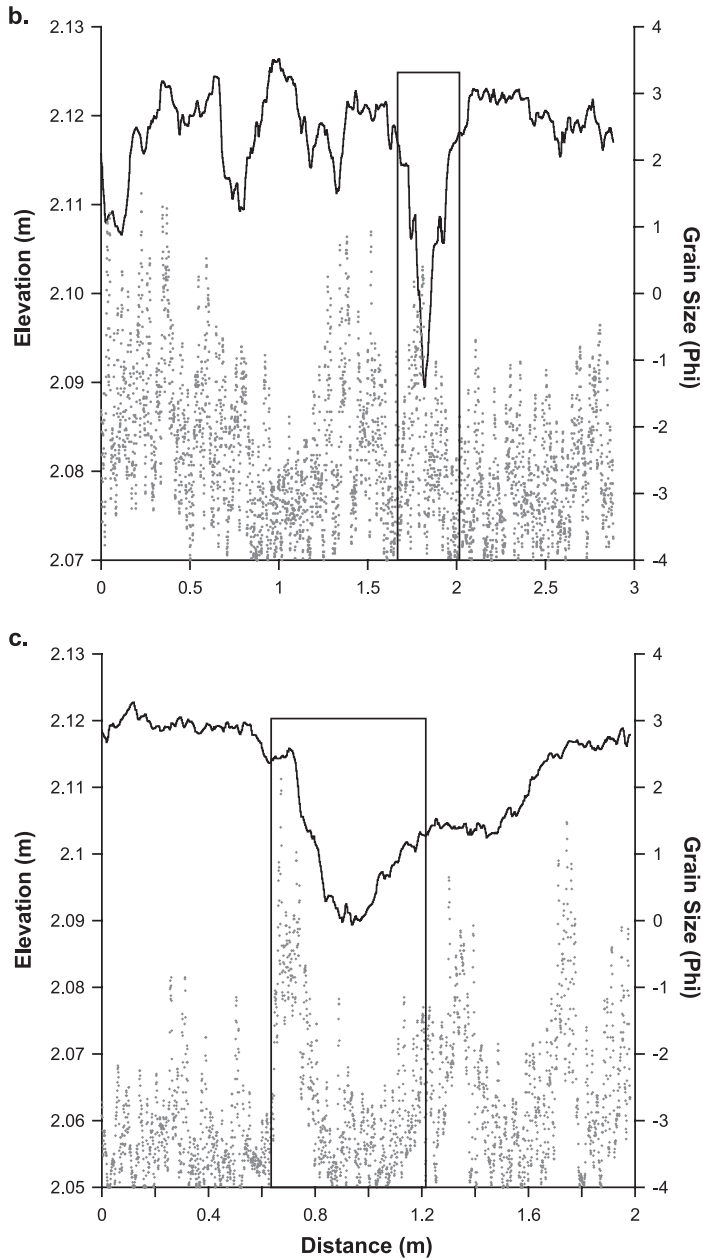


**Figure 7.7** (b) cross-section across the braided river bed showing variable bed elevation and grain size. The confluence zone is outlined. Lateral sorting is evident because finer material enters the confluence from the left anabranch, and secondary flow at the bed sorts the finer material to the margin of the scour hole. The scour hole is relatively coarse-grained but fine-grained 'wings' are prominent; (c) a long profile bisecting the confluence scour hole shows a steep avalanche face with normal fining trend down into the scour. The scour is lined with a coarse lag deposit, and coarse material is prominent along the length of the confluence zone.

flow, morphology and sediment-transport measurement are available for both field and physical model studies.

Beyond the traditional focus of work on confluences, there are almost no data on transport paths and the distribution of path lengths of particles in braided rivers and how these relate to the length scale of the confluence–difffluence units and to the flow structure in the confluence zone. There is scope here for active tracer studies in the field, direct observations in physical models and numerical tracer experiments on path lengths and storage times. Similarly, confluence migration and kinetics are understood conceptually but there has been no analysis of the physical processes by which these adjustments occur beyond the prediction of exit angles in stable confluences. This is important in understanding confluences as distributors of bed material and fine sediment. There is scope for further theoretical development based on work in the 1970s and 1980s, along with new physical experiments.

Spatial and temporal patterns of bedload through confluences and their role in observed fluctuations in bedload-transport rates over time and along the river are a significant aspect of the dynamics of confluences in this setting. Bedload transport rates can, and have, been inferred from measured topographic change in the field and in physical models, but more work is needed based on either direct flux measurements or inferred rates from topographic change (DEMs). Reduced-complexity, exploratory models of braiding exhibit this unstable behaviour in sediment output and there is scope for further theoretical developments using such models to understand the origin and characteristics of these fluctuations.

Finally, high-resolution data from DEMs and image analysis can also provide information on confluence dimensions, persistence and migration distances from which to develop models of confluence stability and controlling conditions and processes. When combined with grain-size mapping, there is the prospect of complete three-dimensional models of braided river sedimentology based on the quantification of river morphodynamics and grain-sorting patterns in physical models and in the field, where sedimentary structure can also be quantified from GPR (ground-penetrating radar) and other geophysical techniques. All of these components of confluence morphology and sedimentology can be seen to connect to one another, and this reflects the significance of unconfined confluences as elements of, and essential to understanding, the morphodynamics of braided rivers.

## Acknowledgements

This chapter is the result of periodic excursions by PA into braided-river confluence dynamics for more than 25 years. It reflects the influence and work of many people, beginning with John Shaw and Gary Parker and including several students (especially Jamie Luce, Duncan Jackson and Fred Varkaris) and collaborators who have worked

in the laboratory and on several field projects related to confluences and other aspects of braided-river dynamics. The research has been made possible by ongoing support from NSERC and by an infrastructure grant from Canada Foundation for Innovation. We are grateful to: Phil Ashworth for permission to use the photograph in Figure 7.1(c), Patricia Connor for preparing Figure 7.4, Fred Varkaris for permission to adapt Figure 7.5 from his thesis, Patrice Carbonneau for his work on automated grain mapping from digital images of the physical model used in Figures 7.6 and 7.7 and Karen van Koerkele for her work on the graphics. We thank André Roy and an anonymous reviewer for their comments.

## References

- Amsler ML, Ramonell CG, Toniolo HA. 2005. Morphologic changes in the Paraná River channel Argentina in the light of the climate variability during the 20th century. *Geomorphology* **70**: 257–278.
- Ashmore PE. 1982. Laboratory modelling of gravel braided river morphology. *Earth Surface Processes and Landforms* **7**: 201–225.
- Ashmore PE. 1985. *Process and Form in Gravel Braided Streams: Laboratory Modelling and Field Observation*, Ph.D thesis, University of Alberta, Edmonton, Alberta, Canada.
- Ashmore PE. 1988. Bed load transport in braided gravel-bed stream models. *Earth Surface Processes and Landforms* **13**: 677–695.
- Ashmore PE. 1991. How do gravel-bed streams braid? *Canadian Journal of Earth Sciences* **28**: 326–341.
- Ashmore PE. 1993. Anabranched confluence kinetics and sedimentation processes in gravel-braided streams. In *Braided Rivers*, Best JL, Bristow CS (eds). Geological Society Special Publication 75: London; 129–146.
- Ashmore P. 2001. Braiding phenomena: Statics and kinetics. In *Gravel-Bed Rivers V*, Mosley MP (ed.). New Zealand Hydrological Society: Wellington; 95–114.
- Ashmore P. 2003. Braided Channels. In *Encyclopedia of Sediments and Sedimentary Rocks*, Middleton GV (ed.). Kluwer: Dordrecht, The Netherlands; 85–87.
- Ashmore PE, Church M. 1998. Sediment transport and river morphology: A paradigm for study. In *Gravel-bed rivers in the Environment*, Klingeman PC, Beschta RL, Komar PD, Bradley JB (eds). Water Resources Publications LLC: Highlands Ranch, Colorado; 115–148.
- Ashmore PE, Parker G. 1983. Confluence scour in coarse braided streams. *Water Resources Research* **19**: 392–402.
- Ashmore PE, Ferguson RI, Prestegard KL, Ashworth PJ, Paola C. 1992. Secondary flow in coarse-grained braided river confluences. *Earth Surface Processes and Landform* **17**: 299–312.
- Ashworth PJ, Ferguson RI, Ashmore PE, Paola C, Powell DM, Prestegard KL. 1992. Measurements in a braided river chute and lobe II: Sorting of bedload during entrainment, transport and deposition. *Water Resources Research* **28**: 1887–1896.
- Benda L, Andras K, Miller D, Bigelow P. 2004. Confluence effects in rivers: Interactions of basin scale, network geometry, and disturbance regimes. *Water Resources Research*, **40**: W05402. DOI: 10.1029/2003WR002583.

- Bertoldi W. 2005. *River Bifurcations*, Ph.D thesis, Universita Degli Studi di Trento, Italy.
- Bertoldi W, Amplatz T, Miori S, Zanoni L, Tubino M. 2006. Bed load fluctuations and channel processes in a braided network laboratory model. In *River Flow 2006*, Ferreira RML, Alves ECTL, Leal JGAB, Cardoso AH (eds). Proceedings of the International Conference on Fluvial Hydraulics, Lisbon, 6–8 September 2006. Taylor and Francis; London.
- Best JL. 1986. The morphology of river channel confluences. *Progress in Physical Geography* **10**: 157–174.
- Best JL. 1988. Sediment transport and bed morphology at river channel confluences. *Sedimentology* **35**: 481–498.
- Best JL, Ashworth PJ. 1997. Scour in large braided rivers and the recognition of sequence stratigraphic boundaries. *Nature* **387**: 275–277.
- Bluck BJ. 1971. Sedimentation in the meandering River Endrick. *Scottish Journal of Geology* **7**: 93–138.
- Bluck BJ. 1974. Structure and directional properties of some valley sandur deposits in southern Iceland. *Sedimentology* **21**: 533–554.
- Bolla Pittaluga M, Repetto R, Tubino M. 2003. Channel bifurcation in braided rivers: Equilibrium configurations and stability. *Water Resources Research* **39**: 1046. DOI: 10.1029/2001WR001112,2003.
- Bradbrook KF, Lane SN, Richards KS. 2000. Numerical simulation of three-dimensional, time-averaged flow structure at river channel confluences. *Water Resources Research* **36**: 2731–2746.
- Bridge JS. 1993. The interaction between channel geometry, water flow, sediment transport and deposition in braided rivers. In *Braided Rivers*, Best JL, Bristow CS (eds). Geological Society Special Publication 75: London; 13–71.
- Bristow CS, Best JL, Roy AG. 1993. Morphology and facies models of channel confluences. In *Alluvial Sedimentation*, Marzo M, Puigdefabregas C (eds). International Association of Sedimentologists Special Publication **17**: 91–100.
- Burge LM. 2005. Wandering Miramichi rivers, New Brunswick, Canada. *Geomorphology* **69**: 253–274.
- Burge LM, Lapointe MF. 2005. Understanding the temporal dynamics of the wandering Renous River, New Brunswick, Canada. *Earth Surface Processes and Landforms* **30**: 1227–1250.
- Cant DJ, Walker RJ. 1978. Fluvial processes and facies sequences in the sandy braided South Saskatchewan River. *Sedimentology* **25**: 625–648.
- Carbonneau PE, Bergeron NE, Lane SN. 2005. Texture-based image segmentation applied to the quantification of superficial sand in salmonid river gravels. *Earth Surface Processes and Landforms* **30**: 121–127.
- Carson MA, Griffiths GA. 1987. Bedload transport in gravel channels. *Journal of Hydrology New Zealand* **26**: 1–151.
- Chandler JH, Ashmore P, Paola C, Gooch M, Varkaris F. 2002. Monitoring river channel change using terrestrial oblique digital imagery and automated digital photogrammetry. *Annals of the Association of American Geographers* **92**: 631–644.
- Collinson JD. 1970. Bedforms of the Tana River, Norway. *Geografiska Annaler* **52A**: 31–55.
- Cowan EJ. 1991. The large-scale architecture of the fluvial Westwater Canyon member, Morrison formation Upper Jurassic, San Juan Basin, New Mexico. In *The Three-Dimensional Facies Architecture of Terrigenous Clastic Sediments and Its Implications for Hydrocarbon Discovery and Recovery*, Miall AD, Tyler N (eds). Society of Economic Palaeontologists and Mineralogists; 84–93.

- Davoren A, Mosley MP. 1986. Observations of bedload movement, bar development and sediment supply in the braided Ohau River. *Earth Surface Processes and Landforms* **11**: 643–652.
- Doeschl A, Ashmore P. 2005. Assessing a cellular braided-stream model with a physical small-scale model of braided-streams. *Earth Surface Processes and Landforms* **30**: 519–540.
- Ferguson RI. 1987. Hydraulic and sedimentary controls of channel pattern. In: *River Channels: Environment and Process*, Richards K (ed.). Institute of British Geographers Special Publication 17. Blackwell: Oxford; 129–158.
- Ferguson RI. 1993. Understanding braiding processes in gravel-bed rivers: Progress and unresolved problems. In *Braided Rivers*, Best JL, Bristow CS (eds). Geological Society Special Publication 75: London; 73–87.
- Ferguson R, Ashmore P, Ashworth P, Paola C, Prestegard K. 1992. Measurements in a braided river chute and lobe I: Flow pattern, sediment transport and channel change. *Water Resources Research* **28**: 1877–1886.
- Fujita Y. 1989. Bar and channel formation in braided streams. In *River Meandering*, Parker G, Ikeda S (eds). American Geophysical Union Water Resources Monograph 12, American Geophysical Union: Washington DC; 417–462.
- Goff JR, Ashmore PE. 1994. Gravel transport and morphological change in braided Sunwapta River, Canada. *Earth Surface Processes and Landforms* **19**: 195–212.
- Gran K, Paola C. 2001. Riparian vegetation controls on braided stream dynamics. *Water Resources Research* **37**: 3275–3283.
- Hein FJ, Walker RG. 1977. Bar evolution and development of stratification in the gravelly, braided, Kicking Horse River, B.C. *Canadian Journal of Earth Sciences* **14**: 562–570.
- Heinz J, Kleinedam S, Teutsch G, Aigner T. 2003. Heterogeneity patterns of Quaternary glaciofluvial gravel bodies S-W Germany: Application to hydrogeology. *Sedimentary Geology* **158**: 1–23.
- Hey RD, Thorne CR. 1986. Stable channels with mobile gravel beds. *Journal of Hydraulic Engineering* **112**: 671–689.
- Hoey TB, Sutherland AJ. 1991. Channel morphology and bedload pulses in braided rivers: A laboratory study. *Earth Surface Processes and Landforms* **16**: 447–462.
- Hoey T, Cudden J, Shvidchenko A. 2001. The consequences of unsteady transport in braided rivers. In *Gravel-Bed Rivers V*, Mosley MP (ed.). New Zealand Hydrological Society: Wellington; 121–140.
- Horton RE. 1945. Erosional development of streams and their drainage basins: Hydrophysical approach to quantitative morphology. *Geological Society of America Bulletin* **56**: 275–370.
- Howard AD. 1971. Optimal angles of stream junction: Geometric, stability to capture, and minimum power criteria. *Water Resources Research* **7**: 863–873.
- Jackson, DJ. 1994. *The Sedimentology of Gravel Bed Rivers*, M.Sc. Thesis, University of Western Ontario.
- Klaassen GJ, Vermeer K. 1988. Confluence scour in large braided rivers with fine bed material. *Proceedings of the International Conference on Fluvial Hydraulics, Budapest, Hungary*; 395–408.
- Luce JJW. 1994. Confluence Zone Sedimentation Processes: Sunwapta River, Alberta, M.Sc. Thesis University of Western Ontario.
- Lunt IA, Bridge JS, Tye B. 2004. A quantitative, three-dimensional depositional model of gravelly braided rivers. *Sedimentology* **51**: 377–414.
- Makaske B. 2001. Anastomosing rivers: A review of their classification, origin and sedimentary products. *Earth Science Reviews* **53**: 149–196.

- McLelland SJ, Ashworth PJ, Best JL. 1996. The origin and downstream development of coherent flow structures at channel junctions. In *Coherent Flow Structures in Open Channels*, Ashworth PJ, Bennett SJ, Best JL, McLelland SJ (eds). John Wiley & Sons: Chichester; 459–490.
- Miall AD, Jones B. 2003. Fluvial architecture of the Hawksbury Sandstone Triassic, near Sydney, Australia. *Journal of Sedimentary Research* **73**: 531–545.
- Mosley MP. 1976. An experimental study of channel confluences. *Journal of Geology* **84**: 535–562.
- Mosley MP. 1981. *Scour depths in branch channel confluences, Ohau River*. Report no. WS 395, Ministry of Works and Development: Christchurch, New Zealand.
- Mosley MP. 1983. Response of braided rivers to changing discharge. *Journal of Hydrology New Zealand* **22**: 18–67.
- Murray AB, Paola C. 2003. Modelling the effect of vegetation on channel pattern in bedload rivers. *Earth Surface Processes and Landforms*, **28**: 131–143.
- Nanson GC, Knighton AD. 1996. Anabranching rivers: Their cause, character and classification. *Earth Surface Processes and Landforms* **21**: 217–239.
- Obermoser A. 2004. *Transport behaviour of coarse particles in a braided gravel-bed stream, Sunwapta River – Canada*, Diploma Thesis, BOKU, University of Natural Resources and Applied Life Sciences, Vienna.
- Paola C. 2001. Modelling stream braiding over a range of scales. In *Gravel-Bed Rivers V*, Mosley MP (ed.). New Zealand Hydrological Society: Wellington; 11–38.
- Paola C, Borgman L. 1991. Reconstructing random topography from preserved stratification. *Sedimentology* **38**: 553–565.
- Parsons D, Best JL, Lane SN, Orfeo O, Hardy RJ, Kostachuk, R. 2007. Form roughness and the absence of secondary flow in a large confluence-diffuence, Rio Parana, Argentina. *Earth Surface Processes and Landforms* **32**: 155–162.
- Powell DM. 1998. Patterns and processes of sediment sorting in gravel-bed rivers. *Progress in Physical Geography* **22**: 1–32.
- Pyrce RS, Ashmore PE. 2005. Bedload path lengths and point bar development in gravel-bed river models. *Sedimentology* **52**: 839–857.
- Roy A. 1985. Optimal models of river branching angles. In *Models in Geomorphology*, Woldenberg M (ed.). Allen and Unwin: Boston; 269–286.
- Roy A, Lane S. 2003. Putting the morphology back into fluvial geomorphology, the case of river meanders and tributary junctions. In *Contemporary meanings in physical geography: From what to why?*, Trudgill S, Roy A (eds). Arnold: London; 103–126.
- Roy NG, Sinha R. 2005. Alluvial geomorphology and confluence dynamics in the Gangetic plains, Farrukhabad-Kannauj are, Uttar Pradesh, India. *Current Science* **88**: 2000–2006.
- Sambrook Smith GH, Ashworth PJ, Best JL, Woodward J, Simpson CJ. 2005. The morphology and facies of sandy braided rivers: Some considerations of scale invariance. In *Fluvial Sedimentology VII*, Blum MD, Marriott SB, Leclair SF (eds). International Association of Sedimentologists Special Publication 35. Blackwell: Oxford; 145–158.
- Sambrook Smith GH, Ashworth PJ, Best JL, Woodward J, Simpson CJ. 2006. The sedimentology and alluvial architecture of the sandy braided South Saskatchewan River, Canada. *Sedimentology* **53**: 413–434.
- Sheets BA, Hickson TA, Paola C. 2002. Assembling the stratigraphic record: Depositional patterns and time-scales in an experimental alluvial basin. *Basin Research* **14**: 287–301.

- Siegenthaler C, Huggenberger P. 1993. Pleistocene Rhine gravel: Deposits of a braided river system with dominant pool preservation. In *Braided Rivers*, Best JL, Bristow CS (eds). Geological Society Special Publication 75: London; 147–162.
- Smith DG. 1973. Aggradation of the Alexandria–North Saskatchewan River, Banff Park, Alberta. In *Fluvial Geomorphology*, Morisawa M (ed.). Proceedings of the 4th Annual Geomorphology Symposium. Binghamton, New York; 201–219.
- Smith ND. 1971. Transverse bars and braiding in the Lower Platte River, Nebraska. *Geological Society of America Bulletin* **82**: 3407–3420.
- Southard JB, Smith ND, Kuhnle RA. 1984. Chutes and lobes: Newly identified elements of braiding in shallow gravelly streams. In *Sedimentology of Gravels and Conglomerates*, Koster EH, Steel RJ (eds). Canadian Society of Petroleum Geologists, Memoir 10: Calgary, Canada; 51–59.
- Stojic M, Chandler J, Ashmore P, Luce J. 1998. The assessment of sediment transport rates by automated digital photogrammetry. *Photogrammetric Engineering and Remote Sensing* **64**: 387–395.
- Tal M, Gran K, Murray AB, Paola C, Hicks DM. 2003. Riparian vegetation as a primary control on channel characteristics in multi-thread rivers. In *Riparian Vegetation and Fluvial Geomorphology*, Bennett SJ, Simon A (eds), American Geophysical Union, Water Science and Application 8: Washington; 43–58.
- Thompson SM. 1985. Transport of gravel by flows up to 500m<sup>3</sup>/s, Ohau River, Otago, New Zealand. *Journal of Hydraulic Research* **23**: 285–305.
- Varkaris F. 1999. *Confluence Sediment Transport Patterns in a Braided River Model*. B.Sc. Thesis, University of Western Ontario.
- Westaway RM, Lane SM, Hicks DM. 2003. Remote survey of large-scale braided rivers using digital photogrammetry and image analysis. *International Journal of Remote Sensing* **24**: 795–816.
- Williams PF, Rust BR. 1969. Sedimentology of a braided river. *Journal of Sedimentary Petrology* **39**: 649–679.
- Wooldridge CL, Hickin EJ. 2005. Radar architecture and evolution of channel bars in wandering gravel-bed rivers: Fraser and Squamish rivers, British Columbia, Canada. *Journal of Sedimentary Research* **75**: 844–860.
- Young WJ, Davies TRH. 1991. Bed load transport processes in a braided gravel-bed river model. *Earth Surface Processes and Landforms* **16**: 499–511.



# **II**

## **Tributary–Main-Stem Interactions**



# 8

## Introduction to Part II: tributary–main-stem interactions

**Stephen P. Rice**

*Department of Geography, Loughborough University, UK*

### Introduction

When viewed at the largest scales, many rivers exhibit incremental downstream changes in key physical characteristics (e.g. discharge, bank strength, bed slope and bed-material grain size) that are associated with downstream changes in channel shape (e.g. Leopold and Maddock, 1953) and planform style (e.g. Church, 1992), with hydraulic properties such as channel roughness (e.g. Bathurst, 1993), with the organization of stream biota (e.g. Vannote *et al.*, 1980) and with the sedimentary architecture of alluvial basin fills. However, these general trends are revealed to be more complex at smaller scales where additional spatial structure is apparent (e.g. Mosley and Schumm, 2001). Variations in lithology, climate, tectonic history and land use may be important sources of structure along some, but the supply of water, sediment and organic materials from tributaries affects longitudinal patterns of channel form and function in all river systems, without exception.

Thus, discharge, width and depth are not smooth, monotonic functions of distance downstream but exhibit step changes wherever large tributaries join a channel (Rhoads, 1987; Richards, 1980). Similarly, downstream fining of bed sediments by abrasion and

sorting processes is repeatedly interrupted by the recruitment of sediment from tributaries (Sternberg, 1875; Miller, 1958; Knighton, 1980; Rice and Church, 1998 and many others). Increases in grain size occur at junctions where coarse sediment is supplied and sudden reductions can occur where fine sediment is supplied in sufficient volume (e.g. Andrews, 1979). These step-like changes in discharge and sediment size may be accompanied by discontinuities in longitudinal profile (Rice and Church, 2001; Hanks and Webb, 2006), changes in planform style (e.g. Russell, 1954; Galay *et al.*, 1998; Mosley and Schumm, 2001), the growth of tributary fans (e.g. May and Gresswell, 2004), shifts in fish and insect community composition (e.g. Rice *et al.*, 2001; Fernandes *et al.*, 2004; Kiffney *et al.*, 2006) and a suite of other geomorphological and ecological impacts (reviewed in Ferguson and Hoey, and Rice *et al.*, Chapters 10 and 11 respectively, this volume).

Physical impacts ultimately reflect the adjustment of channel properties to abrupt changes in the key controls of channel form (discharge, sediment load and sediment calibre) a process that Lodina and Chalov (1971, p.372) point out has implications for channel stability above and below tributary junctions and refer to, wonderfully, as the 'play of tributaries' (see also Large and Petts, 1996). Geomorphological adjustment processes can be particularly dramatic during significant flooding episodes (e.g. Sloan *et al.*, 2001), where tributary sediment yields have been modified by human activities, such as placer mining (e.g. James, 2004), and on regulated rivers where attenuation of main-stem flows or a reduction in their duration, or both, leads to accelerated aggradation below tributary confluences (Petts, 1984; Allen and Hobbs, 1989; Gilvear, 2004 and many others). Aggradation may be exacerbated on regulated rivers if lower water levels in the main stem reduce the tributary base level, inducing tributary rejuvenation and increasing sediment production and delivery (e.g. Petts, 1979).

This last point highlights the fact that there is a two-way interaction between tributaries and their recipient channels such that main-stem processes also impact upon tributary processes and characteristics. For example: main-stem incision may propagate upstream along tributaries via knickpoint retreat (e.g. Brierley and Fryirs, 1999); tributaries may be back flooded by main-stem flows that reverse sediment transport (e.g. Kennedy, 1999) and produce slackwater deposits (e.g. Kochel and Baker, 1982); main-stem processes influence tributary fan development by moderating the amount of sediment deposited in distal tributary reaches (Gomez-Villar *et al.*, 2006) and contributing main-stem overbank sediment to the fan architecture (Florsheim, 2004). The potentially complex geomorphological interaction of main stem and tributary has been compared to that in meso-tidal estuaries by Kennedy (1999). Xu (2001) provides a modern example from China, where rising base level in the Laohahe River and the complex response of its tributary the Yangchangzihe are described by a five-phase qualitative model. The presence of a two-way exchange between tributaries and main stem is particularly important for river ecology, with mobile animals utilizing the contrasting environments between main stem and tributary for various purposes that include

refuge from predators or high flows (Scrivener *et al.*, 1994; Fraser *et al.*, 1995; Power and Dietrich, 2002).

## Individual chapters

The five chapters in Part II tackle several elements of this large field of interest. Their main theme is the reach-scale importance of tributaries for the channels that they join. This is a logical scale of attention for the central part of the book, which links local confluence effects in Part I and the network-scale perspective considered in Part III. Recipient channels are generally referred to as 'main stem' channels throughout these chapters, but this is a linguistic instrument that implies relative size, not that the recipient channel is the principal drainage line: It may refer to the trunk stream or any of its tributary branches.

Kennedy (1999) points out that few studies of tributary–main-stem interactions have considered cases where the tributaries are very small relative to the main stem or where hydrographs are grossly asynchronous (cf. Reid *et al.*, 1989), and Ferguson and Hoey (Chapter 10, this volume) suggest that there is a somewhat inevitable bias in studies of tributary impact towards those junctions where there are large and obvious effects. Many tributaries may have no impact on the channel they join or their impacts may be difficult to disentangle from the background noise. In their respective chapters (11, 12 and 13, this volume), Rice *et al.*, Liebault *et al.* and Benda each emphasize the need to discriminate significant from insignificant tributaries. Part II therefore begins with Torgersen *et al.* identifying tributary-induced impacts amidst general river system heterogeneity. They illustrate various approaches drawing on examples from a range of disciplines. Because broad-scale, spatially explicit investigations of tributary impacts are uncommon, they demonstrate graphical and geostatistical methods of identifying tributary impacts through specific case studies of remotely sensed summer water temperature and Coastal Cutthroat Trout distributions in streams from Oregon, USA. Looking to the future, they suggest that the increasing availability of high-resolution data over long reaches, coupled with the adoption of pattern-recognition and analysis tools developed for similar data by other disciplines, will greatly improve the ability of river scientists to identify tributary-related heterogeneity. This is ultimately necessary in order to test models that aim to predict the style, magnitude and location of tributary influences, such as biodiversity hotspots at network scales (Benda *et al.*, 2004).

Ferguson and Hoey focus on tributary–main-stem geomorphology and particularly the question of how tributary and main-stem characteristics affect the style and extent of reach-scale geomorphological impacts. Alongside a review of available field evidence, they use three models of increasing sophistication to examine this question, including a qualitative, conceptual model, a new quantitative regime theory and a width-averaged sediment routing model. They highlight several areas for further research: better

understanding of width adjustment at junctions, which has a substantial effect on predicted downstream impacts, collection of bedload flux data to help test models, improved understanding of the links between confluence-scale morphology and reach-scale impacts, and more systematic sampling of tributary characteristics and impacts to promote a generic understanding that is not biased towards those tributaries that have obvious and significant effects.

The need for quality datasets with which to test hypotheses and develop better models is also taken up by Rice *et al.* in their examination of tributary impacts on main-stem biota. They argue that tributaries matter ecologically because they can alter environmental conditions and elicit a biological response in the channel that they join, but also because tributaries and confluence zones are sites of intrinsic ecological value where particular biophysical processes and ecosystem services may be concentrated. The chapter uses new field data from multiple confluences to explore the spatial and temporal dynamics of tributary influence on main-stem ecology in the Cascade Mountains, USA and reviews numerical modelling work exploring the controls on physical and thence biotic diversity at confluences. They highlight two key requirements for future research: the need for extensive empirical work to evaluate the abundance, spatial distribution and landscape-scale controls of tributary influence and complementary intensive, perhaps experimental, work focused on understanding the mechanisms that underlie confluence effects.

Liébault *et al.*'s chapter is concerned with the possibility of managing main-stem river problems by the careful manipulation of tributary characteristics. They present conceptual tools and practical examples that indicate how tributaries can be and have been utilized in the management of catchment-scale sediment regimes. Their primary example comes from southern France, where the reactivation of tributary sediment sources is being considered as a tool for managing serious problems of incision and degradation in the main stem of the River Drôme. A gross sediment budget for the river indicates that the extent of the main-stem sediment deficit can only be overcome by assisted replenishment. They present a decision-making tool that may help river managers to implement such a scheme by identifying the bedload supply, transport and delivery potential of individual tributaries. They suggest that the most important challenge in this arena is to understand sediment routing through the channel network by both developing theoretical tools and making observations of channel responses to disturbed sediment regimes.

This is a theme that is further developed by Benda in the final chapter of Part II, which provides a link to the network-scale focus of Part III. Benda uses the term 'confluence environment' to describe main-stem reaches where there are observable tributary impacts on channel and valley morphology. His chapter explores how river network structure and scaling properties may control the number, nature and locations of confluence environments. He also considers the effect of branching networks on the stochastic character of the sediment and organic inputs that create confluence environments, emphasizing

the temporal aspect of tributary impacts. Looking to the future, Benda suggests that a perspective on rivers as networks, that recognizes both confluence and non-confluence environments has the potential to underpin advances in fluvial geomorphology and riverine ecology. For example, given that confluence environments appear to be one type of biological hotspot in river networks, he suggests that an improved understanding of how significant tributary impacts are organized in time and space within networks could benefit the planning and implementation of watershed and channel restoration projects.

## References

- Allen PM, Hobbs R. 1989. Downstream impacts of a dam on a bedrock fluvial system, Brazos River, central Texas. *Bulletin of the Association of Engineering Geologists* **26**: 165–189.
- Andrews ED. 1979. Hydraulic adjustment of the East Fork River, Wyoming to the supply of sediment. In *Adjustments of the Fluvial System*, Rhoades DD, Williams GP (eds). Proceedings of the Tenth Annual Geomorphology Symposia Series, Binghamton, New York, 1979. George Allen and Unwin: London; 69–94.
- Bathurst JC. 1993. Flow resistance through the channel network. In *Channel Network Hydrology*, Beven K, Kirkby MJ (eds). John Wiley & Sons: Chichester; 69–98.
- Benda L, Poff NL, Miller D, Dunne T, Reeves G, Pess G, Pollock M. 2004. The Network Dynamics Hypothesis: How channel networks structure riverine habitats. *BioScience* **54**: 413–427.
- Brierley GJ, Fryirs K. 1999. Tributary-trunk stream relations in a cut-and-fill landscape: A case study from Wolumla catchment, New South Wales, Australia. *Geomorphology* **28**: 61–73.
- Church MA. 1992. Channel morphology and typology. In *The Rivers Handbook, Volume 1*, Calow P, Petts GE (eds). Blackwell: Oxford; 126–143.
- Fernandes CC, Podos J, Lundberg JG. 2004. Amazonian ecology: Tributaries enhance the diversity of electric fishes. *Science* **305**: 1960–1962.
- Florsheim JL. 2004. Side-valley tributary fans in high-energy river floodplain environments: Sediment sources and depositional processes, Navarro River basin, California. *Geological Society of America Bulletin* **116**: 923–937.
- Fraser DF, Gilliam JF, Yip-Hoi T. 1995. Predation as an agent of population fragmentation in a tropical watershed. *Ecology* **76**: 1461–1472.
- Galay VJ, Rood KM, Miller S. 1998. Human interference with braided gravel-bed rivers. In *Gravel Bed Rivers in the Environment*, Klingeman PC, Beschta RL, Komar PD, Bradley JB (eds). Water Resources Publications: Colorado; 471–506.
- Gilvear DJ. 2004. Patterns of channel adjustment to impoundment of the upper River Spey, Scotland (1942–2000). *River Research and Applications* **20**: 151–165.
- Gomez-Villar A, Alvarez-Martinez J, Garcia-Ruiz JM. 2006. Factors influencing the presence or absence of tributary-junction fans in the Iberian Range, Spain. *Geomorphology* **81**: 252–264.
- Hanks TC, Webb RH. 2006. Effects of tributary debris on the longitudinal profile of the Colorado River in Grand Canyon. *Journal of Geophysical Research-Earth Surface* **111**: F02020. DOI: 10.1029/2004JF000257.
- James LA. 2004. Tailings fans and valley-spur cutoffs created by hydraulic mining. *Earth Surface Processes and Landforms* **29**: 869–882.

- Kennedy BA. 1999. Flow and sedimentation at tributary river mouths: A comparison with mesotidal estuaries. In *Varieties of Fluvial Form*, Gupta A, Miller AJ (eds). John Wiley & Sons: Chichester; 409–426.
- Kiffney PM, Greene C, Hall J, Davies J. 2006. Gradients in habitat heterogeneity, productivity, and diversity at tributary junctions. *Canadian Journal of Fisheries and Aquatic Sciences* **63**: 2518–2530.
- Knighton AD. 1980. Longitudinal changes in size and sorting of stream bed material in four English Rivers. *Geological Society of America Bulletin* **91**: 55–62.
- Kochel RC, Baker VR. 1982. Palaeoflood hydrology. *Science* **215**: 353–361.
- Large ARG, Petts GE. 1996. Historical channel-floodplain dynamics along the River Trent – Implications for river rehabilitation. *Applied Geography* **16**: 191–209.
- Leopold LB, Maddock T. 1953. The hydraulic geometry of stream channels and some physiographic implications. *United States Geological Survey Professional Paper* 252.
- Lodina RV, Chalov RS. 1971. Effect of tributaries on the composition of river sediments and deformations of the main river channel. *Soviet Hydrology: Selected Papers* **4**: 370–374.
- May CL, Gresswell RE. 2004. Spatial and temporal patterns of debris-flow deposition in the Oregon Coast Range, USA. *Geomorphology* **57**: 135–149.
- Miller JP. 1958. *High mountain streams: Effects of geology on channel characteristics and bed material*. Memoir 4, State Bureau of Mines and Mineral Resources, New Mexico Institute of Mines and Mining Technology: Socorro, New Mexico.
- Mosley MP, Schumm SA. 2001. Gravel-bed rivers - the view from the hills. In *Gravel bed Rivers* V, Mosley MP (ed.). New Zealand Hydrological Society: Wellington, New Zealand; 479–505.
- Petts GE. 1979. Complex response of river channel morphology to reservoir construction. *Progress in Physical Geography* **3**: 329–362.
- Petts GE. 1984. Sedimentation within a regulated river. *Earth Surface Processes and Landforms* **9**: 125–134.
- Power ME, Dietrich WE. 2002. Food webs in river networks. *Ecological Resources* **17**: 451–471.
- Reid I, Best JL, Frostick LE. 1989. Floods and flood sediments at confluences. In *Floods: Hydrological, Sedimentological and Geomorphological Implications*, Bevan K, Carling P (eds). John Wiley & Sons: Chichester; 135–150.
- Rhoads BL. 1987. Changes in stream channel characteristics at tributary junctions. *Physical Geography* **8**: 346–361.
- Rice SP, Church M. 1998. Grain size along two gravel-bed rivers: Statistical variation, spatial pattern and sedimentary links. *Earth Surface Processes and Landforms* **23**: 345–363.
- Rice SP, Church M. 2001. Longitudinal profiles in simple alluvial systems. *Water Resources Research* **37**: 417–426.
- Rice SP, Greenwood MT, Joyce CB. 2001. Tributaries, sediment sources and the longitudinal organisation of macroinvertebrate fauna along river systems. *Canadian Journal of Fisheries and Aquatic Sciences* **58**: 824–840.
- Richards KS. 1980. A note on changes in channel geometry at tributary junctions. *Water Resources Research* **16**: 241–244.
- Russell RJ. 1954. Alluvial morphology of Anatolian rivers. *Annals of the Association of American Geographers* **44**: 363–391.
- Scrivener JC, Brown TG, Andersen BC. 1994. Juvenile chinook salmon (*Onchorhynchus tshawytscha*) utilization of Hawks creek, a small and non-natal tributary of the upper Fraser River. *Canadian Journal of Fisheries and Aquatic Sciences* **51**: 1139–1146.

- Sloan J, Miller JR, Lancaster N. 2001. Response and recovery of the Eel River, California, and its tributaries to floods in 1955, 1964, and 1997. *Geomorphology* **36**: 129–154.
- Sternberg H. 1875. Untersuchungen über längen- und Querprofil geschiebeführender Flüsse. *Zeitschrift für Bauwesen* **25**: 483–506.
- Vannote RL, Minshall GW, Cummins KW, Sedell JR, Cushing CE. 1980. The River Continuum Concept. *Canadian Journal of Fisheries and Aquatic Sciences* **37**: 130–137.
- Xu JX. 2001. Adjustment of mainstream – Tributary relation upstream from a reservoir: An example from the Laohahe River, China. *Zeitschrift Fur Geomorphologie* **45**: 359–372.



# 9

## Spatial identification of tributary impacts in river networks

**Christian E. Torgersen<sup>1</sup>, Robert E. Gresswell<sup>2</sup>, Douglas S. Bateman<sup>3</sup> and Kelly M. Burnett<sup>4</sup>**

<sup>1</sup>*US Geological Survey, Forest and Rangeland Ecosystem Science Center, Cascadia Field Station, University of Washington, College of Forest Resources, USA*

<sup>2</sup>*US Geological Survey, Northern Rocky Mountain Science Center, USA*

<sup>3</sup>*Department of Forest Sciences, Oregon State University, USA*

<sup>4</sup>*US Department of Agriculture, Forest Service, Pacific Northwest Research Station, USA*

### Introduction

The ability to assess spatial patterns of ecological conditions in river networks has been confounded by difficulties of measuring and perceiving features that are essentially invisible to observers on land and to aircraft and satellites from above. The nature of flowing water, which is opaque or at best semi-transparent, makes it difficult to visualize fine-scale patterns in habitat and biota at close range, and the linear topology of river networks complicates the process of scaling up to detect coarse-scale patterns. This spatially incomplete perspective limits our understanding of lotic systems because the scaled character of biotic and abiotic patterns produces different results depending on the method of data collection (Fausch *et al.*, 2002; Hildrew and Giller, 1994).

Recent changes in the way river scientists collect data are now filling in these gaps to reveal patterns that raise new questions about the structure and function of riverine mosaics and networks. The recent identification of tributary influences on stream channel morphology (Benda *et al.*, 2004b; Benda *et al.*, 2003) and associated data (Fernandes *et al.*, 2004; Kiffney *et al.*, 2006; Rice *et al.*, 2001) has been made possible, in part, by the use of spatially explicit sampling approaches. This chapter focuses on contributions of such approaches to recognizing and describing the impacts of tributaries in river networks. The emphasis here is on identifying patterns as opposed to explaining the processes underlying such patterns. Other sections of this book elucidate the functional impacts of tributaries on spatial heterogeneity in fluvial morphology, water quality, biological response, network topology, hydrology, sediment delivery and contaminant transport. This chapter explains how to see patterns amidst this heterogeneity.

We illustrate various approaches for identifying impacts of tributaries along the receiving channel (hereafter referred to as the main stem) in a river network. Literature examples are drawn from a range of disciplines that apply different sampling designs, data types and data-collection methods. Many of the studies cited in this chapter do not state an explicit intent to evaluate tributary impacts, but their methods hold promise for addressing important questions in this area. Except for terrain analysis of available digital elevation data (e.g. Benda *et al.*, in press), broad-scale, spatially explicit investigations of tributary effects on fluvial features and aquatic biota are uncommon. Therefore, we demonstrate graphical (longitudinal analysis and smoothing) and geostatistical (one-dimensional and network variograms) methods of identifying tributary impacts through specific case studies of (1) remotely sensed summer water temperature in the North Fork John Day River in north-eastern Oregon, USA and (2) coastal cutthroat trout distribution in a headwater stream network of Camp Creek, a tributary to the Umpqua River in western Oregon, USA.

## Data and measurement

The detection of tributary influences requires information on the locations of confluences and spatial variation in the response variables of interest. In this respect, the task of spatial identification of tributary impacts is as much cartographic as it is geomorphologic and ecological. The first challenge in designing a study to identify tributary impacts is to locate the tributaries themselves. Without walking the entire length of the river network, it is difficult – if not impossible – to map first-order tributary junctions in densely forested watersheds. However, analytical tools are now available to automate recognition of tributary junctions from relatively high-resolution digital elevation data ( $< 10 \text{ m}^2$ ) over broad spatial extents ( $> 10\,000 \text{ km}^2$ ) (Benda *et al.*, in press). The ability to locate tributary confluences may depend on the size and intermittency of the

tributaries relative to the main stem (Benda *et al.*, 2004a; Clarke and Burnett, 2003; Wigington *et al.*, 2005). Thus, it is essential to specify the source, scale and date of the map or digital data used to identify the location and relative size of confluences in relation to the main stem. In forested headwater streams, tributaries of 1–2 m in width are very difficult to detect using aerial photography, on which topographical maps are based. The error in maps of various types and scales can often be quite significant. For example, in a forested landscape, a commonly available US Geological Survey (USGS) topographic map with a scale of 1:24 000 represents the best estimate of an aerial photo interpreter on the location and extent of a tributary that is not visible from above due to overhanging riparian vegetation. The USGS standard for horizontal positional accuracy in 1:24 000 data is that 90 per cent of mapped points lie within approximately 12 m of their true positions (USGS, 2007). However, no such standard exists for mapping the occurrence or spatial extent of streams. Errors in spatial accuracy cannot be quantified without field verification. Digital elevation models (DEM) of various resolutions (e.g. 10–30 m for USGS 7.5 minute topographic quadrangles) may give the impression of greater accuracy than the hand-drawn maps from which they were derived. However, these data by definition incorporate additional error during translation from analogue to digital form. Therefore, 10- and 30-metre DEM data must be viewed critically as tools for locating tributary junctions that cannot be viewed in aerial photographs (Clarke and Burnett, 2003; Stock and Dietrich, 2003). Light detection and ranging (LiDAR, or lidar) offers the most promising potential for mapping fine-scale topography of fluvial features in both forested and non-forested landscapes. (Power *et al.*, 2005).

## Sampling design

In the past, traditional sampling methods attempted to avoid biases caused by discontinuities at tributary confluences rather than focus on such discontinuities in physical and biological gradients (Bruns *et al.*, 1984). This was a reasonable approach for pursuing objectives of detecting dominant gradients in environmental conditions and biological communities. For example, broad-scale longitudinal patterns in water temperature are more accurately represented by avoiding sampling locations immediately downstream of confluences, where temperature measurements are likely to be viewed as outliers. However, with rising interests in exploring discontinuities along the river continuum (Poole, 2002), traditional sampling techniques (*sensu* Cochran, 1977) are being adapted (see Hirzel and Guisan, 2002) to address scientific questions that are fundamentally spatial in nature.

Investigations of tributary impacts in river networks employ two kinds of sampling designs that differ in the scale and the spatial arrangement of sample units. In the nomenclature of statistical design in aquatic resource monitoring and assessment, these

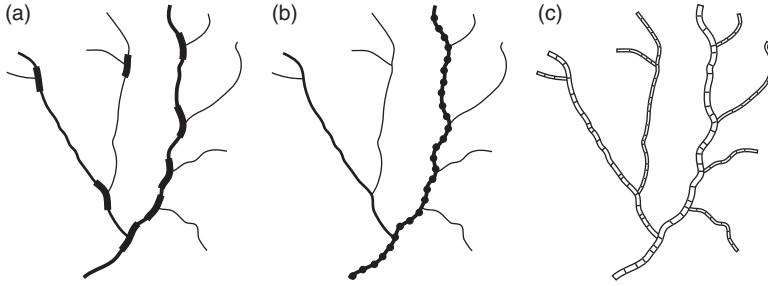


**Figure 9.1** Intensive and extensive sampling approaches for identifying tributary impacts in fluvial networks. An intensive design employs a limited number of (a) sites positioned upstream and downstream of tributary confluences. Extensive designs use (b) sample points or (c) sample areas (pool/riffle units and reaches) that are distributed along the entire main stem or throughout the river network.

types of study designs are termed ‘intensive’ and ‘extensive’ (Conquest and Ralph, 1998). Simplified graphical representations of these approaches are depicted in Figure 9.1.

### *Intensive sampling*

Intensive surveys employ methods that meet specific data requirements at a limited number of sites distributed within and among catchments (Figure 9.1(a)). This survey method focuses sampling effort at sites in the main stem upstream, adjacent to and downstream of tributary confluences. Measurements of biological and physical parameters are collected at a single site, often with an emphasis on establishing long-term records of change. Techniques employed in intensive surveys may be time consuming but offer an advantage in that they usually quantify accuracy and precision. The spatial scale of an intensive survey may range in resolution from 0.1 to 10 m (i.e. the minimum dimension of an individual measurement in terms of length of stream) and in extent from 10 to 1000 m (i.e. the site or length of stream within which individual samples are taken). Within a site, sampling may be conducted hierarchically at points, along transects or over areas to assess variation at microhabitat, pool/riffle and reach scales individually or, using a nested design, collectively (Armitage and Cannan, 1998; Friswell *et al.*, 1986). The number and spatial dimensions of sites in an intensive survey are generally limited by the time it takes to sample multiple parameters accurately and precisely at each site. Thus, considerable effort must be expended to identify sites where tributary impacts are most likely to be detected. Any determination of the appropriate sampled length requires a knowledge or estimation of the downstream and upstream extent of the tributary effects before data are collected and analysed – a difficult task in remote or poorly studied regions where tributary impacts typically occur. In spite

of these logistical challenges, the intensive approach has been used effectively in several studies that have identified tributary impacts on aquatic biota (Bruns *et al.*, 1984; Fernandes *et al.*, 2004; Kiffney *et al.*, 2006; Osborne and John Wiley & Sons, 1992; Stevens *et al.*, 1997).

### *Extensive designs*

Extensive surveys are designed to characterize spatial variation contiguously across many sites to obtain a picture of entire river segments. The distinguishing feature of an extensive survey is the relatively high resolution (0.1–100 m) and density of samples distributed over a relatively large extent of the main stem (> 1000 m) (Figure 9.1(b)). To identify longitudinal patterns in aquatic habitat and biota, data are typically gathered only in the main stem (Rice *et al.*, 2001). Recent recognition that network structure can influence fluvial systems has led aquatic scientists to collect spatially continuous data throughout entire headwater catchments (Figure 9.1(c)) (Gresswell *et al.*, 2006). As in intensive surveys, samples in extensive surveys may be collected at point locations or along transects, but areal sample units, such as geomorphologically defined pools and riffles, are most commonly employed to map aquatic habitat in linear networks (Radko, 1997). The size of the sample unit (i.e. micro-, meso- or macro-habitat features) determines the degree of variability in the data and the patterns observed. For example, extensive surveys typically exclude micro-scale variability by targeting geomorphically defined meso-scale habitat features, such as pools and riffles. Nested sampling designs have potential for evaluating longitudinal patterns in fluvial characteristics and biota at multiple spatial scales, but such approaches are often not combined with extensive surveys (Torgersen and Close, 2004). Certain types of data lend themselves better to point- or area-based sampling techniques. For example, continuous data types – including elevation, water temperature, chemistry, and channel width and depth – may be measured effectively using a point-based sampling technique. Discrete data types, such as counts of fish, invertebrates, sediment particles and logs, are usually quantified in linear or areal units. Counts can be estimated over large areas with point sampling methods (Barker and Sauer, 1995), but these methods are not widely used in rivers (Persat and Copp, 1990).

In spite of the apparent advantages for quantifying spatial pattern in rivers, three key trade-offs are associated with extensive surveys: (1) contiguous sampling along a main stem or a river network, rather than among catchments, generally limits studies to a smaller sampling extent, (2) including a large number of samples can increase data subjectivity if methods are used that rely on indirect measurement and estimation, as opposed to direct measurement with defined levels of accuracy and precision and (3) the large number of observers needed to sample many kilometres of river in a short period increases the cost of field data collection for synoptic assessments.

## Data collection

Spatially extensive, high-resolution data are useful for identifying spatial patterns of geomorphological and biological responses (Cooper *et al.*, 1997). Data of this nature have recently become available in fluvial geomorphology and lotic ecology (Fausch *et al.*, 2002; Power *et al.*, 2005; Walsh *et al.*, 1998), but traditional, intensive approaches for sampling fluvial systems are still the dominant method of data collection. Riverine scientists are beginning to weigh the known precision and accuracy of traditional measurement methods against newer methods with greater capacity to quantify spatial patterns but with less-well-known performance. The continued experimentation and development of such approaches is essential for improving our understanding of tributary confluences and their role in structuring the biotic and abiotic properties of fluvial networks.

The following examples of data collection illustrate techniques across disciplines that have been used successfully to evaluate tributary impacts or have high potential for development and application. The methods are presented according to the nature of data collection: (1) samples that are collected in the field and (2) remotely sensed images that are sampled in the laboratory. The distinction between the two methods is important because field sampling requires an observer to travel to and collect data at a site and so is more time consuming. Moreover, the scales of spatial and temporal variation in some types of field data are not suited for extensive data collection. For example, data types that require near-simultaneous sampling or complicated collection protocols, such as pH and turbidity, cannot be sampled in large numbers of sites without increasing the number of field personnel. The requirement that the observer be present – on the ground – makes it difficult to collect spatially extensive data at a high resolution in river networks. Remotely sensed data, in contrast, can be collected from a variety of platforms (ground, airborne or space) in a short period and offers the advantage that sampling can be streamlined, and even automated, using a computer in the laboratory. As a general rule in collecting data to quantify spatial patterns, the time in the field collecting and processing samples is minimized to increase the number of samples and the distance over which they are collected (Hirzel and Guisan, 2002; Schneider, 1994a).

### *Field measurement*

Data-collection methods for measuring spatial variation in river channel dimensions, substrate composition, water temperature and chemistry, and fish and macroinvertebrate distribution can be modified to increase the spatial resolution and extent of sampling. Using the technique developed by Hankin and Reeves (1988), visual estimates of channel width, depth and pool/riffle length can be corrected for observer bias based on a systematic selection of verified measurements. This dramatically reduces

the time required to map spatial patterns in river morphology so that over 10 km per day may be surveyed by a two-person crew (McIntosh *et al.*, 2000). A similar approach has been developed for visually characterizing and validating gravel-cobble river-bed sediments at the scale of kilometres (Latulippe *et al.*, 2001). In navigable rivers, water temperature, depth and conductivity can be measured in an extensive manner by towing probes behind a boat and continuously logging temperatures every one to three seconds while a global positioning system (GPS) records spatial coordinates. Using this method, Vaccaro and Maloy (2006) mapped thermal patterns and groundwater discharge areas over distances of 5–25 km.

Measurements of water-nutrient concentrations cannot be estimated visually, and it is difficult to collect samples sequentially along a main stem to quantify spatial heterogeneity at the scale of kilometres. However, Dent and Grimm (1999) employed up to 14 different people arrayed along a 10-km stream segment and collected nearly simultaneous water samples every 25 m. The samples were then processed in the laboratory to quantify nutrient concentration (nitrate-nitrogen and soluble reactive phosphorus) and conductivity. This technique provided data of sufficient resolution and extent to identify discontinuities in longitudinal patterns associated with tributary confluences; however, no attempt was made to relate spatial patterns in the measured variables to the positions of tributary junctions.

Quantifying spatial patterns of biological organisms in fluvial systems presents a new set of sampling challenges in addition to those just described. Field equipment required for observing and collecting aquatic organisms and measuring important variables, such as algal biomass and chlorophyll, is bulky and heavy. Moreover, some organisms, such as fish, amphibians and large macroinvertebrates, avoid detection by terrestrial observers and snorkellers. In spite of these difficulties, various techniques have been developed to approximate spatial patterns and thus help identify tributary impacts. Macroinvertebrates are particularly difficult to sample at high spatial resolution and over long distances because collection and laboratory processing techniques are time consuming, and traditional sampling equipment, such as Surber samplers and drift-collection devices, are not easily transportable if one intends to traverse multiple kilometres along a stream (Hauer and Lamberti, 1998). Nevertheless, quantifying patchiness in macroinvertebrate distribution is important for understanding abiotic factors influencing community organization (Downes *et al.*, 1993). Rice *et al.* (2001) employed a two-person crew to collect 10-minute kick samples at 10 different subsamples per site and was able to gather data in 43 sites over 12 days. The distribution of large-bodied macroinvertebrates, such as freshwater mussels, can be mapped also by snorkelling (Howard and Cuffey, 2003). Similar methods are currently being developed for quantifying spatial patterns of large-bodied arthropods, such as stonefly larvae (C.V. Baxter, Idaho State University, USA, *personal communication*).

Stream fishes have long been observed and counted by divers with mask and snorkel (Cunjak *et al.*, 1988; Mullner *et al.*, 1998; Roni and Fayram, 2000). However, only recently have spatially continuous distributions of fish abundance and species composition

been mapped by visual surveys. Such methods are particularly suited for small- to medium-sized rivers that have good visibility due to low turbidity and high water quality (Torgersen *et al.*, 2006). Although visual surveys are considerably more time consuming for quantifying fish than physical habitat, multiple two-person crews, with each mapping up to 4 km per day, can cover tens of kilometres per week. In contrast to snorkelling, electrofishing techniques involve heavy equipment and are generally not employed to map spatially continuous fish distributions, but these methods also have been adapted to increase the resolution and extent of sampling (Bateman *et al.*, 2005).

### **Remote sensing**

Remote-sensing technology is revolutionizing the study of fluvial networks (Hauer and Lorang, 2004; Power *et al.*, 1999; Walsh *et al.*, 1998). New methods have developed at a rapid rate since sensor technology and computer processing capability improved dramatically in the mid-1990s. The remote sensing of rivers and streams is still primarily an airborne application, particularly with regard to identifying tributary impacts in small rivers and streams. However, this is merely a technical challenge of spatial resolution and may be solved in the next decade by improved space-borne sensors. The list of biotic and abiotic features that may be remotely sensed is rapidly growing, and the most comprehensive review of these techniques applied to rivers was compiled by Mertes *et al.* (2004). Remote sensing can now obtain digital data that – with calibration – are nearly identical to field measurements for a variety of parameters used to identify tributary impacts, including topography, surface-suspended sediment concentration, water-surface height, bed material grain size, bathymetry and surface temperature. Moreover, remote sensing data, once considered too costly due to the expense of contracting both a sensor and aircraft, are increasingly recognized as more economical than collecting, entering and processing similar field-collected analogue data.

Airborne remote-sensing methods that have been particularly helpful for quantifying fine-scale spatial patterns over long distances in small- to medium-sized rivers include lidar (Charlton *et al.*, 2003; Reutebuch *et al.*, 2005), multi- and hyperspectral sensors (Legleiter *et al.*, 2004; Lorang *et al.*, 2005; Marcus *et al.*, 2003) and thermal infrared imaging (Cherkauer *et al.*, 2005; Handcock *et al.*, 2006; Torgersen *et al.*, 2001). Direct observations from a helicopter have also been used to map spawning habitat for salmon over hundreds of kilometres (Isaak and Thurow, 2006).

Significant advances have also resulted from very high-resolution digital aerial photography and an automated sampling algorithm to generate a spatially continuous record of the median grain size of substrates in an 80-km river section (Carbonneau *et al.*, 2005). A major limitation of these airborne methods – with the exception of lidar – is that they are effective only when the vertical view of the stream is unobstructed by riparian vegetation. Thus, in some instances it may be necessary to employ

remote-sensing approaches on the ground, underneath the riparian canopy. Traditional methods for characterizing the size of river-bed sediments involve a time-consuming, manual collection of particles (Diplas and Sutherland, 1988; Wolman, 1954), but various ground-based photographic methods can reduce the time spent at each site and thereby increase sampling resolution or extent. Graham *et al.* (2005) developed a transferable ground-based technique using a hand-held digital camera and automated image processing to quantify grain-size variability in rivers and streams that are not suited for airborne applications. In summary, digital imaging and computerized-processing techniques have produced major advances that are just beginning to help establish a spatially explicit template for identifying tributary impacts. Thus, much fertile ground remains for exploring remote-sensing technology and applying it to the study of main-stem-tributary dynamics in fluvial networks.

## Analytical tools

In the section on sampling design, intensive and extensive approaches for identifying tributary impacts were differentiated. Intensive studies, with widely dispersed sample sites, are not spatially explicit in the strictest sense because the gradient across all sites is evaluated, not the actual spatial patterns among sites. Hildrew and Giller (1994) eloquently describe this problem in relation to environmental gradients determined by the statistical analysis of intensive survey data: ‘These gradients are not “real” gradients in space, such as those which might exist along a single river, but are abstracts from all of the sites surveyed.’ A recent study by Kiffney *et al.* (2006 and Chapter 11, this volume) addressed this problem by collecting nested samples in transects spaced along the main stem 500 m upstream and downstream of tributary confluences. Responses of multiple-habitat, water-quality and biological variables to tributary confluences were then averaged among sites, but the spatial locations of transects with respect to the confluence were maintained and included in statistical analysis. In another intensive study, Fernandes *et al.* (2004) statistically identified impacts of tributaries by plotting fish species diversity upstream of tributary confluences against fish diversity downstream; departures from a 1:1 regression relationship provided evidence of tributary effects. Both methods were appropriate and instructive, but they provided limited information about the spatial gradients in species-habitat relationships between confluences, which would, potentially, provide additional insights.

The next sections on analytical tools for identifying tributary impacts focus primarily on the analysis of data acquired through extensive rather than intensive surveys. Additional information on the statistical analysis of intensive survey data can be obtained from a standard statistical text (Sokal and Rohlf, 1995). Extensive survey data, however, require non-traditional approaches to analysis because they are spatially

autocorrelated, non-normally distributed and generally inappropriate for traditional statistical tools, such as least squares regression and analysis of variance (ANOVA) (Legendre and Fortin, 1989).

## Graphical methods

The most basic method for identifying tributary impacts in fluvial systems is graphical analysis of longitudinal data sets, which can be readily generated with new GIS-based analytical tools (Benda *et al.*, in press). Heterogeneity associated with tributary confluences has been effectively characterized in physical attributes (e.g. boulders and wood) through graphical approaches to examining field data (Benda *et al.*, 2003; Bigelow *et al.*, 2007; Macnab *et al.*, 2006). Spatially continuous data from extensive surveys are instructive for evaluating associations between locations of tributary junctions and biotic and abiotic patterns, but certain data types are easier to interpret than others. Measurements of variables, such as water temperature, are relatively stable over short distances and produce plots that are directly interpretable. For example, remotely sensed water-temperature data are well suited to longitudinal analysis in a 80-km section of the North Fork John Day River, a medium-sized wilderness stream (5–30 m in width) (Figure 9.2).

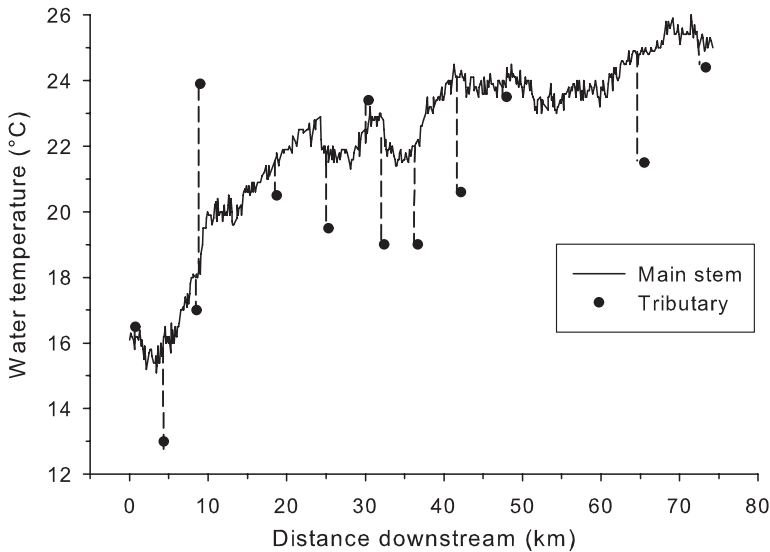


**Figure 9.2** Remotely sensed water temperature in the main stem and tributary confluences of the North Fork John Day River, north-eastern Oregon, USA. Airborne thermal infrared remote sensing was conducted on 4 August 1998. Dashed vertical lines indicate the spatial locations of tributaries with respect to main-stem water temperature.

The fine-scale variation in water temperature in Figure 9.2 is the result of measurement error of approximately 0.5 °C (Torgersen *et al.*, 2001), and broad-scale variation is caused by multiple landscape factors influencing solar inputs, groundwater–surface-water exchange and channel morphology (Poole and Berman, 2001). As with other methods of airborne remote sensing of streams, the aircraft flew upstream and collected overlapping imagery sequentially along the main stem. Geographic coordinates for each image were recorded in flight with a GPS and were used to create maps linking water temperature to locations in the river. Individual temperatures were sampled digitally ( $n = 10$ ) in each image, and the median was calculated and plotted versus distance upstream. Water temperatures measured from the imagery were not corrected for diel changes during the aerial survey, but the duration of the flight was short, approximately 45 minutes. The depiction of the location and temperature of tributaries relative to the main stem facilitated analysis of potential tributary impacts. The precise magnitude of tributary effects on main-stem water temperature was identified in individual high-resolution (< 1 m) thermal images. Thermal variations in main-stem water temperature downstream of river km 25 suggested a cooling influence of some tributaries. The utility of simple graphical representations such as Figure 9.2 is that they provide a broad-scale perspective on longitudinal patterns and the magnitude of the tributary effects.

Graphical analyses of spatial variation in counts of biological organisms and measurements of channel morphology in rivers can be difficult to interpret due to the high degree of heterogeneity in these variables over short distances (*sensu* Downes *et al.*, 1993). Data-smoothing techniques can help sort this fine-scale variation from ecologically meaningful coarse-scale variation. To demonstrate data smoothing in a longitudinal graphical analysis of fish counts, data were selected from Camp Creek, a headwater stream in western Oregon, USA that was surveyed extensively to evaluate spatial and temporal patterns in trout distribution (Gresswell *et al.*, 2006). Counts of trout were obtained using single-pass electrofishing in all pool and cascade habitats throughout the entire fish-bearing sections of the stream network (Bateman *et al.*, 2005) (Figure 9.3). Locations of sampled units were geographically positioned and mapped in a geographical information system (GIS) based on field-measured distances between mapped landmarks, such as tributary junctions and road crossings (Torgersen *et al.*, 2004). The main stem of Camp Creek has eight fishless tributaries and four fish-bearing tributaries. Hydrography for the stream network was derived from 7.5-minute USGS topographic maps.

Similar to spatially continuous counts of other organisms, trout counts in Camp Creek were highly variable among sample units (range 0–22 trout) and gave the appearance of being randomly distributed (Figure 9.4(a)). Such a distribution requires smoothing techniques to identify patterns amidst the heterogeneity. Locally weighted scatterplot smoothing (LOWESS) is a robust, unbiased nonparametric regression technique for identifying trends in ‘noisy’ data (Trexler and Travis, 1993). Many statistical packages

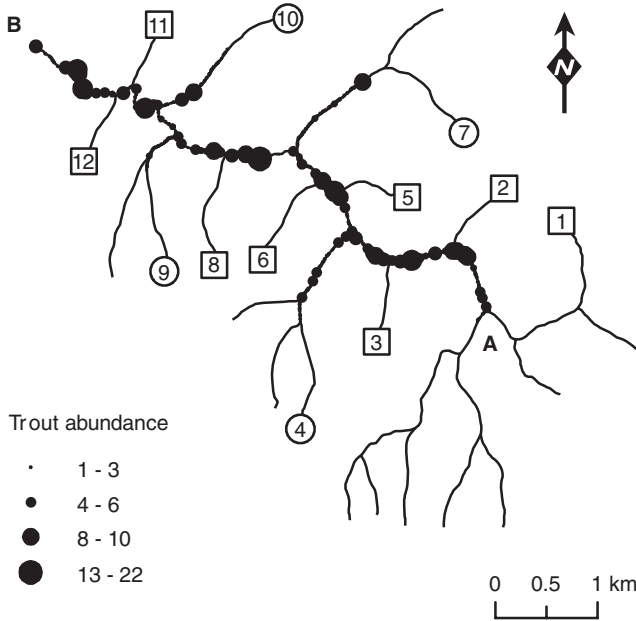


**Figure 9.3** Distribution of fish-bearing (open circles) and fishless (squares) tributaries and counts of coastal cutthroat trout in Camp Creek, western Oregon, USA. The size of the black dots indicates the relative abundance of trout sampled in all pools and cascades in the fish-bearing portion of the stream network. The direction of flow in the main stem (plotted in Figure 9.4) is from A to B.

can perform LOWESS, but SigmaPlot (SPSS, 2004) is particularly flexible in allowing the user to specify two parameters that determine the fit of the model: (1) a smoothing factor that corresponds to the fraction of data points used for each regression and (2) the polynomial degree of the model (SPSS, 2004).

For Camp Creek data, a smoothed trend line of trout counts along the main stem was created with a sampling fraction of 0.2 and a second-order polynomial. The locations of fish-bearing and fishless tributaries were overlaid on the LOWESS trend line to graphically evaluate the correspondence between peaks and valleys in trout abundance and the locations of tributary confluences (Figure 9.4(a)). Fish-bearing and fishless tributaries showed a weak association with valleys and peaks in trout abundance respectively (e.g. tributaries 2, 3, 4 and 5). However, using scaling techniques (Schneider, 1994b; Schneider and Piatt, 1986), counts of trout were smoothed by modifying the bin size of the analysis to 100 m as opposed to plotting raw counts (Figure 4(b)). When LOWESS with the same smoothing factor and polynomial degree was applied to the binned data, the correlation between tributary junctions and the spatial structure of trout distribution became apparent (Figure 9.4(b)). No statistical tests were employed to test the relationship between tributary locations and the distribution of trout because

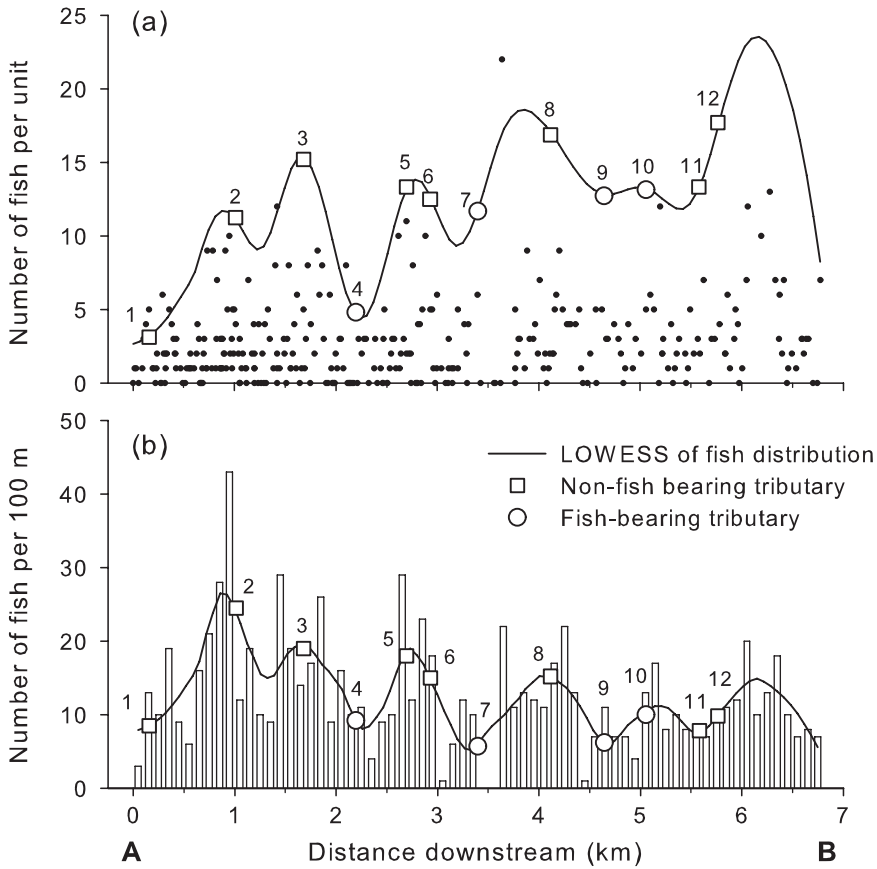


**Figure 9.4** Longitudinal variation in trout counts, and locations of fish-bearing and fishless tributaries in the main stem of Camp Creek (see Figure 9.3). Tributary locations (circles and squares) are overlaid on locally weighted scatterplot smoothing (LOWESS) of trout counts and 100-m bins of trout counts to facilitate graphical analysis. The labels 'A' and 'B' refer to the positions indicated in Figure 9.3.

a complete census of trout was conducted in the study stream. Nine tributary junctions corresponded precisely with peaks and valleys in the LOWESS trend line, and only two of the tributary junctions were not aligned with a peak or a valley. Of particular interest is the association between *fishless* tributaries and *peaks* in trout distribution and the association between *fish-bearing* tributaries and *valleys* in trout distribution.

Trout distribution in headwater streams, such as Camp Creek, reflects complex interactions between physical habitat structure and biological requirements for trout growth and reproduction (Connolly and Hall, 1999; Gresswell *et al.*, 2006; Hicks and Hall, 2003). Further verification of the patterns identified here and their relevance to cutthroat trout ecology require similar analyses in multiple headwater streams. This

is the subject of ongoing work at the present time on multiscale determinants of cut-throat trout distribution, diet and growth in western Oregon (see Gresswell *et al.*, 2006). Examples from the literature in similar headwater streams of the Pacific Northwest suggest that fishless tributary junctions function as localized conduits of invertebrate prey and may be associated with higher densities of fish in the main stem (Wipfli and Gregovich, 2002; Wipfli, 2005). Additionally, fishless streams, although small in drainage area and channel width, can contribute substantially to large wood accumulations transported by debris flows from steep, forested hillslopes of headwater catchments (May and Gresswell, 2003). These large accumulations of wood in the main stem at tributary junctions contribute to channel complexity and may help to explain localized peaks in trout abundance.

## Statistical methods

Graphical analysis of longitudinal patterns may not be sufficient for detecting subtle tributary–main-stem interactions. Therefore, statistical methods may be required to compare multiple longitudinal data sets or explore patterns of within- and between-site variability in stream networks. The careful application of standard statistical tests, such as ANOVA, can be used to parse out sources of variation associated with tributary impacts (Rice and Church, 1998). However, the assumptions of independence and equal variances make ANOVA a problematic tool for analysing closely spaced geographic data (Legendre and Fortin, 1989; Rice and Church, 1998). Geostatistics provides an alternative means to directly evaluate spatial autocorrelation among samples (Rossi *et al.*, 1992). Spatial autocorrelation is the tendency of samples that are collected near to one another to be more similar than samples that are further apart. A semivariogram depicts the variance ( $y$ -axis) between sample points versus the distance at which they are separated ( $x$ -axis) (Palmer, 2002). The shape of the semivariogram provides insights into the spatial structure of the variable of interest (Ettema and Wardle, 2002). Variograms may be calculated for one-dimensional data ( $x$ -coordinate only) and also for two-dimensional data ( $x$ - and  $y$ -coordinates). The Camp Creek data demonstrate how the shape of a semivariogram can provide information on the spacing of peaks and valleys in fish counts.

The semivariograms in Figure 9.5, calculated using the statistical package GS+ for the data depicted in Figure 9.4 (GDS, 2004), illustrate two important phenomena: (1) spatial structure was not discernible from the semivariogram of either the raw fish counts (Figure 9.5(a)) or the binned data (Figure 9.5(b)), but (2) semivariograms of the data smoothed with LOWESS summarized the average spacing between peaks and valleys. The  $x$ -axis location of the first peak in the semivariogram (Figures 9.5(c) and 9.5(d)) indicates the average spacing between peaks and valleys in the smoothed data, and the

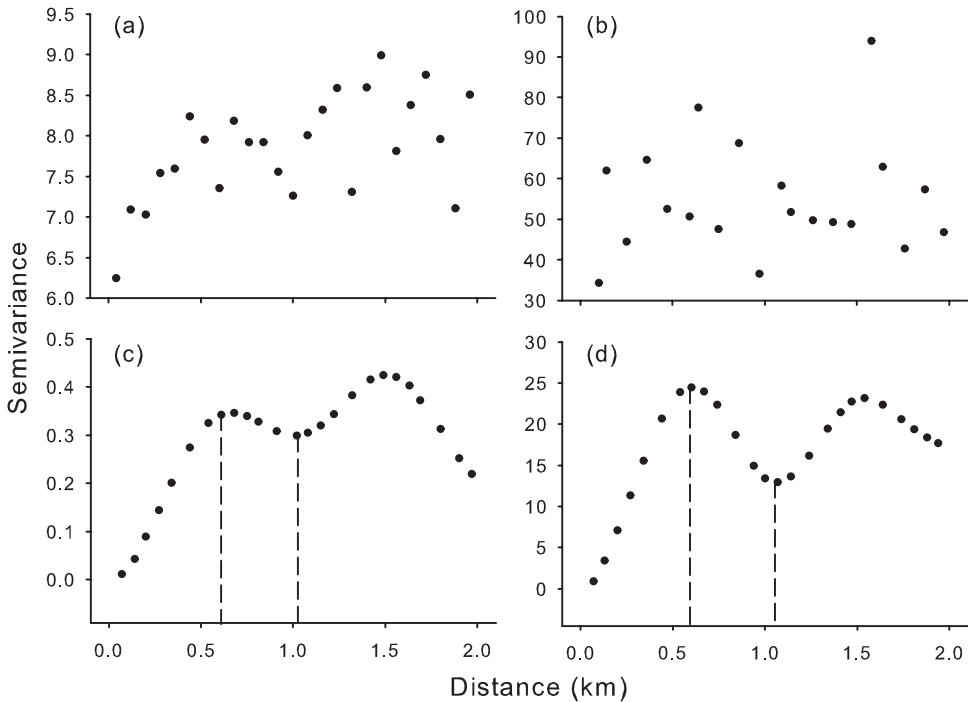


**Figure 9.5** Semivariograms of (a) trout counts, (b) 100-m bins of counts, (c) locally weighted scatterplot smoothing (LOWESS) of counts and (d) LOWESS of 100-m bins in the main stem of Camp Creek (see Figure 9.4). Dashed vertical lines indicate the locations of peaks and valleys in semivariance with respect to the  $x$ -axis.

$x$ -axis location of the first valley indicates the average spacing between successive peaks and valleys (Legendre and Fortin, 1989). The shapes of the variograms from the raw counts (Figure 9.5(c)) and from the binned data (Figure 9.5(d)) differed little. Thus, the underlying spatial structure of fish counts was the same whether it was derived from the LOWESS of the raw counts or the LOWESS of the binned data. Statistical tests were not necessary to evaluate the significance of the variograms of fish counts in the main stem of Camp Creek because the patterns confirmed the results of graphical analysis.

Extending this analysis into the fish-bearing tributaries (Figure 9.3; tributaries 4, 7, 9 and 10) required an automated approach for testing the statistical significance of patterns observed in the semivariogram (Ganio *et al.*, 2005). A network semivariogram was used to simultaneously compare spatial autocorrelation throughout the entire fish-bearing portion of the stream network shown in Figure 9.3. The semivariogram provided a means to compare the patterns of fish counts in the network to

a hypothetical random spatial distribution. If the data are randomly distributed in space, the semivariogram depicts a horizontal cloud of points with no trend in semivariance with increasing separation distance between sample points. Such a pattern confirms that the data are spatially independent (i.e. sample points that are close to one another are not more similar than sample points that are far apart). To determine whether the spatial structure of fish counts depicted in the network semivariogram differed from a random distribution, 5000 permutations of the fish counts were generated, and 2.5th and 97.5th percentiles were calculated. A statistical routine in the S-PLUS statistical package (S-PLUS, 2002) was used to randomly reassign the fish counts to different locations in the stream network for each permutation (Ganio *et al.*, 2005). The characteristic shape and inflection point of the semivariogram in Figure 9.6 indicates that fish counts were non-randomly distributed in the stream network. The departure of semivariance values outside of the horizontal ‘random’ band defined by the percentile boundaries indicated statistically significant spatial structure in the semivariogram at a scale of approximately 1 km – the mean distance between fish-bearing tributaries. This distance is greater than the corresponding peak-to-valley distance (0.5 km) in the main stem alone (Figure 9.4(b)) because it incorporates the entire fish-bearing portion of the stream network. These analyses indicate the potential value of geostatistical techniques for identifying tributary impacts (Torgersen *et al.*, 2004), but more work is needed across multiple stream networks to test specific hypotheses on the role of tributaries in structuring biotic and abiotic gradients in river networks.

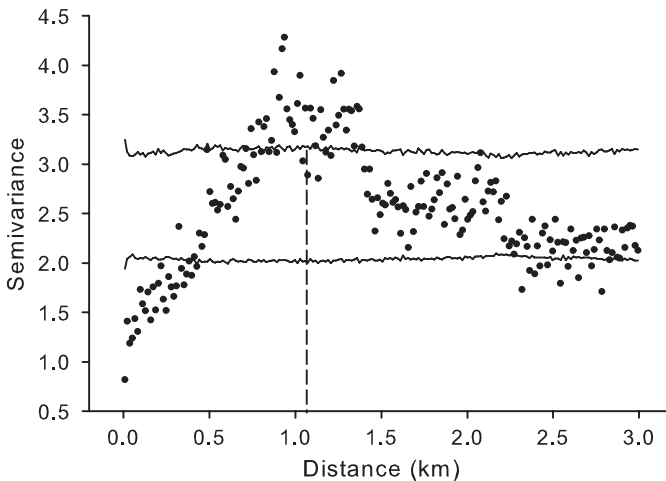


**Figure 9.6** Network semivariogram of trout counts in Camp Creek (see Figure 9.3). Dashed vertical line indicates the location of the peak in semivariance with respect to the x-axis. Horizontal lines are 2.5th and 97.5th percentiles generated from 5000 permutations.

## Future developments and challenges

Methods for identifying tributary impacts in fluvial networks have advanced rapidly due to improvements in sampling, mapping and automated analysis techniques. However, the increasing availability of high-resolution data over long reaches of stream will require riverine scientists to draw upon analysis tools and approaches developed by other disciplines. Intensive approaches to data collection and statistical analysis, which have traditionally derived relationships from a limited number of sites, will need to be adapted to handle large, spatially autocorrelated data sets. Sophisticated statistical tools for pattern detection, such as wavelet analysis, are perfectly suited to evaluating complex spatial patterns but are not commonly applied in rivers (Csillag and Kabos, 2002). These methods were designed for decomposing hierarchical structure in time series and one-dimensional data, which are similar in spatial configuration to the nested spatial pattern of biotic and abiotic features along river channels. An advantage of wavelets over semivariograms is that the wavelet transform function preserves locational information along a transect (i.e. the main stem) (Bradshaw and Spies, 1992). Thus, in wavelet analysis the positions of tributary junctions can be evaluated directly with respect to any hierarchical spatial structure in the data. In contrast, the semivariogram loses locational information due to the averaging of variances across all data points. These two different methods of analysis are complementary but seldom have been used together to elucidate spatial heterogeneity associated with tributary effects (Torgersen *et al.*, 2004).

The spatial analysis of river networks is currently a major focus of environmental monitoring and assessment at local and regional scales and can provide useful tools for understanding and modelling tributary impacts in a network context (Peterson and Urban, 2006; Theobald *et al.*, 2006; Ver Hoef *et al.*, 2006). Other disciplines, such as transportation geography, have developed specialized techniques for studying point patterns in road networks (Yamada and Thill, 2004). Kernel density estimates use a set of probabilities to represent the intensity of spatial point patterns and have been used to examine the spatial clumping of plant species in road networks (Spooner *et al.*, 2004).

The analytical tools and approaches described in this chapter constitute a first step towards understanding tributary impacts using spatially explicit data sets. The application of these and other state-of-the-art methods has significant potential for identifying tributary impacts and developing a better understanding of complex spatial patterns in fluvial networks. Next steps involve the development, testing and transfer of models that predict tributary impacts in systems where data are limited or difficult to collect over large areas (Benda *et al.*, 2004b; Rice, 1998). Recent modelling work on sediment routing at tributary junctions illustrates that longitudinal discontinuities in physical and biological diversity can be predicted at network scales (Ferguson *et al.*, 2006; Rice *et al.*, 2006). Such predictive models can be tested against empirical patterns revealed through the methods outlined in this chapter. The ultimate goal of a combined approach to empirical pattern analysis and modelling is to simulate the spatially dynamic

physical and biological mosaic of tributary–main-stem interactions unfolding through time.

## Acknowledgements

The authors thank all of the dedicated field crews who spent long hours walking, crawling and swimming hundreds of kilometres in rivers and streams to collect the data that were necessary to develop the ideas, concepts and analyses in this chapter. Critical reviews by C. Konrad, C. Mebane, an anonymous reviewer and co-editor Steve Rice significantly improved the clarity and content of earlier versions of this chapter. This work was produced through the Cooperative Forest Ecosystem Research Program, with funding provided by the USGS Forest and Rangeland Ecosystem Science Center and the Oregon Department of Forestry. Additional funding was provided by US Environmental Protection Agency/National Science Foundation Joint Watershed Research Program (R82–4774–010).

## References

- Armitage PD, Cannan CE. 1998. Nested multi-scale surveys in lotic systems: Tools for management. In *Advances in River Bottom Ecology*, Bretschko G, Helesic J (eds). Backhuys Publishers: Leiden, The Netherlands; 293–314.
- Barker RJ, Sauer JR. 1995. Statistical aspects of point count sampling. In *Monitoring Bird Populations by Point Counts*, Ralph CJ, Sauer JR, Droegge S (eds). General Technical Report PSW-GTR-149. USDA Forest Service, Pacific Southwest Research Station: Albany, California; 125–130.
- Bateman DS, Gresswell RE, Torgersen CE. 2005. Evaluating single-pass catch as a tool for identifying spatial pattern in fish distribution. *Journal of Freshwater Ecology* **20**: 335–345.
- Benda L, Veldhuisen C, Black J. 2003. Debris flows as agents of morphological heterogeneity at low-order confluences, Olympic Mountains, Washington. *GSA Bulletin* **115**: 1110–1121.
- Benda L, Andras K, Miller D, Bigelow P. 2004a. Confluence effects in rivers: Interactions of basin scale, network geometry, and disturbance regimes. *Water Resources Research* **40**: WR002583.
- Benda L, Poff NL, Miller D, Dunne T, Reeves GH, Pess GH, Polluck M. 2004b. The network dynamics hypothesis: How channel networks structure riverine habitats. *Bioscience* **54**: 413–427.
- Benda L, Miller D, Andras K, Bigelow P, Reeves G, Michael D. In press. Coupling landscape scale terrain databases with customized analysis tools for watershed analysis and resource management. *Forest Science*.
- Bigelow P, Benda L, Miller D, Burnett K. 2007. On debris flows, river networks, and the spatial structure of channel morphology. *Forest Science* **53**: 220–238.
- Bradshaw GA, Spies TA. 1992. Characterizing canopy gap structure in forests using wavelet analysis. *Journal of Ecology* **80**: 205–215.

- Bruns DA, Minshall GW, Cushing CE, Cummins KW, Brock JT, Vannote RL. 1984. Tributaries as modifiers of the river continuum concept: Analysis by polar ordination and regression models. *Archiv für Hydrobiologie* **99**: 208–220.
- Carbonneau PE, Bergeron N, Lane SN. 2005. Automated grain size measurements from airborne remote sensing for long profile measurements of fluvial grain sizes. *Water Resources Research* **41**: WR003994.
- Charlton ME, Large ARG, Fuller IC. 2003. Application of airborne LiDAR in river environments: The River Coquet, Northumberland, UK. *Earth Surface Processes and Landforms* **28**: 299–306.
- Cherkauer KA, Burges SJ, Handcock RN, Kay JE, Kampf SK, Gillespie AR. 2005. Assessing satellite-based and aircraft-based thermal infrared remote sensing for monitoring Pacific Northwest river temperature. *Journal of the American Water Resources Association* **41**: 1149–1159.
- Clarke S, Burnett K. 2003. Comparison of digital elevation models for aquatic data development. *Photogrammetric Engineering and Remote Sensing* **69**: 1367–1375.
- Cochran WG. 1977. *Sampling techniques*. John Wiley & Sons: Chichester.
- Connolly PJ, Hall JD. 1999. Biomass of coastal cutthroat trout in unlogged and previously clear-cut basins in the central Coast Range of Oregon. *Transactions of the American Fisheries Society* **128**: 890–899.
- Conquest LL, Ralph SC. 1998. Statistical design and analysis considerations for monitoring and assessment. In *River Ecology and Management*, Naiman RJ, Bilby RE (eds). Springer: New York; 455–475.
- Cooper SD, Barmuta L, Sarnelle O, Kratz K, Diehl S. 1997. Quantifying spatial heterogeneity in streams. *Journal of the North American Benthological Society* **16**: 174–188.
- Csillag F, Kabos S. 2002. Wavelets, boundaries, and the spatial analysis of landscape pattern. *Ecoscience* **9**: 177–190.
- Cunjak RA, Randall RG, Chadwick EMP. 1988. Snorkeling versus electrofishing: A comparison of census techniques in Atlantic salmon rivers. *Naturaliste Canadien* **115**: 89–93.
- Dent CL, Grimm NB. 1999. Spatial heterogeneity of stream water nutrient concentrations over successional time. *Ecology* **80**: 2283–2298.
- Diplas P, Sutherland A. 1988. Sampling techniques for gravel sized sediments. *American Society of Civil Engineers, Journal of the Hydraulics Division* **114**: 484–501.
- Downes BJ, Lake PS, Schreiber ESG. 1993. Spatial variation in the distribution of stream invertebrates: Implications of patchiness for models of community organization. *Freshwater Biology* **30**: 119–132.
- Ettema CH, Wardle DA. 2002. Spatial soil ecology. *Trends in Ecology and Evolution* **17**: 177–183.
- Fausch KD, Torgersen CE, Baxter CV, Li HW. 2002. Landscapes to riverscapes: Bridging the gap between research and conservation of stream fishes. *Bioscience* **52**: 483–498.
- Ferguson RI, Cuddin JR, Hoey TB, Rice SP. 2006. River system discontinuities due to lateral inputs: Generic styles and controls. *Earth Surface Processes and Landforms* **31**: 1149–1166.
- Fernandes CC, Podos J, Lundberg JG. 2004. Amazonian ecology: Tributaries enhance the diversity of electric fishes. *Science* **305**: 1960–1962.
- Frissell CA, Liss WJ, Warren CE, Hurlley MD. 1986. A hierarchical framework for stream habitat classification: Viewing streams in a watershed context. *Environmental Management* **10**: 199–214.
- Ganio LM, Torgersen CE, Gresswell RE. 2005. A geostatistical approach for describing spatial pattern in stream networks. *Frontiers in Ecology and Environment* **3**: 138–144.

- GDS. 2004. *GS+ Geostatistics for the Environmental Sciences*, Version 7. Gamma Design Software: Plainwell, Michigan.
- Graham DJ, Rice SP, Reid I. 2005. A transferable method for the automated grain sizing of river gravels. *Water Resources Research* **41**: WR003868.
- Gresswell RE, Torgersen CE, Bateman DS, Guy TJ, Hendricks SR, Wofford JEB. 2006. A spatially explicit approach for evaluating relationships among coastal cutthroat trout, habitat, and disturbance in small Oregon streams. In *Landscape Influences on Stream Habitats and Biological Assemblages*, Hughes RM, Wang L, Seelbach PW (eds). American Fisheries Society: Bethesda, Maryland; 457–471.
- Handcock RN, Gillespie AR, Cherkauer KA, Kay JE, Burges SJ, Kampf SK. 2006. Accuracy and uncertainty of thermal-infrared remote sensing of stream temperatures at multiple spatial scales. *Remote Sensing of Environment* **100**: 457–473.
- Hankin DG, Reeves GH. 1988. Estimating total fish abundance and total habitat area in small streams based on visual estimation methods. *Canadian Journal of Fisheries and Aquatic Sciences* **45**: 834–844.
- Hauer FR, Lamberti GA. 1998. *Methods in stream ecology*. Academic Press: San Diego, CA.
- Hauer FR, Lorang MS. 2004. River regulation, decline of ecological resources, and potential for restoration in a semi-arid lands river in the western USA. *Aquatic Sciences: Research across boundaries* **66**: 388–401.
- Hicks BJ, Hall JD. 2003. Rock type and channel gradient structure salmonid populations in the Oregon Coast Range. *Transactions of the American Fisheries Society* **132**: 468–482.
- Hildrew AG, Giller PS. 1994. Patchiness, species interactions, and disturbance in the stream benthos. In *Aquatic Ecology: Scale, Pattern and Process*, Giller PS, Hildrew AG, Raffaelli DG (eds). Blackwell Science Ltd: Oxford; 21–62.
- Hirzel A, Guisan A. 2002. Which is the optimal sampling strategy for habitat suitability modelling? *Ecological Modelling* **157**: 331–341.
- Howard JK, Cuffey KM. 2003. Freshwater mussels in a California North Coast Range river: Occurrence, distribution, and controls. *Journal of the North American Benthological Society* **22**: 63–77.
- Isaak DJ, Thurow RF. 2006. Network-scale spatial and temporal variation in Chinook salmon (*Oncorhynchus tshawytscha*) redd distributions: Patterns inferred from spatially continuous replicate surveys. *Canadian Journal of Fisheries and Aquatic Sciences* **63**: 285–296.
- Kiffney PM, Greene CM, Hall JE, Davies JR. 2006. Tributary streams create spatial discontinuities in habitat, biological productivity, and diversity in mainstem rivers. *Canadian Journal of Fisheries and Aquatic Sciences* **63**: 2518–2530.
- Latulippe C, Lapointe ML, Talbot T. 2001. Visual characterization technique for gravel-cobble river bed surface sediments; Validation and environmental applications contribution to the Program of CIRSA (Center Interuniversitaire Recherche sur le Saumon Atlantique. *Earth Surface Processes and Landforms* **26**: 307–318.
- Legendre P, Fortin M-J. 1989. Spatial pattern and ecological analysis. *Vegetatio* **80**: 107–138.
- Legleiter CJ, Roberts DA, Marcus WA, Fonstad MA. 2004. Passive optical remote sensing of river channel morphology and in-stream habitat: Physical basis and feasibility. *Remote Sensing of Environment* **93**: 493–510.
- Lorang MS, Whited DC, Hauer FR, Kimball JS, Stanford JA. 2005. Using airborne multispectral imagery to evaluate geomorphic work across floodplains of gravel-bed rivers. *Ecological Applications* **15**: 1209–1222.

- Macnab K, Jacobson C, Brierley G. 2006. Spatial variability of controls on downstream patterns of sediment storage: A case study in the Lane Cove catchment, New South Wales, Australia. *Geographical Research* **44**: 255–271.
- May CL, Gresswell RE. 2003. Processes and rates of sediment and wood accumulation in head-water streams of the Oregon Coast Range, USA. *Earth Surface Processes and Landforms* **28**: 409–424.
- Marcus WA, Legleiter CJ, Aspinall RJ, Boardman JW, Crabtree RL. 2003. High spatial resolution, hyperspectral (HSRH) mapping of in-stream habitats, depths, and woody debris mountain streams. *Geomorphology* **55**: 363–380.
- McIntosh BA, Sedell JR, Thurow RF, Clarke SE, Chandler GL. 2000. Historical changes in pool habitats in the Columbia River basin. *Ecological Applications* **10**: 1478–1496.
- Mertes LAK, Dekker AG, Brakenridge GR, Birkett CM, Letourneau G. 2004. Rivers and lakes. In *Manual of remote sensing, Volume 4: Remote sensing for natural resource management and environmental monitoring*, Ustin SL (ed.). John Wiley & Sons: Hoboken, New Jersey; 345–400.
- Mullner SA, Hubert WA, Wesche TA. 1998. Snorkeling as an alternative to depletion electrofishing for estimating abundance and length-class frequencies of trout in small streams. *North American Journal of Fisheries Management* **18**: 947–953.
- Osborne LL, Wiley MJ. 1992. Influence of tributary spatial position on the structure of warmwater fish communities. *Canadian Journal of Fisheries and Aquatic Sciences* **49**: 671–681.
- Palmer MW. 2002. Scale detection using semivariograms and autocorrelograms. In *Learning Landscape Ecology: A Practical Guide to Concepts and Techniques*, Gergel SE, MG Turner (eds). Springer: New York; 129–144.
- Persat H, Copp GH. 1990. Electric fishing and point abundance sampling for the ichthyology of large rivers. In *Developments in electric fishing*, Cowx IG (ed.). Cambridge University Press: Cambridge, UK; 197–209.
- Peterson E, Urban DL. 2006. Predicting water quality-impaired stream segments using landscape-scale data and a regional geostatistical model: A case study in Maryland. *Environmental Monitoring and Assessment* **121**: 613–636.
- Poole GC. 2002. Fluvial landscape ecology: Addressing uniqueness within the river discontinuum. *Freshwater Biology* **47**: 641–660.
- Poole GC, Berman CH. 2001. An ecological perspective on in-stream temperature: Natural heat dynamics and mechanisms of human-caused thermal degradation. *Environmental Management* **27**: 787–802.
- Power G, Brown RS, Imhof JG. 1999. Groundwater and fish - insights from northern North America. *Hydrological Processes* **13**: 401–422.
- Power ME, Brozovic N, Bode C, Zilberman D. 2005. Spatially explicit tools for understanding and sustaining inland water ecosystems. *Frontiers in Ecology and Environment* **3**: 47–55.
- Radko MA. 1997. *Spatially linking basin-wide stream inventories in a geographic information system*. General Technical Report INT-GTR-345. US Department of Agriculture, Forest Service, Intermountain Research Station: Ogden, Utah, USA.
- Reutebuch S, Andersen H-E, McGaughey RJ. 2005. LIDAR: An emerging tool for multiple resource inventory. *Journal of Forestry* **103**: 286–292.
- Rice S. 1998. Which tributaries disrupt downstream fining along gravel-bed rivers? *Geomorphology* **22**: 39–56.
- Rice S, Church M. 1998. Grain size along two gravel-bed rivers: Statistical variation, spatial pattern and sedimentary links. *Earth Surface Processes and Landforms* **23**: 345–363.

- Rice SP, Greenwood MT, Joyce CB. 2001. Tributaries, sediment sources, and the longitudinal organisation of macroinvertebrate fauna along river systems. *Canadian Journal of Fisheries and Aquatic Sciences* **58**: 824–840.
- Rice SP, Ferguson RI, Hoey TB. 2006. Tributary control of physical heterogeneity and biological diversity at river confluences. *Canadian Journal of Fisheries and Aquatic Sciences* **63**: 2553–2566.
- Roni P, Fayram A. 2000. Estimating winter salmonid abundance in small western Washington streams: A comparison of three techniques. *North American Journal of Fisheries Management* **20**: 683–692.
- Rossi RE, Mulla DJ, Journel AG, Franz EH. 1992. Geostatistical tools for modeling and interpreting ecological spatial dependence. *Ecological Monographs* **62**: 277–314.
- S-PLUS. 2002. *S-PLUS for Windows, Version 6.1*. Insightful Corporation: Seattle, WA.
- Schneider DC. 1994a. *Quantitative ecology: Spatial and temporal scaling*. Academic Press: San Diego, California.
- Schneider DC. 1994b. Scale-dependent patterns and species interactions in marine nekton. In *Aquatic Ecology: Scale, Pattern and Process*, Giller PS, Hildrew AG, Raffaelli DG (eds). Blackwell Science Ltd: Oxford; 441–467.
- Schneider DC, Piatt JF. 1986. Scale-dependent correlation of seabirds with schooling fish in a coastal ecosystem. *Marine Ecology Progress Series* **32**: 237–246.
- Sokal RR, Rohlf FJ. 1995. *Biometry: The principles and practice of statistics in biological research*. W.H. Freeman: New York.
- Spooner PG, Lunt ID, Okabe A, Shiode S. 2004. Spatial analysis of roadside *Acacia* populations on a road network using the network K-function. *Landscape Ecology* **19**: 491–499.
- SPSS. 2004. *SigmaPlot, Version 9.0*. SPSS Science: Chicago, Illinois, USA.
- Stevens LE, Shannon JP, Blinn DW. 1997. Colorado River benthic ecology in Grand Canyon, Arizona, USA: Dam, tributary and geomorphological influences. *Regulated Rivers: Research and Management* **13**: 129–149.
- Stock J, Dietrich WE. 2003. Valley incision by debris flows: Evidence of a topographic signature. *Water Resources Research* **39**: WR001057.
- Theobald DM, Norman JB, Peterson E, Ferraz S, Wade A, Sherburne MR. 2006. *Functional linkage of water basins and streams (FLoWS): ArcGIS tools for network-based analysis of freshwater ecosystems, Version 1*. Natural Resource Ecology Lab, Colorado State University: Fort Collins, CO.
- Torgersen CE, Close DA. 2004. Influence of habitat heterogeneity on the distribution of larval Pacific lamprey (*Lampetra tridentata*) at two spatial scales. *Freshwater Biology* **49**: 614–630.
- Torgersen CE, Faux RN, McIntosh BA, Poage NJ, Norton DJ. 2001. Airborne thermal remote sensing for water temperature assessment in rivers and streams. *Remote Sensing of Environment* **76**: 386–398.
- Torgersen CE, Gresswell RE, Bateman DS. 2004. Pattern detection in stream networks: Quantifying spatial variability in fish distribution. In *GIS/Spatial Analyses in Fishery and Aquatic Sciences (Volume 2)*, Nishida T, Kailola PJ, Hollingworth CE (eds). Fishery-Aquatic GIS Research Group: Saitama, Japan; 405–420.
- Torgersen CE, Baxter CV, Li HW, McIntosh BA. 2006. Landscape influences on longitudinal patterns of river fishes: Spatially continuous analysis of fish-habitat relationships. In *Landscape Influences on Stream Habitats and Biological Assemblages*, Hughes RM, L Wang, PW Seelbach (eds). American Fisheries Society: Bethesda, Maryland; 473–492.

- Trexler JC, Travis J. 1993. Nontraditional regression analysis. *Ecology* **74**: 1629–1637.
- USGS. 2007. *National Map Accuracy Standards (NMAS)*. US Geological Survey, National Mapping Program, <http://rockyweb.cr.usgs.gov/nmpstds/nmas647.html>, accessed 23 January 2008.
- Vaccaro JJ, Maloy KJ. 2006. *A thermal profile method to identify potential ground-water discharge areas and preferred salmonid habitats for long river reaches*. US Geological Survey Scientific Investigations Report 2006–5136: Reston, Virginia.
- Ver Hoef J, Peterson E, Theobald DM. 2006. Spatial statistical models that use flow and stream distance. *Environmental and Ecological Statistics* **13**: 449–464.
- Walsh SJ, Butler DR, Malanson GP. 1998. An overview of scale, pattern, process relationships in geomorphology: A remote sensing and GIS perspective. *Geomorphology* **21**: 183–205.
- Wigington PJ, Moser TJ, Lindeman DR. 2005. Stream network expansion: A riparian water quality factor. *Hydrological Processes* **19**: 1715–1721.
- Wipfli MS. 2005. Trophic linkages between headwater forests and downstream fish habitats: Implications for forest and fish management. *Landscape and Urban Planning* **72**: 205–213.
- Wipfli MS, Gregovich DP. 2002. Export of invertebrates and detritus from fishless headwater streams in southeastern Alaska: Implications for downstream salmonid production. *Freshwater Biology* **47**: 957–969.
- Wolman M. 1954. A method for sampling coarse river-bed material. *American Geophysical Union Transactions* **35**: 951–956.
- Yamada I, Thill J. 2004. Comparison of planar and network *K*-functions in traffic accident analysis. *Journal of Transport Geography* **12**: 149–158.



# 10

## Effects of tributaries on main-channel geomorphology

Rob Ferguson<sup>1</sup> and Trevor Hoey<sup>2</sup>

<sup>1</sup>*Department of Geography, Durham University, UK*

<sup>2</sup>*Department of Geographical and Earth Sciences, University of Glasgow, UK*

### Introduction

All tributaries add to the water discharge of the streams or rivers that they enter, and most also supply additional sediment. The consequences of tributary inputs may be apparent both within the confluence and for some distance up and down the main channel. The local consequences stem from the detailed hydrodynamics of the confluence and include the formation of scour pools and junction bars, as discussed by Best (1988 and Best and Rhoads, Chapter 4, this volume). This chapter is about the more extensive effects that tributaries can have on main-stem geomorphology by inducing discontinuities in channel size, slope and bed composition. These discontinuities and the consequent step changes in flow characteristics and physical habitat are ecologically significant (Rice *et al.* and Benda, Chapters 11 and 13, this volume) but they have received only sporadic attention from geomorphologists. Moreover, this attention has generally been restricted to a speculative interpretation of changes past junctions in particular catchments. The pioneers of hydraulic geometry (Leopold and Maddock, 1953) recognized a general principle that if channel properties scale as power functions of discharge they should change discontinuously with distance (see also Knighton, 1987), but there have been remarkably few attempts to test whether this is actually the case; Richards (1980) is a

notable exception. Tributary inputs of water and sediment also appear to cause discontinuities in main-channel gradient and/or bed grain-size distribution (e.g. Sternberg, 1875; Church and Kellerhals, 1978; Knighton, 1980; Rice and Church, 1998) and are sometimes associated with transformations of channel pattern (e.g. Schumm, 2005, p. 105). Only a few authors have considered what kinds of tributaries have the most impact on main-stem properties, using either qualitative arguments (e.g. Knighton, 1980; Rice, 1998) or statistical analysis of field evidence (Rice, 1998; Benda *et al.*, 2004). In this chapter, we discuss the circumstances in which tributaries have reach-scale impacts on main-stem characteristics and consider how the type and extent of change is related to the characteristics of the tributary, the channel it is joining and the geomorphological setting. We refer extensively to the empirical literature but attempt to complement it by considering the topic from a theoretical point of view, since this can isolate the effects of the multiple controlling factors that are commonly present in field situations.

The structure of the chapter involves an interplay between deductive arguments about how tributaries might be expected to affect the channels they join, based on conceptual and theoretical models which represent fluvial processes in tractable ways, and empirical evidence of what actually happens near tributary junctions. We begin with a conceptual model that suggests why tributaries can be expected to affect main-channel characteristics, particularly in gravel-bed rivers that occupy confined valleys. A survey of the case-study literature shows that the conceptual arguments capture some of what happens in nature but have limitations. Empirical evidence on width change past confluences is considered in this section. The third section reverts to a theoretical approach, developed in two stages. The first is a new mathematical analysis of what downstream changes are necessary past a junction to maintain the sediment-transporting equilibrium of the main stem. This analysis is similar to rational approaches to river regime and downstream hydraulic geometry insofar as it represents the mosaic of bed grain-size distributions in a reach by a single representative diameter. We then relax the assumption of equilibrium and represent the bed by a grain-size distribution which may alter along a reach and, together with the long profile, may evolve over time. Analytical solutions are no longer possible so we resort to using numerical modelling to explore sensitivity to the controlling factors and identify a typology of tributary impacts. In the final section of the chapter we reflect on the increased complexity that is required as additional degrees of freedom are recognized, the limitations this imposes on our ability to understand and predict the effects tributaries have on main-stem geomorphology, and what the research community needs to do to make further progress on this topic.

Attention is mainly directed towards natural situations where tributaries join main stems, but the qualitative and quantitative arguments also apply where the tributary or the main stem is regulated. They even hold in situations where there is no tributary in the usual sense, but natural processes (e.g. debris flows or landslides) or human activities (e.g. waste disposal from alluvial mining) add substantial amounts of sediment to a

river over a very short distance without a significant addition of water. Our conceptual framework is also applicable to mixed alluvial-bedrock river systems, which share a qualitatively similar network structure and downstream hydraulic geometry. However, some of the reach-scale controlling processes differ in bedrock-dominated systems; we consider these differences in our discussion.

## Conceptual considerations

A useful starting point is a qualitative regime model that was proposed by the American engineer Emory Lane (Lane, 1955), has antecedents in the much earlier work of Gilbert (1914) and is mentioned in many textbooks of fluvial geomorphology and river engineering (e.g. Richards, 1982; Chang, 1988). Lane recognized that river regime requires a balance between sediment supply and transport capacity, and expressed this in the pseudo-equation:

$$Q, S \sim L, D \quad (10.1)$$

where  $L, D$  denote the flux and characteristic grain size of bed-material load supplied from upstream and  $Q, S$  denote the water discharge and channel slope. The idea is that if any of the four variables alters at least one other must respond to maintain regime. The variable on the same side of the balance could change in the opposite direction (e.g. the higher the discharge, the lower the gradient required to convey a given amount and calibre of load), or a variable on the opposite side could change in the same direction (e.g. the coarser the sediment in a river, the greater the discharge and/or slope required to convey the same quantity of sediment).

Lane's qualitative balance can be given some quantitative underpinning using standard equations for width-averaged flow and bed-material transport. For example, the transport capacity  $L$  (mass or volume per unit time) of a gravel-bed river is often assessed using the Meyer-Peter and Müller equation, which can be expressed as:

$$L = kw(\tau - \tau_c)^{1.5} \quad (10.2)$$

Here  $k$  is a scaling coefficient that depends on sediment density and the units of measurement of the other variables,  $w$  is channel width,  $\tau$  is the shear stress applied by the flow to the bed and  $\tau_c$  is the critical shear stress to move the bed material. Discharge, slope and grain size do not appear directly in Equation 10.2 but they are implicit in it since  $\tau$  is proportional to the product of depth and slope, depth increases with discharge when other factors are equal and  $\tau_c$  depends mainly on  $D$ . Transport capacity therefore

increases with  $Q$  and  $S$  but decreases with  $D$ . It is far more sensitive to  $D$  in gravel-bed rivers, where  $\tau$  seldom exceeds  $\tau_c$  by more than 50 per cent, than in sand-bed rivers, where  $\tau_c$  is normally at least an order of magnitude smaller than  $\tau$  (e.g. Dade and Friend, 1998). For equilibrium, the transport capacity must balance the supply from upstream, so Equation 10.2 becomes a more specific form of Equation 10.1, as also noted by Church (2006).

Lane (1955) does not apply his conceptual model to what happens past confluences, but it describes the possibilities well. Unless the extra streamflow exactly balances the extra sediment load, Equation 10.1 or Equation 10.2 suggests there will be some adjustment of slope and perhaps also grain size. For example, if  $D$  and  $\tau_c$  were unchanged, a heavily laden tributary would overload the main stem unless there was some increase in channel slope past the junction. This implies aggradation at the junction or a reduction in sinuosity. Conversely, a clearwater tributary (one flowing from a lake or reservoir, with negligible sediment load) increases  $Q$  but not  $L$ , so Equation 10.1 suggests that the main-stem sediment load can be transported over a lower slope below the confluence; this could be achieved by degradation, as commonly observed below dams, or by an increase in sinuosity.

In the light of our present understanding of river processes and response, based on a literature that has grown hugely since 1955, Lane's qualitative arguments remain valid in essence but can be seen to simplify or omit some other relevant considerations. First, the extent to which  $D$  can be a response variable rather than an independent control depends very much on the type of river. Gravel-bed rivers generally have a far wider range of grain sizes present on the bed than do sand-bed rivers, and gravel transport is often size-selective, so the bed can become coarser or finer through preferential entrainment and deposition. For example, rather than a clearwater tributary leading to a reduction in slope it could lead to partial armouring of the bed, or some combination of degradation and armouring, as observed in most of the dam case studies discussed by Williams and Wolman (1984). Sand-bed rivers generally have narrower bed-material size distributions, affording less opportunity for  $D$  to be an adjustable part of the regime, and transport is normally almost unselective. A massive tributary input of gravel to a main stem with a sandy bed can, however, be enough to transform it into a gravel-bed channel, just as a massive input of sand into a gravel channel can blanket the gravel and transform the river bed.

The other factor not considered by Lane (1955), but which complicates the application of his balance concept to adjustments at confluences, is the possibility of a change in main-stem channel width as a result of tributary inflow. The bankfull width of a river channel scales with the discharge it conveys during flood conditions. Statistical data analysis suggests a power-law relationship  $w \propto Q^b$  with an exponent of about 0.5 over the full range from laboratory channels and small streams to the Earth's largest rivers (e.g. Church, 1992). This is one of a set of trends often referred to as 'downstream hydraulic geometry' (Leopold and Maddock, 1953), but 'downstream' is rather misleading here

since discharge does not in fact increase smoothly with distance downstream but in step changes at major junctions; width and depth might therefore be expected to do the same. A change in width past a junction complicates the assessment of change in bedload transport capacity. Considering Equation 10.2 again, transport capacity for given  $Q$ ,  $S$ ,  $D$  increases linearly with width but non-linearly with depth and therefore depends on the width-to-depth ratio. In most situations, the wider the channel below a junction, the lower its transport capacity if all else is equal. This is an example of how rivers have more degrees of freedom than Lane (1955) considered, so that adjustments are shared amongst several channel characteristics each of which alters less than might be supposed on the basis of Equation 10.1.

A third conceptual consideration is the degree of coarse-sediment coupling between tributary and main stem. This is an extension of a concept familiar in relation to hillslope geomorphology and accelerated soil erosion (e.g. Harvey, 2002): a slope separated from the river by a floodplain does not feed water or sediment directly into the river, which in turn does not influence what is happening in or on the hillslope. Tributary flow does normally connect to main rivers, but flood peaks may not be synchronous (especially in regulated systems or large basins spanning different climate zones), and in drylands ephemeral flows in tributary and main stem may not coincide and transmission losses have to be considered (Thornes, 1977; Reid *et al.*, 1989). Tributaries have sedimentary coupling in narrow upland valleys (e.g. Rice and Church, 1996), and also in wide valleys if the recipient channel happens to be up against flanking hills, but where tributaries cross a low-gradient floodplain their coarse load is deposited in fans at the valley margin. This greatly reduces the scope for tributaries to have a major impact on main-stem slope or grain size. In valleys of variable width, it is possible for some tributaries to be coupled in terms of sediment supply but others not (e.g. Rice, 1998).

## Empirical evidence

It is very likely that the majority of tributaries have no perceptible effect on the rivers they join, but it is hard to demonstrate this from the published literature, which understandably emphasizes locations where something ‘interesting’, but possibly unusual, occurs. The meta-study by Benda *et al.* (2004) documented a variety of responses, with aggradation prominent, and noted a statistical tendency for effects to be reported more often for larger tributaries. Rice’s work on the Pine and Sukunka rivers in western Canada (Rice and Church, 1998; Rice, 1998, 1999) emphasized the disruptive effects of tributaries to these confined rivers, but in fact less than 20 per cent of the tributaries had a perceptible effect on main-stem grain size. This is not surprising from a theoretical standpoint: the topology of drainage networks is such that most junctions are between channels of very different link magnitude (= number of fingertip headwaters, a surrogate for catchment area and streamflow), and a tributary that is much smaller

than the stream it joins is unlikely to add enough discharge to require a significant increase in width or enough bedload to have a perceptible impact on bed calibre or slope. Moreover, even large tributaries cannot alter the calibre of the main-channel bed unless the tributary bedload is not merely large in quantity but also appreciably coarser or finer.

Theoretical considerations do nevertheless suggest two kinds of impact that should be discernible in the field: main-stem width should increase appreciably where a major tributary joins and bed grain size and/or slope should alter where a tributary injects a significant quantity of bedload that is substantially finer or coarser than the load from the proximal main stem. We present here a non-exhaustive summary of the literature that either describes situations known to fulfil these conditions or infers the second type of impact from the existence of discontinuities in main-stem character past junctions.

## Channel size

The expectation of step changes in channel size past major confluences is noted by Leopold and Maddock (1953) but there have been few detailed investigations of changes in width and none as far as we know of changes in mean channel depth (as opposed to studies of how confluence scour-pool depth relates to junction angle and discharge ratio). The most detailed study of discontinuities in width is that by Richards (1980), who uses field measurements along streams in upland Britain to show that width is essentially constant along individual network links but increases past junctions in proportion to the 0.6 power of link magnitude. Since magnitude scales with catchment area and discharge generally increase more slowly than area, Richards' result is not inconsistent with  $w \propto Q^{0.5}$ .

Circumstantial evidence supporting the application of traditional hydraulic geometry equations to confluences is illustrated in Figure 10.1. This plot refers to 14 of the biggest river junctions on Earth, located in South America, Siberia, western Africa and northern Canada, and is based on measurements made from satellite images (S.N. Lane, *personal communication*, 2006). Lane's data on the widths of the channels above and below each confluence can be used to test agreement with the assumption that  $w \propto Q^b$  in general and  $w \propto Q^{0.5}$  in particular. Let  $w_p$ ,  $w_t$ , and  $w_d$  denote the widths of the proximal main river (taken to be the wider of the two rivers that join), the tributary and the distal main river respectively. Since few of the rivers concerned are routinely gauged,  $Q_p$ ,  $Q_t$  and  $Q_d$  are unknown, but if  $w \propto Q^b$  applies with a fixed non-zero value of  $b$  then we should find that:

$$w_d = w_p [1 + (w_t/w_p)^{1/b}]^b \quad (10.3)$$

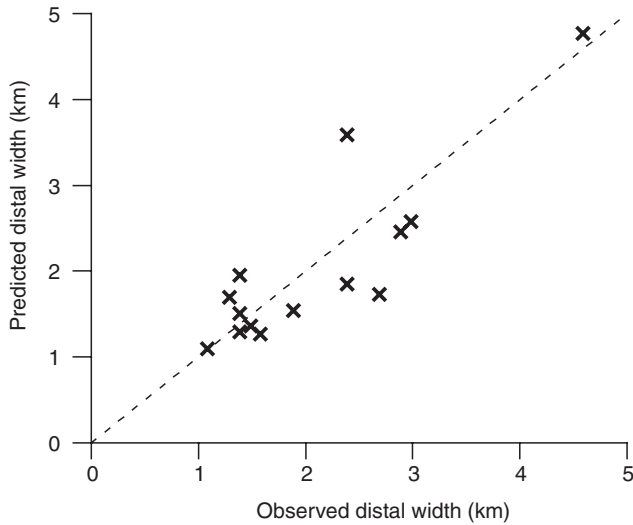


**Figure 10.1** Predictions of width change at major river confluences based on standard hydraulic geometry.

This implies that, for any exponent in the plausible range  $0 < b < 1$ , we expect the combined river to be wider than either of the channels above the junction, but not as wide as the sum of their widths. If the exponent is specified, Equation 10.3 predicts the precise value of  $w_d$  from the values of  $w_p$  and  $w_t$ . Figure 10.1 compares the observed distal widths with those predicted using  $b = 0.5$ . The data points fall on either side of the line of perfect agreement, indicating no obvious bias in the predictions, and when the exponent  $b$  is calibrated to the data the optimum value is found to be very close to 0.5: 0.51 for minimum sum of squares of percentage error, or 0.54 for zero mean percentage error. The data as a whole are therefore consistent with the conventional hydraulic geometry equation.

There is, however, considerable scatter in Figure 10.1, with prediction errors ranging from  $-37$  per cent to  $+49$  per cent, and four of the confluences contradict even the qualitative predictions of Equation 10.3 by having  $w_d < w_p$  or  $w_d > (w_p + w_t)$ . In this particular data set the widths are for discharges below bankfull, and possibly further below bankfull in one tributary than the other since the catchments concerned are so large that it cannot be assumed that they experience synchronous discharge fluctuations. Another factor, relevant at all scales, is that channel width depends on channel materials as well as discharge. Stronger banks can resist a higher shear stress, allowing the channel to be narrower and deeper (e.g. Millar and Quick, 1993). This can happen where a tributary with a high wash load causes deposition of cohesive sediment on the distal channel banks; Schumm (2005, p. 104) gives an example from Kansas, USA. Also, a coarser bed requires a greater shear stress to maintain a given transport capacity, so

the channel must be relatively deeper and narrower. Dimensionally consistent regime equations fitted to river data suggest  $w \propto Q^{0.5} D^{-0.25}$ , or something very close to this (Parker, 1979; Bray, 1982; Parker *et al.*, 2007).

## Sedimentary links

The other anticipated effect of tributaries on main-channel geomorphology is to create discontinuities in slope and/or bed grain size where a significant load of relatively coarse or fine sediment is added. The most obvious example is punctuated downstream fining. This is the situation in which the usual downstream reduction in mean and maximum grain size is disrupted where tributaries enter, segmenting the river into what Rice and Church (1998) call 'sedimentary links'. Punctuated downstream fining is widespread. It is noted by Sternberg (1875) in his classic work on the Rhein and has been identified in many subsequent studies (e.g. Church and Kellerhals, 1978; Knighton, 1980; Dawson, 1988; Rice and Church, 1998). Rice and Church (2001) show that slope as well as grain size tend to decline along sedimentary links, then increase abruptly at the start of the next link. Thus, the longitudinal profile is also segmented in a cusped way: there are multiple concave links with each coarse tributary acting as a local base level. The amount and calibre of bedload in rivers is very rarely monitored, so there is a danger of circular argument here ('punctuated downstream fining supports the hypothesis that coarse tributaries affect main-stem geomorphology' and 'these tributaries disrupt downstream fining, so they must be injecting coarse sediment'), but there is some circumstantial evidence to support the hypothesis. Rice (1998) shows that tributaries which terminate sedimentary links in one Canadian river system tend to be bigger and steeper than those which have a negligible effect on main-stem grain size; by implication, they will also convey more and coarser sediment. Similarly, the meta-study by Benda *et al.* (2004) of 14 case studies in the western United States and Canada found that larger tributaries were more likely to have an impact on main-stem grain size and/or long profile. Counter-examples nevertheless exist; for example, Rengers and Wohl (2007) did not find a consistent pattern of disruption by steep tributaries of a gravel-bed river in the mountains of Panama, and speculate that variations in main-stem width mask the expected discontinuities. This can be understood from Equation 10.2: narrowing of the main stem can increase shear stress sufficiently to convey the added coarse load from a tributary without any increase in slope.

Punctuated downstream fining and segmented long profiles are mainly reported from confined or incised gravel-bed rivers, but they are not restricted to such settings. Discontinuities in slope and grain size have been reported from boulder torrents and rock gorges (e.g. Shimazu, 1994; Hanks and Webb, 2006) which receive occasional injections of coarse material in the form of debris flows down steep tributaries. There are also documented cases of local coarsening and/or aggradation where

tributaries enter sand-bed rivers. Pinter *et al.* (2004) investigated locations along the upper and middle Mississippi that require frequent dredging and identified unregulated tributaries as one of the main causes, and Harmar and Clifford (2006) note that further down the Mississippi the Arkansas River supplies enough gravel to increase the thalweg  $D_{50}$  of the main river from 0.5 mm to over 2 mm for a short distance and cause local steepening. Gravel-bed rivers in wide valleys where tributaries deposit any coarse load before reaching the main channel may still show segmentation as a result of non-point 'supply zones' of coarse sediment such as moraines (Davey and Lapointe, 2007). Whilst almost all the examples mentioned so far are of the effect of relatively coarse tributaries, cases have also been reported where major lateral inputs of fine sediment from dune fields (Smith and Smith, 1984) or waste disposal from alluvial metal mining (Knighton, 1989) have transformed gravel beds to sand.

In summary, there are numerous field case studies which show main-channel width, bed grain size or slope altering past a junction in the direction that would be expected from qualitative conceptual arguments. But not all tributaries have any impact, and some do not have the anticipated direction of impact. Moreover, it is not always possible to make a qualitative prediction; for example, if the bedload injected by a tributary is of a similar calibre to that being transported by the main stem, Lane's balance leaves it unclear whether slope will increase, decrease or stay the same. Even where the direction of impact is predictable from Equation 10.1, its magnitude is not. For quantitative prediction of regime change past junctions, and qualitative prediction in otherwise ambiguous situations, Lane's arguments must be made more precise by adopting mathematical representations of the physical processes involved. They must also be extended to embrace all potentially relevant controlling factors and degrees of freedom for channel response, notably by taking the likely change in width into account. In the next section, we develop a quantitative regime model for tributary effects on recipient channels.

## Theoretical models: (1) Regime analysis of confluences

The balance between bed-material supply from upstream and local transporting capacity can be made precise by using specific equations to make a quantitative link between discharge  $Q$ , slope  $S$ , width  $w$ , grain size  $D$  and load  $L$ . We assume the confluence is in equilibrium (the capacity of the combined river equals the sum of the bed-material supply from the proximal main stem and the tributary) and make the same three simplifications as in other analytical treatments of channel regime: calculations are done on a spatially averaged basis with no consideration of within-reach spatial variation in morphology and flow, there is no allowance for variation over time in discharge and sediment transport, and the bed grain-size distribution is

represented by a single diameter which serves to characterize both the grain roughness of the bed and the grain sizes in transport. These simplifications may be inappropriate in some situations but are necessary to make progress with an analytical approach. Some or all of them can be relaxed in a numerical approach, as discussed later.

The details of the analysis differ between gravel- and sand-bed rivers since some process equations are specific to one or other type of channel, but the general approach is the same. Flow width, mean depth and mean velocity are denoted by  $w$ ,  $d$  and  $v$  respectively, and the proximal main stem, distal main stem and tributary are denoted by subscripts p, d and t, as before. The tributary contributions of water and sediment are defined as ratios:

$$QR = Q_t/Q_p \quad (10.4a)$$

$$LR = L_t/L_p \quad (10.4b)$$

$$DR = D_t/D_p \quad (10.4c)$$

These ratios are assumed to be known, along with all properties of the proximal main stem. The problem is to determine the properties of the distal main stem such that it can just convey the additional sediment from the tributary.

Seven constraints are required to obtain a unique solution. Five are provided by the conservation of water,  $Q_d = Q_p + Q_t = Q_p (1 + QR)$ ; conservation of sediment,  $L_d = L_p + L_t = L_p (1 + LR)$ ; the flow continuity equation  $Q = wdv$ ; a flow resistance equation; and a transport capacity equation. The sixth is a hydraulic geometry relation for width, and we close the system using the same bed mixing model as Sklar *et al.* (2006):

$$D_d = (D_p L_p + D_t L_t)/(L_p + L_t) \quad (10.5a)$$

This estimates distal grain size as a weighted average of the proximal and tributary grain sizes, weighted according to the relative sediment loads. It simplifies to:

$$D_d/D_p = (1 + DR \cdot LR)/(1 + LR), \quad (10.5b)$$

which shows that, unless the tributary load has the same calibre as the proximal main stem, the distal main stem will become finer or coarser to an extent that depends on DR and LR in combination. Figure 10.2 shows the range of possibilities.

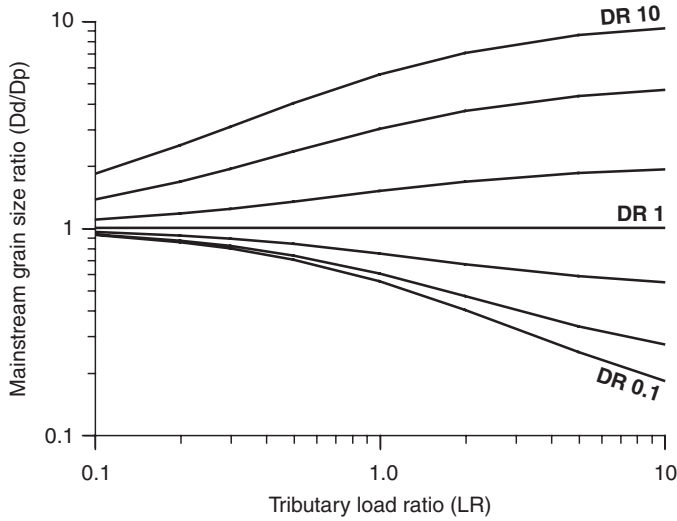


**Figure 10.2** Mixing model (Equation 10.5 for grain-size change past a junction as a function of tributary load ratio (LR) and bedload grain-size ratio (DR).  $D_p$  and  $D_d$  are the grain sizes of the proximal and distal main channel respectively. Curves are for DR = 10, 5, 2, 1, 0.5, 0.2 and 0.1 from top to bottom.

### Sand-bed rivers

These normally have dune beds and we assume that flow resistance can be represented by a constant value of Manning’s  $n$ . Thus,  $v \propto d^{2/3} S^{1/2}$  and:

$$d \propto (Q/w)^{3/5} S^{-3/10} \tag{10.6}$$

An appropriate and tractable equation for total bed-material load, including the suspended component, is that of Engelund and Hansen, which predicts transport capacity per unit width from the friction factor and the 2.5 power of the dimensionless shear stress on the bed. For given  $n$ , sediment density and water density the transport equation can be simplified to

$$L \propto wd^{1/3}(dS)^{5/2}/D \tag{10.7}$$

For the system to be in sediment-transporting equilibrium, the ratio  $L_d/L_p$  calculated using Equation 10.7 must equal  $1 + LR$ . By using Equation 10.5b, Equation 10.6 and the

assumption that  $w \propto Q^{0.5}$  the sediment balance can be solved for the change in slope past the junction:

$$S_d/S_p = (1 + LR \cdot DR)^{20/33} / (1 + QR)^{9/11} \approx (1 + LR \cdot DR)^{0.6} / (1 + QR)^{0.8} \quad (10.8)$$

Even if there is no change in grain size, it is apparent from Equation 10.8 that the effect of the tributary on the main-stream long profile depends on the balance between the discharge ratio QR and the load ratio LR. The tributary injection of load may require an increased channel slope despite the extra streamflow, the tributary addition of water may be sufficient to convey the increased load over a gentler slope or, with particular combinations of LR and QR, the slope could remain unchanged. If the tributary injects relatively coarse or fine sediment, it is the balance between QR and  $LR \cdot DR$  that matters. A sediment-laden tributary with LR much bigger than QR,  $DR > 1$ , or both, requires an increase in main-stem slope if the extra load is to be transported away. Conversely, a lightly loaded or completely clear tributary with negligible LR but appreciable QR enables the combined river to transport the load from upstream over a gentler gradient. In the particular case of a symmetric confluence of two identical rivers, with  $QR = LR = DR = 1$ , Equation 10.8 predicts that the combined river will have a gradient  $S_d = 0.86S_p$ , that is a small but perceptible reduction in gradient. The physical interpretation is that the deeper combined river is more efficient at transporting sediment despite its greater width.

## Gravel-bed rivers

For these we use the Manning–Strickler representation of flow resistance,  $n \propto D^{1/6}$ , which is a good approximation of the theoretically superior Keulegan-style logarithmic resistance law for rivers in which  $d/D$  exceeds 10. It follows that:

$$d \propto q^{3/5} D^{1/10} S^{-3/10} \quad (10.9)$$

The most appropriate but tractable transport equation is now that of Meyer-Peter and Müller, Equation 10.2 above, in which we can assume  $\tau_c \propto D$ . The equilibrium requirement  $L_d/L_p = 1 + LR$  gives:

$$1 + LR = \frac{w_2}{w_1} \left( \frac{\tau_2 - \tau_{c2}}{\tau_1 - \tau_{c1}} \right)^{1.5} = (1 - 1/\Phi)^{-1.5} \left( \frac{w_2}{w_1} \right) \left( \frac{\tau_2}{\tau_1} - \frac{\tau_{c2}}{\Phi \tau_{c1}} \right)^{1.5} \quad (10.10)$$

where the new parameter  $\Phi = \tau/\tau_c$  is the transport stage in the proximal main stem. This has a typical value of 1.2–1.5 in gravel-bed rivers at bankfull discharge (e.g. Dade and

Friend, 1998). By substituting  $\tau \propto dS$  and  $\tau_c \propto D$  an explicit solution can be obtained for the distal slope:

$$\frac{S_d}{S_p} = \left[ \frac{(1/\Phi) (w_d/w_p)^{2/3} (D_d/D_p) + (1 - 1/\Phi) (1 + LR)^{2/3}}{(1 + QR)^{3/5} (w_d/w_p)^{1/15} (D_d/D_p)^{1/10}} \right]^{10/7} \quad (10.11)$$

The distal grain size is again specified using the mixing model (Equation 10.5). Finally, we consider two alternatives for the width: the traditional simple hydraulic geometry relation:

$$w \propto Q^{0.5} \quad (10.12a)$$

or the Parker–Bray relation:

$$w \propto Q^{0.5}/D^{0.25} \quad (10.12b)$$

Substitution of Equation 10.5 and Equation 10.12a or Equation 10.12b in Equation 10.11 allows an analytical solution for the distal slope if QR, LR, DR and  $\Phi$  are known. No broad conclusions can be drawn from the general solution but it simplifies somewhat in special cases. Three interesting cases are (a) the symmetric confluence of two identical rivers, (b) the effect of a clearwater input where there is a lake or dam a short way up the tributary and (c) the effect of natural or anthropogenic inputs of sediment without significant extra streamflow, such as landslides, debris flows and mine waste disposal. We also consider what happens if (d) grain size is assumed the same everywhere, as in most landscape-evolution models.

At a symmetric confluence ( $QR = LR = DR = 1$ ), the slope solution simplifies to  $S_d/S_p = (1.02 - 0.21/\Phi)^{10/7}$  irrespective of which width equation is used. This predicts a substantial reduction in slope below the junction (an 18 per cent reduction for  $\Phi = 1.4$ , for example), as in our sand-bed analysis.

In case (b), the clearwater tributary with  $LR = 0$ , the change in regime slope past the junction depends only on QR and  $\Phi$  irrespective of the width equation. The solution simplified in this way shows that the addition of water without extra sediment always leads to a reduction in slope, more so for higher QR (as would be expected) and also for higher stress ratio  $\Phi$  (Figure 10.3). The effect is quite pronounced for major clearwater tributaries.

Case (c), where there is an addition of sediment but no significant addition of water, is represented by setting  $QR = 0$ . The solution for distal slope in this case does depend to a small extent on the choice of width equation. Figure 10.4 shows predictions using  $w \propto Q^{0.5}$ ; if  $w$  also depends on  $D^{-0.25}$ , the curves plot slightly lower. It can be seen that coarse lateral inputs (DR greater than about 2) can only be transported if there is a substantial increase in distal slope, implying aggradation at the junction.

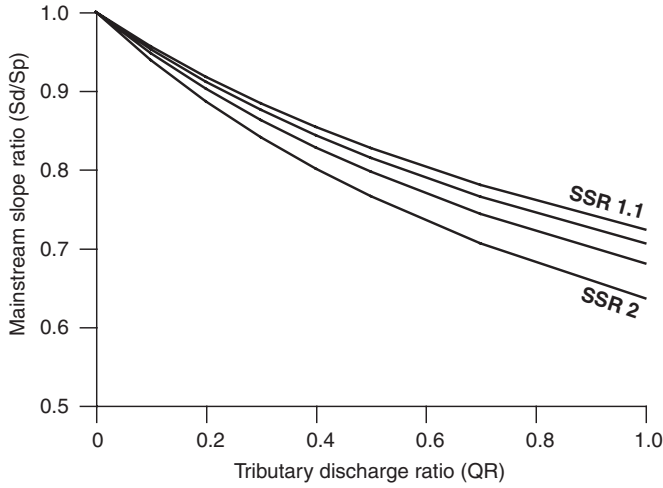


**Figure 10.3** Predicted effect of a clearwater tributary on the regime slope of a gravel-bed river.  $S_d$  and  $S_p$  are the distal and proximal main-channel slopes. Curves are for different ratios (SSR) of actual to critical shear stress in the proximal main channel, with values 1.1, 1.2, 1.4, 2 from top to bottom.

The necessary distal slope increases with the tributary grain size, as would be expected intuitively, and also with tributary load up to a value of  $LR \approx 2$  (the physical interpretation of the downturn in the curves beyond  $LR = 2$  is not immediately obvious). Fine lateral inputs are predicted to have the opposite effect: they can be transported over a reduced gradient because the main-stem bed becomes finer and the critical shear stress is reduced.

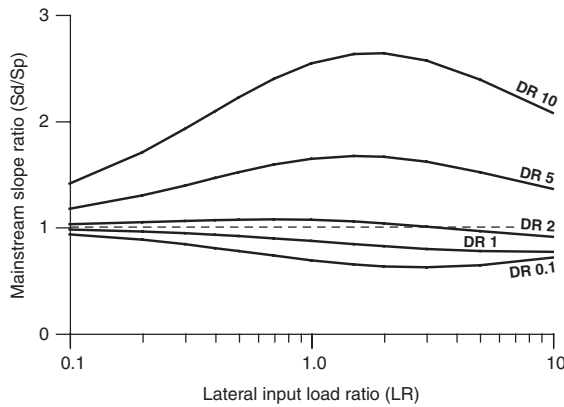


**Figure 10.4** Predicted effect of lateral sediment input on main-stem slope if there is no additional streamflow. Curves are for different bedload grain-size ratios. Calculations assume standard hydraulic geometry and shear stress ratio 1.4.

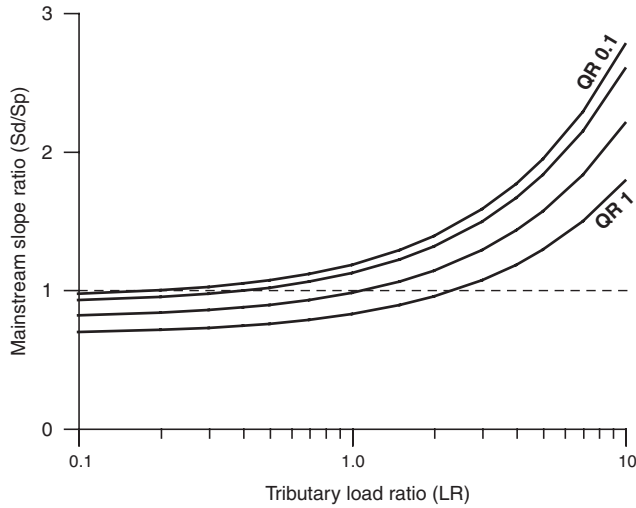


**Figure 10.5** Predicted change in main-channel slope past the confluence of a tributary of specified discharge ratio (QR) and load ratio (LR) and no difference in grain size ( $DR = 1$ ). Curves are for  $QR = 0.1, 0.2, 0.5$  and  $1$  from top to bottom.

Turning finally to case (d), setting  $DR = 1$  in the general solution removes the effect of relatively coarser or finer inputs and focuses attention on the discharge and load ratios. These operate in opposite directions, as in the sand-bed case (Equation 10.8): with other things equal, transporting extra sediment load requires a higher slope, but extra discharge allows a given load to be transported over a lower slope. Figure 10.5 shows the trade-off between these separate effects in typical gravel-bed conditions. Small additions of sediment can be transported on a reduced slope even if there is little extra streamflow, but large additions of sediment require a steepening of the main stem even if the tributary has a substantial water discharge.

This new regime analysis of tributary effects has qualitative implications consistent with interpretations made by field workers and with Lane's balance concept. Most of the ingredients of the analysis are widely accepted process equations, the exceptions being the hydraulic geometry relation and the mixing model for grain size. The equations show that discontinuities arise in main-stem slope and grain size because of trade-offs amongst width, depth, shear stress and bedload transport capacity as they adjust to step changes in water discharge, sediment load and sediment calibre. Despite the number of degrees of freedom involved, the regime analysis provides quantitative predictions of the outcome of any combination of changes in the input variables. It therefore goes beyond Lane's qualitative approach (Equation 10.1), which cannot predict even the sign of change in most situations in which both discharge and load alter past a junction.

Two of the simplifications recognized at the outset (width-averaged calculations and steady discharge) will be discussed later. The next step up towards the full complexity of the real world is to relax the other two simplifications: the assumption that the system is in exact equilibrium, and the use of a single grain size for the bed (in the flow resistance equation) and the bedload (in the transport-capacity equation) even though in reality flow resistance in gravel-bed rivers is dominated by the coarsest grains in the bed whereas transport is usually preferentially of the finer grains.

## Theoretical models: (2) Numerical experiments with adjustable grain-size distributions

A model of how a tributary affects the slope and grain-size distribution (GSD) of a gravel-bed main stem was developed and applied by Ferguson *et al.* (2006). The model, called TRIB, operates on the same basis as the SEDROUT model developed by Hoey and Ferguson (1994) to model the transient co-evolution of long profile and downstream fining. Like the regime analysis of the last section, TRIB is width-averaged, uses the Manning equation for flow resistance and  $w \propto Q^{0.5}$  for width change, and assumes tributary discharge and load are steady over time and can be specified as ratios QR, LR of the discharge and load in the proximal main stem. The two main differences are that the single representative grain size  $D$  for each channel segment is replaced by separate bed and bedload GSDs at each of a large number of nodes along the main channel, and that the bed elevation and GSD at each node are free to evolve over time in accordance with the sediment continuity equations for each size fraction. This necessitates the use of a transport law that is designed for size fractions and allows for hiding and protrusion effects on  $\tau_c$ ; TRIB uses the equations of Wilcock and Crowe (2003). The tributary bedload also has a GSD, which is user-specified to give the desired ratio DR between the median diameters of the tributary and proximal loads. The evolution of the system is computed iteratively using a finite-difference scheme.

Ferguson *et al.* (2006) report a large set of generic simulations in which different combinations of tributary QR, LR and DR were tried for a tributary entering midway along a 10-km main stem. The initial condition for each run was the same: a smoothly concave main-stem long profile with moderate downstream fining, generated by running the model with no tributary until aggradation had fallen to a low rate so that the system was in quasi-equilibrium. The tributary is turned on when the run starts. Adjustment is initially rapid but slows down as the system takes on a segmented form with discontinuities in slope and grain size at the junction. Runs were stopped when the transient changes set into play by adding the tributary had slowed so much that the maximum local rate of aggradation or degradation was no greater than in the absence of a tributary. Continuing a simulation indefinitely leads towards the only possible exact equilibrium, in which the proximal and distal channel segments are both straight but

have different slopes (as in the regime analysis of the previous section). This would take such a long time to achieve in most real-world situations that catchment hydrology, sediment supply or base level would probably have altered meanwhile. It is likely, therefore, that most natural confluences are also in a state of quasi-equilibrium rather than exact equilibrium. We are not aware of any sufficiently detailed repeat surveys with which to test this supposition but it is consistent with Mackin's (1948) interpretation of the widely accepted concept of grade or dynamic equilibrium.

Analysis of the results of over 100 simulations revealed clear links between the tributary parameters QR, LR and DR and the simulated impact of the tributary on the main stem. The quantitative results are specific to the ideal main stem that was considered, but sensitivity analyses reported in Ferguson *et al.* (2006) show that the qualitative trends summarized below are unaffected by altering the initial long profile shape (straight, gently concave or highly concave) or the hydraulic boundary conditions (proximal  $Q$ ,  $w$ ,  $S$ ,  $n$  and  $D$ , all of which are jointly mediated through the proximal shear stress ratio,  $\Phi$  in our regime analysis). A typology of responses was established with the primary criterion being whether the junction itself aggraded, degraded or experienced negligibly small vertical change. As would be expected, very small tributaries (QR and LR both  $< 0.1$ ) have little or no impact, and nor do tributaries with  $DR \approx 1$ . Where larger tributaries inject relatively coarse sediment ( $DR > 1$ ) the outcome depends on the balance between QR and LR but almost always involves aggradation and consequent discontinuities in main-stem slope and grain size. The magnitude of this effect increases with the product  $LR \cdot DR$  but decreases with QR (Figure 10.6, upper curves). Only with  $LR/QR < 0.2$  (almost a clearwater tributary) is there no aggradation or even slight degradation. This neutral or degrading behaviour also occurred in all simulations with an appreciable input of relatively fine sediment ( $DR < 1$ ). Amounts of degradation are generally far smaller than amounts of aggradation; they increase with LR and with QR as shown by the lower pair of curves in Figure 10.6(A). The response close to the junction therefore depends on the balance between the overloading effect of the tributary (higher LR and DR) and the greater transporting capacity of the distal stream (higher QR), in accordance with Lane (1955).

A significant aspect of the results, and a secondary component of the typology proposed by Ferguson *et al.* (2006), is that the simulated effects of a tributary extend some way upstream as well as downstream. Aggradation due to coarse tributaries leads to the development of separate proximal and distal sedimentary links: slope and grain size just above the junction are lower, and slope and grain size just below the junction are higher, than they would be in the absence of a tributary.

Something that is apparent in TRIB simulations, but is unknowable in the field, is that the grain size of the main-stem bed well below a junction is not necessarily the same as it would be without the tributary. If LR is appreciably lower than QR, the distal bed tends to become coarser as fine sediment is winnowed from the bed to build the load up to capacity; if LR is appreciably higher than QR, the distal bed tends to

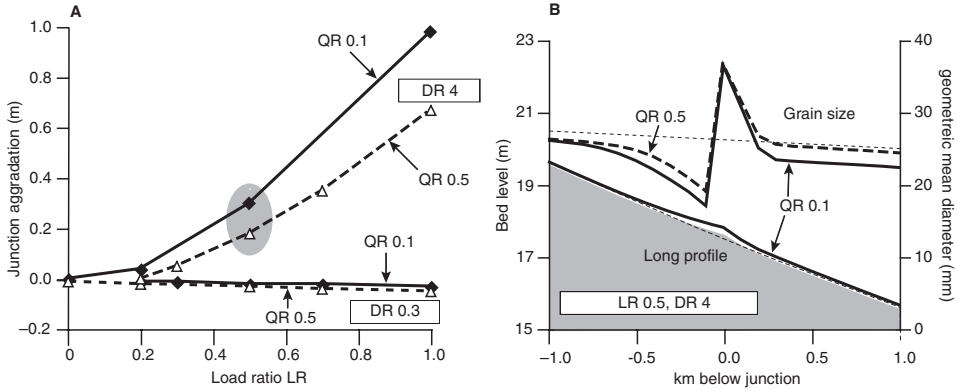


**Figure 10.6** (A) Change in junction bed elevation during simulations using the TRIB model with different combinations of tributary load ratio (LR, on horizontal axis), discharge ratio (QR, distinguished by solid or dashed curves) and grain-size ratio (DR; upper pair of curves showing major aggradation are for coarse input, lower pair showing slight degradation are for fine input). (B) Simulated long profiles and downstream fining profiles for the two runs in the shaded area of part A. Faint dotted lines show the initial (no tributary) situation; solid lines show outcome with QR = 0.5. The outcome for QR = 0.1 is the dashed line (grain size) and upper edge of grey tone (long profile).

coarsen close to the junction but become finer further down the link as excess load is deposited. This is again qualitatively consistent with Lane (1955) and with our regime analysis. Table 10.1 shows how, for a given grain-size ratio DR, different combinations of aggradation (A) or degradation (D) at the junction and coarsening (C) or fining (F) well past the junction (beyond 1 km in our 5-km distal reach) are associated with different

**Table 10.1** Type of main-stem response in simulation experiments at different ranges of the ratio LR/QR, for tributaries injecting relatively coarse (DR = 4) or fine (DR = 0.3) load. Response types A and D denote aggradation or degradation; F and C denote finer or coarser than in the absence of a tributary.

Type of response		Range of LR/QR over which observed	
at junction	1 km downstream	coarse inputs	fine inputs
A	F	1–100	not observed
A		1	not observed
A	C	0.5–0.7	not observed
	C	0.1–0.7	0.05
D	C	0.01–2	0.01–3
D		not found	1–4
D	F	not found	3–500

ranges of the ratio LR/QR. For coarse tributaries, there is a sequence of response types from DC to C, AC, A and finally AF as LR/QR increases. For sandy tributaries, the sequence runs in the opposite direction: C, DC, D, DF as LR/QR increases. All these results are for the standard  $w \propto Q^{0.5}$  hydraulic geometry. If width increases faster than this with discharge, the effect of QR is reduced; conversely, if distal width is restricted, QR has more effect and degradation is more likely. This points to the significance of our earlier discussion of scatter about hydraulic geometry trends and whether channel width depends on grain size as well as discharge.

Running a large number of simulations allowed Ferguson *et al.* (2006) to identify how main stems respond to the three independent controls of tributary discharge, load and load calibre, both individually and in combination. It is almost impossible to do this through field case studies. The validity of the general conclusions rests on that of the assumptions made, but the conclusions are compatible with what has been inferred from case studies. Relatively fine-grained or clear tributaries tend to cause slight degradation, often with distal coarsening. Coarser-grained tributaries cause modest to massive aggradation and coarsening at the junction, with consequences that extend up and downstream. The resulting streamwise pattern of sedimentary links is just as described by Rice and Church (1998) and implies a greater range of substrate, hydraulic conditions and physical habitat than in the absence of tributaries. The ecological implications of this heterogeneity are considered further in Rice *et al.* (2006) and by Rice *et al.*, Chapter 11, this volume.

## Discussion

Many tributaries have no perceptible effect on the geomorphology of the rivers they join, but some do, and the effects vary in style and magnitude. Empirical studies have generated some understanding of when and how tributaries affect main-stem geomorphology, but they provide little basis for predicting the magnitude of any impact. A hydraulic geometry relation can be used to predict how channel width will increase past a junction (Richards, 1980; Figure 10.1 above), but there are no comparably specific relations to predict impacts on slope or grain size. All we have is some indication that aggradation and punctuated downstream fining are more probable where tributaries are relatively large (Rice, 1998; Benda *et al.*, 2004) and perhaps also relatively steep (Rice, 1998). This poverty of empirical knowledge is partly for lack of adequate data. Any impact a tributary has on main-stem slope or grain size must depend on the amount and calibre of bedload that it supplies, but measurement of bedload is difficult, imprecise and rarely undertaken, so very few data are available for statistical analysis.

This chapter has therefore taken a mainly theoretical approach based on widely accepted representations of alluvial river processes at three levels of sophistication, taking progressively more variables and degrees of freedom into account. The simplest

approach, applying the long-standing concept of a qualitative balance between the amount and calibre of bedload and the transporting capacity provided by river discharge and slope, was shown to be applicable to channel changes past confluences and to give some insight into the effects of tributaries. Specifically, it highlights the existence of at least three controlling factors: the ratios of tributary to main-stem discharge (QR) and bed-material load (LR) and the ratio (DR) of the calibre of the respective loads. But qualitative theory cannot predict the magnitude (sometimes not even the direction) of response to a change in one or more controls, and this particular qualitative theory does not allow for changes in channel width past a junction. These deficiencies are overcome in our second contribution: a new quantitative regime theory of how changes in width, slope and grain size past a sand-bed or gravel-bed junction can combine to maintain onward transport of the water and bedload supplied by the tributary. The general solution for distal slope remains to be tested but several special cases of it were shown to be compatible with the qualitative model. The regime theory also predicts whether junctions will aggrade or degrade according to the relative coarseness of the tributary load and the relative amounts of sediment and water that are added. The third and most sophisticated approach, summarized here from the full account in Ferguson *et al.* (2006), is to allow spatially and temporally variable GSDs and transient adjustment of the main channel. This highest level of complexity requires a numerical modelling approach rather than mathematical analysis, but the results remain compatible with the simpler models and have analogues in the field literature.

Because each level of theory is based on physical principles, it can be applied to what-if management questions, for example regarding the potential impacts of flow regulation or land-use change. However, notwithstanding the plausible and mutually consistent results from the quantitative models, they make simplifying assumptions that need to be considered carefully. The simplifications are of two kinds: what's left out and just how the included factors are represented. We think the most problematic issues are of the first kind: the one-dimensional nature of the models, the assumption of steady 'dominant' discharge and the lack of consideration of possible feedback to tributary properties as the main channel adjusts. These are discussed in turn below. One other omission – abrasion of bed material, *in situ* and during transport – is less problematic at the scale of interest in this chapter, though Cui and Parker (2005) and Sklar *et al.* (2006) show its importance over longer distances and at network scale. Our particular choices of flow resistance and bedload transport equations are less important: alternatives would make some difference to quantitative predictions but not to qualitative patterns.

A width-averaged treatment of hydraulic and bedload calculations is standard in regime theory and sediment-routing models, but it probably exaggerates the magnitude of change in the immediate vicinity of a junction. The tributary is assumed to mix immediately and uniformly across the main river, whereas in reality there is some spatial lag and often an asymmetric morphology with the flow concentrated on the side opposite to a tributary junction bar or fan/delta, like the one shown in



**Figure 10.7** Deflection of main-stem flow by a junction delta where a small glacier-fed tributary joins the Hunza River, Karakoram mountains, northern Pakistan. Main river is flowing right to left at about 60 per cent of seasonal maximum discharge. Photo: Robert Ferguson.

Figure 10.7. In such situations, the main flow is likely to be narrower, which usually increases transport capacity since the higher shear stress in Equation 10.2 outweighs the lower width. This must reduce the aggradation rate. A two-dimensional numerical model would be required to simulate such effects in any detail but they can be represented crudely in a one-dimensional model by reducing the width at the junction. Re-running the coarse-tributary examples of Figure 10.6 with a 25 per cent reduction in width at and immediately past the junction makes little difference to the simulated pattern of grain sizes but reduces junction aggradation by over 30 per cent. A related issue that was touched on in relation to Figure 10.1 is that width changes past junctions are not perfectly predictable and probably depend on sediment characteristics as well as the tributary discharge ratio. Since the transport capacity of the distal main stem is sensitive to its width, departures from a simple  $w \propto Q^{0.5}$  scaling could exaggerate or mask the types of response that we predict. As already noted, Rengers and Wohl (2007) speculate that streamwise variations in width might account for the lack of clear punctuated downstream fining along the river they studied. A further complication when attempting one-dimensional modelling of irregular natural channels is the difficulty of specifying the effective width of active transport; it is likely to be less than the bankfull channel width, and the choice has a sensitive influence on simulated transport rates (see, for example, Ferguson *et al.*, 2001), but there is no sure basis for choosing a value.

The assumption of constant high discharge (e.g. bankfull or mean annual flood) is again universal in regime theory and common in sediment-routing models (e.g.

Ferguson *et al.*, 2001; Cui and Parker, 2005). It is justifiable insofar as the main injection of sediment from a tributary will be when it is in flood, and (in gravel-bed rivers at least) onwards transport of the additional load will occur only when the main stem is in flood. But tributary and main-stem flows may not be synchronous, as already noted, and even if they are synchronous the discharge and load ratios may vary from one event to the next so that coarse sediment injected by the tributary is stored before redistribution down the main stem at a later date (e.g. Marutani *et al.*, 1999). The concept of coupling becomes tenuous if the frequency of bedload transport in the tributary is radically different from that in the main stem. This may happen if the main river is regulated, leading to an accumulation of tributary fans (e.g. Church, 1995) or if the material supplied by the tributary (perhaps in the form of a high-magnitude, low-frequency debris flow) is so coarse that it will take centuries to disperse (e.g. Hammack and Wohl, 1996). Such effects cannot be allowed for in a simple regime analysis, but they will arguably tend to cancel out over long periods of time and they could be simulated using numerical models. Benda (Chapter 13, this volume) considers the long-term implications of stochastic debris flow activity and coupling at network scales.

In developing our theoretical treatment of tributary impacts, we chose to specify tributary characteristics through the ratios QR, LR and DR, which quantify how the water discharge, bed-material load and bed-material calibre of the tributary compare with those of the main channel above the junction. This is a natural approach when trying to quantify Lane's balance concept, and is mathematically and computationally tractable, but it is hard to apply to specific field situations with no data on tributary load. Explicit modelling of tributary load using tributary slope, width and bed grain size (or GSD) would be an obvious and computationally straightforward modification of the set-up used in TRIB, though any application to specific situations would require the necessary data on the tributary as well as the main stem. This approach would also open the way to allowing for certain kinds of feedback from main stem to tributary, for example how any incision or widening of the main channel increases the slope and sediment load of the tributary immediately above the confluence (e.g. Cohen and Brierley, 2000) and how tributary fans deflect the main channel towards the far side of the valley and thus reduce the tributary gradient at the confluence. But no simple model can reproduce some of the other observed consequences of deflection by tributary fans: alternation of single-channel and braided planform (Dawson, 1988), interbedding of fan deposits with main-stem floodplain deposits (Florsheim, 2004) and incision of a deflected main channel into the inner spur of a valley bend (James, 2004).

Many of the issues raised in the analysis and discussion above also apply to bedrock-controlled river systems, but there is far less empirical information about such river systems for use in evaluating theoretical predictions. The fundamental importance of bedload transport rate and grain size in controlling the evolution of bedrock rivers has been established (e.g. Sklar and Dietrich, 1998). Incision into bedrock depends on

a supply of abrasive tools, but not in such quantity as to cover and protect the bed. Tributaries (and other lateral inputs of sediment from debris flows or landslides) can alter this supply and therefore affect incision, gradient and long profile. Hanks and Webb (2006) show that the long profile of the Grand Canyon is controlled by episodic injections of large amounts of coarse material from steep tributaries. Recent suggestions that bedrock channel width acts as a control over incision rate (Finnegan *et al.*, 2005) need to be balanced against ongoing uncertainty about the controls over channel width in bedrock settings (Whipple, 2004). Given the long timescales involved in incision, bedrock morphology is sensitive to long-term variations in climate, which affects both hydrology and sediment supply. The assumptions of quasi-equilibrium that are valid in the alluvial case may not be so readily applicable, and caution needs to be exercised in relating bedrock river morphology to averaged measures of present-day conditions (such as mean annual flood).

Several research needs are implicit in the preceding discussion. First, channel-width adjustment past junctions is of interest in itself and has substantial influence on predicted slope discontinuities and junction aggradation in both regime and transient models. The main issue is the extent to which tributary injections of relatively coarse or fine sediment alter the increase in width that would be expected on the basis of discharge alone. Studies of tributaries of contrasting type could help throw light on this, but quite large sample sizes would be required to obtain clear results. Second, the regime model presented here remains to be tested. The main obstacle to doing this is the shortage of data on bedload fluxes. In areas of contrasting lithology, it may be possible to estimate the sediment-load ratio from the dilution of natural sediment tracers (Hoey, 1994). Another indirect approach is to estimate main-channel fluxes inversely from channel change and constrain tributary contributions by hydraulic calculations (Ham and Church, 2000). Conversely, if the regime model is trusted it could be inverted to estimate tributary flux. A third need is to assess the role of within-confluence adjustments in reducing the amplitude of beyond-confluence adjustments. The example given above was the demonstration that narrowing the confluence in a TRIB simulation, to mimic the effect of a junction bar, substantially reduced the amount of aggradation and thus the degree of discontinuity in main-stem slope. Field studies of the extent of narrowing and asymmetry near junctions, or better still flow measurements yielding the spatial distribution of shear stress, would be instructive; so would theoretical investigation using a two-dimensional model or a '1.5-dimensional' model with an effective width and shear stress based on cross-sectional information. A fourth area for further research is junction geomorphology in bedrock or mixed rock/alluvial channels, where basic observational studies are needed. Finally, and more broadly, the literature on tributary impacts is heavily biased towards those tributaries that have obvious and significant impacts on main-stem morphology. More systematic sampling of tributary characteristics and impacts is required if we are to develop generic understanding. Similarly, our understanding is best of small river systems where tributaries

can be considered to be in equilibrium with present-day conditions. Data from a wide range of scales of river system, which adjust over a wide range of characteristic timescales, are required (See Parsons *et al.*, Chapter 5, this volume). Each of these lines of research could add to our understanding of how tributaries affect the main channels they join.

## Acknowledgments

The numerical modelling was supported by NERC grants NER/A/S2000/01199, 01384 and 01385 to Rice, Ferguson and Hoey. We thank Stuart Lane for permission to use his data on channel widths at major confluences, Stephen Rice for advice on drafts of this chapter and an anonymous reviewer for detailed and helpful comments.

## References

- Benda L, Andras K, Miller D, Bigelow P. 2004. Confluence effects in rivers: Interactions of basin scale, network geometry, and disturbance regimes. *Water Resources Research* **40**: W05402.
- Best JL. 1988. Sediment transport and bed morphology at river channel confluences. *Sedimentology* **35**: 481–498.
- Bray DI. 1982. Regime equations for gravel-bed rivers. In *Gravel-Bed Rivers*, Hey RD, Bathurst JC, Thorne CR (eds). John Wiley & Sons: Chichester; 517–552.
- Chang HH. 1988. *Fluvial processes in river engineering*. John Wiley & Sons: Chichester.
- Church M. 1992. Channel morphology and typology. In *The Rivers Handbook, Volume 1*, Calow P, Petts GE (eds). Blackwell: Oxford; 126–143.
- Church M. 1995. Geomorphic response to river flow regulation: Case studies and time-scales. *Regulated Rivers: Research and Management* **11**: 3–22.
- Church M. 2006. Bed material transport and the morphology of alluvial river channels. *Annual Reviews of Earth and Planetary Science* **34**: 325–354.
- Church M, Kellerhals R. 1978. On the statistics of grain size variation along a gravel river. *Canadian J. Earth Sciences* **15**: 1151–1160.
- Cohen TJ, Brierley GJ. 2000. Channel instability in a forested catchment: A case study from Jones creek, East Gippsland, Australia. *Geomorphology* **32**: 109–128.
- Cui YT, Parker G. 2005. Numerical model of sediment pulses and sediment-supply disturbances in mountain rivers. *Journal of Hydraulic Engineering ASCE* **131**: 646–656.
- Dade WB, Friend PF. 1998. Grain-size, sediment-transport regime, and channel slope in alluvial rivers. *Journal of Geology* **106**: 661–675.
- Davey C, Lapointe M. 2007. Sedimentary links and the spatial organization of Atlantic salmon (*Salmo salar*) spawning habitat in a Canadian Shield river. *Geomorphology* **83**: 82–96.
- Dawson M. 1988. Sediment size variation in a braided reach of the Sunwapta River, Alberta, Canada. *Earth Surface Processes and Landforms* **13**: 599–618.
- Ferguson RI, Church M, Weatherly H. 2001. Fluvial aggradation in Vedder River, British Columbia: Testing a one-dimensional sedimentation model. *Water Resources Research* **37**: 3331–3347.

- Ferguson RI, Cudden JR, Hoey TB, Rice SP. 2006. River system discontinuities due to lateral inputs: Generic styles and controls. *Earth Surface Processes and Landforms* **31**: 1149–1166.
- Finnegan NJ, Roe G, Montgomery DR, Hallet B. 2005. Controls on the channel width of rivers: Implications for modeling fluvial incision of bedrock. *Geology* **33**: 229–232.
- Florsheim JL. 2004. Side-valley tributary fans in high-energy river floodplain environments: Sediment sources and depositional processes, Navarro River basin, California. *Geological Society of America Bulletin* **116**: 923–937.
- Gilbert GK. 1914. The transportation of debris by running water. *US Geological Survey Professional Paper* **86**.
- Ham DG, Church M. 2000. Bed-material transport estimated from channel morphodynamics: Chilliwack river, British Columbia. *Earth Surface Processes and Landforms* **25**: 1123–1142.
- Hammack L, Wohl E. 1996. Debris-fan formation and rapid modification at Warm Springs rapid, Yampa River, Colorado. *Journal of Geology* **104**: 729–740.
- Hanks TC, Webb RH. 2006. Effects of tributary debris on the longitudinal profile of the Colorado River in Grand Canyon. *Journal of Geophysical Research (Earth Surface)* **111**: F02020.
- Harmar OP, Clifford NJ. 2006. Planform dynamics of the Lower Mississippi River. *Earth Surface Processes and Landforms* **31**: 825–843.
- Harvey AM. 2002. Effective timescales of coupling within fluvial systems. *Geomorphology* **44**: 175–201.
- Hoey TB. 1994. Relative bed-material discharges at a mountain stream confluence using a natural sediment tracer. *Journal of Hydrology (NZ)* **32**: 16–28.
- Hoey TB, Ferguson RI. 1994. Numerical modelling of downstream fining by selective transport in gravel-bed rivers: Model development and illustration. *Water Resources Research* **30**: 2251–2260.
- James LA. 2004. Tailings fans and valley-spur cutoffs created by hydraulic mining. *Earth Surface Processes and Landforms* **29**: 869–882.
- Knighton AD. 1980. Longitudinal changes in size and sorting of stream-bed material in four English rivers. *Geological Society of America Bulletin* **91**: 55–62.
- Knighton AD. 1987. River channel adjustment – the downstream dimension. In *River Channels: Environment And Process*, Richards KS (ed.). Institute of British Geographers Special Publication 18. Blackwell: Oxford; 95–128.
- Knighton AD. 1989. River adjustment to changes in sediment load: The effects of tin mining on the Ringarooma River, Tasmania, 1875–1984. *Earth Surface Processes and Landforms* **14**: 333–359.
- Lane EW. 1955. The importance of fluvial morphology in hydraulic engineering. *Journal of the Hydraulics Division ASCE* **81**: 1–17.
- Leopold LB, Maddock Jr T. 1953. Hydraulic geometry of stream channels and some physiographic implications. *US Geological Survey Professional Paper* **272**.
- Mackin JH. 1948. Concept of the graded river. *Geological Society of America Bulletin* **59**: 463–512.
- Marutani T, Kasai M, Reid LM, Trustrum NA. 1999. Influence of storm-related sediment storage on the sediment delivery from tributary catchments in the Upper Waipaoa River, New Zealand. *Earth Surface Processes and Landforms* **24**: 881–896.
- Millar RG, Quick MC. 1993. Effect of bank stability on geometry of gravel rivers. *Journal of Hydraulic Engineering* **119**: 1343–1363.
- Parker G. 1979. Hydraulic geometry of active gravel rivers. *Journal of the Hydraulics Division ASCE* **105**: 1185–1201.

- Parker G, Wilcock PR, Paola C, Dietrich WE, Pitlick J. 2007. Physical basis for quasi-universal relations describing bankfull hydraulic geometry of single-thread gravel bed rivers, *Journal of Geophysical Research – Earth Surface* **112**: F04005, doi:10.1029.2006JF000549
- Pinter N, Miller K, Wlosinski JH, van der Ploeg RR. 2004. Recurrent shoaling and dredging, middle and upper Mississippi River, USA. *Journal of Hydrology* **290**: 275–296.
- Reid I, Best JL, Frostick LE. 1989. Floods and flood sediments at river confluences. In *Floods: Hydrological, Sedimentological and Geomorphological Implications*, Beven KJ, Carling PA (eds). John Wiley & Sons: Chichester; 135–150.
- Rengers F, Wohl E. 2007. Trends of grain sizes on gravel bars in the Rio Chagres, Panama. *Geomorphology* **83**: 282–293.
- Rice SP. 1998. Which tributaries disrupt downstream fining along gravel-bed rivers? *Geomorphology* **22**: 39–56.
- Rice SP. 1999. The nature and controls of downstream fining within sedimentary links. *Journal of Sedimentary Research* **69**: 32–39.
- Rice SP, Church M. 1996. Bed material texture in low order streams on the Queen Charlotte Islands, British Columbia. *Earth Surface Processes and Landforms* **21**: 1–18.
- Rice SP, Church M. 1998. Grain size along two gravel-bed rivers: Statistical variation, spatial pattern and sedimentary links. *Earth Surface Processes and Landforms* **23**: 345–363.
- Rice SP, Church M. 2001. Longitudinal profiles in simple alluvial systems. *Water Resources Research* **37**: 417–426.
- Rice SP, Ferguson RI, Hoey TB. 2006. Tributary control of physical heterogeneity and biological diversity at river confluences. *Canadian Journal of Fisheries and Aquatic Sciences* **63**(11): 2553–2566.
- Richards KS. 1980. A note on changes in channel geometry at tributary junctions. *Water Resources Research* **16**: 241–244.
- Richards KS. 1982. *Rivers: Form and Process in Alluvial Channels*. Methuen: London.
- Schumm SA. 2005. *River Variability and Complexity*. CUP: Cambridge.
- Shimazu H. 1994. Segmentation of Japanese mountain rivers and its causes based on gravel transport process. *Transactions of the Japanese Geomorphological Union* **15**: 111–128.
- Sklar LS, Dietrich WD. 1998. River longitudinal profiles and bedrock incision models: Stream power and the influence of sediment supply. In *Rivers over Rock: Fluvial Processes in Bedrock Channels*, Tinkler KJ, Wohl EE (eds). Geophysical Monograph Series 107, American Geophysical Union: Washington; 237–260.
- Sklar LS, Dietrich WE, Foufoula-Georgiou E, Lashermes B, Bellugi D. 2006. Do gravel bed river size distributions record channel network structure? *Water Resources Research* **42**: W06D18.
- Smith ND, Smith DG. 1984. William River: An outstanding example of channel widening and braiding caused by bed-load addition. *Geology* **12**: 78–82.
- Sternberg H. 1875. Untersuchungen uber Langen und Querprofil geschiebefuhrender Flusse. *Zeitschrift für Bauwesen* **25**: 483–506.
- Thornes JB. 1977. Channel changes in ephemeral streams: Observations, problems, and models. In *River Channel Changes*, Gregory KJ (ed.). John Wiley & Sons: Chichester; 317–335.
- Whipple KX. 2004. Bedrock rivers and the geomorphology of active orogens. *Annual Review of Earth and Planetary Sciences* **32**: 151–185.
- Wilcock PR, Crowe JC. 2003. Surface-based transport model for mixed-size sediment. *Journal of Hydraulic Engineering* **129**: 120–128.
- Williams GP, Wolman MG. 1984. Downstream effects of dams on alluvial channels. *US Geological Survey Professional Paper* **1286**.

# 11

## The ecological importance of tributaries and confluences

Stephen P. Rice<sup>1</sup>, Peter Kiffney<sup>2</sup>, Correigh Greene<sup>3</sup> and George R. Pess<sup>3</sup>

<sup>1</sup>*Department of Geography, Loughborough University, UK*

<sup>2</sup>*NOAA – Northwest Fisheries Science Center, Mukilteo Field Station, USA*

<sup>3</sup>*NOAA – Northwest Fisheries Science Center, 2725 Montlake Boulevard East, USA*

### Introduction

Until recently, the ecological importance of tributary confluences had received relatively little attention (e.g. Bruns *et al.*, 1984; Petts and Greenwood, 1985), but this is now changing. It is increasingly clear that tributaries matter, not only because they can alter environmental conditions and elicit a biological response in the channel that they join (e.g. Rice *et al.*, 2001a; Fernandes *et al.*, 2004) but also because tributaries and confluence zones are sites of intrinsic ecological value where particular biophysical processes and ecosystem services may be concentrated (e.g. Power and Dietrich, 2002; Kiffney *et al.*, 2006). There is some evidence that these impacts may extend beyond the channel to affect floodplain biodiversity (Godreau *et al.*, 1999). In the first part of this chapter, we review existing evidence for tributary effects and the mechanisms responsible for them, and the recent theoretical developments that place the role of tributaries in a network context (Poole, 2002; Benda *et al.*, 2004; Thorp *et al.*, 2006; Grant *et al.*, 2007). We argue that developing our understanding of tributary effects is crucial because tributaries and confluence zones fulfil ecosystem functions and provide a variety of ecosystem services

that will only become more important as anthropogenic pressure on riverine ecosystems grows.

While empirical and theoretical evidence for tributary influence is convincing, it is clear that many questions remain to be answered, not least about the spatial extent and temporal characteristics of ecological tributary impacts – which tributaries matter, when and for which plants and animals? These and other information gaps hinder our ability to develop sustainable management strategies that accommodate tributary value. We argue that key limitations include a paucity of sufficiently detailed and extensive empirical data and the difficulties of integrating physical, chemical and biological factors into useful explanations of observed patterns. In the second part of this chapter, we therefore present field data from multiple confluences over several years, integrating physical, chemical and biological information to explore the spatial and temporal dynamics of tributary influence on main-stem ecology in the Cascade Mountains, Washington State, USA.

## **Tributaries, confluences and river ecology**

The distribution and health of in-stream biota in part reflect responses to abiotic environmental conditions. In this context, tributary confluences are important because they are places where the recruitment of water, sediment and organic matter can have a substantial impact on habitat in the recipient channel. In addition, tributaries and confluence zones (those parts of the main-stem channel directly affected by tributaries) are important because they provide unique habitats and support important ecological functions.

### **Changes in main-stem habitat characteristics at tributary confluences**

Principal abiotic effects at tributary confluences can be abrupt changes in main-stem water volume, water chemistry, organic matter and supplied sediment. These, in turn, have implications for a number of important habitat characteristics that include total wetted area, water chemistry and temperature, shading, channel slope, width and depth, substrate characteristics, channel hydraulics and hyporheic flow. It is not too surprising, then, that a number of studies have demonstrated significant shifts in main-stem invertebrate, fish and other communities at individual confluences, for example in association with changes in water temperature (Milner and Petts, 1994; Knispel and Castella, 2003), substrate characteristics (Rice *et al.*, 2001b), nutrient chemistry (Kiffney *et al.*, 2006) and assorted physio-chemical factors (Cianficconi *et al.*, 1991). Below dams, where main-stem disruption of water and sediment regimes means that tributary supplies of water and sediment are of enhanced importance, significant changes in aquatic

communities are widely documented (e.g. Petts and Greenwood, 1985; Vinson, 2001; this is further discussed below).

Beyond these local impacts, tributaries are important for the longitudinal organization of stream biota. An early illustration of this is in Illies' (1953) observation that major transitions between benthic communities along the Fulda River, Germany tended to occur at tributary confluences. In the River Continuum Concept, it was suggested that tributaries accelerate or retard downstream gradients of community development by resetting bioenergetic conditions (Vannote *et al.*, 1980; Minshall *et al.*, 1985). Thus, Bruns *et al.* (1984) found that tributaries along the Snake River, Idaho modified some downstream gradients, particularly the composition of macroinvertebrate functional feeding groups and of transported organic matter. They suggest that small tributaries have the effect of sliding communities forward along the ambient continuum while large tributaries set back community development.

Subsequently, it has been suggested that tributaries might, in fact, define a stepped, river discontinuum (Perry and Schaeffer, 1987; Bravard and Gilvear, 1996) and the Link Discontinuity Concept (Rice *et al.*, 2001a) formalized this by proposing that recruitment of water and sediment at tributaries (and other sediment sources) configures an abiotic framework within which confluence nodes and the intervening channel links are basic spatial elements of biotic organization. Field evidence to support this comes from the Pine and Sukunka Rivers, Canada, where within-link longitudinal trends in macroinvertebrate abundance and richness are disrupted and reset at confluences (Rice *et al.*, 2001a) and differences between macroinvertebrate communities upstream and downstream of confluences are substantially greater than differences between equally spaced sites in the intervening channel links (Rice *et al.*, 2001b). Recent studies have shown that nutrient chemistry, algal biomass and fish communities can also exhibit structured patterns around tributary junctions (Kiffney *et al.*, 2006).

## Biological functions of tributary confluences

It is apparent that tributaries and confluence zones are important sites in their own right, with intrinsic biological value beyond their importance for structuring communities at larger scales. This reflects at least four functions. First, confluences can be associated with increased productivity due to tributary supply of supplemental nutrients, drift and detritus. For example, along 2000 km of the Solimões–Amazon main stem in Brazil, the diversity of electric fishes (*O. Gymnotiformes*), increases close to confluences, especially where the tributary is 'white water' and therefore rich in nutrients, organic matter and invertebrate prey (Fernandes *et al.*, 2004). The cumulative effect may be substantial: in the coastal watersheds of south-eastern Alaska, every kilometre of salmon-bearing channel receives sufficient energy surcharges from fishless tributaries to support between 100 and 2000 young-of-the-year salmonids (Wipfli and Gregovich, 2002).

Second, confluences are sites where the juxtaposition of distinctive upstream, downstream and tributary environments may be usefully exploited by mobile species (Power and Dietrich, 2002). For example, yellow-legged frogs (*Rana boylei*) over-winter in tributary streams but congregate at main-stem confluences to breed on the South Fork Eel River, northern California (Kupferberg, 1996). These patterns probably reflect the higher illumination and algal productivity of the main-stem environment, which is more conducive to tadpole growth, and the presence of coarse sediments supplied by tributaries that provide low-velocity environments for egg clutches. Another example is provided by Scrivener *et al.* (1994), who found that juvenile chinook salmon (*Oncorhynchus tshawytscha*) moved between the main stem of Fraser River, British Columbia and a small non-natal tributary in response to seasonal variations in main-stem flow and turbidity. Elevated numbers of chinook were found in the clear tributary during the period of main-stem nival flooding, presumably because feeding opportunities were temporarily better, but returned to the main river after the flood when turbidity there declined.

The juxtaposition of contrasting environments may also enhance particular ecological processes such as refugia use. For example, tributaries may act as refugia from main-stem predators, as in the northern Range Mountains of Trinidad, where the main-stem presence of the piscivore *Hoplias malabaricus* (Wolf fish) causes higher tributary densities of the killifish *Rivulus hartii*, which is its main prey (Fraser *et al.*, 1995). Similarly, shaded tributaries may provide thermal refugia that mobile fish utilize during warm summer months (Kaeding, 1996; Bramblett *et al.*, 2002). In the Smith River, Oregon tributaries provide cool, thermal refugia that juvenile coho (*Oncorhynchus kisutch*) exploit during warm periods to minimize metabolic demand and reduce parasite infestation (Cairns *et al.*, 2005). The importance of tributaries as thermal refugia may become increasingly important with predicted increases in temperature resulting from global warming.

Third, the morphology and hydraulics of confluences are unusual and may provide unique ecological opportunities for some organisms (Franks *et al.*, 2002). For example, the Irrawaddy river dolphin (*Orcaella brevirostris*) shows a strong preference for confluence areas along the Mahakam River, Borneo. Kreb and Budiono (2005) argue that dolphins congregate at these habitats due to high fish abundances in deep confluence scour holes and the counter-circulating, scour-hole flow structures which trap migrating fish. River dolphins in the Cinaruco River, Venezuela, the Amazon River, Peru and the Yangtze River, China also exhibit a marked preference for confluence locations (McGuire and Winemiller, 1998; Leatherwood *et al.*, 2000; Zhang *et al.*, 2003), possibly for the same reasons. Similarly, deep, clean confluence pools provide important habitat for over-wintering steelhead (*Oncorhynchus mykiss*) in north-western California (Nakamoto, 1994).

Fourth, adjustment of the main-stem channel to tributary water and sediment fluxes can increase physical heterogeneity at confluences, ensuring a wider array of environmental conditions per unit channel length than would otherwise be present (Rice *et al.*,

2006). That is, habitat variability is likely to be greater along a stretch of river including a confluence than along a similar reach without a confluence. In this sense, tributaries are one of many factors, like variations in geology or valley confinement, that enhance in-channel heterogeneity in river systems. The argument that greater habitat heterogeneity was provided by coarse-grained sedimentation downstream of confluences was one of several reasons used to explain increases in taxa richness below tributaries and other sediment sources along the Pine and Sukunka Rivers, Canada (Rice *et al.*, 2001b). More comprehensive evidence for this effect comes from three river basins in Washington, where tributary confluences are associated with habitat discontinuities (in nutrient loading, wood loading, substrate size, channel slope and water depth) and significant shifts in primary productivity (periphyton biomass), sculpin density (*Cottus* sp.) and the abundance of salmonids (Kiffney *et al.*, 2006). Moreover, species richness, measured as species  $\times$  size classes, peaked close to seven of the 12 tributaries studied. Elevated physical heterogeneity may augment biological diversity because of the well-established principle that biological diversity tends to increase with habitat variability (MacArthur and MacArthur, 1961; Benda *et al.*, 2004). This concept led Benda *et al.* (2004) to propose that confluences are biological 'hotspots' (cf. McClain *et al.*, 2003) that contribute disproportionately to the overall aquatic biodiversity of the river network. Benda (Chapter 13, this volume) considers the implications of this model at network scales and the properties of networks that are important for creating widespread heterogeneity.

Numerical experiments utilizing a one-dimensional sediment-routing model, TRIB (details of the model are discussed by Ferguson and Hoey, Chapter 10, this volume) suggest that tributaries are most often responsible for increasing main-stem physical heterogeneity if they introduce coarse sediment in sufficient quantities to generate confluence aggradation (Rice *et al.*, 2006). Under these circumstances, the model predicts that heterogeneity is increased in two ways. First, geomorphological adjustments produce step-changes in environmental variables that define two physically distinct zones where otherwise there would be no zonation. Specifically, the channel upstream develops a flatter gradient with finer sediments, greater sand content and deeper, slower flows, while the downstream channel becomes steeper, coarser and cleaner with faster, shallower flows. Second, adjustment processes produce strong physical gradients within each zone that further diversify environmental conditions. For example, confluence aggradation promotes a size-selective sorting of the bed sediment and this produces downstream fining below the confluence (grain size declines rapidly with distance downstream). These predictions are in broad agreement with field observations (see Ferguson and Hoey, Chapter 10, this volume for a review) and the upstream–downstream zonation is summarized in Benda *et al.*'s (2004) reference to regions of upstream 'interference' and downstream 'mixing' (see their Figure 2).

Scenario modelling using TRIB suggested that the two key controls on confluence aggradation (and thence habitat diversity in this model) are the quantity and size of the tributary bedload relative to the main-stem bedload. Relative discharge was found

to be much less important (Rice *et al.*, 2006). This result emphasizes the importance of identifying and quantifying the significant sediment sources and sediment-routing pathways within the hydrological channel network, because it is these which may be most important for identifying high-heterogeneity confluences and therefore putative biological hotspots. Based on this modelling work, Rice *et al.* (2006) outline some testable hypotheses to guide future work in this area. These included expectations that: (1) as the volume and grain sizes of the tributary bedload increase relative to the main-stem load, there will be increases in overall biotic diversity around tributary confluences and strengthening of biotic gradients, (2) the reaches upstream and downstream from confluences that are affected by tributaries are likely to support assemblages of plants and animals that exhibit lentic and lotic characteristics respectively (because slower, deeper flows upstream are replaced by faster, shallower flows downstream). In the absence of appropriate physical and biological data, these hypotheses remain to be tested in the field.

### **Tributary effects at river network scales**

Work on the inherent biological importance of confluences has occurred alongside broader calls for a 'fluvial landscape ecology' (Fisher, 1997; Poole, 2002; Wiens, 2002), in which it is emphasized that rivers are spatially distributed, heterogeneous systems wherein the shape and topology of the drainage network and the juxtaposition of small and large sub-networks in a hierarchical structure are key controls of ecological functions and the distribution of lotic organisms. The emergence of this network-scale perspective is represented by a raft of theories that seek to explain the spatial and temporal organization of river biota across networks rather than along individual drainage lines; for example, the landscape-scale application by Poole (2002) of Hierarchical Patch Dynamics, the Network Dynamics Hypothesis (Benda *et al.*, 2004) and the River Ecosystem Synthesis (Thorp *et al.*, 2006). Grant *et al.* (2007) broaden this discussion to consider the population- and community-level importance of the architecture, nodes and links of dendritic ecological networks (DENs), of which river systems are one type.

General support for a network-scale perspective is found in a burgeoning array of arguments that food webs, patterns of habitat fragmentation, population dynamics, biogeochemical cycling and genetic differentiation are intimately connected to river network architecture (Power and Dietrich, 2002; Fagan, 2002; Fisher *et al.*, 2004; Lowe *et al.*, 2006a; Grant *et al.*, 2007). Studies at network scales have demonstrated links between the distribution of fish communities and network geometry (Osborne and Wiley, 1992; Grenouillet *et al.*, 2004) and the importance of landscape-scale factors like geology and land-use for understanding the distribution of stream biota (Richards *et al.*, 1996; Steel *et al.*, 2004).

At these network scales, confluences are important system elements (nodes) that have been shown to affect ecosystem organization. For example, in the Osage River,

Missouri confluences act as zoogeographic barriers to the distribution of the Niangua Darter (*Etheostoma nianguae*), where the difference in stream order between tributary and recipient channel is greater than or equal to three. This is most probably because droughts disproportionately affect small tributary channels and force the fish to move into adjacent, main-stem channels (Mattingly and Galat, 2002). Moreover, the density and spatial arrangement of confluences may be an important control on ecosystem form and function. For example, Smith and Kraft (2005) found that the number of confluences downstream from a site is an important determinant of fish assemblage in the Catskills, New York and, in landscape-scale modelling of steelhead (*Oncorhynchus mykiss*) distributions in Oregon watersheds, confluence density was a significant correlate with redd density (Steel *et al.*, 2004; EA Steel, *personal communication*, 2005). Lowe *et al.* (2006b) suggest that the number of confluences in a network might be positively related to network-scale community stability and overall biodiversity.

## Tributaries, ecosystem functions and river management

The preceding review indicates that tributaries and confluence zones fulfil important ecosystem functions that include structuring main-stem habitat, increasing main-stem productivity, providing local refugia and enhancing network heterogeneity. Therefore, tributaries are critical landscape elements affecting patterns of biodiversity and ecosystem function at various river scales. Because of their importance, the degradation or disconnection of tributary streams resulting from in-stream interventions or land-use actions may result in declines in critical ecosystem services locally along reaches and across networks. Just as river managers should recognize the importance of tributaries for managing main-stem sediment dynamics (see Liebault *et al.*, Chapter 12, this volume), so it is clear that protecting, maintaining and/or rehabilitating tributaries and confluence zones is important for the general health of riverine ecosystems. Moreover, where there are strong associations between confluence habitats and particular organisms, the conservation of those organisms may rely upon the careful management of the confluence zone. This may involve the protection of locally scarce organisms, such as the freshwater snail *Gyraulus acronicus* in the United Kingdom (Killeen and McFarland, 2004), or species threatened with global extinction, such as the Yangtze River dolphin (*Lipotes vexillifer*) (Zhang *et al.*, 2003), both of which show a strong preference for confluence environments.

As pressures on riverine ecosystems grow, for example due to global warming, nutrient loading, river regulation and river fragmentation (Meybeck, 2003), the ecosystem value of tributaries will become increasingly important. Global circulation models predict that air temperature will increase by 1–5°C over the next century depending on modelling scenarios. Higher air temperatures coupled with drier summer conditions may lead to metabolically stressful water temperatures in regions with cold-stenothermic

aquatic species (e.g. salmon). Cool, forested, headwater tributary streams, may therefore, provide refuge for cold-stenothermic species from potentially thermally stressful conditions in main-stem rivers (Cairns *et al.*, 2005). It has long been recognized that protecting the riparian vegetation of tributary channels is critical to maintaining the thermal integrity and flow characteristics of downstream channels. If climate change scenarios are accurate, applying this concept to the management of river networks is imperative for the protection of biodiversity and ecosystem function.

Tributaries also perform important nutrient-processing functions that may help to buffer riverine ecosystems from enhanced nutrient loading as a result of human activities. In a comparative study, Petersen *et al.* (2001) found that headwater tributaries retain and transform 50 per cent of inorganic nitrogen inputs from their watersheds. These authors speculate that such streams may be most important in regulating water chemistry in large networks because their large surface-to-volume ratios favour rapid nitrogen uptake and processing.

Confluence zones are of particular importance for the in-stream and floodplain ecology of large rivers that have been channelized and simplified for navigation, flood control and other purposes. For example, along the lower Missouri River, where regulation has eliminated natural backwater habitats, tributaries provide important alternative habitats that help to maintain a diverse native fishery (Brown and Coon, 1994; Braaten and Guy, 1999). In Europe, Pollux *et al.* (2006) found that a lowland tributary to the River Meuse in the Netherlands provided important spawning and rearing habitat with significant benefits for the recruitment of a variety of fish populations in the channelized main river.

Dams are a particular form of river regulation that alter the sediment flux and the quantity, variability, timing and quality (e.g. temperature) of water discharge causing significant changes to in-stream environmental conditions and, therefore, downstream biotic communities (Ward and Stanford, 1983, 1995). The recruitment of water and sediment from unregulated tributaries is then of elevated importance, affecting the main stem in two ways, both of which have implications for river biota. First, tributaries can reintroduce elements of the abiotic environment (water, sediment, heat) that have been removed or restricted by river regulation and, to varying degrees, reset them to pre-impoundment levels. For example, on the Colorado River, significant shifts in the algal and macroinvertebrate communities are observed where the Paria River reintroduces sediment-rich water to the clearwater reach downstream from the Glen Canyon dam (Stevens *et al.*, 1997). Temperature is not reset and, although the community downstream of the tributary is probably more similar to the pre-dam community, releases of cold water from the dam ensure that the macroinvertebrate fauna remains impoverished (Stevens *et al.*, 1997). In other cases, there is greater evidence of full 'recovery' below tributary junctions, for example Stinton Creek, a major tributary of the regulated Canning River, Western Australia, re-establishes discharge and flood frequency sufficiently to replace a predominantly lentic post-dam fauna with a lotic assemblage (Storey

*et al.*, 1991). Sato *et al.* (2005) provide a further example, highlighting the poor reproductive health of curimatã-pacú (*Prochilodus argenteus*) along an impounded reach of the São Francisco river, in south-eastern Brazil, and the stark improvement in reproductive health immediately downstream of an unregulated tributary where hypolimnetic waters are moderated.

Second, regulation is usually associated with a reduction in the magnitude and duration of peak flows and a reduction of sediment supply, so that sediment-transport capacity declines (Andrews, 1986). Aggradation below confluences is a widely reported consequence that reflects the delivery of tributary-bed materials in amounts and sizes that exceed the reduced, post-regulation transport capacity or competence (Petts, 1984; Allen, 1989; Sear, 1995). Physical changes to channel morphology and bed-material characteristics can, in turn, have important biological consequences. On the regulated River Rheidol in Wales, a complex geomorphological response to sediment deposition below the Peithnant tributary has increased habitat diversity and macroinvertebrate richness along an 'adjustment' reach (Petts and Greenwood, 1985; Greenwood *et al.*, 1999). The ecological consequences of such geomorphological adjustments are unlikely to be straightforward or always beneficial, in terms of increasing biotic richness and density. For example, post-impoundment sedimentation below tributaries may result in a channel narrowing and riparian encroachment that reduces the volume of available aquatic habitat along the main stem, as on the Snowy River, Australia (Erskine *et al.*, 1999).

Tributaries are therefore especially critical to ecosystem structure and function along rivers fragmented by impoundments and modified by channelization. River managers should be particularly attentive to the maintenance and protection of tributary functions along rivers with dams and other forms of regulation.

## Constraints on understanding and progress

Given this importance, it is crucial that we evaluate our current understanding, identify information gaps and set objectives that can improve our ability to incorporate tributary values into river management strategies. While the evidence for tributary impacts and functions reviewed above is convincing, it is true that the empirical evidence is still relatively thin and that our understanding of key mechanisms is far from complete, especially at network scales (Grant *et al.*, 2007). We certainly lack empirical data to test the growing number of hypotheses and theories about tributary impacts (Benda *et al.*, 2004; Rice *et al.*, 2006) and to validate and constrain numerical models of network-scale biological processes that explicitly consider confluence nodes (e.g. Muneeppeerakul *et al.*, 2007).

In particular, we do not know how general the affects and mechanisms described above are. This is true within individual regions, where a key question is 'Which

tributaries are most likely to be ecologically important within a river network?’ Given the diversity of impacts and causative mechanisms, allied with the array of biological processes that mediate strictly abiotic ecological responses, a simple answer to this question is unlikely. Answers would, nevertheless, be of significant value, because they might provide the basis for the a priori identification of ecologically important confluences. This would be an important management tool for targeting restoration or conservation efforts (see Benda *et al.*, 2004).

Generality is also an issue at larger spatial scales. For instance, we know little about the importance and role of tributary confluences between different geographic regions that are affected by different land-use patterns, hydroclimatic regimes and lithologies. In the same vein, we know little about the temporal dynamics of tributary importance in relation to any seasonal affects (e.g. variations in climate, riparian vegetation or productivity), the annual hydrologic regime and individual flood hydrographs. In addition, while many of the recent theoretical developments cited above (e.g. confluences as hotspots, the River Ecosystem Synthesis and DENs) are exciting ideas that hold significant promise, many aspects of them remain to be tested. For example, the network-dynamics hypothesis yields a number of testable hypotheses concerning the control of riverine heterogeneity (and by inference biodiversity) by network structure, but quantitative assessments are constrained by a lack of suitable data (Benda *et al.*, 2004).

Indeed, data to evaluate and refine many elements of the ideas reviewed above are scarce, both at confluence and network scales. In part, this reflects the cost of acquiring snapshot biological and environmental information at a high spatial resolution across extensive channel networks. In this regard, novel remote-sensing techniques may become increasingly useful and there is also a need to develop appropriate geostatistical techniques that are tailored to extract meaningful patterns from river network surveys (see Torgersen *et al.*, Chapter 9, this volume and Power *et al.*, 2005). In addition, progress is hindered by a lack of testable hypotheses (though see Benda *et al.*, 2004 and Rice *et al.*, 2006), the difficulty of attaining experimental control in field situations, weaknesses in coupling numerical models of abiotic and biotic processes and insufficient cross-disciplinary expertise to properly integrate physical, chemical and biological information.

## **Tributary nutrient loading, basal stream productivity and higher-order aquatic and terrestrial fauna: a case study**

In the second part of this chapter, we illustrate the value and importance of field data by exploring several aspects of tributary–main-stem ecology in the Cascade Mountains, Washington State, USA. This analysis demonstrates the benefits of collecting data from

multiple confluences over several years and of integrating physical, chemical and biological information to develop an understanding of tributary effects. Field data were collected in western Washington in the foothills of the Cascade Mountains. This area is part of the Pacific Coastal ecoregion (Naiman and Bilby, 1998) and is characterized by mild, wet winters with a pronounced summer dry season. The vegetation is predominantly mixed conifers and broadleaf riparian species (see Kiffney *et al.*, 2006).

Habitat and biological surveys were conducted at 10 sites within the Skagit and Cedar River networks (Figure 11.1) to determine whether locations around tributary junctions exhibited increased habitat heterogeneity, nutrient input, primary and secondary productivity and abundance of aquatic and terrestrial taxa. The impetus for this data collection was an earlier observation on the Cedar River that nutrient loading and fish abundance tended to be higher at tributary confluences (Kiffney *et al.*, 2002). We hypothesized that elevated nutrient loading at confluences is a common phenomenon in this region and that higher nutrient levels would increase main-stem primary productivity. In turn, we speculated that such increases, along with other tributary impacts (e.g. temperature changes and substrate heterogeneity), would increase macroinvertebrate and fish abundances close to confluences and that these effects may consequently enhance insectivorous and piscivorous bird abundances close by.

In addition, we utilized data from a separate study that examined longitudinal patterns of habitat selection by spawning Chinook salmon (*Oncorhynchus tshawytscha*) (Beechie *et al.*, in press) to investigate the relevance of tributaries for an animal of particularly high conservation value. Chinook are the largest salmonids in the Pacific Northwest (PNW) and spawn in the main stems of large river systems (Montgomery *et al.*, 1999). While adult salmon are quite faithful to their natal river system, the selection of spawning sites within rivers can vary compared to their natal egg nest (also called 'redd') site. At river reach and habitat scales, spawners respond to river depth and flow (Healey, 1991), temperature (Torgersen *et al.*, 1999), gravel size (Healey, 1991) and hyporheic flow (Geist, 2000), and these cues correlate with optimal spawning and incubation conditions (Beechie *et al.*, in press). Because tributaries can influence each of these factors, we hypothesized that Chinook salmon redds would occur at relatively higher densities close to tributaries. We speculated that this effect might be enhanced during years when low flows restrict habitat use to colder and deeper areas of the channel network because such areas would be found downstream of tributaries. We examined this prediction by conducting salmon-spawning surveys in the North Fork (NF) Stillaguamish River (Figure 11.1).

By examining nutrient loading, primary productivity and macroinvertebrate, fish (including salmon) and bird taxa, this study provided an opportunity to assess both the trophic extent of tributary influences and whether ecological impacts extend beyond the stream into the terrestrial environment. Collectively, these studies provide compelling evidence that tributary streams affect the ecology of main-stem rivers where they influence a variety of processes and biotic patterns.

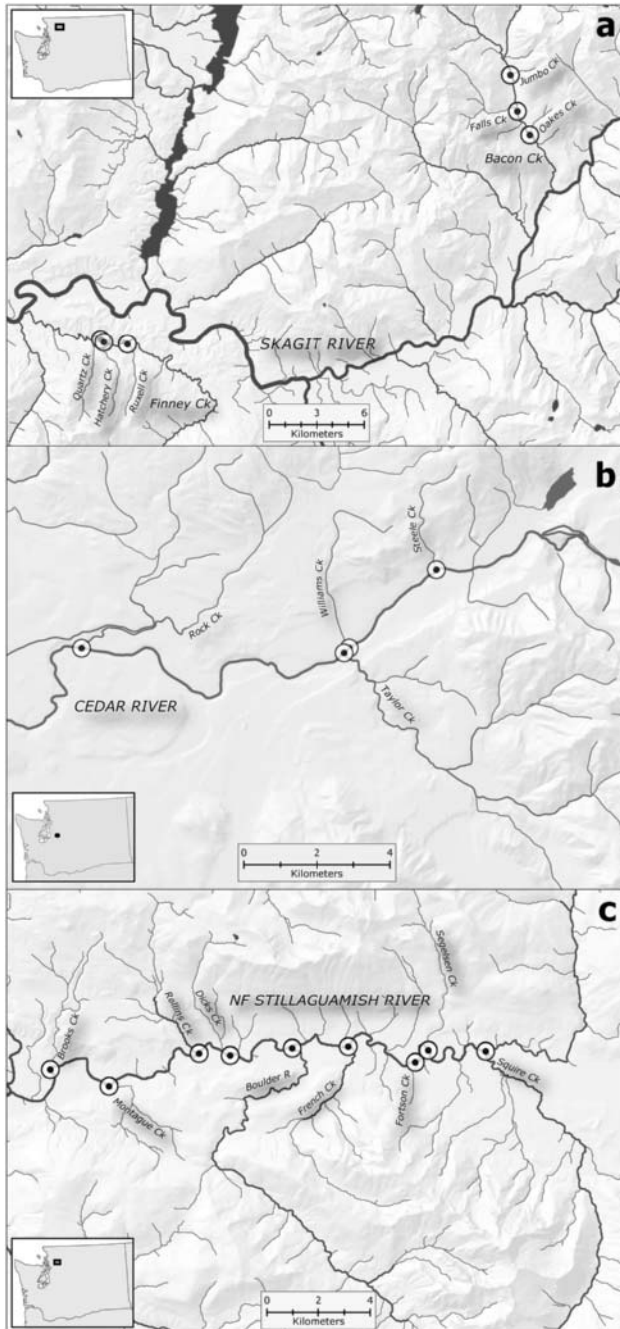


**Figure 11.1** Map of study streams: (a) Skagit River sites, (b) Cedar River and Taylor Creek sites and (c) the NF Stillaguamish River. Circles represent study reaches, with the small dot within each circle representing location of tributary–main-stem confluence. Maps courtesy of Jeremy Davies (Northwest Fisheries Science Center).

## Habitat and biological surveys

Between 2002 and 2004 detailed surveys were conducted of tributary and main-stem (defined here as the larger channel receiving inputs from smaller tributaries) physical, chemical and biological attributes around four confluences in the Cedar River network (on the Cedar main stem) and around three confluences on Bacon Creek and Finney Creek in the Skagit River network (Figure 11.1). The 10 tributary streams are primarily shaded while the main-stem channels are relatively open with cool, clear water and rock-gravel substrates. Main-stem areas range between 1578 and 30 121 ha (measured from above tributary confluences), and the ratio of tributary to main-stem area covers an order of magnitude from 0.046 to 0.49. Although these systems are relatively pristine, it is also important to note that all of our study sites have experienced some anthropogenic impacts (e.g. logging and dams), and these may affect our results.

Our survey design and methods were based on a standardized approach developed by the United States Environmental Protection Agency's Environmental Monitoring and Assessment Program (EMAP; Kaufmann, 2002). We present only a brief description of this approach here; further details can be obtained in Kaufmann (2002) and Kiffney *et al.* (2006). Reach lengths were 40 times the average wetted width of the main stem during our surveys and ranged from 200 to 920 metres (Kaufmann, 2002). Each reach was divided into 11 equally spaced transects that were perpendicular to water flow, with six primary transects upstream and five transects downstream of each tributary (Figure 11.2). Distances between transects differed among the 10 tributary–main-stem reaches because channel width varied among main-stem rivers. To standardize this distance, we divided the length between each transect and the tributary by the intra-transect distance. We called this normalized distance the 'standardized distance unit', or SDU, with this value ranging from  $-5$  to  $5$  (Kiffney *et al.*, 2006). In addition to the primary transects, we placed secondary transects ( $0.5$  to  $-0.5$ ) within each reach to test for tributary effects that might occur at finer spatial scales. Distances between these transects were 12.5, 25 and 50 per cent of the distance between primary transects.

In 2002, grab-water samples were collected from  $-1$  to  $1$  SDU on the Cedar River, and we collected samples from all transects in 2003 at the Finney and Bacon creeks. These samples were analysed for total nitrogen and phosphorus, and dissolved nitrate and nitrite, ammonia and soluble reactive phosphorus.

We used unglazed ceramic tiles to quantify algal biomass and aquatic insect colonization rate above and below tributary confluences of the Cedar River and Finney and Bacon creeks. Four to five tiles ( $25\text{ cm}^2$ ) were attached to wire mesh and anchored to the stream bottom at secondary transects above and below each confluence. Insect density and algal biomass were quantified four times (day 8, 16, 24 and 36 after placement of tiles). Some mayflies were sensitive to observer movement; therefore, we counted these taxa while the tile remained in the water. The tile was then slowly removed from the water and the remaining insects were identified and counted. This approach has been used

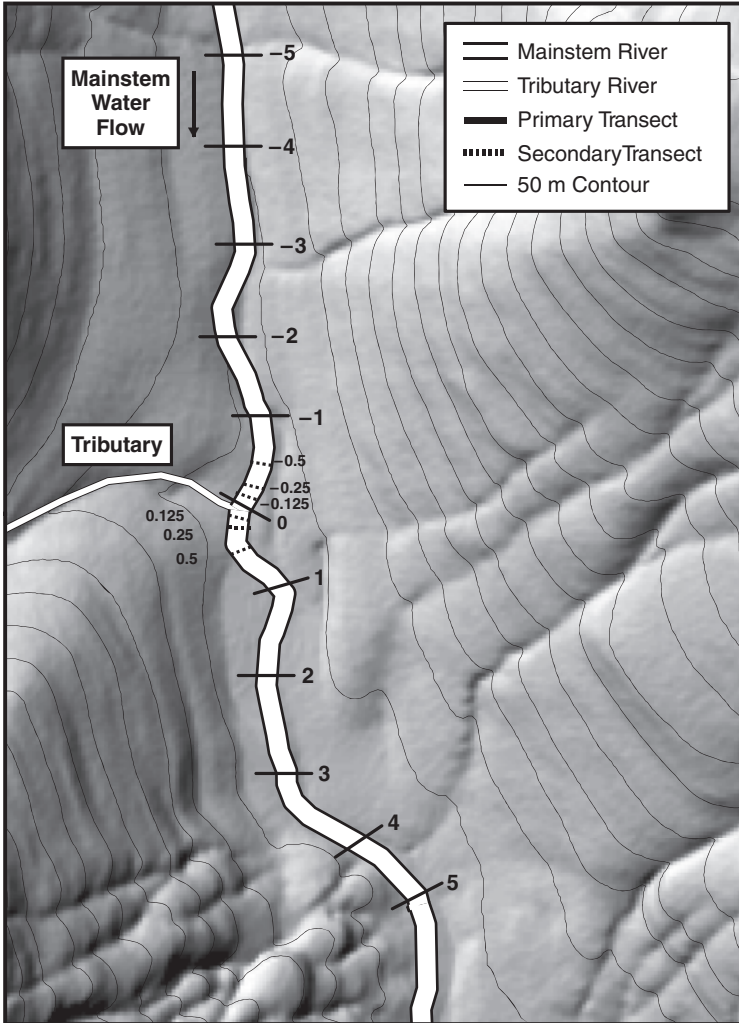


**Figure 11.2** Survey design used for this study. Primary transects were 5 through -5, with the 0 transect immediately upstream of the tributary-main-stem confluence. Secondary transects (0.5 to -0.5) were used to collect additional samples for nutrients, water temperature, algal biomass and density of benthic organisms.

successfully in other studies to quantify effects of light (Kiffney *et al.*, 2003, 2004) and nutrients (Kiffney and Richardson, 2001) on algal biomass and insect consumers. After counting insects, tiles were scrubbed and rinsed with distilled water, with the resultant slurry collected onto a glass-fibre filter (Gelman Type A/E, 0.47  $\mu\text{m}$ ). Chlorophyll *a* was extracted from the filter using 90 per cent acetone for about 18 hours, and chlorophyll *a* concentration was determined using a Turner fluorometer (Kiffney *et al.*, 2003).

To characterize the benthic fauna, surveys were conducted at primary and secondary transects. A square plastic (PVC pipe) frame (0.25 m<sup>2</sup> area) weighed down by sand within the pipes was carefully placed on the stream bottom at three locations (left, middle and right side) across each transect. Within each quadrat, we counted and identified sculpin, a small benthic fish species (*Cottus* sp.) and large caddis flies (primarily *Dicosmoecus gilvipes*).

Bird censuses were conducted above and below tributary junctions at Finney Creek in 2004. We enumerated foraging behaviour of individual birds recording prey type, prey number and foraging-bout duration between -4 and 3 SDU. We also quantified bird abundance and diversity between these same transects by establishing point count stations of 50-m radius, where we recorded all birds observed over eight minutes. Multiple surveys were conducted at Finney Creek in June and July.

## Spawning salmon surveys

Nine tributaries varying in drainage area (Table 11.1; Figure 11.1) enter the NF Stillaguamish in the areas where Chinook salmon spawn, providing a basis for examining

**Table 11.1** Drainage areas of nine tributaries of the NF Stillaguamish, the percentage of each tributary's drainage area out of the NF's drainage at the point of each confluence and the proportion of redds detected 1.1 km below each tributary (compared to one laid 1.1 km above) during 1998 to 2001. Light shading indicates  $p < 0.05$ , dark shading indicates  $p < 0.01$ , as determined by binomial tests on the frequency of redds laid below and above each tributary. Underlining indicates significant attraction to areas above tributary junctions ( $p < 0.05$ ).

Tributary	Drainage area (km <sup>2</sup> )	% of NF drainage at junction	Percentage of redds laid below tributary			
			1998	1999	2000	2001
Squire	69.59	33.75	100	80	36	33
Segelson	10.36	4.52	100	8	39	50
Fortson	3.03	1.29	78	78	48	77
French	20.68	7.57	50	53	73	100
Boulder	65.02	18.67	73	71	52	65
Dicks	8.84	2.41	29	13	33	20
Rollins	20.57	5.30	9	67	50	20
Montague	13.30	3.24	56	43	100	25
Brooks	11.49	2.69	45	67	100	27
<b>Average discharge during spawning (m<sup>3</sup>/s)</b>			6.8	11.9	16.2	17.8

the effects of tributaries on the distribution of redds. The Washington State Department of Fish and Wildlife has conducted redd counts during spawning season annually since 1974. Redd counts are conducted by stream walks every seven to 10 days during the spawning season (August to October, when flow levels are at their annual low point). All redds are flagged when first observed so as not to be recounted in the proceeding surveys. In 1998 through 2001, this effort was intensified and all redds in the NF Stillaguamish were systematically mapped on a weekly basis (Hahn *et al.*, 2001), thereby providing a high spatial and temporal resolution of spawning data that are used in our analysis.

At each of the nine tributaries, we counted the number of redds occurring either 1.1 km above or below each tributary. In order to account for alluvial fans and tributary-associated hyporheic flows, we displaced the starting position for the downstream zone to a point 0.1 km above the tributary junction. Redds were counted in a 1.1-km zone upstream as a paired control in order to examine whether salmon preferred areas downstream or upstream of confluences. The number of redds not associated with tributaries at all (i.e. outside of the 2.2-km area around each tributary) were also counted. Particular attention was paid to Boulder Creek, one of the largest tributaries in the system. Boulder Creek supplies glacial meltwater to the NF Stillaguamish and therefore is a critical source of cold water for the entire system.

Because flows in the NF Stillaguamish become low during the spawning period, we hypothesized that the effects of tributaries might be strongly related to flow levels. Using data from the US Geological Service (USGS) gauge at the mouth of the NF Stillaguamish, we calculated an average discharge during the spawning period (August to October), by weighting monthly average flows by the proportion of redds laid during each month. This weighted average therefore directly relates monthly flow levels to the temporal pattern of spawning abundance, emphasizing the flow at peak spawning times.

## Physical and chemical patterns

Strong temperature gradients were common around tributary confluences. For example, there was a sharp break in water temperature at the confluence of Steele Creek and the main stem Cedar River, with water temperature about 1°C cooler in the immediate vicinity of the junction (Figure 11.3).

We have consistently observed that tributary streams in the Cedar River watershed were richer in nitrogen and phosphorus than the main stem. For example, nutrient concentrations during summer were often higher at sampling stations immediately below tributary junctions: total phosphorus concentrations were 12–69 per cent higher immediately below tributary confluences compared to transects 40–80 m upstream or downstream of the junction (Figure 11.4(a–d)). Similar peaks were observed in Finney and Bacon Creeks (Figure 11.4(e–h)). Although peaks generally occur at

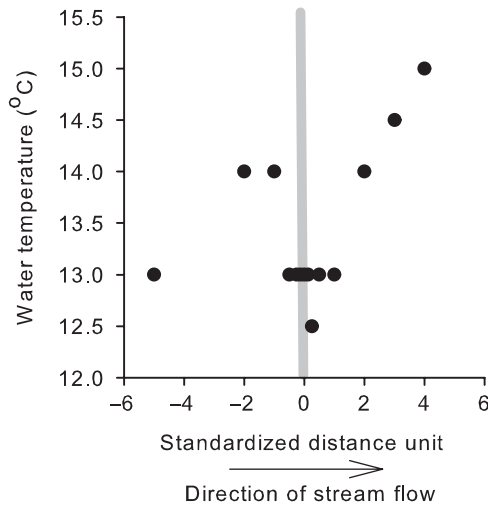


**Figure 11.3** Scatterplot of water temperature vs. SDUs for Steele Creek and main stem Cedar River confluence. Grey bar denotes approximate location of tributary junction.

tributary confluences, concentrations quickly decline downstream, indicating a rapid uptake by primary producers. We also observed that tributary streams in the Cedar River were exporting potentially significant amounts of biologically important materials during winter. Total N and dissolved P concentrations in tributary streams during winter were three times and 1.5 times higher than main-stem sites (Figure 11.5).

## Biological patterns

Summer algal accrual rates were largely concordant with patterns of nutrient concentrations in main-stem habitats. Algal accrual rates were approximately 50 times higher at the transect 25 m downstream of the Rock Creek confluence compared to transects 80 m upstream or downstream of the junction (Figure 11.6(a)). Similar patterns were observed at the confluences of Williams, Taylor and Steele Creeks with the Cedar River (Figure 11.6(b–d)), at the confluences of Jumbo and Falls Creeks with Bacon Creek (Figure 11.6(e–f)), and at several tributary confluences along Finney Creek (Kiffney and Greene, unpublished results).

Insect colonization rates and abundance of benthic organisms on tiles exhibited notable gradients at tributary confluences. In the Cedar River, abrupt shifts in insect colonization rate occurred about 10 m upstream of the Williams and Steele Creek confluences, and at 20 and 40 m downstream of the Taylor and Rock Creek confluences (Figure 11.7). Surveys of benthic organisms in the Skagit River also revealed

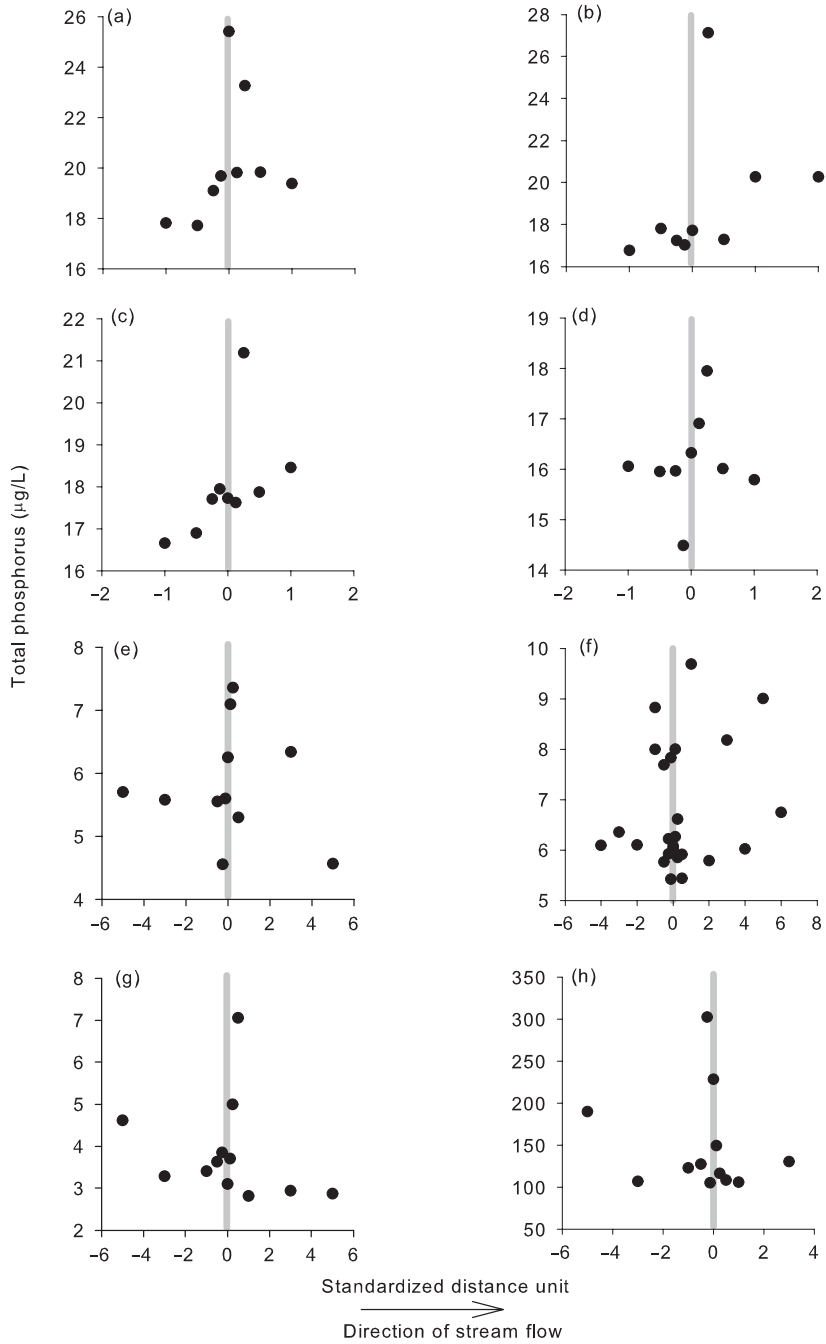


**Figure 11.4** Scatterplots of total phosphorus vs. SDUs for the (a) Rock, (b) Taylor, (c) Williams (d) Steele, (e) Ruxell, (f) Quartz and Hatchery, (g) Jumbo and (h) Falls Creek confluences. Rock, Taylor, Williams and Steele Creeks flow into the Cedar River; Ruxell, Quartz and Hatchery Creek flow into Finney Creek; Jumbo and Falls Creek flow into Bacon Creek.

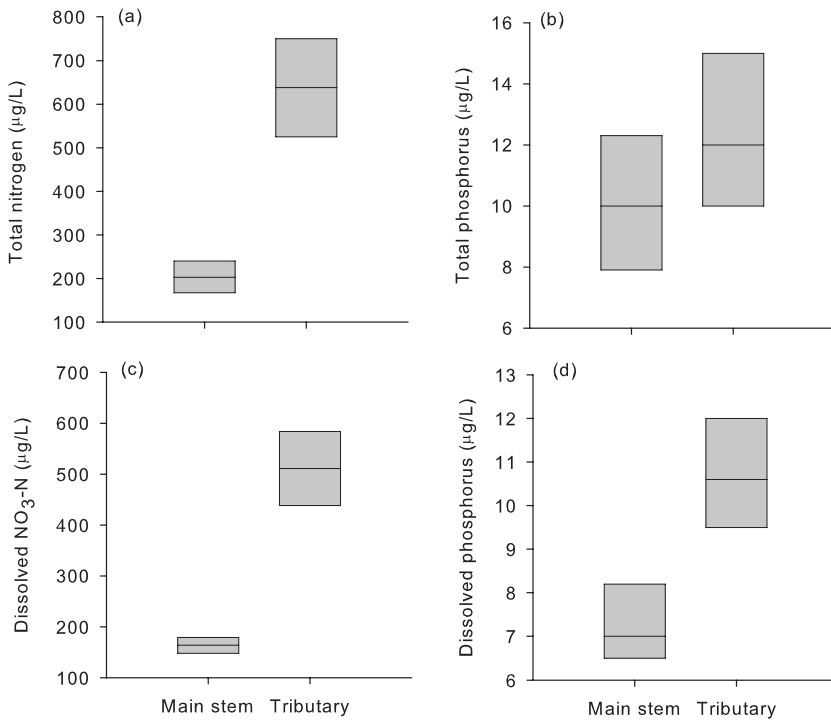


**Figure 11.5** Mean ( $\pm$  95 per cent confidence intervals) (a) total nitrogen, (b) total phosphorus, (c) dissolved nitrogen and (d) dissolved phosphorus for water samples collected at main-stem sampling sites ( $n = 9$ ) and tributary sites ( $n = 4$ ) during winter (November–February) in the Cedar River.

gradients in abundance patterns for multiple taxa at tributary junctions (Figure 11.8). There were two peaks in the density of *Dicosmoecus gilvipes* at the confluence of Ruxell Creek with Finney Creek: one was located at transect -4, followed by a peak immediately upstream of the junction (Figure 11.8(a)). Similarly, mayfly density was 1.3–20 times higher at the same confluence compared to upstream or downstream transects (Figure 11.8(b)). Stonefly predators were more abundant and total insect density was greater in a reach of Finney Creek where two tributaries (Quartz and Hatchery Creeks) entered the main stem very close together (Figure 11.8(c–d)). Total insect density also peaked at the confluences of Jumbo Creek and Falls Creek with Bacon Creek, and remained elevated at some downstream transects (Figure 11.8(e–f)).

Greater standing stocks and accrual rates of primary producers and consumers may promote local abundances and diversity of predators. We observed that densities and diversity of fish generally peaked at tributary confluences (Kiffney *et al.*, 2006). In addition, bird abundance, diversity and foraging rate peaked immediately upstream of tributary confluences. Foraging rate was about 2.5 times higher in the large floodplain complex formed where Quartz and Hatchery Creeks entered Finney Creek (Figure 11.9).

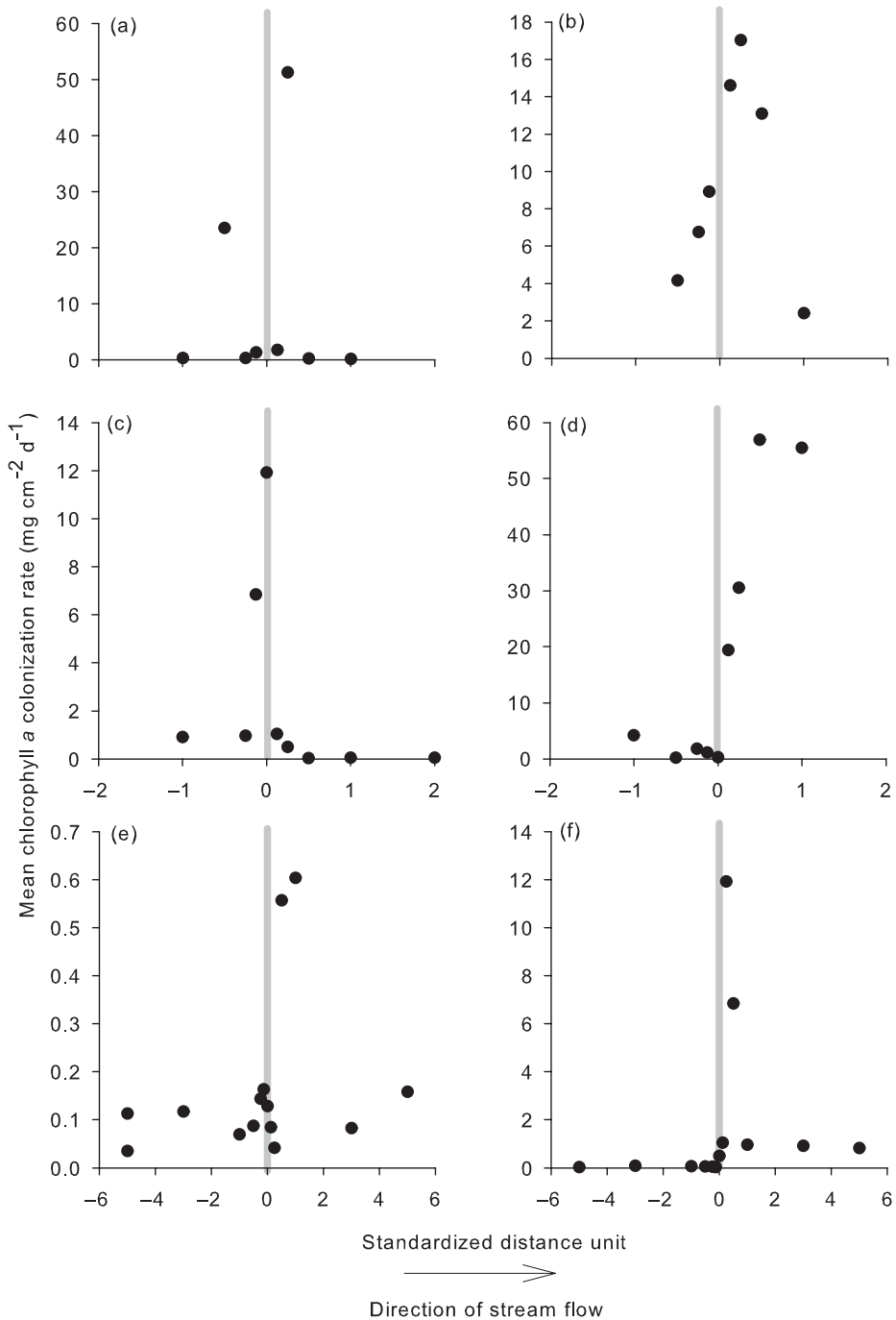


**Figure 11.6** Scatterplots of algal chlorophyll *a* accruing on ceramic tiles averaged across a five-week colonization period vs. SDUs for the (a) Rock, (b), Williams (c) Taylor and (d) Steele Creek confluences on the Cedar River, and the (e) Jumbo and (f) Falls Creek confluences on Bacon Creek.

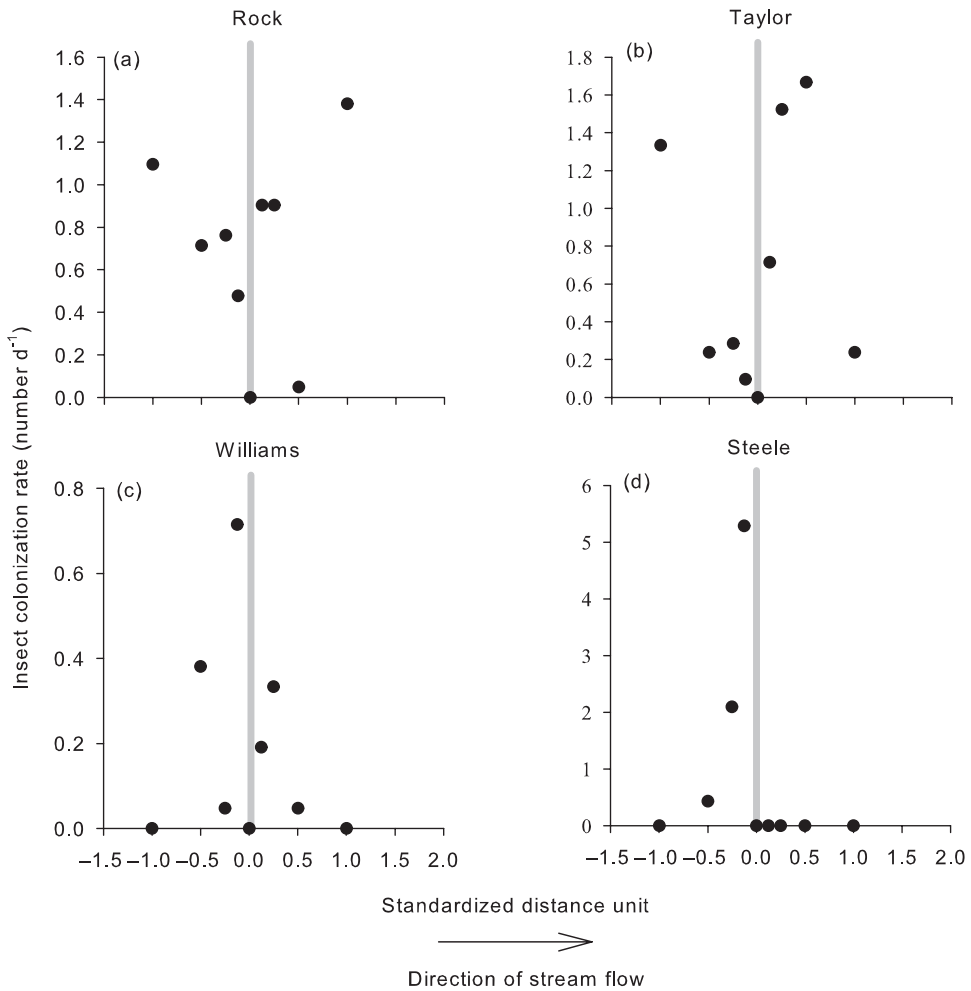


**Figure 11.7** Scatterplots of total insect colonization rate on ceramic tiles averaged across a five-week colonization period vs. SDUs for the main-stem Cedar River confluences (a) Rock, (b) Taylor, (c) Williams and (d) Steel Creeks.

## Spawning patterns

Tributaries were an important predictor of spawning behaviour. At the scale of the entire NF Stillaguamish, approximately one-third of all spawning (34 per cent  $\pm$  2 per cent) occurred at or directly below tributaries (i.e. within 1.1 km including and below any confluence), and this distribution approached the percentage of the entire main stem represented by the 1.1-km segments below confluences (40 per cent). Hence, at the scale

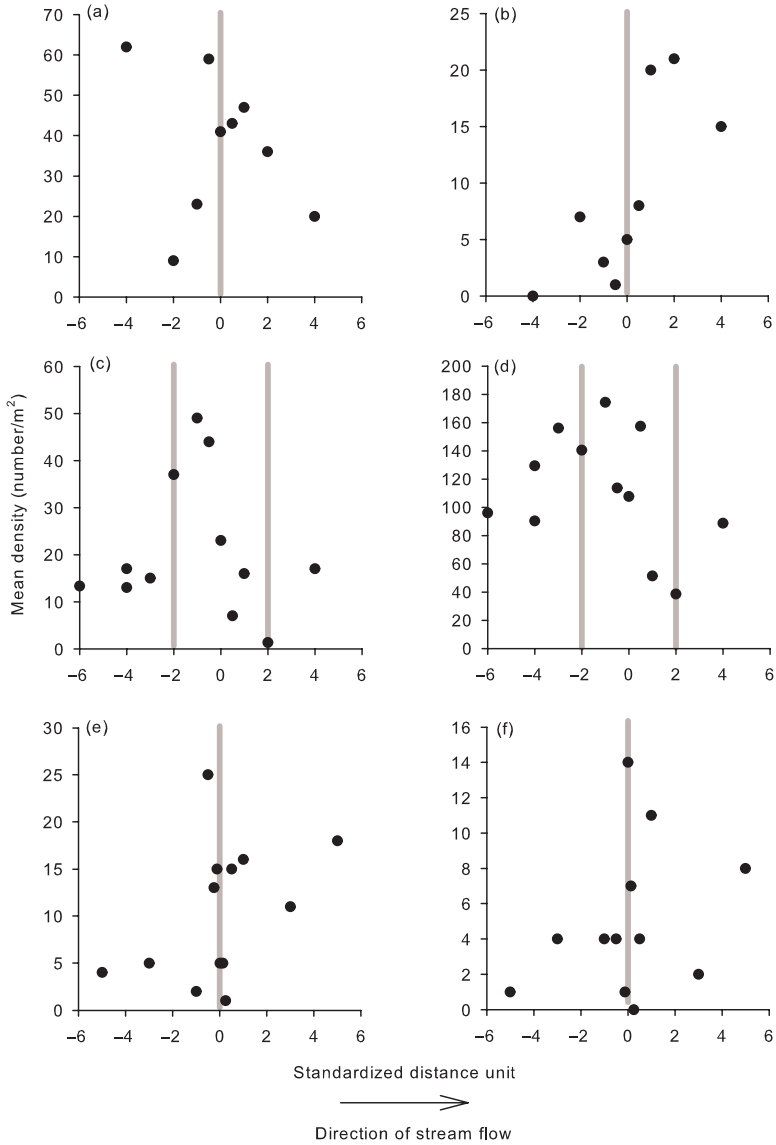


**Figure 11.8** Scatterplots of (a) the caddis fly *Dicosmoecus gilvipes* density and (b) total mayfly density at the confluence of Ruxell and Finney Creeks, (c) stonefly density and (d) total insect density where Quartz and Hatchery Creeks flow into Finney Creek (the two confluences are very close together as indicated by the grey bars), and (e–f) total insect density at the confluence of Jumbo and Bacon Creeks and the confluence of Falls and Bacon Creeks, respectively, versus SDUs. Insect density was quantified during benthic surveys conducted in the summer of 2004.

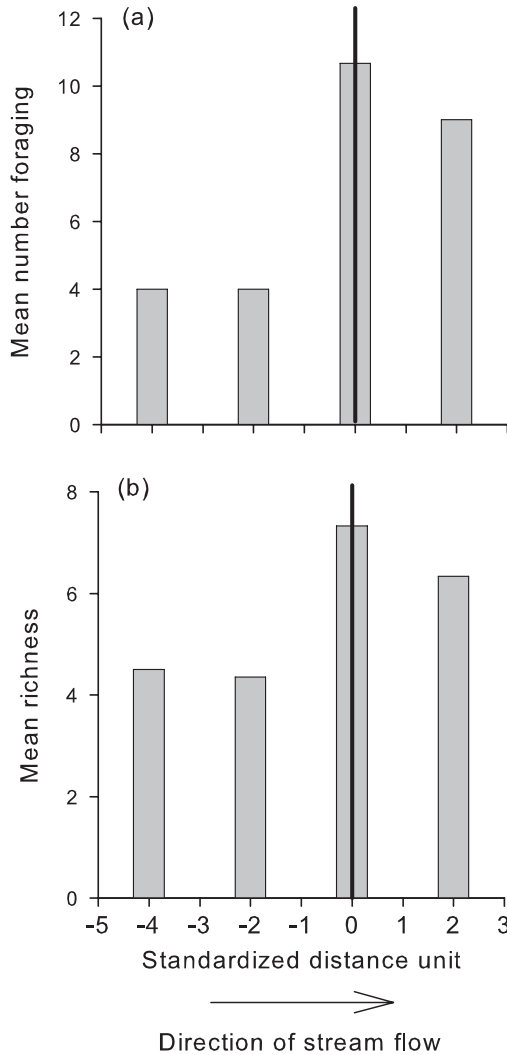


**Figure 11.9** Mean number of (a) birds foraging and (b) bird taxa richness versus SDUs in the reach where Quartz and Hatchery Creeks join Finney Creek during the summer of 2004.

of the entire NF Stillaguamish, patterns of redd distribution below tributary confluences appear to occur no more than expected by chance. However, patterns in spawning were apparent at two smaller spatial scales. First, the proportion of fish spawning above Boulder Creek, the major source of cold water in the North Fork ( $11.13^{\circ}\text{C} \pm 1.26$  below the Boulder River versus  $12.04^{\circ}\text{C} \pm 1.44$  upstream of the Boulder River), was positively related with discharge during spawning (Figure 11.10). This suggests that

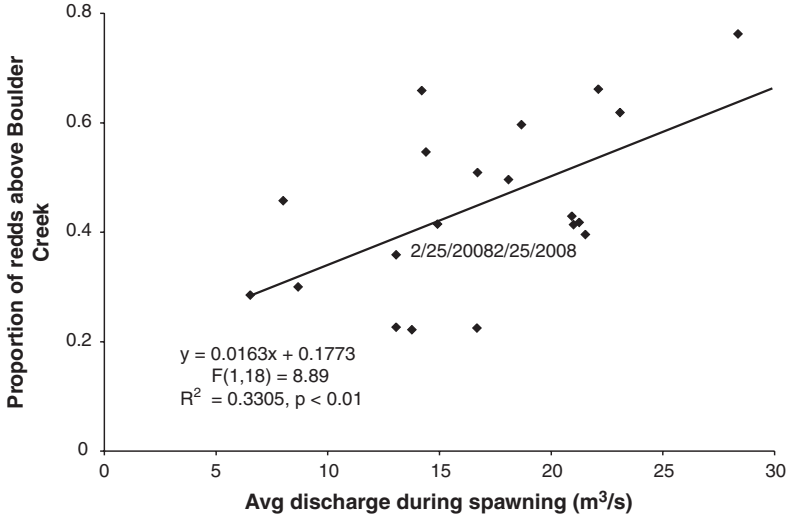


**Figure 11.10** Proportion of Chinook salmon redds laid above Boulder Creek (a major tributary and source of glacial meltwater) as a function of the average discharge (m<sup>3</sup>/s) of the NF Stillaguamish during spawning. Average discharge was weighted across August, September and October using the proportion of redds laid during those months. Each data point is for one year.

during low flows, this large tributary diverts many fish that might have spawned above it to cooler areas downstream. At a smaller spatial scale, we examined whether there was a preference for spawning below each tributary using a binomial test of observed and expected proportions of redds laid within the 1.1-km zones above and below each tributary (Table 11.1). The NF drainage-wide proportion of redds laid below tributaries (32–36 per cent, depending upon the year) was used as the expected proportion in each binomial test. A significant departure downstream of any tributary indicates preferential selection for redd construction of areas below that particular tributary junction (Table 11.1). During low-flow years (1998 and 1999), significant preference for downstream sites was detected for up to two-thirds of the tributaries, while during years with higher flow (2000 and 2001) significant downstream preference occurred at only three of the nine tributary junctions (Figure 11.11). At these three junctions, Chinook preferentially built redds downstream in all years. The first was Boulder Creek, the second-largest tributary in the system with the cold-water input noted above. The second was French Creek, a moderately sized tributary. The third tributary, Fortson Creek, is the smallest drainage in the data set, yet is a significant source of groundwater and hyporheic flow from several large ponds. It is important to note that there are no flow-depth barriers to upstream migration in the main-stem NF Stillaguamish at any of the tributary junctions.

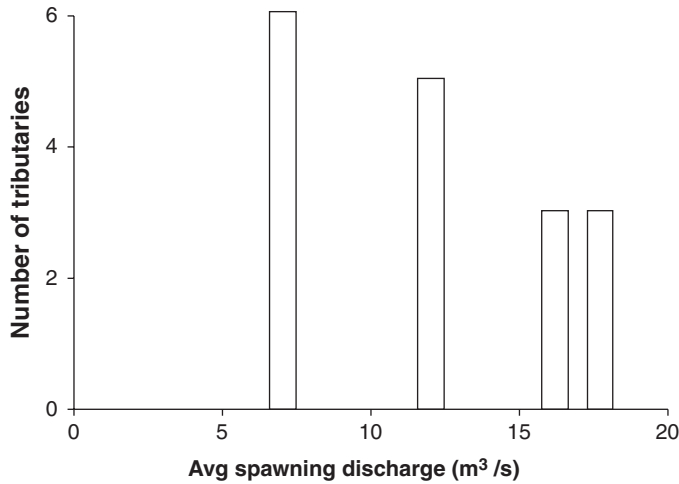


**Figure 11.11** The number of tributaries in the NF Stillaguamish watershed exhibiting significant downstream spawning preferences, as a function of average discharge ( $\text{m}^3/\text{s}$ ) of the NF Stillaguamish during spawning. Average discharge was weighted across August, September and October using the proportion of redds laid during those months.

## Discussion

These results show that tributary streams can alter a variety of ecological characteristics and processes of main-stem rivers, ranging from water temperature and chemistry to bird-foraging behaviour and habitat selection by spawning salmon. For example, stream temperature of the main-stem Cedar River dropped abruptly from 14 to 13°C at the confluence of Steele Creek and recovered to similar levels about 160 m downstream of the confluence. While most tributaries have a cooling effect on main-stem channels, we have also observed that water temperature can be higher at tributary confluences (Kiffney *et al.*, 2006). The size and direction of the tributary temperature effect is likely conditional upon a number of factors, such as the ratio of tributary to main-stem area, substrate characteristics, groundwater characteristics, the riparian condition of the tributary and receiving stream, and the presence of wetlands or lentic habitat. Margolis *et al.* (2001) found that water temperature downstream of beaver impoundments was significantly higher than at upstream sites due to increased solar exposure and longer residence time. Alternatively, beaver-dam complexes have been shown to be sources of cool water by forcing flow through the hyporheic zone (Pollock *et al.*, 2007). Beaver-pond complexes can be important on low-order tributaries in the PNW and may warm or cool tributary water flowing to main-stem habitat, thereby altering stream temperature within the confluence zone.

The results in this study confirm the earlier finding that tributary streams tend to increase main-stem nutrient levels close to confluences. In the PNW and other forested temperate regions, it is likely that small headwater streams are particularly important nutrient sources for otherwise oligotrophic main-stem rivers. Small tributary streams are typically heavily shaded so that primary productivity is constrained by light limitation (Kiffney *et al.*, 2003). The uptake of essential nutrients such as nitrogen and phosphorus is therefore low (Hill *et al.*, 2001) and unused nutrients are exported to sunlit main-stem rivers where they are available for uptake by primary producers (Power and Dietrich, 2002).

The composition of the riparian tree community may also enhance nutrient levels in tributary streams, which, in turn, influence nutrient levels in the main stem. Of particular importance is red alder (*Alnus rubra*), a nitrogen-fixing species that is commonly found along riparian corridors in the PNW (Volk *et al.*, 2003). Volk (2004) found that dissolved nitrate+nitrite concentration in six headwater streams was positively correlated with the proportion of riparian trees represented by alder. Red alder made up 10–30 per cent of the riparian vegetation in tributaries to the Cedar River, which may partially explain the almost three-fold difference in total nitrogen between tributary and main-stem sampling stations. It is likely that the combination of nutrient-rich inputs from alder and low nutrient uptake by primary producers contributes to the increased nutrient concentrations we have observed in confluence zones.

The results support the hypothesis that tributary streams are biologically important sources of main-stem nutrients because algal colonization rate peaked immediately adjacent to all four tributary streams entering the Cedar River (Figure 11.4), as well as confluences in Finney Creek and Bacon Creek (Kiffney *et al.*, 2006). The wetted channel of the main stem Cedar is approximately 20–30 m wide allowing ample inputs of solar radiation that, in combination with the high nutrient loads, promote primary productivity around confluences. A number of studies have shown that the primary productivity of freshwater habitats is partially limited by nutrients and light (Hill *et al.*, 1995; Kiffney and Richardson, 2001). If tributary streams subsidize main-stem rivers with essential nutrients increasing primary productivity, then we would predict that higher trophic levels, such as insects, fish and birds, would be attracted to some tributary confluences because of higher basal productivity.

In fact, we observed multiple lines of evidence to support this prediction. First, insect colonization rates in three of four Cedar River tributaries were higher in confluence zones than transects further away. Second, the density of some insect herbivores and predators generally peaked around the confluence zone. Third, we showed in an earlier study that fish density, especially that of juvenile fish, peaked at tributary confluences (Kiffney *et al.*, 2006). Finally, preliminary analysis indicates that bird-foraging rates and richness peaked in the confluence zone of Quartz, Hatchery and Finney Creeks. We speculate that the increased foraging rate around these confluences was a result of multiple factors, including suitable habitat and high secondary productivity. For example,

at the Quartz–Hatchery confluence zone on Finney Creek we observed abundant gravel bars used by spotted sandpipers and robins, wood jams used for perching by flycatchers and kingfishers and deep pools used by diving birds such as common mergansers. In addition, we observed increased secondary productivity leading to a greater biomass of benthic and emerging insects feeding benthic foragers (e.g. the American dipper) and flycatchers. Because juvenile-fish density generally peaked around tributary confluences, it is also possible that piscivorous birds were attracted to these locations because of more abundant food resources. Because we were only able to conduct detailed bird surveys at one tributary on Finney Creek, more study is clearly needed to further examine the generality of these patterns and whether tributary confluences provide ecologically significant locations for terrestrial as well as aquatic biota. Despite this limitation, results of the bird surveys were in agreement with results for a wide variety of physical, chemical and biological endpoints and provide preliminary evidence that tributary impacts can cascade up from aquatic to terrestrial food webs.

On the Stillaguamish River, tributaries are a strong predictor of spawning behaviour at multiple spatial scales (see also Beechie *et al.*, in press). Tributaries appear particularly important during low-flow years, when low water or higher temperatures may constrain the areas in which salmon spawn. Tributaries might serve other functions for spawners, for example by providing gravel substrate, although we could not evaluate these effects in this case study. Similarly, the provision of particular mixes of trace elements by tributaries might serve as olfactory signposts for salmon homing for natal spawning grounds. However, the fact that we were able to detect flow-dependent patterns indicates that signposts are likely facultative.

Together, these results support the hypothesis that in the PNW basal productivity (defined here as nutrient levels, algal and insect colonization) is higher close to confluences than at sites further away. Elevated abundances of fish and birds close to confluences support the suggestion that this impact can affect the reach-scale distribution of animals in higher trophic levels. There is also some evidence (in elevated bird abundances) that the influence of tributaries extends into the terrestrial environment. Moreover, the importance of tributaries for the main-stem distribution of Chinook spawning sites highlights the importance of tributaries and confluences for maintaining the integrity of high-level ecosystem services in river networks, especially during low-flow years.

## Conclusion

We have presented a review of earlier work and new data from field studies in western Washington which suggests that, by supplying sediment, water and wood as well as essential nutrients and food resources, tributary streams can influence the habitat complexity, biodiversity and productivity of main-stem rivers. Geomorphologists have

long recognized the physical changes associated with tributary confluences; however, we show that these physical changes can be associated with ecological changes. At local scales, tributary junctions might be ecologically important and even act as biodiversity hotspots because they are sites where: supplemental nutrients and energy are supplied, the juxtaposition of distinctive environments enhance particular ecological processes (such as refugia use), water quality, hydraulics and channel morphology are atypical and there is enhanced environmental heterogeneity. At larger scales, confluences are locations where water-borne tributary inputs and main-stem geomorphological adjustments are most acute. Confluences are therefore important sites of longitudinal discontinuity that contribute to the landscape-scale structure of lotic ecosystems. In the context of emerging theories that emphasize the ecological relevance of whole-network architecture, particularly the hierarchical branching topology of stream systems, the number and distribution of confluence nodes appears to be important for a variety of processes, including interspecific interactions (e.g. predator–prey relationships), population dispersal and food availability (Power and Dietrich, 2002; Grant *et al.*, 2007; Muneeppeerakul *et al.*, 2007).

Notwithstanding the convincing field evidence and modelling results that support these arguments, empirical data are scarce and our understanding of key mechanisms remains inadequate. Reasons for this include the difficulty of obtaining data over large spatial scales, a paucity of testable hypotheses and the interdisciplinary nature of the topic. Looking forward, there are two key areas where progress is required. These requirements complement the call from those working at network scales for continued field research to address a number of key issues in that area (Lowe *et al.*, 2006b; Grant *et al.*, 2007).

First, there is an urgent need for additional empirical work to evaluate the abundance, spatial distribution and landscape-scale controls of tributary effects (both within individual drainage systems and between regions). For example, although the numerical-modelling work reviewed here indicates that the relative quantity and character of the sediment supplied by a tributary are crucial controls on physical and thence biotic diversity at confluences, data to test the hypotheses generated by this modelling are not available (Rice *et al.*, 2006). Similarly, the case study presented here adds to a growing body of work which suggests that tributaries are important for river ecology in the PNW (Rice *et al.*, 2001a, 2001b; Benda *et al.*, 2004; Kiffney *et al.*, 2006; Bigelow *et al.*, 2007), additional studies are needed to evaluate the importance of tributaries in other regions where landscape, land-use, seasonality, vegetation, climate and geology are different.

Second, the extensive studies required to address these questions should be supported by intensive work that seeks to develop a fuller understanding of the mechanisms that underlie confluence effects. Most work to date has demonstrated associations between tributaries and ecological phenomena and offered reasonable explanations for them, but there have been relatively few attempts to isolate key processes and examine them in detail. For example, the case study from Washington indicates the potential for tributary

influence to extend into high trophic levels, across the terrestrial–aquatic interface and into high-order ecosystem services. Water-temperature changes, tributary nutrient loading and the consequent cascade of energy all appear to be important factors that help to explain these observations, but we can only speculate about the details of these relationships and the extent to which other processes might be relevant.

River confluences are just one example of the important connections that characterize river networks, and further research is needed to determine the relative importance of this connection within the broader context of river basins. Other examples include lake inlets and outlets, wetland connections to lakes or streams, hyporheic connections across the river corridor, river bifurcations in deltas and the transition from non-tidal to estuarine environments. Lateral connections are also a critical component of habitat heterogeneity within river basins (e.g. between channels and their floodplains) contributing to overall river biodiversity and ecosystem function (Malard *et al.*, 2006). Our arguments about the importance of tributary confluences support the general proposition that maintaining the ecological function of such connections and adopting a network-scale perspective are critical for maintaining biological diversity and sustaining ecosystem services.

## Acknowledgements

The numerical modelling was supported by NERC grants NER/A/S2000/01199, 01384 and 01385 to Rice, Ferguson and Hoey. The Northwest Fisheries Science Centre and the Earthwatch Institute provided support for the tributary junction survey work, while the NOAA-Smith College internship programme provided a number of excellent interns. Greene and Kiffney also thank the numerous Earthwatch volunteers who tirelessly helped collect the data. We especially thank J. Hall for his efforts. We would like to thank the Tulalip Tribe, the Stillaguamish Tribe and the Washington Department of Fish and Wildlife for their assistance in the collection of salmonid habitat data and for the use of salmonid redd data in the Stillaguamish River Basin.

## References

- Allen PM, Hobbs R. 1989. Downstream impacts of a dam on a bedrock fluvial system, Brazos River, central Texas. *Bulletin of the Association of Engineering Geologists* **26**: 165–189.
- Andrews ED. 1986. Downstream effects of Flaming Forge Reservoir on the Green River, Colorado and Utah. *Geological Society of America Bulletin* **97**: 1012–1023.
- Beechie T, Moir HJ, Pess G. In press. Hierarchical physical controls on salmonid reproductive biology. In *Physical Factors Affecting Salmon Spawning and Egg Survival to Emergence: Integrating Science and Remediation Management*, DeVries P, Sear D (eds). American Fisheries Society: Bethesda, Maryland.

- Benda L, Poff NL, Miller D, Dunne T, Reeves G, Pess G, Pollock M. 2004. The Network Dynamics Hypothesis: How channel networks structure riverine habitats. *BioScience* **54**: 413–427.
- Bigelow PE, Benda LE, Miller DJ, Burnett KM. 2007. On debris flows, river networks, and the spatial structure of channel morphology. *Forest Science* **53**: 220–238.
- Braaten PJ, Guy CS. 1999. Relations between physicochemical factors and abundance of fishes in tributary confluences of the lower channelized Missouri River. *Transactions of the American Fisheries Society* **128**: 1213–1221.
- Bramblett RG, Bryant MD, Wright BE, White RG. 2002. Seasonal use of small tributary and main-stem habitats by juvenile steelhead, coho salmon, and Dolly Varden in a southeastern Alaska drainage basin. *Transactions of the American Fisheries Society* **131**: 498–506.
- Bravard J, Gilvear DJ. 1996. Hydrological and geomorphological structure of hydrosystems. In *Fluvial Hydrosystems*, Petts GE, Amoros C (eds). Chapman and Hall: London; 98–116.
- Brown DJ, Coon TG. 1994. Abundance and assemblage structure of fish larvae in the lower Missouri River and its tributaries. *Transactions of the American Fisheries Society* **123**: 718–732.
- Bruns DA, Minshall GW, Cushing CE, Cummins KW, Brock JT, Vannote RL. 1984. Tributaries as modifiers of the river continuum concept: Analysis by polar ordination and regression models. *Archiv fur Hydrobiologie* **99**: 208–220.
- Cairns MA, Ebersole JL, Baker JP, Wigington PJ, Lavigne HR, Davis JA. 2005. Influence of summer stream temperatures on black spot infestation of juvenile Coho salmon in the Oregon Coast Range. *Transactions of the American Fisheries Society* **134**: 1471–1479.
- Cianficconi F, Pirisinu Q, Tucciarelli F. 1991. Ecological influence of the tributaries on the macrobenthos in the Umbrian Tiber River (1974–75). *Archiv Fur Hydrobiologie* **122**: 229–244.
- Erskine WD, Terrazzolo N, Warner RF. 1999. River rehabilitation from the hydrogeomorphic impacts of a large hydro-electric power project: Snowy River, Australia. *Regulated Rivers: Research and Management* **15**: 3–24.
- Fagan WF. 2002. Connectivity, fragmentation, and extinction risk in dendritic metapopulations. *Ecology* **83**: 3243–3249.
- Fernandes CC, Podos J, Lundberg JG. 2004. Amazonian ecology: Tributaries enhance the diversity of electric fishes. *Science* **305**: 1960–1962.
- Fisher SG. 1997. Creativity, idea generation, and the functional morphology of streams. *Journal of the North American Benthological Society* **16**: 305–318.
- Fisher SG, Sponseller RA, Heffernan JB. 2004. Horizons in stream biogeochemistry: Flowpaths to progress. *Ecology* **85**: 2369–2379.
- Franks CA, Rice SP, Wood PJ. 2002. Hydraulic habitat in confluences: An ecological perspective on confluence hydraulics. In *The Structure, Function and Management Implications of Fluvial Sedimentary Systems*, Dyer FJ, Thoms MC, Olley JM (eds). International Association Hydrological Sciences Publication 276: Wallingford, UK; 61–67.
- Fraser DE, Gilliam JE, Yip-Hoi T. 1995. Predation as an agent of population fragmentation in a tropical watershed. *Ecology* **76**: 1461–1472.
- Geist D. 2000. Hyporheic discharge of river water into fall chinook salmon (*Oncorhynchus tshawytscha*) spawning areas in the Hanford Reach, Columbia River. *Canadian Journal of Fisheries and Aquatic Sciences* **57**: 1647–1656.
- Godreau V, Bornette G, Frochot B, Amoros C, Castella E, Oertli B, Chambaud F, Oberti D, Craney E. 1999. Biodiversity in the floodplain of Saone: A global approach. *Biodiversity and Conservation* **8**: 839–864.

- Grant EHC, Lowe WH, Fagan WF. 2007. Living in the branches: Population dynamics and ecological processes in dendritic networks. *Ecology Letters* **10**: 165–175.
- Greenwood MT, Bickerton MA, Gurnell AM, Petts GE. 1999. Channel changes and invertebrate faunas below Nant-y-Moch dam, River Rheidol, Wales, UK: 35 years on. *Regulated Rivers: Research and Management* **15**: 99–112.
- Grenouillet G, Pont D, Herisse C. 2004. Within-basin fish assemblage structure: The relative influence of habitat versus stream spatial position on local species richness. *Canadian Journal of Fisheries and Aquatic Sciences* **61**: 93–102.
- Hahn P, Kraemer C, Hendrick D, Castle P, Wood L. 2001. *Washington state chinook salmon spawning escapement assessment in the Stillaguamish and Skagit Rivers, 1998*. Washington Department of Fish and Game; 165pp.
- Healey MC. 1991. Life history of Chinook salmon (*Oncorhynchus tshawytscha*). In *Pacific Salmon Life Histories*, Groot C, Margolis, L (eds). University of British Columbia Press: Vancouver, British Columbia; 311–394.
- Hill WR, Ryon MG, Schilling EM. 1995. Light limitation in a stream ecosystem: Responses by primary producers and consumers. *Ecology* **76**: 1297–1309.
- Hill WR, Mulholland PJ, Marzolf ER. 2001. Stream ecosystem responses to forest leaf emergence in spring. *Ecology* **82**: 2306–2319.
- Illies J. 1953. Die Besiedlung der Fulda (insbes. das Benthos der Salmonidenregion) nach dem jetzigen Stand der Untersuchung. *Ber.Limnol.Flussstat.Freudenthal* **5**: 1–28.
- Kaeding LR. 1996. Summer use of coolwater tributaries of a geothermally heated stream by rainbow and brown trout, *Oncorhynchus mykiss* and *Salmo trutta*. *American Midland Naturalist* **135**: 283–292.
- Kaufmann PR. 2002. Physical habitat characterization. In *Environmental Monitoring and Assessment Program – Surface Waters: Western Pilot Study Field Operations Manual for Wadeable Streams*, Jackson WL, Lazorchak JM, Klemm DJ (eds). US Environmental Protection Agency: Washington, DC; 103–160.
- Kiffney PM, Richardson JS. 2001. Effects of nutrient enrichment on periphyton and vertebrate (*Ascapus truei*) and invertebrate grazers in experimental channels. *Copeia* **422**–429.
- Kiffney PM, Volk CJ, Hall J. 2002. *Community and ecosystem attributes of the Cedar River and tributaries before arrival of anadromous salmonids*. Technical report submitted to Seattle Public Utilities. NMFS – Watershed Program: Seattle, WA.
- Kiffney PM, Richardson JS, Bull JP. 2003. Responses of periphyton and insects to experimental manipulation of riparian buffer width along forest streams. *Journal of Applied Ecology* **40**: 1060–1076.
- Kiffney PM, Richardson JS, Bull JP. 2004. Establishing light as a causal mechanism structuring stream communities in response to experimental manipulation of riparian buffer width. *Journal of the North American Benthological Society* **23**: 542–555.
- Kiffney PM, Greene C, Hall J, Davies J. 2006. Gradients in habitat heterogeneity, productivity, and diversity at tributary junctions. *Canadian Journal of Fisheries and Aquatic Sciences* **63**: 2518–2530.
- Killeen IJ, McFarland B. 2004. The distribution and ecology of *Gyraulus acronicus* (Ferussac, 1807) (Gastropoda : Planorbidae) in England. *Journal of Conchology* **38**: 441–456.
- Knispel S, Castella E. 2003. Disruption of a longitudinal pattern in environmental factors and benthic fauna by a glacial tributary. *Freshwater Biology* **48**: 604–618.

- Kreb D, Budiono YK. 2005. Conservation management of small core areas: Key to survival of a critically endangered population of Irrawaddy river dolphins *Orcaella brevirostris* in Indonesia. *Oryx* **39**: 178–188.
- Kupferberg SJ. 1996. Hydrologic and geomorphic factors affecting conservation of a river-breeding frog (*Rana boylii*). *Ecological Applications* **6**: 1332–1344.
- Leatherwood S, Reeves RR, Wuersig B, Shearn D. 2000. Habitat preferences of river dolphins in the Peruvian Amazon. In *Biology and Conservation of Freshwater Cetaceans in Asia*, Reeves RR, Smith BD, Kasuya T (eds). Occasional papers of the IUCN Species Survival Commission 23. IUCN: Gland, Switzerland; 131–144.
- Lowe WH, Likens GE, McPeck MA, Bussers JC. 2006a. Linking direct and indirect data on dispersal: Isolation by slope in a headwater stream salamander. *Ecology* **87**: 334–339.
- Lowe WH, Likens GE, Power ME. 2006b. Linking scales in stream ecology. *Bioscience* **56**: 591–597.
- MacArthur R, MacArthur JW. 1961. On bird-species diversity. *Ecology* **42**: 594–598.
- Malard F, Uehlinger U, Zah R, Tockner K. 2006. Flood pulses and riverscape dynamics in a braided glacial river. *Ecology* **87**: 704–716.
- Margolis BE, Castro MS, Raesly RL. 2001. The impact of beaver impoundments on the water chemistry of two Appalachian streams. *Canadian Journal of Fisheries and Aquatic Sciences* **58**: 2271–2283.
- Mattingly HT, Galat DL. 2002. Distributional patterns of the threatened Niangua darter, *Etheostoma nianguae*, at three spatial scales, with implications for species conservation. *Copeia* 573–585.
- McClain ME, Boyer EW, Dent CL, Gergel SE, Grimm NB, Groffman PM, Hart SC, Harvey JW, Johnston CA, Mayorga E, McDowell WH, Pinay G. 2003. Biogeochemical hotspots and hot moments at the interface of terrestrial and aquatic ecosystems. *Ecosystems* **6**: 301–312.
- McGuire TL, Winemiller KO. 1998. Occurrence patterns, habitat associations, and potential prey of the river dolphin, *Inia geoffrensis*, in the Cinaruco river, Venezuela. *Biotropica* **30**: 625–638.
- Meybeck M. 2003. Global analysis of river systems: From Earth system controls to Anthropocene syndromes. *Proceedings Royal Society of London B* **358**: 1935–1955.
- Milner AM, Petts GE. 1994. Glacial rivers: Physical habitat and ecology. *Freshwater Biology* **32**: 295–307.
- Minshall GM, Cummins KW, Petersen RC, Cushing CE, Bruns DA, Sedell JR, Vannote RL. 1985. Developments in stream ecosystem theory. *Canadian Journal of Fisheries and Aquatic Sciences* **42**: 1045–1055.
- Montgomery DR, Beamer EM, Pess GR, Quinn TP. 1999. Channel type and salmonid spawning distribution and abundance. *Canadian Journal of Fisheries and Aquatic Sciences* **56**: 377–387.
- Muneepeerakul R, Weitz JS, Levin SA, Rinaldo A, Rodriguez-Iturbe I. 2007. A neutral metapopulation model of biodiversity in river networks. *Journal of Theoretical Biology* **245**: 351–363.
- Naiman RJ, Bilby RE. 1998. River ecology and management in the Pacific Coastal Ecoregion. In *River Ecology and Management*, Naiman RJ and Bilby RE (eds). Springer-Verlag: New York: 1–12.
- Nakamoto RJ. 1994. Characteristics of pools used by adult summer steelhead overwintering in the New River, California. *Transactions of the American Fisheries Society* **123**: 757–765.
- Osborne LL, Wiley MJ. 1992. Influence of tributary spatial position on the structure of warmwater fish communities. *Canadian Journal of Fisheries and Aquatic Sciences* **49**: 671–681.

- Perry JA, Schaeffer DJ. 1987. The longitudinal distribution of riverine benthos: A river discontinuum? *Hydrobiologia* **148**: 257–268.
- Petersen BJ, Wollheim WM, Mulholland PJ, Webster JR, Meyer JL, Tank JL, Martí E, Bowden WB, Valett HM, Hershey AE, McDowell WH, Dodds WK, Hamilton SK, Gregory S, Morrall DD. 2001. Control of nitrogen export from watersheds by headwater streams. *Science* **292**: 86–90.
- Petts GE. 1984. *Impounded Rivers: Perspectives for ecological management*. John Wiley & Sons: Chichester.
- Petts GE, Greenwood M. 1985. Channel changes and invertebrate faunas below Nant-y-Moch dam, River Rheidol, Wales, UK. *Hydrobiologia* **122**: 65–80.
- Pollock M, Beechie T, Jordan C. 2007. Geomorphic changes upstream of beaver dams in Bridge Creek, an incised stream in the interior Columbia River basin, eastern Oregon. *Earth Surface Processes and Landforms* **32**: 1174–1185.
- Pollux BJA, Korosi A, Verberk WCEP, Pollux PMJ, van der Velde G. 2006. Reproduction, growth, and migration of fishes in a regulated lowland tributary: Potential recruitment to the river Meuse. *Hydrobiologia* **565**: 105–120.
- Poole GC. 2002. Fluvial landscape ecology: Addressing uniqueness within the river discontinuum. *Freshwater Biology* **47**: 641–660.
- Power ME, Dietrich WE. 2002. Food webs in river networks. *Ecological Research* **17**: 451–471.
- Power ME, Brozovič N, Bode C, Zilberman D. 2005. Spatially explicit tools for understanding and sustaining inland water ecosystems. *Frontiers in Ecology and the Environment* **3**: 47–55.
- Rice SP, Greenwood MT, Joyce CB. 2001a. Tributaries, sediment sources and the longitudinal organisation of macroinvertebrate fauna along river systems. *Canadian Journal of Fisheries and Aquatic Sciences* **58**: 824–840.
- Rice SP, Greenwood MT, Joyce CB. 2001b. Macroinvertebrate community changes at coarse-sediment recruitment points along two gravel-bed rivers. *Water Resources Research* **37**: 2793–2803.
- Rice SP, Ferguson RI, Hoey T. 2006. Tributary control of physical heterogeneity and biological diversity at river confluences. *Canadian Journal of Fisheries and Aquatic Sciences* **63**: 2553–2566.
- Richards C, Johnson LB, Host GE. 1996. Landscape-scale influences on stream habitats and biota. *Canadian Journal of Fisheries and Aquatic Sciences* **53**: 295–311.
- Sato Y, Bazzoli N, Rizzo E, Boschi MB, Miranda MOT. 2005. Influence of the Abaete River on the reproductive success of the neotropical migratory teleost *Prochilodus argenteus* in the Sao Francisco River, downstream from the Tres Marias Dam, southeastern Brazil. *River Research and Applications* **21**: 939–950.
- Sear DA. 1995. Morphological and sedimentological changes in a gravel-bed river following 12 years of flow regulation for hydropower. *Regulated Rivers: Research and Management* **10**: 247–264.
- Scrivener JC, Brown TG, Andersen BC. 1994. Juvenile chinook salmon (*Oncorhynchus tshawytscha*) utilization of Hawks Creek, a small and non-natal tributary of the upper Fraser River. *Canadian Journal of Fisheries and Aquatic Sciences* **51**: 1139–1146.
- Smith TA, Kraft CE. 2005. Stream fish assemblages in relation to landscape position and local habitat variables. *Transactions of the American Fisheries Society* **134**: 430–440.
- Steel EA, Feist BE, Jensen DW, Pess GR, Sheer MB, Brauner JB, Bilby RE. 2004. Landscape models to understand steelhead (*Oncorhynchus mykiss*) distribution and help prioritize barrier

- removals in the Willamette basin, Oregon, USA. *Canadian Journal of Fisheries and Aquatic Sciences* **61**: 999–1011.
- Stevens LE, Shannon JP, Blinn DW. 1997. Colorado River benthic ecology in Grand Canyon, Arizona, USA: Dam, tributary and geomorphological influences. *Regulated Rivers: Research and Management* **13**: 129–149.
- Storey AW, Edward DH, Gazey P. 1991. Recovery of aquatic macroinvertebrate assemblages downstream of Canning Dam, Western Australia. *Regulated Rivers: Research and Management* **6**: 213–224.
- Thorp JH, Thoms MC, Delong MD. 2006. The riverine ecosystem synthesis: Biocomplexity in river networks across space and time. *River Research and Applications* **22**: 123–147.
- Torgersen CE, Price DM, Li HW, McIntosh BA. 1999. Multiscale thermal refugia and stream habitat associations of Chinook salmon in northeastern Oregon. *Ecological Applications* **9**: 301–319.
- Vannote RL, Minshall GW, Cummins KW, Sedell JR, Cushing CE. 1980. The River Continuum Concept. *Canadian Journal of Fisheries and Aquatic Sciences* **37**: 130–137.
- Vinson MR. 2001. Long-term dynamics of an invertebrate assemblage downstream from a large dam. *Ecological Applications* **11**: 711–730.
- Volk CJ. 2004. *Nutrient and biological responses to red alder (Alnus rubra) presence along headwater streams: Olympic Peninsula, Washington*, Ph.D thesis, University of Washington.
- Volk CJ, Kiffney PM, Edmonds RL. 2003. Role of riparian red alder (*Alnus rubra*) in the nutrient dynamics of coastal streams of the Olympic Peninsula, WA, USA. *American Fisheries Society Special Publication* **34**: 213–228.
- Ward JV, Stanford JA. 1983. The serial discontinuity concept of lotic ecosystems. In *Dynamics of Lotic Ecosystems*, Fontaine TD, Bartell SM (eds). Ann Arbor Science: Ann Arbor, Michigan; 29–42.
- Ward JV, Stanford JA. 1995. The serial discontinuity concept: Extending the model to floodplain rivers. *Regulated Rivers: Research and Management* **10**: 159–168.
- Wiens JA. 2002. Riverine landscapes: Taking landscape ecology into the water. *Freshwater Biology* **47**: 501–515.
- Wipfli MS, Gregovich DP. 2002. Export of invertebrates and detritus from fishless headwater streams in southeastern Alaska: Implications for downstream salmonid production. *Freshwater Biology* **47**: 957–969.
- Zhang X, Wang D, Liu R, Wei Z, Hua Y, Wang Y, Chen Z, Wang L. 2003. The Yangtze River dolphin or baiji (*Lipotes vexillifer*): Population status and conservation issues in the Yangtze River, China. *Aquatic Conservation-Marine and Freshwater Ecosystems* **13**: 51–64.

# 12

## Tributaries and the management of main-stem geomorphology

**Frédéric Liébault<sup>1</sup>, Hervé Piégay<sup>2</sup>, Philippe Frey<sup>1</sup> and Norbert Landon<sup>3</sup>**

<sup>1</sup>*Cemagref Groupement de Grenoble, Unité de Recherche ETNA (Erosion Torrentielle, Neige et Avalanches), France*

<sup>2</sup>*Université de Lyon, UMR 5600 CNRS, Site ENS-LSH, Plateforme ISIG, France*

<sup>3</sup>*Université de Lyon, UMR 5600 CNRS, Site Université Lumière – Lyon 2, Institut de Recherche en Géographie, France*

### Introduction

The sustainable management of river channels cannot be achieved without a catchment-scale approach in which management strategies avoid actions that may be cancelled by network-scale interactions. Recognizing and understanding the influence of tributaries on physical dynamics in the recipient channel is, therefore, important. Conceptually, tributaries may be considered as 'source sites', where management actions designed to alter sediment and/or water regimes can be implemented with the aim of restoring or preserving main-stem physical processes. Tributaries are major physical links between hillslopes and the main stem, so that when planning any basin-scale management scheme (e.g. soil-conservation programmes for sediment-transport regulation)

it is also important to understand their sediment-routing properties. River management financial budgets are often tight and it is usually necessary to maximize returns on a limited investment. The identification of the key tributaries, in terms of their source and routing characteristics, may then be very useful at network scales, for example in targeting erosion-control works to particular tributary basins and thereby saving substantial funds.

Regulating low-order streams to promote the sustainable management of the recipient river channels downstream requires a robust understanding of the geomorphic processes that govern tributary impacts. These impacts are driven by water and sediment supply. Their magnitude will depend on the abundance of these outputs, but also on the water and sediment regime in the recipient channel, which can be in equilibrium, supply-limited or transport-limited, and on the relative nature of the delivered sediment (grain-size distribution, resistance to abrasion and clast shape) (Ferguson *et al.*, 2006). The geomorphic impact of tributaries thus implies a comparison of tributary and main-stem regimes and physical attributes (Benda *et al.*, 2004). Depending on these boundary conditions and fluxes, the geomorphic impact may be significant or insignificant. Significant impacts from tributaries will reinforce or reverse the morphological and sedimentary trends of the recipient channel. Several examples document channel aggradation following dramatic sediment supply events from tributaries (Pitlick, 1993; Benito *et al.*, 1998; Brierley and Fryirs, 1999; Gomez *et al.*, 2003). It is also recognized that channel degradation can be induced or aggravated by reductions in sediment supply from tributaries (Wyzga, 1991; Landon *et al.*, 1998; Rinaldi and Simon, 1998; Liébault *et al.*, 1999). Tributary impacts on the size and composition of river-bed sediments is also well known (Knighton, 1980; Rice, 1998; Pitlick and Cress, 2002; Surian, 2002). The disruption of downstream fining by the tributary-induced coarsening of bed-material is the most common effect (Rice and Church, 1998).

These geomorphic impacts may have positive or negative effects on main-stem ecological conditions and flooding risk, two issues of primary concern for contemporary river management. Excessive channel aggradation may provoke a loss of habitat diversity that can affect biological communities, as in the case of sediment slugs originating from destabilized tributaries (Bartley and Rutherford, 2005). Conversely, it has been shown that fish habitats may be improved downstream of tributary junctions that deliver bed-load to the main stem and sustain braided reaches (Piégay *et al.*, 2000; see Rice *et al.*, Chapter 11, this volume, for further examples). Changes in bed-material affect hydraulic conditions by modifying the bed roughness and subsequently hydro-ecological conditions (i.e. modification of flow depth and velocity distributions). Tributary-induced discontinuities in main-stem morphology and grain size may lead to a greater physical diversity that is positive in terms of biological diversity (Rice *et al.*, 2001). The role of low-order tributaries as sources of large woody debris may be important in this regard (Benda *et al.*, 2003). When sediment inputs from tributaries decline, there may be negative impacts. For example, in sediment-starved river basins, channel incision can have

negative ecological impacts on riparian forests and in-channel biological communities (Bravard *et al.*, 1997). Main-stem flood risk can be amplified by tributary impacts. This is particularly the case in upland environments where sediment deposition from debris flows or extreme floods in low-order mountain streams may create obstructions in the recipient channel (Lahousse and Romelé, 2000) sometimes forming temporary lakes that empty catastrophically (Marnezy, 1993).

The objectives of this paper are (1) to present a conceptual framework for evaluating the geomorphic impacts from tributaries, with special emphasis on management issues at different linked scales (main-stem–tributary and network scales, the confluence scale being addressed in Ettema, Chapter 6, this volume) and (2) to illustrate this theoretical framework with some case studies of the management approaches adopted in the Drôme River basin in the Southern French Prealps.

## **A conceptual framework for assessing the geomorphological impact of tributaries and their importance for main-stem management**

### **General considerations**

Within a theoretical context of uniform rainfall and geology, it is possible to have a simple gradient of main-channel properties from upstream to downstream under the control of network architecture, basin relief and shape. In this context, the relief controls the channel gradients and the energy available for bedload transport and morphological adjustment. However, in reality, because of differences in geology and hydrology, each sub-catchment has its own sensitivity and critical thresholds to change, and also its own temporal behaviour and adjustment duration to a given flood event. Thus, even where human impacts (including intentional management strategies) are homogeneous in space and time across a given catchment (e.g. widespread deforestation and pasture development), we can expect variable tributary reactions, according to variable natural conditions.

The main geomorphic processes of main-stem adjustment to tributary impact are incision, with progressive erosion spreading through the stream network, and aggradation, with sediment wave propagation downstream. Key issues are the time taken for adjustment, the duration of the propagation of the effects downstream and upstream and the attenuation of these effects from the impact site to other locations. Remote impacts may occur several decades after the initial cause, and as a result their intensity may be much lower than at the impact point some distance away.

In a catchment, the main-channel geometry is the result of cumulative interactions between its upstream branches and their associated sub-catchments. Tributaries are sensitive to human actions and their changes may propagate downstream. In the Yzeron

catchment near Lyon, in south-east France, urbanization has generated higher peak flows that have subsequently caused widespread channel degradation of the tributary network and aggradation in the main stem, where sand waves have disrupted fish habitat (Grosprêtre and Schmitt, 2006). Tributaries are the first affected by land-use changes, and thus can be indicators of future changes on the main channel. Tributaries can also be affected by changes in the main stem through an adjustment to local base level, as in the central Mississippi in the United States, where main-stem straightening induced regressive erosion in tributary rivers (see Schumm *et al.*, 1984; Simon and Hupp, 1986).

## Assessing the geomorphic impact of tributaries

Basin-scale approaches for managing tributary impact are of particular relevance when disturbances (e.g. channel degradation, aggradation or bank erosion) are expanding along most of the main-stem channel. In such a situation, it may be useful to regulate the water and sediment supplied by tributary sub-basins. It is first important to evaluate whether tributaries are an important part of the problem by understanding the overall magnitude of the tributary impact. In turn, it is important to understand which tributaries trigger the most significant impacts. The answer to the first question requires an evaluation of the relative influence of tributaries on the main-stem response, as compared to other potential forcings of the fluvial system. The answer to the second question requires a comparative analysis of tributaries, ideally coupled to analysis of the main-stem disruption.

## Understanding geomorphological adjustments

For retrospective analysis, the effects of past disturbances can be assessed using data and information from various sources, including existing images and maps, and field evidence. Changes in tributary morphology can also be highlighted from field surveys that focus on present-day processes and adjustment stages. In this context, the geographical comparison of tributaries is a meaningful tool for identifying critical factors and understanding ongoing geomorphological adjustments. Retrospective analyses of changes in sediment supply can reveal the sediment regime within tributary channels. For example, Liébault (2005) uses the date of tree establishment along the Sure Torrent, a tributary to the Drôme River, to demonstrate the downstream propagation of channel incision due to a decrease in bedload delivery.

In the case of Pine Creek, Idaho, we used historical photos to characterize channel widening in the tributaries and the main stem, as well as archive data to identify the potential factors affecting the sediment supply and channel resistance to mining activity

and deforestation (Kondolf *et al.*, 2002). By comparing a catchment unaffected by mining with affected catchments, we demonstrated that mining activity resulted in a much larger channel response than deforestation (Figure 12.1(A) and (B)). This approach also showed that some tributaries have already recovered and exhibit channel widths similar to those before the impact, while other tributaries are still reacting to the impact. There is an asymmetry in the evolution of the channel system, with an immediate widening (within 10 years) but a slow process of recovery (50 years at least).

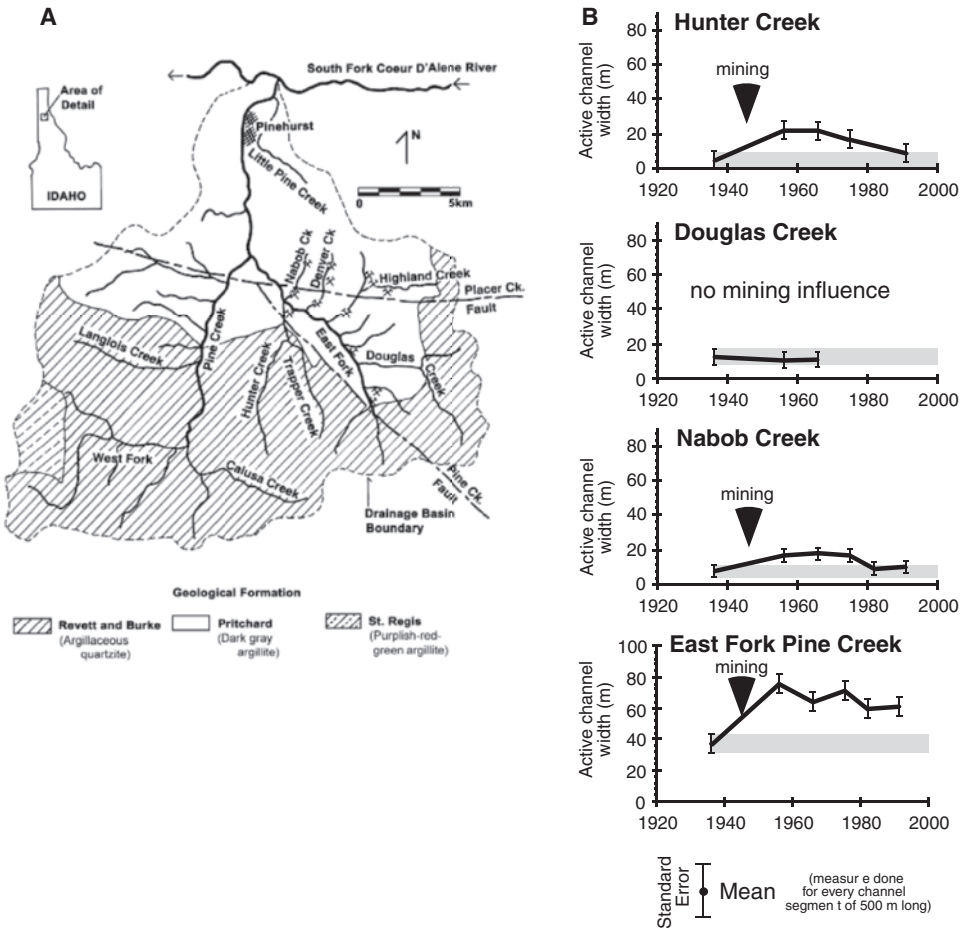


**Figure 12.1** (A) Location map of Pine Creek catchment in Idaho, showing major tributaries and generalized geology. Pick-and-shovel symbols denote mines, the largest of which were located along eastern tributaries to the East Fork. Geology based on Jones (1919), mine locations from Mitchell (1996). (B) Changes over time in unvegetated, active channel width for East Fork Pine Creek and its tributaries, as measured from aerial photographs. Error bars are based on precision of aerial-photo measurements (reprinted from Kondolf *et al.*, 2002, with permission from Elsevier).

Another catchment scale approach was used in the Eygues River basin (south-east France), where tributaries are adjusting to catchment reforestation linked to rural depopulation (Liébault *et al.*, 2002). Active channel narrowing and incision has propagated through the drainage network in response to a decrease in sediment supply. Aerial photographs were used to characterize the spatial variability of this channel narrowing within tributary sub-basins for the 1948–1996 period (Figure 12.2(A)). The spatial pattern of the sub-basin response is complex, suggesting heterogeneous land-use changes and catchment controls on the geomorphic response of individual tributaries. We used normalized Principal Component Analysis (Figure 12.2(B)) to develop a model

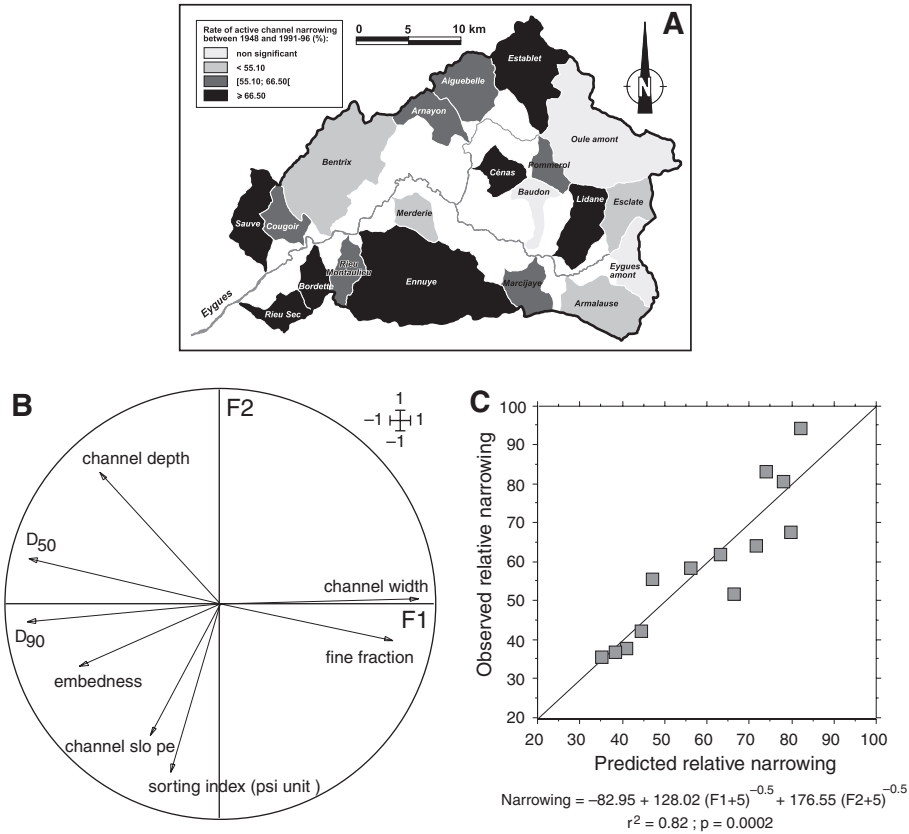


**Figure 12.2** Prediction of channel narrowing in tributary catchments of the Eygues River, south-east France from tributary grain-size and geometry characteristics: (A) the sub-basin variability in the rate of channel narrowing in the mountainous part of the Eygues basin; (B) projection of channel morphology variables on the first factorial map of a normalized PCA; (C) observations versus predictions of channel narrowing between 1945 and 1995 from the first two components of the PCA (modified from Clément and Piégay, 2003).

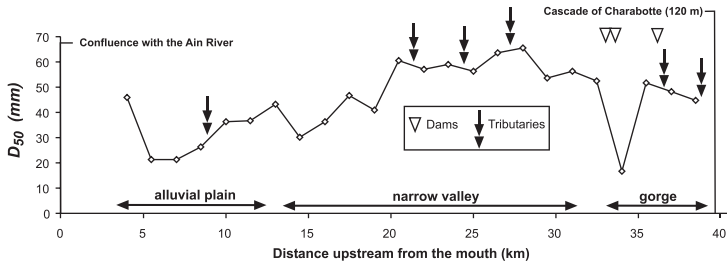
of channel narrowing that can be used to predict the magnitude of tributary response from present-day measurements of grain size and bankfull geometry. This may be useful for the identification of highly impacted tributaries at a regional scale. In turn, because the tributary incision generated sediment which moved off downstream, this may help to identify those tributaries that are most likely to have an impact on the geomorphological regime of the main stem.

## Identifying tributary impacts along the recipient channel

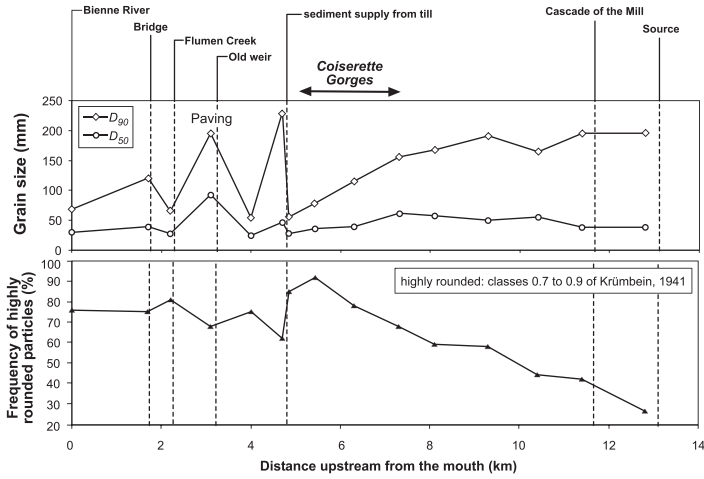
The longitudinal pattern of sedimentary characteristics can be used to evaluate the importance of individual tributaries relative to other sediment sources. Studies on the Albarine and Tacon Rivers, two tributaries to the Ain River in south-east France, illustrate this approach (Figure 12.3(A) and (B)). In the case of the Albarine (Figure 12.3(A)), two main  $D_{50}$  trends are observed along the river course. A coarsening is observed in the gorges between 29 and 40 km upstream. Downstream from the coarsest peak, the  $D_{50}$  decreases at a nearly constant rate. The short tributaries observed all along this reach have no effect on this trend, suggesting that their contribution is limited. In the Tacon example (Figure 12.3(B)), the morphology of the valley is important with fining in the gorge upstream, which is wooded and does not supply sediment to the main stem, and coarse peaks downstream associated with local supplies for example from a glacial deposit. In some cases, other sedimentary parameters, such as particle roundness, can be used to trace active sources (Figure 12.3(B)). Roundness analysis might be particularly useful where grain-size analysis is inconclusive because of factors other than sediment supply disrupting trends along the channel course. Along the Tacon (Figure 12.3(B)) grain-size decreases are associated with roundness increases which demonstrates the effects of abrasion during transport and the absence of additional sediment supply through the gorge. The supply of angular particles from adjacent glacial deposits is also clearly shown. In this case, it is clear that the combination of sedimentary parameters makes the interpretation more robust, although, once again, tributary streams are not important sediment sources for this river.

Lithology is also a useful indicator of tributary inputs when the geological settings are significantly different between sub-catchments. This approach has been used in the Ouvèze River, a right-side tributary to the Rhône draining areas of granite and basalt but crossing limestone, schists and marly environments. Trends in lithology along the Ouvèze (Figure 12.3(C)) show that there is a significant substitution of lithology from upstream to downstream. In the Mézayon catchment, cristallophilous rocks other than schists are dominant upstream and a consistent increase in schists is then observed downstream. In the Ouvèze branch, limestone dominates upstream whereas basalt introduced from the Bayonne Stream is observed downstream. Comparative analysis of the lithology downstream from the confluence of the Mézayon and the Upper Ouvèze

A) The Albarine, a tributary to the Ain River draining the southern Jura mountains



B) The Tacon, a tributary to the Biemme River, draining the northern Jura mountains



C) The Ouvèze River, a tributary to the Rhône River

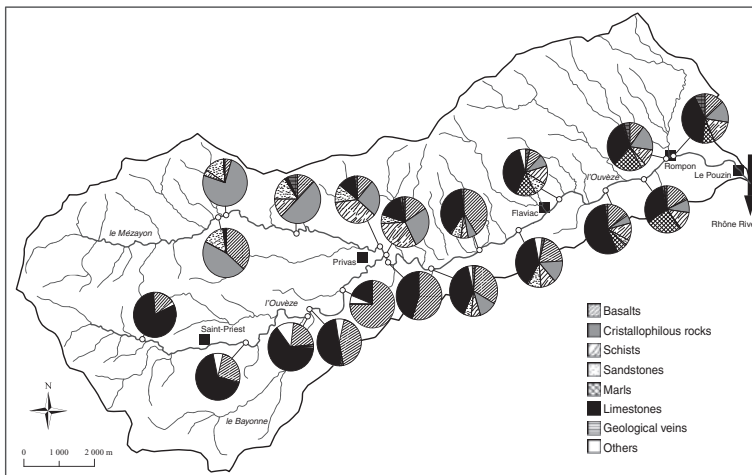


**Figure 12.3** (A) Downstream variation of  $D_{50}$  along the Albarine, a tributary to the Ain River in the Jura Mountains; (B) downstream variations of  $D_{50}$ ,  $D_{90}$  and frequency of highly rounded pebbles along the Tacon, a tributary to the Biemme River in the Jura Mountains; (C) lithological signature within a catchment, the case of the Ouvèze River: a tool for identifying the main tributary contributions to sediment downstream.

with upstream reaches reflects the different source-area contributions. The frequency of schists downstream from the confluence is low compared to the values observed along the Mézayon, but the frequency of the cristallophilous rocks and the sandstones are those expected if we assume an equal bedload contribution of the sub-basins. For other lithologies, the basalt frequency is similar to the frequency expected, but the limestone frequency is higher than expected. These different observations support the conclusion that the Ouvèze branch has a slightly higher contribution downstream than the Mézayon. Between Privas and Flaviac, the lithological signal is consistent, demonstrating the low contribution of sediment from the local tributaries. Marl, which is totally absent upstream from Flaviac, is then more frequent downstream, demonstrating the significant contribution of the most downstream tributaries to the lower Ouvèze.

## **Managing the geomorphological impact of tributaries: the case of the Drôme River, SE France**

The Drôme River is a gravel-bed river that drains 1680 km<sup>2</sup> of mainly marl and limestone terrains in the Southern French Prealps. Channel responses to changing sediment supply have been a management issue since the nineteenth century and contrasting efforts to regulate coarse-sediment inputs from tributaries have been implemented in the catchment. During the nineteenth century, the challenge was to act against the aggradation of a wide and active braided channel and the consequent increased flooding risk across the floodplain. This situation was triggered by accelerated erosion on hillslopes due to both climatic and anthropogenic forcing, the respective influence of both being an important research question (Bravard, 2002a; Liébault *et al.*, 2005). Conversely, since the 1990s, managers have been trying to stop accelerated channel incision induced by the cumulative impact of gravel mining, channel embankment, torrent-control works and catchment-scale reforestation (Landon *et al.*, 1998). In each of these contrasting geomorphic contexts, tributaries have been considered as source sites that may be manipulated to counter adverse conditions in the main stem. Research studies were conducted here (1) to assess the geomorphic impact of erosion-control works completed in tributaries for sediment-supply regulation and (2) to evaluate the bedload replenishment potential of tributaries for reversing channel degradation.

### **Channel aggradation and torrent-control works**

The Drôme River was an aggrading braided river during the nineteenth century. This is clearly illustrated in old pictures and maps, and can also be found in written accounts (Landon, 1999; Bravard, 2002b). This situation was the result of a very high sediment supply from deforested hillslopes that were destabilized by an increasing frequency of

high-rainfall events, in a period of high agricultural pressure. Land-use statistics from the beginning of the nineteenth century reveal that the forest cover occupied only ~30 per cent of the catchment, while the present-day value is ~70 per cent (Liébault, 2003). Accelerated erosion was not exclusive to the Drôme: most upland environments in France were affected. Laws were therefore enacted in 1860, 1862 and 1884 to implement an ambitious programme of soil conservation in French mountains, known as the RTM (*Restauration des Terrains en Montagne*, mountain land restoration) scheme. The planned reforestation of eroded hillslopes and construction of engineering works in active gullies and torrents were considered at that time as the best remedial strategy for reducing flooding and erosion risks that threatened the socio-economic development of mountain territories (Surell, 1841). The old French forest and water administration was then in charge of purchasing land highly degraded by erosion to implement reforestation, grazing and torrent-control works, including constructing check-dams in headwater channels.

In the Drôme River basin, records from the National Forest Office archives show that these works were mostly constructed between 1860 and 1914. Fifty-three RTM zones were delimited and purchased, within which 13 217 ha were reforested, mostly by planting exogenous black pine (*pinus nigra*), and 13 554 check-dams were constructed along tributaries (Liébault and Zahnd, 2001). Some complementary works were also carried out, including turfing, the construction of fascines and wattlings (small check-dams made of wood) and 'brush gully check' (use of brush mulch or fascines in gullies to aid in revegetation). Most of the main tributaries to the Drôme River were regulated by RTM works. Only one of the 25 main tributaries (drainage basin >10 km<sup>2</sup>) to the middle and upper Drôme has not been affected.

The evaluation of the geomorphic responses of tributaries and the main stem to RTM works was addressed by means of different approaches. Given the substantial spatial extent of RTM works in the Drôme catchment, it was not possible to conduct a representative comparative analysis of channel responses in the Drôme catchment alone. However, by enlarging the study area to include the Eygues and Roubion River basins, located south of the Drôme in the same physiographic environment, both regulated and non-regulated sub-basins could be examined.

A total of 51 sub-basins can be selected, nine of them being non-regulated. The comparison of geomorphic responses revealed that regulated and non-regulated tributaries experienced similar channel adjustments from the 1950s onward, namely active channel narrowing and incision (Liébault *et al.*, 2005). Unit rates of active channel narrowing (area of vegetated active channel between two dates divided by the length of the study reach) measured between 1948 and 1991 by means of aerial-photograph analysis are similar between regulated and non-regulated tributaries. A Mann-Whitney U-test revealed no significant difference of mean values ( $p = 0.4585$ ), which are 0.66 and 0.77 ha km<sup>-1</sup> for regulated and non-regulated tributaries respectively. On the basis of this result, we concluded that the geomorphic impact of RTM works likely occurred

in the first half of the twentieth century along tributary channels, a hypothesis that we cannot assess directly because the photographic archive begins in 1948.

A field survey conducted along the Archiane Torrent (86 km<sup>2</sup> drainage basin), a tributary to the Bez River in the upper part of the Drôme River basin, revealed that the 1950s active channel incised into a terrace, named T2, that may correspond to the braided channel prior to RTM works (Figure 12.4(A)). Dating of the older pioneer trees on the T2 terrace showed that the forest encroachment started between 1908 and 1921, according to the ages of the five oldest trees found in this level (Figure 12.4(B)). It is likely that the T2 terrace was formed by incision in response to the reduced sediment availability caused by the RTM works. According to the National Forest Office archives, 126 ha were reforested in the catchment, 645 fascines, 6698 wattlings and 892 cut-stone check-dams were built in active gullies and a length of 14 956 m of low-order channels were vegetated by brush gully check. Notwithstanding the importance of these interventions, the T2 terrace cannot be attributed solely to RTM works, as it also coincides with the end of the Little Ice Age, a period during which climatic-driven hillslope geomorphic processes were more frequent (Kotarba, 1997; Jomelli and Pech, 2004).

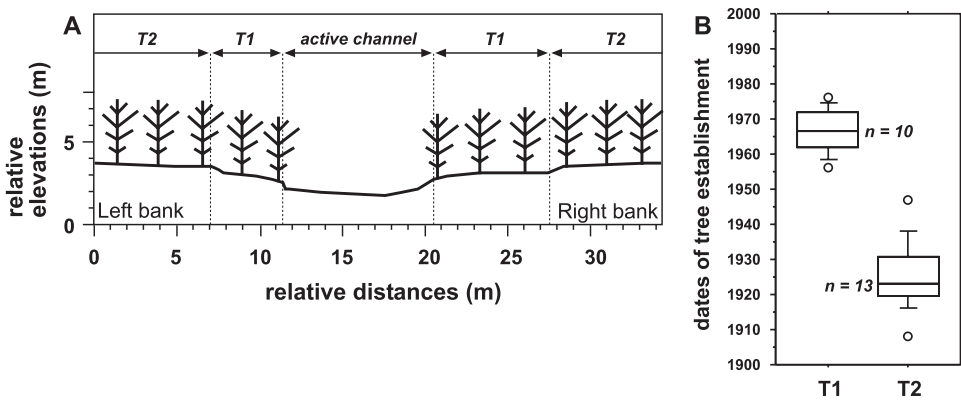


**Figure 12.4** Surveyed cross section of the Archiane Torrent showing two recent levels of forested terraces (A) and distributions of dates of forest establishment on T1 and T2 terraces based on dendrochronological dating (B); boxes represent upper and lower quartiles; vertical lines represent upper and lower tenths; open circles are extreme values; n is the number of dated trees.

To summarize, RTM works assisted by climatic changes induced a first phase of channel degradation and narrowing in tributaries at the beginning of the twentieth century. This may have sustained the sediment supply to the main stem by routing a substantial mass of sediment from the nineteenth-century braid plains of larger tributaries. The main-stem response to the RTM-induced decrease in sediment supply may therefore have been delayed and likely occurred during the second half of the twentieth

century, with some important chronological differences between reaches according to their position relative to the regulated tributaries.

In order to determine the spatial distribution of main-stem reaches that should have been highly affected by RTM works, a simple procedure of tributary-impact classification was performed. The RTM impact probability index ( $RIP_i$ ) was calculated for each tributary along the middle and upper Drôme River, upstream from Die:

$$RIP_i = \left( \frac{Ad_t}{Ad_m} \right) RTM, \quad (12.1)$$

where  $Ad_t$  is the drainage area of the tributary catchment,  $Ad_m$  is the drainage area of the main-stem catchment upstream from the confluence and  $RTM$  is the relative area of RTM zones in the tributary catchment.  $Ad_t$  and  $Ad_m$  were estimated from 1:25 000 topographic maps and  $RTM$  was determined by means of digitized RTM zones provided by the National Forest Office. The  $Ad_t$ - $Ad_m$  ratio is a simple index for evaluating the potential geomorphic effect of a tributary on the recipient channel, based on the postulate that the larger the size of the tributary relative to the main stem, the higher the potential geomorphic effect (Rice, 1998; Benda *et al.*, 2004). The  $RTM$  index gives an estimate of the degree to which the tributary catchment was regulated by reforestation and torrent engineering works.

This procedure makes it possible to identify a general spatial pattern of decreasing predicted RTM impact from upstream to downstream (Figure 12.5(A)). This is explained by the higher geomorphic effect of upstream regulated tributaries (Boulc, Gâts, Maravel and Haute-Drôme), their drainage area being large relative to the size of the main-stem catchment. Leaving aside these upstream impacts, about 10 reaches can be identified along the Drôme and Bez Rivers where substantial impacts are expected. Those can be compared to the distribution of main-stem incision (Figure 12.5(B)), determined by a diachronic analysis of the longitudinal profile. The long profiles of the Drôme and Bez Rivers were surveyed in 1928. These profiles were compared to (1) a 1995 survey of the Bez River and the Drôme River downstream of the confluence with the Bez (see Landon *et al.*, 1998 for details), (2) a 1996 survey of the Drôme River upstream from the Claps landslide (see Piégay *et al.*, 2004 for details) and (3) a 2003 survey of the Drôme River between the confluence with the Bez and Luc-en-Diois. Reaches characterized by a significant decrease in channel elevation (> 30 cm) during the period are mapped on Figure 12.5(B). A good spatial correlation is observed between the distribution of RTM impact along the main stem and incised reaches, especially in the vicinity of the Béoux, Blanchon, Bains, Mians, Valcroissant and Meyrosse Torrents. The main-stem incision was therefore likely induced by a decreasing sediment supply due to the reforestation and construction of torrent-control works in these sub-basins, though it appears that in contrast to the tributary systems the main-stem impact occurred in the second half of the twentieth century.

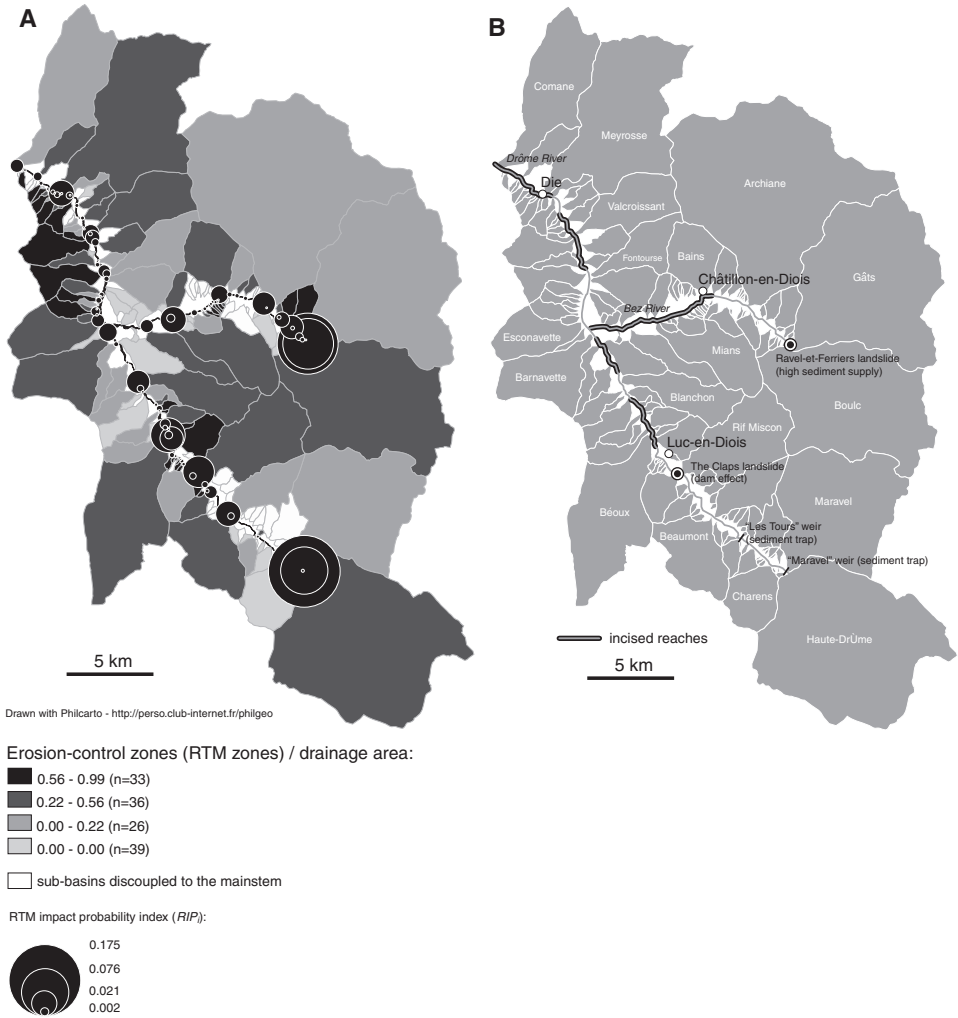


**Figure 12.5** Estimated impact on main-stem geomorphology of RTM works in tributary sub-basins based on the *RIP*; calculated for each tributary to the Drôme River upstream of Die (A); sub-basins are classified according to the relative area of RTM zones. The distribution of incised reaches along the main stem (B), established by long-profiles comparisons, correlates with the distribution of estimated RTM impacts.

The absence of incision downstream of some large tributaries where an impact was expected can be explained by local conditions. The upstream course of the Bez River, where the predicted RTM impact is very high, is characterized by channel aggradation. This is due to a sediment wave that propagates downstream from a very active deep-seated landslide, the Ravel-et-Ferriers slump, reactivated in 1994. This landslide supplies  $\sim 4000 \text{ m}^3 \text{ yr}^{-1}$  of coarse sediments to the Bez River (Bravard and Landon,

2003). No degradation is observed in the Upper Drôme River, upstream from the Claps landslide, although sub-basins were highly regulated by RTM works. The Claps is a large translational landslide ( $1.5 \text{ Mm}^3$ ) that occurred in 1442 in a narrow gorge. The obstruction effect of the landslide, which created a 70-m-high natural dam, is still active today and the Upper-Drôme acts as a bedload trap. This trapping effect is amplified by two large artificial weirs built in the active channel in 1962 and 1984 to prevent channel aggradation downstream (Figure 12.5(B)). Upstream of the slide, coarse sediments coming from incised regulated tributaries are accumulating in the main stem, and channel aggradation is observed (Piégay *et al.*, 2004). A third case is the reach of the Drôme downstream of the Esconavette and Barnavette Torrents. The absence of channel incision here may be explained by a high bedload supply from the highly incised downstream end of the Bez River.

The case study of the Drôme River and its tributaries illustrates that the effect of sediment-transport regulation in tributaries on main-stem morphology and sediment regime is not straightforward. The prediction of channel responses, both in space and time, needs to take into account the routing processes of coarse sediments through the fluvial system (Schumm, 1977). These processes may lead to significant delays between the instigation of source-area management in tributaries and the expected response downstream. The geomorphic response may be the inverse of the expected one, as sediment remobilization from alluvial stores located downstream of source areas induces aggradation further downstream. Moreover, concomitant forcings may reinforce or reverse the geomorphic effect of management strategies, making it difficult to predict geomorphic responses to predefined management scenarios. Lastly, the management scheme may induce unexpected disturbances many decades later. This is the case with the Drôme basin, where current channel incision is the long-term and somewhat ironic consequence of the successful RTM schemes of the late nineteenth century.

## Contemporary channel degradation and bedload replenishment

Accelerated channel incision of the Drôme River in the second half of the twentieth century, induced by in-channel gravel mining, embankment and a decrease in sediment supply from hillslopes (spontaneous reforestation and RTM works) has led to the undermining of bridges and dikes and the lowering of the groundwater table beneath adjacent floodplains (Landon *et al.*, 1998). A bridge collapsed in 1995 and a second bridge was destabilized and closed to traffic in 2003. A list of recommendations concerning the preservation of in-channel sediment stores was proposed and published in a regional water master plan adopted in 1997; the plan calls for the prohibition of gravel mining in the active channel and the promotion of artificial sediment replenishment in the most degraded reaches, eventually by the managed reactivation of bedload transport along some tributaries.

## The role of tributaries in the Drôme's sediment budget

Bedload-transport measurements on three tributaries to the Drôme River between 1997 and 2002 (Liébault, 2003), combined with complementary regional data of bedload yields from sediment traps and morphological estimates (Table 12.1), were used to develop a predictive model for bedload yield based on drainage basin area:

$$V_b = 28.72 A_d^{0.978}, \quad (12.2)$$

where  $V_b$  is the bedload yield in  $\text{m}^3 \text{yr}^{-1}$  and  $A_d$  is the drainage area in  $\text{km}^2$  ( $R^2 = 0.830$ ;  $p = 0.0006$ ;  $n = 9$ ) (Figure 12.6). This equation shows that bedload transport increases linearly with drainage area. Equation 12.2 was used to calculate the mean annual bedload supply from tributaries in the Drôme basin (Figure 12.7). The cumulative bedload input from all tributaries at the downstream end of the mountainous part of the basin are  $29\,500 \text{ m}^3 \text{yr}^{-1}$ . The annual bedload transport of the lower Drôme River, known from a sediment trap at the Rhône confluence, is  $\sim 35\,000 \text{ m}^3 \text{yr}^{-1}$  (Landon, 1999). Sediment input from bank erosion is

**Table 12.1** Bedload yields for rivers and streams of the Southern French Prealps, used for calibrating Equation 12.2.

Study sites	Drainage areas ( $\text{km}^2$ )	Bedload yields ( $\text{m}^3 \text{yr}^{-1}$ )	Methods	References
Barnavette Torrent (D)	14	712	Scour chains and painted tracers (1997–2002)	Liébault (2003)
Béoux Torrent (D)	28	565	Scour chains and painted tracers (1997–2002)	Liébault (2003)
Bine Torrent (R)	19	618	Morphological estimate (1956–1991)	Liébault and Piégay (2001)
Esconavette Torrent (D)	10	651	Scour chains and painted tracers (1997–2002)	Liébault (2003)
Eygues River (E)	1100	66 000	Morphological estimate (1948–1996)	Landon <i>et al.</i> (1999)
Lower-Drôme River (D)	1640	35 000	Sediment trap (1961–1997)	Landon (1999)
Soubriou Torrent (R)	26	183	Morphological estimate (1956–1991)	Liébault and Piégay (2001)
Upper-Drôme River (D)	93	3530	Sediment trap (1928–2002)	Piégay <i>et al.</i> (2004)
Upper-Roubion River (R)	132	1016	Morphological estimate (1956–1991)	Liébault and Piégay (2001)

D: Drôme River basin; E: Eygues River basin; R: Roubion River basin

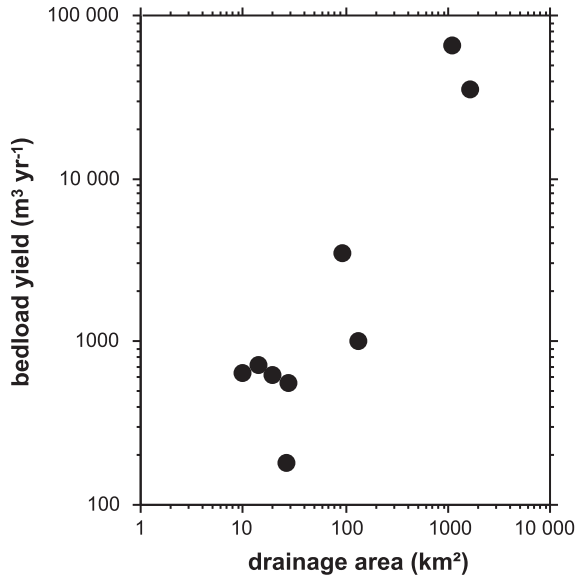


**Figure 12.6** Annual bedload yield plotted versus drainage area for rivers and streams of the Southern French Prealps (Liébault, 2003).

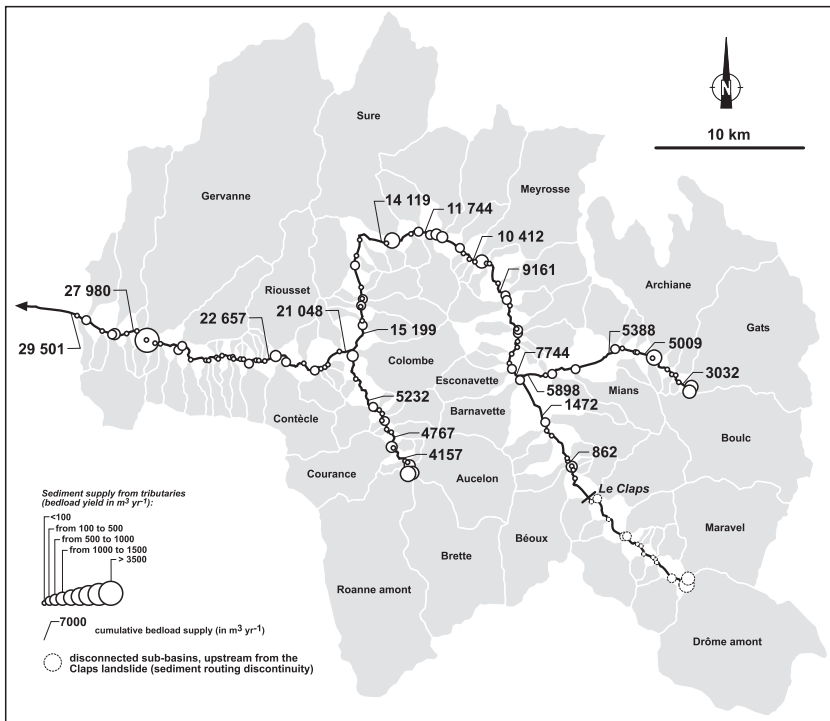


**Figure 12.7** Basin-scale assessment of the annual bedload supply from tributaries to the Drôme River, based on the power relation in Figure 12.6. Cumulative bedload supplies are calculated by summing bedload yields of tributaries located upstream from calculation points.

negligible because the Drôme River has been characterized by strong active channel narrowing since the 1950s (bank accretion > bank erosion; Kondolf *et al.*, 2002). Despite uncertainties inherent in these estimates, we therefore found a global sediment deficit of  $\sim 5500 \text{ m}^3 \text{ yr}^{-1}$ . This suggests that the tributaries are supplying insufficient sediment to balance the current output rate into the Rhône River. This budget does not account for the abrasion of coarse sediments along the river course, a process that may amplify the deficit between inputs and outputs in distal reaches. Moreover, bedload yields used for the sediment-budget computation can be considered as an upper limit because bedload transport in most of the streams studied, reconstructed for the last 50 years (Table 12.1), was sustained by degradation into alluvial stores that are not renewed by the supply of sediment from hillslope sources. As a result, sediment stores are shrinking along tributaries and the gravel deficit of the Drôme River will probably increase over the next few decades. It is then likely that the prohibition of gravel mining in the active channel will not be sufficient by itself to stop current channel degradation.

## A decision-making tool for bedload replenishment

For this reason, sediment replenishment of highly degraded reaches is under consideration as a management strategy, and here we propose a decision-making tool that may help river managers to implement such a scheme. There are two parts to this tool that correspond to the conceptual ideas laid out above: the identification of bedload-supply potential and the evaluation of bedload-transport potential.

Aerial photographs (1991 infra-red colour 1:17 000 scale) were used to map all the sediment sources located upstream from degraded reaches. The most common sources of sediment in the Drôme River basin are active gullies, incised into alternating marl and limestone sequences. The bedload-supply potential of each sediment source was qualitatively assessed as the product of three parameters: (1) lithology, (2) distance to the closest incised reach and (3) hazard potential. The first parameter characterizes the potential of the sediment source to deliver coarse-grained sediment to channels and depends only on the nature of the rocks or surficial deposits that are affected by erosion processes. This was determined using 1:50 000 geological maps and 1:17 000 1991 aerial photographs. The second parameter is the distance between the source and the target reach. The closer a source is to the reach, the stronger is the likelihood of it being important. The third parameter characterizes the potential of the source to deliver sediment without increasing flood or geomorphic hazards for human infrastructures that are located along the sediment routing pathway. This parameter was assigned according to the presence or absence of human infrastructure between the source and the target reach.

The bedload supply potential was calculated semi-automatically using MapInfo (the detailed procedure of computation can be found in Liébault *et al.*, 2001). Maps were then constructed for each of the target reaches which classified sediment sources according to

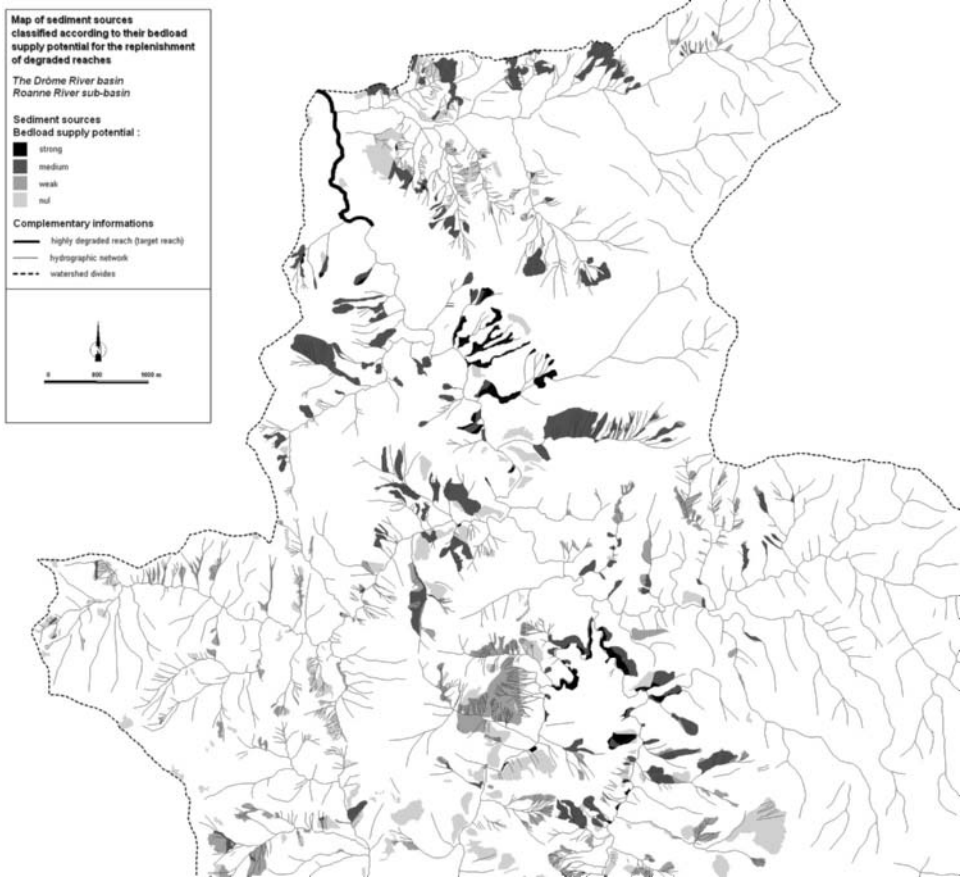


**Figure 12.8** Map of the sediment sources that could be reactivated for artificial bedload replenishment: the example of the Roanne River, a tributary to the Drôme River; the most appropriate sites for bedload replenishment are those characterized by a high bedload supply potential.

their potential of being used in design strategies for the artificial supply of sediment (Figure 12.8). These maps can help managers to identify the areas where erosion should be maintained and/or accelerated for the replenishment of degraded reaches. For the entire Drôme River basin, sediment sources with a high potential for bedload replenishment represent 155 ha. The artificial replenishment of degraded reaches could be envisaged through several operations, involving different sediment stores. For example, vegetated colluvial deposits, scree slopes, alluvial fans or low terraces coupled with active tributary channels in the vicinity of degraded reaches could be reactivated by deforestation.

However, activating potentially useful sediment stores is not sufficient. It is also important to evaluate the bedload-transport capacity of the tributaries which would route

**Table 12.2** General characteristics of the tributaries of the Drôme River used to evaluate sediment-transport capacity.  $A$ : drainage area,  $S$ : slope,  $d_{xx}$ : diameters for which xx per cent is finer than  $d_{xx}$ ,  $W$ : bankfull width.  $S$ ,  $d_x$  and  $W$  pertain to the studied reach, usually the reach upstream from the Drôme confluence.

Tributaries	$A$ (km <sup>2</sup> )	$S$	$d_{50}$ (mm)	$d_{30}$ (mm)	$d_{90}$ (mm)	$W$ (m)
Barnavette	14.0	0.013	21	13	44	5.2
Béoux	28.2	0.016	21	15	44	5.0
Comane	23.1	0.012	133	54	243	2.9
Esconavette	9.5	0.021	27	12	101	5.0
Meyrosse	44.9	0.010	49	22	151	7.1
Valcroissant	12.5	0.022	45	17	103	4.0

activated sediment to the main stem where it is needed. Bedload-transport formulas were used to estimate transport capacity for the tributaries along a 21-km reach located between Die and Luc-en-Diois. This reach is severely affected by incision and is therefore in the greatest need of a management strategy. We selected those six tributaries with drainage areas between 10 and 100 km<sup>2</sup> (Table 12.2) as these were considered to be the most favourable bedload candidates. Our objective was to identify the most appropriate tributaries for implementing a sediment-supply replenishment programme to mitigate channel incision along the main stem.

Many transport formulas are available in the literature (Gomez, 1989). Most formulas were established for relatively low slopes. For example, Meyer-Peter and Müller (1948) investigated slopes up to 0.022 but with very few data above 0.012. As the investigated tributary reaches show slopes ranging from 0.01 to 0.02, we chose the Rickenmann formula (Rickenmann, 2001) valid for a large range of slopes (0.001 to 0.1). This formula is a simplified form of a fitting procedure using data from Meyer-Peter and Müller (1948), Smart and Jaeggi (1983) and Rickenmann (1991). With a density for solids of 2.68, the formula is:

$$q_s = 1.5 \left( \frac{d_{90}}{d_{30}} \right)^{0.2} S^{1.5} (q_w - q_c), \quad (12.3)$$

where  $S$  is the slope,  $d_x$  the diameter for which x per cent is finer,  $q_s$  and  $q_w$  the volumic unit-width discharge of bedload and water, respectively. The volumetric unit-width incipient motion critical discharge established by Bathurst *et al.* (1987) is  $q_c$ :

$$q_c = 0.065 (s - 1)^{1.67} \sqrt{g} d_{50}^{1.5} S^{-1.12}, \quad (12.4)$$

where  $s$  is the solid-to-liquid density ratio. The latter formula is the result of a fitting procedure for a range of slopes between 0.0025 and 0.2. The  $\left( \frac{d_{90}}{d_{30}} \right)^{0.2}$  factor is a rather

coarse but simple way to account for non-uniform sediments. Refined approaches would need fractional grain-size analysis.

This formula does not take into account sediment-supply conditions but rather gives the maximum transport capacity under unlimited sediment supply. In addition, it has the same limitations as many other bedload formulae, including the assumption of steady, uniform flow. Nevertheless, application to the Barnavette Torrent, where bedload-transport volumes were measured between 1997 and 2002 using scour chains and painted tracers (Liébault, 2003), gave fair values of event-based bedload volumes (De Block, 2004). To identify the most powerful of the six selected tributaries for bedload transport, we calculated the non-dimensional volumetric solid-to-water discharge ratio  $q_s/q_w$  for increasing water discharges (Figure 12.9(A)). This ratio is hereafter named 'concentration'.

For each tributary, a representative reach of the lower course was selected for bedload computation. Study reaches were not always the lowest reach. For example, the downstream end of the Esconavette Torrent is a small alluvial fan with a wandering pattern where the Rickenmann bedload formula is not applicable. In this case, the reach immediately upstream was chosen. The length over which the slope was computed was chosen carefully, for example between two major break of slopes, and over a sufficient distance to avoid an unrepresentative local slope value.

For each tributary, Figure 12.9(A) shows the critical discharge for incipient motion and the asymptotic concentration at high discharges. The asymptotic concentration mainly depends on slope and, weakly, on the grain-size range. From a lower asymptotic concentration of about 0.15 to 0.6 per cent for slopes varying between 0.012 and 0.022, the tributaries can be classified as follows, from lower to higher concentration: Comane, Meyrosse, Barnavette, Béoux, Valcroissant and Esconavette. Incipient motion critical discharges depend mainly on slope, grain size and width. Four tributaries out of six effectively present a comparable critical discharge between 0.7 and 1.3 m<sup>3</sup>s<sup>-1</sup>, the order being Béoux, Esconavette, Barnavette and Valcroissant. In contrast, the Meyrosse and the Comane streams, which are characterized by the lowest slopes and the coarsest grain sizes, exhibit higher critical discharges. When examined in the field, those tributaries, and especially the Comane, are characterized by strong armouring in the downstream reaches and densely vegetated riverbanks, indicating channel stability.

Among the four tributaries exhibiting a relatively low critical discharge, the Esconavette Torrent and the Valcroissant Torrent display similar concentrations. However, field examination confirms that the Esconavette is a very active tributary, whereas the Valcroissant is totally inactive due to a very low sediment supply. This example illustrates the limits of this straightforward hydraulic approach and the need for the two-part tool, which also considers supply potential.

Moreover, this analysis does not take into account the hydrology of the catchment. Obviously, the larger the drainage area, the larger the water discharge. Figure 12.9(B) shows the concentration  $q_s/q_w$  as a function of specific discharge. The patterns are

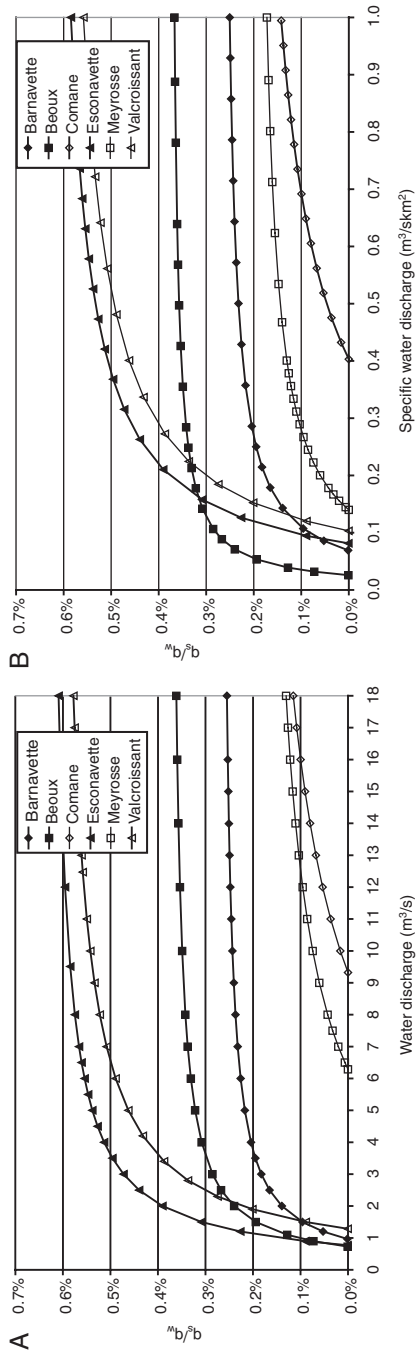


**Figure 12.9** Concentrations  $q_s/q_w$  for each tributary versus (A) water discharge and (B) specific water discharge.

similar but there is one important difference: because the drainage area of the Béoux is about three times that of the Esconavette, the Béoux has a much lower specific discharge although they have the same absolute critical discharge. For high-flow events, the Esconavette presents an asymptotic concentration of about 0.6 per cent compared to about 0.4 per cent for the Béoux Torrent, which means that the Esconavette is likely to yield 50 per cent more coarse sediment. In contrast, for the low-flow events there is a higher yield for the Béoux. For example, at a specific discharge of  $0.1 \text{ m}^3\text{s}^{-1}\text{km}^{-2}$ , the concentration of the Béoux is about 0.28 per cent, whereas it is only 0.13 per cent in the Esconavette. This observation is of great importance when the problem is to determine which of the two streams – Béoux or Esconavette – is likely to provide the greater total volume of sediment to the Drôme River over a certain period of time. The Esconavette is the best candidate for the Drôme replenishment programme in terms of high-discharge events, whereas the Béoux has a better yield for low flows near the critical discharge.

Although this case study is not necessarily extendable to other sites, some useful general conclusions can be drawn: (1) this simple analysis based on bedload-transport formulae with a threshold of motion allowed us to identify the potential tributaries to implement a replenishment program; (2) as illustrated by the Valcroissant tributary, a full analysis of the sediment recharge potential of a river basin requires two complementary steps, the first being the determination of potential sediment sources and the second being the determination of the sediment-transport capacity of the fluvial network.

## Practical management outcomes for sediment replenishment

What has been the practical outcome of the geomorphological investigations of the Drôme tributaries? First, they contributed to the development of a number of management principles for the Drôme catchment (Bravard *et al.*, 1999): (1) preserve bedload transport in tributaries, (2) maintain coupling between eroding slopes producing coarse sediments and the channel network, (3) limit future erosion-control works on marly slopes, (4) preserve aggrading reaches when flooding risks are acceptable, (5) in aggrading reaches where flooding risks are unacceptable, promote sediment-transport enhancement actions (vegetation removal, remobilization trenches) instead of dredging operations, (6) delimit an erodible river corridor to preserve sediment recharge from bank erosion. These recommendations were approved by the local management commission and registered in a regional water master plan. This has been followed by artificial replenishments of gravel related to specific opportunities. The dredging of a sediment trap at the Rhône–Drôme confluence permitted the replenishment of  $20\,000 \text{ m}^3$  of gravels to an upstream reach where embankments had been destabilized by incision. The construction of a tunnel in the upper part of the basin provided an

opportunity to recharge 25 000 m<sup>3</sup> of fragmented excavated limestones in the Boulc stream, a tributary to the Bez River.

Since 2005, the sediment replenishment of degraded reaches along the Drôme River has been funded within the framework of an EU LIFE-Environment project ('Forests for Water'). The general objective of this project is to promote the integration of the forest in the EU Water Framework Directive (Ferry, 2004). The Drôme River basin is one of the European sites that have been selected for testing the applicability and efficiency of forest-management actions for hydrosystem restoration. The specific objective in the Drôme is to evaluate the forest influence on sediment supply from hillslopes and valley-floor alluvial stores. Two experimental sites have been proposed by river scientists and approved by stakeholders. The first is composed of paired and partially wooded gullies considered to be representative of the dominant sediment source of the Drôme basin. Drainage areas are between 0.14 and 0.17 ha. After a calibration period, one of the two catchments has been deforested. Coarse-sediment traps located at the output of the catchments allow measurement of the potential increase of sediment supply induced by deforestation. The second site for experimental sediment recharge is along the Béoux Torrent, which exhibits post-1950 forested alluvial terraces along its alluvial fan. A portion of these terraces, located 2 km upstream from the Drôme confluence, has been deforested in order to facilitate sediment recharge by bank erosion (Figure 12.10). These two sites have been monitored since July 2005. An analysis of the geomorphic effect of deforestation is not yet possible because there have not been any substantial rainfall events to date. However, these experiments will provide valuable quantitative data for the evaluation of sediment-replenishment programmes based on the reactivation of hillslope and valley-floor sediment in tributary valleys.

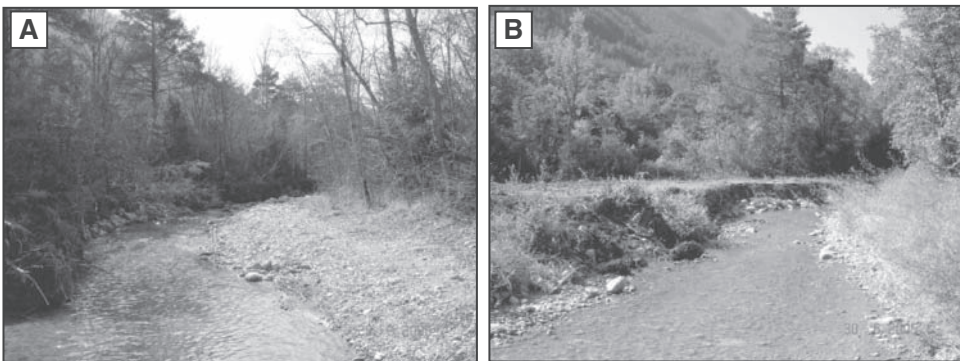


**Figure 12.10** Experimental bedload replenishment site on the Béoux Torrent (drainage basin: 30 km<sup>2</sup>), a tributary to the Drôme River, before (A) and after (B) deforestation works. A portion of a low wooded recent alluvial terrace was deforested in May 2005 to enhance sediment supply from bank erosion. Upstream views.

## Conclusion

This chapter presents some conceptual tools and practical examples that indicate how tributaries can be and have been utilized in the management of catchment-scale sediment regimes. Tributaries are recognized as physical links by which the spatial and temporal variability of catchment processes are transmitted to the recipient channel. Therefore, both the spatial arrangement of tributaries in the drainage network and the intrinsic characteristics of sub-basins play an important role in the magnitude and spatial pattern of the tributary impact along trunk streams. This impact is driven by the water and sediment supply; the higher these are relative to the main-stem water discharge and sediment load, the higher the potential impact will be (see Ferguson and Hoey, Chapter 11, this volume).

If tributary basins are to be manipulated to manage main-stem channel geomorphology, then other important parameters need to be considered, such as the geomorphic sensitivity and sediment-routing dynamics of the main stem, plus the relative cumulative influence of other lateral sediment sources (e.g. landslides and bank erosion). Thus, in some catchments, it has been demonstrated that tributaries only have a small effect on the longitudinal patterns of main-stem morphology and sedimentology, these patterns being mostly controlled by the processes of sediment-wave propagation through the drainage network (Jacobson and Gran, 1999). The diachronic study of the changing nature of tributaries is presented as a possible approach for evaluating their geomorphic impact. This can help to predict future main-stem-channel responses and to determine reaches where such responses are likely to occur. It is also possible to infer tributary impact from the analysis of downstream trends in main-stem bed-material grain-size shape, and lithological composition. This may be useful for identifying the most active tributaries in terms of sediment supply. More quantitative approaches, based on bedload-transport modelling and measurement are also possible. They provide valuable information about the tributary impact if they are integrated in a sediment-budget framework, as illustrated for the Drôme tributaries.

Management actions to mitigate the impact of tributaries mostly concern the regulation of sediment and water regimes by catchment-scale management actions (i.e. reforestation and erosion-control works). The effectiveness of such programmes requires the predetermination of those tributaries that have a significant effect on the main stem's geomorphological regime. In such cases, it is important to consider the time lag between the management action and its effect on the main channel downstream. The example of the Drôme River basin is particularly illustrative, since it shows that regulation works conducted along some tributaries between 1860 and 1914 have probably sustained a braided pattern in the main channel by the downstream propagation of incision along small torrents. It also shows a contrasting perception of tributaries through time. Their sediment supply was considered as having a negative effect on the main-stem corridor at the beginning of the twentieth century, when the main stem was

aggrading, and now this is viewed as a positive contribution in the present-day context of accelerating channel degradation in the main valley.

Some future research directions can be proposed for improving our understanding of tributary geomorphic impact and the development of more appropriate management tools. We think that the most important challenge is to understand sediment routing through the channel network. This can be achieved through both the development of theoretical tools that address this spatial scale (Benda and Dunne, 1997; Sklar *et al.*, 2006) and field observations and measurements of channel responses to disturbed sediment regimes in adjusting river systems (Jacobson and Gran, 1999; Kasai *et al.*, 2004). It is the confrontation of such approaches that will give us the opportunity to develop and test decision-making tools adapted for the integrative management of fluvial systems.

## Acknowledgements

We are grateful for the field assistance of the ONF Drôme-Ardèche (French National Forest Office). Thank you to John Pitlick and Stephen Rice for the constructive reviews. Funding was provided by the 'Forests for Water' LIFE programme (LIFE03/ENV/S/000601).

## References

- Bartley R, Rutherford I. 2005. Measuring the reach-scale geomorphic diversity of streams: Application to a stream disturbed by a sediment slug. *River Research and Applications* **21**: 39–59.
- Bathurst JC, Graf WH, Cao HH. 1987. Bedload discharge equations for steep mountain rivers. In *Sediment Transport in Gravel-Bed Rivers*, Thorne CR, Bathurst JC, Hey RD (eds). John Wiley & Sons: Chichester; 453–477.
- Benda L, Dunne T. 1997. Stochastic forcing of sediment routing and storage in channel networks. *Water Resources Research* **33**: 2865–2880.
- Benda L, Veldhuisen C, Black J. 2003. Debris flows as agents of morphological heterogeneity at low-order confluences, Olympic Mountains, Washington. *Geological Society of America Bulletin* **115**: 1110–1121.
- Benda L, Andras K, Miller D, Bigelow P. 2004. Confluence effects in rivers: Interactions of basin scale, network geometry, and disturbance regimes. *Water Resources Research* **40**: W05402. DOI: 10.1029/2003WR002583.
- Benito G, Grodek T, Enzel Y. 1998. The geomorphic and hydrologic impacts of the catastrophic failure of flood-control-dams during the 1996-Biescas flood (Central Pyrenees, Spain). *Zeitschrift für Geomorphologie* **42**: 417–437.
- Bravard JP. 2002a. Les réponses des systèmes fluviaux à une réduction des flux d'eau et de sédiments sous l'effet du reboisement en montagne. *La Houille Blanche* **3**: 68–71.

- Bravard JP. 2002b. Le “traitement” des versants dans le département de la Drôme, des inondations de 1840 à la loi du 27 juillet 1860. *Annales des Ponts et Chaussées* **103**: 37–43.
- Bravard JP, Landon N. 2003. Les ajustements du Bez, un torrent du Diois (Alpes du Sud), essai de micro-histoire géomorphologique. In *Eau et Environnement, Tunisie et Milieux Méditerranéens*, Arnould P, Hotyat M (eds). ENS éditions: Lyon; 115–128.
- Bravard JP, Amoros C, Pautou G, Bornette G, Bournaud M, Creuzé des Châtelliers M, Gibert J, Peiry JL, Perrin JF, Tachet H. 1997. River incision in South-East France: Morphological phenomena and ecological effects. *Regulated Rivers: Research and Management* **13**: 1–16.
- Bravard JP, Landon N, Peiry JL, Piégay H. 1999. Principles of engineering geomorphology for managing channel erosion and bedload transport, examples from French rivers. *Geomorphology* **31**: 291–311.
- Brierley GJ, Fryirs K. 1999. Tributary-trunk stream relations in a cut-and-fill landscape: A case study from Wolomla catchment, New South Wales, Australia. *Geomorphology* **28**: 61–73.
- Clément P, Piégay H. 2003. Statistics and fluvial geomorphology. In *Tools in Fluvial Geomorphology*, Kondolf MG, Piégay H (eds). John Wiley & Sons: Chichester; 597–630.
- De Block B. 2004. *Etude du transport solide d'affluents de la Drôme dans le cadre de la recharge sédimentaire*, Unpublished Ms thesis, Ecole Nationale du Génie de l'Eau et de l'Environnement de Strasbourg.
- Ferguson RI, Cudden JR, Hoey TB, Rice SP. 2006. River system discontinuities due to lateral inputs: Generic styles and controls. *Earth Surface Processes and Landforms* **31**: 1149–1166.
- Ferry O. 2004. La forêt au service de l'eau: Une perspective européenne. *Revue Forestière Française* **1**: 47–64.
- Gomez B. 1989. An assessment of bedload sediment transport formulae for gravel bed rivers. *Water Resources Research* **25**: 1161–1186.
- Gomez B, Banbury K, Marden M, Trustrum NA, Peacock DH, Hoskin PJ. 2003. Gully erosion and sediment production: Te Weraroa Stream, New Zealand. *Water Resources Research* **39**: 1187–1194.
- Grosprêtre L, Schmitt L. 2006. *Etude hydro-géomorphologique de l'Yzeron et définition d'indicateurs de suivi*. Unpublished technical report. Université Lyon 2, CNRS-UMR 5600.
- Jacobson RB, Gran KB. 1999. Gravel sediment routing from widespread, low-intensity landscape disturbance, Current River basin, Missouri. *Earth Surface Processes and Landforms* **24**: 897–917.
- Jomelli V, Pech P. 2004. Effects of the Little Ice Age on avalanche boulder tongues in the French Alps (Massif des Ecrins). *Earth Surface Processes and Landforms* **29**: 553–564.
- Jones Jr EL. 1919. A reconnaissance of the Pine Creek district, Idaho. *United States Geological Survey Bulletin* **710-A**: 1–36.
- Kasai M, Marutani T, Brierley GJ. 2004. Patterns of sediment slug translation and dispersion following typhoon-induced disturbance, Oyabu Creek, Kyushu, Japan. *Earth Surface Processes and Landforms* **29**: 59–76.
- Knighton AD. 1980. Longitudinal changes in size and sorting of stream-bed material in four English rivers. *Geological Society of America Bulletin* **91**: 55–62.
- Kondolf GM, Piégay H, Landon N. 2002. Channel response to increased and decreased bedload supply from land use change: Contrasts between two catchments. *Geomorphology* **45**: 35–51.
- Kotarba A. 1997. Formation of high-mountain talus slopes related to debris-flow activity in the High Tatra Mountains. *Permafrost and Periglacial Processes* **8**: 191–204.

- Lahousse P, Romelé C. 2000. Le Ravin des Sables (Hautes-Alpes, France): Une nouvelle source de risque dans la vallée de la Clarée. *Géographie Physique et Quaternaire* **54**: 271–280.
- Landon N. 1999. *L'évolution contemporaine du profil en long des affluents du Rhône moyen, constat régional et analyse d'un hydrosystème complexe, la Drôme*. Unpublished PhD thesis, Université Paris IV-Sorbonne.
- Landon N, Piégay H, Bravard JP. 1998. The Drôme River incision (France): From assessment to management. *Landscape and Urban Planning* **43**: 119–131.
- Landon N, Piégay H, Clément P, Kondolf GM, Liébault F, Rogers C, Colangelo C, Michel V. 1999. *Mission d'expertise réalisée sur le bassin de l'Eygues pour le compte du Syndicat d'Aménagement Rural de la Drôme et des Syndicats drômois et vauclusiens de l'Eygues, propositions pour une gestion physique équilibrée du lit de l'Eygues et de son bassin*. Unpublished technical report, Laboratoire Environnement-Ville-Société, UMR5600 CNRS: Lyon, France.
- Liébault F. 2003. *Les rivières torrentielles des montagnes drômoises: Évolution contemporaine et fonctionnement géomorphologique actuel (massifs du Diois et des Baronnies)*, Unpublished Ph.D thesis, Université Lumière Lyon 2.
- Liébault F. 2005. Morphological response of an alpine torrent to watershed reforestation (The Sure Torrent, Southern French Prealps). *Studia Geomorphologica Carpatho-Balcanica* **XXXIX**: 50–69.
- Liébault F, Piégay H. 2001. Assessment of channel changes due to long-term bedload supply decrease, Roubion River, France. *Geomorphology* **36**: 167–186.
- Liébault F, Zahnd E. 2001. La Restauration des Terrains en Montagne en Diois – Baronnies. *Terres Vocances* **3**: 27–48.
- Liébault F, Clément P, Piégay H, Landon N. 1999. Assessment of bedload delivery from tributaries: The Drôme River case, France. *Arctic, Antarctic, and Alpine Research* **31**: 108–117.
- Liébault F, Clément P, Piégay H. 2001. *Analyse géomorphologique de la recharge sédimentaire des bassins versants de la Drôme, de l'Eygues et du Roubion*. Unpublished technical report, CNRS – UMR 5600.
- Liébault F, Clément P, Piégay H, Rogers C, Kondolf GM, Landon N. 2002. Contemporary channel changes in the Eygues basin, Southern French Prealps: The relationship of sub-basin variability to watershed characteristics. *Geomorphology* **45**: 53–66.
- Liébault F, Gomez B, Page M, Marden M, Peacock D, Richard D, Trotter CM. 2005. Land-use change, sediment production and channel response in upland regions. *River Research and Applications* **21**: 739–756.
- Marnezy A. 1993. Un exemple de catastrophe hydrologique évitée: L'obstruction de l'Arc par une crue du torrent de l'Envers en juin 1992. *Revue de Géographie de Lyon* **68**: 193–202.
- Meyer-Peter E, Müller R. 1948. Formulas for bed-load transport. In *Proceedings of the International Association of Hydraulic Research, 3rd Annual Conference, Stockholm*; 39–64.
- Mitchell V. 1996. *Inventory of Mines in the Pine Creek Basin*. Idaho Department of Mines and Geology, Moscow, ID.
- Piégay H, Thévenet A, Kondolf GM, Landon N. 2000. Physical and human factors influencing potential fish habitat distribution along a mountain river, France. *Geografiska Annaler* **82A**: 121–136.
- Piégay H, Walling DE, Landon N, He Q, Liébault F, Petiot R. 2004. Contemporary changes in sediment yield in an alpine montane basin due to afforestation (the Upper-Drôme in France). *Catena* **55**: 183–212.

- Pitlick J. 1993. Response and recovery of a subalpine stream following a catastrophic flood. *Geological Society of America Bulletin* **105**: 657–670.
- Pitlick J, Cress R. 2002. Downstream changes in the channel geometry of a large gravel bed river. *Water Resources Research* **38**: 1216–1226.
- Rice S. 1998. Which tributaries disrupt downstream fining along gravel-bed rivers? *Geomorphology* **22**: 39–56.
- Rice S, Church M. 1998. Grain size along two gravel-bed rivers: Statistical variation, spatial pattern and sedimentary links. *Earth Surface Processes and Landforms* **23**: 345–363.
- Rice S, Greenwood MT, Joyce CB. 2001. Macroinvertebrate community changes at coarse sediment recruitment points along two gravel bed rivers. *Water Resources Research* **37**: 2793–2803.
- Rickenmann D. 1991. Hyperconcentrated flow and sediment transport at steep slopes. *Journal of Hydraulic Engineering* **117**: 1419–1439.
- Rickenmann D. 2001. Comparison of bedload transport in torrents and gravel bed streams. *Water Resources Research* **37**: 3295–3305.
- Rinaldi M, Simon A. 1998. Bed-level adjustments in the Arno River, central Italy. *Geomorphology* **22**: 57–71.
- Schumm SA. 1977. *The fluvial system*. The Blackburn Press: Caldwell, New Jersey.
- Schumm SA, Harvey MD, Watson CC. 1984. *Incised channels: 'nitiation, evolution, dynamics, and control*. Water Resources Publication: Littleton.
- Simon A, Hupp CR. 1986. Channel evolution in modified Tennessee channels. In *Proceedings of the Fourth Federal Interagency Sedimentation Conference, Las Vegas, March 24–27, 2*, 5–71: 5–82.
- Sklar LS, Dietrich WE, Foufoula-Georgiou E, Lashermes B, Bellugi D. 2006. Do gravel bed river size distributions record channel network structure? *Water Resources Research* **42**: DOI: 10.1029/2006WR005035.
- Smart GM, Jaeggi M. 1983. *Sediment transport in steilen Gerinnen*. ETH: Zürich.
- Surell A. 1841. *Etude sur les Torrents des Hautes-Alpes*. Dunod: Paris.
- Surian N. 2002. Downstream variation in grain size along an Alpine river: Analysis of controls and processes. *Geomorphology* **43**: 137–149.
- Wyzga B. 1991. Present-day downcutting of the Raba River channel (western Carpathians, Poland) and its environmental effects. *Catena* **18**: 551–566.

# 13

## Confluence environments at the scale of river networks

**Lee Benda**

*Earth Systems Institute, USA*

### Introduction

The focus on tributary confluences in this book aims to advance our understanding of rivers as branching networks in which populations of tributary junctions create zones of mixing in the transport of water, sediment and organic material that lead to unique and heterogeneous fluvial and riparian confluence environments. In this chapter, the term ‘confluence environment’ refers to observable differences in channel and valley morphology that occur at or near confluences due to abrupt influxes of water, sediment and organic material from tributary basins. The terms ‘confluences’ and ‘tributary junctions’ refer only to the physical intersection point between two channels that may or may not have observable morphological effects. The potential controls on populations of confluence environments are evaluated within the context of the structure and scaling properties of river networks, including network patterns, drainage density and the power law of stream sizes. In addition, because confluence environments are affected by the temporal variability of sediment supply from tributary basins, the effect of branching networks on the stochastic nature of sediment inputs is also considered. New perspectives of rivers as networks that are comprised of both confluence and non-confluence environments have the potential to underpin advances in fluvial geomorphology and riverine ecology, and related endeavours pertaining to resource management and restoration science.

The abrupt influx of water, sediment and organic material from tributaries to main rivers creates potentially significant aquatic and riparian confluence environments. Changes in attributes such as flow discharge, sediment storage, wood storage, substrate size, floodplain dimensions, terrace ages and valley widths that occur at or near confluences have important geomorphic and ecological implications (Best, 1986; Rice *et al.*, 2001; Benda *et al.*, 2004a; Kiffney *et al.*, 2006; Hoffman and Gabet, 2007; and see Ferguson and Hoey, and Rice *et al.*, Chapters 10 and 11, in this volume). In addition, because of morphological changes that occur at confluences, the diversity of riparian and in-stream morphologies (including their ages) may increase as one approaches confluence environments from upstream or downstream (Benda *et al.*, 2003a; Rice *et al.*, 2006).

Exploring the relationships between confluence environments and the structure and scaling properties of river networks opens new avenues for study. River networks have many interesting properties that can influence the organization of confluence environments in space and time. Although the structure of river networks varies in detail from one watershed to another, thereby creating unique watershed environments, there should be universal patterns across watersheds. For example, trellis-shaped river networks (in rectangular basins) have distinct distributions of tributary basin sizes compared to dendritic networks (in oval basins), and stream orders (Strahler, 1952) and tributary basins are hierarchically arrayed by their numbers and sizes, factors that can affect the creation of confluence environments.

Episodically occurring erosion and sediment transport during or following storms, floods and fires often form or rejuvenate tributary confluence environments, particularly in upland landscapes. Consequently, fans at tributary mouths and their up- and downstream zones of influence expand and contract over time in response to the timing of watershed disturbances (Benda *et al.*, 2003b; Hoffman and Gabet, 2007). During periods of low watershed erosion, riparian and stream morphology associated with confluences can become eroded and thus diminish. Conversely, fans and their associated stream morphology can expand during periods of heightened watershed disturbance. Confluences can also amplify channel dynamics. The frequency and magnitude of sediment fluctuations may be higher proximal to and downstream of confluences due to the episodic inputs of sediment and water from the tributary. Additionally, areas upstream of confluences that may be wider and lower-gradient due to increased sediment storage may interfere with the transport and storage of sediment and organic material from upstream, altering the dynamic regime. Because the frequency and magnitude of sediment supply and transport fluctuations are influenced by river network structure and basin scale, the dynamic characteristics of confluence environments can vary with position in the network.

## River network structure and confluence environments

In this chapter, river network structure is considered in terms of (1) basin size and shape, (2) network pattern, (3) the size difference between confluent tributaries, (4) the

power law of stream sizes, (5) drainage and confluence density and (6) local network geometry, including sequences of tributary intersections (Figure 13.1). The focus is on the morphological properties of channels and valleys that occur at or near confluences due to abrupt influxes of sediment, organic material and water. These include alluvial and debris fans that impinge on channels, alluvial terraces, increased channel sinuosity, variation in width-to-depth ratios, finer or coarser channel substrates and increased variability of near-stream (riparian) and in-stream morphology close to confluences (Table 13.1). Confluence effects are not reviewed in detail and readers are referred to other chapters and to the sources referred to in Table 13.1.

## Symmetry ratios and confluence environments

There are many factors that determine the type and magnitude of confluence environments, including the size difference between two intersecting channels, the erosion and sediment-transport characteristics of tributary basins, the grain size of transported sediment, the longevity of tributary-related deposits, the geometry of the valley and channel at confluences and downstream and the timing of stochastic watershed disturbances such as fires, storms and floods. Since one goal of this chapter is to examine how river network structure can influence spatial patterns of confluence environments, the two factors that are known to vary universally with basin-scale and network-branching patterns are addressed here: the size difference between two intersecting channels and the frequency and magnitude of erosion and sediment-transport processes.

Early work on tributary effects focused primarily on changes in hydraulic geometry (i.e. width, depth and form ratio) due to changes in discharge between tributaries and main stems (Mosley, 1976; Best, 1988) and focused on the ratio between discharge (or its surrogate drainage area; see Miller, 1958) among the minor tributary ( $Q_2$ ), major tributary ( $Q_1$ ) and the main stem downstream of the confluence ( $Q_0$ ) (Roy and Woldenberg, 1986). Consistent morphological changes in the anticipated directions (i.e. channel-width increases below the confluence; see Leopold *et al.*, 1964) occurred when the ratio between the minor and major tributaries ( $Q_2/Q_1$ ), called the 'symmetry ratio', was equivalent to 0.6 to 0.7, indicating a threshold relationship between tributary and main-stem river sizes (Rhoads, 1987). In this chapter, a similar approach is taken but the emphasis is on changes in channel and valley morphology at confluences due to influxes of sediment and organic material from tributaries. Impacts are evaluated according to the symmetry ratio, and that analysis is used to create a statistical model to examine the role of river network structure on confluence environments.

Fourteen field studies that document confluence environments at 168 tributary junctions in the western United States and Canada are used to construct the model (Table 13.1). These confluences are located along 730 km of river channels, with drainage areas that span seven orders of magnitude. The reader is referred to the individual studies for details. In all cases, confluence environments were identified as those where there

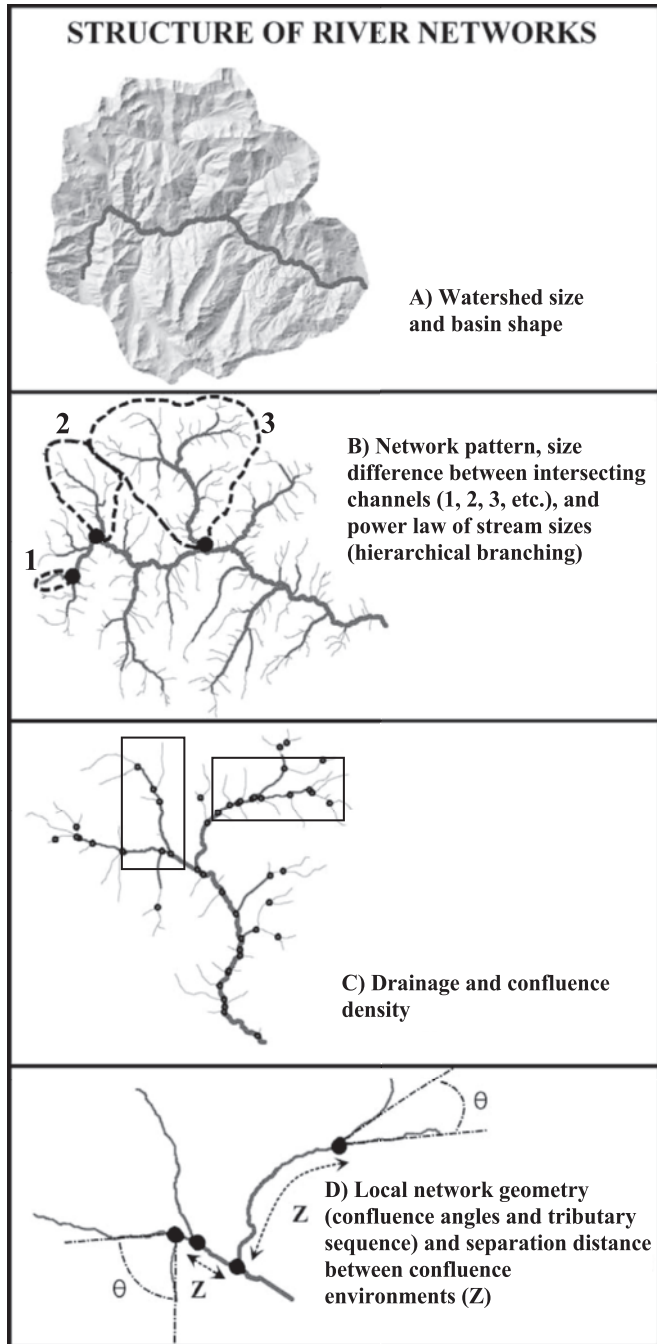


**Figure 13.1** Elements of river network structure that may affect the development of confluence environments include (A) watershed size and basin shape, (B) size difference between the tributary and the channel it joins and the power law of stream sizes, (C) drainage and confluence density and (D) local network geometry.

**Table 13.1** Studies documenting confluence environments across the western United States and Canada are used in the development of a model discussed in this chapter.

Location	Climatic Region	Type of Sediment Transport	Contributing Stream Area (km <sup>2</sup> )	Receiving Stream Area (km <sup>2</sup> )	Morphological Effects
Olympic Mts., WA, Sekiu <sup>1</sup>	Humid	Debris flow	0.02–0.73	0.67–4.2	A, B, D, G, K
Ash Cr, Arizona <sup>2</sup>	Arid	Flash flood	0.42	9.8	D, F
Queen Charlotte Islands, British Columbia <sup>3</sup>	Humid	Debris flow	0.11–5.6	0.3–12.0	K
Olympic Mts., WA, Matheny and Sitkum <sup>1</sup>	Humid	Debris flow	0.37	20.3	A, B, D, G, J, K
Coast Range, Oregon <sup>4</sup>	Humid	Debris flow	0.08–0.27	0.8–30	A, B, C, D, E, F, G, H, J, K, L, N
Sheep Creek, Idaho <sup>5</sup>	Semi-arid	Alluvial	26.6	64.6	A, B, C, D, G
Oregon Cascades <sup>6</sup>	Humid	Debris flow	0.11–3.0	51–71	E, F, G
Crooked River, Idaho <sup>5</sup>	Semi-a rid	Alluvial	3.4	219	A, B, C, D, G
Bear Creek, CO <sup>7</sup>	Semi-a rid	Flash flood	5.9–23.9	193–407	E
North Fork Boise River, Idaho <sup>5</sup>	Semi-a rid	Alluvial	0.6–29	322–461	A, B, C, D, F, G, H
Wenaha River, Oregon <sup>8</sup>	Semi-a rid	Alluvial	18–71	446–516	F, G
Snoqualmie River, Washington <sup>14</sup>	Humid	Alluvial	85–750	712–1794	A, B, C, D
Pine and Sukunka Rivers, British Columbia <sup>9</sup>	Semi-a rid	Alluvial	2.3–203	1579–2145	D
South Fork Payette River, Idaho <sup>10</sup>	Semi-a rid	Flash flood	0.55	2470	E
Bella Coola River, British Columbia <sup>11</sup>	Humid	Alluvial	12.8–285	4779–5421	M
Middle Fork Salmon River <sup>12</sup>	Semi Arid	Debris Flow/ Flash Flood	2.5–295	1,176–7,096	A, B, E
Grand Ronde, Oregon <sup>8</sup>	Semi Arid	Alluvial	764–1,342	6,953–7,781	F, G
Snake River, Oregon <sup>10</sup>	Semi Arid	Alluvial	9,137	240,765	G, F
Colorado River/pre-dam <sup>13</sup>	Arid	Debris Flow/ Flash Flood	14.3–6,076	280,000–386,800	A, D, E, I

Characteristics of confluence environments: (A) gradient steeping, (B) gradient lowering, (C) upstream sediment deposition, (D) changing substrate size, (E) boulders and/or rapids, (F) terraces, (G) floodplains, (H) side channels, (I) mid-channel bars, (J) ponds, (K) log jams, (L) meanders and (M) channel instability. <sup>1</sup>Benda *et al.* (2003a), <sup>2</sup>Wohl and Pearthree (1991), <sup>3</sup>Hogan *et al.* (1998), <sup>4</sup>Everest and Meehan (1981) and Benda (1990), <sup>5</sup>Benda *et al.* (2003b), <sup>6</sup>Grant and Swanson (1995), <sup>7</sup>Grimm *et al.* (1995), <sup>8</sup>Baxter (2002), <sup>9</sup>Rice *et al.* (2001), <sup>10</sup>Meyer and Pierce (2003), <sup>11</sup>Church (1983), <sup>12</sup>Meyer and Liedeker (1999), <sup>13</sup>Melis *et al.* (1995), <sup>14</sup>Booth *et al.* (1991).

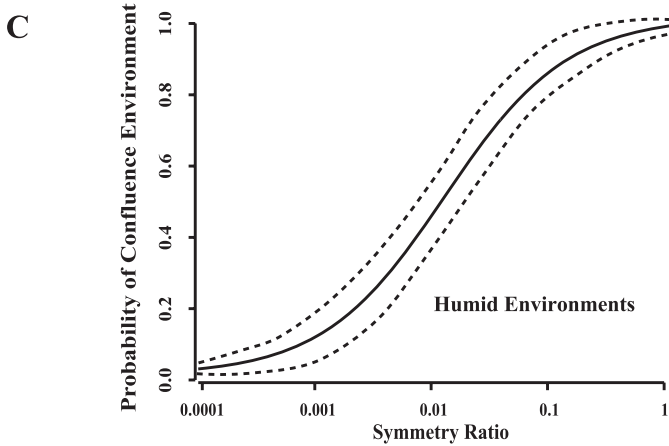
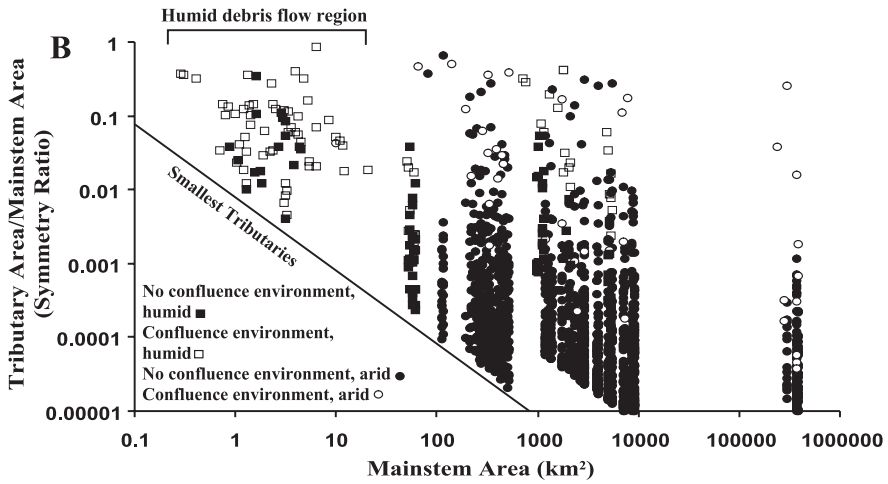
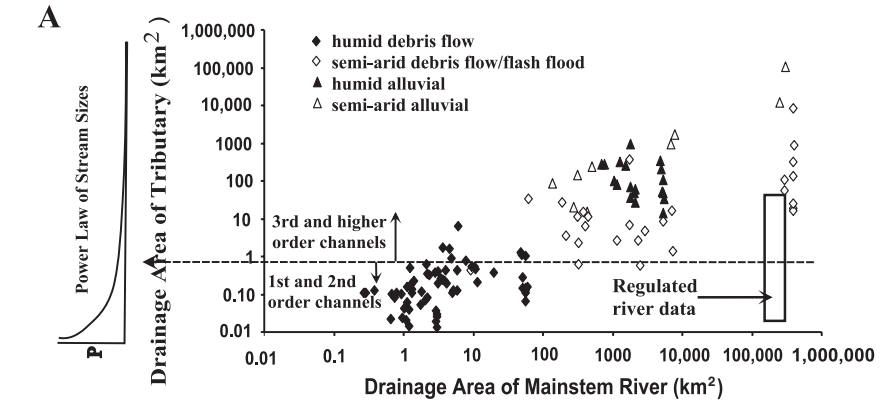
were clear and observable geomorphological impacts in the recipient channel. Symmetry ratios for these junctions are then assumed to be characteristic of those where confluence environments are likely.

The data on confluence environments in Table 13.1 represent a range of sediment-transporting mechanisms, including debris flow, flash flood and fluvial processes (Figure 13.2(A)). In humid landscapes, the data are partitioned by two transport mechanisms across watershed sizes. Debris flows occur within basins typically less than 1 km<sup>2</sup> and the confluence environments they form (boulder deposits, log jams, gradient knick-points and channel meanders) are restricted to main stems of less than approximately 50 km<sup>2</sup>. Also in humid areas, confluence environments constructed by fluvial processes (represented by changes in grain size, increases in sediment storage, and increased meanders and channel anastomosing) dominate in streams with drainage areas that range from 50 km<sup>2</sup> to 2000 km<sup>2</sup> (Table 13.1, Figure 13.2(A)). The relationship is less distinct in semi-arid rivers: there is a large degree of overlap between alluvial processes and debris-flow/flash-flood processes across the entire range of main-stem drainage areas, from 100 to 400 000 km<sup>2</sup>. These data indicate that flash-flood, debris-flow and alluvial processes occur across the same range of tributary basin areas, likely reflecting landscapes susceptible to episodic high-intensity thunderstorms on land surfaces with sparse vegetative cover. Thus, flash floods may occur at certain times and less intense runoff events during other times.

Overall, larger tributary basins are associated with confluence environments in larger rivers (Figure 13.2(A)) (see Benda *et al.*, 2004a for further details). For example, debris flows that originate from small basins (0.01 to 1 km<sup>2</sup> in drainage area) create confluence environments in basins of 1 to 50 km<sup>2</sup>. By contrast, confluence environments in larger rivers (1000–400 000 km<sup>2</sup>) are associated with larger tributaries (10–10 000 km<sup>2</sup>). The data also reveal a threshold in which tributary basins less than approximately 1 km<sup>2</sup> do not affect main-stem rivers greater than approximately 50 km<sup>2</sup>. This is significant because it indicates how the power-law distribution of channel sizes (e.g. ‘the law of stream numbers’, Horton, 1945), and by analogy the confluence environments linked

---

**Figure 13.2** (A) Comparison of tributary basin area and main-stem drainage area for 168 tributaries where confluence environments have been documented. Data are taken from the studies listed in Table 13.1. The dashed horizontal line represents the approximate drainage area threshold for first- and second-order streams that comprise the majority of stream sizes and their confluences. The power relationship to the left of the y axis illustrates the decreasing proportion of large tributary basin sizes within a basin. (B) Ratio of tributary to main-stem drainage area (symmetry ratio) for confluence environments and tributary junctions without confluence environments for both humid and semi-arid environments. The diagonal line corresponds to the smallest tributaries considered. (C) Logistic regression is used to estimate the probability of a confluence environment using symmetry ratios (B) for humid environments. Dashed lines show maximum likelihood 95 per cent confidence intervals. Reproduced from *Water Resources Research* 40: W05402, (2004)



to those channels, constrains the formation of confluence environments at the scale of entire networks. For example, in humid landscapes the majority (70 to 80 per cent) of tributary basins are of first- and second-order and are less than 1 km<sup>2</sup> in drainage area (Benda and Dunne, 1997a). This implies that only 20 to 30 per cent of tributary junctions (of third- and higher- order) are available to create confluence environments in rivers with a drainage area greater than approximately 50 km<sup>2</sup>. Although not shown in Figure 13.2, data from regulated rivers (see Table 13.1) reveal that small tributaries can trigger confluence effects in large, dammed rivers pointing to the effects of reduced flooding erosion on confluence-related landforms (see also Melis *et al.*, 1995).

The data in Figure 13.2(A) were used to identify symmetry ratios for the tributary junctions where confluence environments were observed and/or measured. Similarly, the symmetry ratios for tributaries along the same 730 km of channel where confluence environments were not observed and recorded were computed (Figure 13.2(B)). The symmetry ratios reveal that for any main-stem drainage area, the proportion of all tributary junctions that create confluence environments increases as the symmetry ratio increases (Figure 13.2(B)).

Why should higher symmetry ratios correspond to confluence environments as shown in Figure 13.2? Larger tributaries produce more sediment and commonly have larger alluvial fans compared to smaller basins (Bull, 1977) and this principle extends to small headwater basins (< 1 km<sup>2</sup> in area), where larger catchments produce debris flows of larger volumes. Larger tributary basins also have a higher frequency of sediment-transporting events (Benda and Dunne, 1997b). Thus, the overall pattern where larger tributaries are associated with confluence environments in larger main-stem rivers likely corresponds to larger tributaries producing more sediment and a greater number of events that promote the formation and increased longevity of confluence-related riparian and channel morphology. The ability of coarse-textured debris-flow deposits to survive in-stream erosion should be greater than finer-textured alluvial deposits. Nevertheless, debris-flow deposits are not recorded in channels greater than approximately 50 km<sup>2</sup>, and thus are also sensitive to symmetry-ratio constraints.

That larger tributaries are associated with confluence environments in larger rivers likely reflects other factors in addition to the symmetry ratio, including variation in erosion and sedimentation regimes, grain size of transported sediment and valley morphology. These factors for the most part are not known in the studies and hence could not be incorporated into the model. For example, debris-flow deposits in streams that contain boulders (limited in the data to rivers of less than 50 km<sup>2</sup>) may have a higher longevity compared to alluvial deposits, and debris flows can be of a high volume, even from small tributary basins, because they are a form of mass wasting. This may help to explain the non-distinct separation of confluence from non-confluence environments based on symmetry ratio, a pattern evident in the data in the humid, debris-flow region of Figure 13.2(B).

Stochastic sediment pulses contribute to the formation of confluence environments, particularly in mountain terrains (e.g. Meyer *et al.*, 2001; Meyer and Pierce, 2003). Identifying confluence environments may therefore depend on the length of time since the last erosion and sediment-transport event, and this may be specific to individual tributary basins. Thus, for a given symmetry ratio, some proportion of junctions may have confluence environments and some may not, simply because of the time elapsed since the last formative event. Confluence environments formed at the mouths of larger tributaries, however, may be more frequently active because of an increase in sediment-transport frequency with distance downstream in river networks (Benda and Dunne, 1997b). There is some evidence of this in Figure 13.2(B), where the overall proportion of confluence to non-confluence environments increases with increasing drainage area.

Because of the lack of specificity about the types, length scales, composition and ages of observed confluence environments in the literature as a whole (e.g. Table 13.1), logistic regression was used to specify the relation between symmetry ratio and the binomial response: 'confluence environment' or 'no confluence environment' (Benda *et al.*, 2004b). The data in Figure 13.2(B) were binned by symmetry ratio and logistic regression used to describe the proportion of confluence environments within each bin. The logistic model specifies the probability of a confluence environment as:

$$P_e = \exp(g(x))/(1 + \exp(g(x))) \quad (13.1)$$

where  $P_e$  is the probability of a confluence environment and  $g(x)$  is fitted to the data shown in Figure 13.2(B). Confluence environments are defined very generally as those listed in Table 13.1 and are not differentiated according to type or magnitude.

Using data for humid environments only for illustration, the regression is:

$$g(x) = 3.79 + 1.96 * \log(t_a/m_a) \quad (13.2)$$

where  $t_a/m_a$  is the ratio of tributary-to-main-stem drainage area (symmetry ratio). Based on this equation, there is an 85 per cent probability that a tributary with a drainage area one-tenth that of the main stem will create a confluence environment (Figure 13.2(C)). The probability decreases to less than 10 per cent for tributary basins with symmetry ratios below 0.001. No distinction is made for location of confluences within the river network and thus deposit survivability or the frequency of sediment pulses that can affect confluence environments; the effect of network structure on stochastic sediment supply is considered later in the chapter.

## Basin shape, network patterns and confluence environments

The scaling relationship between the symmetry ratio of confluent tributaries and the probability of confluence effects (Figure 13.2(C) and Equation 13.2) is used to consider how spatial controls on tributary sizes can influence the distribution of confluence environments within watersheds, specifically the morphological changes listed in Table 13.1. First and foremost, the shapes of drainage basins that correspond to geometric patterns of river networks place first-order constraints on the spatial pattern (number and spacing) of confluence environments. For instance, dendritic networks tend to create heart- or pear-shaped basins (e.g. compact basins), while trellis networks tend to create elongate or rectangular basins (Figure 13.3(A) and (B)). Increasing basin width downstream in compact basins leads to a coalescing of many small channels into channels of increasing size (i.e. increasing stream order) thereby creating larger tributary streams that intersect main-stem channels. A series of larger tributary channels intersecting a main-stem river creates higher symmetry ratios and thus the occurrence of higher probabilities of confluence environments downstream (Figure 13.3(C)). In contrast, basin width does not increase as significantly downstream in rectangular watersheds resulting in less opportunity for encountering larger tributaries, and consequently the symmetry ratio (and thus the probability of confluence environments) should decline downstream (Figure 13.3(C)).

The control of network pattern and basin shape on confluence environments is illustrated in an 1800 km<sup>2</sup> drainage basin in the Oregon Coast Range (USA) using the logistic regression for humid basins (Equation 13.2). The Siuslaw River basin contains both compact and rectangular sub-basins and thus a large range of predicted confluence probabilities (Figure 13.4(A)). In the rectangular basin containing the trellis network, the predicted confluence probabilities get smaller downstream, in most cases below  $p = 0.5$  in the lower half of the basin, and hence there may be few confluence environments in that area (Figure 13.4(B)). In contrast, in the compact sub-basin, the probability of confluence environments starts high at the head of the basin but remains high intermittently (often approaching  $p = 1$ ) due to the intersection of large tributaries in the dendritic network (Figure 13.4(C)).

Confluence environments, however, are not limited to the intersection point between two tributaries, but rather confluence-related landforms and stream morphology can extend downstream considerable distances (Rice *et al.*, 2001; Benda *et al.*, 2003a; Hoffman and Gabet, 2007). To account for this, the statistical confluence model is extended in this chapter to illustrate how the spatial pattern of confluence environments may change downstream in river networks beyond individual confluence points. In this model, tributaries are viewed in terms of sedimentary links with a downstream decay in confluence-related environments, including a decrease in grain size downstream of

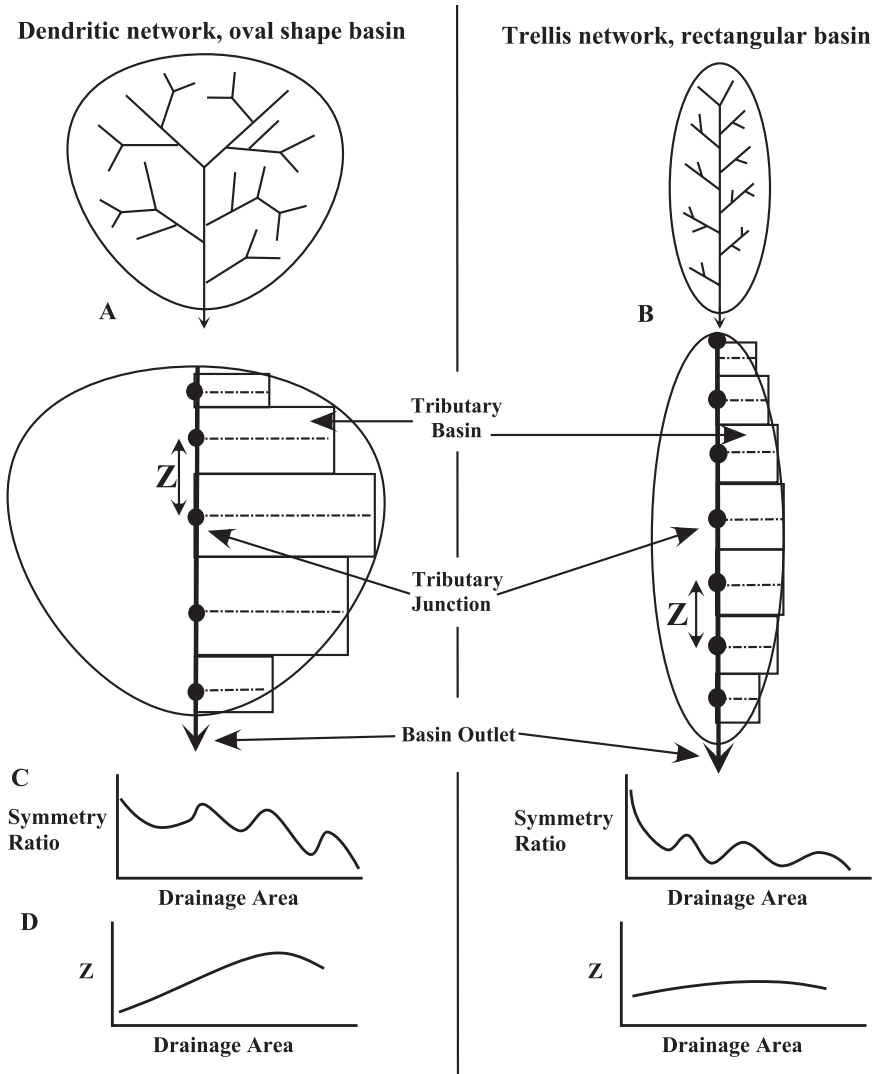


**Figure 13.3** Basin shape and network patterns affect the downstream distribution of tributary basin sizes. (A) Oval basins (with dendritic networks) promote an increase in the size of tributaries (length and width) downstream. (B) Rectangular basins (with trellis networks) limit the sizes of tributaries downstream. (C) Oval basins should promote higher symmetry ratios (and thus a higher probability of confluence environments) downstream compared to trellis networks. (D) Dendritic networks also promote larger spacing,  $z$ , between confluence environments.

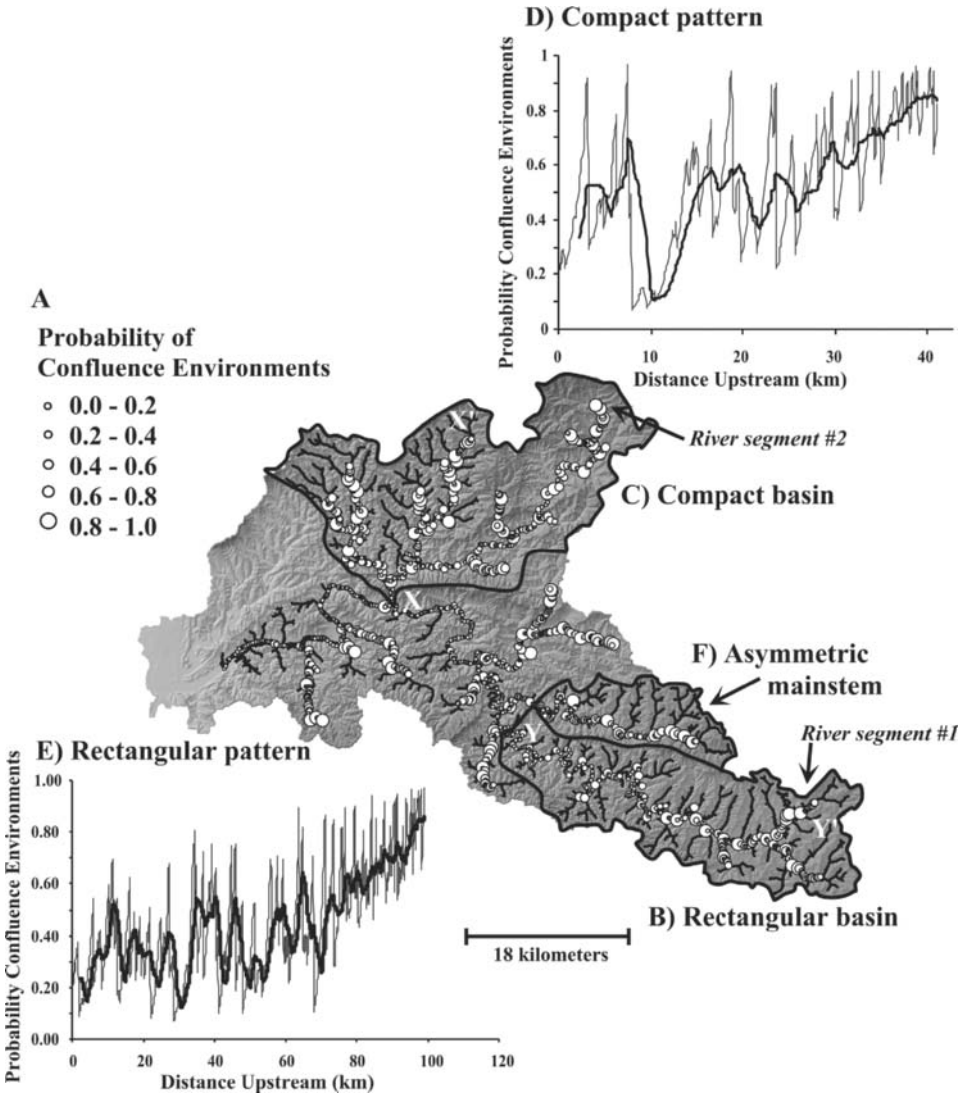


**Figure 13.4** (A) The probability of confluence environments is predicted for an 1800-km<sup>2</sup> basin in the Oregon Coast Range (USA) using the logistic regression in Figure 13.2(C). The compact (C) and rectangular (B) sub-basins have very different downstream patterns of predicted confluence environments. Using an updated model (since Benda *et al.*, 2004b) that predicts the downstream decay of confluence probabilities along the channel network, the longitudinal patterns of confluence environments vary between compact (D) and rectangular (E) basins; the darker, smoother lines represent a 1000-m moving average. The asymmetric location of the main stem within a basin (F) affects patterns of confluence probabilities. River segments #1 and #2 refer to Figure 13.6(C). Maps and plots of confluence environments generated by NetMap. Reproduced from *Forest Sciences*. **53**: 206–209 (2007).

sediment sources, and specifically tributary junctions (*sensu* Rice, 1998; Rice *et al.*, 2001). To apply this concept here, the probability of confluence environments (e.g. Figure 13.2(C)) is applied to main-stem channels downstream of each tributary junction, with a magnitude that decays exponentially with distance downstream from confluences using:

$$p_x = p_{x0}e^{-\alpha x} \quad (13.3)$$

where  $p_x$  is the probability of confluence environments at a distance  $x$  downstream from the tributary,  $p_{x0}$  is the confluence probability associated with specific tributaries and  $\alpha$  is a decay coefficient (also called a 'diminution rate'). A decay coefficient of  $0.5 \text{ km}^{-1}$  is used here for illustration.

Using this updated model in the Siuslaw basin reveals two different patterns of fluctuating confluence environments along channel networks between the trellis (rectangular basin) and dendritic (compact) networks (Figure 13.4). In both networks, the upper region of the basins has the highest frequency and the consistently highest predicted probabilities of confluence environments (Figure 13.4(D) and (E)). This is because numerous, small, headwater tributary confluences have high symmetry ratios, a pattern that breaks down lower in networks as small headwater tributaries encounter increasing main-stem channel sizes. This has implications for the spatial scale of channel morphological diversity driven by confluences, a process discussed later in the chapter. The compact sub-basin in the Siuslaw watershed is characterized by intermittent high probability values of confluence environments downstream (Figure 13.4(D)), corresponding to the conceptual model in Figure 13.3(C). The trellis network in the rectangular basin, in contrast, shows a consistent downstream decline in probabilities of confluence environments (Figure 13.4(E)), also in agreement with the conceptual model (Figure 13.3(C)). Specific fluctuations in confluence probabilities along the channels in both basins reflect variations in local network geometry that create either long stretches of channels with no major junctions or a tight spacing of several large tributaries (e.g. Figure 13.1(D)).

In addition to basin shape and network pattern, the location of the main channel within a basin should also influence the spatial pattern of tributary basin sizes. A channel that is asymmetrically oriented within its basin (Figure 13.4(F)) will reduce tributary sizes (and hence the likelihood of confluence effects) on one side of the basin while increasing tributary sizes (and hence confluence effects) on the other side.

The channel-asymmetry factor, along with different network patterns and basin shapes, illustrates how network structure can potentially organize the spatial distribution of confluence environments in a watershed. Such network factors could be used to create classification systems for differentiating among spatial patterns of potential confluence environments and hence the degree of physical heterogeneity in river systems driven by confluences (e.g. Benda *et al.*, 2007). The relationships among basin

size, network configuration, basin shape and orientation of main-stem rivers can be expressed as a set of testable hypotheses that emphasize river systems as networks comprising confluence and non-confluence environments (see **Discussion**, below).

## Local network geometry

The roles of basin shape and network geometry on confluence environments describe general tendencies about how confluence environments can be organized by the structure of drainage networks. However, local network geometry may cause deviations from these central tendencies (e.g. Figure 13.1(D)). For example, confluence environments can be separated by long distances because of resistant bedrock or the random evolution of river networks (e.g. low probability of confluence environments between 8 and 15 km in the compact basin, Figure 13.4(D)). Likewise, structural controls, such as faults or mechanically weak rocks, may lead to a concentration of confluences in certain parts of networks.

Another aspect of local network geometry, the angle between two intersecting tributaries, may also influence the spatial distribution of confluence environments. Mosley (1976) and Best (1986) document how bar size, bar location and scour depth increased as the confluence angle increased. In addition, confluence angles greater than  $70^\circ$  promoted the deposition of debris flows and the creation of fans at confluences of first- and second-order streams with higher-order channels in a humid mountain landscape (Benda and Cundy, 1990). In headwater areas of watersheds, narrow tributary-junction angles may dominate with the deposition of debris flows creating spatially contiguous valley fills (Lancaster *et al.*, 2001). The opposite appears to hold in larger channels that are characterized by larger tributary-confluence angles (Lubowe, 1964) where discrete fans are more likely to create confluence effects (Bigelow *et al.*, 2007).

The constraint of junction angles on confluence environments has implications for populations of confluences in river networks. Low junction angles, characteristic of parallel and sub-parallel drainage networks (Zernitz, 1932), often in rectangular basins, may reduce the opportunity for confluence environments in contrast to dendritic networks (in oval basins) characterized by higher junction angles that may create a greater likelihood of confluence environments. In general, junction angles increase as the size or stream order of the receiving stream increases, ranging from approximately  $40^\circ$  at stream order one to approximately  $90^\circ$  at stream order four (Lubowe, 1964).

## Drainage and confluence density

Variations in drainage density and hence junction density may influence the occurrence of confluence environments across watersheds (e.g. Figure 13.1(C)). Confluence density should theoretically scale with drainage density, although network patterns could also

moderate this. Drainage densities in semi-arid to humid landscapes can range from approximately 2 to 12 km km<sup>-2</sup>, reflecting variations in climate, vegetation, bedrock and landscape age (Abrahams, 1972; Grant, 1997). Presently, little is known about how confluence density varies across watersheds or landscapes.

For illustration in this chapter, confluence density (number km<sup>-2</sup>) was estimated in sub-basins of the Hunter Creek watershed (115 km<sup>2</sup>) in western Oregon, USA and ranged from less than one to approximately eight (Figure 13.5(A)). Confluence density should reflect drainage density, and the total length of channels in a basin depends on locations of channel heads. To define channel heads in the Hunter Creek basin, the channel head slope–area relationship for the Oregon Coast Range was used (Montgomery and Foufoula-Georgiou, 1993). The variation in total junction density, however, may not relate directly to the variation in the density of confluence environments. For example, the proportion of confluence environments associated with a  $p > 0.7$  (using Equation 13.2) reveals somewhat different patterns and ranged from less than 16 per cent to approximately 70 per cent (Figure 13.5(B)). The highest proportions of predicted confluence environments are generally located in sub-basins at the heads of networks, probably reflecting the concentration of high probability values due to small tributary basins intersecting small- to moderate-size main-stem channels (this effect is also apparent in Figure 13.4(D) and (E)). Overall, there is a weak dependence of junction density with drainage density across the Hunter Creek sub-basins ( $n = 26$ ); a linear regression revealed an  $r^2$  of 0.31.

It is likely that areas of watersheds with higher probabilities of confluence environments should have more confluence-related morphology, thereby affecting fluvial geomorphic processes and associated riverine ecosystems, including differences in channel and valley-floor heterogeneity (Table 13.2).

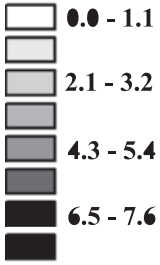
## River network scaling properties of confluence environments

### Separation distance of confluence environments

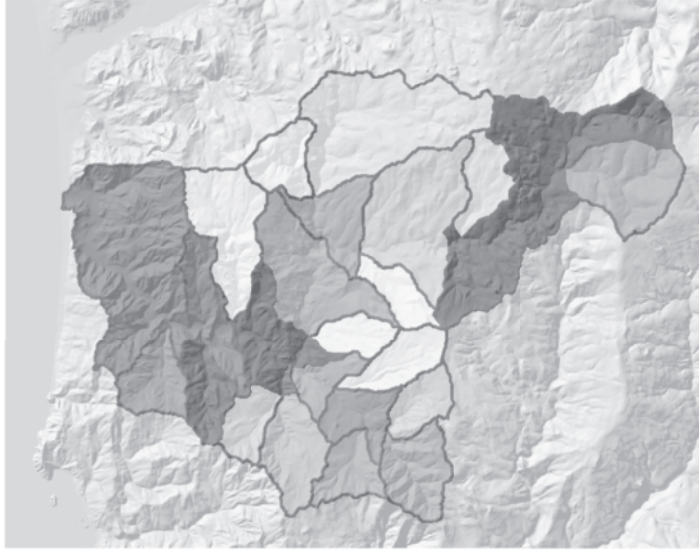
The observation that larger tributary basins are required to create confluence environments in larger main-stem channels (Figure 13.2) introduces a scaling effect in a watershed's confluence environments. Larger tributary basins are characterized by greater length as well as width (Hack, 1957). Thus, tributaries of increasing width take up more space, and therefore confluence environments associated with larger tributaries should be separated by an increasing distance downstream along river channels (Abrahams, 1984). This prediction is apparent in the Siuslaw example (Figure 13.4(D) and (E)) and supported by field data from the studies listed in Table 13.1 (Figure 13.6(A)). For example, in the upper portions of humid drainage basins, confluence environments are

(A)

**Confluence Density**  
(#/km<sup>2</sup>)



0 1.25 2.5 5 Kilometers

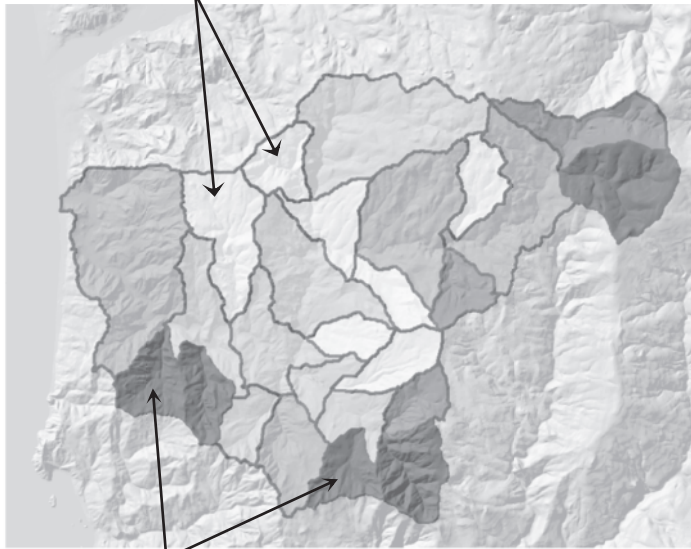


(B)

**Proportion of**  
**Confluences**  
**with P > 0.7**



**Less confluence environments**



**More confluence environments**

**Figure 13.5** (A) Confluence density ( $\# \text{ km}^{-2}$ ) varies across Hunter Creek, a 115-km<sup>2</sup> basin in western Oregon (USA). (B) The proportion of confluence environments with a predicted high probability ( $p > 0.7$ ) shows different spatial patterns; sub-basins with the highest junction density may or may not have the highest density of significant confluences.

**Table 13.2** Combining the geometric structure and scaling properties of river networks with principles of stochastic watershed processes leads to a series of testable hypotheses. Adapted from Benda *et al.*, 2004a.

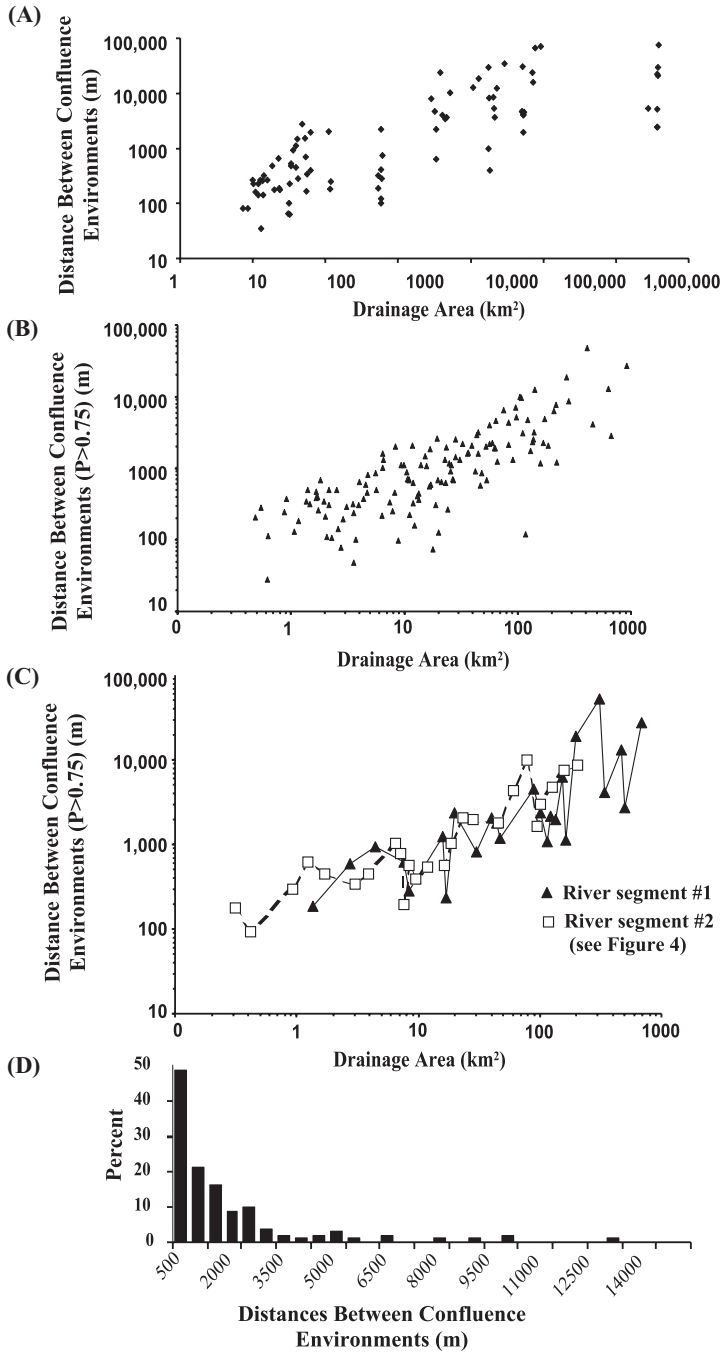
---

**Predictions related to geometric structure and scaling properties of river networks**

- 1) The probability of confluence environments increases with the ratio of tributary to main-stem sizes (symmetry ratio), with all other things being approximately equal.
- 2) Compact basins (i.e. heart- or pear-shaped basins) that contain dendritic networks favour increasing tributary size and hence increasing confluence environments downstream compared to rectangular basins containing trellis or parallel networks.
- 3) Local (km-scale) patterns of tributary intersections can dictate the number and proximity of confluence environments. Closely spaced tributaries will yield valley segments of higher physical heterogeneity compared to valley segments that do not contain closely spaced tributary junctions.
- 4) Basins with higher drainage density and corresponding higher junction density will have more confluence environments.
- 5) The separation distance between confluence environments increases downstream with increasing basin size, particularly in dendritic networks.
- 6) The channel length and area affected by confluence environments will increase with increasing drainage area (at the confluence).
- 7) The overall proportion of channel area affected by confluence environments may be tens of per cent and approach 50 per cent in some regions of networks, although it will likely be less due to the stochastic nature of confluence environments where only a proportion will be active at any one time.
- 8) The law of stream sizes (Horton, 1945) indicates that the majority of confluence environments are located relatively close to one another (less than approximately 500 m) and within relatively small basins ( $< 50 \text{ km}^2$ ).

**Predictions related to stochastic watershed processes**

- 9) In sufficiently large basins ( $\sim 10^2 \text{ km}^2$ ), the age distribution of confluence-related landforms (i.e. fans, terraces, floodplains) will be shifted to older geomorphic features in upper regions of networks and towards younger features in downstream portions of basins (particularly in oval-shaped basins) based on network scaling of sediment supply, transport and storage frequency and magnitude.
  - 10) There may be regions within channel networks that have heightened sediment-supply, -transport and -storage dynamics due to patterns of intersecting tributaries. In dendritic networks, this area may be located in the central portion of the network.
  - 11) Channelized disturbances (i.e. floods and accelerated sediment and wood supply) will have increased frequency and magnitude proximal and immediately downstream of confluences, leading to greater physical heterogeneity, including the age distribution of fluvial landforms.
  - 12) Channelized disturbances will be magnified immediately upstream of significant confluence environments leading to greater physical heterogeneity, including the age distribution of fluvial landforms. Consequently, confluences are disturbance loci because of the mixing and interfering effects of fluxes of water, sediment and organic material.
-



spaced, on average, several hundred metres apart, reflecting the spacing of low-order tributaries prone to debris flows (Hogan *et al.*, 1998; Benda *et al.*, 2003a; Bigelow *et al.*, 2007). In contrast, in larger basins of up to 300 000 km<sup>2</sup>, the distance separating confluence environments is in the order of several kilometres to tens of kilometres (Baxter, 2002; Benda *et al.*, 2003b). The confluence environment model (Figure 13.2(C), Equation 13.2) applied to the Siuslaw watershed and using  $p > 0.75$  as an illustrative threshold for the presence of confluence environments also reveals a pattern of increasing distance between confluence environments as the main-stem's drainage area increases (Figure 13.6(B)). The patterns revealed in Figures 13.6(A) and (B) represent central tendencies, but actual patterns of confluence separation distance are highly variable, depending on local network geometry (Figure 13.6(C)). Nevertheless, the field data and the Siuslaw model show that confluence environments are more closely spaced in smaller streams compared to larger rivers. This highlights the variable spatial scale of morphological diversity driven by confluences in watersheds.

## The law of stream sizes and the spatial scale of morphological diversity related to confluences

Another scaling property of confluence environments relates to the power-law distribution of stream sizes within channel networks (e.g., Horton, 1945). There are many smaller tributaries than larger tributaries within a watershed and consequently the majority of confluence environments should be located relatively close to one another in relatively small basins. For example, in the 1800 km<sup>2</sup> Siuslaw watershed, approximately 50 per cent of tributaries with a large probability of creating confluence effects (e.g.  $p > 0.75$ ) are predicted to be within 500 m of each other in small- to moderate-size basins (Figure 13.6(D)). Confluence separation distances of less than 500 m correspond to main-stem drainage areas of approximately 1 to 50 km<sup>2</sup> in the Siuslaw basin (Figure 13.6(B)). Hence, the spatial scale of morphological diversity created by confluence environments in watersheds is defined by a power law (e.g. Figure 13.6(B)), a pattern reflecting the hierarchical branching of river networks.

←

**Figure 13.6** (A) The distance separating confluence environments increases downstream in the studies listed in Table 13.1. (B) Spacing for tributaries with predicted confluence environments of  $p > 0.75$  increases downstream in the Siuslaw River basin (see also Figure 13.4). (C) Individual river segments in the Siuslaw River basin (starting from headwaters) reveal large variability in spacing of confluence environments (with  $p > 0.75$ ) due to variations in local network geometry (see Figure 13.4 for locations of river segments #1 and #2). (D) The distance between confluence environments (with  $p > 0.75$ ) within the Siuslaw River basin is non-linearly distributed reflecting the power law of stream sizes.

## Longitudinal extent and size of confluence environments

A third scaling property of confluence-related morphology is that the sizes of confluence environments associated with tributaries increase downstream (Figure 13.7). Although the field data are sparse (Studies #1, 5, 6, 11 and 14 in Table 13.1), the length of channels affected by confluences ranges from approximately 100 m in basins less than approximately 10 km<sup>2</sup> to several kilometres in basins between approximately 10 000 and 300 000 km<sup>2</sup> (Figure 13.7). This pattern is anticipated since the channel gradient declines with increasing river size. Hence, any vertical obstruction in a channel that interferes with the transport of sediment or wood (e.g. boulders or woody debris associated with tributary inputs), and thus contributes to the production of a confluence environment, should influence a channel distance upstream at least equivalent to the height of the obstruction divided by the tangent of the underlying stream gradient.

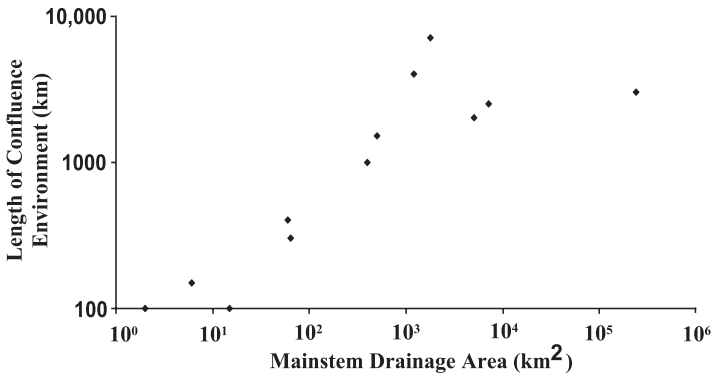


**Figure 13.7** The length of confluence environments increases downstream (data from Table 13.1).

## The relative proportion of confluence environments in networks

Two of the scaling properties described above lead to a third. The proportion of channel length potentially affected by confluences (i.e. physical effects such as changes in grain size, channel slope etc.) along a continuum of drainage areas can be estimated by dividing the length of confluence effects (Figure 13.7) by the average separation distance between confluence environments (Figure 13.6(A)). Linear regressions are fitted to the data on spacing between confluence environments and the length of confluence environments. The estimated proportion of confluence-affected environments in channels according to drainage area remains approximately constant across drainage areas and is about 40 per cent. This is due to the non-linear increase in both confluence-environment separation distance and length that increase similarly downstream. The

proportion of channel length affected by confluences, however, should be strongly influenced by the timing and location of watershed disturbances, such as storms, floods and fires.

There are few field data to compare with the predicted proportion of confluence environments. For moderate-size mountain streams in the Oregon Coast Range (10 km<sup>2</sup>), Bigelow *et al.* (2007) document that debris fans (formed at the mouths of first- and second-order channels) that can affect channel morphology bordered approximately 50 per cent of the channel length. The occurrence of channels intersecting small streams from both sides of the valley often cause overlaps of confluence-related deposits that can increase the difficulty of differentiating one confluence environment from another (Bigelow *et al.*, 2007). At a larger basin scale (450–500 km<sup>2</sup>), Baxter (2002) classifies approximately 20 per cent of the length of the Wenaha River in eastern Oregon, USA as confluence environments.

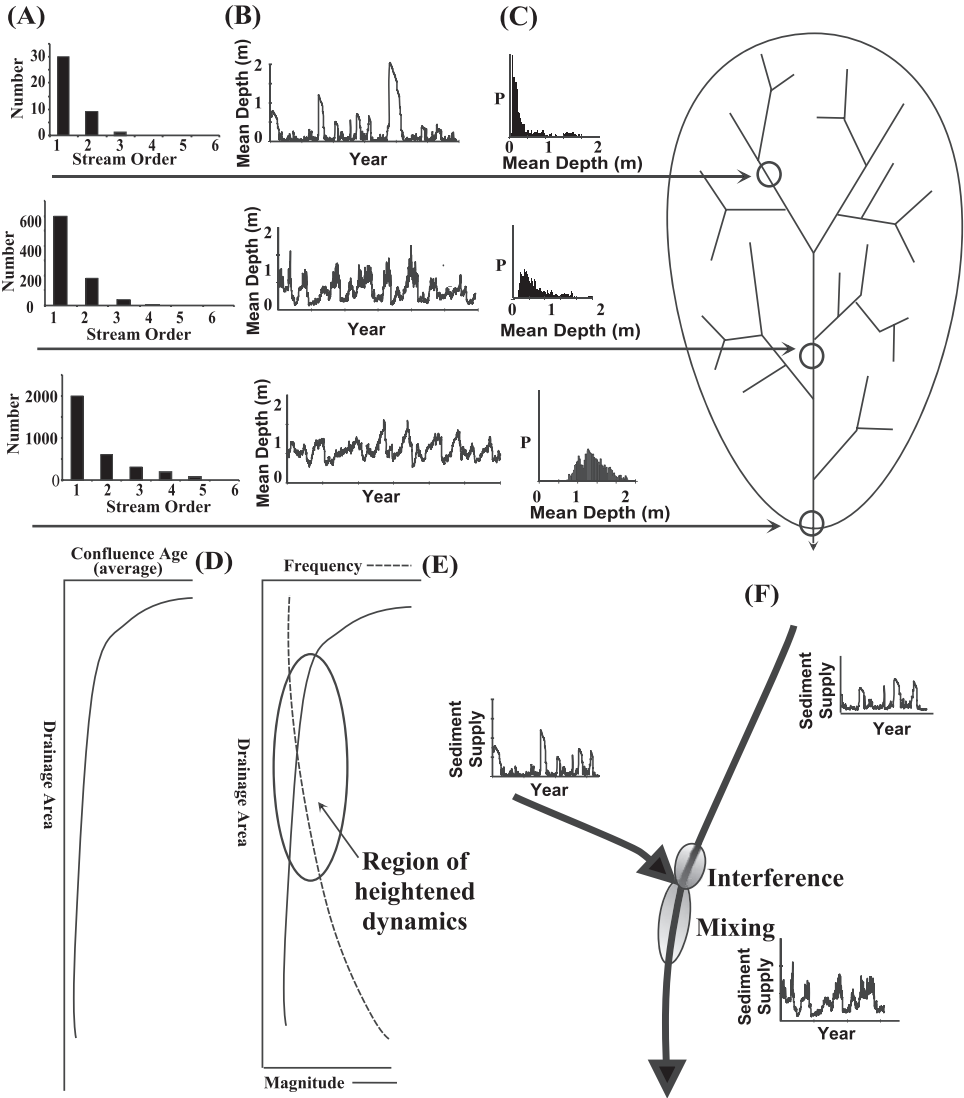
## **Stochastic watershed processes: river network organization of erosion and sediment-supply dynamics**

The preceding portion of this chapter describes controls that river networks can impose on the spatial distribution of confluence environments. Many confluence environments are strongly influenced by the stochastic nature of storms, floods and erosion that create episodic sediment supply and transport, particularly in upland catchments. Consequently, confluence environments may have a distinct temporal dimension that can also vary according to river network structure and basin scale. The role of river network structure on the stochastic dimension of confluence environments is the topic of this section.

It is the episodic nature of sediment and organic material flux that creates many of the observed confluence-related landforms (Miller *et al.*, 2003), particularly in the studies recorded in Table 13.1. For example, the highly episodic nature of debris flows and flash floods driven by large storms creates, at confluences, debris and alluvial fans, fan-induced elevation knickpoints (leading to changes in channel gradients and channel widths), boulder accumulations (leading to rapids), log jams and terraces of various ages (Benda, 1990; Grant and Swanson, 1995; Melis *et al.*, 1995; Benda *et al.*, 2003b; Hoffman and Gabet, 2007). In larger channels, flood events that transport large volumes of bedload create other types of fluvial environments, including persistent changes in channel-substrate size, patterns of bar accumulation (e.g. Church, 1983; Rice, 1998), channel meanders, pools, fans and terraces. Thus, confluence environments can be rejuvenated during and immediately following periods of accelerated supply and transport of sediment, but they can diminish during periods of low watershed disturbance due to the fluvial erosion of confluence-related deposits.

# The role of hierarchical branching networks on the frequency and magnitude of sediment supply, transport and storage

The hierarchical branching of river networks introduces an interesting scaling effect in the frequency and magnitude of sediment supply and thus sediment transport in watersheds. Because of the spatial patchiness and stochastic nature of the climate system



and the heterogeneity of land-surface properties, channels receive a series of sediment pulses over time (rather than a continuous supply of sediment) (Hack and Goodlett, 1960; Dietrich and Dunne, 1978; Pearce and Watson, 1986). In the context of sediment supply to channel networks, the majority of sediment source areas within a hierarchically branching river network are small tributary sub-basins less than one square kilometre in area. Simulation modelling has illustrated that channels receive sediment from a multitude of tributary sources (0.01 to 1 km<sup>2</sup>) over time, the number of which increases rapidly and non-linearly downstream (Figure 13.8(A)). This leads to a fluctuating time series (10<sup>2</sup>–10<sup>3</sup> yr) of sediment supply, transport, and storage in main-stem channels that is illustrated hypothetically in Figure 13.8(B). Upper portions of watersheds with few sediment sources are characterized by infrequent and high-magnitude sediment pulses. With increasing distance downstream, sediment supply and storage fluctuations increase in frequency but decrease in magnitude.

Because of the stochastic nature of storms that trigger erosion, the predicted probability density of sediment supply and storage (defined by frequency and magnitude) is generally right skewed in the upper parts of basins (Figure 13.8(C)) (Benda and Dunne, 1997a). However, the probability density of sediment supply and storage in channels is predicted to evolve downstream from right-skewed (in upper basins) to more symmetrical forms (Figure 13.8(C)). This is because a hierarchical network leads to the summing, or convolution, of the large number of probability densities (e.g. skewed sediment-supply distributions) in headwater basins over time. It is therefore likely that a more symmetrical or normal probability distribution evolves as the number of sediment

---

**Figure 13.8** This figure illustrates aspects of the stochastic dimension of sediment supply and storage downstream in a river network using simulation modelling (adapted from Benda and Dunne, 1997). (A) The number of tributary sediment sources increases rapidly downstream along the North Fork of the Smith River in the central Oregon Coast Range, USA. (B) The computer-simulated time series of sediment supply (represented as channel-sediment storage using channel-sediment depth as a surrogate) is shown at three spatial scales within an actual watershed. Note the variation in frequency, magnitude and average sediment storage with drainage area. (C) Time series of fluctuating sediment storage (depth) in channels are represented by probability density functions. (D) The evolving probability density of sediment flux and storage (C) leads to a hypothesis (Table 13.2): a higher proportion of older confluence-related morphology occurs in upper networks and a higher proportion of younger confluence-related morphology and hence more persistent confluence environments will be found in the lower portions of networks (Benda *et al.*, 2004b). (E) The simulation modelling leads to another hypothesis regarding river network dynamics: the highest frequency of intermediate-size disturbances occurs in the central network potentially creating a zone of heightened channel dynamics (see Table 13.2). (F) An inference that can be drawn from the field data on confluence environments (Figure 13.1, Table 13.1) and simulation modelling is that channel disturbances (from fires, storms and floods) are locally amplified at confluences thus creating unique regions of channel dynamics.

sources increases downstream, a physical manifestation of the central limit theorem (Benda and Dunne, 1997b). Other factors are also involved in this likely downstream shift, including selective transport and temporary sediment storage (e.g. in bars or behind log jams), particle breakdown that causes diffusion and attrition of bed-material pulses downstream, and an increasing store of sediment in larger and lower-gradient channels that reduces the ability of lower-magnitude sediment-supply fluctuations to alter storage and thus channel morphology.

Pulses of channel-sediment supply and corresponding changes in channel-sediment storage that are predicted to increase in frequency but decrease in magnitude downstream have ramifications for the age distribution of confluence-related landforms, including fans, terraces and associated fluvial features. Fans constructed by debris flows or flash floods at outlets of small headwater basins are formed during high-magnitude events having a frequency in the order of many decades to centuries (Wohl and Pearthree, 1991; Benda and Dunne, 1997a; Meyer *et al.*, 2001; May and Gresswell, 2003). Hence, at any point in time, the observed age distribution of fans at the mouths of small basins (and associated confluence-related riparian and fluvial features) should be, by inference, skewed towards older, eroded features (see Figure 13.8(D) and also Figure 11 in Benda *et al.*, 2004b). Moving downstream in larger networks, the skew of sediment supply and storage that rejuvenates confluence environments is predicted to be lower (i.e. higher frequency but lower magnitude) primarily because of an increasing number of runoff-generated floods. Therefore, on average, the age distribution of fans and related fluvial landforms both up- and downstream of confluences at the mouths of larger basins should have a higher proportion of younger- to middle-aged features (perhaps less than 50 to 100 years and commonly in the range of decades). These temporally averaged patterns can be locally altered by very large storms or fires that trigger widespread basin erosion (e.g. during hurricanes; see Hack and Goodlett, 1960). For instance, during periods of wildfires and large storms, the age distribution of fans can shift towards younger ages, and a higher proportion of confluences can significantly affect main-stem channel morphology. Likewise, climate change or changes in landslide rates associated with land use (e.g. Montgomery *et al.*, 2000) should alter the age distribution of fan deposits and hence the degree of physical heterogeneity linked to them (Benda *et al.*, 2003a).

The pattern of sediment-related frequency of channel dynamics increasing downstream while the magnitude diminishes may create a zone in river networks where sediment-related channel (and floodplain) changes may be most pronounced. In the upper network, disturbances may be of the highest magnitude and have the largest geomorphic effect but occur rarely (decades to centuries). In the lower network, disturbances may be of a much lower magnitude, occur commonly (years) but do relatively less geomorphic work. Thus, there may be a region in the central part of the network where intermediate-magnitude, sediment-related disturbances (that can trigger changes in channel and floodplain morphology), including at confluences, occur with

a sufficient frequency (decades) to create a zone of highest sediment-supply, -transport and -storage dynamics (Figure 13.8(E)) (see hypotheses in Table 13.2).

## Discussion

### Confluence environments in the context of river networks: testable hypotheses

The relationships among network structure, the scaling properties of river networks, stochastic watershed processes and the spatial and temporal organization of confluence environments can be cast as a set of testable hypotheses. The most fundamental hypothesis is that as the ratio of tributary-to-main-stem drainage area increases so does the probability of observing a confluence effect (Hypothesis #1, Table 13.2), although the disturbance regime in a watershed should influence the probability. There are a series of more interesting hypotheses pertaining to how basin shape, network geometry (including drainage density) and stream-scaling laws may influence the spatial pattern of confluence environments and confluence-related heterogeneity in river basins (Hypotheses #2–8, Table 13.2). Stochastic watershed processes reflecting regional-disturbance regimes, basin size and network geometry also lead to testable hypotheses about the organization of confluence environments. For example, a higher frequency of lower-magnitude sediment pulses is predicted to lead to a higher proportion of younger-age confluence environments in the lower portion of river networks (Hypothesis #9, Table 13.2).

For the most part, these hypotheses pertain to the characteristics of populations of confluences within a large watershed or across a series of watersheds. They will be challenging to evaluate, considering the intensity of field analysis that may be necessary. Even determining how a single confluence environment (or a contiguous series of confluence environments) affects the morphology of channels is not trivial, based on the detailed information that must be collected and analysed (e.g. Rice *et al.*, 2001; Benda *et al.*, 2003a; Kiffney *et al.*, 2006; Hoffman and Gabet, 2007). In addition, since confluence environments can wax and wane based on the time that has elapsed since the last local disturbance, the historical timing of watershed events, such as storms, floods and fires, introduces additional complexity to the analyses of confluence environments in space and time. Despite the potential difficulties, the study of the river network organization of geomorphic processes (and related ecological processes) at confluences should prove fruitful but may require new and innovative types of analyses. For example, high-resolution topographic data (light detection and ranging, or LiDAR) may prove valuable in resolving confluence effects over large geographic areas. See Torgersen *et al.*, Chapter 9, this volume, for further consideration of this issue.

## **A network runs through it: support for emerging concepts in watershed and river ecology**

Principles of geomorphology have provided the physical templates for river ecology. A good example is the River Continuum Concept (RCC; Vannote *et al.*, 1980), which was based on early principles of fluvial geomorphology that emphasized spatially and temporally averaged downstream changes in channel morphology over many orders of magnitude (e.g. Leopold *et al.*, 1964). The RCC emphasized gradual adjustments of biota and ecosystem processes in rivers and de-emphasized habitat dynamics and heterogeneity. The linear-homogeneous (non-network-variable) perspective embodied in the RCC dominated river ecology in the latter portion of the twentieth century (Fisher, 1997), despite the fact that downstream interruptions in channel and valley morphology due to a host of factors including tributary confluences and alternating canyons and floodplains have long been observed (Bruns *et al.*, 1984; Minshall *et al.*, 1985; Perry and Schaeffer, 1987).

In what amounted to a marked evolution in riverine ecology during the two decades straddling the turn of the century, current perspectives focus on physical and biological heterogeneity, dynamics (disturbance) and scale, described variously as: (1) 'hierarchical patch dynamics' (Frissel *et al.*, 1986; Wu and Loucks, 1995; Townsend, 1989; Poole, 2002), (2) 'riverscapes', or a landscape view of rivers that embrace physical heterogeneity (Schlosser, 1991; Ward *et al.*, 2002; Fausch *et al.*, 2002; Wiens, 2002) and (3) 'natural disturbance', or dynamics in aquatic systems (Resh *et al.*, 1988; Reeves *et al.*, 1995; Poff *et al.*, 1997). Geomorphic perspectives that evaluate rivers as networks affecting fluvial processes, forms and physical heterogeneity driven by drainage structure, scaling properties and dynamic processes can provide support for emerging perspectives in river ecology. Future advances in the fields of geomorphology and river ecology may consider how network structure organizes other watershed processes relevant to aquatic and riparian environments, such as longitudinal profiles, valley morphology and the flux and storage of organic material. Conceptual and numerical frameworks that consider rivers as networks but circumscribed within watersheds containing variation in lithology, topography, climate and vegetation await further development and refinement.

## **River networks, resource management and river restoration**

One obvious application for emerging geomorphic and ecological principles that focus on rivers as networks and on watershed dynamics is in the field of river restoration. Significant time and capital are spent on the restoration of watersheds and their stream networks to reverse decades and sometimes centuries of the impact of human land use on aquatic ecosystems. One pervasive impact is the reduction of riverine diversity through diking, dredging, the removal of log jams and damming. Consequently, a major objective of restoration has been to restore heterogeneity to near-natural levels.

Because of the recognized importance of confluences in creating riverine heterogeneity, restoration might be focused on maintaining certain watershed processes that maintain confluence environments.

Another objective of river restoration is to focus energy in the best places (i.e. to restore the intrinsically best habitats). Although in an early stage of investigation, tributary confluences appear to be one type of biological hotspot for a variety of reasons, including thermal refugia, physical heterogeneity (and hence biological diversity) and dispersal corridors (see Rice *et al.*, Chapter 11, this volume). Consequently, an improved understanding about how confluences function over time and how confluence environments are organized within networks can help when planning and implementing watershed and channel restoration projects. Specifically, adding confluence environments to stream and habitat classification systems and computerized terrain analysis could highlight the geomorphological and ecological relevance of confluence environments and thus the ecosystem significance of stream networks, basin shapes, sizes and disturbance regimes (e.g. Bigelow *et al.*, 2007; Benda *et al.*, 2007).

## Acknowledgements

This chapter draws heavily on many published studies of confluence environments (Table 13.1) and on several recent papers on confluence environments at network scales (Benda *et al.*, 2004a, 2004b). I would like to acknowledge the contribution of all those authors and co-authors, specifically pertaining to the network papers including LeRoy Poff, Daniel Miller, Kevin Andras, Thomas Dunne, Gordon Reeves, Paul Bigelow, George Pess and Michael Pollock. This chapter was improved by comments and suggestions from an anonymous reviewer and co-editor Steve Rice.

## References

- Abrahams AD. 1972. Drainage densities and sediment yields in eastern Australia. *Australian Geographical Studies* **10**: 19–41.
- Abrahams AD. 1984. Channel networks: A geomorphological perspective. *Water Resources Research* **20**: 161–188.
- Baxter CV. 2002. *Fish movement and assemblage dynamics in a Pacific Northwest Riverscape*, Doctoral Dissertation, Oregon State University, Corvallis, OR.
- Benda L. 1990. The influence of debris flows on channels and valley floors in the Oregon coast range, USA. *Earth Surface Processes and Landforms* **15**: 457–466.
- Benda L, Cundy TW. 1990. Predicting deposition of debris flows in mountain channels. *Canadian Geotechnical Journal* **27**: 409–417.
- Benda L, Dunne T. 1997a. Stochastic forcing of sediment routing and storage in channel networks. *Water Resources Research* **33**: 2865–2880.
- Benda L, Dunne T. 1997b. Stochastic forcing of sediment supply to channel networks from landsliding and debris flow. *Water Resources Research* **33**: 2849–2863.

- Benda L, Veldhuisen C, Black J. 2003a. Debris flows as agents of morphological heterogeneity at low-order confluences, Olympic Mountains, Washington. *Geological Society of America Bulletin* **115**: 1110–1121.
- Benda L, Miller D, Bigelow P, Andrus K. 2003b. Effects of Post-Wildfire Erosion on Channel Environments, Boise River, Idaho. *Journal of Forest Ecology and Management* **178**: 105–119.
- Benda, L, Miller D, Dunne T, Poff L, Reeves G, Pess G, Pollock M. 2004a. Network dynamics hypothesis: How channel networks structure river habitats. *BioScience* **54**: 413–428.
- Benda L, Andras K, Miller D, Bigelow P. 2004b. Confluence effects in rivers: Interactions of basin scale, network geometry, and disturbance regimes. *Water Resources Research* **40**: W05402. DOI: 10.1029/2003WR002583.
- Benda L, Miller D, Andras K, Bigelow P, Reeves G, Michael D. 2007. NetMap: A new tool in support of watershed analysis and resource management. *Forest Science* **53**: 206–219.
- Best JL. 1986. Sediment transport and bed morphology at river channel confluences. *Sedimentology* **35**: 481–498.
- Best JL. 1988. Sediment transport and bed morphology at river channel confluences. *Sedimentology* **35**: 481–498.
- Bigelow P, Benda L, Miller D, Reeves G, Burnett K. 2007. On the constructive effects of debris flows in aquatic habitats. *Forest Science* **53**: 239–253.
- Booth DB, Bell K, Whipple KX. 1991. *Sediment transport along the South Fork and Mainstem of the Snoqualmie River*. King County Surface Water Management Division: Seattle, Washington.
- Bruns DA, Minshall GW, Cushing CE, Cummins KW, Brock JT, Vannote RC. 1984. Tributaries as modifiers of the river continuum concept: Analysis by polar ordination and regression models. *Archiv für Hydrobiologie* **99**: 208–220.
- Bull WB. 1977. The alluvial fan environment. *Progress in Physical Geography* **1**: 222–270.
- Church M. 1983. Pattern of instability in a wandering gravel bed channel. In *Modern and Ancient Fluvial Systems*, Collinson JD, Lewin J (eds). Blackwell: Oxford; 169–180.
- Dietrich WE, Dunne T. 1978. Sediment budget for a small catchment in mountainous terrain. *Zeitschrift für Geomorphologie Supplemenaryt Band* **29**: 191–206.
- Everest FH, Meehan WR. 1981. Forest management and anadromous fish habitat productivity. In *Transactions of the 46th North American Wildlife and Natural Resources Conference*; 521–530.
- Fausch, KD, Torgersen CE, Li H. 2002. Landscapes to riverscapes: Bridging the gap between research and conservation of stream fishes. *BioScience* **52**: 483–498.
- Fisher SG. 1997. Creativity, idea generation, and the functional morphology of streams. *Journal of North American Benthological Society* **16**: 305–318.
- Frissell CA, Liss WJ, Warren WJ, Hurley MD. 1986. A Hierarchical Framework for Stream Habitat Classification: Viewing Streams in a Watershed Context. *Environmental Management* **10**: 199–214.
- Grant G. 1997. A geomorphic basis for interpreting the hydrologic behavior of large river basins. In *River Quality: Dynamics and Restoration*, Laenen A, Dunnette DA (eds). CRC Press Inc.: Boca Raton, FL; 105–119.
- Grant GE, Swanson FJ. 1995. Morphology and processes of valley floors in mountain streams, Western Cascades, Oregon. In *Natural and Anthropogenic Influences in Fluvial Geomorphology, Geophysical Monograph Series 89*, Costa JE, Miller AJ, Potter KW, Wilcock PR (eds). American Geophysical Union: Washington; 83–101.
- Grimm MM, Wohl EE, Jarett RD. 1995. Coarse-sediment deposition as evidence of an elevation limit for flash flooding, Bear Creek, Colorado. *Geomorphology* **14**: 199–210.

- Hack JT. 1957. Studies of longitudinal stream profiles in Virginia and Maryland. United States Geological Survey Professional Paper, 294B.
- Hack JT, Goodlett JC. 1960. *Geomorphology and Forest Ecology of a Mountain Region in the Central Appalachians*. Geological Survey Professional Paper 347, United States Geological Survey.
- Hogan DL, Bird SA, Hassan MA. 1998. Spatial and temporal evolution of small coastal gravel-bed streams: The influence of forest management on channel morphology and fish habitats. In *Gravel-Bed Rivers in the Environment, Gravel Bed Rivers IV*, Klingeman PC, Beschta RL, Komar PD, Bradley JB (eds). Water Resources Publications: Highlands Ranch, CO, USA; 365–392.
- Hoffman DF, Gabet EJ. 2007. Effects of sediment pulses on channel morphology in gravel bed rivers. *Geological Society of America Bulletin* **119**: 116–125.
- Horton RE. 1945. Hydrophysical approach to the morphology of hillslopes and drainage basins. *Geological Society of America Bulletin* **56**: 275–370.
- Kiffney PM, Greene CM, Hall JE, Davies JR. 2006. Tributary streams create spatial discontinuities in habitat, biological productivity, and diversity in mainstem rivers. *Canadian Journal of Fisheries and Aquatic Science* **63**: 2518–2530.
- Lancaster S, Hayes SK, Grant GE. 2001. Modeling sediment and wood storage and dynamics in small mountainous watersheds. In *Geomorphic Processes and Riverine Habitat*, Dorava JM, Montgomery DR, Palcsak BB, Fitzpatrick FA (eds). American Geophysical Union: Washington DC.; 85–102.
- Leopold LB, Wolman MG, Miller JP. 1964. *Fluvial Processes in Geomorphology*. H.W. Freeman: San Francisco.
- Lubow J. 1964. Stream junction angles in the dendritic drainage pattern. *American Journal of Science* **262**: 325–339.
- May CL, Gresswell RE. 2003. Processes and Rates of Sediment and Wood Accumulation in Headwater Streams of the Oregon Coast Range, USA. *Earth Surface Process and Landforms* **28**: 409–424.
- Melis TS, Webb RH, Griffiths PG, Wise TW. 1995. *Magnitude and frequency data for historic debris flows in Grand Canyon National Park and Vicinity, Arizona*. Water-Resources Investigations Report 94-4214, US Geological Survey.
- Meyer GA, Leidecker ME. 1999. Fluvial terraces along the Middle Fork Salmon River, Idaho, and their relation to glaciation, landslide dams, and incision rates: A preliminary analysis and river-mile guide. In *Guidebook to the Geology of Eastern Idaho*, Hughes SS, and Thackray G.D (eds). Idaho Museum of Natural History: Pocatello, Idaho; 219–235.
- Meyer GA, Pierce JL. 2003. Climatic controls on fire-induced sediment pulses in Yellowstone National Park and Central Idaho: A long-term perspective. *Forest Ecology and Management* **178**: 89–104.
- Meyer GA, Pierce JL, Wood SH, Jull AJT. 2001. Fires, storms, and sediment yield in the Idaho batholith. *Hydrological Processes* **15**: 3025–3038.
- Miller DJ, Luce CH, Benda LE. 2003. Time, space, and episodicity of physical disturbance in streams. *Forest Ecology and Management* **178**: 121–140.
- Miller JP. 1958. *High Mountain Streams: Effects of Geology on Channel Characteristics and Bed Material*. Socorro: New Mexico.
- Minshall WG, Cummins KW, Peterson BJ, Cushing CE, Bruns DA, Sedell JR, Vannote RL. 1985. Developments in stream ecosystem theory. *Canadian Journal of Fisheries and Aquatic Sciences* **42**: 1045–1055.
- Montgomery DR, Foufoula-Georgiou E. 1993. Channel network source representation using digital elevation models. *Water Resources Research* **29**: 3925–3934.

- Montgomery DR, Schmidt KM, Greenberg HM, Dietrich WE. 2000. Forest clearing and regional landsliding. *Geology* **28**: 311–314.
- Mosley MP. 1976. An experimental study of channel confluences. *Journal of Geology* **84**: 535–562.
- Pearce AJ, Watson A. 1986. Geomorphic effectiveness of erosion and sedimentation events. *Journal of Water Resources* **5**: 551–567.
- Perry JA, Schaeffer DJ. 1987. The longitudinal distribution of riverine benthos – a river dis-continuum. *Hydrobiologia* **148**: 257–268
- Poff NL, Allen JD, Bain MB, Karr J, Prestegard KL, Richter BD, Sparks RE, Stromberg JC. 1997. The natural flow regime: A paradigm for river conservation and restoration. *BioScience* **47**: 769–784.
- Poole GC. 2002. Fluvial landscape ecology: Addressing uniqueness within the river discontinuum. *Freshwater Biology* **47**: 641–660.
- Reeves G, Benda L, Burnett K, Bisson P, Sedell J. 1995. A disturbance-based ecosystem approach to maintaining and restoring freshwater habitats of evolutionarily significant units of anadromous salmonids in the Pacific Northwest. In *Evolution and the Aquatic System: Defining Unique Units in Population Conservation*. American Fisheries Society Symposium **17**: 334–349.
- Resh VH, Brown AV, Covich AP, Gurtz ME, Li HW, Minshall GW, Reice SR, Sheldon AL, Wallace JB, Wissmar R. 1988. The role of disturbance in stream ecology. *Journal of the North American Benthological Society* **7**: 433–455.
- Rhoads BL. 1987. Changes in stream characteristics at tributary junctions. *Physical Geography* **8**: 346–361.
- Rice SP. 1998. Which tributaries disrupt downstream fining along gravel-bed rivers? *Geomorphology* **22**: 39–56.
- Rice SP, Greenwood MT, Joyce CB. 2001. Tributaries, sediment sources, and the longitudinal organization of macroinvertebrate fauna along river systems. *Canadian Journal of Fisheries and Aquatic Sciences* **58**: 828–840.
- Rice SP, Ferguson RI, Hoey TB. 2006. Tributary control of physical heterogeneity and biological diversity at river confluences. *Canadian Journal of Fisheries and Aquatic Sciences* **63**: 2553–2566.
- Roy AG, Woldenberg MJ. 1986. A model for changes in channel form at a river confluence. *Journal of Geology* **94**: 402–411.
- Schlosser IJ. 1991. Stream Fish Ecology: A Landscape Perspective. *BioScience* **41**: 704–712.
- Strahler AN. 1952. Hypsometric (area-altitude) analysis of erosional topography. *Geological Society of America Bulletin* **63**: 1117–1142.
- Townsend CR. 1989. The patch dynamics concept of stream community ecology. *Journal of the North American Benthological Society* **8**: 36–50.
- Vannote RL, Minshall GW, Cummins, KW, Sedell JR, Cushing CE. 1980. The River Continuum Concept. *Canadian Journal of Fisheries and Aquatic Sciences* **37**: 130–137.
- Ward JV, Tockner K, Arscott DB, Claret C. 2002. Riverine landscape diversity. *Freshwater Biology* **47**: 517–539.
- Wiens JA. 2002. Riverine landscapes: Taking landscape ecology into the water. *Freshwater Biology* **47**: 501–515.
- Wohl EE, Pearthree, PP. 1991. Debris flows as geomorphic agents in the Huachuca Mountains of southeastern Arizona. *Geomorphology* **4**: 273–292.
- Wu JG, Loucks OL. 1995. From balance of nature to hierarchical patch dynamics: A paradigm shift in ecology. *Quarterly Review of Biology* **70**: 439–466.
- Zernitz E. 1932. Drainage patterns and their significance. *Journal of Geology* **40**: 498–521.

# **III**

## **Channel Networks**



# 14

## Introduction to Part III: channel networks

**Bruce L. Rhoads**

*Department of Geography, University of Illinois, USA*

### Introduction

Since the cycle of erosion was proposed by William Morris Davis (1899), the structure and development of drainage networks has been of central concern in geomorphology. Davis viewed the development of stream networks as a necessary consequence of the evolutionary 'maturation' of landscapes via fluvial erosion. Glock (1931) expanded Davis's framework to provide a detailed conceptual model on the evolutionary development of networks. The seminal work by Robert Horton (1945) grounded the study of network development on principles of physics and ushered in an era of the quantitative analysis of networks led by Art Strahler (1952, 1964) and his students (Schumm, 1956; Morisawa, 1964; Woldenberg, 1969). The development and testing of the random topology model, which focused on the arrangement of stream segments within drainage networks, dominated inquiry from the mid-1960s (Shreve, 1966, 1967) through to the early 1980s (see Abrahams, 1984 for an overview). A growing dissatisfaction with this statistical approach to network analysis led to the emergence of process-oriented studies of drainage networks. The major themes of this work include the influence of drainage-network structure on hydrological response, the dynamics of sediment transfer within drainage networks, the dispersion of solutes through networks, the modelling of drainage-network development in the context of landscape evolution

and the formation of fluvial networks on other planets, especially Mars. These themes provide the basis for the five chapters in the final section of this volume.

## Individual chapters

The structure of a drainage network can be viewed as a filter for inputs of runoff from hillslopes that transforms these inputs into a pattern of watershed output, known as a 'hydrograph'. This idea provides the foundation for modelling watershed runoff based on the concept of a geomorphologic instantaneous unit hydrograph (Rodríguez-Iturbe and Valdes, 1979). The primary effect of the stream network is to act as a dispersive filter for runoff by creating differences in travel times of water to the basin outlet as it moves along discrete pathways through the network. In the lead chapter, Saco and Kumar (Chapter 15, this volume) provide a critical overview of how the research into geomorphological influences of watershed, channel and stream-network properties on hydrological dispersion has evolved since the 1980s and also identify future directions for research into the connection between geomorphology and hydrology. Linking dispersive hydrological processes with space–time variability in rainfall characteristics and with sediment dynamics are two important issues warranting further investigation.

The linkages among sediment dynamics, hillslope, and channel networks are examined by Lu and Richards (Chapter 16, this volume). Most attempts to evaluate the connection between upland erosion and sediment yield have been based on the concept of the sediment-delivery ratio, which treats the watershed as a black-box 'sink' that traps a certain percentage of sediment on an average annual basis on its way to the outlet. Some attempts have been made to refine this conception, mostly through the notion of a spatially distributed sediment budget (Trimble, 1983) that partitions sinks and sources of sediment throughout watersheds. Most of this work has been empirical, however, and little or no attempt has been made to model sediment dynamics at the watershed scale. Building on work by Lu *et al.* (2005), Lu and Richards (Chapter 16, this volume) describe a model that treats sediment dynamics within an event-based, spatially distributed framework. Their simple model contains only two sediment stores: one for hillslopes and the other for the channel network, but the basic framework can readily be extended to partition the watershed system into multiple stores representing different parts of the hillslope and channel system.

The dispersion of solutes in river systems should have a close connection with hydrological dispersion. Gooseff *et al.* (Chapter 18, this volume) explore this issue in detail, emphasizing differences in the processes that control solute dynamics at different locations in river networks. At the network scale, systematic downstream changes in channel morphology, flow hydraulics and hyporheic exchange result in general patterns of solute transport. Local complexity at the reach scale, including the influence of stream confluences, often produces substantial departures from network-scale trends. The

relationship between local- and network-scale controls is a problem in need of further investigation.

Over geological timescales, geomorphological and hydrological processes interact via the dynamics of drainage-basin and channel-network evolution. The rapid growth in computer-based modelling in geomorphology has produced a veritable explosion of research on this topic. Gasparini *et al.* (Chapter 17, this volume) use the CHILD numerical model to predict the changes that might occur in channel slope, grain-size characteristics and sediment load at the network scale in response to a change in climate, namely an increase in precipitation. The predictions show that transient responses to the precipitation increase are complex, varying with position in the channel network. The complex response noted here expands empirical ideas on network-scale channel dynamics proposed by Schumm (1973) and provides a caution for interpreting past climate changes from empirical evidence on changes in channel slope or grain size.

Channel networks are not unique to Earth, but have been documented on other planets, especially Mars. Irwin *et al.* (Chapter 19, this volume) highlight that the networks on Mars are clearly fluvial features. The fluvial erosion of ancient surfaces of Mars was episodic and perhaps discontinuous; thus, many networks are less well developed than those on Earth and strongly reflect an imposed topography that formed billions of years ago. The channels and networks of Mars provide an extraordinary opportunity to investigate fluvial erosion under circumstances that differ from conditions on Earth. Such investigations have only just begun.

## References

- Abrahams AD. 1984. Channel networks: A geomorphological perspective. *Water Resources Research* **20**: 161–188.
- Davis WM. 1899. The geographical cycle. *Geographical Journal* **14**: 481–504.
- Glock WS. 1931. The development of drainage systems: A synoptic view. *Geographical Review* **21**: 475–482.
- Horton RE. 1945. Erosional development of streams and their drainage basins: Hydrophysical approach to quantitative morphology. *Geological Society of America Bulletin* **56**: 275–370.
- Lu H, Moran CJ, Sivapalan M. 2005. A theoretical exploration of catchment-scale sediment delivery. *Water Resources Research* **41**: W09415. DOI: 10.1029/2005WR004018.
- Morisawa ME. 1964. Development of drainage systems on an upraised lake floor. *American Journal of Science* **262**: 340–354.
- Rodríguez-Iturbe I, Valdes JB. 1979. The geomorphological structure of hydrological response. *Water Resources Research* **15**: 1409–1420.
- Schumm SA. 1956. Evolution of drainage systems and slopes in badlands at Perth Amboy, New Jersey. *Geological Society of America Bulletin* **67**: 597–646.
- Schumm SA. 1973. Geomorphic thresholds and the complex response of drainage systems. In *Fluvial Geomorphology*, Morisawa M (ed.). New York State University Publications in Geomorphology: Binghamton; 299–310.

- Shreve RL. 1966. Statistical law of stream numbers. *Journal of Geology* **74**: 17–37.
- Shreve RL. 1967. Infinite topologically random channel networks. *Journal of Geology* **75**: 178–186.
- Strahler AN. 1952. Hypsometric (area-altitude) analysis of erosional topography. *Geological Society of America Bulletin* **63**: 1117–1142.
- Strahler AN. 1964. Quantitative geomorphology of drainage basins and channel networks. In *Handbook of Applied Hydrology*, Chow VT (ed.). McGraw-Hill: New York; 4-39–4-76.
- Trimble SW. 1983. A sediment budget for Coon Creek basin in the driftless area, Wisconsin, 1853–1977. *American Journal of Science* **283**: 454–74.
- Woldenberg MJ. 1969. Spatial order in fluvial systems: Horton's laws derived from mixed hexagonal hierarchies of drainage basin areas. *Geological Society of American Bulletin* **80**: 97–112.

# 15

## Hydrologic dispersion in fluvial networks

**Patricia M. Saco<sup>1</sup> and Praveen Kumar<sup>2</sup>**

<sup>1</sup>*Civil and Environmental Engineering, School of Engineering, University of Newcastle, Australia*

<sup>2</sup>*Environmental Hydrology and Hydraulic Engineering, Department of Civil and Environmental Engineering, University of Illinois, USA*

### Hydrologic dispersion effects on runoff response

This chapter attempts to bring together and summarize the results from recent research analysing the role of hillslope, channel and network processes on the hydrologic response of basins (Wang *et al.*, 1981; Mesa and Mifflin, 1986; van der Tak and Bras, 1990; JIN, 1992; Naden, 1992; Robinson *et al.*, 1995; Yen and Lee, 1997, among others). In doing so, particular emphasis is placed on understanding how different processes act at various scales, from individual channels to the network scale, to produce the dispersive, or ‘spreading’, effects that shape the basin’s hydrologic response. These processes not only have an impact on the hydrograph’s shape by determining the way water is routed to the outlet but also on the way sediments, nutrients, chemicals, aquatic organisms, seeds, bacteria and a number of other substances are redistributed along the basin and/or transported to the outlet by the flow. Consequently, the advances presented in this chapter are relevant not only for hydrology and other fields like fluvial geomorphology and ecology but also for interdisciplinary research in a number of emerging fields, like ecohydrology hydroecology and ecogeomorphology.

Overland or surface flow is potentially produced by every point in the basin and delivered to the channels composing the stream network, through which it is transported to the basin's outlet. It is the combined effect of the transport processes through both hillslopes and the network of channels that shapes the hydrologic response of river basins. The effect of the geomorphologic characteristics of the river network on the hydrologic response was first studied by Kirkby (1976) and Lee and Delleur (1976). However, the complete formalization of these effects within the framework of the instantaneous unit hydrograph (IUH) was first achieved with the development of the theory of the geomorphologic instantaneous unit hydrograph (GIUH). The GIUH (Rodriguez-Iturbe and Valdes, 1979; Gupta *et al.*, 1980) provided a significant leap forward in hydrologic science because for the first time the basin's IUH was analytically linked to the geomorphologic structure of the river network.

Hydrologic dispersion is the combined effect of all the dispersive mechanisms that produce spread in the travel times of water drops to the watershed's outlet and, consequently, it has a direct impact on the shape of the direct runoff hydrograph. At the scale of individual channels, surface flow experiences both advective and dispersive processes. In the case of pure advection, an input water wave (i.e. a hydrograph) at the channel inlet is routed downstream without changing its shape. In this case, all the water drops entering the channel have the same velocity and equal travel times to the channel outlet. Hydrodynamic dispersion processes account for the effects of storage, turbulence and shear stresses. Owing to these effects, some of the water drops entering the channel travel slower than others, producing spread in the distribution of arrival times at the channel's outlet. Figure 15.1a shows the effect of hydrodynamic dispersion on the hydrologic response of individual channels.

At the scale of a watershed, the existence of a network of channels has a direct impact on the hydrograph owing to the spreading effect induced by the existence of numerous different pathways for water travelling to the basin outlet (Figure 15.1b). In this case, hydrologic dispersion effects are due to both hydrodynamic dispersive processes and network dispersive processes arising from the variability of travel times along different flowpaths. The concept of geomorphologic dispersion (Rinaldo *et al.*, 1991; Snell and Sivapalan, 1994) explains the effect of variable travel distances along different pathways on the hydrologic response (Figure 15.2a). The concept of kinematic dispersion (Saco and Kumar, 2002a and b; 2004; Snell *et al.*, 2004) is an additional form of network dispersion that arises due the effect of velocities varying in different channels along the network (Figure 15.2b). Figure 15.2c represents the network spreading effect of both geomorphologic dispersion (quantified by the geomorphologic dispersion coefficient  $D_G$ ) and kinematic dispersion (quantified by the kinematic dispersion coefficient  $D_K$ ) on the total hydrologic dispersion of the hydrograph. It is the combination of these three hydrologic dispersive processes (hydrodynamic, geomorphologic and kinematic dispersion) that characterizes the spread of the watershed's hydrograph (Figure 15.2d). Hydrologic dispersion has an impact not only on the duration of the hydrograph but

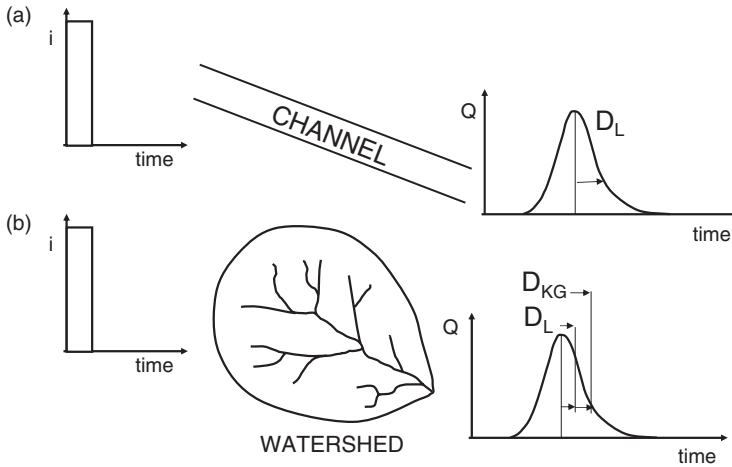


**Figure 15.1** Schematic adapted from White *et al.* (2004), showing the different contributions to hydrologic dispersion in channels and watersheds. (a) For individual channels, the total variance of the arrival time distribution is induced by hydrodynamic dispersion effects only (captured by the hydrodynamic-dispersion coefficient  $D_L$ ). (b) In a watershed, the total variance of the arrival time distribution is induced by both hydrodynamic dispersion effects and network dispersive effects due to variability in flow paths(captured by the dispersion coefficient  $D_{KG}$ ).

also on the magnitude of the peak discharge and the time to peak (Robinson *et al.*, 1995; Saco and Kumar, 2002a, and b; Paik and Kumar, 2004; Snell *et al.*, 2004).

This chapter is organized as follows. First, we review the GIUH, which is generally used as the framework to analytically derive the contribution of each dispersive process and to understand its role in shaping the hydrograph. This leads to consideration of the concept of geomorphologic dispersion and, in turn, the use of Instantaneous Response Functions (IRFs) to account for non-linear effects on the hydrologic response of basins. The concept of kinematic dispersion and the effect of basin scale and rainfall intensity and the dynamics of surface runoff over hillslopes are then considered. Meta-channel approaches to capture network effects on the dispersive mechanisms are then discussed. Finally, a number of open questions that might be tackled through future research are introduced.

## Runoff response as travel-time distributions: the GIUH

The geomorphologic instantaneous unit hydrograph (GIUH) was the first approach in which the basin's IUH was explicitly linked to the geomorphologic structure of the river network. The GIUH is derived as the probability distribution of the arrival times of water drops at the basin's outlet, given an instantaneous input of a unit volume of

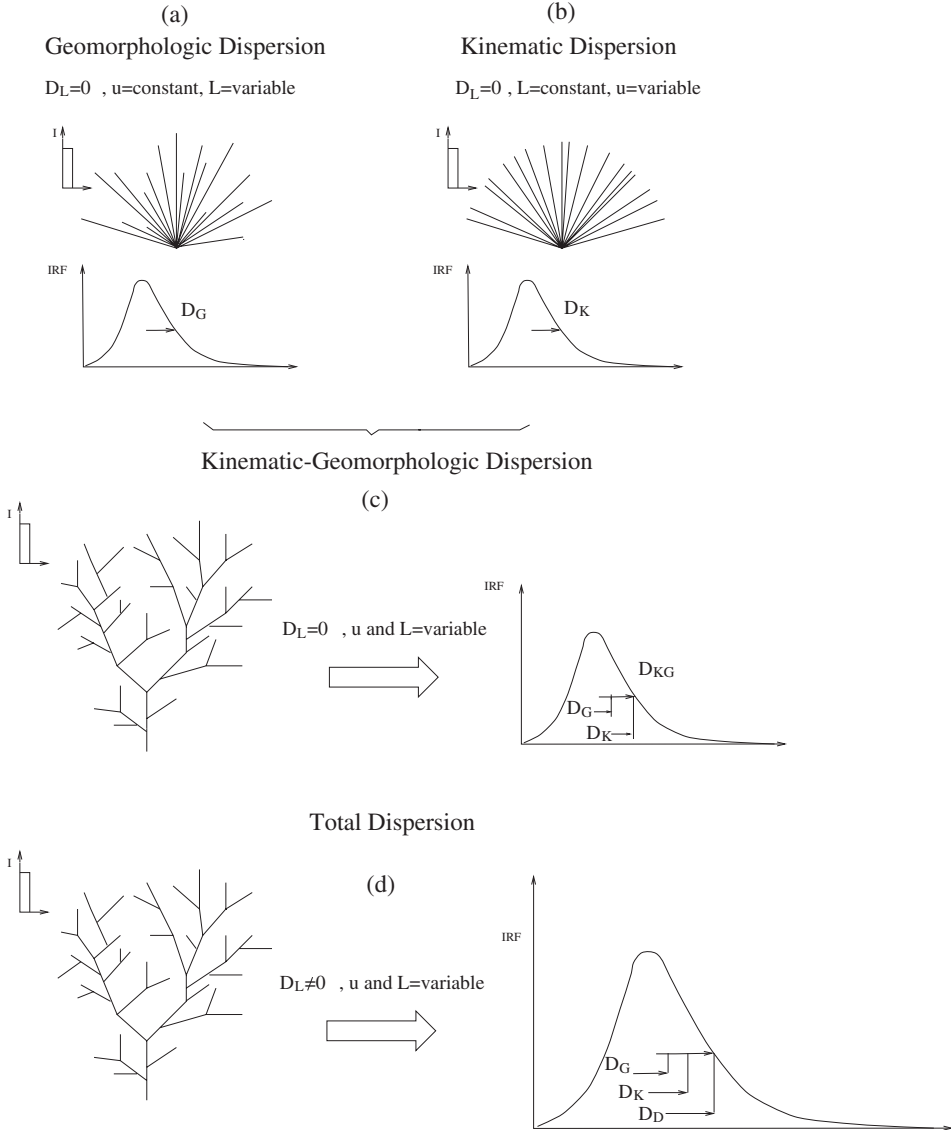


**Figure 15.2** Schematic to illustrate the concepts of geomorphologic and kinematic dispersion. (a) System of channels with varying lengths connected to a single outlet, in which hydrodynamic effects are considered negligible and the celerities are the same for all channels. The spread of travel times is completely induced by geomorphologic dispersion. (b) System of channels with identical lengths but different celerities in which hydrodynamic effects are considered negligible. The spread of travel times is completely induced by kinematic dispersion. (c) In a river network the effects of geomorphologic and kinematic dispersion act together and give rise to the kinematic-geomorphologic dispersion. (d) Partition of the total dispersion when the geomorphologic dispersion ( $D_G$ ), the kinematic dispersion ( $D_K$ ), and the hydrodynamic dispersion ( $D_D$ ) act together. Reproduced from *Water Resources Research* **38**: 1244, © American Geophysical Union.

rainfall excess uniformly distributed over the basin (Rodriguez-Iturbe and Valdes, 1979; Gupta *et al.*, 1980). In its original derivation the arrival times were estimated for a set of pathways derived by representing the network geometry and topology using Horton ratios and the Strahler ordering scheme (Rodriguez-Iturbe and Valdes, 1979).

Using the Strahler ordering scheme (Strahler, 1957), a pathway can be defined as a set of transitions from the initial order of a droplet (the order of the stream into which the droplet is initially injected), into higher and higher-order streams until the outlet (highest-order stream) is reached. For example, in a third-order basin the collection of all paths  $\Gamma = \{\gamma_1, \gamma_2, \gamma_3, \gamma_4\}$  is given as:

$$\begin{aligned} \gamma_1 &: o_1 \rightarrow \omega_1 \rightarrow \omega_2 \rightarrow \omega_3 \rightarrow \text{outlet} \\ \gamma_2 &: o_1 \rightarrow \omega_1 \rightarrow \omega_3 \rightarrow \text{outlet} \\ \gamma_3 &: o_2 \rightarrow \omega_2 \rightarrow \omega_3 \rightarrow \text{outlet} \\ \gamma_4 &: o_3 \rightarrow \omega_3 \rightarrow \text{outlet} \end{aligned}$$

where  $o_i$  denotes an overland state contributing directly to a stream of order  $\omega_i$ . This proposition can be easily extended to a basin of arbitrary order  $\Omega_i$ .

Each path  $\gamma$  is defined by the collection of states  $\gamma = \{x_1, x_2, \dots, x_k\}$  where  $x_1 = o_i$ ,  $x_2 = \omega_i$  with  $i$  one of  $\{1, \dots, \Omega\}$ ,  $x_j$  with  $j = 3, \dots, k - 1$  is one of  $\{i + 1, \dots, \Omega - 1\}$  and  $x_k = \omega_\Omega$ . The probability  $p(\gamma)$  of following any path to the outlet is given by the probability,  $\pi_{x_1}$ , of a water drop starting out in the state  $x_1$ , times each of the probabilities of making a transition to the streams of higher order along that path:

$$p(\gamma) = \pi_{x_1} \times p_{x_1, x_2} \times p_{x_2, x_3} \times \dots \times p_{x_{k-1}, x_k} \tag{15.1}$$

where  $p_{x_i, x_j}$  is the transition probability from the state  $x_i$  to  $x_j$ . The travel time through a path is the sum of the travel times through each of its individual states:  $T_\gamma = T_{x_1} + \dots + T_{x_k}$ . The travel-time distribution  $f_b(t)$  at the basin's outlet, when the rainfall is instantaneously and uniformly distributed over the entire basin, is obtained by randomizing over all possible paths:

$$f_b(t) = \sum_{\gamma \in \Gamma} p(\gamma) \{ f_{x_1} * f_{x_2} * \dots * f_{x_k}(t) \}_\gamma \tag{15.2}$$

where  $*$  denotes convolution,  $f_{x_i}(t)$  is the travel time distribution through each of the individual states of network path  $\gamma$ . Alternatively, the above formulation can be separated into hillslope and network responses as:

$$f_b(t) = f_h * \sum_{\gamma \in \Gamma} p(\gamma) f_\gamma(t) \tag{15.3}$$

where  $f_h = f_{x_1}$  is the hillslope (or overland) response and the network response is given as:

$$f(t) = \sum_{\gamma \in \Gamma} p(\gamma) f_{\gamma}(t) \quad (15.4)$$

Note that  $f_{\gamma}(t) = f_{x_2} * f_{x_3} * \dots * f_{x_k}(t)$  is the travel time distribution through the network portion of each individual path  $\gamma$ . There are several expressions in the literature to obtain the hillslope IUH (Henderson and Wooding, 1964; Kirkby, 1976; Mesa and Mifflin, 1986; van der Tak and Bras, 1990; Naden, 1992; Robinson *et al.*, 1995; Lee and Yen, 1997). The effect of hillslopes on the unit hydrograph is discussed below in the section entitled **Hillslope dispersive effects**.

In order to completely characterize the network GIUH  $f(t)$ , given by Equation (15.4), it is necessary to determine the:

- initial state probabilities  $\pi_{x_1}$
- state-to-state transition probabilities  $p_{x_i, x_j}$
- residence time distribution in each state  $f_{x_i}(t)$ .

The initial probability for a particular state  $x_i = o_{\omega}$  is simply the fraction of the basin area that contributes overland flow to a stream of order  $\omega$ . The expressions for state-to-state transition probabilities are more involved and can be derived using the Horton ratios (Rodriguez-Iturbe and Valdes, 1979) or directly from the Strahler ordered network (Snell and Sivapalan, 1994), which is equivalent to using the network tributary structure (Peckham, 1995; Saco and Kumar, 2002b).

Different methodologies have been used to derive the residence time distributions in individual streams or states. In the original GIUH derived by Rodriguez-Iturbe and Valdes (1979), the residence time distributions in each state were assumed to be exponential. Gupta *et al.* (1980) used a uniform distribution and van der Tak and Bras (1990) proposed a gamma distribution. Recent research has used the inverse Gaussian distribution (Mesa and Mifflin, 1986; Rinaldo *at al.*, 1991; Snell and Sivapalan, 1994; Saco and Kumar, 2002a, b and 2004; Paik and Kumar, 2004) to describe the residence time distribution. The inverse Gaussian distribution constitutes a solution to the linear advection dispersion equation that describes the flow through individual streams (Rodriguez-Iturbe and Rinaldo, 1997):

$$\frac{\partial h_{\omega}}{\partial t} + u_{\omega} \frac{\partial h_{\omega}}{\partial x} = D_{L\omega} \frac{\partial^2 h_{\omega}}{\partial x^2} \quad (15.5)$$

where  $h_\omega$ ,  $D_{L\omega}$  and  $u_\omega$  are the flow depth, the coefficient of hydrodynamic dispersion ( $m^2/s$ ) and the kinematic wave celerity ( $m/s$ ) for the state  $\omega$ , respectively. The latter two can be computed as:

$$u_\omega = \frac{3}{2}v_\omega^* \tag{15.6}$$

and

$$D_{L\omega} = \frac{u_\omega h_\omega^*}{3\bar{S}_\omega} \tag{15.7}$$

where  $v_\omega^*$  and  $h_\omega^*$  are respectively the reference flow velocity and depth for steady state uniform flow conditions in the state  $\omega$ , and  $\bar{S}_\omega$  is the mean bed slope for the state  $\omega$ .

For the special case in which the kinematic celerity and the hydrodynamic-dispersion coefficient ( $u$  and  $D_L$  respectively) can be considered spatially invariant throughout the basin, the network's travel-time distribution is obtained as (Rinaldo *et al.*, 1991):

$$f(t) = \frac{1}{\sqrt{4\pi D_L t^3}} \sum_{\gamma \in \Gamma} p(\gamma) \bar{L}_\gamma \exp \left\{ -\frac{(\bar{L}_\gamma - ut)^2}{4D_L t} \right\} \tag{15.8}$$

where  $\bar{L}_\gamma = \sum_{\omega \in \gamma} \bar{L}_\omega$  is the mean length of path  $\gamma$ .

An alternative and useful representation of the GIUH is through the width-function or link-based approach (Troutman and Karlinger, 1985; Mesa and Mifflin, 1986; Snell and Sivapalan, 1994; Robinson *et al.*, 1995; Naden, 1992; Rinaldo *et al.*, 1995; Saco and Kumar, 2004). The width function is defined as the frequency distribution of the number of channel links as a function of distance to the basin's outlet. If the area contributing to each channel is constant, the width function is equal to the area function of the basin. Therefore, the width (or area) function defines the amount of drainage area located at a given distance from the outlet. Early research linking the width function and the hydrologic response came from the work of Lee *et al.* (1972), Lee and Delleur (1976) and Kirkby (1976). The main difference between the original (Horton-based) approach described above and the one based on the width function resides in the way in which the network pathways, followed by the individual water drops to the outlet, are represented. In the GIUH defined using the link-based approach, a pathway is defined for each link or individual channel in the network, and this complete set of paths can be described in terms of the width function.

For the particular case in which the channel response is assumed to be uniform or to vary as a function of the distance to the basin's outlet, the network GIUH can be written in terms of the width function following the formulation proposed by Mesa and

Mifflin (1986):

$$f(t) = \int_0^{\infty} W(x) f(x, t) dx \quad (15.9)$$

where  $f(x, t)$  is the residence time distribution for a channel located at a distance  $x$  from the outlet and  $W(x)$  is the normalized width function. Gupta *et al.* (1986) consider the simplified but important case in which the flow dynamics is assumed to be driven by pure convection processes (with constant velocity  $v$ ), which implies that water drops that arrive at the outlet at time  $t$  were initially (at  $t = 0$ ) at a distance  $x = vt$ . Therefore, in this case, the GIUH is proportional to the width function re-scaled as:

$$f(t) \propto W(vt) \quad (15.10)$$

which clearly establishes the strong link between the width function, which captures the organization of the river network, and the basin's hydrologic response. Some of the questions that arise from this simple example and have led to substantial research are: 'Under what circumstances will the network geomorphology captured in the width or area distance function drive the shape of the hydrograph?' and 'Under what conditions will other processes (e.g. overland flow on hillslopes) dominate the hydrograph?' It is obvious that the width/area function is not necessarily positively skewed, yet empirical hydrographs are. What processes are responsible for inducing this positive skew? These are some of the issues addressed in the following sections.

## Geomorphologic dispersion in stream networks

Rinaldo *et al.* (1991) and Snell and Sivapalan (1994) propose an approach to identify and quantify the relative contributions of hydrodynamic and network effects on the basin's hydrologic response. The variance of the travel time distribution, for the case in which celerities and hydrodynamic dispersion can be considered invariant along the river network, can be obtained from Equation 15.8 as:

$$\text{Var}(T) = \frac{2\bar{L}(\Omega)}{u^3} (D_L + D_G) \quad (15.11)$$

where  $\bar{L}(\Omega) = \sum_{\gamma \in \Gamma} p(\gamma) \bar{L}_{\gamma}$  is the mean path length of the network.

The first term in the right-hand side of Equation 15.11 represents the contribution due to the effect of hydrodynamic dispersion. The second term corresponds to the

geomorphologic dispersion coefficient ( $D_G$ ) defined by Rinaldo *et al.* (1991) as:

$$D_G = \frac{u}{2\bar{L}(\Omega)} \left\{ \sum_{\gamma \in \Gamma} p(\gamma) (\bar{L}_\gamma)^2 - \left( \sum_{\gamma \in \Gamma} p(\gamma) \bar{L}_\gamma \right)^2 \right\} \quad (15.12)$$

which appears because of the presence of the river network and accounts for the variance of travel times induced by the existence of paths of different lengths  $\bar{L}_\gamma$ .

Equation 15.12 can be expressed in terms of the first two moments of the distribution of path lengths (Snell and Sivapalan, 1994) as:

$$D_G = \frac{u \text{Var}_\gamma(\bar{L}_\gamma)}{2E_\gamma(\bar{L}_\gamma)} \quad (15.13)$$

where the subscript  $\gamma$  will be used to denote a moment which is computed over all possible paths  $\gamma$ .

Therefore, in this case, there are two mechanisms that contribute to the variance of the travel time distribution:

- Part of the variance of the water drops' travel times is due to the dispersion along the individual paths which is induced by the hydrodynamic effects. If all paths had the same length, this would constitute the only mechanism contributing to the variance since the rate of arrivals through different paths would coincide. This portion is captured by the hydrodynamic dispersion coefficient  $D_L$  in Figure 15.1b.
- The remaining variance is due to the heterogeneity of path lengths in the stream network, which produces the spread in the arrival rates referred to as 'geomorphologic dispersion'. This portion is captured by the network dispersion coefficient  $D_{KG}$  in Figure 15.1b, which in this case is equal to  $D_G$  because the celerity is the same in all channels.

Snell and Sivapalan (1994) and Robinson *et al.* (1995) show that hydrodynamic dispersion is only a small component of the total dispersion, and thus it has only a relatively minor impact on the shape of the unit hydrograph for both small and large catchments. They found that the main contribution to the variance of the network travel-time distribution is due to geomorphologic dispersion. The results from White *et al.* (2004) for eight large basins in Illinois are consistent with the results of Snell and Sivapalan (1994) and Robinson *et al.* (1995), that is they found that geomorphologic dispersion plays a dominant role at all scales. However, in the analysis of White *et al.* (2004) though both dispersion coefficients increased with increasing scale and decreasing flow frequency, the hydrodynamic dispersion coefficient increased at a faster rate than the geomorphologic

dispersion coefficient with increasing scale. That is, the influence of geomorphologic dispersion on the hydrologic response is greatest in the smaller watersheds and at high flow frequencies; nonetheless, its influence is still larger than that of hydrodynamic dispersion for all scales of interest.

The results from these studies have important practical implications for hydrologic data modelling. It means that surveying channel characteristics, such as flow depth, top width, discharge, channel-bed roughness and channel cross-sectional area, which in the past used to be considered as the critical data needed for hydrologic modelling, is not as important as obtaining the correct characterization of the network morphology. The network structure parameters, needed to determine the magnitude of geomorphologic dispersion effect, are relatively simple to extract from DEMs, which under the assumptions analysed in this section (spatially invariant hydrodynamic characteristics) means that the hydrologic response can be reasonably approximated without a large amount of expensive field work. The validity of these assumptions will be further discussed in the following sections.

## Non-linear effects and the use of hydraulic geometry relations

The analysis by Rinaldo *et al.* (1991) and Snell and Sivapalan (1994), presented in the previous section, on the physical processes that contribute to the variance of the travel-time distributions, considers the particular case in which the hydrodynamic parameters ( $u$  and  $D_L$ ) can be assumed to be spatially invariant along the river network. However, flow through the channel network is inherently non-linear and shows a strong dependence on scale (i.e. the size of the basin). In a general case, the hydrodynamic parameters depend on the local flow conditions due to the non-linear nature of the momentum equations. This dependence can be quantified using Equations 15.6 and 15.7, which are stated in terms of local reference flow conditions. Moreover, empirical evidence shows that flow velocities vary non-linearly with flow discharge both in time and space along the river network (Minshall, 1960; Pilgrim, 1976). In particular, Pilgrim (1976) shows, using tracer studies, that average flow velocities are a non-linear function of discharge but reach an asymptotic value at high flows. Many researchers have invoked Pilgrim's observations to justify the assumption of spatially invariant velocities, which though valid for high (over-bankfull) flows is not a good approximation for the lower flow conditions under which the velocities vary downstream.

The non-linearity of the hydrologic response in the time domain can be accounted for by the use of IRFs (Valdes *et al.*, 1979; Wang *et al.*, 1981; Robinson *et al.*, 1995; Yen and Lee, 1997; Saco and Kumar 2002a and b; Paik and Kumar, 2004), which describe a time-variant basin response. The IRF formulation is similar to that of the IUH in

that the system response is still linear and given by its convolution with the effective rainfall, but, unlike the IUH, the IRF is allowed to vary with time as a function of the rainfall history. The IRF may or may not account for the non-linearity that takes place in the space domain. For example, in the work by Valdes *et al.* (1979) the residence time distributions are estimated considering a time-varying but spatially invariant velocity (i.e. the velocity varies with the effective rainfall but is spatially constant on the basin). Wang *et al.* (1981) derive expressions for the mean travel time over both hillslopes and channels of varying Strahler order which implicitly account for changes in flow velocities. Velocity changes in their work are based on numerical experiments performed with the linear geomorphic model proposed by Gupta *et al.* (1980). Lee and Yen (1997) apply kinematic-wave theory and derive explicit equations to compute the mean travel time for equilibrium flow conditions on hillslopes and channels of different Strahler orders. Robinson *et al.* (1995) use hydraulic-geometry relations to obtain time-varying but spatially invariant equivalent hydrodynamic parameters to derive the basin's IRF, and to compute the relative importance of geomorphologic versus hydrodynamic dispersion as a function of the excess rainfall.

Saco and Kumar (2002a and b) and Paik and Kumar (2004) use hydraulic geometry relations (Leopold and Maddock, 1953) to characterize the variation of the celerity and the hydrodynamic-dispersion coefficient in the travel-time distribution (Equation 15.4) as a function of both space (i.e. along the river network) and rainfall excess. In this way, the characteristics of network geometry were effectively coupled to hydraulic geometry relations which implicitly characterize the non-linearity of flow dynamics. We should note that when considering a uniformly distributed rainfall excess rate over the basin, the frequency of the corresponding accumulated discharge (used in the hydraulic geometry relations) varies downstream along the network. The hydraulic geometry relations state that the water surface width ( $w$ ), the hydraulic depth ( $h$ ) and the mean velocity ( $v$ ) vary as power functions of discharge as:

$$Q = a_S Q^{b_S} ; h = c_S Q^{f_S} ; \text{ and } v = k_S Q^{m_S} \quad (15.14)$$

for at-a-station relationships, and as:

$$Q = a_D Q^{b_D} ; h = c_D Q^{f_D} ; \text{ and } v = k_D Q^{m_D} \quad (15.15)$$

for downstream relationships corresponding to a discharge of a given frequency. The approach by Saco and Kumar (2002 a and b), explained in the following section, extends the framework developed by Rinaldo *et al.* (1991) (described earlier in this chapter), to analyze the dispersion mechanisms which contribute to the variance of the travel time distribution as a result of non-linearity, as captured in the hydraulic-geometry relations. Alternative approaches to investigate the effect of non-linear flow effects on the hydrologic response are described in Reggiani *et al.* (2001) and Snell and Sivapalan

(2004). These studies use the full Saint Venant equations to model the propagation of the flood waves that results from an instantaneous pulse of rainfall. The results of Snell and Sivapalan on the impact of non-linearity of the dispersion mechanisms are discussed in the section entitled **Kinematic dispersion effects using the meta-channel approach**.

## Kinematic dispersion in stream networks

Saco and Kumar (2002a) show that when considering spatially varying celerities there are three dispersion mechanisms that contribute to the variance of the travel-time distribution. Two of these mechanisms, geomorphologic and hydrodynamic dispersion, are the ones identified when considering spatially invariant hydrodynamic coefficients. The third mechanism arises due to the presence of spatially varying celerities and is referred to as 'kinematic dispersion'.

Figure 15.2 illustrates the concepts of geomorphologic and kinematic dispersion. Figure 15.2a shows a system of channels with varying lengths connected to a single outlet, in which hydrodynamic effects are considered negligible and the celerities are the same for all channels. The spread of travel times for water instantaneously and uniformly poured into this system will be completely induced by geomorphologic dispersion effects. On the other hand, in the system shown in Figure 15.2b, the channels have all the same length but different celerities, and again hydrodynamic effects are assumed to be negligible. The spread of travel times in Figure 15.2b will be completely induced by differences in celerities termed as 'kinematic dispersion'. In a stream network (such as the one represented in Figure 15.2c) the geomorphologic and kinematic dispersion effects act together and give rise to what we refer to as 'kinematic-geomorphologic dispersion'.

The assumption of spatial invariance of the coefficient of hydrodynamic dispersion and the kinematic wave celerity is relaxed in the work by Saco and Kumar (2002a) by assuming that they are a function of the Strahler order  $\omega$  of the stream. An equivalent celerity  $u_\gamma$  and hydrodynamic-dispersion coefficient  $D_{L\gamma}$ , which preserve the mean and variance of the travel-time distribution for each path  $\gamma$ , can then be obtained as (Saco and Kumar, 2002a):

$$u_\gamma = \frac{\bar{L}_\gamma}{E(T_\gamma)} = \frac{\bar{L}_\gamma}{\sum_{\omega \in \gamma} \frac{\bar{L}_\omega}{u_\omega}} \quad (15.16)$$

and

$$D_{L\gamma} = \frac{u_\gamma^3 \text{Var}(T_\gamma)}{\bar{L}_\gamma} = \frac{u_\gamma^3}{\bar{L}_\gamma} \left( \sum_{\omega \in \gamma} \frac{\bar{L}_\omega D_{L\omega}}{u_\omega^3} \right) \quad (15.17)$$

where  $\bar{L}_\omega$  is the mean length of a stream of order  $\omega$ ,  $\bar{L}_\gamma = \sum_{\omega \in \gamma} \bar{L}_\omega$  is the mean path length for path  $\gamma$  and  $T_\gamma$  is the travel time in path  $\gamma$ .

An equivalent network celerity, that preserves the mean travel time over the network, can be defined in terms of the mean path length of the network ( $\bar{L}(\Omega)$ ) and the network's mean travel time ( $E(T_n) = E_\gamma(E(T_\gamma))$ ) as follows:

$$u_n = \frac{\bar{L}(\Omega)}{E(T_n)} = \frac{\sum_{\gamma \in \Gamma} p(\gamma) \bar{L}_\gamma}{\sum_{\gamma \in \Gamma} p(\gamma) \frac{\bar{L}_\gamma}{u_\gamma}} \quad (15.18)$$

where  $p(\gamma)$  is the probability of a water drop following a particular path  $\gamma$ . The geomorphologic dispersion coefficient ( $D_G$ ) is then obtained by replacing this equivalent network celerity into Equation 15.13:

$$D_G = \frac{u_n}{2\bar{L}(\Omega)} \left\{ \sum_{\gamma \in \Gamma} p(\gamma) (\bar{L}_\gamma)^2 - \left( \sum_{\gamma \in \Gamma} p(\gamma) \bar{L}_\gamma \right)^2 \right\} \quad (15.19)$$

The kinematic–geomorphologic dispersion coefficient, which captures the combined effects of the heterogeneity of flow velocities and length of path, is obtained as (Saco and Kumar, 2002a):

$$D_{KG} = \frac{u_n^3}{2\bar{L}(\Omega)} \left\{ \sum_{\gamma \in \Gamma} p(\gamma) \left( \frac{\bar{L}_\gamma}{u_\gamma} \right)^2 - \left( \sum_{\gamma \in \Gamma} p(\gamma) \frac{\bar{L}_\gamma}{u_\gamma} \right)^2 \right\} \quad (15.20)$$

Therefore, the dispersive effect due to the existence of different celerities along different paths, called ‘kinematic dispersion’, can be captured by the kinematic dispersion coefficient defined as:

$$D_K = D_{KG} - D_G \quad (15.21)$$

Hydrodynamic dispersion effects are captured by the coefficient  $D_D$ , computed as the weighted average of the contributions of hydrodynamic dispersion over each path ( $D_{L\gamma}$ ), as:

$$D_D = \frac{u_n^3}{\bar{L}(\Omega)} \sum_{\gamma \in \Gamma} p(\gamma) \frac{\bar{L}_\gamma D_{L\gamma}}{u_\gamma^3} \quad (15.22)$$

which shows that spatially varying celerities alter the expression of the hydrodynamic dispersion as well. The variance of the travel-time distribution  $f(t)$  (IRF) results from the superposition of the three dispersion mechanisms and can be expressed as:

$$\text{Var}(T_n) = \frac{2E_\gamma(\bar{L}_\gamma)}{u_n^3}(D_D + D_G + D_K) \quad (15.23)$$

It is important to note that the kinematic dispersion coefficient,  $D_K$ , can take positive or negative values. A negative contribution implies that the velocities over different paths are such that longer paths have higher equivalent path celerities, which tends to reduce the geomorphologic dispersion that would otherwise be caused by the longer path length. To illustrate this, let us consider an extreme example in which the hydrodynamic dispersion for all paths is zero and the celerities are such that all the raindrops travelling over different paths arrive simultaneously to the control section. In this case, the travel time or, equivalently, the ratio of the path length to the equivalent path celerity ( $\bar{L}_\gamma/u_\gamma$ ) is the same for all paths. Therefore, the variance of the travel times over the different paths is zero and  $D_K = -D_G$ . Conversely, the contribution of kinematic dispersion becomes positive and large when the path celerities over longer paths are lower than those of the shorter paths. Finally, kinematic dispersion is zero when the celerities are spatially invariant (Rinaldo *et al.*, 1991; Snell and Sivapalan, 1994; Robinson *et al.*, 1995), since  $u_n = u_\gamma = u_\omega = u$  and  $D_{KG} = D_G$ .

In real basins, longer paths tend to have lower celerities and consequently  $D_K$  is positive. Saco and Kumar (2002a and b) found that the contribution of kinematic dispersion to the total variance of the travel-time distribution is comparable to that of the geomorphologic dispersion, and significantly larger than the hydrodynamic dispersion. Therefore, if this contribution is ignored in models, the spread of the computed hydrologic response, more specifically the hydrograph, will be underestimated. As a consequence, the computed hydrograph will overestimate the peak flow and underestimate the time to peak and duration. This means that modelling efforts should not only focus on getting the correct characterization of the network geometry (as suggested by the studies summarized in the earlier section **Geomorphologic dispersion in stream networks**) but also the correct representation of the downstream increase in flow velocity.

## The effect of scale and rainfall intensity on the dispersive mechanisms

The main goal of this section is to analyse how the relative importance of geomorphologic, kinematic and hydrodynamic effects changes for basins of different scales and for storms of varying intensity. This information is important to guide our modelling

efforts under different situations. More specifically, this type of insight will help us to answer the following questions: ‘Are network effects important at all scales of interest?’, ‘Is the effect of varying channel velocities negligible for small basins?’ ‘Does the impact of kinematic dispersion increase for increasingly larger basins?’, ‘Does the relative importance of the various dispersion effects change for storms of varying intensity?’ and ‘How does the shape of the hydrograph change for both varying scale and intensity?’

Saco and Kumar (2002a and b) estimate the contributions of hydrodynamic, geomorphologic and kinematic dispersion using spatially varying hydraulic characteristics computed from hydraulic-geometry relations. Their analysis is based on the results for two basins (the Mackinaw and Vermilion) in Illinois, which are characterized by a very low relief. In this section, we present a similar analysis for the Upper Susquehanna River basin near Waverly (New York) and the Rogue River basin near Central Point (Oregon). These two additional basins were selected to provide physiographic, climatic and hydrologic conditions very different from those in Illinois. The spatially varying celerities and hydrodynamic dispersion coefficients were obtained using hydraulic-geometry relations derived by Stall and Yang (1970).

Table 15.1 shows the equivalent network celerity and dispersion coefficients for the Susquehanna and Rogue River basins, obtained for rainfall excess rates of 1 and 5mm/hr for both basins (order 6) and for their sub-basins of order  $\Omega = 3$  to 5. All coefficients increase with both basin order and rainfall excess rate. Moreover, the fractional contribution of each dispersion coefficient to the total dispersion ( $D_T = D_K + D_G + D_D$ ) does not change significantly with basin scale. The relative contribution of the hydrodynamic dispersion is very small (less than 10 per cent in both basins). The relative contribution of  $D_K$  is less than that of  $D_G$ , but still significant for both basins. In the

**Table 15.1** Equivalent network celerity and hydrodynamic-dispersion coefficients for rainfall excess rates of 1 and 5 mm/hr in the Upper Susquehanna and the Rogue River basins.

$\Omega$	$u_n(m/s)$		$D_G(m^2/s)$		$D_D(m^2/s)$		$D_K(m^2/s)$	
	$I = 1$	$I = 5$	$I = 1$	$I = 5$	$I = 1$	$I = 5$	$I = 1$	$I = 5$
Upper Susquehanna								
3	0.26	0.49	23.4	44.3	0.6	2.1	8.6	16.3
4	0.30	0.57	73.8	139.6	2.5	8.6	27.4	51.9
5	0.36	0.68	180.9	342.0	10.3	35.2	61.9	117.0
6	0.44	0.82	708.6	1339.2	45.8	157.0	305.3	576.9
Rogue								
3	0.21	0.49	22.2	52.0	0.2	0.7	10.1	23.5
4	0.25	0.59	61.4	143.7	0.7	2.8	27.5	64.3
5	0.31	0.73	198.0	463.5	2.7	10.8	88.7	207.7
6	0.39	0.9	352.6	825.4	10.4	41.5	179.2	419.5

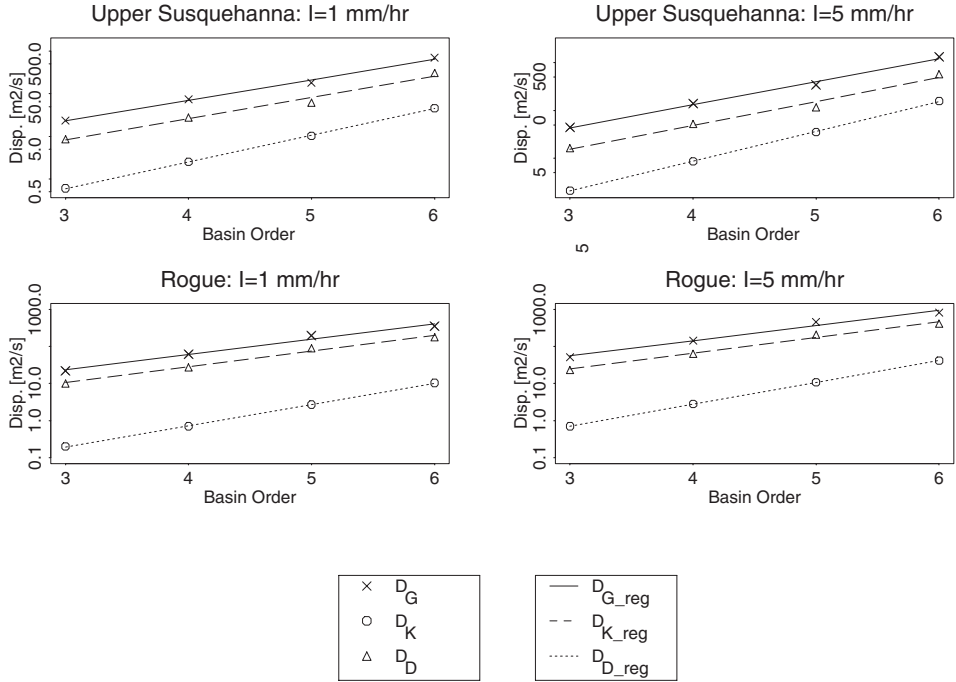


**Figure 15.3** Geomorphologic ( $D_G$ ), kinematic ( $D_K$ ), and hydrodynamic ( $D_D$ ) dispersion coefficients for rainfall excess rates of 1 and 5 mm/hr in the Upper Susquehanna and Rogue River basins. The points in the plots correspond to the values estimated from Equations (15.19), (15.21) and (15.22). The lines represent the regression lines for orders 3 to 6.

Susquehanna river basin,  $D_K$  corresponds to about 25 per cent of the total dispersion for both rainfall rates analysed. In the Rogue River basin,  $D_K$  contributes about 30 per cent of the variance. The combined contribution of kinematic and geomorphologic dispersion is very important for both basins and is significantly larger than that of the hydrodynamic dispersion at all scales. These results are in agreement with those reported by Saco and Kumar (2002a and b) for the Vermilion and Mackinaw River basins.

Figure 15.3 shows that the logarithms of all the dispersion coefficients exhibit a remarkable linear trend as a function of basin order. As seen in Figure 15.3, changes in the rainfall excess rate do not affect these linear trends. These results are also in agreement with those of Saco and Kumar (2002b). The linear trend provides evidence for the existence of power-law behaviour as a function of the area of the Strahler order sub-basins. A physically based analytical explanation for the existence of these linear trends is given by Saco and Kumar (2002b), which result from the inherent self-similar geometric and topologic characteristics of the river network as captured by Horton’s laws of stream lengths, areas and slopes.

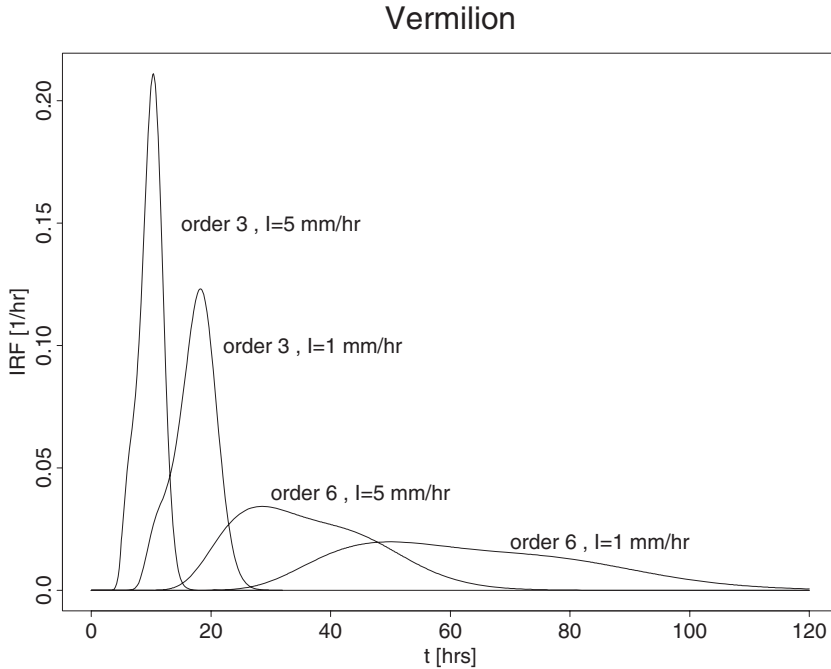


**Figure 15.4** Network IRFs for the Vermilion river basin for rainfall excess rates of 1 and 5 mm/hr and basin orders  $\Omega = 3$  and 6. Reproduced from *Water Resources Research* **38**: 1245, © American Geophysical Union.

Figure 15.4 shows the non-linear characteristics of the network IRF for the Vermilion river basin. The network IRF is strongly dependent on both the rainfall excess rate and basin order. For a basin of given order  $\Omega$ , as  $I$  increases, the hydrograph's peak value increases, whereas the time to peak and the spread decrease because the celerity increases. For a rainfall excess rate  $I$ , as the order of the basin increases, the hydrograph's peak value decreases, whereas both the time to peak and the spread increase.

The effect of non-linear celerity variations on time to peak and hydrograph duration is further explored by Paik and Kumar (2004). They postulate that celerity variations might be responsible for the observed non-linear dependence of the IRF on rainfall. Their results show that the time to peak  $t_p$  and the peak response vary as  $t_p \propto I^{-m_s}$  and  $f(t_p) \propto I^{+m_s}$ , where  $m_s$  is the exponent in the hydraulic geometry relation for velocity (Equation (15.14)). They found that these power-law relations are supported by the analysis based on direct convolution IRFs of river basins in Illinois. Figure 15.5 shows the variation of the time to peak and the IRF's peak as a function of rainfall excess rates for the Vermilion river basin in Illinois. This figure illustrates the power-law dependence on the rainfall excess for the basin, which is consistent with the theoretical

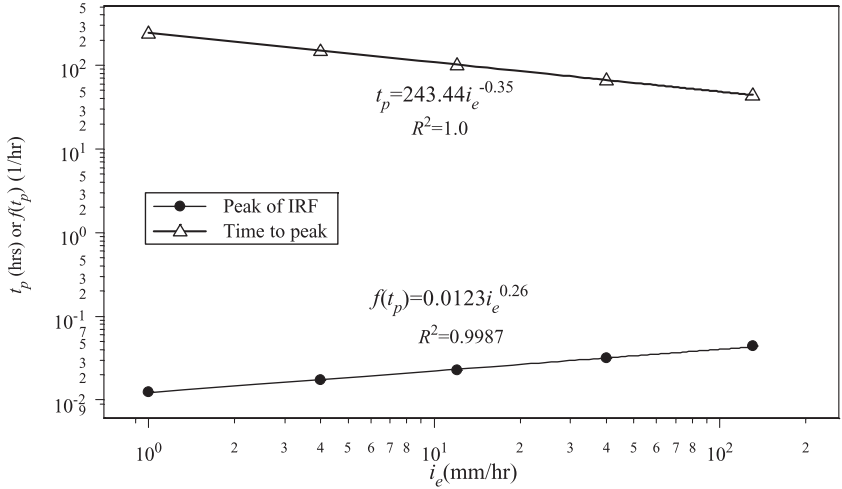


**Figure 15.5** Relationship between  $t_p$  (time to peak) and  $f(t_p)$  (peak of the IRF) and rainfall excess rates ( $i_e$ ) for the Vermilion river basin in Illinois. The time to peak and the peak of the IRF were obtained by the direct convolution for different rainfall excess rates. Logarithmically transformed regression models are used to fit trend lines. Reproduced from *Water Resources Research* 40: W03602 © American Geophysical Union.

predictions. The fitted exponent value matches the theoretical value of  $-m_s$  for the  $t_p$  relationship. The fitted exponent value for the  $f(t_p)$  relationship in Figure 15.5 is also close to the theoretical value. These results show that, owing to the non-linear relation between celerity and flow rate, different (albeit uniform) rainfall rates induce different downstream variations in the flow-celerity fields. As a consequence, the geomorphologic and kinematic dispersion effects change and so does the shape of the basin’s travel-time distribution. These equations that relate the change in time to peak and peak response to rainfall intensity and hydraulic geometry can be incorporated in non-linear models of hydrologic response to account for both scale and rainfall intensity effects (not incorporated in most of the current models).

### Hillslope Dispersive effects

The analysis of the impact of hillslope dynamics in the hydrologic response has been the subject of active research (Henderson and Wooding, 1964; Kirkby, 1976; Mesa and Mifflin, 1986; van der Tak and Bras, 1990; Naden, 1992; Robinson *et al.*, 1995; Rinaldo *et al.*, 1995; Lee and Yen, 1997; Olivera and Maidment, 1999; D’Odorico and Rigon, 2003; Botter and Rinaldo, 2003; Saco and Kumar, 2004). The relative importance of hillslope and network response determines the shape of the hydrograph because of their direct effect on travel times. Kirkby (1976) shows that in small basins the shape

of the hydrograph is dominated by the hillslope hydrograph, while for large basins the shape of the hydrograph tends to resemble the network-width function and the effects of channel routing tend to reduce and delay the peak of the hydrograph. The studies by Mesa and Mifflin (1986) and Naden (1992) compare hillslope versus network effects in various study basins. Mesa and Mifflin explore the relative importance of hillslope response and stream network routing using a width-function approach, for a small basin in Mississippi. They conclude that even for such small basins the stream network geometry strongly influences the basin hydrograph. On the other hand, Naden (1992) investigates the impact of spatial variability of soils and rainfall on the Thames River basin at Cookham (UK) and reports that, despite the large size of the basin, the hillslope response is dominant in this basin.

Robinson *et al.* (1995) analyse the impact of hillslope and network dynamics on the shape of the hydrograph using physically based hillslope response functions that account for both surface and sub-surface processes. Their results suggest that for large basins the emphasis of a hydrologic model should lie on correctly capturing the network response (i.e. geomorphologic dispersion), while for small basins the effort should be on correctly representing the hillslope response. Botter and Rinaldo (2003) study the effect of catchment size on the relative importance of hillslope and network contributions to the basin's hydrologic response. Their results suggest that channel-based kinematic-dispersion mechanisms are less important than a proper characterization of hillslope-channel transitions in a wide range of spatial and dynamic scales. They report that the dominance of these effects depends on the difference between hillslope and channel velocities and suggest that the dominant features of the hydrologic response were not strictly of geomorphologic nature (i.e. due to the variability of the path-lengths in the river network). They conclude that kinematic effects stemming from non-stationary, downstream-increasing mean advection along channelized pathways are not always dominant, and report that it is a combination of kinematic and geomorphological effects derived from hillslope-channel transitions that has a dominant effect on the travel-time distributions at all the scales analysed. D'Odorico and Rigon (2003) analyse the catchment's travel-time distribution accounting for variations of the fraction of saturated areas and report that for small values of the saturated fraction the mean and variance of the travel-time distribution is mostly controlled by the channel network.

Rinaldo *et al.* (1995) analyse how the differences in the dynamics of hillslopes and channels affect the skewness and variance of the hydrograph. They demonstrate that, as the ratio of channel to hillslope celerities ( $u_c/u_h$ ) increases, the mean and variance of the hydrograph also increase. Saco and Kumar (2004) provide additional insight on these issues, through the analysis of hillslope versus network dispersive mechanisms and their relative impacts on the IRF's variance and skewness. They use the approach described in **Kinematic dispersion in stream networks** to compute the relative contributions of geomorphologic and kinematic dispersion due to hillslope celerities. In

their study, hillslope flow is described using an advection–dispersion equation similar to that used for channels Equation 15.5, which results in the following hillslope’s travel time distribution (Rinaldo *et al.*, 1991, 1995):

$$f_h(t) = \frac{L_h}{\sqrt{4\pi D_{L_h} t^3}} \exp \left\{ -\frac{(L_h - u_h t)^2}{4 D_{L_h} t} \right\} \quad (15.24)$$

where  $L_h$ ,  $y_h$ ,  $D_{L_h}$  and  $u_h$  are respectively the length, flow depth, coefficient of hydrodynamic dispersion and kinematic wave celerity of the hillslopes. Using this approximation, the equivalent basin celerity that preserves the first moment of the IRF can be computed as (Saco and Kumar, 2004):

$$u_b = \frac{\bar{L}_b}{E(T_b)} = \frac{\sum_{\gamma \in \Gamma} p(\gamma) L_{b\gamma}}{\sum_{\gamma \in \Gamma} p(\gamma) \frac{L_{b\gamma}}{u_{b\gamma}}} \quad (15.25)$$

where  $\bar{L}_b = \bar{L}_h + \bar{L}_\gamma$ , and  $u_{b\gamma}$  is the equivalent path celerity which takes into account the effect of hillslope celerities, defined as  $u_{b\gamma} = (L_h + L_\gamma) / (\frac{L_h}{u_h} + \frac{L_\gamma}{u_\gamma})$ , where the sub-index  $b\gamma$  refers to attributes of the complete path (i.e. hillslope and channel portions of the path).

The basin geomorphologic dispersion coefficient  $D_{G_b}$ , which takes into account both network and hillslope effects, is obtained by replacing  $u_n$  in Equation 15.19 by the equivalent basin celerity  $u_b$ , as (Saco and Kumar, 2004):

$$D_{G_b} = \frac{u_b}{2E_\gamma(L_{b\gamma})} \left\{ \text{Var}_\gamma(L_h) + \text{Var}_\gamma(L_\gamma) \right\} \quad (15.26)$$

Similarly, the basin kinematic–geomorphologic dispersion coefficient (Equation 15.20) can be expressed as:

$$D_{KG_b} = \frac{u_b^3}{2E_\gamma(L_{b\gamma})} \left\{ \text{Var}_\gamma \left( \frac{L_h}{u_h} \right) + \text{Var}_\gamma \left( \frac{L_\gamma}{u_\gamma} \right) \right\} \quad (15.27)$$

In order to isolate the hillslope kinematic effects, the effect of varying channel celerities was not considered, that is the velocity in the channels was assumed to be spatially constant. The resulting ‘hillslope’ kinematic–geomorphologic dispersion coefficient,  $D_{KG_h}$ , is obtained by rewriting Equation 15.27 as:

$$D_{KG_h} = \frac{u_b}{2E_\gamma(L_{b\gamma})} \left\{ \left( \frac{u_b}{u_h} \right)^2 \text{Var}_\gamma(L_h) + \left( \frac{u_b}{u_c} \right)^2 \text{Var}_\gamma(L_\gamma) \right\} \quad (15.28)$$

The ‘hillslope’ geomorphologic dispersion coefficient  $D_{G_h}$  is equal to  $D_{G_b}$  (Equation 15.26) since  $u_b$  is the only term affected by the hillslope dynamics. And the ‘hillslope’ kinematic dispersion coefficient  $D_{K_h}$  is obtained as the difference between the previous two coefficients.

Comparing  $D_{KG_h}$  and  $D_{G_h}$  and noting that  $\frac{u_b}{u_h} > 1$  and  $\frac{u_b}{u_c} < 1$ , it becomes evident that the first term in the right-hand side of Equation 15.28 is larger than the first term in the right-hand side of Equation 15.26, while the second term in the right-hand side of Equation 15.28 is smaller than the second term in the right-hand side of Equation 15.26. Therefore, depending on the relative contributions of hillslopes and channels,  $D_{KG_h}$  can be smaller (negative kinematic dispersion) or larger (positive kinematic dispersion) than  $D_{G_h}$ .

Figure 15.6 displays the magnitude of the normalized dispersion coefficients as a function of the ratio of hillslope-to-channel celerities  $u_h/u_c$ . As shown in this figure, as the ratio  $u_h/u_c$  decreases from a starting value of 1 (in which kinematic-dispersion effects are absent) and as long as the ratio  $u_h/u_c$  is less than 0.015, geomorphologic dispersion is larger than the dispersion due to the combined influence of the geomorphologic and advective effects ( $D_{KG_h}$ ). For  $1 < u_h/u_c < 0.015$ , the kinematic dispersion is negative and partially compensates for the effect of geomorphologic dispersion, reaching a minimum for a ratio  $u_h/u_c$  of 0.04 (largest negative kinematic dispersion coefficient). Within this interval, hillslope celerities partially compensate for the geomorphologic dispersion that the basin would experience if all water drops were travelling at the equivalent basin celerity. The influence of hillslope celerities is larger in the shorter paths. As a

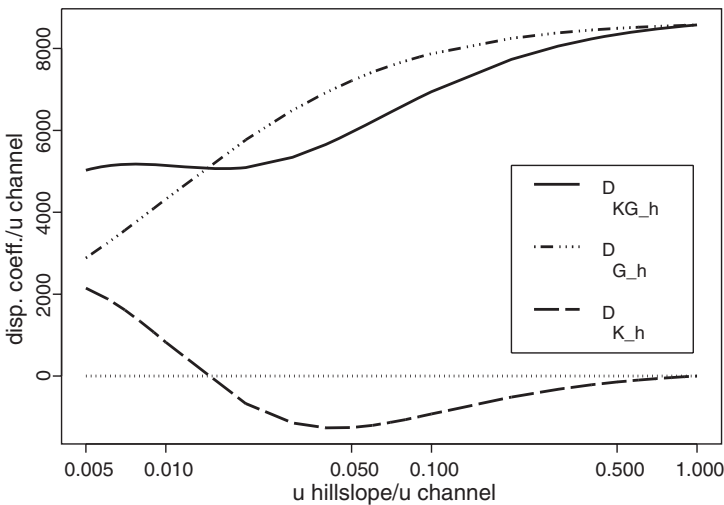


**Figure 15.6** Magnitude of the different dispersion mechanisms as a function of  $u_h/u_c$  for the Mackinaw River basin. Reproduced from *Water Resources Research* 40: W03602 © American Geophysical Union.

consequence, the longer paths tend to have larger equivalent path celerities ( $u_y$ ) than the shorter paths which results in the aforementioned compensation effect induced by the kinematic dispersion. As  $u_h/u_c$  decreases, the travel time in the hillslopes increases and becomes of the same order of magnitude as the travel time in the channels. Therefore, as travel times in channels become relatively small as compared to that on hillslopes, the geomorphologic-dispersion effect becomes less important. As  $u_h/u_c$  continues to decrease the kinematic-geomorphologic dispersion becomes larger than the geomorphologic dispersion and the kinematic dispersion coefficient becomes positive. The total geomorphologic-kinematic dispersion has a decreasing trend for  $u_h/u_c < 0.005$ . After that, the variance continues to increase, as  $u_h/u_c$  decreases, because of the decrease in the equivalent basin celerity and not because of the hillslope kinematic dispersion effects. In summary, the kinematic dispersion induced by hillslopes does not tend to reinforce the effect of geomorphologic dispersion; rather, it tends to counteract it.

Figure 15.7 shows the area–distance function and the rescaled area–distance function for the Mackinaw River basin. The increase in the positive skewness of the rescaled area–distance is in agreement with the results reported by Rinaldo *et al.* (1995). The geomorphologic dispersion coefficient can be obtained from the variance of the area–distance function and the geomorphologic-kinematic dispersion coefficient can be

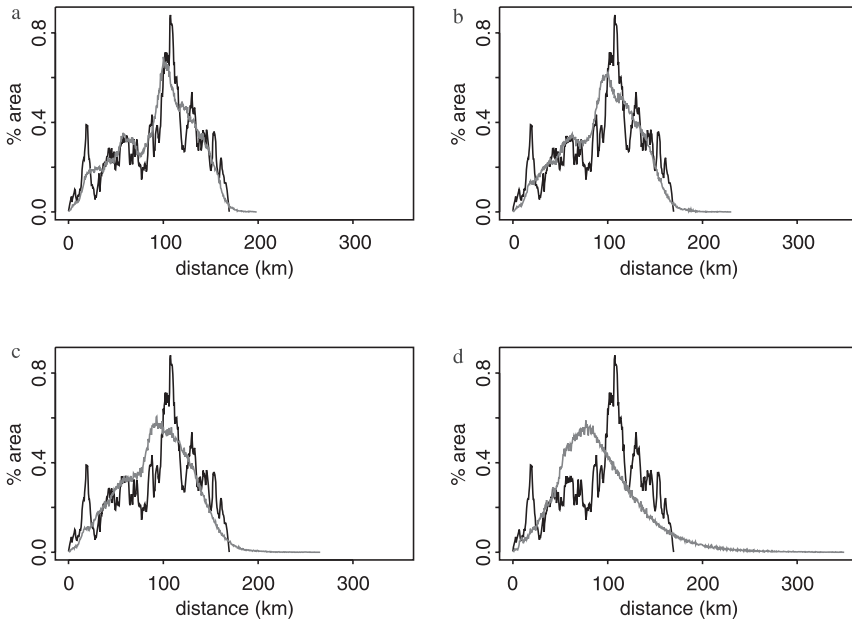


**Figure 15.7** Area–distance (black line) and rescaled area–distance function (grey line) for the Mackinaw River basin when (top left)  $u_h/u_c = 0.1$ , (top right)  $u_h/u_c = 0.06$ , (bottom left)  $u_h/u_c = 0.04$ , and (bottom right)  $u_h/u_c = 0.01$ . Reproduced from *Water Resources Research* 40: W03602 © American Geophysical Union.

obtained from the variance of the rescaled area–distance function, both shown in Figure 15.7 for  $u_h/u_c = 0.1, 0.06, 0.04$  and  $0.01$ . As seen in this figure, the variance of the travel-time distribution (rescaled area–distance function) increases with decreasing ratio  $u_h/u_c$  due to the thickening of the tail of the distribution (which is also responsible for the increase in skewness).

The results from the different studies presented in this section emphasize that both hillslope dynamics (i.e. the distribution of hillslope lengths and velocities) and network dynamics (i.e. the distribution and spatial variability of channel lengths and velocities) play important roles in shaping the hydrograph at all scales of interest. In particular, these findings show that the variance and skewness (and therefore the duration) of the hydrograph is driven by both network and hillslope processes. The later results suggest that it is crucial to correctly incorporate in the model the distribution of hillslope lengths since for small hillslope velocities the increase in variance is driven by the effect of paths with long hillslope (not channel) lengths.

## Kinematic dispersion effects using the meta-channel approach

Snell and Sivapalan (2004) use an alternative methodology, the so-called ‘meta-channel approach’, to incorporate the spatial variability of the network and channel geomorphology and analyse its impact on the hydrologic response. They use this formulation and a simplified version of the full Saint Venant equations to model the propagation of the flood wave that results from an instantaneous pulse of rainfall, and to investigate the effects of spatial heterogeneity and non-linearity on the shape of a basin’s hydrologic response function. They also investigate the concept of kinematic dispersion as a possible explanation for the positive skewness of the hydrologic response, particularly for large basins in which the effect of hillslopes is weaker and so is its influence on determining the hydrograph’s positive skewness as identified in the previous section.

The meta-channel approach models the network as a single channel using effective parameterizations that capture the spatial variation of the various components of the network. It uses the equations of conservation of continuity and mechanical energy to collapse the two-dimensional branched channel network into a single one-dimensional channel. This single-channel representation incorporates the network pattern expressed through the width function of the basin and the variation of channel hydraulic geometry in space and time expressed as a combination of at-a-site and downstream hydraulic geometry relations. The meta-channel has varying cross-sections and perimeters that follow the shape of the width function.

Snell and Sivapalan (1995) derive the hydraulic geometry for every point of a meta-channel for the Hutt catchment in New Zealand. The meta-channel hydraulic geometry is expressed in terms of an effective wave celerity and dispersion coefficient, both of which are a function of the discharge and spatial location. These are the hydrodynamic

parameters needed for the generalized non-linear diffusion wave equation derived by Sivapalan *et al.* (1997), which combines the continuity and momentum equations for an arbitrary river channel reach into a single second-order, non-linear partial-differential equation in discharge  $Q$ . Using this non-linear routing model (which incorporates hydrodynamic dispersion parameters that vary both in space and time), Snell *et al.* (2004) analyse the roles of non-linearity and scale effects on the hydrograph shape for the Hutt catchment.

Using the Hutt catchment, Snell *et al.* (2004) study the effects of catchment scale on the channel network's response function. They extract several sub-catchments from the Hutt ranging in size from 0.86 to 86.7 km<sup>2</sup> and use several storm events ranging from 0.1 to 1000 mm. They quantify the relative contributions to the total dispersion of the hydrodynamic, geomorphologic and kinematic components. The dispersion coefficients are computed following the analysis from Rinaldo *et al.* (1991) and Saco and Kumar (2002a) as:

$$D_{NK} = D_T - D_G - D_L \tag{15.29}$$

where  $D_{NK}$  is a kinematic dispersion coefficient derived using the non-linear routing model on the meta-channel,  $D_T$  is the total dispersion derived from the moments of the IRF,  $D_G$  is the geomorphological dispersion computed from Equation 15.13 and  $D_L$  is a linear hydrodynamic dispersion estimated from a steady linear routing using an estimated mean celerity  $u$  obtained from the non-linear routing.

Their results are summarized in Figure 15.8 which shows that  $D_{NK}$  increases with increasing catchment size, with no apparent falloff at any stage. The rate of increase did not appear to be dependent on the magnitude of the event. Snell *et al.* (2004) also compute a non-dimensional kinematic dispersion coefficient from their

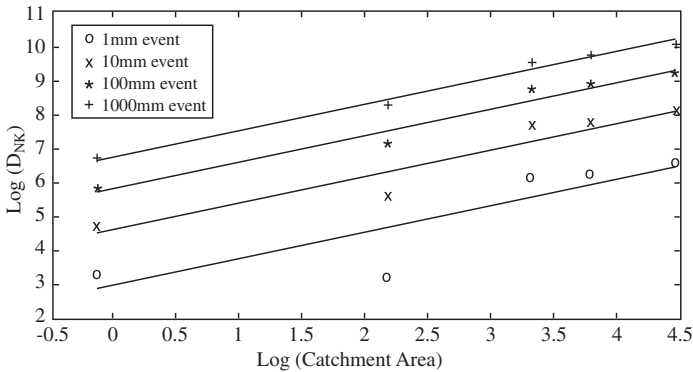


**Figure 15.8** Kinematic dispersion coefficient that includes the effect of nonlinear wave routing in the metachannel ( $D_{NK}$ ) as a function of catchment size and event magnitude. Reproduced from *Advances in Water Research* 30: 2311–2323, (2004) © Elsevier.

non-linear routing model,  $D_{NK}^*$ , as the ratio between the kinematic and geomorphological dispersion coefficients and found that for larger catchments (greater than 25 km<sup>2</sup>)  $D_{NK}^*$  remained invariant with catchment size for any given event. This implies that  $D_{NK}^*$  increases at the same rate as  $D_G$  and therefore that kinematic effects have a significant impact on network responses at all catchment scales, which is consistent with previous results. They report that the combination of channel non-linearity and spatial heterogeneity, on their own, appear to explain the transformation of underlying negatively skewed geomorphological functions, such as the width function, into smooth and positively skewed unit hydrographs. They also report that the kinematic effects, due to the presence of spatially and temporally variable velocity fields, have a dominant impact on the shape of the catchment's instantaneous response function, confirming the results of Saco and Kumar (2002a).

## Summary and future research directions

'Hydrologic dispersion' refers to the combined effect of all dispersive processes that contribute to the variance (spread) in the arrival-time distribution of water drops to the watershed's outlet and, consequently, has a direct impact on the shape of the direct runoff hydrograph. Hydrologic-dispersive processes have an impact not only on the duration of the hydrograph but also on the magnitude of the peak discharge and the time to peak. The hydrologic dispersion is mainly driven by three main processes:

- **Hydrodynamic dispersion**, which is induced by and accounts for storage, turbulence and shear-stress processes along the individual channels. Owing to this effect, some of the water drops entering the channel travel slower than others, producing spread in the distribution of arrival times at the channel's outlet. If all paths were equal (same length and hydraulic geometry), this would constitute the only mechanism contributing to hydrologic dispersion.
- **Geomorphologic dispersion**, arising from the heterogeneity of path lengths in the stream network that introduces spread in the arrival times of water drops to the basin's outlet. The effect of geomorphologic dispersion is significantly more important than that of hydrodynamic dispersion at all catchment scales (Rinaldo *et al.*, 1991; Snell and Sivapalan, 1994; Robinson *et al.*, 1995; Saco and Kumar, 2002a and b; White *et al.*, 2004).
- **Kinematic dispersion**, induced by the effect of spatially varying celerities along the stream network. Different studies have demonstrated that kinematic dispersion contributes a significant portion of the total hydrologic dispersion and has a substantial impact on the shape of the network-response function (Saco and Kumar, 2002a and b; Snell *et al.*, 2004; Paik and Kumar, 2004).

The GIUH framework has allowed the derivation of analytical formulations to investigate the role of different dispersive mechanisms on shaping the hydrograph. It has also enabled us to understand the role of network versus channel processes and the role of network geomorphologic versus kinematic effects. This understanding is extremely important because it not only guides our efforts for modelling and data acquisition related to engineering and management applications but also opens new questions for future research. As mentioned in the previous sections, the importance of geomorphologic dispersion, which explains most of the variance of the travel-time distribution, implies that the correct representation of the network characteristics in hydrologic models is extremely important. It has been shown that the correct characterization of kinematic dispersion processes in hydrologic models is also important to reproduce the basin's hydrologic response. Therefore, it is necessary to include an adequate characterization of the channel hydraulic geometry not only for GIUH-type formulations, as the ones explored in the previous sections, but also for distributed models of runoff response.

Though significant advances have been achieved in our understanding of hydrologic dispersion processes, many questions remain unanswered. We have made remarkable progress in our understanding of the role of non-linearity, scale effects and the mechanisms responsible for the skewness of the hydrograph. However, some of these issues still require further research. For example, as explained in the previous sections, both hillslope effects and kinematic effects through non-linear space–time variations of velocities have been found to be responsible for inducing skewness in the travel-time distribution. It is still not clear under which conditions each of these mechanisms dominates the travel-time distribution and if the prevailing mechanism changes with scale and/or rainfall intensity. Another question that requires further investigation is the effect of the spatial variability of rainfall fields. Most of the research presented in this chapter was done under the assumption of spatially uniform rainfall, which is reasonable for small- to medium-size basins. However, as catchment scale increases, this assumption is no longer valid. Further research is needed to assess the impact of the time–space rainfall variability (and particularly its interaction with the network structure) on the dispersion mechanisms and the hydrograph shape.

There are also numerous interdisciplinary open questions related to the role of hydrologic dispersion on various ecogeomorphological basin characteristics. For example, Sklar *et al.* (2006) show that the distribution of travel distances and transport pathways through the drainage network might, in some cases, affect the size distribution and flux rates of the bed material at a control section. They found that though the source of sediment from hillslopes (and particularly its resistant to abrasion) is key to the understanding of the spatial trends and variability in bedload-size distributions, the drainage network can also play a very important role. They observed that basin shape and the internal branching pattern can either amplify or dampen the effects of spatial variability in the size of sediments delivered to channels by hillslopes. The influence on bedload

variability of channel-network properties (such as the width function and the spacing between tributary junctions) depends on the fundamental length scale imposed by particle abrasion. In this way, sediments of intermediate durability will display the greatest variability in bedload mass, since the tributary junction spacing and basin width are likely to occur at length scales that allow for the significant wear – but not the complete destruction – of sediments supplied from upstream and therefore would have an important influence on the distribution of bed material sizes. An immediate question that arises from the results of Sklar *et al.* (2006) is about the impact of hydrologic-dispersion processes on the bedload variability. Hydrologic dispersion would account not only for the distribution of travel distances (geomorphologic component) but also for velocity variations (kinematic component) in the river network, giving a more complete description of travel times in the network that might influence abrasion.

Finally, recent research has looked at the role of river networks as ecological corridors (Bertuzzo *et al.*, 2007). This type of analysis is relevant for understanding the impact of hydrologic controls imposed by river networks on invasion processes (of species, populations, propagules or infective agents). Such research opens the possibility of investigating the effect of the interaction between hydrologic-dispersion processes and the spreading of species along ecological corridors defined by the river network structure.

## Acknowledgments

We would like to thank Bruce Rhoads and Murugesu Sivapalan for offering advice and providing comments and constructive criticisms, which have helped to substantially improve the article.

## References

- Bertuzzo E, Maritan A, Gatto M, Rodriguez-Iturbe I, Rinaldo A. 2007. River networks and ecological corridors: Reactive transport on fractals, migration fronts, hydrochory. *Water Resources Research* **43**: W04419. DOI: 10.1029/2006WR005533.
- Botter G, Rinaldo A. 2003. Scale effect on geomorphologic and kinematic dispersion. *Water Resources Research* **39**: 1286. DOI: 10.1029/2003WR002154.
- D'Odorico P, Rigon R. 2003. Hillslope and channel contributions to the hydrologic response. *Water Resources Research* **39**: 1113. DOI: 10.1029/2002WR001708.
- Gupta VK, Waymire E, Wang CT. 1980. A representation of an instantaneous unit hydrograph from geomorphology. *Water Resources Research* **16**: 855–862.
- Gupta VK, Waymire EC, Rodríguez-Iturbe I. 1986. On scales gravity and network structure in basin runoff. In *Scale Problems in Hydrology*, Gupta VK, Rodríguez-Iturbe I and Wood EF (eds). Reidel, Dordrecht: Holland; 159–184.

- Henderson FM, Wooding RA. 1964. Overland flow and groundwater flow from a steady rainfall of finite duration. *Journal of Geophysical Research* **69**: 1531–1540.
- Jin C. 1992. A deterministic Gamma-type geomorphologic instantaneous unit hydrograph based on path types. *Water Resources Research* **28**: 476–486.
- Kirkby MJ. 1976. Tests of a random network model and its application to basin hydrology. *Earth Surface Processes* **1**: 197–212.
- Lee KT, Yen BC. 1997. Geomorphologic and kinematic-wave-based hydrograph derivation. *Journal of Hydraulic Engineering ASCE* **123**: 73–80.
- Lee MT, Blank D, Delleur JW. 1972. A program for estimating runoff from Indiana watersheds, Part II. Assembly of hydrologic and geomorphologic data for small watersheds in Indiana, Technical Report No. 23, Purdue University<sup>7</sup> Water Resources Research Center, Lafayette, Indiana.
- Lee MT, Delleur JW. 1976. A variable source area model of the rainfall runoff process based on the watershed stream network. *Water Resources Research* **12**: 1029–1036.
- Leopold LB, Maddock T. 1953. The hydraulic geometry of stream channels and some physiographic implications. *US Geological Survey Professional Paper* **252**: 57.
- Mesa OJ, Mifflin ER. 1986. On the relative role of hillslope and network hydraulic geometry in hydrologic response. In *Scale Problems in Hydrology*, Gupta VK, Rodriguez-Iturbe I and Wood EF (eds), D. Reidel, Norwell, MA; 1–17.
- Minshall NE. 1960. Predicting storm runoff on small experimental watersheds. *Journal of the Hydraulics Division, American Society of Civil Engineers* **86**(HY8): 17–38.
- Naden PS. 1992. Spatial variability in flood estimation for large catchments: The exploitation of channel network structure. *Hydrology Sciences Journal* **37**: 53–71.
- Olivera F, Maidment D. 1999. Geographic Information Systems (GIS)-based spatially distributed model for runoff routing. *Water Resources Research* **35**: 1155–1164.
- Paik K, Kumar P. 2004. Hydraulic geometry and the nonlinearity of the network instantaneous response. *Water Resources Research* **40**: W03602. DOI: 10.1029/2003WR002821.
- Peckham SD. 1995. New results for self-similar trees with applications to river networks. *Water Resources Research* **31**: 1023–1030.
- Pilgrim DH. 1976. Travel times and nonlinearity of flood runoff from tracer measurements on a small watershed. *Water Resources Research* **12**: 487–496.
- Reggiani P, Sivapalan M, Hassanizadeh SM, Gray WG. 2001. Coupled equations for mass and momentum balance in a stream network: Theoretical derivation and computational experiments. *Proceedings of the Royal Society (London), Series A: Mathematical, Physical Engineering Sciences* **457**: 157–189.
- Rinaldo A, Marani A, Rigon R. 1991. Geomorphological dispersion. *Water Resources Research* **27**: 513–525.
- Rinaldo A, Vogel GK, Rigon R, Rodriguez-Iturbe I. 1995. Can one gauge the shape of a basin?. *Water Resources Research* **31**: 1119–1127.
- Rodriguez-Iturbe I, Valdes JB. 1979. The geomorphologic structure of hydrologic response. *Water Resources Research* **15**: 1409–1420.
- Robinson JS, Sivapalan M, Snell JD. 1995. On the relative roles of hillslope processes, channel routing, network geomorphology in the hydrologic response of natural catchments. *Water Resources Research* **31**: 3089–3101.
- Saco PM, Kumar P. 2002a. Kinematic dispersion in stream networks 1. Coupling hydraulic and network geometry. *Water Resources Research* **38**: 1244. DOI: 10.1029/2001WR000695.

- Saco PM, Kumar P. 2002b. Kinematic dispersion in stream networks 2. Scale issues and self-similar network organization. *Water Resources Research* **38**: 1245. DOI: 10.1029/2001WR000694.
- Saco PM, Kumar P. 2004. Kinematic dispersion effects of hillslope velocities, *Water Resources Research* **40**: W01301. DOI: 10.1029/2003WR002024.
- Sivapalan M, Bates BC, Larsen JE. 1997. Generalized nonlinear diffusive wave equation: theoretical development and application. *Journal of Hydrology* **192**: 1–16.
- Sherman LK. 1932. Stream flow from rainfall by the unit-graph method. *Engineering News-Record* **108**: 501–505.
- Sklar LS, Dietrich WE, Foufoula-Georgiou E, Lashermes B, Bellugi D. 2006. Do gravel bed river size distributions record channel network structure?, *Water Resources Research* **42**: W06D18. DOI: 10.1029/2006WR005035.
- Snell JD, Sivapalan M. 1994. On geomorphological dispersion in natural catchments and the geomorphological unit hydrograph. *Water Resources Research* **30**: 2311–2323.
- Snell JD, Sivapalan M. 1995. Application of the meta-channel concept: construction of the hydraulic geometry for a natural catchment. *Hydrological Processes* **9**: 485–505.
- Snell JD, Sivapalan M, Bates B. 2004. Nonlinear kinematic dispersion in channel network response and scale effects: application of the meta-channel concept. *Advances in Water Resources* **27**: 141–154.
- Stall JB, Fok YS. 1968. Hydraulic geometry of Illinois streams. *University of Illinois Water Resources Research Report* **15**: 47.
- Stall JB, Yang CH. 1970. Hydraulic geometry of 12 selected stream systems of the United States. *University of Illinois Water Resources Center Report* **32**: 73.
- Strahler AN. 1957. Quantitative analysis of watershed geomorphology. *Eos Transactions American Geophysical Union* **38**: 913–920.
- Troutman BM, Karlinger MR. 1985. Unit hydrograph approximation assuming linear flow through topologically random channel networks. *Water Resources Research* **21**: 743–754.
- Valdes JB, Fiallo Y, Rodriguez-Iturbe I. 1979. A rainfall-runoff analysis of the geomorphic IUH. *Water Resources Research* **15**: 1421–1434.
- van der Tak LD, Bras RL. 1990. Incorporating hillslope effects into the geomorphological instantaneous unit hydrograph. *Water Resources Research* **26**: 2393–2400.
- Wang CT, Gupta VK, Waymire E. 1981. A geomorphologic synthesis of nonlinearity in surface runoff. *Water Resources Research* **17**: 545–554.
- White AB, Kumar P, Saco PM, Rhoads BL, Yen BC. 2004. Hydrodynamic and geomorphologic dispersion: Scale effects in the Illinois river basin. *Journal of Hydrology* **288**: 237–257.
- Yen BC, KT Lee. 1997. Unit hydrograph derivation for ungauged watersheds by stream order laws. *Journal of Hydrologic Engineering, ASCE* **2**: 1–9.



# 16

## Sediment delivery: new approaches to modelling an old problem

Hua Lu<sup>1</sup> and Keith Richards<sup>2</sup>

<sup>1</sup>*British Antarctic Survey, UK*

<sup>2</sup>*Department of Geography, University of Cambridge, UK*

### Introduction

River channel networks transport both water delivered to them by catchment runoff processes and sediments acquired by various erosion processes as the runoff occurs over slopes and in the channels themselves. These networks are dynamic systems with branching structures that exhibit a high degree of complexity, but also regularity and organization; this spatial and temporal organization within river basins emerges from a large number of interconnected physical and biological processes. Sediment delivered to the river network, and then routed through it, is thus derived from many different sources within a catchment, including areal production from hillslope soil erosion (both sheet-wash and gully erosion) and point and line sources, such as mass movements and river-bed and bank erosion. During transport, this sediment may be partly and temporarily stored en route, in sediment sinks such as colluvium on the lower-gradient hillslopes, alluvium (in the floodplain and river terraces) and in lakes, reservoirs and estuaries.

Models developed to account for sediment transport at the catchment and river network scale have varying degrees of complexity. The simplest consist of empirical

relationships for sites within the network for which sediment-yield and stream-flow data are available; these include methods combining sediment-rating relationships and flow-duration curves (Gregory and Walling, 1973; Crawford, 1991; Horowitz, 2003), and those based on surveys of lake and reservoir sedimentation (Verstraeten and Poesen, 2000). These empirical relationships based on site-specific observations and data may be useful for the particular site where the data were collected, but extrapolation to other catchments is unlikely to be generally successful. Semi-empirical relationships have been derived between sediment yield and variables defining climate forcing (rainfall properties) and catchment morphology, such as catchment area, soil type, geology, topography, vegetation and land-use management (Milliman and Meade, 1983; Restrepo and Kjerfve, 2000). Both the empirical and semi-empirical models contain weak representations of transport mechanisms, lack explicit evaluation of sediment sources, and focus on temporal variability while ignoring both the spatial heterogeneity of sources and sediment-routing processes. The earliest spatially distributed models of sediment yield were multivariate linear regression models (Anderson, 1954; Anderson, 1957; André and Anderson, 1961). These models were later developed as grid-based methods involving systematic inventories of land-surface attributes in ungauged basins (Solomon and Gupta, 1977; Cluis *et al.*, 1979; and see below).

The second category of model seeks to build on fundamental hydrologic and hydraulic processes, where the separate effects of climate forcing, catchment conditions and anthropogenic influences can all be identified (e.g. Flanagan and Nearing, 1995; Morgan *et al.*, 1998). Their process descriptions may include runoff generation and routing, flow hydraulics, particle detachment by raindrop impact, deposition and remobilization, and coupling between water flow and sediment (Young *et al.*, 1989; Krysanova *et al.*, 1998; Bouraoui and Dillaha, 1996). These models are often extremely data-demanding, requiring input data such as digital elevation models (DEMs), climate, soil, vegetation cover, land use and other management factors, all at relatively fine spatial and temporal resolutions. They are used by engineers, water-quality managers and water-resources planners to analyse critical process interactions affecting water quality, to evaluate the effectiveness of alternative control strategies and to provide data to perform cost-benefit analysis and decision-making. It is not our intention to review these models in detail, but it is worth noting that their reliability tends to decrease with increased catchment size and complexity (Novotny and Olem, 1994).

A third category of models includes those that treat sediment transport stochastically, although the number of these is limited. For example, Moore and Clarke (1983) propose a probabilistic sediment-transport model in the form of the well-known time-invariant linear system assumed by the unit-hydrograph method. By extending the advection–diffusion equation by adding a term to account for sediment deposition, they show that, for sediment transport, the channel-response function can be expressed as a stochastic function of the distance to the outlet, the time since erosion begins and the average flow velocity. They use the hydrodynamic–dispersion coefficient to describe the

sediment-routing efficiency within the channel network, and a proportionality constant to define a linear relationship between deposition and storage. The channel response in the model of Moore and Clarke is conceptually equivalent to the sediment-delivery ratio, only it is allowed to vary with both the distance to the outlet and the time.

The ultimate goal of developing sediment-yield models is to improve our understanding of sediment-transport processes in the river network, that is of the supply, delivery, storage and yield of sediment over various time and space scales. However, the degree of complexity of these processes over a whole catchment and river network means that it is necessary to strike a balance between theoretical and empirical approaches, especially when dealing with practical catchment-management issues, such as the downstream sedimentation effects of upstream soil erosion. Physically based sediment-transport models remain overly complex in relation to the data available to estimate or calibrate their many parameters, or to validate them. This problem is not unique to sediment-transport modelling, but applies to most models coupled to spatially distributed hydrologic drivers (Beven, 1989; Jakeman and Hornberger, 1993). The lack of available data (of sediment yield and environmental variables) and the associated parameterization difficulties lead modelled sediment-transport rates to be highly uncertain. Furthermore, simplifications, such as state-steady flow assumptions, fail to take into account the threshold-dependent, hysteretic and highly intermittent nature of sediment transport; and improperly scaled sediment routing may give rise to non-linear error propagation. It therefore remains difficult to elucidate the direct linkages between detailed descriptions of processes operating at small scales and observed macroscopic features of sediment-yield variability at the catchment scale.

Biron and Lane (Chapter 3, this volume) demonstrate that modelling sediment transport at river cross-sections can be approached by detailed coupling of hydrologic and hydraulic models, and Gasparini *et al.* (Chapter 17, this volume) contend that, to understand and model network evolution, the sediment-transport rate is often necessarily described by simplified transport laws (power functions of discharge and slope, shear stress under steady-state runoff, and discharge as a power function of contributing area). Sediment transport, as described in the present chapter, requires an approach between these end-member cases because of the increased complexity of spatial and temporal heterogeneities at the catchment scale, even on timescales for which the catchment characteristics remain constant. Here, the greatest challenges to understanding and modelling sediment transport occur not only because of non-linear interactions of the processes of erosion, deposition and remobilization of sediment but also because of our inability to represent its non-equilibrium nature and the spatial and temporal scales over which heterogeneities occur (Richards, 1993; Lane *et al.*, 1997).

This chapter therefore provides a critique of the current knowledge of the processes that control sediment transport at the catchment scale and introduces alternative approaches to this complex transport phenomenon, in which transport coefficients based on the mean and variance of velocities are dependent on temporal and spatial

scales of measurement. By contrast with models that attempt to capture finer details of physical processes, the primary focus in this chapter is to explain the macroscopic features of sediment transport, such as the scaling issues related to temporal and spatial variability, the interplay between climatic, hydrological and geomorphological controls and mathematical representations of controlling processes. We begin by defining ‘sediment yield’, ‘sediment-delivery ratio’ and tackling the issues related to their empirical estimation. We then demonstrate the similarity between sediment-delivery and catchment-runoff processes, and show that this similarity motivates the development of a simple model that provides a physical interpretation of observed scaling behaviours of specific sediment-yield and sediment-delivery ratios with travel time and catchment area. We then examine a distributed model of sediment production and delivery, which is based on similar principles and is applicable to practical environmental management problems. To make the problem tractable, this chapter is limited to suspended sediment transport and omits processes such as bedload transport and landslides.

## The concept of sediment delivery

‘Sediment yield’ is defined as the quantity of eroded material transported by water flow from a defined area of the landscape to a specific location, such as the outlet of a drainage basin for a given measurement period. As a catchment-scale measure of soil erosion, transport and deposition, the sediment yield reflects characteristics of the catchment, its climate and morphological conditions. For comparative purposes, it is expressed as a weight per unit area and time [ $M L^{-2} T^{-1}$ ], as its spatial and temporal averages vary with both the area and time period of measurement. A dimensionless empirical variable, the sediment-delivery ratio (SDR), is often used to relate the space-time average of catchment sediment yield and gross erosion, by:

$$y = \gamma e_{x,y} \quad (16.1)$$

where  $y$  ( $M L^{-2} T^{-1}$ ) is the average sediment yield,  $e_{x,y}$  ( $M L^{-2} T^{-1}$ ) is the average gross erosion rate (also expressed per unit area and time for dimensional consistency) and  $\gamma$  is the SDR (Walling, 1983; Richards, 1993). The time period over which  $y$  and  $e$  are estimated is often an annual average, although both upland erosion rate and sediment yield may vary widely between and within years. The SDR concept that links them provides a simple basis for investigating problems relating to the downstream consequences of upstream erosion (such as sedimentation and pollution), but in practice its value varies significantly with the size of areal unit, the length of time period over which it is averaged and various environmental properties, and it remains a factor of limited practical value.

A proper definition for the time-averaged sediment yield would be:

$$\bar{y} = \int_{T_y} y(t) dt / T_y = \int_{T_y} C(t) Q(t) dt / AT_y \quad (16.2)$$

where  $y(t)$  is the time-varying area-averaged sediment yield, or specific sediment yield at the measuring location [ $M L^{-2} T^{-1}$ ],  $T_y$  is the characteristic timescale for sediment transport from contributing area  $A$ ,  $Q(t)$  is the time-varying water discharge [ $L^3 T^{-1}$ ] and  $C(t)$  [ $M L^{-3}$ ] is the sediment concentration at time  $t$ . Similarly, a proper definition of SDR is:

$$\gamma = \frac{\int_{T_y} y(t) dt / T_y}{\int_{T_e} e_{x,y}(t) dt / T_e} = \frac{\int_{T_y} C(t) Q(t) dt / AT_y}{\int_{T_e} e_{x,y}(t) dt / T_e} \quad (16.3)$$

where  $T_e$  is the characteristic timescale of hillslope erosion within the catchment,  $e_{x,y}(t) = \frac{1}{A} \iint_A e(x, y, t) dx dy$  is the spatially averaged upland erosion rate [ $M L^{-2} T^{-1}$ ], and  $e(x, y, t)$  [ $M L^{-2} T^{-1}$ ] is the spatially varying plot-scale upland erosion rate at time  $t$  over the contributing area  $A$ . Equation 16.2 implies that a statistically meaningful ensemble mean  $\bar{y}$  can only be obtained where  $y(t)$  is at least quasi-stationary during time  $T_y$ , and Equation 16.3 means that a statistically meaningful ensemble mean for  $\gamma$  can only be obtained when  $e_{x,y}(t)$  is relatively stationary during  $T_e$  and when the conditions for a statistical equilibrium in  $\bar{y}$  are also obeyed. Thus, a statistically meaningful average sediment yield or SDR for a catchment with particular environmental properties (soil erodibility, rainfall characteristics, topography and network geometry) can only occur if it is estimated for a time period over which both erosion rate and sediment yield are at statistical equilibrium.

## Difficulties in measuring and estimating sediment yield and SDR

Understanding sediment transport is complicated by the lack of long-term data on sediment flux within river networks, which are essential for the development and testing of a variety of theories and methods. As noted above, common sources of data are (a) measurements from combined river gauging and sediment-sampling stations and (b) sedimentation records for lakes and reservoirs. Sediment records derived from the former are often too short (only a few decades at most), and those derived from the latter often lack temporal resolution. There are also means of measuring (using erosion pins or soil caesium inventories), or estimating (using soil-erosion models) at-a-point

erosion rates within catchments, and integrating these over a catchment leads to an estimate of the gross erosion rate. Most available datasets relate to agricultural plots and small experimental catchments, and do not represent the interacting processes and spatial heterogeneities occurring at larger spatial scales.

As a result, the statistical requirements outlined in the previous section are rarely met in practice, particularly because the characteristic timescale for sediment delivery  $T_y$  can be much larger than the characteristic erosional timescale  $T_e$ . Wischmeier and Smith (1978) suggest that at least 20 to 25 years of rainfall data are needed to define a long-term average for rainfall erosivity. Thus, at the plot scale, a few decades of erosion measurements are needed for statistically meaningful long-term average erosion rates. Studies of travel distance in flumes and in small catchments suggest that most entrained sediment is transported only a few metres before being redeposited (e.g. Parsons and Stromberg, 1998). In comparison with the rate of change of land-surface conditions, the rate of change of fluvial suspended sediment concentration is small. The travel distance for suspended sediment (i.e. the wash fraction of the load) increases considerably once those fine particles reach the streams. Viewing the hillslope and river network as an integrated system, the characteristic timescale of catchment sediment yield must be longer than that at the plot scale, but remains largely unknown at present. This long timescale for sediment yield places a limit on the degree to which the yield of particulate sediment from a river network can be isolated from considerations of chemical weathering and solute yield, since fine sediments in storage for long periods in large catchments may be remobilized by chemical processes and eventually exported in solution (Dietrich and Dunne, 1978).

In a steady-state system, sediment yield would be approximately equal to the amount eroded from upstream slopes, and there is no net change in storage (Slaymaker, 1972). Such a condition rarely exists in river basins (Trimble, 1983), and certainly cannot be assumed for much of the United States (Trimble, 1975) and Australia (Wasson *et al.*, 1998) since European settlement. In the last 200 years in Australia, the erosion of hillslopes and stream banks has increased significantly (Edwards, 1993), supplying large quantities of sediment to the rivers (Rutherford, 2000). Much of this sediment is still stored within the river system (Wasson *et al.*, 1996). In large catchments, the characteristic timescale of catchment-sediment yield is related to prolonged sediment storage (Dietrich and Dunne, 1978; Trimble, 1983; Meade, 1988; Meade *et al.*, 1990). For example, Church (2002) suggests that in Canadian drainage basins the characteristic time of sediment transfer is of the order of  $10^2$ – $10^6$  yr, reflecting this long-term storage effect. In small catchments, the main stores are in fans, footslopes and terraces; in large rivers, the floodplains, reservoirs and the river bed are more important. Sediment-residence times are measurable via appropriate observations of sediment body age and turnover rate. The non-steady-state nature of sediment transport renders the concept of a stationary sediment yield or SDR effectively meaningless beyond a limiting catchment area. For any time period, the SDR can be used to link the upland erosion rate to

sediment yield only when no significant change of sediment storage occurs (Trimble, 1983). A question thus arises as to whether the concept of the SDR should be restricted to catchments small enough that the integral time in Equations 16.2 and 16.3 is of the order of the sediment-transit time from hillslope to channel.

To make the situation even worse, measurements of upland erosion and sediment yield are often made during different time periods, and the values of  $T_e$  and  $T_y$  are determined by data availability rather than theoretical necessity. For these practical reasons, various different approximations to Equations 16.2 and 16.3 have been used, and they are often reduced to:

$$\bar{y} = c_0 \sum_{j=1}^M Q_j C_j \quad (16.4)$$

and

$$\gamma = \frac{c_0 \sum_{j=1}^M Q_j C_j}{\bar{e} A M} \quad (16.5)$$

where  $Q_j$  and  $C_j$  are discrete samples of discharge and sediment concentration respectively.  $M$  is the total number of samples,  $\bar{e}$  is the average annual spatially averaged upland erosion rate,  $c_0$  is a dimensionless factor representing the ratio of the units of  $\bar{e}$  and the units of specific sediment yield estimated from discrete samples. Sometimes, further approximation is applied by focusing only on hydrograph events, or hydrograph peaks. Frequently, the measured concentration  $C$  is replaced by a concentration estimated from a sediment-rating relationship, then applied to a discharge record that is more continuous and long-standing than the sediment record. Furthermore, inadequate sampling may also cause large errors in estimates of sediment yield (Walling, 1977; Yorke and Ward, 1986). Few estimates of catchment-averaged  $\bar{y}$  or SDR are therefore based on data allowing true statistical averaging, and accordingly most estimations of  $\bar{y}$  or SDR can rarely be compared directly between catchments. A general source of problems in cross-catchment comparisons of SDRs and  $\bar{y}$  is the failure of the analyst to scale the data to equivalent areas for comparison. Church *et al.* (1999) examined fluvial sediment yield in Canada and found that the specific sediment yield  $\gamma$  increases downstream in most regions, indicating a regional degradation of river valleys. Aggradation, however, occurs regionally over the southern Prairies, while specific sediment yields are on average similar at all scales in southern Ontario. Church *et al.* (1999) also note the danger of a simple presentation of unadjusted specific sediment yields in cross-catchment comparisons. The scale dependence of specific sediment yield means that sediment yields must be scaled to a standard area for comparison between basins and regions.

A practical reason for deriving the SDR ( $\gamma$ ) using Equation 16.3 or its approximations for a series of catchments is that, if a good correlation can then be established between  $\gamma$  and measured catchment properties, Equation 16.1 can be used to estimate the sediment yield from erosion estimates for ungauged catchments. The latter have been based, for example, on erosion estimates using the Universal Soil Loss Equation (Roehl, 1962; Trimble, 1983) or an equivalent soil-loss model. However, the only strong signal that emerges in attempts to derive such a relationship between  $\gamma$  and catchment properties is the well-known  $\gamma$ - $A$  relationship (Roehl, 1962; ASCE, 1975), examples of which are shown in Figure 16.1. These suggest a power-function relationship:

$$\gamma = \alpha A^\phi \tag{16.6}$$

where  $\alpha$  and  $\phi$  are empirical parameters. Observational studies show that the exponent  $\phi$  is commonly but not universally negative, and mostly of the order of  $-0.01$  to  $-0.04$ . Similar inverse power functions have also been found for annual average sediment yield (Milliman and Meade, 1983). There are grounds for expecting an inverse relationship of the  $\bar{y}$  or SDR with area, such as the decreasing average gradient of larger catchments, and the associated increasing potential for intervening storage between locations of sediment detachment and sites where sediment yield is measured. Furthermore, in large catchments, erosive rainstorms are unlikely to cover the whole basin, and this also implies decreasing SDR with increasing area.

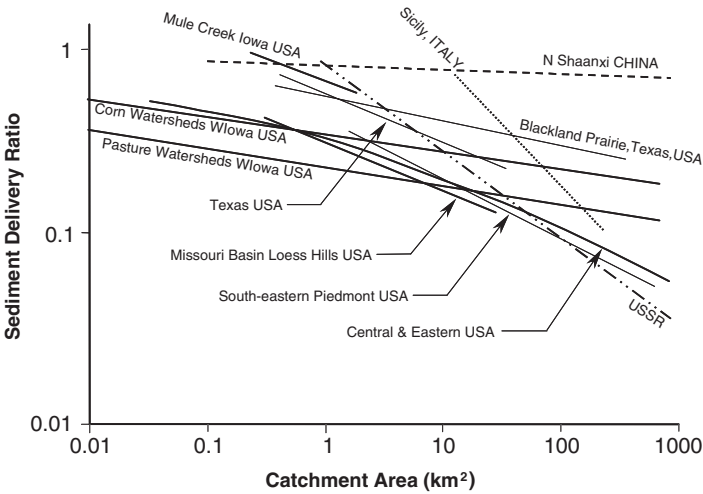


**Figure 16.1** Relationships of the SDR to catchment area based on historical empirical data. Various different sampling methods were employed in developing the different relationships. The trend for Sicily was from Ferro and Minacapilli (1995). The rest are redrawn from Walling (1983).

However, Figure 16.1 shows that considerable variation exists in  $\gamma$ - $A$  relationships in different regions, with  $\gamma$  varying by a factor of two or more for a given area, suggesting that a variation of  $\gamma$  depends on properties other than catchment area. Equation 16.6 therefore appears to be only a weak scaling relationship rather than a basis for the regionalization of sediment delivery. In addition, as a counter example, data from Canada and Australia (Church and Slaymaker, 1989; Wasson, 1994; Wasson *et al.*, 1998) shows that the SDR may sometimes increase with catchment area, in association with channel incision, or remobilization of paraglacial sediment supply. A number of studies where both cases of  $\gamma < 1$  and  $> 1$  are present are summarized by Birkinshaw and Bathurst (2006). Faced with such evidence of unpredictable variation in the SDR, some researchers have even completely dismissed it as a useful concept (Trimble and Crosson, 2000; Kinnell, 2004). However, it may be less the concept itself that is the problem than the way it has been misused.

One problem with the  $\gamma$ - $A$  relationship is that the values of  $\gamma$  are lumped at the whole catchment scale, and there is no information in the catchment scale measure (area) about the structure of the drainage network and the organization of sub-catchments. The importance of these issues was recognized by Boyce (1975), who noted that downstream flow-through channels (interior links in the drainage network) have lower delivery ratios for their area than exterior links, but are unrepresented in the  $\gamma$ - $A$  relationships shown in Figure 16.1. Boyce (1975) considers a hypothetical watershed in which the exterior links have a high delivery ratio and the whole drainage basin a lower one (consistent with the  $\gamma$ - $A$  relationship). If the production of sediment per unit area across the whole catchment is assumed to be uniform, the interior link areas must have an even lower delivery ratio than the complete catchment. The conclusions to be drawn from this simple thought experiment are that the  $\gamma$ - $A$  relationship cannot be used to examine within-catchment variation in the delivery ratio (since it is based on between-catchment statistical analysis), that it cannot be used for reliable comparison between catchments when it fails to define the variation between them in network structure (and sediment routing) and that the appropriate way to treat the delivery-ratio concept is in a spatially distributed manner, applying it to small sub-catchments and defining whole-catchment delivery ratios in terms of chained sediment budgets to downstream sites (see below).

Limiting the applicability of the SDR to small catchments and treating in-channel sediment transport as a separate issue may largely neutralize the existing critique of the usefulness of the SDR. In fact, Equation 16.6 merely represents a general area-scaling relation for sediment yield. The scaling exponent  $\phi < 0$  (or  $> 0$ ), or  $\gamma < 1$  (or  $> 1$ ) in Equation 16.6 implies aggradation (or degradation) over the specific measuring time period. This holds either at field edges or, at the usual larger scale of observations, in floodplains or along a river channel. The scaling exponent  $\phi$  essentially plays the same role, for sediment transport, as the extensively studied fractal scaling relations do for runoff. It represents a generalized and alternative approach to the catchment scaling of sediment transport for a shorthand summary of regional sediment-yield trends and

patterns. In our view, it would make more physical sense to restrict the commonly used steady-state SDR to small catchments, where statistical-equilibrium conditions are more likely to be met. The scaling perspective of Equation 16.6 then must be generalized when applied to the channel phase, where the parameter  $\phi$  needs to be treated as a function of time and catchment conditions because the system is no longer stationary.

In a practical sense, an ability to estimate the SDR would be valuable as a means of linking upland erosion and downstream sediment yield and of informing the assessment of the operational life of a new reservoir in terms of storage depletion caused by sedimentation. Methods to estimate the trap-efficiency (TE per cent) of a reservoir of given geometry and operational characteristics (TE is the percentage of inflowing sediment retained in the reservoir), including the Brune (1953) and Churchill (1948) curves, are essentially similar to the SDR–area relationship. The former relates TE to the ratio of the reservoir’s water-storage capacity and the annual water inflow; the latter relates the sediment throughput (defined as 100-TE per cent) to an index based on the reservoir retention time and throughflow velocity (Verstraeten and Poesen, 2000; Richards, 2002). The theoretical significance of the SDR is that it defines a relationship between sediment-production locations in a drainage basin and the attenuation and depositional losses associated with the routing of material through the drainage network to a downstream location. The SDR thus defines how the erosional history of a drainage basin is modulated by temporary storage, as erosional products are moved discontinuously through the landscape. However, this is only true if the SDR is treated as a spatially distributed index for much smaller spatial domains (where the statistical equilibrium conditions are more likely to be satisfied), rather than simply as a lumped index for the entire basin; and if its dependence on the network structure of a basin is explicitly considered.

The importance of storage along the river network is evident both in understanding landscape evolution and in environmental management. In the former case, for example, it is not straightforward to interpret dated sedimentary units in downstream sediment sinks in relation to environmental (e.g. climate change) drivers without knowing the time constants for the upstream landscape, which themselves may vary with climate. Also, sediment may enter storages during periods of catchment disturbance, especially at river confluences (Richards, 1993), in the form of alluvial fans, and then be reworked into downstream floodplains later, in a version of the complex response model (Schumm and Parker, 1973), in which external stimuli such as climatic changes cause multiple aggradation-incision cycles. These issues imply that lags between the production of sediment and its deposition in temporary storage are highly variable both within and between catchments, depending on sediment-routing pathways. This means that attempts to infer the timing of climatic change from histograms of  $^{14}\text{C}$  dates obtained from organic material preserved in alluvial sediments must be treated with caution, since the intervals between erosion and burial will vary considerably depending on catchment size and network structure (Knox, 1975; Macklin, 1999; Richards, 2002).

In the latter case, the environmental problems associated with sediment yield include sedimentation and loss of storage capacity in reservoirs, increased flooding as a result of channel aggradation and water-quality problems that reflect the fact that sediment serves as a carrier for nutrients and pesticides (Scheffer, 1998; Woodroffe *et al.*, 1993; McCulloch *et al.*, 2003). The management of such sediment-related problems must be based on understanding both upstream sediment production and downstream effects. Thus, there are practical needs to regionalize or extrapolate observed sediment yield (or the SDRs) from gauged sites to ungauged sites. Additional physiographic and hydrological attributes have been suggested as a basis for regionalization; these include mean annual runoff, average catchment relief, channel-network bifurcation ratio, catchment relief/length ratio, main channel slope and mean travel time of sediment (Roehl, 1962; Renfro, 1975; Walling, 1983; Khanbilvardi and Rogowski, 1984; Ferro and Minacapilli, 1995). This implies that the empirical scaling relation, e.g. Equation 16.6, is likely to suffer from the effect of 'the devil's own variable', catchment area (Anderson, 1957), with which many of these other controlling factors are correlated.

The mixture of methods, timescales and definitions used in the past, and the resulting lack of consistency in the data employed, all imply that not only are more process-based insights into sediment delivery needed but, equally, so is a suitable theoretical framework. Theoretical development needs to focus on the interactions amongst the diverse array of processes controlling sediment supply, the system heterogeneity at the catchment scale and the routing of sediment through the drainage network, which together have given rise to a wide variation of relationships between sediment production and sediment yield, with multiscale coherence lengths and potentially very long sediment-retention times. In the following sections, therefore, we explore some alternative, related, theoretical approaches to sediment production, delivery and yield. These examine the relationship between hydrology and sediment yield, and the spatial structure of production, storage and yield defined by routing through the river network. They range from theoretical models that explore how some interactions amongst system components may arise in the real world, and may lead to the formulation of testable hypotheses that can be evaluated through empirical studies, to simplified models that have demonstrable utility in practical environmental management.

## **Links between hydrology and sediment production and yield**

Rainfall-runoff processes are the ultimate drivers of erosional processes and sediment transport, so certain parallels should exist between the relationships of runoff and sediment yield to catchment properties. Close correlation between suspended sediment yield and discharge has commonly been observed in small agricultural catchments (Lane *et al.*, 1997; Krysanova *et al.*, 1998), and in many cases, mean runoff depth (runoff per

unit area) and sediment yield scale with basin area in similar ways, with inverse power-function relationships and similar scaling exponents (e.g. Benson, 1962; Goodrich *et al.*, 1997). A similar scale transition in behaviour exists in hydrology to that which exists in the transition from hillslope erosion, in which sheetwash and rill erosion supply sediment to the river network, to channel erosion, in which the sediment supply is generated by river bank erosion. This transition has been recognized by Calver *et al.* (1972) and Kirkby (1976) as a scale-dependent change in the relative importance of the hillslope-runoff process and the network-dependent channel-routing process in determining the temporal characteristics of the hydrograph (e.g. its time of rise, time of concentration and time base).

In Figure 16.2, a connection to hydrological scaling is illustrated by plotting empirical SDR data (Roehl, 1962) in relation to catchment area  $A$  and comparing these against average peak-flow (flood) responses (the plotted lines) for similar-sized catchments, using parameters defined by Robinson and Sivapalan (1997a) from simple theoretical reasoning. The SDR values (dots) were derived from eastern USA regions where hillslope erosion dominates. The average peak-flow response,  $E(S)$ , is defined as the ratio between average peak runoff at the catchment outlet and the average rainfall intensity. For rectangular pulses of rainfall falling on a catchment, and assuming a triangular unit hydrograph of flood response, Robinson and Sivapalan (1997a) derived an analytical expression for  $E(S)$  of the form:

$$E(S) = 2 (t_r / t_c) \{ 1 - (t_r / t_c) + (t_r / t_c) \exp [ - (t_c / t_r) ] \} \tag{16.7}$$

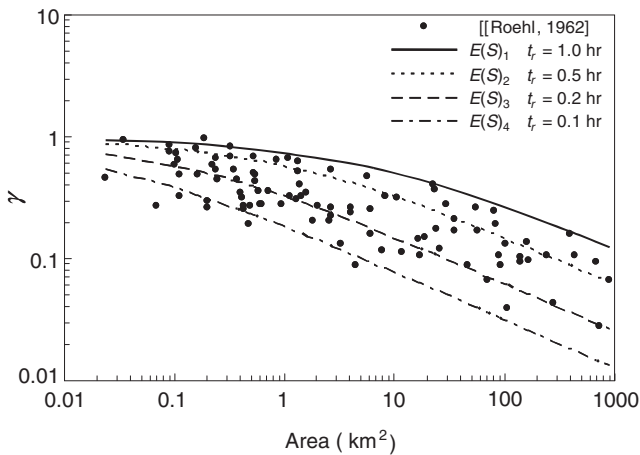


**Figure 16.2** Comparison of sediment delivery ratio  $\gamma$  derived from measurements (Roehl, 1962) and peak-flow response  $E(S)$  (Equation 16.5) with different values of excess rainfall duration  $t_r$ . It is assumed that  $t_c$  in Equation 16.5 is expressed as a function of basin area  $A$  of the form:  $t_c = \xi A^\nu$ , where values of 1 and 0.4 were used for  $\xi$  and  $\nu$ .

where  $t_r$  and  $t_c$  are the duration of rainfall excess (rainfall minus infiltration), and the catchment's time to concentration, respectively. Figure 16.2 shows that with the choice of a realistic range of values of  $t_r$ ,  $E(S)$  expressed by Equation 16.7 is able to represent the variability in observed values of the SDR. This indicates that in environments dominated by hillslope erosion, the SDR may be closely related to (or analogous with) catchment runoff response, with similar scaling behaviour. Since  $E(S)$  is a ratio of rates of runoff discharge and runoff generation, while the SDR is a ratio of sediment discharge to sediment generation, the comparability in these two ratios shown in Figure 16.2 might imply a similar form of relationship for sediment yield, particularly for small agricultural catchments where hillslope erosion dominates.

Both observational data and simulated lines in Figure 16.2 suggest that the slope of the  $\gamma$ - $A$  relationship changes while catchment area increases. This reflects a typical multifractal feature and is consistent with the change in physical control of the sediment yield or runoff processes while the catchment area increases. One key feature of Equation 16.7 is that peak runoff response  $E(S)$  is merely a function of the ratio between two timescales,  $t_r$  and  $t_c$ , representing the interplay between catchment geomorphological conditions and hydrological controls. Such interplay can be conceptually illustrated by Figures 16.3 and 16.4, which are intuitive pictures showing advection, dispersion and deposition processes occurring along a hillslope profile (Figure 16.3) and sediment transport within a catchment with Strahler order of three (Figure 16.4). These figures show how the dual relationship between hillslope/catchment travel time and rainfall

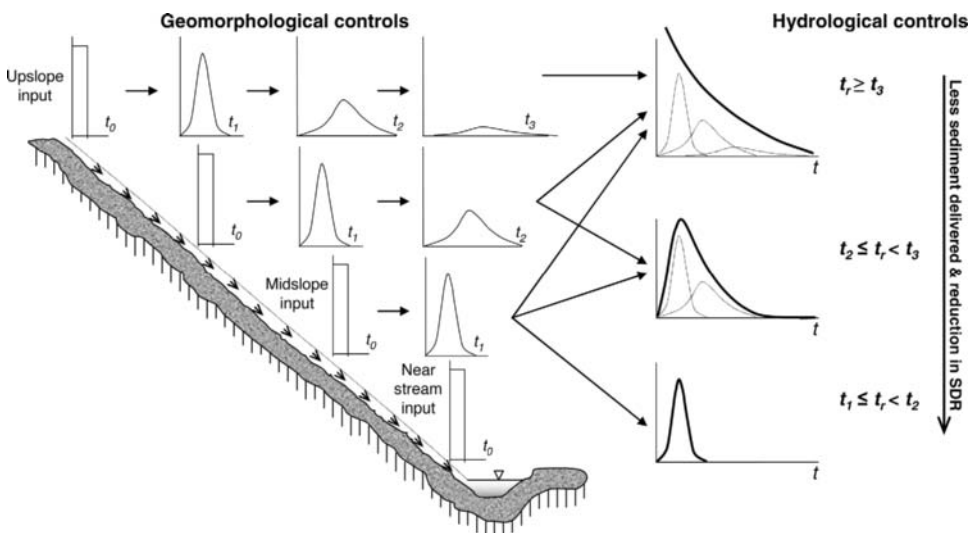
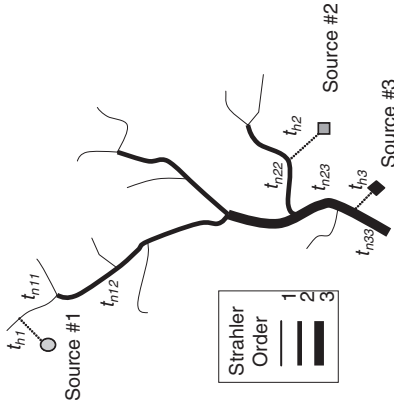


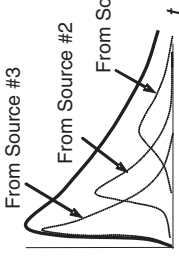
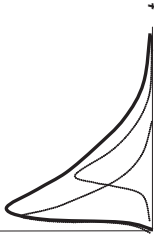
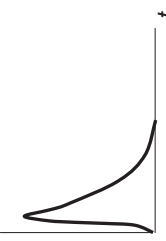
**Figure 16.3** A conceptual model of sediment transport from spatially uniform erosion sources for a hypothetical hillslope.



$$t_{c1} = t_{n1} + t_{n11} + t_{n12} + t_{n13}$$

$$t_{c2} = t_{n2} + t_{n22} + t_{n23}$$

$$t_{c3} = t_{n3} + t_{n33}$$

Typical shape of sedigraph	Control conditions	Catchment characteristics
	$t_{er} \gg t_c$	<p>Small catchments, or those in regions whose climate is characterised by long duration rainfall. The shape of the sedigraph may closely resemble the associated hydrograph. Both sedigraph and hydrograph may show similar power function scaling exponents in relation to catchment area. SDR values near unity may be feasible. Statistically meaningful time-averaged SDR values may occur.</p>
	$t_{er} \sim t_c$	<p>Medium-sized catchments, or those in temperate regions in which morphological and climatic controls interact. Sediment production is partially delivered and partially stored. Scalings for sediment yield and hydrological variations differ. The SDR varies from event to event, and must be treated as a function of time.</p>
	$t_{er} \ll t_c$	<p>Arid, semi-arid, or large catchments with short storm durations. Only sediment derived near the outlet, or from stream bank erosion, is exported. Most eroded sediment is more or less permanently stored. Even if great disturbance occurs in the catchment, limited change in sediment yield is observed at the outlet. The sedigraph is of a "first flush" type, and may differ in shape from the associated hydrograph. No statistically meaningful time-averaged SDR can be estimated as SDR effectively approaches zero.</p>

**Figure 16.4** The same concept as in Figure 16.3, but for a hypothetical network of order three with uniformly distributed sediment source supply. This shows that the travel time for source #1 is the longest (i.e.  $t_{c1} > t_{c2} > t_{c3}$  and  $t_c$  is the longest sediment travel time within the catchment. The table (right) illustrates the importance of the interplay between a catchment's geomorphological and hydrological controls in determining the shape of the sedigraph and its relation to macroscopic catchment characteristics. Note that the shape of sedigraphs may alter with spatially varying erosion sources.

duration may result in different shapes of sedigraph, and why values of SDR tend to reduce when the source area gets larger. Suppose that the total sediment yield received by a channel is the integral of the contributions from each point along the length of the hillslope (see Figure 16.3). At time  $t_0$ , upland erosion occurs. Sediment travelling downhill from sources near the channel reaches the channel promptly (occurring at time  $t_0$ ), with the smallest amount of sediment deposition on the hillslope. Sediment eroded at the top of a slope has a lower chance of reaching the channel as it must travel further. There is a time delay between the sediment production and its final receipt by the channel. During this time, proportionally more sediment gets deposited *en route* before it reaches the channel. During an erosion–sediment transport event, sediment yield in the channel may be determined by comparing the hillslope-sediment travel time  $t_h$  with the effective upland erosion duration  $t_r$  (i.e. during which local erosion occurs). When  $t_r$  is longer than  $t_h$  (e.g.  $t_h = t_3$ , as shown in Figure 16.3), sediment from all sources has an opportunity to be delivered. The total time-dependent sediment yield has a positively skewed shape (e.g. a peak at short time lags with a long tail in order to account for the first flush and delaying effects). Conversely, sediment yield may resemble the near-stream erosion distribution if  $t_r \ll t_h$  (e.g. the duration of upland erosion is particularly short). In this case, the total time-dependent sediment yield has a less skewed shape, similar to that of a Gaussian distribution. Figure 16.4 shows that this concept can be applied to sediment transport in a channel network, in which the sediment yield is measured at the catchment outlet. Similarly, sediment near the catchment outlet becomes sediment yield promptly, while the sediment contributing to the total sediment yield from the upstream sources will be reduced and more spread out in time. The upstream sediment contribution is further constrained by the rainfall duration.

For hillslopes, de Ploey (1984) suggests a physical mechanism for this by linking the basal sediment yield to the relationship between the duration of storm rainfall and overland-flow travel time, with deposition occurring when rain ceases because of reduced turbulence in sheetwash when raindrop impact ceases. In small catchments in which hillslope runoff dominates, sediment delivery is therefore likely to reflect the intensity and duration of rainfall, while in larger catchments where hydrological routing and sediment storage are dominant factors sediment production and transfer mainly reflect the interactions among bank erosion, channel incision and floodplain storage. For the latter case, Equation 16.7, or Figures 16.3 and 16.4, cannot account for the full range of variations in the relationships amongst sediment yield, SDR and catchment area, since there are cases where channelized phenomena, such as secondary reworkings of valley-floor deposits and channel incision, may even lead to increases in SDR with basin area (Church and Slaymaker, 1989; Church *et al.*, 1999). Therefore, the interaction between runoff generation and sediment-storage spatial distributions must be modelled, and additional sediment-mobilization processes must be represented. A

simple linear storage model developed to account for these factors is described in the following section.

## Physical inferences of sediment delivery based on a simple lumped model

The idea of geomorphological and hydrological controls on sediment transport described in the previous section can be made mathematically more explicit using a simple linear storage model, such as that illustrated in Figure 16.5(a) (Lu *et al.*, 2005b). This model is a modified version of the hydrological scaling model (Sivapalan *et al.*, 2002) and can be used to explore how catchment hydrological response, erosion source type and intensity, and depositional processes influence sediment transport. This event-based model consists of two linear sediment stores, one for hillslopes and one for the channel network. The hillslope store is supplied with sediment by upland erosion at the rate  $e_h(t)$  [ $M L^{-2} T^{-1}$ ] over an effective storm duration  $t_{er}$  (sediment transport only occurs during this period). At time  $t$ , some eroded sediment is redeposited within the hillslope at the rate  $r_h$  [ $M L^{-2} T^{-1}$ ], and the rest is delivered to the channel network store at rate  $y_h$  [ $M L^{-2} T^{-1}$ ]. The mass of sediment stored in the hillslope per unit area is denoted by  $S_h$  [ $M L^{-2}$ ] and can be estimated by the balance between the erosion rate  $e_h(t)$ , the redeposition rate  $r_h(t)$  and the rate of delivery to the channel,  $y_h(t)$ . Similarly, at a given time  $t$ , the channel store is supplied with sediment from the hillslope store at the rate  $y_h(t)$  plus the stream-bank erosion rate  $e_n(t)$  [ $M L^{-2} T^{-1}$ ]. This therefore captures the two states, or sub-systems – the hillslope and the channel network – that relate, respectively, to surface runoff and soil erosion, and hydrograph routing and bank erosion, as discussed in the previous section.

Some sediment in the channel store is redeposited in the channel at the rate  $r_n$  [ $M L^{-2} T^{-1}$ ], while some is transported to the catchment outlet and leaves the catchment at the rate  $y$  [ $M L^{-2} T^{-1}$ ] (the area-specific sediment yield). The mass of sediment stored in the channel network is  $S_n$  [ $M L^{-2}$ ] and can be estimated by a balance between the hillslope delivery rate,  $y_h(t)$ , the channel network erosion rate,  $e_n(t)$ , the rate of redeposition within the channel network,  $r_n(t)$ , and the rate of sediment delivery to the catchment outlet,  $y(t)$ . The continuity equation of sediment for the two stores can thus be expressed as:

$$\begin{aligned}\frac{dS_h(t)}{dt} &= e_h(t) - r_h(t) - y_h(t) \\ \frac{dS_n(t)}{dt} &= e_n(t) + y_h(t) - r_n(t) - y(t)\end{aligned}\tag{16.8}$$

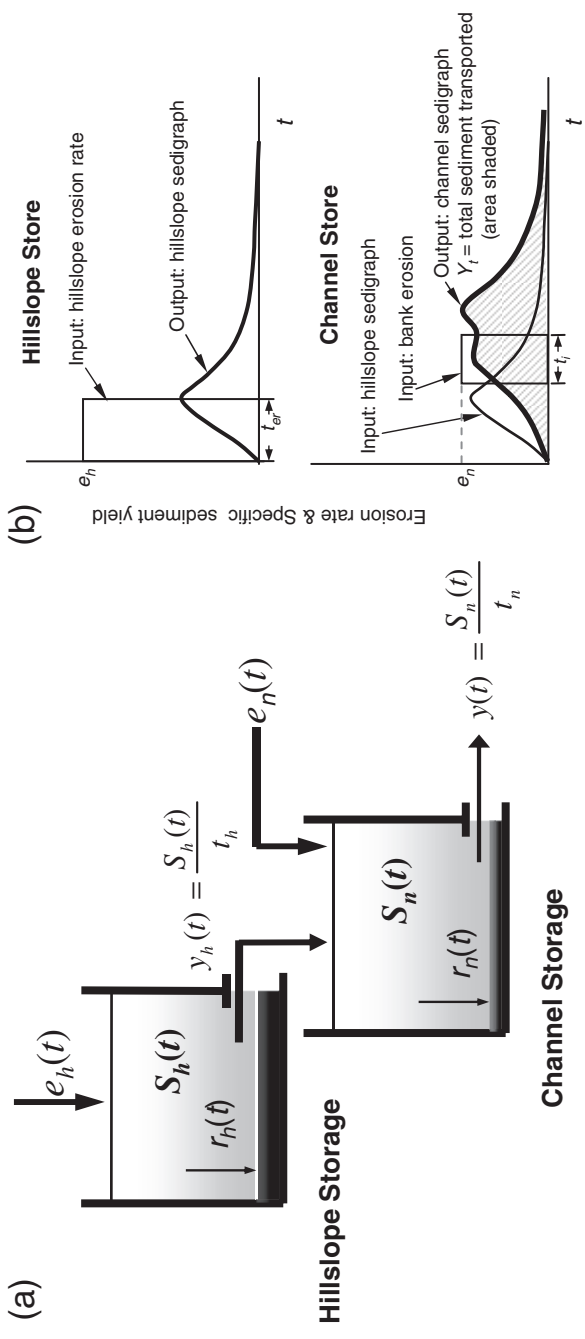


**Figure 16.5** (a) A two-store lumped linear model of sediment transport at the catchment scale; (b) temporal representation of (a) for a single event. Constant hillslope ( $e_h$ ) and bank erosion ( $e_n$ ) rates occur for the effective erosion durations  $t_{er}$  and  $t_t$ . The shaded area of the sedigraph is the total sediment yield  $Y_t$ , and this is less than the total area of the sediment inputs of the two stores, because of deposition.

We assume that hillslopes are eroded at a constant rate  $e_h$  during the entire duration of effective sediment transport  $t_{er}$  and that channels are eroded at a constant rate  $e_n$  for a duration  $t_i$ , which is shorter than the time base of the sedigraph. This event-based sediment-transport model can be represented schematically as shown in Figure 16.5(b). Linear relationships between the transport fluxes and storage are assumed, and Equation 16.8 can then be rewritten as linear ordinary differential equations in the dependent variables of  $y_h$  and  $y$ :

$$t_n \frac{dy_h(t)}{dt} = e_h(t) - (\lambda_h t_h + 1)y_h(t) \quad (16.9)$$

$$t_n \frac{dy(t)}{dt} = e_n(t) + y_h(t) - (\lambda_n t_n + 1)y(t) \quad (16.10)$$

where  $t_h$  and  $t_n$  are the mean residence times within the hillslope store and the channel store, and  $\lambda_h$  and  $\lambda_n$  are deposition parameters both of which have the units of  $[T^{-1}]$ . Physically,  $\lambda_h$  ( $\lambda_n$ ) represents the proportion of sediment in the hillslope (channel) store that is redeposited per unit time, here, as a first approximation, treated as constant over an event.

Equations 16.9 and 16.10 are standard first-order ordinary differential equations that can be solved analytically to give time-dependent sediment yield at the catchment outlet:

$$y(t) = y_h(t) + y_n(t) \quad (16.11)$$

where  $y_h$  and  $y_n$  are the sediment contributions from the hillslope and channel stores, respectively at time  $t$ . Both  $y_h$  and  $y_n$  can be expressed as:

$$y_h(t) = \begin{cases} 0, & t \leq 0 \\ \frac{e_h}{A_h B_n} \left( 1 - \exp\left(-\frac{B_n t}{t_n}\right) - \frac{\exp\left(-\frac{A_h t}{t_h}\right) - \exp\left(-\frac{B_n t}{t_n}\right)}{1 - \frac{A_h t_h}{B_n t_n}} \right), & 0 < t \leq t_{er} \\ \frac{e_h}{A_h B_n} \left( \frac{1 - \exp\left(-\frac{A_h t_{er}}{t_h}\right)}{1 - \frac{A_h t_h}{B_n t_n}} \exp\left(-\frac{A_h(t - t_{er})}{t_h}\right) + \frac{1 - \exp\left(-\frac{B_n t_{er}}{t_n}\right)}{1 - \frac{B_n t_h}{A_h t_n}} \exp\left(-\frac{B_n(t - t_{er})}{t_n}\right) \right), & t > t_{er} \end{cases} \quad (16.12)$$

$$y_n(t) = \begin{cases} 0 & t \leq t_i \\ \frac{e_n}{B_n} \left( 1 - \exp\left(-\frac{B_n(t - t_i)}{t_n}\right) \right), & t_i < t \leq t_{i2} \\ \frac{e_n}{B_n} \left( \exp\left(\frac{B_n t_{i2}}{t_n}\right) - \exp\left(\frac{B_n t_i}{t_n}\right) \right) \exp\left(-\frac{B_n t}{t_n}\right), & t > t_{i2} \end{cases} \quad (16.13)$$

where  $A_h = 1 + \lambda_h t_h$  and  $B_n = 1 + \lambda_n t_n$ . In essence, Equations 16.11 to 16.13 suggest that, for a given time  $t$ , sediment yield  $y(t)$  is the sum of sediment yield from hillslope supply  $y_h(t)$  and channel supply  $y_n(t)$ , and the actual shape of  $y(t)$  is mostly determined by the various dimensionless time-scaling parameters, namely  $A_h, B_n, t_{er}/t_h$  and  $t_i/t_n$ , and by the relative importance of hillslope and bank erosion. Because of the multiple sources, by using Equations 16.11 to 16.13, it can be shown that  $y(t)$  can have single, flat or multiple peaks, and the peak may occur at a time when  $t < t_{er}$  or  $t > t_{er}$ . Furthermore, large values of  $t_h, t_n, A_h$  or  $B_n$  often result in smaller values of  $y(t)$  with less dispersion in shape, suggesting a different sampling frequency may be needed to capture fully the variability of  $y(t)$  under such conditions.

Some simple relationships can be derived using such a model. For instance, the total sediment yield (per unit area per storm,  $Y_t$ ) can be estimated as:

$$Y_t = \int_0^\infty y(t)dt = \frac{1}{B_n} \left( \frac{e_h t_{er}}{A_h} + e_n t_i \right) \tag{16.14}$$

Substituting Equation 16.14 into Equation 16.1, and assuming that total erosion  $e$  is estimated only as hillslope erosion  $e_h$ , results in an expression for the SDR,  $\gamma_e$ :

$$\gamma_e = \frac{t_{er}}{t_i} \frac{1}{B_n} \left( \frac{1}{A_h} + \frac{e_n t_i}{e_h t_{er}} \right) \tag{16.15}$$

Equations 16.14 and 16.15 state that the total sediment yield  $Y_t$  is a fraction ( $1/A_h B_n$ ) of the total hillslope erosion ( $e_h t_{er}$ ) plus a fraction ( $1/B_n$ ) of the total bank erosion ( $e_n t_i$ ). These fractions are scaling parameters that depend on the sediment depositional timescale relative to the travel times in the hillslope and channel stores. Equation 16.15 can be used to fit to SDR data such as those of Roehl (1962), as shown in Figure 16.6. Here, simulated curves of  $\gamma_e$  are plotted in comparison to these data, the curves being obtained by using Equation 16.15, and setting  $\frac{e_n t_i}{e_h t_{er}} = 0$  (implying negligible bank erosion),  $t_h = 0.1$  hr (rapid hillslope delivery) and  $\lambda_h = 0.01$  hr<sup>-1</sup> (low hillslope depositional timescale). This plot implies that the variation in Roehl’s data can be explained by the channel depositional parameter  $\lambda_n$ . Of course, Figure 16.2 has already suggested that, for cases in which hillslope erosion dominates, the  $\gamma$ - $A$  relationship can be represented by a hydrological model based on the duration of excess rainfall and the time of concentration. It is likely that some combination of the hydrological and geomorphological models will provide a more complete physical explanation of the  $\gamma$ - $A$  relationship. Figure 16.6 explicitly demonstrates that the  $\gamma$ - $A$  curves must be based on properly defined timescales in the identification of sediment yield and on-site erosion rates; each curve in the diagram is specific for two timescales.

This simple lumped model (i.e. Equation 16.8 and its analytical solution) can provide qualitative process-based insights into the causes of variation in the SDR. For

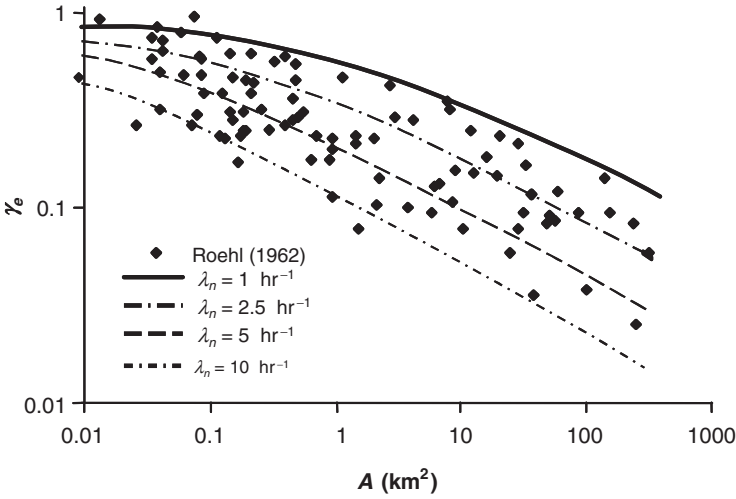


**Figure 16.6** Simulated curves of total-volume-based SDR  $\gamma_e$  in comparison to the SDR estimates of Roehl (1962). The curves were calculated using Equation 16.15 with parameters set as explained in the text. The physical interpretation of these curves is that variations of  $\gamma_e-A$  are controlled by the channel depositional parameter  $\lambda_n$ .

example, when hillslope erosion dominates ( $e_h \gg e_n$ , or  $e_n \rightarrow 0$ ), the SDR increases when the timescale required for either hillslope or channel deposition increases. As channel erosion increases relative to hillslope erosion, the SDR increases and could even exceed unity. This suggests that the physical meaning of SDR may change from being an indicator of upland sediment delivery efficiency, as traditionally defined, to that of relative contribution of hillslope and channel erosion. The shift between these interpretations begins to take place for  $\frac{1}{A_h} < \frac{e_n t_i}{e_h t_{er}}$ . It is possible to infer, indirectly, the effect of an increase in channel-bed particle size, which is likely to reduce the channel erosion rate and reduce the timescale required for channel deposition; this results in lower SDR values unless the ratio of hillslope to channel erosion rate is high. For small steep catchments, and for the general case where hillslope erosion is dominant, Equation 16.8 reduces to that of Sivapalan *et al.* (2002) for the runoff case. In such situations, the  $\gamma-A$  ( $\gamma-A$ ) relationships closely mirror that for runoff and area, so that variation in suspended sediment yield can be largely explained by variation in runoff, and the scaling exponents of SDR and unit sediment yield are similar to that for unit runoff. In larger catchments, both the depositional parameter  $\lambda_n$  and the channel erosion rate,  $e_n$ , are likely to increase, and thus control the SDR, which will no longer relate to area in the same way as runoff. The deposition capacity of the channel store controls both the  $\gamma_p-A$  and  $\gamma_e-A$  relationships, regardless of the effective duration of upland erosion. In these cases, even though sediment yield may exhibit a strong correlation

with the runoff rate at a sampling point, this is only local and does not imply a potential for regionalization.

In Figures 16.1 and 16.2, it is evident that the slope of the  $\gamma_e$ - $A$  relationship is not constant, but changes from near-zero for small catchment area  $A$  to  $-0.4$  as  $A$  increases. For small values of the channel depositional parameter  $\lambda_n$ , in catchments with areas smaller than about  $1000 \text{ km}^2$ , the  $\gamma_e - A$  slope tends to remain close to zero, as long as the catchment lacks sediment storage and the sediments are mainly fine-grained (as in the Chinese Loess region; Walling, 1983). This is consistent with the expectation that the transport of suspended sediment is mostly restricted by hillslope supply and that channels tend to export much of the fine wash load delivered to them. However, such system equilibrium cannot be sustained for individual events, especially in large catchments, so the  $\gamma_e$ - $A$  slope becomes more negative when the area is larger. This is consistent with patterns reported in the literature on catchment sediment delivery (Walling, 1983; Richards, 1993). Equations 16.14 and 16.15 also explain that if the hillslope erosion rate  $e_h$  is fixed, and the channel erosion rate  $e_n$  increases linearly with the channel travel time  $t_n$ , both  $Y_t$  and the SDR increase with  $A$ . This pattern has been observed empirically (Church *et al.*, 1999) in catchments with increasing sediment supply downstream.

The inferences discussed above show how a simple model can give rise to a rich array of testable hypotheses, and can suggest relationships that can be further explored in empirical research. This theoretical model provides a way to explore how the sources and sinks of sediment, along with the time and space scales of sediment movement for hillslopes versus channel networks, influence the dynamics of sediment delivery from drainage basins. Another example is provided by Lisle and Church (2002), who present a conceptual model of sediment movement and storage in large drainage basins, based on a cascade of linear reservoirs in which sediment is transferred through a series of channel/valley segments (natural sediment storage reservoirs) that are distinguished from their neighbours by their particular capacity to store and transport sediment. The sediment-transport capacity of each reservoir is assumed to be a function of storage volume, which influences sediment mobility and availability through variations in bed-surface texture, channel gradient and the availability of valley-floor sediments for erosion. This conceptual model has two phases. In phase I, a reservoir (e.g. a channel segment) linearly responds to the variations of sediment supply and proportional changes occur in the volume of stored sediment. In phase II, the reservoir non-linearly responds to the changes in the volume of stored sediment through armouring and changes in roughness. Lisle and Church (2002) propose that phase I may represent an idealized transport-limited state, while phase II represents a supply-limited condition. Their simulations of the degradation of an alluvial reservoir with channel and valley-floor surfaces indicate that interactions between channel lowering and lateral erosion are critical in the manifestation of a transport-storage relation. This implies that further research into transport-storage relations could lead to improved sediment-routing

models for drainage basins in which component sediment reservoirs adjust dynamically to varying sediment loads.

## Practical large-scale application using a distributed model

One practical need in catchment management is to develop process-based and spatially distributed sediment-delivery models that can be used in catchments with limited hydrological and sediment data. For example, Phillips (1991) proposes a process-based formula that estimates catchment-sediment yield by separately considering landslides/debris flows, hillslope sheet and rill erosion, and channel erosion:

$$y = e \gamma_h \gamma_l \gamma_c, \quad (16.16)$$

where  $e$  is average sediment erosion rate,  $\gamma_h$ ,  $\gamma_l$  and  $\gamma_c$  are the SDRs related to hillslope sheet and rill erosion, landslides/debris flows, and channel flow. Colluvial and alluvial storages are defined by:

$$S_c = (1 - \gamma_s) (1 - \gamma_l) e A \quad (16.17)$$

and

$$S_A = (1 - \gamma_c) \gamma_c \gamma_l e A \quad (16.18)$$

where  $A$  is the catchment area. Equations 16.16 to 16.18 simply and usefully represent sediment yield in relation to distinct processes and have been applied by both Phillips (1991) and Reid and Dunne (1996). However, this model lacks spatial information about where the sediment sources and storages are located, and how the SDRs are spatially distributed.

Several spatially distributed models constructed in a geographical information systems (GIS) environment have been developed recently, some including novel ideas, such as the runoff travel time concept (Ferro and Minacapilli, 1995; Ferro and Porto, 2000; Jain and Kothiyari, 2000; Fernandez *et al.*, 2003). The GIS is used to generate, manage and determine the model input factors. One objective of such studies is to develop an SDR model that incorporates key elements of the catchment-storm response and the sediment-delivery process, in a spatially distributed manner structured by the river network. Conceptually similar to the Phillips (1991) model, and operationally similar to GIS-based sediment-delivery models, Prosser *et al.* (2001) takes a further step by treating different erosion sources, including bank erosion, separately. This simple sediment-transport model has been used within a broad-scale sediment budget framework, in which the spatially distributed SDR of hillslope delivery is estimated by using

an SDR based on sedigraph peaks and derived from Equation 16.11 (Prosser *et al.*, 2003; Lu *et al.*, 2004; Lu *et al.*, 2005a). This was implemented using a GIS framework at a very large scale (for the  $c.1.1 \times 10^6$  km<sup>2</sup> basin of the Murray-Darling in eastern Australia), and evaluated as a spatially distributed phenomenon dependent on the probabilities of rainfall intensity and rainfall duration, and on sediment routing through the whole river network. The aim was to assess spatial patterns of erosion, to target erosion-control practices and to optimize the associated expenditure.

During this modelling exercise, the river network of the basin was divided into about 10 000 river links, separated by tributary junctions or nodes, each with an associated drainage area of 50–100 km<sup>2</sup>. These links are the basic spatial units for the sediment budget model, and the area contributing to each is referred to as a ‘link element’. Each link,  $i$ , receives an input of sediment from its upstream tributaries ( $T_i$ ), to which is added a mean annual supply of suspended sediment from bank erosion along the link itself ( $B_i$ ), from gully erosion ( $G_i$ ), and from hillslope sheet wash and rill erosion ( $E_i$ ) in the link element, the last of which is moderated by a hillslope sediment-delivery ratio ( $\gamma_i$ ). The total supply to each link is  $S_i$  (the sum of the upstream and within-link supplies). There is also a within-element loss to the sediment budget, in the form of a deposition or loss term ( $D_i$ ). These within-element quantities are estimated using various empirical procedures, appropriate for this scale and including the use of remotely sensed data, a form of the Universal Soil Loss Equation, and long-term rainfall records.

The suspended sediment output from a link is:

$$Y_i = T_i + B_i + G_i + (E_i * \gamma_i) - D_i = T_i + I_i - D_i = S_i - D_i \quad (16.19)$$

with units of tons per year ( $\text{t yr}^{-1}$ ), where  $I_i$  is the sediment supply within the element. The within-element loss from the element sediment budget is the deposition term  $D_i$ , which may be disaggregated into losses in floodplains, lakes and reservoirs. If the budget for each element is estimated, an element-scale delivery ratio can be defined as the ratio of the output from the element to the total sediment supply to the element, thus:

$$\gamma_i = Y_i/S_i = 1 - D_i/S_i \quad (16.20)$$

The mean annual delivery of sediment from any link,  $i$ , to an arbitrary downstream link to which it is tributary,  $k$ , is  $\lambda_{ik}$  ( $\text{t yr}^{-1}$ ). The location  $k$  may be the downstream link of a catchment within which practices to control sediment production and delivery are to be implemented, and where the consequences for sediment yield are to be measured in order to assess costs and benefits;  $\lambda_{ik}$  is the sediment supply ( $I_i$ ) from within the link element  $i$  multiplied by the sediment delivery efficiency through all river links along

the route to  $k$ :

$$\lambda_{ik} = I_i \prod_{j=1}^{M_{ik}} \gamma_j \quad (16.21)$$

where  $M_{ik}$  is the total number of river links along the route from link  $i$  to the sediment control location  $k$ . The  $\gamma_j$  values are the successive link element SDRs, each being the probability of sediment passing through a river link  $j$ , as determined by the amount of deposition. If all probabilities are equal, the contribution of a link element  $i$  to the sediment control location  $k$  is proportional to the intervening travel distance. In reality, the probabilities vary because deposition varies through a river network.

The sediment produced in a given element is thus routed through all intervening elements to a downstream control site, and the contribution of this sediment production to the sediment yield at the downstream site is the sediment production successively multiplied by the fractional SDRs of all elements along the transport path (Equation 16.21). This macro-scale application thus allows for the spatial distribution of both hillslope- and catchment-scale SDRs. The total sediment yield at the downstream sediment control location  $k$  is given by:

$$T_k = \sum_{i=1}^N \lambda_{ik} \quad (16.22)$$

where  $N$  is the total number of link elements contributing to sediment control location  $k$ . Although this implementation is at a very large scale, in principle its formulation follows the theoretical structure outlined in the previous sections, with sediment being generated by several mechanisms within individual elements of a catchment; the  $\gamma_j$  being within-catchment delivery ratios applicable to individual link elements; and the sediment yield contributed at the catchment outlet by each element reflecting the routing and intervening loss of sediment from 'source' to 'sink', through the network structure.

Once this model has been set up, it is possible to experiment in a GIS with the consequences of different erosion-control policies and to measure the on-site and downstream benefits of each against the costs of implementation. These policies can be quite different in terms of their spatial targeting. One approach is simply to select sites for treatment at random, to mimic a practice which simply takes advantage of willing landowners. Another is to target the locations with the highest within-element sediment supply ( $I_i$ ), whatever the erosional process may be, or by focusing especially on the soil- or bank-erosion hotspots. Finally, it is possible using this methodology to target the elements that, by virtue of the delivery efficiency to the downstream site, contribute most to sediment yield at this point. Approaches which target erosional hotspots are in cost-benefit terms little better than random selection methods, but the last scenario is consistently the most cost-effective method of sediment control, and it is the one that is enabled only through a spatially disaggregated approach to sediment delivery.

While this particular application may be employed mainly in the context of the contemporary management of catchment erosion and sediment yield, the event-based framework of Equation 16.8 could also be used to model longer-term sediment yield, by incorporating the probability distributions of erosive rainfall intensities, rainfall durations and the durations between events, all within a Monte Carlo simulation framework (Robinson and Sivapalan, 1997b). This could lead to a more rigorous, process-based framework within which the controlling factors for sediment transport can be explored for a given catchment, and for particular histories of sediment production and transporting events. It would also provide an opportunity to examine the characteristic response times of catchments, to assess how catchments of different sizes filter the effects of climatic variations of different temporal scales, and therefore to underpin interpretations of the relationship between climatic change and sediment storage within catchments of different size and geometry.

## Conclusions

It has long been recognized that the basis for understanding and modelling sediment delivery in catchments has been inadequate for both theoretical and practical purposes. The persistence of the simple inverse, power-function  $\gamma-A$  relationship has reflected limited innovation in the analysis of sediment delivery, and new approaches have clearly been needed. This is particularly necessary where this simplified approach to sediment delivery is used to obtain values of the SDR ( $\gamma$ ) to then adjust estimates of upland erosion to allow for intervening deposition before downstream control locations, such as reservoirs, where estimates of sedimentation rates are required.

The discussion in this chapter has focused on five key requirements for a new approach to sediment delivery: a physical basis for understanding and modelling sediment delivery; the underling relationship of sediment delivery to driving hydrological processes; explicit spatial disaggregation of both sediment production and delivery within catchments, structured by the channel network through which sediment is routed; recognition of scale-dependent changes of the dominant processes; and explicit attention to the appropriate timescales for measuring, averaging and comparing sediment delivery. The theoretical discussion of the relationship between sediment delivery and hydrology has highlighted the roles of rainfall and runoff intensity and the duration of effective events as controls of sediment delivery at the small scale, giving way to a different set of controls at larger scales (in larger catchments) where routing through the network dominates. It is necessary to draw specifically on channel network structure, address the stochastic nature of sediment transport, and allow disaggregation of both erosional processes (sheetwash, gully erosion and river-bank erosion) and sites of differential erosional intensity. From a practical point of view, we would recommend that the SDR concept be restricted to small catchments where hillslope erosion dominates,

so that an unambiguous interpretation of fractional sediment yield from land-surface erosion to channels can be made.

Rainfall-driven sediment production is explicitly a stochastic process depending on spatial and temporal variations in erosion, transport and deposition. A practicable sediment-transport model will require a framework in which processes of sediment production on the hillslopes and in individual channels are treated probabilistically, while routing through the whole channel network is handled in a spatially distributed manner. Such a framework would provide a useful tool for exploring the ways in which interactions among system components occur in the real world and for developing hypotheses about how different combinations of the factors influence sediment delivery. The formulation of testable hypotheses can be evaluated through focused empirical studies, and the results from such empirical studies may then guide investigations of sediment budgets in ungauged basins. More specifically, such a modelling framework may provide the opportunity to account for much of the variability observed in aggregate sediment-delivery ratios, the deviations from fractal scaling  $\gamma$ - $A$  relationships and the apparently anomalous evidence of increasing rates of sediment yield with basin area where channel incision is dominant. It also underpins a practical implementation of sediment-delivery modelling that is able to optimize spatially targeted sediment-control policies in a large catchment, revealing that the traditional approach that links hillslope soil erosion to downstream sedimentation via an aggregate SDR may focus attention on entirely the wrong sources of sediment. It might be expected, therefore, that this will also increasingly provide a basis for a more theoretically informed approach to sediment production, delivery, storage and yield in process-based models of longer-term drainage basin evolution.

## Acknowledgements

Part of this chapter draws on previous collaborative work with Chris Moran at the University of Queensland, Ian Prosser at CSIRO Land and Water, and Murugesu Sivapalan at the University of Illinois at Urbana-Champaign. We are grateful for the constructive comments on an earlier draft made by Michael Church at the University of British Columbia.

## References

- Anderson HW. 1954. Suspended sediment discharge as related to streamflow, topography, soil and land use. *AGU Transactions* **35**: 269–281.
- Anderson HW. 1957. Relating sediment yield to watershed variables. *Transactions of the American Geophysical Union* **45**: 307–321.

- André JE, Anderson HW. 1961. Variation of soil erodibility with geology, geographic zone, elevation and vegetation type in northern California. *Journal of Geophysical Research* **66**: 3351–3358.
- ASCE. 1975. *Sedimentation Engineering*. American Society of Civil Engineers Manuals and Reports on Engineering Practice, No. 54: New York.
- Benson MA. 1962. Factors influencing the occurrence of floods in a humid region of diverse terrain, *US Geological Survey Water Supply Paper*, 1580-B.
- Beven KJ. 1989. Changing ideas in hydrology – the case of physically-based models. *Journal of Hydrology* **105**: 157–172.
- Birkinshaw SJ, Bathurst JC. 2006. Model study of the relationship between sediment yield and river basin area. *Earth Surface Processes and Landforms* **31**: 750–761.
- Bouraoui F, Dillaha TA. 1996. ANSWERS-2000: Runoff and sediment-transport model, *Journal of Environmental Engineering, ASCE* **122**: 493–502.
- Boyce RC. 1975. Sediment routing with sediment-delivery ratios. In *Present and Prospective Technology for Predicting Sediment Yields and Sources*. US Department of Agriculture Publication ARS-S-40; 61–65.
- Brune GM. 1953. Trap efficiency of reservoirs. *Transactions of the American Geophysical Union* **34**: 407–18.
- Calver A, Kirkby MJ, Weyman DR. 1972. Modelling hillslope and channel flow. In *Spatial Analysis in Geomorphology*, Chorley RJ (ed.). Methuen: London; 197–218.
- Church M. 2002. Fluvial sediment transfer in cold regions. In *Landscapes of Transition: Landform Assemblages and Transformations in Cold Regions*, Hewitt K, Byrne M-L, English M, Young G (eds). Kluwer Academic: Netherlands; 93–117.
- Church M, Slaymaker O. 1989. Disequilibrium of Holocene sediment yield in glaciated British Columbia. *Nature* **337**: 452–454.
- Church M, Ham D, Hassan M, Slaymaker O. 1999. Fluvial clastic sediment yield in Canada: Scaled analysis. *Canadian Journal of Earth Sciences* **36**: 1267–1280.
- Churchill MA. 1948. Discussion of 'Analyses and use of reservoir sedimentation data' by L.C. Gottschalk. In *Proceedings of the federal interagency sedimentation conference, Denver, Colorado*; 139–40.
- Cluis DA, Couillard D, Potvin L. 1979. A grid square transport model relating land use exports to nutrient loads in rivers. *Water Resources Research* **15**: 630–636.
- Crawford CG. 1991. Estimation of suspended-sediment rating curves and mean suspended-sediment loads. *Journal of Hydrology* **129**: 331–348.
- de Ploey J. 1984. Hydraulics of runoff and loess loam deposition. *Earth Surface Processes and Landforms* **9**: 533–539.
- Dietrich WE, Dunne T. 1978. Sediment budget for a small catchment in mountainous terrain. *Zeitschrift für Geomorphologie, Supplement Band* **29**: 191–206.
- Edwards K. 1993. Soil erosion and conservation in Australia. In *World Soil Erosion and Conservation*, Pimental D (ed.). Cambridge University Press: Cambridge; 147–169.
- Fernandez C, Wu JQ, McCool DK, Stöckle CO. 2003. Estimating water erosion and sediment yield with GIS, RUSLE, and SEDD. *Journal of Soil and Water Conservation* **58**: 128–136.
- Ferro V, Minacapilli M. 1995. Sediment delivery processes at basin scale. *Hydrological Sciences Journal* **40**: 703–718.
- Ferro V, Porto P. 2000. Sediment delivery distributed (SEDD) model. *Journal of Hydrologic Engineering* **5**: 633–647.

- Flanagan DC, Nearing MA (eds). 1995. *USDA-Water Erosion Prediction Project: Hillslope Profile and Watershed Model Documentation*. NSERL Report No. 10, USDA-ARS National Soil Erosion Research Laboratory: West Lafayette, Indiana.
- Goodrich DC, Lane LJ, Shillito RA, Miller SN, Syed KH, Woolhiser DA. 1997. Linearity of basin response as a function of scale in a semi-arid watershed. *Water Resources Research* **33**: 2951–2965.
- Gregory KJ, Walling DE. 1973. *Drainage Basin Form and Processes: A Geomorphological Approach*. John Wiley & Sons: Chichester.
- Horowitz AJ. 2003. An evaluation of sediment rating curves for estimating suspended sediment concentrations for subsequent flux calculations. *Hydrological Processes* **17**: 3387–3409.
- Jain MK, Kothiyari UC. 2000. Estimation of soil erosion and sediment yield using GIS. *Hydrological Sciences Journal* **45**: 771–786.
- Jakeman AJ, Hornberger GM. 1993. How much complexity is warranted in a rainfall-runoff model? *Water Resources Research* **29**: 2637–2649.
- Khanbilvardi RM, Rogowski AS. 1984. Quantitative evaluation of sediment delivery ratios. *Water Resources Bulletin* **20**: 865–874.
- Kinnell PIA. 2004. Sediment delivery ratios: A misaligned approach to determining sediment delivery from hillslopes. *Hydrological Processes* **18**: 3191–3194.
- Kirkby MJ. 1976. Tests of the random network model, and its application to basin hydrology. *Earth Surface Processes* **1**: 197–212.
- Knox JC. 1975. Concept of the graded stream. In *Theories of Landform Development*, Melhorn WN, Flemal RC (eds). Publications in Geomorphology, State University of New York: Binghamton; 169–198.
- Krysanova V, Muller-Wohlfeil DI, Becker A. 1998. Development and test of a spatially distributed hydrological/water quality model for mesoscale watersheds. *Ecological Modeling* **106**: 261–289.
- Lane LJ, Hernandez M, Nichols MH. 1997. Processes controlling sediment yield from watersheds as functions of spatial scale. *Environmental Modelling and Software* **12**: 355–369.
- Lisle TE, Church M. 2002. Sediment transport-storage relations for degrading alluvial reservoirs. *Water Resources Research* **38**: DOI: 10.1029/2001WRR001086.
- Lu H, Moran CJ, Prosser IP, DeRose R. 2004. Investment prioritization based on broadscale spatial budgeting to meet downstream targets for suspended sediment loads. *Water Resources Research* **40**: DOI: 10.1029/2003WR002966.
- Lu H, Moran CJ, Prosser IP. 2005a. Modelling sediment delivery ratio over the Murray Darling Basin. *Environmental Modelling and Software* **21**: DOI: 10.1016/j.envsoft.2005.04.021.
- Lu H, Moran CJ, Sivapalan M. 2005b. A theoretical exploration of catchment-scale sediment delivery. *Water Resources Research* **41**: 10.1029/2005WR004018 (Correction: **42**: DOI: 10.1029/2006WR004917, 2006).
- Macklin MG. 1999. Holocene river environments in prehistoric Britain: Human interaction and impact. *Journal of Quaternary Science* **14**: 521–530.
- McCulloch M, Fallon S, Wyndham T, Henry E, Lough J, Barnes D. 2003. Coral record of increased sediment flux to the inner Great Barrier Reef since European settlement. *Nature* **421**: 727–730.
- Meade RH. 1988. Movement and storage of sediment in river systems. In *Physical and Chemical Weathering in Geochemical Cycles*, Lermund A, Meybeck M (eds). Kluwer Academic Publishers: Dordrecht, Holland; 165–179.

- Meade RH, Yuzyk TR, Day TJ. 1990. Movement and storage of sediment in rivers of the United States and Canada. In *Surface Water Hydrology*, Wolman MG, Riggs HC (eds). Geological Society of America: Boulder, Colorado; 255–280.
- Milliman JD, Meade RH. 1983. World-wide delivery of river sediment to oceans. *Journal of Geology* **91**: 1–21.
- Moore RJ, Clarke RT. 1983. A distribution function approach to modelling basin sediment yield. *Journal of Hydrology* **65**: 239–257.
- Morgan RPC, Quinton JN, Smith RE, Govers G, Poesen JWA, Auerswald K, Chisci G, Torri D, Styczen ME. 1998. The European Soil Erosion Model (EUROSEM): A dynamic approach for predicting sediment transport from fields and small catchments. *Earth Surface Processes and Landforms* **23**: 527–544.
- Novotny V, Olem H. 1994. *Water Quality: Prevention, Identification and Management of Diffuse Pollution*. Van Nostrand Reinhold: New York.
- Parsons AJ, Stromberg GL. 1998. Experimental analysis of size and distance of travel of unconstrained particles in interill flow. *Water Resources Research* **34**: 2377–2381.
- Phillips JD. 1991. Fluvial sediment budgets in the North Carolina Piedmont. *Geomorphology* **4**: 231–241.
- Prosser IP, Rutherford ID, Olley JM, Young WJ, Wallbrink PJ, Moran CJ. 2001. A large-scale patterns of erosion and sediment transport in river networks, with examples from Australia. *Marine Freshwater Research* **52**: 81–99.
- Prosser IP, Moran CJ, Lu H, Olley J, DeRose R, Cannon G, Croke B, Hughes A, Jakeman A, Newham L, Scott A, Weisse M. 2003. *Basin-Wide Mapping of Sediment and Nutrient Exports in Dryland Regions of the Murray-Darling Basin*. Technical Report 33/03, CSIRO Land and Water: Canberra.
- Reid LM, Dunne T. 1996. *Rapid evaluation of sediment budgets*. Geoecology Paperback. Catena Verlag: Reiskirchen, Germany.
- Renfro GW. 1975. Use of erosion equations and sediment-delivery ratios for predicting sediment yield. In *Present and Prospective Technology for Predicting Sediment Yield and Sources*, ARS-S-40. Agricultural Research Service, USDA; 33–45.
- Restrepo JD, Kjerfve B. 2000. Water discharge and sediment load from the western slopes of the Colombian Andes with focus on Rio San Juan. *Journal of Geology* **108**: 17–33.
- Richards KS. 1993. Sediment transport into and through the network. In *Channel Network Hydrology*, Kirkby MJ, Beven K (eds). John Wiley & Sons: Chichester; 221–54.
- Richards KS. 2002. Drainage basin structure, sediment delivery and the response to environmental change. In *Sediment Flux to Drainage Basins: Causes, Controls and Consequences*, Jones SJ, Frostick LE (eds). Geological Society of London, Special Publication 191; 149–160.
- Robinson JS, Sivapalan M. 1997a. An investigation into the physical causes of scaling and heterogeneity of regional flood frequency. *Water Resources Research* **33**: 1045–1059.
- Robinson JS, Sivapalan M. 1997b. Temporal scales and hydrological regimes: Implications for flood frequency scaling. *Water Resources Research* **33**: 2981–2999.
- Roehl JE. 1962. Sediment source areas, delivery ratios and influencing morphological factors. *International Association for Hydrological Sciences Publication* **59**: 202–213.
- Rutherford I. 2000. Some human impacts on Australian stream channel morphology. In *River Management: The Australasian Experience*, Brizga S, Finlayson B (eds). John Wiley & Sons: Chichester.

- Scheffer M. 1998. *Ecology of shallow lakes*. Chapman and Hall: London.
- Schumm SA, Parker RS. 1973. Implications of complex alluvial response of drainage systems for Quaternary alluvial stratigraphy. *Nature* **243**: 99–100.
- Sivapalan M, Jothityangkoon C, Menabde M. 2002. Linearity and non-linearity of basin response as a function of scale: Discussion of alternative definitions. *Water Resources Research* **38**: 10.1029/2001WR000482, 4.1–4.5.
- Slaymaker HO. (1972) Patterns of present sub-aerial erosion and landforms in Mid-Wales. *Transactions, Institute of British Geographers* **55**: 47–68.
- Solomon SI, Gupta SK. 1977. Distributed numerical model for estimating runoff and sediment discharge of ungauged rivers. *Water Resources Research* **13**: 619–625.
- Trimble SW. 1975. Denudation studies: Can we assume stream steady state? *Science* **188**: 1207–1208.
- Trimble SW. 1983. A sediment budget for Coon Creek basin in the Driftless Area, Wisconsin, 1853–1977. *American Journal of Science* **283**: 454–74.
- Trimble SW, Crosson PUS. 2000. Soil erosion rates – myth and reality. *Science* **289**: 248–250.
- Verstraeten G, Poesen J. 2000. Estimating trap efficiency of small reservoirs and ponds: Methods and implications for the assessment of sediment yield. *Progress in Physical Geography* **24**: 219–251.
- Walling DE. 1977. Assessing the accuracy of suspended sediment rating curves for a small basin. *Water Resources Research* **13**: 531–538.
- Walling DE. 1983. The sediment delivery problem. *Journal of Hydrology* **65**: 209–237.
- Wasson RJ. 1994. Annual and decadal variation of sediment yield in Australia, and some global comparisons. *International Association for Hydrological Sciences Publication* **224**: 269–279.
- Wasson RJ, Olive LJ, Rosewell CJ. 1996. Rates of erosion and sediment transport in Australia. *International Association of Hydrological Sciences Publication* **236**: 139–148.
- Wasson RJ, Mazari RK, Starr B, Clifton G. 1998. The recent history of erosion and sedimentation on the Southern Tablelands of southeastern Australia: Sediment flux dominated by channel incision. *Geomorphology* **24**: 291–308.
- Wischmeier WH, Smith DD. 1978. *Predicting Rainfall Erosion Losses: A Guide to Conservation Planning*. US Department of Agriculture, Agriculture Handbook No. 537.
- Woodroffe CD, Mulrennan ME, Chappell J. 1993. Estuarine infill and coastal propagation, Southern van Diemen Gulf, Northern Australia. *Sedimentary Geology* **83**: 257–275.
- Yorke TH, Ward JR. 1986. Accuracy of sediment discharge estimates. In *Proceedings of the Fourth Federal Interagency Sedimentation Conference: Las Vegas, Nevada, March 24–27*, 1; 4–49–4–59.
- Young RA, Onstad CA, Bosch DD, Anderson WP. 1989. AGNPS: A non-point source pollution model for evaluating agricultural watersheds. *Journal for Soil Water Conservation* **44**: 168–173.

# 17

## Numerical predictions of the sensitivity of grain size and channel slope to an increase in precipitation

Nicole M. Gasparini<sup>1</sup>, Rafael L. Bras<sup>2</sup>  
and Gregory E. Tucker<sup>3</sup>

<sup>1</sup>*School of Earth and Space Exploration, Arizona State University, USA*

<sup>2</sup>*Department of Civil and Environmental Engineering, Massachusetts Institute of Technology (MIT), USA*

<sup>3</sup>*Cooperative Institute for Research in Environmental Sciences (CIRES) and Department of Geological Sciences, University of Colorado, USA*

### Introduction

Well-known correlations between sediment yield and climate properties have inspired the widespread view that climate-driven variation in sediment supply is often the cause of fluctuations in sedimentation rate over geologic time. Yet, we know surprisingly little at a quantitative level about the nature and relative importance of climate controls. For example, while Zhang *et al.* (2001) argued that late-Cenozoic global cooling drove enhanced rates of erosion and deposition worldwide; some studies have shown a negligible correlation between climate and millennial-scale or longer denudation rates (e.g. Riebe *et al.*, 2001; Burbank *et al.*, 2003; von Blanckenburg, 2005). This uncertainty underscores

the need for a process-level understanding of climate controls on denudation. In this study, we use a physically based numerical model to quantitatively describe some of the possible effects of climate change on erosion rates throughout a drainage network.

Climate influences the quantity and timing of water delivered to a river network, and also the volume and texture of sediment. Changes in water or sediment supply can potentially lead to a wide range of adjustments throughout a channel network, including: changes in gradient due to aggradation, degradation or sinuosity adjustment; bed fining or coarsening, which affects transport rates and roughness; and adjustments in channel width and depth (e.g. Schumm, 1977). All of these variables are tightly coupled with the channel's ability to convey water and sediment, and in that sense the river network can be seen as a complex dynamic system with many degrees of freedom. The behaviour of such systems often defies intuition, making mathematical models virtually essential to understanding system dynamics and framing testable hypotheses. Therefore, it is natural that researchers have developed a number of mathematical models, nearly always implemented numerically, in order to provide a theoretical framework for understanding river network form and dynamics.

For example, Rinaldo *et al.* (1995) used a numerical model to investigate potential changes in drainage density with climate. They modelled fluvial processes as 'threshold-limited' (i.e. once the fluvial shear stress surpassed the critical shear stress, slopes were lowered back to threshold conditions). Fluvially eroded material could not be redeposited. Their model also contained an algorithm for diffusive hillslope erosion and deposition. During wetter periods, which they modelled by lowering the threshold for erosion, they found that drainage density increased. In contrast, the drainage density decreased during drier periods. Their study suggests that evidence of past climatic patterns is more likely to be preserved in landscapes with little to no tectonic forcing.

Tucker and Slingerland (1997) modelled network response to changes in rainfall magnitude, rainfall frequency and the critical shear stress for the entrainment of sediment. Their model included both fluvial and hillslope processes. Physically based sediment-transport equations were used to calculate rates of erosion or deposition throughout the fluvial network. They found that an increase in the magnitude of rainfall or a decrease in the erosion threshold both resulted in initial expansion and erosion of the channel headwaters and deposition at larger drainage areas. Eventually, as erosion in the headwaters continued, the drainage density increased. On the other hand, a decrease in the magnitude of rainfall or an increase in the erosion threshold resulted in a period of slow aggradation throughout the fluvial network. A decrease in rainfall frequency also resulted in a period of slow aggradation, while an increase in rainfall frequency resulted in a slower expansion of the fluvial network and no deposition of sediment. Tucker and Slingerland (1997) also found that landscape response varied depending on the state of the landscape before a perturbation in climate. As a result, climate oscillations that occur more quickly than the timescale of landscape response could have different signatures on the landscape.

Howard (1999) explored the response of gully erosion to a disturbance in vegetation, which could result perhaps from fire, overgrazing or drought. He modelled fluvial erosion using physically based equations for the detachment and transport of sediment. Vegetation disturbances were simulated by reducing the critical shear stress for erosion for a discrete period. During the disturbance, erosion rates accelerated, with the highest erosion rates concentrated in low-order channels and steep hillslopes. After the disturbance period, vegetation was only re-established in areas which were eroding below a threshold rate, while in areas that were still eroding too fast it was assumed that the vegetation could not take root. Howard (1999) found that the proportion of the landscape that experienced accelerated erosion rates varied depending on the relative strength of the vegetation and the underlying material and the threshold erosion rate at which vegetation could grow back. However, he notes that once gullies were established their headwall advance could often continue even after vegetation completely grew back.

The network response between permafrost and non-permafrost conditions was explored by Bogaart *et al.* (2003). Permafrost inhibits infiltration and leads to Hortonian runoff. In contrast, during warm periods, rainfall infiltrates more readily into non-frozen soils, and saturation-excess runoff occurs. Bogaart *et al.* (2003) modelled alternating periods of permafrost and non-permafrost conditions by changing the runoff production mechanism in their model. They found that during temperate periods, when more water was transmitted through the sub-surface, the drainage density decreased. A cooling period following temperate conditions led to a peak in the sediment load as the smaller-order channels expanded into the areas which were hillslopes under a warmer climate. However, the sediment load did not remain high throughout the entire cool period and began to decline once the drainage density adjusted to the cooler climate.

Coulthard *et al.* (2000) explored how changes in both vegetation cover and rainfall magnitude could affect erosion and sedimentation over time periods of 10 to 100 years. Their study modelled the erosion, transport and deposition of nine different grain-size fractions on a very fine spatial scale using a cellular model. Changes at a location, or cell on the landscape, are a function only of changes in the immediately surrounding cells. (The cellular model differs from the sediment- and water-routing schemes used by Tucker and Slingerland (1997), Howard (1999) and Bogaart *et al.* (2003), and from the model used in this study.) They found that either an increase in rainfall magnitude or a decrease in vegetation cover alone could result in a 100 per cent or 25 per cent increase in sediment discharge respectively. However, when both rainfall magnitude was increased and vegetation cover was decreased, the sediment discharge increased by 1 300 per cent. Similarly to the other studies, the increase in sediment discharge was linked to headword expansion of the network, or an increase in drainage density.

In this study, we use the CHILD numerical model (Tucker *et al.*, 2001a, 2001b) to explore how an increase in runoff, as a result of an increase in precipitation rate, affects the channel slope and bed texture throughout a drainage network. We model the bed material as a mixture of sand and gravel and track changes in the proportion of sand

(versus gravel) on the bed. We explore changes throughout a network, both spatially and temporally, over hundreds to thousands of years. We model only fluvial processes, and therefore we are not able to make predictions about changes in drainage density, as previous studies have done.

As we have discussed, previous studies have already addressed the patterns of erosion and deposition throughout a network in response to an increase in rainfall magnitude. However, our study is unique because it explores how the coupling between channel slope and bed texture control erosion rates throughout a network over both short and long timescales. We use the model to address the following questions: ‘Does a change in climate lead to a direct change in the texture of fluvial deposits?’, ‘When considering the mutual adjustment of both channel slope and surface texture, as opposed to adjustments in channel slope alone, is the network response dampened or does it become more complex?’ and ‘Are steady-state predictions of channel slope and bed texture good indications of how a network will respond to a perturbation in climate?’

## Landscape-evolution models

In this study, we use the CHILD model to explore the morphology of a network responding to a change in precipitation rate. Before describing the details of the CHILD model, we give a brief history of physically based, two-dimensional landscape-evolution models. CHILD and other similar models are referred to as two-dimensional because the processes operating in these models are calculated in two-dimensional space ( $x, y$ ); in other words, the state variables (elevation and sediment texture) are functions of two independent spatial dimensions. The processes in the model shape a three-dimensional surface ( $x, y, z$ ) which evolves through time.

The background below is not exhaustive and is limited only to two-dimensional surface-process models. We do not discuss one-dimensional, single-thread channel models. In comparison with landscape models, many single-thread channel models contain more sophisticated flow and sediment-transport algorithms (e.g. Paola *et al.*, 1992; Vogel *et al.*, 1992; Cui *et al.*, 1996; Hoey and Ferguson, 1997; Robinson and Slingerland, 1998; Marr *et al.*, 2000; Ferguson and Hoey, Chapter 10, this volume; Rice *et al.*, Chapter 11, this volume). However, these models address research questions on different spatial and temporal scales. Our discussion also excludes tectonic models of mountain-belt evolution, which are often coupled with surface-processes models but focus on the sub-surface deformation of rock (e.g. Willett *et al.*, 2001; Stolar *et al.*, 2006).

## Background

In this section, we briefly review several of the relevant landscape-evolution models. These models share the common thread of describing the interplay among runoff,

sediment transport and the dynamic evolution of a topographic surface. More extensive reviews of landscape-evolution theory and models can be found in Coulthard (2001), Willgoose (2005) and Tucker and Hancock (in review).

Ahnert's SLOP3D (e.g. 1976, 1977, 1987) was one of the earliest landform models. SLOP3D is a model of hillslope processes and contains algorithms for the mechanical and chemical weathering of rocks, soil creep, slope failure or landslides and slope wash. Ahnert (1987, p. 3) described the structure of his model as follows: 'An initial land surface is defined, optionally with its underlying geological structures and rocks of varying resistance. This surface is then modified by processes of weathering, stream work, and denudation. Every iteration of the main program loop (in which all process steps are contained) represents one time unit of development. The resulting land surface at the end of each iteration becomes the initial surface for the next. The processes are defined by equations in accordance with empirical knowledge. Tectonic uplift is represented by gross fluvial downcutting  $z/t$  (= rate of lowering of the slope foot).'

In essence, Ahnert's description of the model structure applies to all landscape-evolution models. During a single model time step, any number of physical processes can be simulated, each contributing to the net change in elevation at every point in the landscape. The final evolved landscape after a model time step becomes the initial condition for the following time step, and so on. What has changed since Ahnert's original model are the details of the physical processes included in numerical models and the number of processes modelled. Also, as computing speed increases, numerical models can now simulate landscape evolution over greater spatial and temporal scales.

The SIBERIA model (e.g. Willgoose *et al.*, 1991a, 1991b, 1991c) was designed to explicitly differentiate between hillslope and channel processes. SIBERIA was a significant advance in landform-development models because it simulates drainage-network development along with hillslope processes. In SIBERIA (and other models) water is assumed to flow down the path of steepest descent, and the fluvial discharge at any location on the landscape is a function of the upstream drainage area. The transition from hillslope to channel is modelled according to a channel-initiation function, which varies non-linearly with fluvial discharge and slope. The rate of downslope soil creep is assumed to be proportional to slope gradient (e.g. Culling, 1960). The fluvial transport rate is assumed to be proportional to bed shear stress ( $\tau$ ), and shear stress is modelled as a non-linear function of drainage area ( $A$ ) and slope ( $S$ ) ( $\tau \propto A^m S^n$ , where  $m \approx 0.5$ ,  $n$ , see the next section for a derivation of the shear stress relationship). SIBERIA tracks the sediment flux at every location in the landscape. Continuity of mass, or the difference between the incoming sediment flux and the local transport rate, determines the rate of erosion or deposition across the landscape. Willgoose *et al.* (1991d) used SIBERIA to interpret the natural relationship between channel slope and drainage area (e.g. Hack, 1957; Flint, 1974) as a natural consequence of downstream changes in the efficiency of creep (on hillslopes) and water transport (in channels).

The application of a transport-limited model, as used in SIBERIA, applies to settings where there is an abundant supply of easily entrained sediment, such as alluvial rivers.

However, in bedrock rivers or channels lined with coarse or cohesive material, the rate-limiting process may be the removal of material from the bed. These settings are referred to as 'detachment-limited'. Two studies, Howard (1994) and Tucker and Slingerland (1994), introduced models that include both alluvial channels (transport-limited) and non-alluvial channels (detachment-limited). As with SIBERIA, both DELIM (Howard, 1994) and GOLEM (Tucker and Slingerland, 1994) treat sediment-transport rates as a function of bed shear stress, and continuity of mass determines the erosion rate in alluvial channels. Howard (1994) models the detachment rate of sediment as a function of shear stress (again modelled as a non-linear function of drainage area and slope). Tucker and Slingerland (1994) model the detachment rate as proportional to the product of drainage area and slope, or stream power, following Seidl and Dietrich's (1992) bedrock-erosion study in the Oregon coast range (see also Rosenbloom and Anderson, 1994).

Although details differ between DELIM and GOLEM, both models differentiate between detachment-limited and transport-limited channels in roughly the same way. Where the detachment rate of bedrock is smaller than the erosion rate calculated according to the divergence of sediment flux, the channel is detachment-limited. However, where the erosion rates are limited by the sediment-transport rate, the channel is transport-limited. Neither DELIM nor GOLEM included a channel-initiation function. Rather, hillslope and valley topography arise naturally from the competition of mass transport (creep) and water transport, both of which are active at all points on the terrain.

SIBERIA, DELIM and GOLEM have significantly evolved since these initial studies. However, the basic model structure, as described above, has not changed. It is the details of the processes that have changed. For example, the GOLEM model now includes algorithms for simulating a number of different hillslope processes (Tucker and Bras, 1998). DELIM now includes the formation of impact craters in order to study the evolution of the surface of Mars (Howard, 2007). And SIBERIA can now be used to model soil production as a function of soil moisture (Saco *et al.*, 2006).

There have been other approaches to modelling landscape development. For example, using the principle that local and global rates of energy expenditure are minimized, Optimal Channel Network (OCN) models create networks which have similar structures to those observed in nature (e.g. Rinaldo *et al.*, 1992; Rodríguez-Iturbe *et al.*, 1992; Ijjász-Vásquez *et al.*, 1993; Rigon *et al.*, 1993; Rinaldo *et al.*, 1995). Although OCNs resemble natural networks, they are obtained using rules, rather than the physically based relationships. Similarly, cellular-automata models evolve a landscape by iteratively applying a set of erosion rules. Chase (1992) and Crave and Davy (2001) describe models in which a 'precipiton' falls on the landscape, diffusion acts around the site of the precipiton landing, and erosion or deposition (calculated as a function of slope) shapes the landscape downstream of the precipiton. Chase (1992) is able to produce multifractal topographies with fractal dimensions similar to three mountain ranges

in Southern Arizona. These studies illustrate that branching valley networks can be simulated by many different types of models, as long as they contain a mechanism for increasing the net transport rates where water converges.

## The CHILD model

This section discusses only the processes contained within CHILD that are used in this study. For more details on the structure of CHILD, see Tucker *et al.* (2001a, 2001b). We explore the response of a transport-limited network to a change in climate. It is highly likely that sediment delivery from hillslopes and changes in vegetation will affect the fluvial response to a change in climate, and this has been explored in previous studies (e.g. Tucker and Slingerland, 1997; Howard, 1999; Collins, 2006). However, even though CHILD can simulate both hillslope erosion and the effects of vegetation on fluvial erosion, we do not include these processes in our study. We keep the experiment as simple as possible in order to isolate how changes in sediment texture affect erosion rates after a period of increased runoff due to an increase in precipitation.

In CHILD, the landscape is described by a set of nodes, which are connected by a triangular irregular network. Every node location  $(x, y)$  has an elevation  $(z)$ , which describes the surface topography. Precipitation falls uniformly across the landscape and produces runoff. As water flows downstream (following the steepest slope), sediment can be entrained, transported or deposited. Eroded sediment is added to the downstream sediment load,  $Q_s$ . CHILD tracks both the volume and texture of eroded material and the sediment load at every location in the landscape.

Continuity of mass determines the erosion or deposition rate throughout the network:

$$\frac{dz}{dt} = \sum_i \frac{Q_{s_i} - Q_{t_i}}{a} \quad (17.1)$$

where  $z$  is the channel elevation,  $t$  is the time step,  $Q_{s_i}$  is the volumetric incoming bedload sediment flux of the  $i$ -th grain-size fraction,  $Q_{t_i}$  is the volumetric bedload transport capacity of  $i$ -th grain-size fraction and  $a$  is the area over which the erosion rate is calculated. We assume that all suspended sediment is transported out of the network and does not interact with the bed, and therefore we consider only bedload transport in this study. CHILD tracks the texture of the bed-surface layer and the layers beneath the surface, so that if the system changes from depositional to erosional the model retains a history of the texture of deposits. (For a detailed description of the layering algorithm see Gasparini *et al.* (2004).) In all of the experiments described here, there is a substrate layer, or a deep layer of sediment below the surface layer, which replenishes the surface layer during periods of erosion. In all examples illustrated in this

chapter, the texture of this substrate material does not vary spatially, even though the texture of the surface layer varies throughout the network as a result of selective erosion and deposition.

We apply the Wilcock (2001) sand and gravel-transport model to calculate sediment-transport rates. Wilcock (2001) used field data (Oak Creek, Oregon (Milhous, 1973); East Fork River, Wyoming (Emmett, 1980; Emmett *et al.*, 1980, 1985); Jacoby Creek, California (Lisle, 1989); Goodwin Creek, Mississippi (Kuhnle, 1992)) and flume data (Wilcock and McArdell, 1993) to show that the sediment-transport rates in sand and gravel mixtures could be calculated using only the median sand and gravel grain sizes. The equations he developed for gravel- and sand-bedload transport ( $Q_{t_g}$  and  $Q_{t_s}$ , respectively) are:

$$Q_{t_g} = \frac{11.2 W f_g}{\left(\frac{\rho_s}{\rho} - 1\right) g} \left(\frac{\tau}{\rho}\right)^{1.5} \left[1 - \frac{\tau_{c_g}}{\tau}\right]^{4.5} \quad (17.2)$$

and

$$Q_{t_s} = \frac{11.2 W f_s}{\left(\frac{\rho_s}{\rho} - 1\right) g} \left(\frac{\tau}{\rho}\right)^{1.5} \left[1 - \sqrt{\frac{\tau_{c_s}}{\tau}}\right]^{4.5} \quad (17.3)$$

where 11.2 is a dimensionless parameter,  $W$  is the channel width,  $f_g$  and  $f_s$  are the proportions of the gravel and sand fractions, respectively, in the surface layer,  $\rho_s$  is the sediment density,  $\rho$  is the water density,  $g$  is the acceleration of gravity,  $\tau$  is the basal shear stress and  $\tau_{c_g}$  and  $\tau_{c_s}$  are the critical shear stress for entrainment of gravel and sand, respectively.

Interactions among sediment of different sizes affect the value of the critical shear stress for entrainment. As a result, the critical shear stress varies not only as a function of the grain size to be entrained (e.g. Shields, 1936) but also with the distribution of grain sizes on the channel bed (e.g. Komar, 1987; Kuhnle, 1992; Wilcock and McArdell, 1993; Wilcock, 1998; Weiming *et al.*, 2000; Shvidchenko *et al.*, 2001). Larger grains often become easier to entrain (the critical shear stress value decreases in comparison with the homogeneous value) in the presence of smaller grains because they protrude above the bed. Similarly, smaller grains become harder to entrain (the critical shear stress value increases in comparison with the homogeneous value) in the presence of larger grains because they can get hidden amongst the larger sediment (e.g. Komar, 1987).

In this study, we calculate the critical shear stresses for entrainment of gravel and sand based on the data of Wilcock (1998). Following Gasparini *et al.* (1999) and (2004), we partition the critical shear stress data (as a function of bed sand content) presented

by Wilcock (1998) into three separate regions and describe them using a linear fit (see Figure 1 in Gasparini *et al.*, 1999). On a sand-poor bed (<10 per cent sand), the interlocked gravel framework inhibits the entrainment of both sand and gravel, and the critical shear stress for entrainment remains constant and large. As the bed becomes sandier (between 10 and 40 per cent sand in the surface layer), the gravel framework is broken. Both sand and gravel become easier to entrain as the proportion of sand increases. In this region, the critical shear stress for both sand and gravel decreases as the proportion of sand on the bed increases. When the bed contains greater than 40 per cent sand, the critical shear stress again becomes largely insensitive to variations in the relative proportions of sand and gravel and the critical shear stress for each grain size again becomes constant. The critical shear stress relationships are shown in both Gasparini *et al.* (1999) and (2004).

We make some assumptions in order to calculate the bed shear stress ( $\tau$ ) in Equations 17.2 and 17.3. We assume that flow is uniform, steady and wide, and the cross-section averaged bed shear stress ( $\tau$ ) follows as:

$$\tau = \rho g D S \quad (17.4)$$

where  $D$  is the channel depth and  $S$  is the channel slope.

We assume that channel width ( $W$ ) varies as a power-law function of fluvial discharge ( $Q$ ), as has been shown for many alluvial channels (e.g. Leopold and Maddock, 1953; Wolman, 1955; Leopold *et al.*, 1964):

$$W = k_w Q^b \quad (17.5)$$

where  $k_w$  varies between rivers and  $b$  is often close to 0.5. Throughout this study, we set  $b = 0.5$  and  $k_w = 1.0 \text{ m}^{-0.5} \text{ s}^{0.5}$ .

We assume that flow velocity ( $V$ ) follows the Manning Equation (e.g. Chow, 1959):

$$V = N^{-1} D^{2/3} S^{1/2} \quad (17.6)$$

where  $N$  is the roughness coefficient.

Fluvial discharge is assumed to be a function of the drainage area ( $A$ ):

$$Q = P A^c \quad (17.7)$$

where  $c$  depends on the hydrology of the network and is less than or equal to one (e.g. Slingerland *et al.*, 1994; O'Connor and Costa, 2004; Solyom and Tucker, 2004). Throughout this study, we set  $c = 1$ .  $P$  is the effective precipitation rate, which is that part of the precipitation that contributes to runoff.

A relationship for channel depth ( $D$ ) as a function of drainage area ( $A$ ) and slope ( $S$ ) results from combining and rearranging the continuity of mass relationship for

fluvial discharge ( $Q = VWD$ ) with Equations 17.5 to 17.7. Substituting for the channel depth in Equation 17.4, we obtain a relationship for bed shear stress as a function of the drainage area and channel slope:

$$\tau = k_{\tau} P^{3/10} A^{3/10} S^{7/10} \quad (17.8)$$

where

$$k_{\tau} = \rho g \left( \frac{N^{3/5}}{k_w^{3/5}} \right) \quad (17.9)$$

In the simulation presented in this chapter, we use Equations 17.2 and 17.3 to calculate the sediment-transport rates of gravel and sand respectively at every location in the network. Channel width and fluvial discharge are calculated using Equations 17.5 and 17.7 respectively. The bed shear stress is calculated using Equation 17.8. The critical shear stress depends on the local texture of the channel bed and is calculated using the critical shear stress relationship illustrated in Figure 1 of Gasparini *et al.* (1999). In the upper-most reach of the channel, or points in the landscape which have no upstream contributions, there is no incoming sediment load and the transport rate determines the erosion rate (Equation 17.1). The volume and texture of material eroded is routed downstream and becomes part of the incoming sediment load at the downstream point. At all other points in the network, the erosion rate is a function of both the local transport rate and the incoming sand and gravel load (Equation 17.1).

## Example simulation of network evolution

In this section, we illustrate how the CHILD model can be used to gain an insight into network evolution that is not readily seen by investigating the sediment-transport equations outside of the model. We examine channel-slope and surface-texture changes in response to an increase in discharge, resulting from an increase in the precipitation rate. We first illustrate the steady-state channel-slope–area and surface-texture–area relationships as predicted using Equations 17.2 and 17.3 and the iterative method described by Gasparini *et al.* (2004). Both the slope–area and surface-texture–area relationships are sensitive to changes in the precipitation rate. Using the CHILD model, we then illustrate how the erosion rate, channel slope and surface texture evolve as a fluvial network transitions from steady-state with a low precipitation rate to steady-state with a higher precipitation rate. The numerical example highlights the value of numerical models for simulating conditions which are not readily understood by examining transport equations alone.

## Steady-state network sensitivity to precipitation

Before proceeding to the CHILD model results, we discuss the predicted steady-state slope–area and surface-texture–area relationships. An entire river network reaches steady state when, at every location, the erosion rate matches the rate of base-level fall at the network outlet. In natural systems, the rate of base-level fall is set by the channel into which the network drains, the rate of sea-level fall or local tectonic conditions. In the CHILD model, the rate of base-level fall is a boundary condition which remains constant in all of the numerical results presented here.

Ideally, we could derive analytical expressions for the steady-state slope–area and surface-texture–area relationships. Unfortunately, analytical solutions are intractable given the complexity of the sediment-transport equations (e.g. Equations 17.2 and 17.3). However, for the special case of steady, uniform erosion and uniform substrate composition, the slope–area and surface-texture–area relationships can be found using an iterative method. For a complete description of the iterative solution, see Gasparini *et al.* (2004). Here we present only the results of this method.

The steady-state slope–area and texture–area relationships for three different precipitation rates are illustrated in Figure 17.1(A) and (B). For any given precipitation rate, the channel slope decreases downstream and the sand content of the bed increases downstream (or with drainage area). For a given drainage area, the channel slope and surface-sand content decrease as the precipitation rate increases.

An increase in precipitation causes an increase in the fluvial discharge. One might expect that a steady-state network with higher discharge would, all else being equal, have higher bed shear stresses. However, Figure 17.1(C) indicates that this is not necessarily the case; in fact, the steady-state solutions show that bed shear stress is relatively insensitive to discharge. In the upper parts of the network (smaller drainage area), the shear stress slightly increases with an increase in the rate of precipitation, but in the lower parts of the network the shear stress slightly decreases with an increase in precipitation. In most parts of the network, the critical shear stress for the entrainment of gravel and sand slightly increases when the precipitation rate increases, as illustrated by the thick and thin grey lines, respectively, in Figure 17.1(C).

The bed shear stress and critical shear stress adjust with the precipitation rate so that the transport rate, for a given drainage area, is just sufficient to carry the sediment flux from upstream (which is given by the product of drainage area and base-level lowering rate). Changes in channel slope affect the bed shear stress; changes in the surface texture affect the critical shear stress. Throughout the network, for a given drainage area, the surface-sand content decreases as the precipitation rate increases, causing the critical shear stress for both gravel and sand to increase. Changes in both channel width (not shown) and bed shear stress counteract the changes in critical shear stress so that the transport rate does not change (Equations 17.2 and 17.3). In some regions of the network, the bed shear stress actually decreases under greater runoff and discharge,

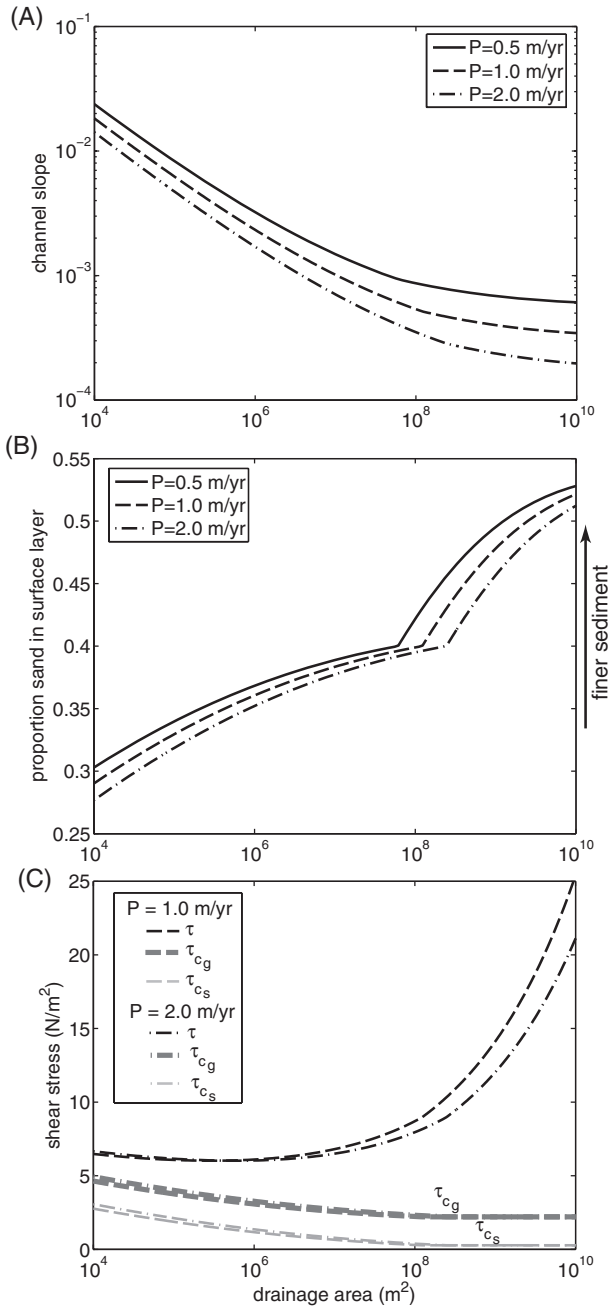


**Figure 17.1** Sensitivity of the slope–area (A) and surface–texture–area (B) relationships to a change in the precipitation rate. (C) illustrates the changes in bed shear stress (black lines) and the critical shear stress for the entrainment of gravel (thick-grey lines) and sand (thin-grey lines) for the two larger precipitation rates illustrated in (A) and (B). Erosion rate and substrate texture do not vary between the curves.

even though the critical shear stress has increased. At first this seems paradoxical, but the reason lies in the mutual adjustment of slope, width and bed texture. Consider two channels with an equal sediment flux, but with different widths. In order to carry the same sediment load, the wider channel must have lower a transport rate per unit width. This requires either a higher transport threshold or a lower bed shear stress, or both. The curves in Figure 17.1 illustrate that both effects contribute to lowering the transport rate per unit width.

In summary, for a given drainage area and sediment flux, an increase in the precipitation rate results in a coarser bed texture and a correspondingly larger critical shear stress. An increase in the precipitation rate also results in a decrease in channel slope. Changes in bed shear stress with drainage area are generally small relative to the magnitude of change in discharge, and the patterns of stress change are somewhat complex. Note that the steady-state predictions for channel slope and bed texture apply at any location in the fluvial network with a given drainage area, not just in the main stem of the network.

### Transient network adjustment to changes in precipitation

In this section, we use the CHILD model to explore the network response to an abrupt increase in the precipitation rate. The initial condition for this experiment is a steady-state network with a uniform erosion rate of 0.1 mm/yr and an annual precipitation rate of 1.0 m/yr. We use a synthetic square drainage network that has no-flux boundaries on all four sides and a single corner outlet through which water and sediment can pass out of the network. The point downstream from the outlet (the outlet is at point (0,0) in Figure 17.2) has a constant base-level fall rate of 0.1 mm/yr. The average cell size for the numerical experiments is 10 000 m<sup>2</sup>, and the total domain size is 6 250 000 m<sup>2</sup>. The maximum time step used in the model is  $5 \times 10^{-4}$  yr or approximately 4.4 hr.

The substrate texture is 50 per cent 0.5 mm sand and 50 per cent 16 mm gravel. The composition of the substrate is uniform in space. Given these boundary conditions, at steady-state, regardless of the precipitation or erosion rates, each point along the channel network must transport a load consisting of 50 per cent sand and 50 per cent gravel. However, as the network adjusts to the change in precipitation, the relative erosion and transport rates of each grain-size fraction vary in both space and time.

We illustrate the network response after an instantaneous increase in the precipitation rate to 2.0 m/yr. The change in the precipitation rate is the only perturbation to the network. An instantaneous doubling of precipitation may seem extreme, and the large change in the precipitation rate exaggerates the changes in the network. However, similar patterns of change would also occur with smaller perturbations to the precipitation rate.

Even though the precipitation rate changes uniformly across the entire network, the erosion response is not uniform in space or time. Figure 17.2(A) illustrates a map of

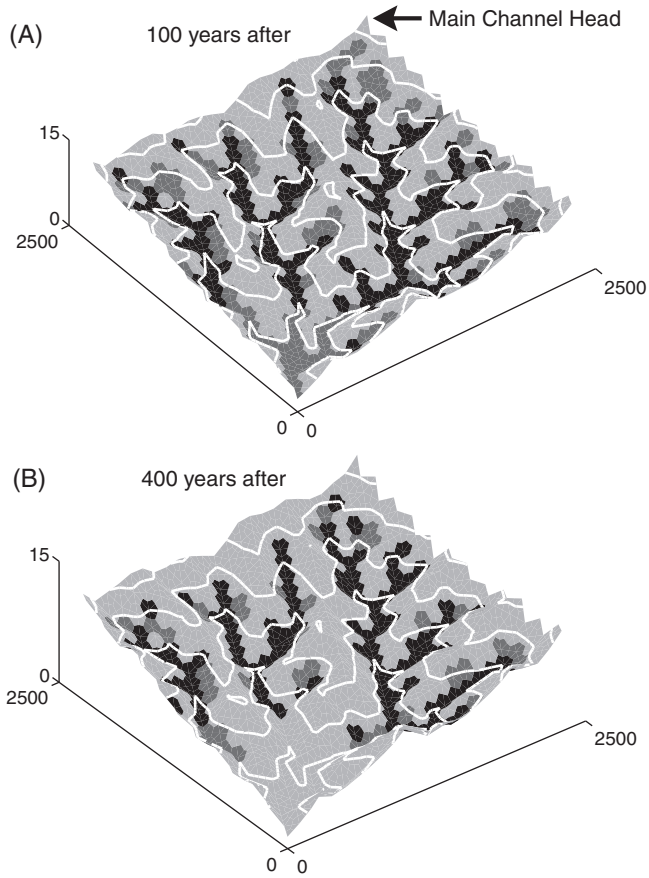


**Figure 17.2** Locations of erosion and deposition across the network at (A) 100 and (B) 400 years after an increase in the precipitation rate. Light-grey represents total erosion; dark-grey represents the erosion or transport of sand and the deposition of gravel; black represents the deposition of both sand and gravel. The white lines are two-metre contour lines, and the axes scales are in metres. The network configuration does not change between (A) and (B), and therefore the channel head remains in the same location.

erosion rates for a single time step 100 years after the increase in precipitation. In this figure, areas in which both sand and gravel are eroded from the bed are illustrated in light grey; areas in which gravel is deposited but sand is either eroded or transported are illustrated in dark grey; areas in which both sand and gravel are deposited are illustrated in black. Even after 100 years, the rates of erosion and deposition vary greatly throughout the network. The uppermost parts of the network, which have little to no contributing area, respond to the increase in fluvial discharge by eroding both

sand and gravel (light grey). More sediment is sent downstream and the sediment load quickly increases, and gravel is deposited (dark-grey areas). As the load continues to increase downstream, both sand and gravel are deposited in the lower reaches of larger tributaries and in the main channel (black areas). Further downstream from the areas in which both sand and gravel are deposited, the sediment load is reduced and the main channel is able to transport all of the sand load, but the channel does not have the capacity to transport the gravel load, and gravel continues to be deposited (dark-grey areas).

The selective erosion and deposition of sediment (as illustrated across the network in Figure 17.2) causes a change in the channel slope and surface texture. Figure 17.3 illustrates changes in the channel slope, surface texture and net erosion rate in the main channel only. We simplify the data by only showing those from the main channel, but the pattern of changes at a given drainage area is the same across the network. Before the increase in the precipitation rate, the channel slope and surface texture are at steady-state, illustrated by the light-grey line labelled 'P' in Figure 17.3(A) and (B). The new steady-state relationships given the doubling of the precipitation rate are shown by the dark-grey line and are labelled '2P'.

After 100 years, the channel slope has noticeably increased only near the outlet (see black solid line in Figure 17.3(A)), whereas the slope has decreased only slightly throughout the rest of the channel. Changes in the channel slope result from changes in the net erosion/deposition rate (of both sand and gravel), which are illustrated in Figure 17.3(C). (For reference, the steady-state erosion rate is illustrated by the light-grey line in Figure 17.3(C) and positive values (above the dark-grey line) indicate net erosion, while negative values indicate net deposition.) The erosion/deposition rates illustrated in Figure 17.3(C) are only for a single time step, but the pattern over the first 100 years stays roughly the same; only the point of greatest deposition migrates upstream. In areas in which the deposition rate is decreasing downstream (near the outlet), the slope increases. In the rest of the channel, where the deposition rate is increasing downstream (or the erosion rate is declining downstream), the slope decreases. However, after 100 years, the decline in slopes in the upper reaches is so slight that it is not noticeable in the data (see black solid line in Figure 17.3(A)).

The selective erosion/deposition shown in Figure 17.2 leads to the changes in surface texture in the main channel, as illustrated in Figure 17.3(B). In the upper-most parts of the main channel where the net erosion rate is high (black solid line in Figure 17.3(C)) and both sand and gravel are being eroded (light-grey areas in Figure 17.2(A)), the proportion of sand in the surface layer increases (black solid line in Figure 17.3(B), small drainage area). The surface-sand content increases because the gravel transport rate increases and the surface layer is stripped of its coarse material. However, in the rest of the channel, gravel is being deposited at a greater rate than sand (Figure 17.2(A)), and the sand content of the surface layer decreases (black solid line in Figure 17.3(B)).

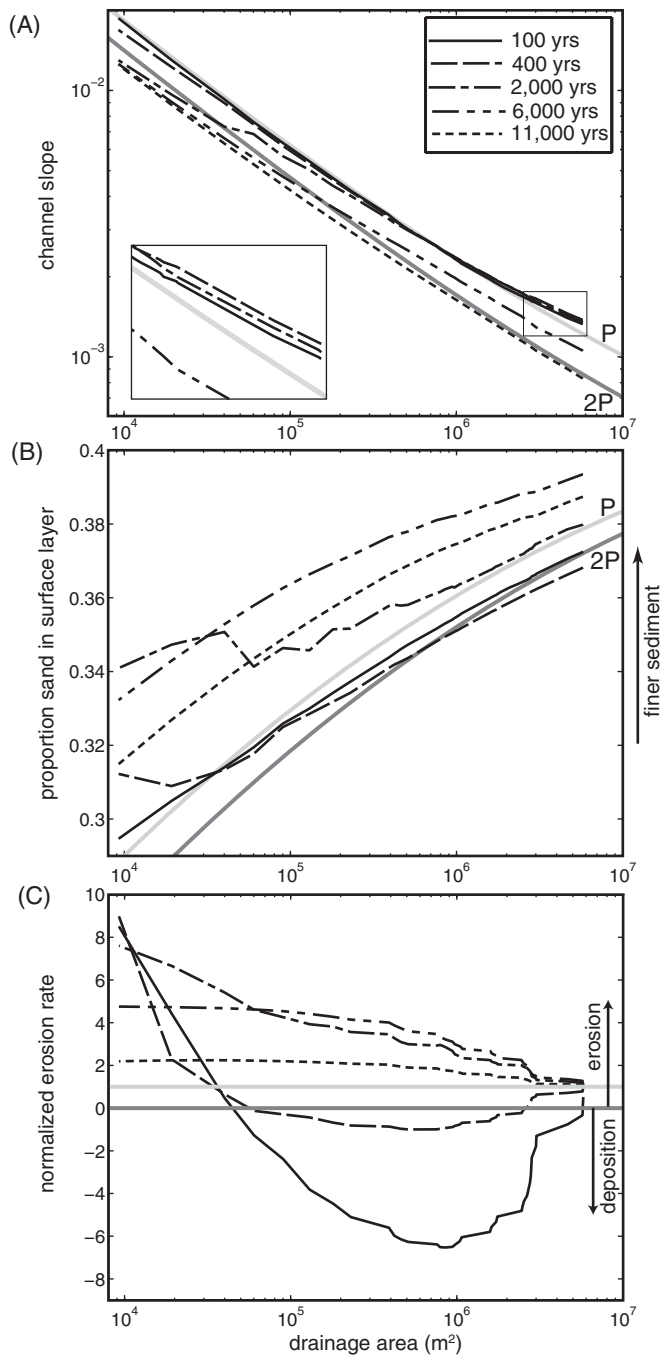


**Figure 17.3** Temporal changes in (A) channel slope, (B) surface texture and (C) the erosion rate (relative to base-level fall rate) in the main channel in response to an increase in the precipitation rate. (continued)

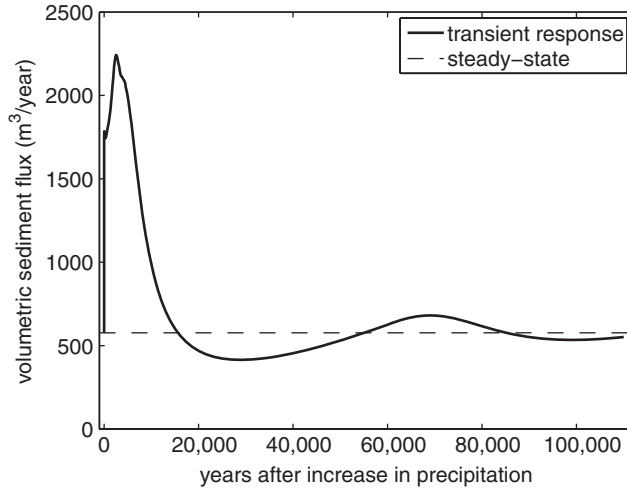


**Figure 17.4** Sediment flux at the outlet after the precipitation increase. For reference, the steady-state sediment flux is illustrated with a dashed line.

The sediment flux at the outlet is illustrated in Figure 17.4. The steady-state sediment flux at the outlet is a function of the drainage area and rate of base-level lowering, and therefore it does not vary with the precipitation rate (as illustrated by the dashed line in Figure 17.4). However, the sediment flux does vary greatly during the transient response. After the increase in the precipitation rate, the sediment flux at the outlet rapidly increases above the steady-state value. The deposition in some parts of the network after the first 100 years (as illustrated in Figure 17.2(A)) results in a small decline in the sediment flux at the outlet. This decline occurs between approximately 50 and 300 years. (This decline is barely visible in Figure 17.4 because of the scale.) However, even though the sediment flux at the outlet declines during this period, it still remains greatly elevated above the steady-state value.

After 400 years, the area of the network in which both sand and gravel are being eroded has expanded (compare the extent of light-grey areas between Figure 17.2(A) and (B)). Because the slope has increased near the outlet (dashed line in Figure 17.3(A), see inset),



**Figure 17.3** In (A) and (B), the channel slope and surface texture before the increase in precipitation is shown by the light-grey line, labelled 'P'; the final channel slope and surface texture is illustrated by the dark-grey line, labelled '2P'. The inset in (A) gives a closer view of the initial changes in the slope near the outlet. The legend in (A) applies to the entire figure. In (C), the light-grey lines represent the steady-state erosion rate, both before and after the change in precipitation; the dark-grey horizontal line demarcates erosion (above) and deposition (below). Note that erosion and deposition in this figure are the net change in elevation, even though in some locations only gravel may be deposited (see Figure 17.2).

transport rates increase and, at the large drainage area, the channel begins to erode rather than accumulate material (dashed line in Figure 17.3(C)). However, deposition is still occurring throughout much of the network. Because gravel was deposited at a greater rate than sand, the sand content of the surface throughout much of the main channel has decreased even further after 400 years (dashed line in Figure 17.3(B)).

Changes in the surface texture throughout the network follow the same pattern as in the main channel. Figure 17.5 illustrates the sand content across the network, and shows that much of the network has a lower surface-sand content than it did originally (compare the initial network, Figure 17.5(A) with the network after 400 years, Figure 17.5(B)). Only in the upper-most parts of the network, where both sand and gravel have been continually eroded and the surface armour has been stripped (Figure 17.2), has the sand content of the network actually increased (compare upper-most parts of the network in Figure 17.5(A) and (B)).

Through time, the areas of the network in which sand and gravel are deposited continue to shrink. Eventually, the entire network begins to erode again, as it will in steady-state. After the relatively brief period of deposition in some parts of the network, the erosion rates increase beyond the steady-state value, and the sediment flux at the outlet continues to increase (Figure 17.4). By 2000 years after the increase in the precipitation rate, the erosion rate throughout the main channel (dash-dot line in Figure 17.3(C)) has increased beyond the steady-state value. The channel slope has declined throughout the main channel (compare the dash-dot with the dashed line in Figure 17.3(A)), although near the outlet the slope still remains steeper than the initial condition. The surface texture throughout the network has become finer than it was initially, in contrast to the coarsening that occurred throughout most of the network after 400 years (compare the dashed line (400 years) with the dash-dot line (2000 years) in Figure 17.3(B)).

The trend of increasing erosion rate continues throughout much of the main channel until about 6000 years (dash-dot-dot line in Figure 17.3(C)). However, the sediment flux at the outlet starts to decline after approximately 2500 years (Figure 17.4), when erosion rates in the upper parts of the network decline. Between 2000 and 6000 years, channel slopes decline throughout the main channel and the surface-sand content increases throughout most of the main channel (compare dash-dot (2000 years) and dash-dot-dot (6000 years) lines in Figure 17.3(A) and (B) respectively). In comparison with the initial network and after 400 years, the surface-sand content has increased throughout the network (compare Figure 17.5(C) with Figure 17.5(A) and (B)).

Between 6000 and 11 000 years after the increase in the precipitation rate, erosion rates in the main channel decline (compare dash-dot-dot (6000 years) and dotted (11 000 years) lines in Figure 17.3(C)). The channel slope continues to decline throughout the main channel (dotted line in Figure 17.3(A)) because the erosion rate at any given time step is declining downstream. The surface-sand content also declines in this time period but remains well above the new steady-state value (dotted line in Figure 17.3(B)). The

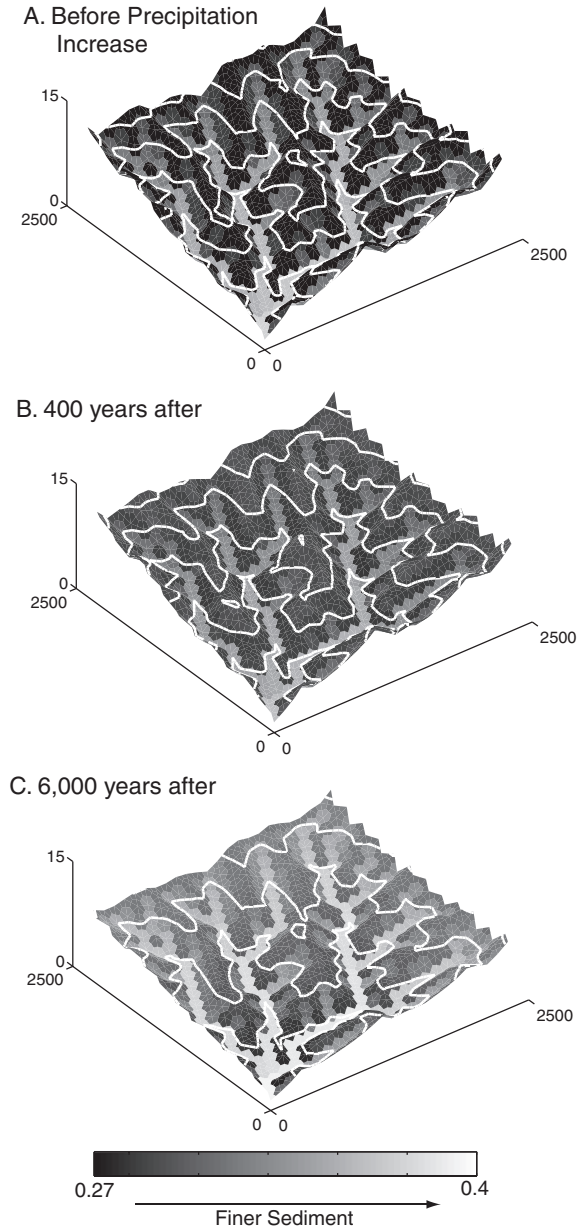


**Figure 17.5** Topography of the drainage network shaded by the proportion of sand in the surface layer, as indicated by the colour bar. The same scale applies to all three figures. The white lines are two-metre contour lines, and the axes scales are in metres. (A) illustrates the initial steady-state network; (B) and (C) illustrate changes in the surface texture at two different times following the change in precipitation. The network configuration does not change between the figures. A colour reproduction of this figure can be seen in the colour section towards the centre of the book.

sediment flux is declining but still remains above the steady-state value because the entire network is eroding faster than the steady-state rate.

Given the conditions in the network at 11 000 years after the rainfall perturbation, the channel slope must increase and the surface-sand content must decrease in order for the network to reach the new steady-state conditions. However, the network goes through a number of cycles of coarsening and fining, steepening and shallowing before the network reaches its new steady-state conditions. These cycles appear as a series of damped oscillations in the sediment-yield curve (Figure 17.4), which resemble those observed by Schumm *et al.* (1987) in an experimental drainage basin that was perturbed by a base-level drop. Later changes in slope, surface texture and erosion rates are not illustrated, but the oscillations in sediment flux at the outlet (Figure 17.4) indicate later periods of both increasing and decreasing erosion rates throughout the network. Even after 100 000 years, the network is still adjusting, although the changes in channel slope and surface texture are so slight that the network has effectively reached steady-state. Part of the reason for the gradual convergence on steady-state is the different timescales of adjustment in different parts of the network. Because any point in the network must adjust to both upstream and downstream changes in the erosion rate, the network response is more complex than a simple, direct adjustment in channel slope and surface texture.

## Discussion

Our model predicts that under steady, uniform erosion, higher precipitation rates lead ultimately to channels with shallower slopes and coarser bed material. Intuitively, the results seem reasonable. A higher precipitation rate results in a higher fluvial discharge, and with a higher discharge, a lower gradient is required to transport the incoming sediment load. Similarly, the bed coarsens, causing the critical shear stress values to increase. Under different climatic conditions, both channel slope and grain size mutually adjust in order to produce a constant erosion rate at steady-state.

Given the general links between fluvial discharge, channel slope and grain size, it is tempting to try to infer climatic conditions from fluvial deposits, and many studies have done so (e.g. Schumm, 1968; Knox, 1972, 1983; Costa, 1978; Blum and Valastro, 1989; Sugai, 1993; Arbogast and Johnson, 1994; Fuller *et al.*, 1998; Reid *et al.*, 1999). However, the non-steady example illustrated here suggests that direct inference of flow conditions from slope and texture in a single part of the network can be deceptive. The local channel response to any type of perturbation is not isolated from the response of the upstream reach, the local tributaries and the hillslopes which supply the local sediment load (e.g. Schumm, 1973; Butzer, 1980; Rinaldo *et al.*, 1995; Tucker and Slingerland, 1997).

The complex link between the texture of fluvial deposits and climate has been recognized in field studies. Blum and Valastro (1989) found that the Pedernales River, Texas

was carrying a coarser sediment load during more humid conditions 1000 years ago, in comparison with the current more arid conditions and a finer sediment load. They also point out that other studies have observed the opposite trend, that coarser-grained sediment loads occur during arid periods.

Our numerical results suggest that even a single uniform increase in the precipitation rate does not lead to a direct change in slope and surface texture. Erosion rates of both grain-size fractions vary in time and throughout the network. All parts of the network experience periods of increasing and decreasing channel slopes, but the slope response is not necessarily spatially uniform. Similarly, the surface texture coarsens and fines throughout the network, but, again, the bed may be armouring in some reaches of the network, while the armour is being stripped in other reaches of the network. Coarsening of the bed occurs during periods of deposition, when gravel is deposited at a greater rate than sand, and also during periods of erosion, when sand is eroded at a greater rate than gravel. These numerical results suggest that there may not be a direct link between grain size and climate, or channel slope and climate, when the network is not in steady conditions or, in other words, that a network's response to climate change is complex (Schumm, 1973).

Although the response is complex, some patterns also arise. The general pattern of initial upstream erosion and downstream deposition was also observed by Tucker and Slingerland (1997). In the results presented here, erosion upstream leads to a fining of the bed sediment, whereas in downstream areas, deposition leads to a coarsening of the bed sediment. The bed texture and erosion/sediment behaviour in the lower reaches of the network then go through an oscillatory cycle, consisting first of deposition and coarsening, followed by erosion and fining, then back to erosion and coarsening, until the new equilibrium is established. Given these time and space variations, the results suggest that field observations of fluvial erosion or aggradation, or sediment texture fining or coarsening, could represent one particular component of a cycle, and will depend on the position in the network and the elapsed time since the initial perturbation. Although there may not be a general relationship between climate change and fluvial behaviour, there are potentially identifiable spatial and temporal patterns within a network.

Because the large drainage-area reaches experience prolonged deposition, the lower parts of the network may be the areas that are most likely to preserve deposits and potential information about past climate perturbations. However, the initial period of deposition does not last indefinitely, and eventually the lower parts of the network begin to erode again. These results suggest that an understanding of the response time to climate change is critical for interpreting perturbations to a network.

Many of the erosion and sedimentation patterns in our numerical study are similar to the complex geomorphic response described by Schumm (1973). As an example of complex response, Schumm (1973) discussed the analogue experiments of Lewis (1944), in which he carved a network into a sand and mud mixture which drained on to a floodplain. Lewis then introduced water into the main channel and the two tributaries.

At the contact between the main channel and the floodplain, a knickpoint, or locally steep region, developed and migrated up the network. This initiated rapid erosion in the headwaters and deposition in the lower reaches of the network. As the upper reaches stabilized, the sediment load decreased downstream and the lower reaches began to incise again.

In our numerical experiments, we saw almost the same pattern as described by Lewis (1944), with the exception of an initial knickpoint. The knickpoint described by Lewis (1944) was initiated in a location where there was a break in slope, and this break in slope migrated headward. Numerical experiments of bedrock rivers, or detachment-limited rivers, produce knickpoints when a network experiences an increase in the base-level lowering rate or an instantaneous drop in the base-level. These perturbations cause a locally steep region to form which then migrates upstream (e.g. Whipple and Tucker, 2002; Crosby *et al.*, 2007). However, the same perturbation in a transport-limited river, or alluvial river, creates a diffusive response. Transport-limited rivers cannot sustain an abrupt change in a slope (e.g. Whipple and Tucker, 2002; Gasparini, 2003; Crosby *et al.*, 2007). We simulate an alluvial network and do not change the base-level fall rate, and therefore our model does not create a knickpoint. However, the erosional response described by Lewis (1944) after the knickpoint has moved through the network is very similar to the erosional patterns produced in our numerical experiment.

The experiment that we present here is idealized in many ways. For example, the response would likely be different if the network had not reached steady-state before the precipitation rate was changed (e.g. Rinaldo *et al.*, 1995). Other variables that we have not considered, such as vegetation, respond to climate change and affect the sediment load (e.g. Huntington, 1924; Bryan, 1928; Slaymaker, 1990; Prosser *et al.*, 1994; Wilcox *et al.*, 1996; Mulligan, 1998; Howard, 1999; Collins, 2006). We also make the assumption that the hydraulic geometry relationship does not vary during transient conditions. However, studies have shown that changes in both fluvial and sediment inputs downstream of a dam often cause a spatially and temporally variant response in channel geometry (e.g. Phillips *et al.*, 2005; Brandt, 2000; Petts and Gurnell, 2005). The scope of this study was limited in order to focus on changes in slope and bed texture. However, any number of complications could be added in future experiments in order to explore whether more variability in the system enhances or reduces the complexity of the response (Bras *et al.*, 2003).

## Conclusions

When the erosion rate is uniform throughout a drainage network, both channel slope and surface texture vary with drainage area in a predictable manner. Our steady-state theory predicts that channel slopes decrease and the bed material coarsens when the precipitation/runoff rate is higher. However, transitions from one steady-state

climate regime to another are complex. The numerical simulation suggests that the response of both channel gradient and surface texture varies in space and time. Initially, small tributaries respond to an increase in the precipitation rate by eroding at a faster rate. The increased erosion in small tributaries strips the bed of its armour, and the sand content of the bed increases. However, in the lower reaches of the network, the sediment load increases and coarse sediment is deposited. The spatial pattern in erosion rates causes the channel gradient to increase in some parts of the network and decrease in others. After the initial response, the network begins to erode throughout; however, the sand- and gravel-transport rates vary in space, causing later periods of both coarsening and fining, and an increasing and decreasing channel gradient. The results indicate that climate change can cause a complex response, in the form of damped oscillations in sediment yield, bed texture and the erosion/deposition rate. The oscillatory nature of the response, and the fact that its phase and amplitude depend on network position, suggest that it would be oversimplistic to invoke a direct connection between climate state and fluvial properties (such as bed slope or texture) unless the network has reached a steady, graded form.

## Acknowledgements

Reviews by Rudy Slingerland and Bruce Rhoads are gratefully acknowledged. The authors also thank Stephen Rice, André Roy and Bruce Rhoads for their efforts in putting together this volume. This work was funded by the US Army Research Office (grants DACA88-95-C-0017, DAAD19-99-1-0338 and DAAD19-0101-0513), the Italian National Research Council and the NASA Earth System Science Fellowship. Post-doctoral funding for NMG was provided by Kelin Whipple.

## References

- Ahnert F. 1976. Brief description of a comprehensive three-dimensional process-response model of landform development. *Zeitschrift für Geomorphologie Suppl.* **25**: 29–49.
- Ahnert F. 1977. Some comments on the quantitative formulation of geomorphological processes in a theoretical model. *Earth Surface Processes* **2**: 191–201.
- Ahnert F. 1987. Approaches to dynamic equilibrium in theoretical simulations of slope development. *Earth Surface Processes and Landforms* **12**: 3–15.
- Arbogast AF, Johnson WC. 1994. Climatic implications of the Late Quaternary alluvial record of a small drainage basin in the Central Great Plains. *Quaternary Research* **41**: 298–305.
- Blum MD, Valastro S. 1989. Response of the Pedernales River of Central Texas to late Holocene climate change. *Annals of the Association of American Geographers* **79**: 435–456.
- Bogaart PW, Tucker GE, de Vries JJ. 2003. Channel network morphology and sediment dynamics under alternating periglacial and temperate regimes: A numerical simulation study. *Geomorphology* **54**: 257–277.

- Brandt SA. 2000. Classification of geomorphological effects downstream of dams. *Catena* **40**: 375–401.
- Bras RL, Tucker GE, Teles V. 2003. Six myths about mathematical modeling in geomorphology. In *Prediction in Geomorphology*, Wilcock PR, Iverson RM (eds). American Geophysical Union: Washington DC; 63–79.
- Bryan K. 1928. Historic evidence on changes in the channel of the Rio Puerco, a tributary of the Rio Grande in New Mexico. *Journal of Geology* **36**: 265–282.
- Burbank DW, Blythe AE, Putkonen J, Pratt-Situala B, Gabet E, Oskin M, Barros A, Ojha TP. 2003. Decoupling of erosion and precipitation in the Himalayas. *Nature* **426**: 652–655.
- Butzer KW. 1980. Holocene alluvial sequences: Problems of dating and correlation. In *Timescales in Geomorphology*, Cullingford RA, Davidson DA, Lewin J (eds). John Wiley & Sons: Chichester; 131–142.
- Chase CG. 1992. Fluvial land sculpting and the fractal dimension of topography. *Geomorphology* **5**: 39–57.
- Chow VT. 1959. *Open-channel hydraulics*. McGraw-Hill: New York.
- Collins DBG. 2006. Geomorphology and ecohydrology of water-limited ecosystems: A modeling approach. PhD thesis, Massachusetts Institute of Technology.
- Costa JE. 1978. Holocene stratigraphy in flood frequency analysis. *Water Resources Research* **14**: 626–632.
- Coulthard TJ. 2001. Landscape evolution models: A software review. *Hydrological Processes* **15**: 165–173.
- Coulthard TJ, Kirkby MJ, Macklin MG. 2000. Modeling geomorphic response to environmental change in an upland catchment. *Hydrological Processes* **14**: 2031–2045.
- Crave D, Davy P. 2001. A stochastic ‘precipiton’ model for simulation erosion/sedimentation dynamics. *Computers and Geosciences* **27**: 815–827.
- Crosby BT, Whipple KX, Gasparini NM, Wobus CW. 2007. Formation of fluvial hanging valleys: Theory and simulation. *Journal of Geophysical Research* **112**: 10.1029/2006JF000566.
- Cui Y, Parker G, Paola C. 1996. Numerical simulation of aggradation and downstream fining. *Journal of Hydraulic Research* **34**: 185–204.
- Culling WEH. 1960. Analytical theory of erosion. *Journal of Geology* **68**: 336–344.
- Emmett WW. 1980. A field calibration of the sediment-trapping characteristics of the Helley-Smith bedload sampler. *USGS Professional Paper* **1139**.
- Emmett WW, Myrick RH, Meade RH. 1980. *Field data describing the movement and storage of sediment in the East Fork River, Wyoming, Part 1. River hydraulics and sediment transport, 1979*. Open-File Report 80-1189, US Geological Survey.
- Emmett WW, Myrick RH, Martinson HA. 1985. *Hydraulic and sediment-transport data, East Fork River, Wyoming*. Open-File Report 85-486, US Geological Survey.
- Flint JJ. 1974. Steam gradient as a function of order, magnitude, and discharge. *Water Resources Research* **10**: 969–973.
- Fuller IC, Macklin MG, Lewin J, Passmore DG, Wintle AG. 1998. River response to high-frequency climate oscillations in southern Europe over the past 200 k.y.. *Geology* **26**: 275–278.
- Gasparini NM. 2003. Equilibrium and transient morphologies of river networks: Discriminating among fluvial erosion models, PhD thesis, Massachusetts Institute of Technology.
- Gasparini NM, Tucker GE, Bras RL. 1999. Downstream fining through selective particle sorting in an equilibrium drainage network. *Geology* **27**: 1079–1082.

- Gasparini NM, Tucker GE, Bras RL. 2004. Network-scale dynamics of grain-size sorting: Implications for downstream fining, stream-profile concavity and drainage basin morphology. *Earth Surface Processes and Landforms* **29**: 401–421.
- Hack JT. 1957. Studies of longitudinal stream profiles in Virginia and Maryland. *United States Geological Survey Professional Papers* **294-B**, 45–97.
- Hoey TB, Ferguson RI. 1997. Controls of strength and rate of downstream fining above a river base level. *Water Resources Research* **33**: 2601–2609.
- Howard AD. 2007. Simulating the development of martian highland landscapes through the interaction of impact cratering, fluvial erosion, and variable hydrologic forcing. *Geomorphology* **91**: 332–363.
- Howard AD. 1994. A detachment-limited model of drainage basin evolution. *Water Resources Research* **30**: 2261–2285.
- Howard AD. 1999. Simulation of gully erosion and bistable landforms. In *Incised River Channels: Processes, Forms, Engineering and Management*, Darby SE, Simon A (eds). John Wiley & Sons: Chichester; 277–299.
- Huntington E. 1924. *The Climatic Factor as Illustrated in Arid America*. Carnegie Institution Publication.
- Ijjász-Vásquez E, Bras RL, Rodríguez-Iturbe I, Rigon R, Rinaldo A. 1993. Are river basins optimal channel networks? *Advances in Water Resources* **16**: 69–79.
- Knox JC. 1972. Valley alluviation in Southwestern Wisconsin. *Annals of the association of American geographers* **62**: 401–410.
- Knox JC. 1983. Responses of river systems to Holocene climates. In *Late Quaternary Environments of the United States: Volume 2, The Holocene*, Wright HE, Porter SC (eds). University of Minnesota Press: Minneapolis; 26–41.
- Komar PD. 1987. Selective grain entrainment by a current from a bed of mixed sizes: A reanalysis. *Journal of Sedimentary Petrology* **57**: 203–211.
- Kuhnle RA. 1992. Fractional transport rates of bedload on Goodwin Creek. In *Dynamics of Gravel-Bed Rivers*, Billi P, Hey RD, Thorne CR, Tacconi P (eds). John Wiley & Sons: Chichester; 141: 145
- Leopold LB, Maddock T. 1953. The hydraulic geometry of stream channels and some physiographic implications. *United States Geological Survey Professional Paper* **252**: 1–57.
- Leopold LB, Wolman MG, Miller JP. 1964. *Fluvial Processes in Geomorphology*. Dover Publications.
- Lewis WV. 1944. Steam trough experiments and terrace formation. *Geological Magazine* **81**: 241–253.
- Lisle T. 1989. Sediment transport and resulting deposition in spawning gravels, north coastal California. *Water Resources Research* **25**: 1303–1319.
- Marr JG, Swenson JB, Paola C, Voller VR. 2000. A two-diffusion model of fluvial stratigraphy in closed depositional basins. *Basin Research* **12**: 381–398.
- Milhous RT. 1973. Sediment transport in a gravel-bottomed stream, Ph.D dissertation, Oregon State University.
- Mulligan M. 1998. Modeling the geomorphological impact of climatic variability and extreme events in a semi-arid environment. *Geomorphology* **24**: 59–78.
- O'Connor J, Costa JE. 2004. Spatial distribution of the largest rainfall-runoff floods from basins between 2.6 and 26,000 km<sup>2</sup> in the United States and Puerto Rico. *Water Resources Research* **40**: 10.1029/2003WR002247.

- Paola C, Heller PL, Angevine CL. 1992. The large-scale dynamics of grain-size variation in alluvial basins, 1: Theory. *Basin Research* **4**: 73–90.
- Petts GE, Gurnell AM. 2005. Dams and geomorphology: Research progress and future directions. *Geomorphology* **71**: 27–47.
- Phillips JD, Slattery MC, Musselman ZA. 2005. Channel adjustments of the lower Trinity River, Texas, downstream of Livingston Dam. *Earth Surface Processes and Landforms* **30**: 1419–1439.
- Prosser IP, Chappell J, Gillespie R. 1994. Holocene valley aggradation and gully erosion in head-water catchments, South-Eastern Highlands of Australia. *Earth Surface Processes and Landforms* **19**: 465–480.
- Reid I, Laronne JB, Powell DM. 1999. Impact of major climate change on coarse-grained river sedimentation: A speculative assessment based on measured flux. In *Fluvial Processes and Environmental Change*, Brown AG, Quine TA (eds). John Wiley & Sons: Chichester; 105–115.
- Riebe CS, Kirchner JW, Granger DE, Finkel RC. 2001. Minimal climatic control on erosion rates in the Sierra Nevada, California. *Geology* **29**: 447–450.
- Rigon R, Rinaldo A, Rodríguez-Iturbe I, Bras RL, Ijász-Vásquez E. 1993. Optimal channel networks: A framework for the study of river basin morphology. *Water Resources Research* **29**: 1635–1646.
- Rinaldo A, Dietrich WE, Rigon R, Vogel GK, Rodríguez-Iturbe I. 1995. Geomorphological signatures of varying climate. *Nature* **374**: 632–635.
- Rinaldo A, Rodríguez-Iturbe I, Rigon R, Bras RL, Ijász-Vásquez E, Marani A. 1992. Minimum energy and fractal structures of drainage networks. *Water Resources Research* **28**: 2183–2195.
- Robinson RAJ, Slingerland RL. 1998. Origin of fluvial grain-size trends in a foreland basin: The Pocono Formation in the central Appalachian basin. *Journal of Sedimentary Research* **68**: 473–486.
- Rodríguez-Iturbe I, Rinaldo A, Rigon R, Bras RL, Marani A, Ijász-Vásquez E. 1992. Energy dissipation, runoff production, and the three-dimensional structure of river basins. *Water Resources Research* **28**: 1095–1103.
- Rosenbloom NA, Anderson RS. 1994. Hillslope and channel evolution in a marine terraced landscape, Santa Cruz, California. *Journal of Geophysical Research* **99**: 14013–14029.
- Saco PM, Willgoose GR, Hancock GR. 2006. Spatial organization of soil depths using a landform evolution model. *Journal of Geophysical Research* **111**: 10.1029/2005JF000351.
- Schumm SA. 1968. *River adjustment to altered hydrologic regime – Murrumbidgee River and paleochannels, Australia*. Professional Paper 598, US Geological Survey.
- Schumm SA. 1973. Geomorphic thresholds and complex response of drainage systems. In *Fluvial Geomorphology*, Morisawa M (ed.). Publications in Geomorphology, State University of New York: Binghamton, NY; 299–310.
- Schumm SA. 1977. *The Fluvial System*. John Wiley & Sons: Chichester.
- Schumm SA, Paul MM, Weaver WE. 1987. *Experimental fluvial geomorphology*. John Wiley & Sons: Chichester.
- Seidl MA, Dietrich WE. 1992. The problem of channel erosion into bedrock. *Catena Supplement* **23**: 101–124.
- Shields A. 1936. Application of similarity principles and turbulence research to bedload movement, Mitteilungen der preussischen versuchsanstalt für wasserbau und schiffbau, 26, Berlin. In *W. M. Keck Laboratory of Hydraulics and Water Resources Report 167*, Ott WP, Uchelen JC, translators. California Institute of Technology: Pasadena, California.

- Shvidchenko AB, Pender G, Hoey TB. 2001. Critical shear stress for incipient motion of sand/gravel streambeds. *Water Resources Research* **37**: 2273–2283.
- Slaymaker O. 1990. Climate change and erosion processes in mountain regions of Western Canada. *Mountain Research and Development* **10**: 171–182.
- Slingerland R, Furlong K, Harbaugh JW. 1994. *Simulating Clastic Sedimentary Basins*. Prentice-Hall: Old Tappan, N. J.
- Solyom PB, Tucker GE. 2004. Effect of limited storm duration on landscape evolution, drainage basin geometry, and hydrograph shapes. *Journal of Geophysical Research – Earth Surface* **109**: DOI: 10.1029/2003JF000032.
- Stolar DB, Willett SD, Roe GH. 2006. Climatic and tectonic forcing of a critical orogen. In *Tectonics, climate and landscape evolution. Geological Society of America Special Paper 398, Penrose Conference Series*, Willett SD, Hovius N, Brandon MT, Fisher DM (eds). Geological Society of America: Boulder, CO; 241–250.
- Sugai T. 1993. River terrace development by concurrent fluvial processes and climatic changes. *Geomorphology* **6**: 243–252.
- Tucker GE, Bras RL. 1998. Hillslope processes, drainage density, and landscape morphology. *Water Resources Research* **34**: 2751–2764.
- Tucker GE, Hancock GR. In review. Landform characterization and evolution. In *Handbook of Geomorphology*, Gomez B, Baker V, Goudie AS, Roy A (eds). Sage Publications.
- Tucker GE, Slingerland RL. 1994. Erosional dynamics, flexural isostasy, and long-lived escarpments: A numerical modeling study. *Journal of Geophysical Research* **99**: 12 229–12 243.
- Tucker GE, Slingerland RL. 1997. Drainage basin responses to climate change. *Water Resources Research* **33**: 2031–2047.
- Tucker GE, Lancaster ST, Gasparini NM, Bras RL. 2001a. The channel-hillslope integrated landscape development model (CHILD). In *Landscape Erosion and Evolution Modeling*, Harmon RS, Doe WW (eds). Kluwer Academic/Plenum Publishers: New York; 349–388.
- Tucker GE, Lancaster ST, Gasparini NM, Bras RL, Rybarczyk SM. 2001b. An object-oriented framework for distributed hydrologic and geomorphic modeling using triangulated irregular networks. *Computers and Geosciences* **27**: 959–973.
- Vogel KR, van Niekerk A, Slingerland R, Bridge JS. 1992. Routing of heterogeneous sediments over movable bed: Model verification. *Journal of Hydraulic Engineering* **118**: 263–279.
- von Blanckenburg F. 2005. The control mechanisms of erosion and weathering at basin scale from cosmogenic nuclides in river sediment. *Earth and Planetary Science Letters* **237**: 462–479.
- Weiming W, Wang SSY, Jia Y. 2000. Nonuniform sediment transport in alluvial rivers. *Journal of Hydraulic Research* **38**: 427–434.
- Whipple KX, Tucker GE. 2002. Implications of sediment-flux dependent river incision models for landscape evolution. *Journal of Geophysical Research, B, Solid Earth and Planets* **107**: 10.1029/2000JB000044.
- Wilcock PR. 1998. Two-fraction model of initial sediment motion in gravel-bed rivers. *Science* **280**: 410–412.
- Wilcock PR. 2001. Toward a practical method for estimating sediment-transport rates in gravel-bed rivers. *Earth Surface Processes and Landforms* **26**: 1395–1408.
- Wilcock PR, McArdell BW. 1993. Surface-based fractional transport rates: Mobilization thresholds and partial transport of a sand-gravel sediment. *Water Resources Research* **29**: 1297–1312.

- Wilcox BP, Pitlick J, Allen CD, Davenport DW. 1996. Runoff and erosion from a rapidly eroding pinyon-juniper hillslope. In *Advances in Hillslope Processes*, Anderson MG, Brooks SM (eds). John Wiley & Sons: Chichester; 61–77.
- Willett SD, Slingerland R, Hovius N. 2001. Uplift, shortening, and steady state topography in active mountain belts. *American Journal of Science* **301**: 579–582.
- Willgoose GR. 2005. Mathematical modeling of whole landscape evolution. *Annual Reviews of Earth and Planetary Sciences* **33**: 443–459.
- Willgoose GR, Bras RL, Rodríguez-Iturbe I. 1991a. A coupled channel network growth and hillslope evolution model, 1. Theory. *Water Resources Research* **27**: 1671–1684.
- Willgoose GR, Bras RL, Rodríguez-Iturbe I. 1991b. A coupled channel network growth and hillslope evolution model, 2. Nondimensionalization and applications. *Water Resources Research* **27**: 1685–1696.
- Willgoose GR, Bras RL, Rodríguez-Iturbe I. 1991c. Results from a new model of river basin evolution. *Earth Surface Processes and Landforms* **16**: 237–254.
- Willgoose GR, Bras RL, Rodríguez-Iturbe I. 1991d. A physical explanation of an observed link area-slope relationship. *Water Resources Research* **27**: 1697–1702.
- Wolman MG. 1955. *The natural channel of Brandywine Creek Pennsylvania*. Professional Paper 271, United States Geological Survey.
- Zhang P, Molnar P, Downs WR. 2001. Increased sedimentation rates and grain sizes 2–4 Myr ago due to the influence of climate change on erosion rates. *Nature* **410**: 891–897.

# 18

## Solute transport along stream and river networks

**Michael N. Gooseff<sup>1</sup>, Kenneth E. Bencala<sup>2</sup>  
and Steven M. Wondzell<sup>3</sup>**

<sup>1</sup>*Department of Civil and Environmental Engineering, Pennsylvania State University, USA*

<sup>2</sup>*US Geological Survey, USA*

<sup>3</sup>*USDA Forest Service, Pacific Northwest Research Station, Olympia Forestry Sciences Laboratory, USA*

### Introduction

Since the 1950s, the science of solute transport in streams has burgeoned. Significant advances have been made in our understanding of the controls on solute transport at the reach scale (hundreds of metres), but few studies have scaled beyond continuous reaches of a few kilometres. Notable exceptions include theoretical studies of solute transport throughout river networks (e.g. Zhan, 2003; Zhang and Aral, 2004; Lindgren *et al.*, 2004; Gupta and Cvetkovic, 2002). Laenen and Bencala (2001) summarize a number of reach-scale stream-tracer experiments throughout the Willamette River basin in Oregon, and there have been recent efforts to examine the factors controlling the transport of nitrogen through the entire Mississippi River basin (Alexander *et al.*, 2000) and of large, Arctic river networks (Holmes *et al.*, 2000). These latter studies generally rely upon discharge-monitoring data, potentially lumped both in space and time (i.e. a single value to represent a basin and a single annual-discharge estimate) and water-quality

data throughout respective basins. Thus, our current understanding of solute transport at the river network scale is limited.

In this chapter, we focus on the processes that control solute transport in rivers and explore how those controls change from headwaters to higher-order streams. Fluvial geomorphologists have long studied how channel geometry and resulting hydraulics change predictably along the network continuum (Leopold and Maddock, 1953). We propose that the predictable changes in morphology and hydraulics have predictable impacts on the physical processes of stream-solute transport. This issue is critical to understanding stream ecology and contaminant transport at the network scale. For example, network-scale solute transport is important to conceptual ecological models, such as the River Continuum Concept, that propose ecosystem processes and forcing factors along streams vary systematically with location along the river due to changes in river size and connectivity to the adjacent landscape (Vannote *et al.*, 1980; Fisher *et al.*, 1998). Thus, we have structured this chapter to open with an introduction of solute-transport processes in streams (see Fischer *et al.* (1979) and Rutherford (1994) for additional details). We then link these processes to morphologic and hydraulic domains within the stream network. Finally, we offer a perspective on future research foci that will improve our understanding of solute transport from headwater streams to large rivers.

## Review of current knowledge

Material transport in streams is influenced by two major categories of processes: physical and chemical, where the latter may include geochemical and biochemical reactions. Here, we mostly focus on the physical hydrological controls on the fate and transport of dissolved materials (solutes). We do not address the larger field of biogeochemistry directly but rather show how hydrological processes influence the potential occurrence of a variety of biogeochemical transformations. Much of the basic knowledge about solute transport is derived from experiments in which tracer solutes are released into streams and their movement monitored at one or more sampling points downstream. Consequently, transport processes of solutes, especially conservative or non-reactive solutes, through short sections of stream networks are relatively well understood. In contrast, the movement of particulate (e.g. viruses or bacteria), sediment-sorbed (phosphorus), colloidal (trace metals) or immiscible (oil) contaminants is poorly known. Sources of most solutes in streams are found across landscapes, proximal and distal from the stream network. The hydrologic connections between landscapes and stream networks control the source amounts and fluxes of solutes to streams. Further, the transport of some contaminants occurs in several phases simultaneously. For example, Montana's Clark Fork was initially contaminated by erosion and the redistribution of mine tailings throughout large portions of the stream network. Today, trace-metal transport

occurs both in dissolved and colloidal forms (Nimick *et al.*, 2003). Additionally, during high flows, erosion continues to transport and redistribute sediment within the stream network. A thorough review of these complexities, for a multitude of contaminants, is beyond the scope of this chapter.

There are four physical hydrologic processes that strongly affect the transport of solutes in stream networks: advection, dispersion, transient storage and the mixing of stream water with inflows (Ramaswami *et al.*, 2005). The processes of longitudinal advection and dispersion are well known and commonly described by one-dimensional transport models. In these models, ‘transient storage’ refers to the movement of channel water and associated solutes into either in-channel dead zones or subsurface flowpaths of the hyporheic zone (Harvey and Wagner, 2000). The process of mixing with inflows refers to (1) groundwater–surface-water exchange with local or regional aquifers (gaining or losing reaches), at a spatial and temporal scale beyond hyporheic exchange, and (2) tributary junctions throughout the stream network, where waters from different parts of the network are combined. In the context of stream-solute transport, research has focused on shorter reaches (100–1000 m in length) because they (1) are of appropriate size to contain channel heterogeneity, (2) represent particular morphologies or stream types, (3) are easily comparable to similar channel lengths of different stream types and (4) represent a scale that is tractable for current methods and reasonable field-research logistics.

The movement of water through landscapes and down stream networks links a variety of potential sources and sinks of solutes throughout watersheds. The spatial distribution of landscape elements within watersheds (including land use types) and their connection to the hydrologic network will largely control the movement of water and solutes between stream networks and the catchment. For example, runoff from urban lands is likely to be flashy – reflecting rapid response to hydrologic inputs – and likely to provide a mix of solutes foreign to streams in less human-affected settings. Alternatively, irrigation demand removes both water and associated solutes from streams and applies those waters and solutes across portions of the watershed. Thus, distributed sources and sinks of contaminants or other solutes to streams exist throughout watersheds (Todd *et al.*, 2003).

The delivery of solutes to streams occurs via a complex mixture of point-source inflows (e.g. waste-water treatment-plant effluent) and less obvious groundwater contributions. One of the simplest and most common conceptualizations of a stream (Figure 18.1(A)) shows a well-defined channel, with distinct inflows from tributaries, seeps and groundwater discharge pathways. In this conceptual view, a stream reach is either gaining or losing water, but never both simultaneously. A more complex and realistic view (Figure 18.1(B) and (C)) envisions an ill-defined channel with dispersed inflows from both surface and subsurface sources. In this conceptualization, a stream may be both gaining and losing water, possibly with hyporheic exchange flows (Bencala, 2005) returning water to the stream. The dispersed inflows to the stream may originate

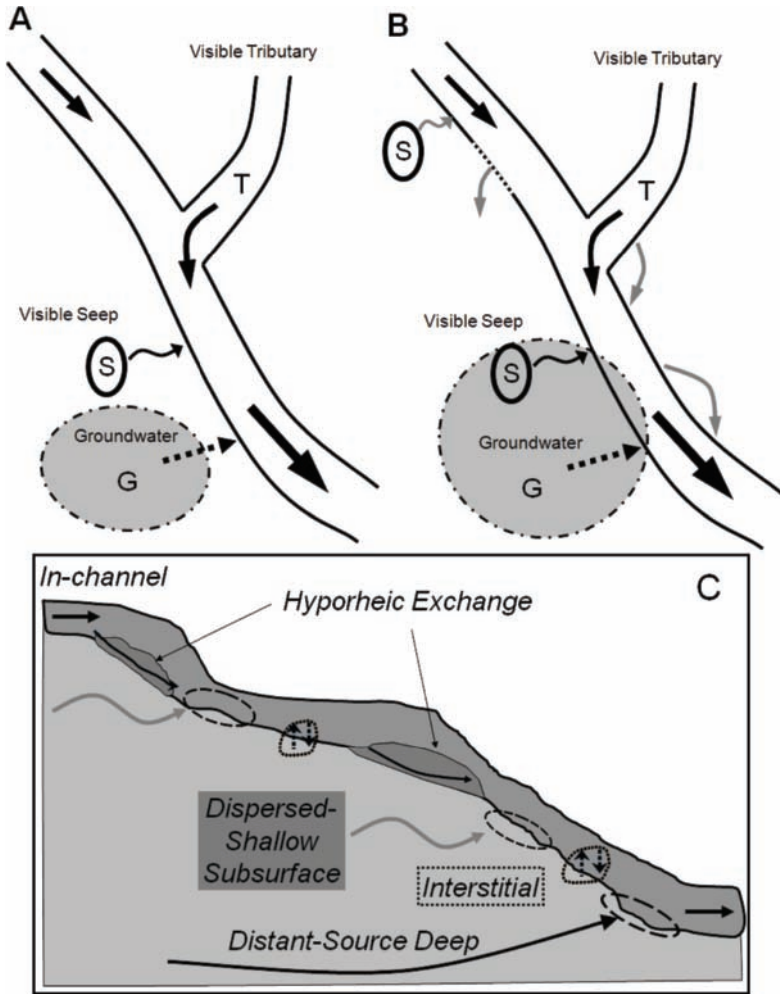


**Figure 18.1** Conceptual diagrams of streamflow exchanges with groundwater in which (A) stream water sources are visible at the surface and (B) a more realistic conceptualization where, surface and subsurface sources as well as subsurface sinks may all exist in the same reach (e.g. within 100 m); and (C) a vertical cross-section conceptual model of stream–groundwater exchanges with associated locations of localized mixing noted. S indicates a seep, G indicates groundwater and T indicates tributary.

(Figure 18.2) on the hillslope ‘near’ the stream or at some greater distance further up-gradient from the stream. Further complexity (Figure 18.2) in the interpretation of solute sources arises due to the mixing of water in the riparian zone (Chanat and Hornberger, 2003).

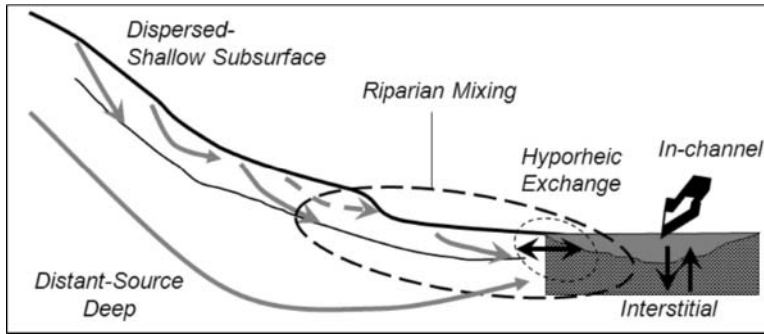


**Figure 18.2** Conceptual model of stream–groundwater interactions representing proximate and distal flowpaths interacting with streams and proposing lateral flowpaths to streams mixing prior to directly interacting with streams.

The details of groundwater–stream connections may be significant to the discharge of water in large river systems (Konrad, 2006). In streams, the significance may most clearly be evident in the variability observed in the concentrations of solutes in inflowing waters. For example, in metal-rich streams that are either in relatively undisturbed catchments (Bencala *et al.*, 1990) or in highly impacted catchments (Kimball *et al.*, 2002), the magnitude of the signal of metal concentrations, from either groundwater seeps or tributaries, allows for variations in concentrations to be observed on the scale of tens of metres along streams.

## Processes

The spatial and temporal distributions of solute concentrations and loads (as the product of discharge and concentration) throughout stream networks are controlled by sources and the processes of transport, mixing and storage. Solute inputs to streams vary in time and space. Instantaneous, focused inputs or point sources are generally episodic and localized (e.g. the accidental spill of a solute at a particular location). Inputs of longer distributions can be both point sources, such as sewage outfalls, or more widely distributed, non-point sources, such as atmospheric deposition. Solutes may reach the stream network at the surface (e.g. spill) and via the subsurface (e.g. mineral weathering). Regardless of the source type, changes in stream-solute concentrations are not necessarily coincident with a change in solute load, as, for example, water entering streams with low solute concentrations will dilute stream concentrations, but increase stream discharge. Here, we discuss the processes of solute transport and fate, rather than sources in a watershed.

Four processes influence solute transport and solute load throughout a stream network: these are advection, dispersion, transient storage and the mixing of different

source waters. All solutes are subject to these physical processes. Additionally, non-conservative solutes are likely to be subject to chemical reactions and transformations. As such, the role of transient storage may be especially important because of the increased travel time either in surface dead zones, where photochemical reactions may occur, or in the subsurface, where solutes are in close contact with biofilms on sediment surfaces. Non-conservative solutes may also be influenced by mixing, if inflows introduce other mutually reactive solutes. We focus only on the conservative nature of solute transport throughout stream networks, and the potential for non-conservative transformations altered by or controlled by transient storage and mixing with inflows, in particular. Here, we introduce the four hydrologic processes, and then discuss the ways in which conditions throughout a stream network modify the magnitude of these processes and their consequential influence on stream-solute transport.

Advection is the bulk transport of a solute in the channel downstream. One approach to directly measure the advection of solutes is performing a stream-solute tracer experiment. In a pulse-stream tracer experiment within an advection-dominated transport regime (i.e. most streams of moderate or high gradient), the arrival of the highest concentrations of the solute at a downstream location indicates the timescale of advection between the points of injection and recovery. Advection is controlled by stream flow velocity, which is related to discharge, by longitudinal gradient and by channel roughness, which can be described by several metrics, including the Manning Equation. Thus, changes in channel morphology and discharge from headwaters to outlet will generally lead to increases in advection rates downstream (Leopold and Maddock, 1953; Jobson, 1996). However, the reach-scale variability in channel morphology, as well as the temporal changes in discharge, can lead to deviations from general trends on local-spatial and short-time scales.

Longitudinal dispersion is the hydrodynamic spreading of solute both ahead of and behind the centre of the solute pulse. Spatial variability in flow velocity across the width and depth of the channel drives hydrodynamic dispersion. Dispersion is present in even the simplest of channels because velocity gradients in the flow are created by friction at the channel boundaries. The spatial variability in the distribution of flow velocity increases as the channel complexity increases, so that it is expected that dispersion is positively correlated to increasing channel complexity. Furthermore, longitudinal dispersion is generally expected to increase with increasing discharge (Wallis and Manson, 2004), as complex turbulence structures develop within the water column. Thus, as a pulse of an injected tracer or spilled contaminant moves downstream, longitudinal dispersion tends to spread the solute out, leading to reduced peak concentrations, but an increased duration of exposure.

Transient storage is the movement of solute into and out of channel dead zones (side pools, eddies, slackwater etc.) or the subsurface, along hyporheic flowpaths. Transient storage slows the movement of water and solutes relative to that expected from advection and dispersion alone (Runkel, 2002). Typically, there is a wide range in the distribution

of transient-storage times within any given stream reach, ranging from small pools or eddies, that retain water for only a few seconds, to off-channel wetlands or long hyporheic flowpaths where stream water may be retained for days or weeks. In all cases, transient storage provides additional opportunities for non-conservative solutes in the stream water to contact surficial sediments or aquatic macrophytes. These surfaces are usually colonized by bacteria, fungi and algae, forming biofilms in which chemical and biological processes can transform many non-conservative solutes (Battin *et al.*, 2003). Hyporheic exchange flows are especially important in this regard because the stream water flows through the sediment filling the stream valleys, bringing solutes into intimate contact with sediment surfaces.

Channel roughness, as a function of bed material and morphology, has been shown to be an important control on hyporheic exchange (e.g. Bencala and Walters, 1983; Harvey and Bencala, 1993). At a small spatial scale ( $< 1 \text{ m}^2$ ), bed material and its arrangement control the local texture and shear between the water and bed. This influence of channel friction on the moving water affects advection and hydrodynamic dispersion. Also at these scales, Elliot and Brooks (1997) demonstrate that the pressure variation along sandy streambeds that were dominated by dune and ripple bedforms induces hyporheic exchange. Their 'pumping-exchange' model has been applied in various flume settings (see Packman and Bencala (2000) for a summary) and is likely to explain hyporheic exchange processes in most lowland sand-bed rivers. At the channel-unit scale, flow velocity is highly variable, with deeper, slower water in pools, compared to shallower and faster water in riffles, at low to moderate discharges. Because of the dynamics of channel hydraulics, an uneven hydraulic pressure distribution is realized across the streambed (longitudinally and laterally). Flowing water and subsurface water near the channel boundary react to these pressure differences, driving stream water into the bed at some locations (downwelling) and allowing subsurface water to flow into the surface channel at other locations (upwelling). The patterns of upwelling and downwelling locations are largely driven by breaks in the channel slope. Thus, the pattern of steps, pools and riffles will dictate exchange patterns (Anderson *et al.*, 2005; Gooseff *et al.*, 2006). Channel morphology is typically determined by the balance between sediment supply and transport capacity, which tend to vary. However, in some streams, inputs of large wood from adjacent forests can also control channel morphology (Figure 18.3).

The net effect of hyporheic exchange flows on solute transport depends on both physical and biogeochemical processes (Bencala, 2005). The physical controls are succinctly summarized by Darcy's Law:  $Q_{\text{HEF}} = -kA(\Delta H/\Delta L)$ , where:  $Q_{\text{HEF}}$  is the hyporheic exchange flow,  $k$  is the saturated hydraulic conductivity,  $A$  is the cross-sectional area through which flow occurs and  $\Delta H/\Delta L$  is the head gradient. Clearly, high-gradient streams with coarse-textured bed sediment (large  $k$ ) have a great potential for hyporheic exchange. Conversely, low-gradient streams flowing over fine-textured bed sediment have a much smaller potential for hyporheic exchange. It is important to consider the

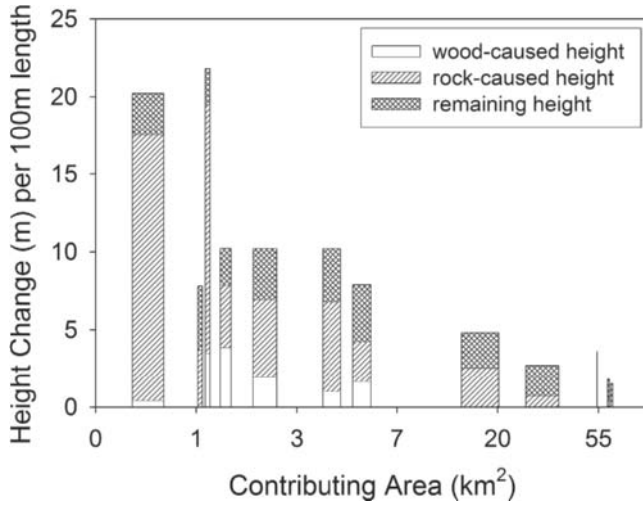


**Figure 18.3** Change in elevation over 100 m of stream length for 12 reaches surveyed in the Lookout Creek basin, Oregon, a fifth-order catchment, as a result of general gradient, steps created by boulders and steps created by wood. The width of the bars is not indicative of any metric. Wood-caused steps have a maximum impact on bed height change around 1–2 km<sup>2</sup> contributing area, whereas headwater reaches (< 1 km<sup>2</sup> contributing area) have the greatest change in height due to rock-caused steps. Data from Anderson (2002).

amount of hyporheic exchange flow ( $Q_{HEF}$ ) that occurs over a given length of stream channel, relative to the stream discharge ( $Q$ ) flowing through that channel. In small, steep mountain streams ( $1.0 \text{ L/s} < Q < 10 \text{ L/s}$ ), hyporheic exchange flows at any given point in the channel can be large relative to the total stream discharge, such that the entire surface stream flow is cycled through the hyporheic zone over distances of less than 100 m (Kasahara and Wondzell, 2003; Wondzell, 2006). As streams increase in size,  $Q$  increases more rapidly than does  $Q_{HEF}$ , so that in larger mountain streams and rivers the amount of hyporheic exchange flow is usually small relative to the total stream discharge, and turnover lengths are very long. From the point of view of simple mass transport, then, the hyporheic zone can have a substantial effect on solute transport in small headwater streams with generally rough channels but is unlikely to have a substantial effect on solute transformations in low-gradient streams with fine-textured bed sediment or in larger streams and rivers.

The net effect of hyporheic exchange flows on water quality also depends on both the rates of biogeochemical processes and the stream-water residence time in the hyporheic zone (Gooseff *et al.*, 2003, Figure 7). Hyporheic exchange flows in small, steep mountain streams tend to have short residence times because flowpaths are relatively short, head gradients steep and hydraulic conductivities large. In contrast, moderate-gradient, larger streams flowing through wide, mountain stream valleys provide opportunities

for long flowpaths with long residence times (Kasahara and Wondzell, 2003). In both cases studied by Kasahara and Wondzell (2003) of low-order and mid-order reaches, hyporheic residence time distributions were highly skewed, with two- to four-hour residence time dominant, but median residence times were only 18 hours in the small stream and 27 hours in the large stream. In both streams, flowpaths with a residence time of 20 or more days were present (Kasahara and Wondzell, 2003). The relative importance of the residence time and quantity of hyporheic exchange in controlling the flux of non-conservative solutes in stream networks has yet to be determined, though it varies along the channel network, in response to changes in corroborating factors (e.g. fluvial geomorphology) from headwaters to larger-order streams.

The potential influence of the hyporheic zone on contaminants moving down the stream network is complex because of the variety of environmental conditions found throughout the hyporheic zone, the variety of chemical and biological reactions that can occur there and the wide variety of the types of possible contaminants. While we cannot explore these issues in depth, there are several generalizations that should be considered. First, because hyporheic exchange significantly retards the transport of some portion of solutes moving through the channel, hyporheic return flows could potentially extend the period of exposure to, or the total watershed residence time of, a contaminant from an accidental spill. Contaminant concentrations will be low in the extended late-time tail of the contaminant plume, however, so that this would present a concern only for contaminants that pose a water-quality threat in low concentrations. Alternatively, the hyporheic zone could store large amounts of contaminants introduced from long duration inputs. In this case, long periods may be necessary to realize the benefits of eliminating sources. Secondly, if contaminants entering the hyporheic zone are highly reactive, it is possible that they could be bound to sediment or organic particles and removed from downstream transport. Eventually, however, erosion is likely to liberate contaminated sediment, which may pose problems at some later time. Alternatively, a variety of contaminants will be transformed by biogeochemical processes in the hyporheic zone. For example, where nitrate is transported to anoxic locations, it can be permanently removed from a solution by denitrification (Peterson *et al.*, 2001).

Lateral inflows and outflows can alter stream-solute loads, depending on solute concentrations in inflowing water. There are a number of studies that document solute and water inflow to streams, particularly in the interest of headwater contributions of diffuse any metal-rich drainage to streams (e.g. Bencala *et al.*, 1990; Kimball *et al.*, 2002). There are also some studies documenting streamflow losses throughout watersheds, primarily reporting the results of seepage meter runs (several distributed points of discharge measurement throughout the stream network) (e.g. Konrad, 2006; Laenen and Risley, 1997; Ruehl *et al.*, 2006; Zellweger, 1994). Such methods do not account for reach-scale gross gains and losses of water, considering only the net gain or loss (as the difference between gross gains and losses) between measurement locations. Hence, reach-scale gains and losses of solute are generally derived from net changes throughout the stream

network. The likelihood of a complex pattern of gross streamflow gains and losses along streams (Payn *et al.*, 2005) suggests that there is a coincident complex pattern of solute mixing with inflows along stream networks.

All four of these processes (advection, dispersion, transient storage and mixing) are reasonably easy to investigate in reach-scale stream experiments but are much more difficult to study at the scale of the entire stream network. We know, however, that these processes affect solute transport at the reach scale. Therefore, we expect the combined influence of these processes on solute transport to be manifest in the cumulative stream network signal. The cumulative effects are not strictly additive, particularly in the cases of hyporheic exchange or streamflow gains and losses, both of which may potentially operate over significant spatial scales to link shorter reaches. We are currently limited if we want to develop field experiments or empirically analyse solute transport through entire stream networks. Transient storage and mixing processes are especially problematic because hyporheic exchange and groundwater inflows are heterogeneous in both time and space. Furthermore, because they are greatly influenced by subsurface processes, they are difficult to measure. For example, the practice of sampling only tributaries and visible surface seeps will 'miss' solute inflows deep beneath the stream from distal sources in the catchment (Figure 18.1(C)), and yet it is not feasible to sample truly representative groundwater without expensive equipment, which is not necessarily available to all. Furthermore, the field characterization of mixing with inflows and transient storage is limited by the resolution of tracer analyses (Harvey and Wagner, 2000), tracer-concentration analytical limitations and the properties of current tracers.

## Linking transport processes with the fluvial geomorphic template

### Network controls on solute-transport processes

Examining solute transport within whole networks presents substantive challenges. Although transport is controlled by advection, dispersion, transient storage and mixing with inflows, it is difficult to quantify any of these at the scale of an entire watershed. Therefore, we examine higher-order controls on physical transport. These are: discharge, channel form (geomorphology and network topology) and near-stream hydraulic gradients. These controls vary spatially throughout a watershed and at different temporal scales as well. Discharge is the primary control on solute transport in the channel, affecting advection and dispersion processes through hydraulic characteristics, as well as bulk dilution for solute mass. The relationship between discharge and flow velocity (Leopold and Maddock, 1953) is critically important, showing that transport times will be much faster at higher discharges. In humid areas, discharge is usually proportional to drainage

area so that, in conventional characterizations, stream discharge and transport velocity increase downstream. This pattern may not hold in arid regions, however, where stream losses to evaporation or aquifer recharge may lead to a diminishing discharge with accumulated drainage area. Even in humid regions, discharge does not increase smoothly with accumulated drainage area or distance from source. For example, in a  $\sim 2$ -km section of a second-order stream in Montana, we characterized stream discharge and advection by synoptically releasing salt-slug tracers approximately every 100 m. The results (Figure 18.4) show a spatially inconsistent increase in discharge and associated velocity, including some locations where discharge and velocity both decreased. Similar dynamics have been observed in the main stem of the Willamette River in Oregon, USA (Laenen and Risley, 1997, Figure 14), suggesting that such patterns are likely present in many larger rivers as well.

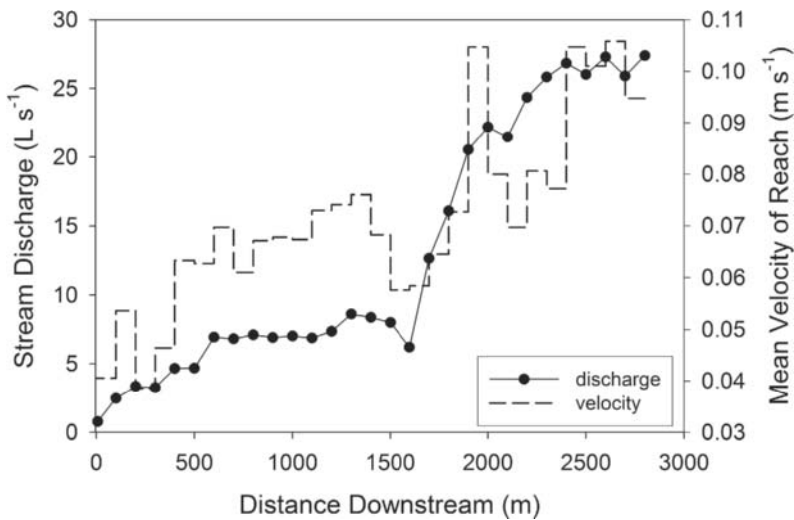


**Figure 18.4** Spatial distribution of flow velocity and discharge measured with salt-tracer injections in consecutive 100-m reaches in a second-order watershed in Montana (RA Payn, unpublished data).

The simple metrics of channel shape often exhibit characteristic patterns in relation to either basin area or discharge. Early work by Leopold and Maddock (1953) showed that both channel width and depth increase with increasing annual average discharge (see also Saco and Kumar, Chapter 15, this volume). The combination of discharge and channel morphology – especially the downstream increases in discharge, width and depth – have important implications for contaminant transport. In general, small streams will be much more retentive than large rivers, but this is not just a consequence of increasing the flow velocity. The water-sediment interface is a highly reactive surface for some solutes (e.g. metals, nutrients, dissolved organic carbon, hormones etc.). In small streams, the size of the wetted streambed area is high relative to discharge, and

water depths are relatively shallow, allowing for a substantial interaction between solutes in the water column and the streambed (Peterson *et al.*, 2001). The situation is reversed in large rivers where flow velocities tend to be much higher, water depths greater and the wetted streambed area is small relative to discharge, all of which combine to limit solute retention. Table 18.1 demonstrates these relationships for the 64 km<sup>2</sup> Lookout Creek watershed in central Oregon. The reduction in the ratio of wetted perimeter to annual mean *Q* at higher stream orders indicates a restriction for hyporheic exchange, compared to low-order reaches. Rivers with large quantities of aquatic macrophytes might be an exception to this general trend, as the stems and leaves provide large surface areas that are also colonized by biofilms and can add substantial roughness to the channel so that they also slow water velocity (Ovesen, 2001), making the river more retentive than would otherwise be expected.

**Table 18.1** Summary network characteristics for the fifth-order Lookout Creek catchment in central Oregon, USA, where *Q* is the mean annual discharge and ‘Area’ refers to the total catchment area contributing to reaches in each stream order, throughout the basin. Data from Wondzell (1994).

Stream Order	Total Network		<i>Q</i> (m <sup>3</sup> s <sup>-1</sup> )	Wetted	
	Length (%)	Area (%)		Perimeter <i>P</i> (m)	<i>P</i> / <i>Q</i>
1	53	66	0.005	2.36	487.60
2	23	16	0.026	4.36	167.37
3	13	10	0.369	8.34	22.59
4	5	4	1.558	12.10	7.77
5	6	4	3.256	15.30	4.70

Hyporheic exchange flows also are an important determinant of solute retention, as described above. Substantial research has shown that exchange flows are strongly controlled by channel morphology (the shape of the channel and the valley floor) (see Wondzell (2006) for more detailed discussion). In turn, channel morphology often shows characteristic patterns in relation to either basin area or discharge (Montgomery and Buffington, 1997, Figures 4 and 5). Detailed morphologic studies have shown that channel morphology broadly results from the balance between sediment supply and transport capacity (Montgomery and Buffington, 1998). Within areas with reasonably similar bedrock lithology, climate and topographic relief, both sediment supply and transport capacity will follow characteristic patterns so that reach slope, channel constraint (the width of the channel relative to the width of the floodplain) and watershed area will be the primary determinants of channel morphology (Chartrand and Whiting, 2000; Montgomery and Buffington, 1998).

The consequence of systematic changes in channel morphology on a gradient of increasing stream size is an increase in median hyporheic residence time and a concurrent

decrease in the amount of hyporheic exchange flow, relative to stream discharge, as drainage area accumulates (Kasahara and Wondzell, 2003). Data collected from small mountain streams in the fifth-order Lookout Creek basin showed that variation in the longitudinal profile of the stream channel (steps or riffles) was a primary driver of hyporheic exchange flow (Kasahara and Wondzell, 2003; Anderson *et al.*, 2005). Steep head gradients around abrupt changes in channel elevation, such as steps, tend to drive abundant exchange flows, but both flowpath length and residence times tend to be short. The prevalence of steps changes systematically through the stream network, accounting for 80 per cent, or more, of the elevation change along headwater streams, but only 50 per cent in mid-order streams (Figure 18.3). While mountain streams of all sizes show lateral complexity as measured by channel sinuosity and the presence of secondary channels, these features tend to be poorly developed in small headwater streams and increasingly better developed as the stream size increases and longitudinal gradients weaken. The actual expression is, however, controlled by channel constraint. Narrow valley floors, constrained by bedrock or other factors, leave little room for streams to develop lateral complexity. Conversely, in wide alluvial valleys, channels are often complex and support relatively large hyporheic exchange flows between main and secondary channels (Kasahara and Wondzell, 2003) driven by increasingly steep lateral head gradients (Figure 18.5). We know of no similar systematic, network-scale analysis of the geomorphic factors driving hyporheic exchange flows in either foothill or lowland rivers. Therefore, we do not know if the trends observed in mountain-river networks can be extended to river networks in other geomorphologic settings.

To demonstrate some of these temporal and spatial changes in solute transport, we present data from repeated stream-tracer experiments in Stringer Creek, a second-order mountain stream in the Little Belt Mountains of Montana (Figure 18.6). We conducted slug injections of Rhodamine-WT (RWT) at the head of the reach in June and July and monitored RWT breakthrough curves (BTCs) at the upper (1660 m downstream) and lower (1408 m further downstream) stream gauges. Discharge was too low in August to perform additional injections above the upper gauge. A third slug injection was performed from the upper stream gauge to lower stream gauge in early September (Figure 18.6(B)). As stream discharge receded throughout the summer, advection decreased substantially (as indicated by the later arrivals of peak concentrations), and dispersion increased (indicated as the spread of the arriving 'hump' of the BTCs), and apparent transient storage increased (as indicated by the total lengths of the BTCs), in both sections of the stream (Figures 18.6(C) and 18.6(D)). The third injection in the lower reach shows evidence of further decreasing advection, but dispersion and transient storage comparisons are not valid because the tracer was released at the upper gauge rather than the stream head.

Whereas large-scale patterns in discharge, flow velocity and channel shape influence general network-scale trends, reach-scale variability in channel morphology can lead to a substantial departure from expected trends. Especially important in mountain stream

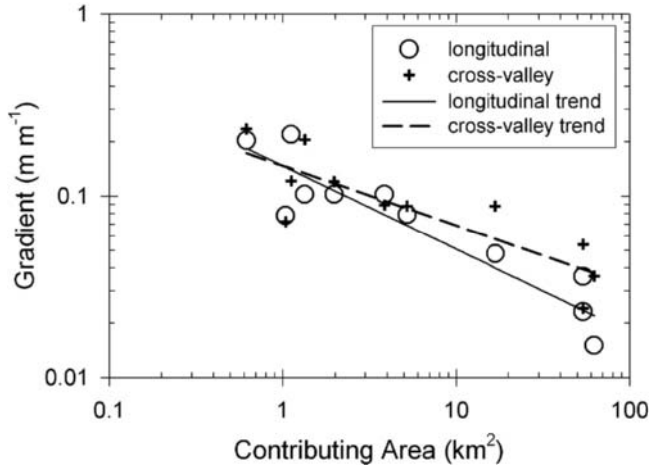


**Figure 18.5** Longitudinal topographic gradients along the thalweg of the stream, and cross-valley gradients in water-surface elevation measured normal to stream flow direction, as surveyed in 10 reaches throughout the Lookout Creek basin, Oregon, USA. Note the tendency for cross-valley gradients to increase, relative to longitudinal gradients, with increased drainage area. Data from Anderson (2002).

networks are wide alluvial valleys whose presence can be controlled by large-scale geologic factors, such as faulting patterns and bedrock contact, by past patterns of glaciation and also by sediment deposition from tributary channels. Stream confluences are often hotspots (locations of enhanced activity) of biological and chemical activity (Fisher *et al.*, 2004; Rice *et al.*, Chapter 11, this volume), driven in part by the complexity of environments found in these locations. In large mountain rivers, confluences often mark major knickpoints in the longitudinal gradient, caused by the deposition of sediment transported into the main-stem channels by tributaries during major floods or by debris flows (Benda *et al.*, 2003). Large boulders tend to dam the main channel, leading to a subsequent deposition upstream of the confluence, building wide, complex valley floors. Such valley-floor environments, with multiple channels and increased sinuosity, have been shown to be important locations for hyporheic exchange flow (Kasahara and Wondzell, 2003).

The general trends in discharge and channel shape and morphology with increasing basin area discussed so far ignore anthropogenic effects on river networks. Throughout the world, river networks have been reshaped by humans (Gregory, 2006), changes that have potentially large effects on solute transport. Obviously, large impoundments will dramatically slow network transport times (Vitousek *et al.*, 1997). Conversely, channelization and dike construction have dramatically simplified some rivers (Sedell and Froggatt, 1984; Triska, 1984), and the resulting straightened and narrowed channels should have much faster transport times. The associated losses of side channels and other lateral complexity combined with increased fine-sediment inputs are also likely

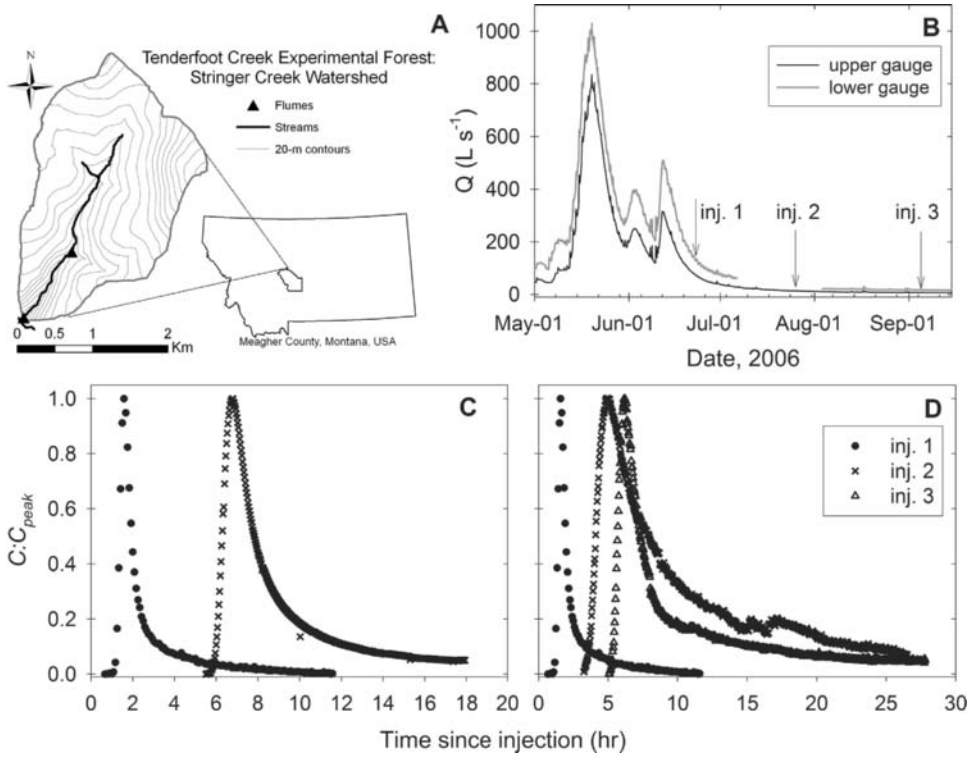


**Figure 18.6** Stream-tracer dynamics in Stringer Creek, Montana in 2006; map of study site (A), hydrograph for the upper and lower gauges on Stringer Creek (B), and Rhodamine WT breakthrough curves at the upper gauge, 1660 m downstream of injection point for injections 1 and 2, which was the eastern stream head (C), and the lower stream gauge, 1408 m downstream of the upper gauge. Injections 1 and 2 were performed on 23 June and 26 July respectively. A third injection was performed on 5 September, starting at the upper gauge. Travel times in panel (D) represent travel from the upper gauge to the lower gauge, to facilitate the comparison of times to peak concentration. Some discharge data from the lower gauge is missing in panel (B), owing to equipment failure.

to restrict hyporheic exchange flows. In many intensively farmed landscapes, the entire drainage network, from buried field drains and the smallest headwater channels to the largest rivers, have been modified to speed the movement of water off the landscape. Water and solute retention is poor in such networks. In large river settings, floodplains can be important locations of solute processing (particularly nutrients) (Mitsch *et al.*, 2005). However, the propensity to create flood-control structures, such as levees, disconnects rivers from their floodplains (Mitsch *et al.*, 2001).

From a simple mixing-model approach, the mixing of stream waters at tributaries or with inflowing groundwater causes a change in solute load, the product of discharge and solute concentration. The spatial distribution of solute loads throughout a stream net-

work at any moment is dictated by the balance of distributed lateral loads to the stream. Dilute lateral inflows of water to streams from groundwater (assuming conservative mixing) will not change loads of a particular stream solute because the mixing of these waters in the channel will increase discharge and proportionally decrease channel solute concentration. However, solute-rich inflows, such as metal loads from acid mine/rock drainage, will increase stream loads of those constituents, until chemical reactions take place to reduce their stream loads. Temporal trends of solute loads at any one point in a channel network are driven by changes in channel discharge and the associated upstream inputs of water and solute.

Temporal changes in discharge, be they seasonal, event responses or diurnal, will affect processes that control solute transport in stream networks. At high-flow conditions, advection and dispersion will increase, but transient storage will diminish because of fewer in-channel dead zones, and because of the reduced relative hyporheic exchange (i.e. in proportion to total discharge). The reduction in the relative hyporheic exchange flow to channel discharge lessens at high-flow conditions because the effect of channel morphology on the energy grade line is dampened and more continuous, thus reducing the local head gradients that drive hyporheic exchange. However, hydraulic conductivity of the bed does not necessarily change from high- to low-flow conditions. Therefore, a reduction in head gradient and a consistency in hydraulic conductivity will result in reduced hyporheic exchange flows. Solute transport is generally enhanced through stream networks at high flow because there is less buffering capacity of the network to retard solute transport.

## Forward-looking perspective

There are several perspectives in which we can advance our understanding and analysis of solute transport along stream and river networks. The process of solute transport along stream and river networks is by-definition integrative. Three fundamental questions from physical hydrology control this transport: (1) 'Where does the water moving to a stream come from?', (2) 'How long does it stay in the channel?' and (3) 'How long does it take to get (back) into the channel?'. Although these questions have been partially answered, we know of no synthetic study that examines these three questions within a large river network and examines how such relations change with time and with location. Answering these questions at a network scale remains a challenge for understanding hydrologic processes, distributed stream-solute loading and solute transport.

## Concepts

Three directions are apparent for advancing a process-based interpretation of solute loading to, and transport along, river networks. The stream does not stand alone,

rather it is intimately connected to its catchment, often in ways that are not easily visible. As such, spatially and temporally distributed mixing processes influence solute concentration, and at any one point the solute signal is an integration of upstream mixing processes and concurrent transport processes in the stream channel.

### **Stream–catchment connections**

The significance of the components of inflow and exchange shift spatially with distance downstream through the catchment, and temporally in response to catchment flow periods. In the upland reaches a stream will gain, and lose, water in visible and relatively shallow flow systems of dispersed seeps and springs. Further downstream spatially distributed connections between the stream and groundwater flow systems will develop. As the network of streams and rivers develops, changes in flow where tributaries meet effectively become point sources. As these changes in water inflow sources occur, there will be changes in stream-solute loads throughout the stream network.

### **Mixing of inflows and hyporheic flows**

Mixing through the riparian zone and along hyporheic exchange flowpaths brings further complexity to the identification of ‘true’ inflow (Cox *et al.*, 2003; Hinkle *et al.*, 2001). This mixing among distal, near-stream and stream waters (Figure 18.2) complicates our notion of end-member contributions to streams, as end-member hillslope, groundwater and stream waters are masked by the mixing process prior to reaching the stream network.

### **Integration within the stream channel**

Catchment, near-stream and in-stream characteristics all are significant in determining the fate of solutes entering the stream channel. As the network of streams and rivers develops, the downstream reaches are necessarily integrations of upstream and up-valley characteristics and processes. However, within this integration, the downstream-solute concentrations are not necessarily the well-mixed sum of the inputs. The relative roles of in-stream biogeochemical and physical processes will vary.

### **Analysis tools**

The progress made in conceptual understanding needs to be realized in the quantitative descriptions of solute fate. The advection–dispersion transport equation has long been

the standard tool for the analysis of solute transport in streams and rivers. Particularly applicable in upland streams, the transient storage model has been useful in drawing our attention to the significance of catchment-stream and hyporheic connections. At the beginning of this century, several modelling approaches are being developed and applied, which further our abilities to quantify transport processes.

Simulations of solute transport using general residence time distribution models (Haggerty *et al.*, 2002; Gooseff *et al.*, 2003) enable the identification of the timescales of exchange, particularly along hyporheic flowpaths, which are varied and possibly quite long compared to in-stream transport.

At the process level, the methods of environmental fluid mechanics (e.g. Ren and Packman, 2004; Marion *et al.*, 2002; Cardenas *et al.*, 2004) are quite successful in interpreting solute transport in flumes. The future challenge is to bring these models and results to field situations. The complexities of flow at the stream–catchment interface have been well simulated (e.g. Kasahara and Wondzell, 2003; Lautz and Siegel, 2006) using the MODFLOW representation of groundwater flow. This approach has required appreciable investments in monitoring the physical systems over relatively small areas. The application of groundwater-flow modelling to define hyporheic flowpaths (e.g. Gooseff *et al.*, 2006) requires refinements in the characterization of the spatial variability of subsurface hydraulic conductivity and the representation of stream-boundary conditions (Tonina and Buffington, 2007).

Models are only one set of analytical tools which need development to transfer our knowledge and approaches from individual streams to networks. In part, the reason that we have made significant advances in understanding discrete reach-scale solute transport and fate, but not moved to larger spatial scales, is that the spatial scale of the reach and the corresponding timescales of processes are most appropriate for the current stream tracer methodology (Harvey and Wagner, 2000; Gooseff *et al.*, 2005). However, these experimental approaches are constrained by analytical limits of tracer-concentration measurement and the properties of the tracers currently available. Thus, there is a clear need to develop and apply more robust conservative hydrologic tracers, detectable at very low concentrations.

## Field studies

There is no one measurement approach for identifying the inflow of water and solutes as the connections of a stream to its catchment shifts. Rather, the challenge to our thinking and our practice is to be aware of the spatially changing nature of these connections. Field observations of the actual paths are needed, and may be facilitated by the application of geophysical field methods to studies of the transport of stream solute. New techniques that corroborate geophysical measurements with hydrologic techniques will in the future provide the spatial data needed to expand this mod-

elling effort to longer stream reaches. Challenges in incorporating connections to the catchment include the matching of detailed field studies to the in-stream modelling of solute transport to develop a better understanding of the effects of channel evolution (Harvey *et al.*, 2003), the characterizations of transport most significant to solute dynamics (Runkel, 2002), and scaling up our process-understanding of river systems (Fernald *et al.*, 2001).

Ultimately, our understanding of solute transport and fate at the scale of river networks will be advanced by developing new conceptual models, testing those models through the acquisition of field data and subsequently developing new numerical models to characterize solute transport in river networks. This process will be iterative as, for example, new advances in field methods may better inform further refined conceptual or numerical models. The succinct characterization of solute transport through river networks remains a challenge for environmental scientists, though the recent advancements in conceptual framework, modelling and field studies point to significant advances in the coming years.

## Acknowledgements

The authors are grateful to R. Runkel, D. Scott and A. Sukhodolov for their constructive reviews of this chapter, which provided much improvement, and to R. Payn, who assisted with data presented here. Support for this work was partly funded through the US National Science Foundation's Geosciences Directorate, EAR 05-30873 and 03-37650. Any opinions, findings and conclusions or recommendations expressed in this material are those of the author(s) and do not necessarily reflect the views of the National Science Foundation.

## References

- Alexander RB, Smith RA, Schwarz GE. 2000. Effect of stream channel size on the delivery of nitrogen to the Gulf of Mexico. *Nature* **403**: 758–761.
- Anderson JK. 2002. Patterns in stream geomorphology and implications for hyporheic exchange flow, Master's thesis, Department of Forest Sciences, Oregon State University.
- Anderson JK, Wondzell SM, Gooseff MN, Haggerty R. 2005. Patterns in stream longitudinal profiles and implications for hyporheic exchange flow at the H.J. Andrews Experimental Forest, Oregon, USA. *Hydrological Processes* **19**: 2931–2949.
- Battin TJ, Kaplan LA, Newbold JD, Hansen CME. 2003. Contributions of microbial biofilms to ecosystem processes in stream mesocosms. *Nature* **426**: 439–442.
- Bencala KE. 2005. Hyporheic Exchange Flows. In *Encyclopedia of Hydrological Sciences*, Anderson M (ed.). John Wiley & Sons: Chichester; 1733–1740.
- Bencala KE, Walters RA. 1983. Simulation of solute transport in a mountain pool-and-riffle stream: A transient storage model. *Water Resources Research* **19**: 718–724.

- Bencala KE, McKnight DM, Zellweger GW. 1990. Characterization of transport in an acidic and metal-rich mountain stream based on a lithium tracer injection and simulations of transient storage. *Water Resources Research* **26**: 989–1000.
- Benda L, Miller D, Bigelow P, Andras K. 2003. Effects of post-wildfire erosion on channel environments, Boise River, Idaho. *Forest Ecology and Management* **178**: 105–119.
- Cardenas MB, Wilson JL, Zlotnik VA. 2004. Impact of heterogeneity, bed forms, and stream curvature on subchannel hyporheic exchange. *Water Resources Research* **40**: W08307. DOI: 10.1029/2004WR003008.
- Chanat JG, Hornberger GM. 2003. Modeling catchment-scale mixing in the near-stream zone – Implications for chemical and isotopic hydrograph separation. *Geophysical Research Letters* **30**: 1091. DOI: 10.1029/2002GL016265.
- Chartrand SM, Whiting PJ. 2000. Alluvial architecture in headwater streams with special emphasis on pool-step topography. *Earth Surface Processes and Landforms* **25**: 583–600.
- Cox MH, Mendez GO, Kratzer CR, Reichard EG. 2003. *Evaluation of tracer tests completed in 1999 and 2000 on the upper Santa Clara River, Los Angeles and Ventura Counties, California*. US Geological Survey, Water-Resources Investigations Report 03-4277, <http://water.usgs.gov/pubs/wri/wrir034277/>, accessed 23 January 2008.
- Elliot AH, Brooks NH. 1997. Transfer of nonsorbing solutes to a streambed with bed forms: Laboratory experiments. *Water Resources Research* **33**: 137–152.
- Fernald AG, Wigington PJ, Landers DH. 2001. Transient storage and hyporheic flow along the Willamette River, Oregon: Field measurements and model estimates. *Water Resources Research* **37**: 1681–1694.
- Fischer HB, List EJ, Koh RYC, Imberger J, Brooks NH. 1979. *Mixing in Inland and Coastal Waters*, Academic Press: New York.
- Fisher SG, Grimm NB, Marti E, Holmes RM, Jones Jr JB. 1998. Material spiraling in stream corridors: A telescoping ecosystem model. *Ecosystems* **1**: 19–34.
- Fisher SG, Sponseller RA, Heffernan JB. 2004. Horizons in stream biogeochemistry: Flowpaths to progress. *Ecology* **85**: 2369–2379.
- Gooseff MN, Wondzell SM, Haggerty R, Anderson J. 2003. Comparing transient storage modeling and residence time distribution (RTD) analysis in geomorphically varied reaches in the Lookout Creek basin, Oregon, USA. *Advances in Water Resources* **26**: 925–937.
- Gooseff MN, Bencala KE, Scott DT, Runkel RL, McKnight DM. 2005. Sensitivity analysis of conservative and reactive stream transient storage models applied to field data from multiple-reach experiments. *Advances in Water Resources* **28**: 479–492.
- Gooseff MN, Anderson JK, Wondzell SM, LaNier J, Haggerty R. 2006. A modeling study of hyporheic exchange pattern and the sequence, size, and spacing of stream bedforms in mountain stream networks, Oregon, USA. *Hydrological Processes* **20**: 2443–2457.
- Gregory KJ. 2006. The human role in changing river channels. *Geomorphology* **79**: 172–191.
- Gupta A, Cvetkovic V. 2002. Material transport from different sources in a network of streams through a catchment. *Water Resources Research* **38**: 1098. DOI: 10.1029/2000WR000064.
- Haggerty R, Wondzell SM, Johnson MA. 2002. Power-law residence time distribution in the hyporheic zone of a 2nd-order mountain stream. *Geophysical Research Letters* **29**: 1640. DOI: 10.1029/2002GL014743.
- Harvey JW, Bencala KE. 1993. The effect of streambed topography of surface-subsurface water exchange in mountain catchments. *Water Resources Research* **29**: 89–98.

- Harvey JW, Wagner BJ. 2000. Quantifying hydrologic interactions between streams and their subsurface hyporheic zones. In *Streams and Ground Waters*, Jones JA, Mulholland P (eds). Academic Press: San Diego; 3–43.
- Harvey JW, Conklin MH, Koelsch RS. 2003. Predicting changes in hydrologic retention in an evolving semi-arid alluvial stream. *Advances in Water Resources* **26**: 939–950.
- Hinkle SR, Duff JH, Triska FJ, Laenen A, Gates EB, Bencala KE, Wentz DA, Silva SR. 2001. Linking hyporheic flow and nitrogen cycling near the Willamette River – a large river in Oregon, USA. *Journal of Hydrology* **244**: 157–180.
- Holmes RM, Peterson BJ, Gordeev VV, Zhulidov AV, Meybeck M, Lammers RB, Vörösmarty CJ. 2000. Flux of nutrients from Russian rivers to the Arctic Ocean: Can we establish a baseline against which to judge future changes? *Water Resources Research* **36**: 2309–2320.
- Jobson H. 1996. *Prediction of traveltime and longitudinal dispersion in rivers and streams*. US Geological Survey, Water-Resources Investigations Report 96–4013.
- Kasahara T, Wondzell SM. 2003. Geomorphic controls on hyporheic exchange flow in mountain streams. *Water Resources Research* **39**: 1005. DOI: 10.1029/2002WR001386.
- Kimball BA, Runkel RL, Walton-Day K, Bencala KE. 2002. Assessment of metal loads in watersheds affected by acid mine drainage by using tracer injection and synoptic sampling: Cement Creek, Colorado, USA. *Applied Geochemistry* **17**: 1183–1207.
- Konrad CP. 2006. Location and timing of river-aquifer exchanges in six tributaries to the Columbia River in the Pacific Northwest of the United States. *Journal of Hydrology* **329**: 444–470.
- Laenen A, Bencala KE. 2001. Transient storage assessments of dye-tracer injections in rivers of the Willamette Basin, Oregon. *Journal of the American Water Resources Association* **37**: 367–377.
- Laenen A, Risley J. 1997. Precipitation-Runoff and Streamflow-Routing Models for the Willamette River Basin. US Geological Survey, Water-Resources Investigations Report 95-4284, [http://or.water.usgs.gov/pubs\\_dir/Pdf/95-4284.pdf](http://or.water.usgs.gov/pubs_dir/Pdf/95-4284.pdf), accessed 23 January 2008.
- Lautz LK, Siegel DI. 2006. Modeling surface and ground water mixing in the hyporheic zone using MODFLOW and MT3D. *Advances in Water Resources* **29**: 1618–1633.
- Leopold LB, Maddock Jr T. 1953. *The hydraulic geometry of stream channels and some physiographic implications*. US Geological Survey, Professional Paper No. 252.
- Lindgren GA, Destouni G, Miller AV. 2004. Solute transport through the integrated groundwater-stream system of a catchment, *Water Resources Research* **40**: W03511. DOI: 10.1029/2003WR002765.
- Marion A, Bellinello M, Guymier I, Packman A. 2002. Effect of bed form geometry on the penetration of nonreactive solutes into a streambed. *Water Resources Research* **38**. DOI: 10.1029/2001WR000264.
- Mitsch WJ, Day JW, Gilliam JW, Groffman PM, Hey DL, Randall GW, Wang NM. 2001. Reducing nitrogen loading to the Gulf of Mexico from the Mississippi River Basin: Strategies to counter a persistent ecological problem. *Bioscience* **51**: 373–388.
- Mitsch WJ, Zhang L, Anderson CJ, Altor AE, Hernandez ME. 2005. Creating riverine wetlands: Ecological succession, nutrient retention, and pulsing effects. *Ecological Engineering* **25**: 510–527.
- Montgomery DR, Buffington JM. 1997. Channel-reach morphology in mountain drainage basins. *Geological Society of America Bulletin* **109**: 596–611.
- Montgomery DR, Buffington JM. 1998. Channel processes, classification, and response. In *River Ecology and Management: Lessons from the Pacific Coastal Ecoregion*, Naiman RJ, Bilby RE (eds). Springer-Verlag: New York; 13–42.

- Nimick DA, Gammons CH, Cleasby TE, Madison JP, Skaar D, Brick CM. 2003. Diel cycles in dissolved metal concentrations in streams – occurrences and possible causes. *Water Resources Research* **39**: 1247. DOI: 10.1029/2002WR001571.
- Ovesen NB. 2001. Diurnal fluctuation in stage and discharge induced by aquatic plants in a Danish lowland stream. *Verhandlungen internationale Vereinigung für theoretische und angewandte Limnologie* **27**: 3729–3732.
- Packman AI, Bencala KE. 2000. Modeling surface-subsurface hydrological interactions. In *Streams and Ground Waters*, Jones JA, Mulholland P (eds). Academic Press: San Diego; 45–80.
- Payn RA, Gooseff MN, McGlynn BL, Benkala KE, Wondzell SM, Jencso K. 2005. Water balance and residence time in stream functional units of differing scales. *Eos Transactions of the AGU*, 86(52), Fall Meeting Supplement, Abstract H43C-0508.
- Peterson BJ, Wollheim WM, Mulholland PJ, Webster JR, Meyer JL, Tank JL, Marti E, Bowden WB, Valett HM, Hershey AE, McDowell WH, Dodds WK, Hamilton SK, Gregory S, Morrall DD. 2001. Control of nitrogen export from watersheds by headwater streams. *Science* **292**: 86–90.
- Ramaswami A, Milford JB, Small MJ. 2005. *Integrated Environmental Modeling: Pollutant Transport, Fate, and Risk in the Environment*. John Wiley & Sons: Hoboken, New Jersey.
- Ren J, Packman AI. 2004. Stream-substream exchange of zinc in the presence of silica and kaolinite colloids. *Environmental Science and Technology* **38**: 6571–6581.
- Ruehl C, Fisher AT, Hatch C, Los Huertos M, Stemler G, Shennan C. 2006. Differential gauging and tracer tests resolve seepage fluxes in a strongly-losing stream. *Journal of Hydrology* **330**: 235–248.
- Runkel RL. 2002. A new metric for determining the importance of transient storage. *Journal of the North American Benthological Society* **21**: 529–543.
- Rutherford JC. 1994. *River Mixing*. John Wiley & Sons: Chichester.
- Sedell JR, Froggatt JL. 1984. Importance of streamside forests to large rivers: The isolation of the Willamette River, Oregon, USA, from its floodplain by snagging and streamside forest removal. *Verhandlungen Internationale Vereinigung für theoretische und angewandte Limnologie* **22**: 1828–1834.
- Todd A, McKnight D, Wyatt L. 2003. Abandoned mines, mountain sports, and climate variability: Implications for the Colorado tourism economy. *Eos Transactions of the AGU* **84**: 377.
- Tonina D, Buffington JM. 2007. Hyporheic exchange in gravel bed rivers with pool-riffle morphology: Laboratory experiments and three-dimensional modeling. *Water Resources Research* **43**: W01421. DOI: 10.1029/2005WR004328.
- Triska FJ. 1984. Role of wood debris in modifying channel geomorphology and riparian areas of a large lowland river under pristine conditions: An historical case study. *Internationale Vereinigung für Theoretische und Angewandte Limnologie* **22**: 1876–1892.
- Vannote RL, Minshall GW, Cummings KW, Sedell JR, Cushing CE. 1980. The river continuum concept. *Canadian Journal of Fisheries and Aquatic Sciences* **37**: 130–137.
- Vitousek PM, Mooney HA, Lubchenco J, Melillo JM. 1997. Human domination of Earth's ecosystems. *Science* **277**: 494–499.
- Wallis SG, Manson JR. 2004. Methods for predicting dispersion coefficients in rivers. *Water Management* **157**: 131–141.
- Wondzell SM. 2006. Effect of morphology and discharge on hyporheic exchange flows in two small streams in the Cascade Mountains of Oregon, USA. *Hydrological Processes* **20**: 267–287.

- Zellweger GW. 1994. Testing and comparison of four ionic tracers to measure stream flow loss by multiple tracer injection. *Hydrological Processes* **8**: 155–165.
- Zhan X. 2003. Simulation of unsteady flow and solute transport in a tidal river network. *Engineering Computations* **20**: 754–767.
- Zhang Y, Aral MM. 2004. Solute transport in open-channel networks in unsteady flow regime. *Environmental Fluid Mechanics* **4**: 225–247.



# 19

## Fluvial valley networks on Mars

Rossman P. Irwin III<sup>1</sup>, Alan D. Howard<sup>2</sup>  
and Robert A. Craddock<sup>1</sup>

<sup>1</sup>*Center for Earth and Planetary Studies, National Air and Space Museum, Smithsonian Institution, USA*

<sup>2</sup>*Department of Environmental Sciences, University of Virginia, USA*

### Introduction

The Earth, Mars and Saturn's moon Titan are the only planetary surfaces known to have widespread, branching, fluid-carved channels or valley networks. Lava channels and collapsed lava tubes formed relatively few sinuous valleys with few to no tributaries on the volcanic plains of Venus (where the average air temperature is  $\sim 450^{\circ}\text{C}$ ), the Moon (Figure 19.1(c)) and Jupiter's moon Io (e.g. Wilhelms, 1987; Baker *et al.*, 1997; McEwen *et al.*, 2000). Venus also has some valley networks with rectangular, labyrinthic, pitted or irregular network structure, reflecting a joint volcanic and tectonic origin (Baker *et al.*, 1997). Dense branching networks occur on Titan (Figure 19.1(a)), but liquid methane is the erosive fluid under its 1.6-bar nitrogen atmosphere at  $-180^{\circ}\text{C}$ , and water ice comprises most of the bedrock and sediment (Tomasko *et al.*, 2005). The current Martian atmosphere is too thin and cold to maintain water in liquid state, but the older terrains have been heavily eroded and incised by valley networks (Figure 19.1(b)), suggesting that past geologic or climatic conditions supported flowing water. These ancient networks are similar in some respects to their modern terrestrial counterparts, but they are immature if formed by runoff (e.g. Howard *et al.*, 2005), and many authors attribute them primarily or exclusively to groundwater sapping (e.g. Pieri, 1980; Carr

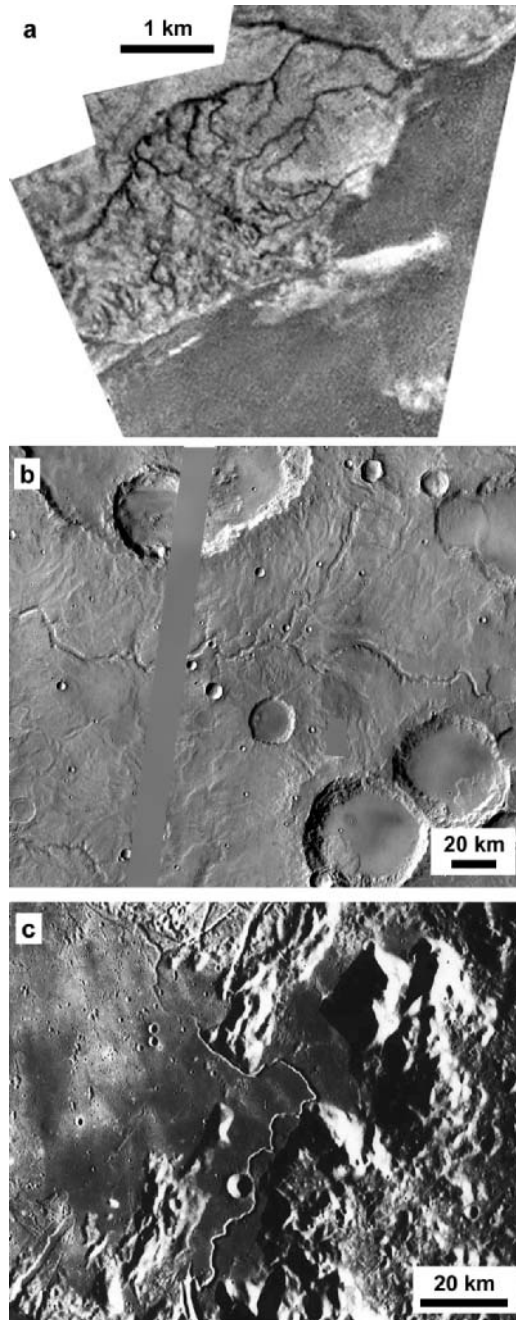


**Figure 19.1** Sinuous valleys formed by flowing methane, water and lava respectively. (a) Networks on Saturn's moon Titan debouched to dark plains (descent image from European Space Agency Huygens probe (credit: ESA/NASA/JPL/University of Arizona). (b) Evros Vallis on Mars ( $12.5^{\circ}\text{S}$ ,  $14.5^{\circ}\text{E}$ , THEMIS daytime infrared image mosaic, credit: University of Arizona). (c) Hadley Rille on the Moon (Apollo 15 image AS15-1135[M]).

and Clow, 1981; Carr and Malin, 2000; Gulick, 2001). The investigation of aqueous processes on early Mars is a major focus of NASA's Mars Exploration Program, because environmental conditions suitable for liquid water may have supported life or prebiotic chemistry on Mars, and much of the geologic record from the first billion years of Earth's history has been lost to erosion, metamorphism and subduction.

In this chapter, we describe the history and present state of Martian fluvial geomorphology, emphasizing quantitative analyses of drainage networks, watershed topography and hydrology. Most studies to date have focused on valley rather than channel characteristics, because aeolian processes and small meteorite impacts have slowly degraded and partially filled the valleys for  $\sim 3.7$  Gyr since the epoch of widespread fluvial erosion (absolute, numerical age estimates herein follow Hartmann and Neukum, 2001), leaving few interior channels exposed (e.g. Carr and Malin, 2000; Irwin *et al.*, 2005a). Moreover, the available orbital imaging has a resolution of  $\sim 0.3$ –250 m/pixel, with limited spatial coverage at high resolution, and robotic landers have not yet visited a valley network. Despite these limitations, investigators have used counts of superimposed impact craters, analyses of valley planform and topography, basic channel morphometry and theoretical modelling to constrain the age, formative processes, developmental history, hydrology, and climatic implications of Martian valley networks.

## Early observations

Johannes Kepler's laws of planetary motion, published in 1609 and 1618, were largely based on Tycho Brahe's earlier observations of Mars. The seventeenth- and eighteenth-century astronomers Christiaan Huygens, Giovanni Cassini, Giacomo Miraldi and William Herschel recognized the Martian polar ice caps and estimated the planet's orbit (1.52 AU), diameter (6792 km), rotation period (24 hours, 37 minutes) and axial tilt ( $25^\circ$ ) (modern data in parentheses are from Kieffer *et al.*, 1992 and Smith *et al.*, 2001). Formal telescopic maps succeeded early sketches during the nineteenth century, interpreting relatively bright and dark regions as continents and seas respectively (summarized by Flammarion, 1892, 1909). Even today, the best ground-based telescopes can resolve few other surface features. Popular conceptions of 'Mars as the Abode of Life' were also founded on perceived observations of dark-toned lineations on the surface, which Percival Lowell (1895, 1906, 1908) interpreted as bands of vegetation along artificial canals used to transport water from the ice caps to arid equatorial regions. Some contemporaries of Lowell who could not see the lineations were sceptical of these claims (e.g. Evans and Maunder, 1903; Wallace, 1907), and spacecraft data later showed that, with the possible exception of the Valles Marineris canyon system, the mapped 'canals' generally do not correspond to obvious valleys or other topographic features (Sagan and Fox, 1975). Nineteenth-century astronomers also observed the Martian atmosphere with clouds and global dust storms. Stoney (1898) correctly proposed that

the polar caps might contain frozen carbon dioxide (the wintertime caps at both poles and the top of the perennial southern cap), although most of their mass is water ice (Kuiper, 1952; Kieffer *et al.*, 1976; Bibring *et al.*, 2004). Theoretical calculations and infrared measurements suggested that Mars has an average surface temperature well below freezing ( $-63^{\circ}\text{C}$ , with extremes below the  $-133^{\circ}\text{C}$  freezing point of  $\text{CO}_2$ ) (e.g. Wallace, 1907; Coblentz, 1925; Sinton and Strong, 1960). Kuiper (1952) made the first spectral identification of  $\text{CO}_2$  in the atmosphere, although it was originally thought to be a minor component (now known to be 95 per cent by volume). The average atmospheric pressure was gradually revised below Lowell's (1908) 87-mbar estimate to  $\sim 5.6$  mbar, which is below the 6.1-mbar triple point where water first becomes stable as a liquid.

More detailed data from interplanetary spacecraft record conditions that are even less favourable for life. The first successful flyby mission to Mars, Mariner 4 in 1965, returned 22 images of a cratered landscape in the southern hemisphere, and the Mariner 6 and 7 flybys imaged a similar region at higher resolution in 1969. The preservation of ancient impact craters seemed to defeat the long-lived paradigm of a water-rich planet, but many of the Martian craters had been substantially modified (Leighton *et al.*, 1965). Erosion rates on Mars were interpreted to be very low, but higher than on the Moon (Anders and Arnold, 1965; Baldwin, 1965; Hartmann, 1966; Öpik, 1966; Murray *et al.*, 1971), and the low atmospheric pressure favoured wind over water as the erosive fluid (Sharp, 1968). Then in 1971, Mariner 9 became the first successful Mars orbiter, returning images of the entire surface at 1 km/pixel resolution with local imaging at 100 m/pixel scale. This mission revealed a planet much more diverse than the flyby missions had suggested, including giant volcanoes and canyons, circumpolar layered deposits, grabens, smooth plains, large outflow channels that resemble flood-carved features on the Earth and smaller valley networks (McCauley *et al.*, 1972). Outflow channels are distinguished from valley networks by their large size (tens to  $\sim 200$  km wide and up to thousands of kilometres long), origin from a point source, anabranching path, streamlined islands and erosional bedforms (Figure 19.2). They are thought to have originated from very large, short-lived groundwater discharges of  $\sim 10^6 - 10^8$  m<sup>3</sup>/s (Baker and Milton, 1974; Carr, 1979, 1996; Baker, 1982; Wilson *et al.*, 2004), but overflow of enclosed basins also contributed to some large channels and valleys (e.g. Parker, 1985; Grant and Parker, 2002; Irwin *et al.*, 2004).

## Distribution, age, origin and morphology of valley networks

### Geologic, topographic and regional distribution

Valley networks primarily occupy the most heavily cratered regions on Mars and are uncommon on younger surfaces (Pieri, 1976, 1980; Carr and Clow, 1981; Carr, 1996).

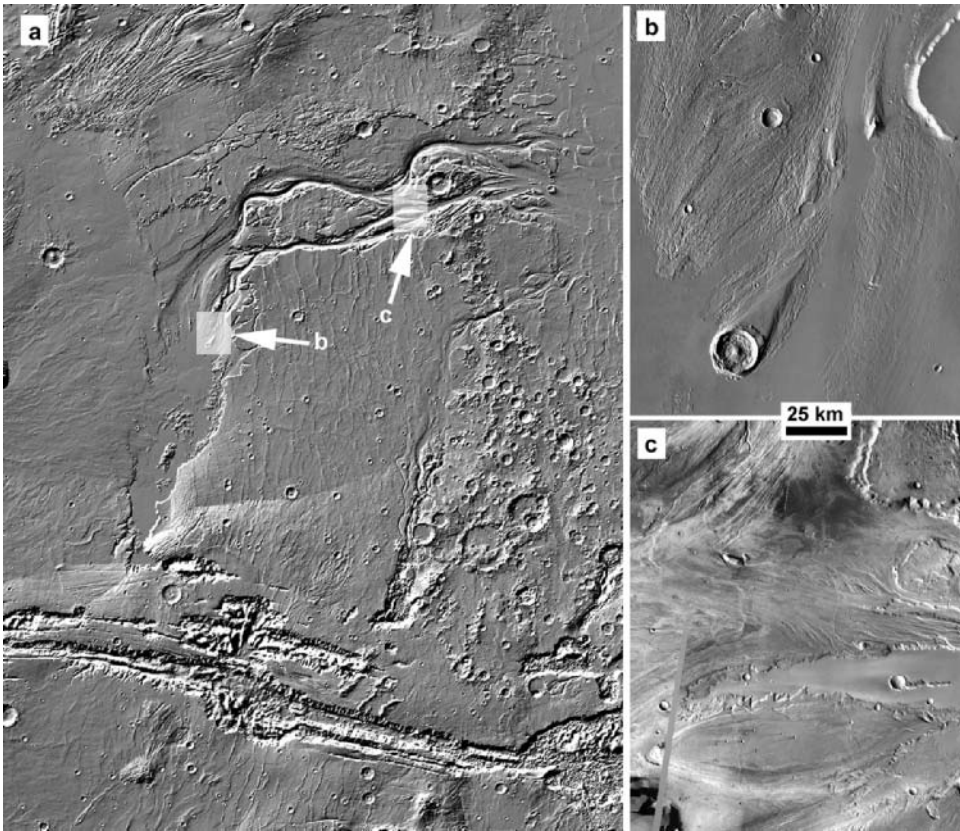


**Figure 19.2** The Martian Kasei Vallis outflow channel, the largest channel in the solar system. (a) Shaded relief of region bounded by  $90^{\circ}\text{W}$ ,  $45^{\circ}\text{W}$ ,  $20^{\circ}\text{S}$  and  $40^{\circ}\text{N}$ . The image is 2507 km across at the bottom. Boxes and arrows indicate the locations of (b) and (c). (b) Streamlined forms in the lee of impact craters and other obstacles to flow ( $16.3^{\circ}\text{N}$ ,  $74.8^{\circ}\text{W}$ ). (c) Longitudinal grooving and incision of the channel bed upstream of a larger crater obstacle ( $25.6^{\circ}\text{N}$ ,  $60.6^{\circ}\text{W}$ ). (b) and (c) are excerpts from the THEMIS daytime infrared mosaic.

These ancient terrains are found on the southern highland plateau, whereas the northern lowland plains and western equatorial Tharsis volcanic province have been resurfaced since widespread valley development ceased (e.g. Tanaka, 1986) (Figure 19.3). Valleys are relatively sparse below about  $-1500$  to  $-1900$  m elevation, which may be attributable to thick volcanic and airfall mantling or contemporary base level control below that topographic level. Pieri (1976) and Carr and Clow (1981) showed that valley networks are concentrated in the dark-toned regions seen in telescopes, but that thick, brighter dust mantles may overlie valleys in the high-albedo areas. Valleys are evident but poorly developed in middle to high latitudes, owing to dust mantling (Soderblom *et al.*, 1974;

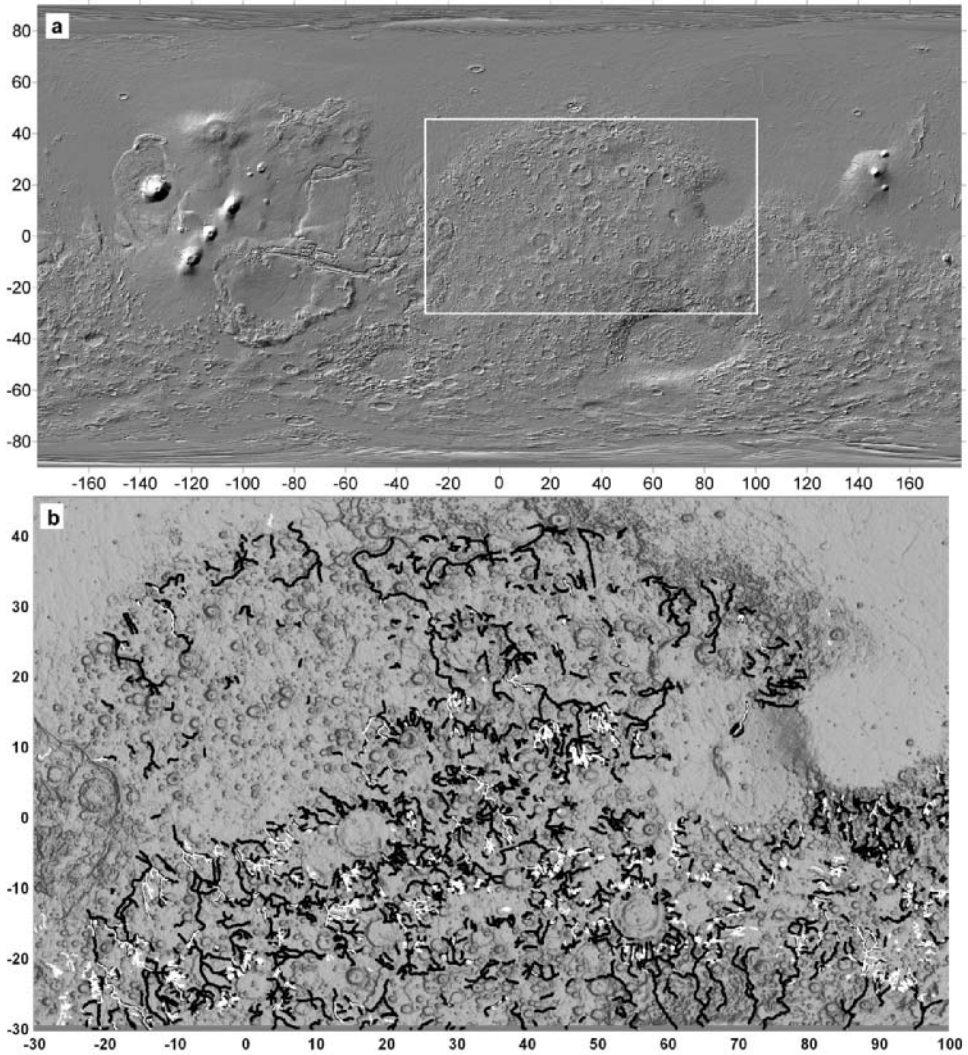


**Figure 19.3** (a) Global shaded relief map of Mars, with outlined location of (b). Valley networks are concentrated in the heavily cratered region that dominates the southern hemisphere. The northern lowland plains and the Tharsis and Elysium volcanic regions ( $\sim 0^\circ\text{N}$ ,  $110^\circ\text{W}$  and  $20^\circ\text{N}$ ,  $150^\circ\text{E}$  respectively) have been completely resurfaced since the epoch of major fluvial activity. The circumference of Mars is 21 339 km at the equator, or 59.275 km per degree. (b) Valley networks mapped in an equatorial highland region by Carr and Chuang (1997) using Viking Orbiter imaging at 1:2-M scale (white lines), compared with major valley networks mapped by A. D. Howard using recent THEMIS imaging and MOLA topography (black lines). Martian valley networks are longer and more numerous than was evident in earlier imaging, but network integration does not approach that found on the Earth.

Pieri, 1976; Carr and Clow, 1981) or less favourable paleoclimates (Williams and Phillips, 2001). Many small valleys occur on intercrater plains, but some originate at crater rims or other sharp ridge crests where no upslope aquifers were available (e.g. Milton, 1973; Masursky *et al.*, 1977; Craddock and Maxwell, 1993; Craddock and Howard, 2002; Irwin and Howard, 2002; Grant and Parker, 2002; Hynes and Phillips, 2003; Stepinski and Collier, 2004) (Figure 19.4). Most Martian valley networks are incised into darker layers of impact ejecta and sedimentary rocks (Malin, 1976a; Malin and Edgett, 2001), which were derived from basaltic igneous rocks (Christensen *et al.*, 2001) during the epoch of heavy meteorite bombardment.

## Ages of valley networks

The unexpected discovery of branching valleys on Mars (initially termed ‘small channels’, ‘runoff channels’ or ‘furrows’) raised the questions of when and for how long the valleys had been active. Unfortunately, we have no rocks from known locations on Mars that could provide absolute age estimates. Relative ages of planetary geologic units are determined using superposition relationships and impact crater populations, as surfaces accumulate craters with time (e.g. Carr, 1981, pp. 54–64). These crater counts are not easily converted to absolute ages, however, because the Martian impact cratering rate and how it declined over time are not precisely known (e.g. Hartmann and Neukum, 2001; Strom *et al.*, 2005). Early workers concluded that the outflow channels and valley networks were relatively old and did not form during more recent cycles of lower-magnitude climate change (Hartmann, 1974; Sharp and Malin, 1975; Pieri, 1976). Malin (1976a, 1976b) dated the valley networks to the epoch of heavy meteorite bombardment, which declined about 3.85 Ga on the Moon and  $\sim 3.7$  Ga on Mars, and later workers have confirmed this relative age (Masursky *et al.*, 1977; Pieri, 1980; Carr and Clow, 1981; Baker and Partridge, 1986; Craddock and Maxwell, 1990; Maxwell and Craddock, 1995; Irwin and Howard, 2002; Ansan and Mangold, 2006). Fluvial activity primarily occurred within the Noachian Period at the base of Tanaka’s (1986) three-period stratigraphic scheme. Valley network activity was contemporary with the more rapid erosional modification and infilling of Noachian impact craters, whereas younger craters of the Hesperian and Amazonian Periods ( $< 3.7$  Ga) have a relatively fresh morphology (Craddock and Maxwell, 1990, 1993; Craddock *et al.*, 1997; Forsberg-Taylor *et al.*, 2004) (Figure 19.4(a)). Fresh crater populations constrain the end of the period of valley network activity. Short-lived, episodic outflow channel activity occurred over a much longer interval of time, from the Noachian and Hesperian to the Amazonian Periods (e.g. Mouginis-Mark, 1990; Zimbleman *et al.*, 1992; Tanaka, 1997), and at least one channel potentially formed within the last  $10^8$  yr (Burr *et al.*, 2002; Berman and Hartmann, 2002).

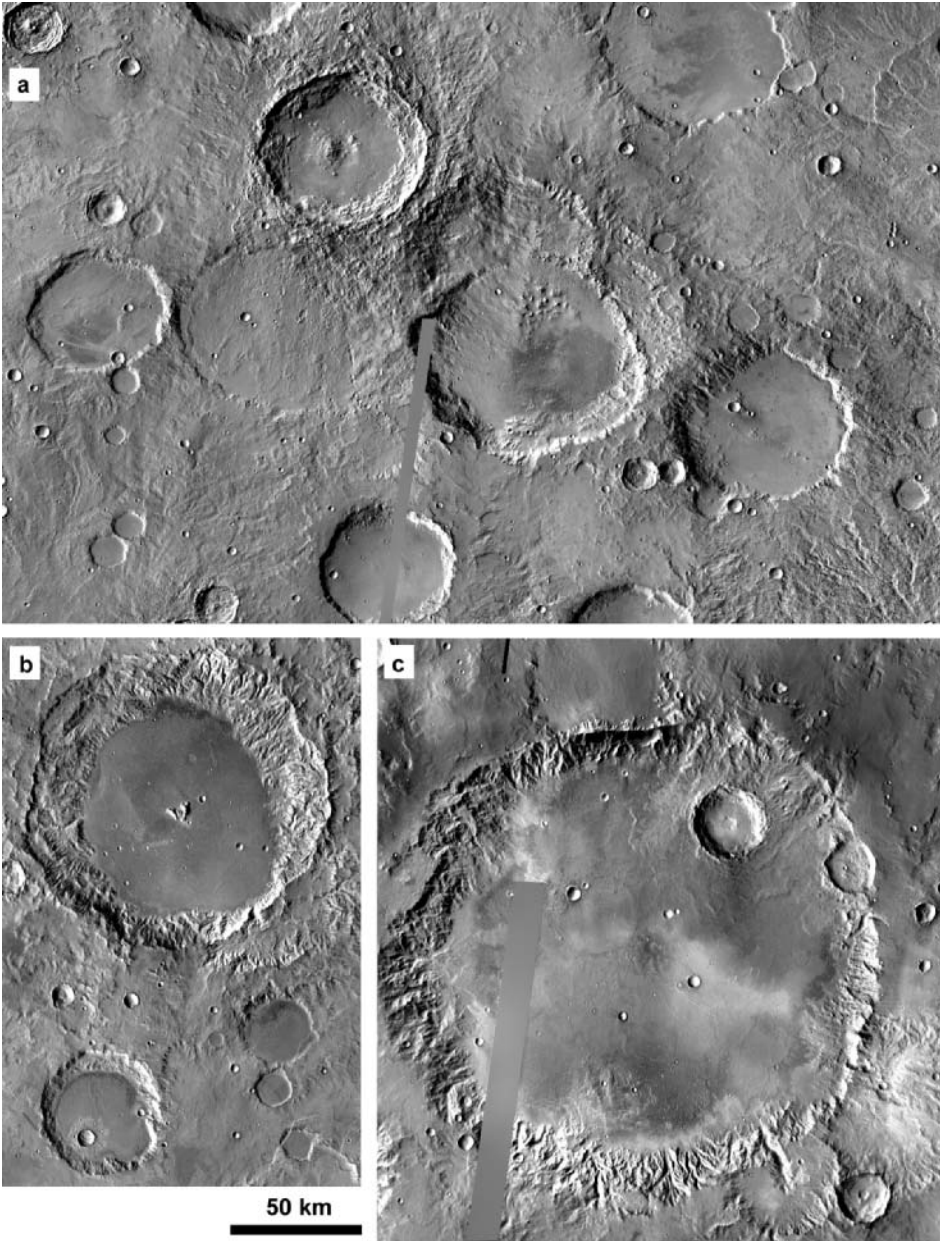


**Figure 19.4** The fluvial modification of impact craters included reworking the rough ejecta, eroding and widening the crater rim, gullying the interior wall and burying the central peak with material shed from the walls. (a) Overlapping fresh (top, left of centre) and modified impact craters in the Terra Sirenum region ( $25^{\circ}\text{S}$ ,  $141.5^{\circ}\text{E}$ ). More heavily modified impact craters stratigraphically underlie fresher craters, unless the more degraded one is much smaller. (b) Impact crater with a densely dissected rim and a still-exposed central peak in Libya Montes, Terra Tyrrhena region ( $5^{\circ}\text{S}$ ,  $72.6^{\circ}\text{E}$ ). (c) The more heavily modified Dawes crater in the Terra Sabaea region ( $9^{\circ}\text{S}$ ,  $38.1^{\circ}\text{E}$ ). All are excerpts from the THEMIS daytime infrared mosaic.

Another issue is whether the highland valley networks were continuously active over a long period or whether they experienced multiple reactivations of regional to global extent early in Martian history (Grant, 1987; Grant and Schultz, 1990; Baker *et al.*, 1991; Gulick *et al.*, 1997). Some spatially localized valley networks dissect volcanoes and volcanic plains of Early to Late Hesperian age (Gulick and Baker, 1990; Scott *et al.*, 1995; Mangold *et al.*, 2004; Quantin *et al.*, 2005), or they originate in the Noachian highlands and cross into younger terrains (Irwin *et al.*, 2005b). Howard *et al.* (2005) and Irwin *et al.* (2005b) showed examples of late-stage valley entrenchment, overflow of previously enclosed basins and coarse sedimentation that occurred sometime between the Noachian/Hesperian boundary ( $\sim 3.7$  Ga) and the middle of the Hesperian Period ( $\sim 3.6$  Ga). This epoch of fluvial activity lasted in the order of  $\sim 10^5$  yr and temporarily exceeded the erosion rates that prevailed before that time. Others have suggested that an early epoch of runoff declined to a regime dominated by groundwater sapping, which downcut the lower reaches of older valleys (Baker and Partridge, 1986; Harrison and Grimm, 2005). Some small impact craters and other steep slopes in the mid-latitudes have very fresh gullies, but these youngest features are localized and conveyed relatively little sediment (Malin and Edgett, 2000b).

Weathering and erosion rates declined severely when fluvial activity ended (Carr and Clow, 1981). Modified impact craters record denudation rates of  $\sim 0.1$ – $10$  m/Myr during the time of fluvial activity, whereas later Hesperian and younger craters ( $< 3.6$  Ga) are little modified (Craddock and Maxwell, 1993; Carr, 1996; Craddock *et al.*, 1997). Small contemporary valleys on intercrater slopes (Figure 19.5) are typically 0.5–4 km wide (median 1.6 km) by 20–250 m deep (median 80 m), but they have experienced only  $\sim 20$  m of infilling in 3.6 Gyr since the mid-Hesperian (Goldspiel *et al.*, 1993a; Williams and Phillips, 2001). Weathering and the aeolian modification of plains have also been extremely slow. The infilling of impact craters limits the total redistribution of plains material since the Noachian to  $< 0.01$  m/Myr (Arvidson *et al.*, 1979; Carr, 1996). Lander observations suggest aeolian denudation rates of plains basalt on the order of centimetres per billion years since the Noachian Period (Golombek and Bridges, 2000; Golombek *et al.*, 2006), although the wind has deeply eroded less resistant, presumably fine-grained, layered sedimentary rocks or tephra in some areas (Ward, 1979; Malin and Edgett, 2000a). The water cycle appears to have declined suddenly, as interior channels do not record gradual declines in discharge, some valleys have V-shaped cross-sections that suggest active downcutting with little subsequent modification and most delta surfaces were not entrenched with declining water level in lake basins (Irwin *et al.*, 2005b) (Figure 19.6).

## Water-source hypotheses and implications for paleoclimate

The most contentious issue regarding valley networks is their water source. The first papers on Martian fluvial landforms compared the common theatre-headed valley

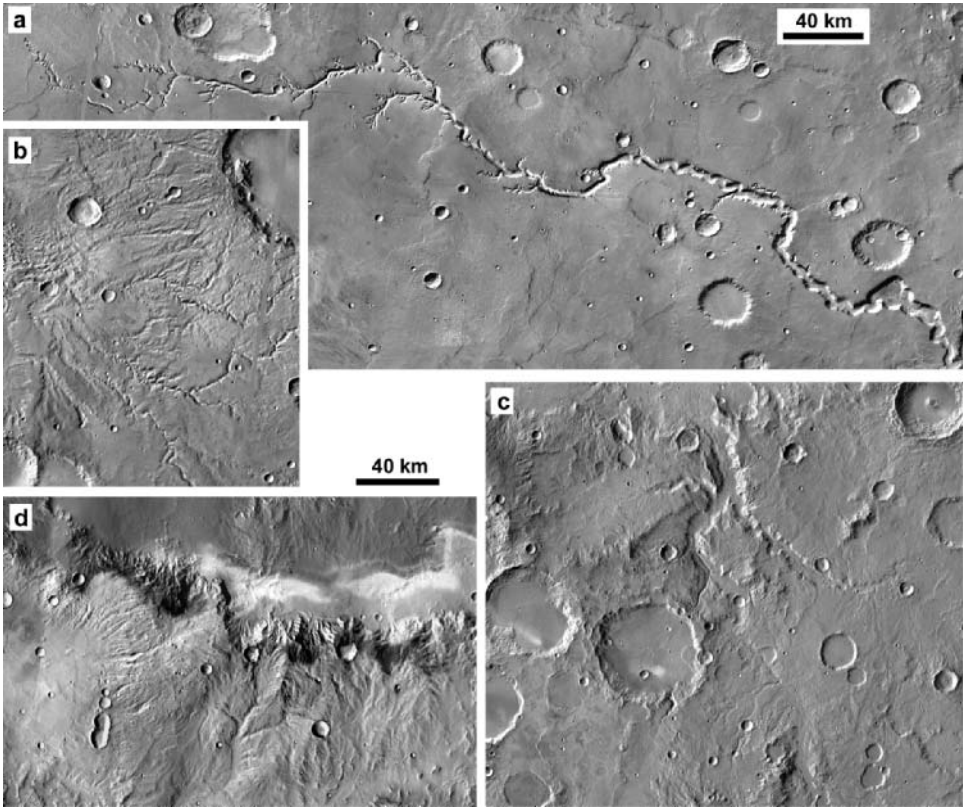


**Figure 19.5** Classification of Martian valley networks. (a) Nirgal Vallis, a large stem valley with entrenched meanders and relatively few, stubby tributaries (28.3°S, 41.4°W). (b) Parana Valles, a typical valley network with poorly dissected interfluvial surfaces, a relatively constant width down-slope and tributary valleys that are similar in width to the stem (22.4°S, 10.4°W). (c) Durius Vallis, a large stem valley with increasing width downslope and much smaller tributaries (16.6°S, 172°E). (d) Dense slope valleys on the southern rim of Schiaparelli crater (6.6°S, 16°E). Note origin of valleys near sharp drainage divides. All are excerpts from the THEMIS daytime infrared mosaic.

networks to box canyons with headwall springs in the south-western United States and Hawaii (Milton, 1973; Sharp and Malin, 1975; Malin, 1976a, 1976b; Pieri, 1976, 1980; Masursky *et al.*, 1977; Carr and Clow, 1981; Baker, 1982; Mars Channel Working Group, 1983; Laity and Malin, 1985; Kochel and Piper, 1986; Howard *et al.*, 1988). Groundwater sapping depends on spring discharge, which weathers the aquifer material, undermines the surface and extends a valley headward (Dunne, 1980). The hypothesis that groundwater alone carved the valley networks gained wide acceptance during and after the Viking missions (1976–1982). Later workers developed this concept, suggesting that prolonged groundwater sapping could occur without atmospheric recharge, if volcanic

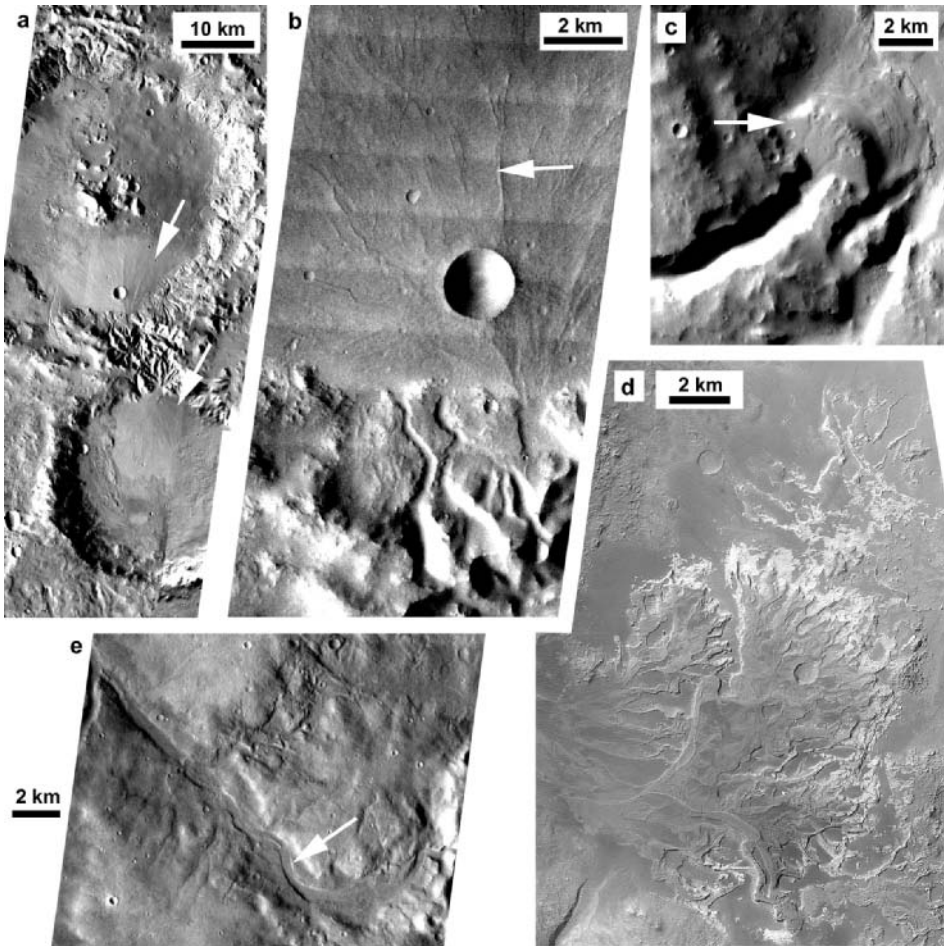


**Figure 19.6** Fluvial deposits and channels on Mars. (a) Large alluvial fans (arrows) were sourced from densely dissected alcoves in the rim of two adjacent impact craters (23.9°S, 28.1°E, THEMIS daytime infrared imaging, (b), (c) and (e) are THEMIS visible wavelength imaging). (b) Distributary channels (arrow) on the northern fan in (a) occur in inverted relief due to selective erosion of fine-grained overbank deposits. (c) A likely delta in a Martian impact crater (12°N, 52.7°W). (d) Meandering distributary channels on the surface of a delta in Eberswalde crater (23.8°S, 33.7°W, MOC image mosaic credit Malin Space Science Systems). (e) Exposed interior channel in Samara Vallis (arrow, 31.5°S, 13°W).

intrusions caused sub-surface heat fluxes to vary over time. The geothermal heating of groundwater would encourage upward diffusion of vapour, which would accumulate near the surface as permafrost (Clifford, 1991, 1993; Clifford and Parker, 2001). This ice would later melt when a magma body was intruded (Wilhelms and Baldwin, 1989; Gulick and Baker, 1989, 1990; Brakenridge, 1990; Gulick, 1998, 2001; Harrison and

Grimm, 2002). The resulting spring discharge might flow for long distances on the surface under an ice cover, as long as the ice remained intact and adequate heat was carried from the aquifer to balance heat lost to the atmosphere (Wallace and Sagan, 1979; Carr, 1983; Goldspiel and Squyres, 2000). Other authors suggested that impact heat would melt ground ice and release water from impact crater rims, forming gullies at higher elevations (Maxwell *et al.*, 1973; Brakenridge *et al.*, 1985). Investigators pointed to the primary igneous rather than weathered or evaporitic spectral signature of most regions (Bandfield *et al.*, 2000, 2003; Christensen *et al.*, 2001; Gaidos and Marion, 2003), and the incomplete dissection of the highlands by theatre-headed valleys as evidence against a warmer, wetter paleoclimate with widespread precipitation (e.g. Carr and Malin, 2000).

The groundwater-sapping hypothesis suffers from a number of weaknesses, summarized by Craddock and Howard (2002): (1) even flows with high sediment concentrations would require recharge to transport sediment equivalent to the measured volumes of valley networks (Howard, 1988; Gulick and Baker, 1990; Goldspiel and Squyres, 1991; Goldspiel *et al.*, 1993b; Grant, 2000; Gulick, 2001). Storm runoff is responsible for much of the aquifer recharge and sediment transport in terrestrial desert rivers (e.g. Howard *et al.*, 1988). (2) Geothermal mechanisms for near-surface ice accumulation and melting in equatorial regions are theoretical and lack empirical support, particularly as most valley networks formed in cratered rather than volcanic terrains. Reasonable geothermal heat fluxes might have supported liquid water at least 300 m below the surface (Goldspiel and Squyres, 2000; Travis *et al.*, 2003), but most valley networks are not, and never were, that deep (Goldspiel *et al.*, 1993a; Williams and Phillips, 2001; Howard *et al.*, 2005). (3) Flowing water must have been spatially ubiquitous, temporally long-lived (at least episodic over  $> 2 \times 10^8$  yr) and volumetrically abundant to modify impact craters. Where adjacent Noachian craters of similar size are observed, the stratigraphically older ones are more heavily modified (Figure 19.4(a)). Fluvial erosion and sedimentation are required to explain the concave profile at the transition between a crater wall and floor (Craddock *et al.*, 1997; Forsberg-Taylor *et al.*, 2004). (4) Theatre headwalls are not unique to groundwater sapping but are found in many valleys where waterfalls sap (i.e. undercut) a resistant caprock and erode a weaker basal layer. (5) The lack of massive carbonate deposits on Mars may reflect an acidic environment rather than a lack of surface water (Fairén *et al.*, 2004). Adequate impact gardening and aeolian erosion have occurred to expose fresh basaltic surfaces to orbiting sensors (Mars Exploration Rover findings have recently supported both of these claims, e.g. Squyres *et al.*, 2004, Golombek *et al.*, 2006). (6) Climatic models and morphometric analyses often yield ambiguous results, as discussed below.

To carve valleys by overland flow, Mars would require a thicker, warmer atmosphere capable of supporting more intense rainfall or snowmelt and long-distance flow without freezing (Sagan *et al.*, 1973; Pollack *et al.*, 1987). Climate modellers have raised the main

objection to this concept, with most finding that a thick CO<sub>2</sub> greenhouse alone could not warm Mars above a globally averaged 0°C (Kasting, 1991; Squyres and Kasting, 1994; Haberle, 1998; Colaprete and Toon, 2003), because changes in the Sun's elemental composition through time imply that it was only ~ 75 per cent as bright at 3.7 Ga (Gough, 1981). Recent studies have suggested that the early Sun may have been a few percent more massive than at present, making it less dim than otherwise expected (e.g. Boothroyd *et al.*, 1991; Graedel *et al.*, 1991; Whitmire *et al.*, 1995). Other greenhouse gases (Sagan and Chyba, 1997), including water vapour excavated by large impacts (Segura *et al.*, 2002; Colaprete *et al.*, 2005) and volcanism (e.g. Baker *et al.*, 1991), would also contribute to greenhouse warming. This issue has not yet been resolved, but a combination of the above factors may have contributed to a long-lived or episodic water cycle on early Mars.

## Valley morphology and diversity

Published classification schemes have differentiated Martian valleys by size, morphology and network planform. Excluding troughs related to volcanoes, crustal extension and collapse, three basic categories include: (1) 'fretted' valleys with a gridded planform and little evidence of through-flowing water (the origin of these valleys remains unclear, Carr, 2001), (2) the monolithic outflow channels (Figure 19.2) and (3) smaller valley networks. Early authors also subdivided the latter category in a qualitative but broadly consistent manner (Figure 19.5), summarized as: (3a) large, widely spaced, sinuous stem valleys that are ~ 10 km wide and ~ 1 km deep ( $\pm 50$  per cent), increase in width downslope and have tributaries much smaller than the stem; (3b) small valley networks with more closely spaced tributaries, which have similar width to higher-order segments downslope; and (3c) dense, sub-parallel slope valleys (Masursky, 1973; Sharp and Malin, 1975; Pieri, 1976; Masursky *et al.*, 1977). Valley spacing and length decrease from category 3a to 3c. Pieri (1980) refined his earlier work to include eight classes of network planform, including digitate (fanned), stem (category 3a), parallel (category 3c), rectilinear, radial centrifugal (away from central highs) and two types of radial centripetal planform (exterior and interior drainage into central basins). True dendritic patterns reflecting the full development of network structure under homogenous geological conditions have not been seen on Mars, although the term has been casually applied in planetary literature.

Most Martian fluvial valleys have either flat-floored or V-shaped cross-sectional profiles. The former category (including much of 3b above) includes a trapezoidal cross-section with sidewalls near the angle of repose, a nearly constant valley width downstream, an amphitheatre headscarp and poorly dissected interfluvial areas between major tributaries (e.g. Pieri, 1980; Baker, 1982; Mars Channel Working Group, 1983). This morphology is most common on low-gradient intercrater plains. Most valleys

with V-shaped cross-sections occur on steeper headwater slopes (Figure 19.5(d)) or at downstream sites where a valley incised a convex break in slope, such as a crater rim (Figure 19.6(c)) (Baker and Partridge, 1986; Williams and Phillips, 2001). Fully dissected surfaces, leaving sharp divides between tributaries, are uncommon and are usually restricted to steep interior walls of impact craters and other slopes (Figures 19.5(d) and 19.6(a)) (e.g. Moore and Howard, 2005; Quantin *et al.*, 2005).

The two types of cross-sections may represent different formative processes or lithologic controls, or they may be gradational forms. The V-shaped valleys probably represent late, rapid downcutting by runoff along a steep gradient, with little subsequent modification. Valley measurements show that width increased in proportion to depth of incision until the longitudinal profile stabilized, and valleys continued to widen afterwards to produce the flat-floored shape (Williams and Phillips, 2001). Rapid headward erosion or downcutting, possibly due to runoff bottlenecks in a cratered landscape, with little time afterwards for widening would produce a nearly constant valley width downstream in a runoff-dominated regime. Alternatively, if headward extension was due to slow groundwater sapping, the valley width and cross-section indicate that nearly all water originated at the valley head (e.g. Goldspiel *et al.*, 1993a; Grant, 2000). The common valley headscarps are likely attributable to sapping (i.e. undercutting) in layered rocks, either by springs or waterfalls.

## Morphometry

A number of investigators have tested the overland flow and groundwater hypotheses by comparing the morphometry (length, sinuosity, drainage density, cross-sectional profiles, network planform and longitudinal grading) of Martian valley networks to mature terrestrial networks. These studies have all shown significant differences between Martian drainage basins and the ideal quasi-equilibrium condition, but it remains uncertain to what degree these differences represent immaturity or a different water source.

Between 1997 and 2001, the Mars Orbiter Laser Altimeter (MOLA) on the Mars Global Surveyor (MGS) orbiter returned the first precise topographic map of Mars at < 0.5-km resolution. Previously, global-scale topography had very poor resolution and incorporated vertical errors up to a kilometre, as elevation estimates were based on the topographic and atmospheric occultation of a spacecraft's radio signal as it passed behind the planet (Kliore *et al.*, 1973; Smith *et al.*, 2001). Studies of valley network development were thus restricted to the plan view of orbital imaging, although less precise local measurements of valley slopes and depths were made using stereo imaging, brightness contrasts across an image (photoclinometry), Earth-based radar tracks and shadows (e.g. Thornhill *et al.*, 1993; Goldspiel *et al.*, 1993a, 1993b; Lucchitta and Dembosky, 1994).

## Planimetric measurements

Quantitative studies based on  $\sim 230$ -m/pixel orbital imaging showed that Martian valley networks are relatively short and discontinuous, with common lengths of tens to hundreds of kilometres (Carr and Clow, 1981; Baker and Partridge, 1986; Carr, 1995; Cabrol and Grin, 2001). Martian watersheds are poorly integrated, and the many enclosed impact craters and intercrater basins include sites where cratering disrupted earlier fluvial pathways. Some basins (particularly craters that formed on pre-crater slopes) are infilled or breached, but most larger basins drained internally (Grant, 1987; Goldspiel and Squyres, 1991; Maxwell and Craddock, 1995; Irwin and Howard, 2002; Kramer *et al.*, 2003). Some significant exceptions have lengths of 1000–4700 km, including larger stem valleys and other networks that crosscut multiple basins on long regional slopes (e.g. Carr and Clow, 1981; Irwin *et al.*, 2005b) (Figure 19.3(b)).

In a study of 71 typical valley networks, Cabrol and Grin (2001) found that most were of Horton (1945) order 3–4, reflecting short length with limited tributary development. In 14 large networks with a maximum Strahler (1952) order of 4, Carr (1995) found bifurcation ratios of 2.9 to 7.6 (average 4.3), similar to terrestrial networks. Length ratios were also comparable but had a relatively large range of 1 to 6.9 (average 2.9), possibly reflecting underdeveloped drainage basins. Using higher-resolution imaging, Ansan and Mangold (2006) report similar results but a higher network order of 5–7 for Warrego Valles. On some volcanoes with dense valleys, Gulick and Baker (1990) measured Shreve (1966) network magnitudes from 2 to 34.

Most Martian valleys have low sinuosity (Grant, 2000), as do their interior channels where evident (Irwin *et al.*, 2005a). Many investigators have attributed this relative straightness to a structural control of groundwater flow (e.g. Pieri, 1980; Brakenridge, 1990); however, new topographic data show that nearly all Martian valley networks follow the steepest topographic gradient, regardless of the local structure. Straight or braided (as opposed to meandering) reaches of terrestrial streams occur where stream power, bank erodibility and a relative supply of bedload are all very low or very high respectively (Knighton, 1998). Few meandering alluvial channels are evident on Mars, either because these channels were too shallow to be preserved or because the required sets of conditions were not often met, but some Martian stem valleys have entrenched meanders (Figure 19.5(a)). These features record meandering surface flowpaths, which can develop over  $\sim 100$ - to 1000-year timescales, that experienced longer-term down-cutting due to excess transport capacity (i.e. stream power) relative to sediment supply. Tectonic uplift does not appear to have been important on Mars, but most valleys with entrenched meanders extend from a low-gradient plain onto a steeper surface, such as an impact crater rim or the wall of a deep stem valley, encouraging headward incision.

Many investigators have measured drainage density, the total length of valleys per unit area, in local to regional study areas. Most studies have found values in the order of  $10^{-2}$  to  $10^{-1}$  km/km<sup>2</sup> on dissected surfaces, one to three orders of magnitude less than typical terrestrial values (Grant and Boothroyd, 1985; Baker and Partridge, 1986; Grant, 1987; Grant and Schultz, 1993; Tanaka *et al.*, 1998; Grant, 2000; Cabrol and Grin, 2001; Gulick, 2001; Irwin and Howard, 2002; Craddock and Howard, 2002; Hynes and Phillips, 2003; Stepinski and Collier, 2004; Ansan and Mangold, 2006; Luo and Stepinski, 2006). Drainage densities above 1.0 have been measured only in Valles Marineris (Mangold *et al.*, 2004) and on some volcanoes (Gulick and Baker, 1990), and the reasons for this variability across Mars remain uncertain (Luo and Stepinski, 2006). Carr and Chuang (1997) made the first effort to quantify Martian drainage densities on a global scale (Figure 19.3(b)). They compared valley networks digitized on Viking Orbiter imaging ( $\sim 230$  m/pixel, 1:2-M scale) with Landsat images of Arizona, Nebraska, New York, Texas and Washington that were degraded to a similar resolution. They found that the average drainage density on Noachian plains is approximately 0.0032 km/km<sup>2</sup>, but that terrestrial values were 0.065–0.209 km/km<sup>2</sup> over the range of climates studied. Several issues complicate such direct comparisons. (1) Viking Orbiter images were taken with different viewing geometries, times of day and atmospheric conditions, so that a feature visible in one image is often difficult to distinguish in the adjacent image. (2) The Landsat spectral bandpasses were selected primarily to monitor vegetation, which is often concentrated around stream channels, whereas images of Mars show little contrast except on steep slopes or compositionally distinct geological units. (3) Terrestrial rivers have been recently active, whereas Martian valleys have experienced 3.7 Gyr of degradation by wind, mass wasting and small impacts. Martian valleys may be evident only where they were deeply incised and not deeply buried, particularly in low-resolution imaging. (4) Regional measurements of drainage density incorporate recent deposits as well as ancient depositional basins, where a shallow channel network would have been easily buried or erased.

In general, new imaging at 1–100 m/pixel from the Mars Orbiter Camera (MOC) on MGS and the Thermal Emission Imaging System (THEMIS) on Mars Odyssey revealed more tributaries, a higher drainage density and better integration than was previously evident (e.g. Hynes and Phillips, 2003; Figure 19.3(b)), but Martian valley networks still appear underdeveloped relative to their terrestrial counterparts. All previous studies have concluded that poor development (i.e. formation, incision or preservation) of headwater tributaries is the main cause of low drainage density on Mars. If widespread precipitation was available, high infiltration capacities maintained by cratering may have impeded runoff production (Baker and Partridge, 1986; Gulick and Baker, 1990; Grant and Schultz, 1993; Carr and Malin, 2000). Alternatively, an Earthlike climate may have prevailed for a limited period.

## Network-junction angles and drainage-basin topography

One of the few characteristics of valley networks that can be quantitatively assessed using Mariner 9 and Viking images is the angular structure of the network, particularly the angles of valley junctions. Early geomorphic literature (e.g. Horton, 1932) suggested that the planimetric form of valley networks was inherited from the topography at the time of initial channel incision (this may be largely true for Mars). Howard (1971) suggested, however, that junction angles dynamically adjust as topography evolves and proposed geometric and minimum power criteria for junction angles. A consequence of these models is that mean junction angles increase with concavity of the drainage network (e.g. Howard, 1990; Sun *et al.*, 1994) and small tributaries merge with large rivers at high junction angles, relative to smaller angles between tributaries of equal size and order. Pieri (1980) showed that Martian junction angles tend towards small values and a high degree of irregularity, which he suggested was due to the immature state of the valley network, with strong structural controls and a lack of sufficient net erosion to develop a highly concave profile. The structure of the network also varies with the scale at which it is observed, a feature not seen in true dendritic networks on Earth.

Several investigators have used the D8 algorithm (Tarboton *et al.*, 1991) to extract information on drainage basins (Hynek and Phillips, 2003; Stepinski and Collier, 2004). In this method, the surface flow direction is the steepest downward slope from the centre of a given pixel to the centre of the eight surrounding it. Flow direction is then integrated to determine the most probable flowpaths for surface water over the given DEM. Streams of different order and magnitude are also identified following several conventions (Horton, 1945; Strahler, 1952; Shreve, 1967). This information can then be used to characterize a number of parameters useful for describing a valley network system (e.g. contributing area, relief and stream order). However, an uncritical application of D8-based methods to MOLA topography leads to the artificial generation of drainage patterns on both dissected and undissected surfaces. Fresh craters have modified the surface since the time of valley network activity, and the derived order and drainage density of a network are functions of the DEM's resolution. Manual editing of computationally identified networks is therefore required.

Although valley networks do not fully dissect the Martian surface, topography can be used to evaluate the cratered landscape's adjustment to hypothetical fluvial processes. Stepinski *et al.* (2002, 2004) showed that runoff on Mars would organize with fractal planar characteristics similar to terrestrial networks. However, drainage basin length ( $L$ ), area ( $A$ ), slope and drainage-density characteristics reflect significant influences from both fluvial erosion and contemporary impact cratering. More densely dissected surfaces show a better adherence to Hack's (1957) Law ( $L \propto A^{0.6}$ ) than other highland areas with similar crater populations, but Martian drainage basins tend to be more

elongated ( $L \propto A^{0.73}$ ). The poor longitudinal grading on Mars caused more energy to be dissipated in high-order segments downstream, a likely indicator that the networks were still growing headward and incising when the water supply declined. They also found that latitude and elevation have no net influence on watershed development (see also Luo and Stepinski, 2006). Luo (2000, 2002) compared the hypsometry of Martian and terrestrial drainage basins, finding that some have deeply incised stem valleys that are often attributed to groundwater sapping, whereas others have hypsometric characteristics more similar to graded watersheds. Topographic analyses using a circularity function (a plot of changes in a drainage basin's shape at different topographic levels) suggest that Martian valley networks are entrenched below a precursor surface that has not been fully regraded by prolonged fluvial erosion (Stepinski and Coradetti, 2004; Stepinski and Stepinski, 2005; Luo and Howard, 2005). These studies favourably compared Martian drainage basins to terrestrial analogues in hyper-arid climates. Valley longitudinal profiles are commonly irregular, reflecting modest total erosion (e.g. Aharonson *et al.*, 2002; Howard *et al.*, 2005; Irwin *et al.*, 2005b; Kereszturi, 2005). An arid climate with ephemeral runoff or a short duration of conditions favourable to precipitation may be responsible for low fluvial incision.

## Alluvial deposits

Both alluvial fans and likely deltas have been recognized along the margins of Martian basins. These landforms provide a depositional record of past fluvial activity that is broadly similar in magnitude but shorter in duration relative to terrestrial desert environments.

### Fans

Noachian impact craters with diameters of 10–70 km typically have 500 to 1000 m of sedimentary fill, and many have lost their well-defined rims to erosion (Figure 19.4) (Craddock *et al.*, 1997; Craddock and Howard, 2002; Forsberg-Taylor *et al.*, 2004). These crater floors typically decline towards the centre with slopes of about  $0.5\text{--}1^\circ$ , suggesting that the floor materials are fluvial bajadas supplied by parallel gullies on the craters' interior walls. Lava eruptions or intrusions as well as airfall deposition may also have contributed to basin infilling, particularly in craters above this size range that often have flatter floors (Craddock and Howard, 2002). Well-developed, cone-shaped alluvial fans, with lengths of tens of kilometres and gradients of a few degrees, occur in some deep craters that formed late in the period of fluvial erosion on Mars (Moore and Howard, 2005). These fans typically radiate from deep, thoroughly dissected alcoves in the crater walls (Figure 19.6(a)). The gradients, size and concavity

of the alluvial fans quantitatively relate to the size and slope of the eroded alcoves in a manner that closely approximates relationships for large terrestrial alluvial fans. On some of the fans, the selective aeolian erosion of fines has revealed distributary channels in inverted relief (Figure 19.6(b)). The distributary network structure, fan gradients and channel-width suggest fluvial sedimentation rather than debris flows (Moore and Howard, 2005).

## Deltas

Most valley networks debouch into impact craters or enclosed intercrater basins, but valley floors are usually graded to the terminal basin floor, with no positive-relief fan or delta at the valley mouth. This characteristic suggests that deep paleolakes were rare or short-lived. Either water was delivered to most basins less rapidly than evaporation and infiltration removed it or water levels fluctuated widely across the basin floors, keeping thick sedimentary deposits from accumulating at the basin margins. These comments are speculative, as the environmental and physiographic conditions that favoured paleolake development have not yet been constrained.

Irwin *et al.* (2005b) reviewed the literature on Martian paleolakes and listed 33 scarp-fronted deposits where valleys debouch into impact craters or other basins (e.g. Figure 19.6(c), (d)). Many of the putative deltas recognized by Cabrol and Grin (1999) could not be relocated in new, higher-resolution imaging. The deposits resemble deltas due to the steep scarp along their outer margins, although the aeolian deflation of fine sediments around an alluvial lag might yield a similar form. Several of these deposits have distributary channels, occasionally in inverted relief (Figure 19.6(d)). In other cases, distributary channels have been mantled, reworked or did not form (although the latter case would imply that these are not subaerial deltas). Other likely deltas have since been discovered, reflecting multiple lake levels (e.g. Di Achille *et al.*, 2006; Weitz *et al.*, 2006).

Few of the putative Martian deltas have been studied in detail, as most were discovered in the last several years when decametre- to metre-scale imaging became available. Malin and Edgett (2003) and Moore *et al.* (2003) described the most spectacular fluvial deposit on Mars, an 11- by 13-km ( $6\text{--}13\text{ km}^3$ ) distributary fan in the 64-km Eberswalde crater (Figure 19.6(d)). This deposit has at least three lobes at different elevations, suggesting two stands of lake level and a complex network of meandering distributary channels that show evidence of lateral migration, vertical aggradation and avulsion. Fassett and Head (2005) described a broadly similar pair of deltas on the opposite side of the planet.

Well-developed alluvial fans and deltas appear to have formed during a terminal epoch of relatively intense fluvial erosion on Mars (Howard *et al.*, 2005; Irwin *et al.*, 2005b; Moore and Howard, 2005). There is little evidence for similar degraded, cone-shaped, gravely alluvial fans and deltas dating from earlier in the Noachian, but the

significance of this absence is uncertain. Such features may have been degraded by wind erosion or buried as the craters filled with sediment; alternatively, the earlier erosional and depositional environment may have been less intense than the later period when well-developed valleys, fans and deltas formed.

## Hydrology

The dominant discharge, annual runoff volume runoff per unit area, and flow longevity of Martian valley networks are all poorly constrained at present. The few recognized interior channels have experienced prolonged dry conditions with aeolian infilling and some modification of the channel banks, and only one basin has been used for an input/evaporation balance that loosely constrains the annual water budget (Irwin *et al.*, 2005a, 2005b). However, where channel and basin dimensions can be measured, quantitative techniques applicable to alluvial channels are available to constrain the hydrology of ancient Martian rivers.

## Scaling equations to Martian gravity

Both theoretical and empirical fluid flow equations can be adjusted for 0.38 times the terrestrial gravitational acceleration to estimate discharge, flow velocity, particle-settling velocity, bed shear stress, critical shear stress for entrainment and sediment-transport rates on Mars. The discharge  $Q$  ( $\text{m}^3/\text{s}$ ) of a channel can be calculated using a combination of the unit-balanced continuity and Darcy-Weisbach equations (the latter is similar in form to the Manning equation):

$$Q = HWV = H^{1.5} W(8gS/f)^{0.5} \quad (19.1)$$

where  $H$  is mean flow depth (m) for channels with high width/depth ratio,  $W$  is channel width (m),  $g$  is gravitational acceleration ( $\text{m}/\text{s}^2$ ),  $S$  is slope and  $f$  is the Darcy-Weisbach friction factor. Equation (19.1) is only useful where depth is known, and measurement errors are significant as depth is the most important contributor to discharge. Measuring the depth of a channel with stereo imaging or shadows and assuming bankfull conditions may yield large errors, since the channel may be either deeply entrenched below a terrace or partly filled with sand. The friction factor must also be estimated, but this is a smaller source of error given the natural range of values and its exponent of 0.5.

A simpler method uses only channel width and assumes that a dominant discharge controls this and other channel dimensions, which has been demonstrated in a variety of terrestrial settings. In humid regions, this flood has a recurrence interval of one to two years (Knighton, 1998), but less frequent floods often dominate arid-zone rivers

(Graf, 1988). Meander wavelength  $\lambda$  scales with channel width as:

$$\lambda = k_\lambda W \quad (19.2)$$

on both Earth and Mars (Moore *et al.*, 2003; Irwin *et al.*, 2005a), and  $W$  scales with discharge as:

$$W = k_w Q^{0.5} \quad (19.3)$$

where the coefficients  $k_\lambda$  and  $k_w$  are  $\sim 10$ – $14$  and  $\sim 3$ – $5$  respectively. Solving for  $Q$  yields:

$$Q = (W/k_w)^2 = (\lambda/k_\lambda k_w)^2 \quad (19.4)$$

The coefficients depend on the contemporary resistance of the channel banks, as more resistant banks yield narrower and deeper channels with a somewhat smaller wavelength, but bank strength is unknown for Mars. Equation (19.1) shows that decreasing gravity reduces flow velocity, so, if slope and roughness are held constant, width and depth must be greater per unit discharge on Mars. The greater depth increases velocity above the factor 0.62 that would result from reducing gravity with a channel of the same dimensions (Pieri, 1980; Komar, 1980b). Empirical data show that  $H \propto W^{0.69}$  (Williams, 1988), a relationship that approximately yields Equation (19.4) if substituted into Equation (19.1). In this case, width, depth and velocity on Mars would be 1.27, 1.18 and 0.67 times their value on Earth, and the discharge resulting from Equation (19.4) would be multiplied by 0.62 ( $1.27^{-2}$ ).

The algebraic manipulation of regression equations introduces significant errors, however, so a function determined with  $Q$  as the dependent variable is favoured (Williams, 1988). For a conservative estimate of discharge, Irwin *et al.* (2005a) measured the channel floor width rather than the bank-to-bank width (in case later mass wasting had modified the banks), and they applied an equation for sand-bed/sand-bank channels that are relatively wide per unit depth (Osterkamp and Hedman, 1982):

$$Q = 1.9 W^{1.22} \quad (19.5)$$

If  $H \propto W^{0.15}$ , an extreme case that may apply to some sand-bank channels, the width, depth and velocity scaling would be 1.48, 1.06 and 0.64 the terrestrial values respectively. To scale Equation (19.5) to Martian gravity, the result must also be multiplied by 0.62 ( $1.48^{-1.22}$ ). Based on this derivation, the channel-forming discharges calculated by Irwin *et al.* (2005a) could be reduced by 18 per cent (they used a scaling coefficient of 0.76 assuming a smaller ratio of width to depth) to provide as conservative an estimate as the data and regression functions could reasonably support. If the channel banks were

more cohesive, the dominant discharges for the larger drainage basins would be higher than they reported.

Nummedal (1977), Komar (1980a, 1980b) and Pieri (1980) compared a similarly sized channel rather than a similar discharge between Earth and Mars, but the same discharge would form a wider and deeper channel on Mars, increasing a flow's erosional efficiency beyond the effect of lower gravity. The critical shear stress  $\tau_c$  ( $\text{N/m}^2$ ) needed to mobilize a particle scales directly with gravity as:

$$\tau_c = 0.06(\rho_s - \rho_w)gD \quad (19.6)$$

where  $\rho_w$  is fluid density,  $\rho_s$  is particle density ( $\text{kg/m}^3$ ) and  $D$  is the particle diameter (m). Bed shear stress  $\tau$  also scales with gravity as:

$$\tau = \rho_w gHS \quad (19.7)$$

However, for a given discharge and slope, the shear stress applied to a channel bed would be 0.40–0.45 or more of the terrestrial value, depending on the ratio of channel width to depth that is controlled by the resistance of channel-bank material. The gravitational force applied to a suspended particle scales with  $g$ , thus the settling velocity for coarse particles is multiplied by 0.62 ( $\sqrt{0.38}$ ) and smaller factors for smaller particles, but flow velocity is at least 0.64–0.67 times the terrestrial value. These relationships impart a slight efficiency to gravel transport on Mars, but, once mobilized, smaller particles would remain suspended much longer in Martian rivers (Nummedal, 1977; Komar, 1979, 1980b; Pieri, 1980), increasing their transport rate by a factor of  $\sim 1.5$ .

In contrast, the lower bed shear stress and particle settling velocities would reduce the abrasion rate of channel bedrock. Corrosion depends on pH, which is unknown but likely more acidic in an atmosphere rich in  $\text{CO}_2$  and  $\text{SO}_2$ . The onset velocity for cavitation scales with  $g^{0.5}$ , so lower gravity provides little benefit, but a hypothetically lower atmospheric pressure would enable the process at lower mean velocities (Baker, 1979). For example, in a 100-mbar atmosphere, flows 1- and 10-m deep would undergo cavitation at velocities of 3 and 6 m/s respectively. These values correspond to fairly steep threshold slopes of 0.03 ( $1.64^\circ$ ) and 0.005 ( $0.3^\circ$ ) at downslope locations where contributing area is sufficient to accumulate flows of that depth. Considering these environmental effects, the incision of small headwater tributaries would take longer for a given flow rate, requiring a longer period of erosion (and more total water) or more rapid weathering for the same amount of bedrock erosion. Moreover, runoff production per unit precipitation is low where tributaries are poorly developed, reducing the effectiveness of flash floods (Patton and Baker, 1976). Scaling arguments suggest that Martian channels should have more bedrock- and gravel-floored reaches and distal fine-grained deposits with lower gradients.

## Applications

Weihaupt (1974) was the first to apply paleohydrologic methods to a Martian fluvial system, Nirgal Vallis, which has well-developed, entrenched meanders along its main stem (Figure 19.5(a)). Meandering is not a recognized attribute of valleys carved by groundwater sapping, but the much smaller, straighter, theatre-headed tributaries to the main valley have no apparent overland drainage. Weihaupt (1974) estimated the mean annual flood based on the meander wavelength of the bedrock valley, and the bankfull discharge was based on the width of the valley floor, taking that to be a channel bed rather than a floodplain or terrace. These methods suggested discharges of  $2700 \text{ m}^3/\text{s}$  and  $100\,000 \text{ m}^3/\text{s}$  respectively, which were not scaled for gravity. Malin and Edgett (2001) identified an interior channel that is locally exposed on the valley floor. This channel's width is 12 per cent of the meander wavelength, as expected from Equation (19.2), so the discharge estimate is reduced to  $4800 \text{ m}^3/\text{s}$ , scaled for gravity and assuming poorly resistant channel banks (Irwin *et al.*, 2005a).

Moore *et al.* (2003) found that the channel width on the Eberswalde crater delta was 14.5 per cent of the meander wavelength and that bankfull discharge was about  $700 \text{ m}^3/\text{s}$ , using Equation (19.4). Jerolmack *et al.* (2004) calculated the discharge at  $410 \text{ m}^3/\text{s}$ , using an equilibrium model for channelized alluvial fans. Given that discharge, the channel-bed materials would be too coarse for wind to remove, but the suspended load deposited on the floodplain would be susceptible to aeolian erosion. This feature explains why the channel beds were preserved as ridges while much of the floodplain had been blown away. The development of meanders by lateral accretion was also consistent with the estimated stream power (Irwin *et al.*, 2005b). Based on reasonable sediment yields and timescales for meander development and avulsion, the longevity of the contributing valley network ranges from  $10^3$ – $10^6$  yr (Moore *et al.*, 2003), with a favoured timescale of at least  $\sim 10^5$  yr (Bhattacharya *et al.*, 2005) that is comparable to the time required to construct large alluvial fans in some Martian impact craters (Moore and Howard, 2005). A reasonable evaporation rate on the order of  $\sim 1 \text{ m/yr}$  from the lake would suggest  $\sim 0.1 \text{ m/yr}$  of runoff from the contributing basin (Irwin *et al.*, 2005b).

Pieri (1980), Irwin *et al.* (2005a, 2005b), Jaumann *et al.* (2005) and Howard *et al.* (2005) have also recognized interior channels within valley networks (Figure 19.6(e)). Larger drainage basins typically yield wider channels, and their discharge from Equation (19.5) divided by a topographically defined contributing area suggests that runoff production rates locally exceeded  $1 \text{ cm/day}$  at times. Runoff production rates were smaller for larger drainage basins, which incorporate low-gradient plains and which may have been larger than the individual storm cells.

## Summary

In many respects, the surface of Mars is intermediate between the cratered Moon and the deeply eroded Earth. Early telescopic observations suggested conditions favourable for life, but later observations and spacecraft imaging revealed a hyperarid planet with very low long-term erosion rates. The Martian highland landscape reflects the prolonged fluvial erosion of Noachian impact craters (Craddock *et al.*, 1997), but this process may have been discontinuous and was not intense enough to fully regrade the landscape into a set of mature drainage basins. As a result, the length, order, network structure, junction angles, sinuosity, drainage density, cross-sectional and longitudinal profiles, and watershed topography of relict valley networks still reflect imposed crater topography. These generally sparse, immature valleys with poorly dissected interfluvial areas were incised during one or more epochs of more intense fluvial activity around the Noachian/Hesperian transition (3.7 Ga). Dominant runoff comparable to terrestrial mean annual floods was associated with local ponding and the deposition of alluvial fans and deltas. The short longevity of Earth-like conditions, the inefficiency of fluvial abrasion under lower gravity and possible high infiltration capacities inhibited the development of headwater tributaries on a relatively cool and arid planet. Erosion rates declined suddenly and severely following this epoch, leaving undissected delta surfaces and well preserved channels and V-shaped valleys. Aeolian erosion and gardening by small impacts has degraded the valley networks somewhat, but their preserved morphometric characteristics are useful in deciphering the environmental conditions of early Mars.

## Acknowledgements

Helpful comments by Vic Baker, Bruce Rhoads, Rebecca Williams and Nicolas Mangold improved the manuscript.

## References

- Aharonson O, Zuber MT, Rothman DH, Schorghofer N, Whipple KX. 2002. Drainage basins and channel incision on Mars. *Proceedings of the National Academy of Sciences* **99**: 1780–1783.
- Anders E, Arnold JR. 1965. Age of craters on Mars. *Science* **149**: 1494–1496.
- Ansan V, Mangold N. 2006. New observations of Warrego Valles, Mars: Evidence for precipitation and surface runoff. *Planetary and Space Science* **54**: 219–242.
- Arvidson RE, Guinness EA, Lee S. 1979. Differential eolian redistribution rates on Mars. *Nature* **278**: 533–535.

- Baker VR. 1979. Erosional processes in channelized water flows on Mars. *Journal of Geophysical Research* **84**: 7985–7993.
- Baker VR. 1982. *The channels of Mars*. University of Texas Press: Austin.
- Baker VR, Milton DJ. 1974. Erosion by catastrophic floods on Mars and Earth. *Icarus* **23**: 27–41.
- Baker VR, Partridge J. 1986. Small Martian valleys: Pristine and degraded morphology. *Journal of Geophysical Research* **91**: 3561–3572.
- Baker VR, Strom RG, Gulick VC, Kargel JS, Komatsu G, Kale VS. 1991. Ancient oceans, ice sheets and the hydrological cycle on Mars. *Nature* **352**: 589–594.
- Baker VR, Komatsu G, Gulick VC, Parker TJ. 1997. Channels and valleys. In *Venus II*, Bougher SW, Hunten DM, Phillips RJ (eds). University of Arizona Press: Tucson; 757–793.
- Baldwin RB. 1965. Mars: An estimate of the age of its surface. *Science* **149**: 1498–1499.
- Bandfield JL, Hamilton VE, Christensen PR. 2000. A global view of Martian surface compositions from MGS-TES. *Science* **287**: 1626–1630. DOI: 10.1126/science.287.5458.1626.
- Bandfield JL, Glotch TD, Christensen PR. 2003. Spectroscopic identification of carbonate minerals in the Martian dust. *Science* **301**: 1084–1087.
- Berman DC, Hartmann WK. 2002. Recent fluvial, volcanic and tectonic activity on the Cerberus Plains of Mars. *Icarus* **159**: 1–17.
- Bhattacharya JP, Payenberg THD, Lang SD, Bourke MC. 2005. Dynamic river channels suggest a long-lived Noachian crater lake. *Geophysical Research Letters* **32**: L10201. DOI: 10.1029/2005GL022747.
- Bibring J-P, Langevin Y, Poulet F, Gendrin A, Gondet B, Berthé M, Sonfflot A, Drossart P, Combes M, Bellucci G, Moroz V, Mangold N, Schmitt B, OMEGA team. 2004. Perennial water ice identified in the south polar cap of Mars. *Nature* **428**: 627–630. DOI: 10.1038/nature02461.
- Boothroyd AI, Sackmann I, Fowler FA. 1991. Our Sun, II, Early mass loss of 0.1M and the case of the missing lithium. *Astrophysical Journal* **377**: 318–329.
- Brakenridge GR. 1990. The origin of fluvial valleys and early geologic history, Aeolis quadrangle, Mars. *Journal of Geophysical Research* **95**: 17 289–17 308.
- Brakenridge GR, Newsom HE, Baker VR. 1985. Ancient hot springs on Mars: Origins and paleoenvironmental significance of small martian valleys. *Geology* **13**: 859–862.
- Burr DM, Grier JA, McEwen AS, Keszthelyi LP. 2002. Repeated aqueous flooding from the Cerberus Fossae: Evidence for very recently extant, deep groundwater on Mars. *Icarus* **159**: 53–73.
- Cabrol NA, Grin EA. 1999. Distribution, classification, and ages of Martian impact crater lakes. *Icarus* **142**: 160–172.
- Cabrol NA, Grin EA. 2001. Composition of the drainage network on early Mars. *Geomorphology* **37**: 269–287.
- Carr MH. 1979. Formation of Martian flood features by release of water from confined aquifers. *Journal of Geophysical Research* **84**: 2995–3007.
- Carr MH. 1981. *The Surface of Mars*. Yale University Press: New Haven.
- Carr MH. 1983. Stability of streams and lakes on Mars. *Icarus* **56**: 476–495.
- Carr MH. 1995. The Martian drainage system and the origin of valley networks and fretted channels. *Journal of Geophysical Research* **100**: 7479–7507.
- Carr MH. 1996. *Water on Mars*. Oxford University Press: New York.
- Carr MH. 2001. Mars Global Surveyor observations of Martian fretted terrain. *Journal of Geophysical Research* **106**: 23 751–23 593.

- Carr MH, Chuang FC. 1997. Martian drainage densities. *Journal of Geophysical Research* **102**: 9145–9152.
- Carr MH, Clow GD. 1981. Martian channels and valleys: Their characteristics, distribution, and age. *Icarus* **48**: 91–117.
- Carr MH, Malin MC. 2000. Meter-scale characteristics of Martian channels and valleys. *Icarus* **146**: 366–386.
- Christensen PR, Bandfield JL, Hamilton VE, Ruff SW, Kieffer HH, Titus TN, Malin MC, Morris RV, Lane MD, Clark RL, Jakosky BM, Mellon MT, Pearl JC, Conrath BJ, Smith MD, Clancy RT, Kuzmin RO, Roush T, Mehall GL, Gorelick N, Bender K, Murray K, Dason S, Greene E, Silverman S, Greenfield M. 2001. Mars Global Surveyor Thermal Emission Spectrometer experiment: Investigation description and surface science results. *Journal of Geophysical Research* **106**: 23 823–23 872. DOI: 10.1029/2000JE001370.
- Clifford SM. 1991. Role of thermal vapor diffusion in the subsurface hydrologic evolution of Mars. *Geophysical Research Letters* **18**: 2055–2058.
- Clifford SM. 1993. A model for the hydrologic and climatic behavior of water on Mars. *Journal of Geophysical Research* **98**: 10 973–11 016.
- Clifford SM, Parker TJ. 2001. The evolution of the Martian hydrosphere: Implications for the fate of a primordial ocean and the current state of the northern plains. *Icarus* **154**: 40–79.
- Coblentz WW. 1925. Temperature estimates of the planet Mars. *Scientific Papers of the Bureau of Standards*, 512, US Department of Commerce: Washington DC.
- Colaprete A, Toon OB. 2003. Carbon dioxide clouds in an early dense Martian atmosphere. *Journal of Geophysical Research* **108**(E4): 5025. DOI: 10.1029/2002JE001967.
- Colaprete A, Haberle RM, Segura TL, Toon OB, Zahnle K. 2005. The effect of impacts on the Martian climate. In *Workshop on the Role of Volatiles and Atmospheres on Martian Impact Craters*, LPI Contribution 1273. Lunar and Planetary Institute: Houston, Texas; 32–33.
- Craddock RA, Howard AD. 2002. The case for rainfall on a warm, wet early Mars. *Journal of Geophysical Research* **107**(E11): 5111. DOI: 10.1029/2001JE001505.
- Craddock RA, Maxwell TA. 1990. Resurfacing of the Martian highlands in the Amenthes and Tyrrena region. *Journal of Geophysical Research* **95**: 14 265–14 278.
- Craddock RA, Maxwell TA. 1993. Geomorphic evolution of the Martian highlands through ancient fluvial processes. *Journal of Geophysical Research* **98**: 3453–3468.
- Craddock RA, Maxwell TA, Howard AD. 1997. Crater morphometry and modification in the Sinus Sabaeus and Margaritifer Sinus regions of Mars. *Journal of Geophysical Research* **102**: 13 321–13 340.
- Di Achille G, Marinangeli L, Ori GG, Hanber E, Gwinner K, Reiss D, Neukum G. 2006. Geological evolution of the Tyras Vallis paleolacustrine system, Mars. *Journal of Geophysical Research* **111**: E04003. DOI: 10.1029/2005JE002561.
- Dunne T. 1980. Formation and controls of channel networks. *Progress in Physical Geography* **4**: 211–239.
- Evans JE, Maunder EW. 1903. Experiments as to the actuality of the ‘canals’ observed on Mars. *Monthly Notices of the Royal Astronomical Society* **63**: 488–499.
- Fairén AG, Fernández-Remolar D, Dohm JM, Baker VR, Amils R. 2004. Inhibition of carbonate synthesis in acidic oceans of early Mars. *Nature* **431**: 423–426.
- Fassett CI, Head III JW. 2005. Fluvial sedimentary deposits on Mars: Ancient deltas in a crater lake in the Nili Fossae Region. *Geophysical Research Letters* **32**: L14201. DOI: 10.1029/2005GL023456.

- Flammarion C. 1892. *La planète Mars et ses conditions d'habilité, vol. I*. Gauthier-Villars et Fils: Paris.
- Flammarion C. 1909. *La planète Mars et ses conditions d'habilité, vol. II*. Gauthier-Villars et Fils: Paris.
- Forsberg-Taylor NK, Howard AD, Craddock RA. 2004. Crater degradation in the Martian highlands: Morphometric analysis of the Sinus Sabaeus region and simulation modeling suggest fluvial processes. *Journal of Geophysical Research* **109**: E05002. DOI: 10.1029/2004JE002242.
- Gaidos E, Marion G. 2003. Geological and geochemical legacy of a cold early Mars. *Journal of Geophysical Research* **108**(E6): 5055. DOI: 10.1029/2002JE002000.
- Goldspiel JM, Squyres SW. 1991. Ancient aqueous sedimentation on Mars. *Icarus* **89**: 392–410.
- Goldspiel JM, Squyres SW. 2000. Groundwater sapping and valley formation on Mars. *Icarus* **148**: 176–192.
- Goldspiel JM, Squyres SW, Jankowski DG. 1993a. Topography of small Martian valleys. *Icarus* **105**: 479–500.
- Goldspiel JM, Squyres SW, Slade MA, Jurgens RF, Zisk SH. 1993b. Radar-derived topography of low southern latitudes of Mars. *Icarus* **106**: 346–364.
- Golombek MP, Bridges NT. 2000. Erosion rates on Mars and implications for climate change: Constraints from the Pathfinder landing site. *Journal of Geophysical Research* **105**: 1841–1854. DOI: 10.1029/1999JE001043.
- Golombek MP, Grant JA, Crumpler LS, Greeley R, Arvidson RE, Bell III JF, Weitz CM, Sullivan R, Christensen PR, Soderblom LA, Squyres SW. 2006. Erosion rates at the Mars Exploration Rover landing sites and long-term climate change on Mars. *Journal of Geophysical Research* **111**: E12S10. DOI: 10.1029/2006JE002754.
- Gough DO. 1981. Solar interior structure and luminosity variations. *Solar Physics* **74**: 21–34.
- Graedel TE, Sackmann IJ, Boothroyd AI. 1991. Early solar mass loss: A potential solution to the weak sun paradox. *Geophysical Research Letters* **18**: 1881–1884.
- Graf WL. 1988. *Fluvial processes in dryland rivers*. Blackburn Press: Caldwell, New Jersey.
- Grant JA. 1987. The geomorphic evolution of eastern Margaritifer Sinus, Mars. *Advances in Planetary Geology*. NASA Technical Memorandum 89871; 1–268.
- Grant JA. 2000. Valley formation in Margaritifer Sinus, Mars, by precipitation-recharged groundwater sapping. *Geology* **28**: 223–226.
- Grant JA, Boothroyd JC. 1985. Drainage basin areas and densities, Samara and Parana/Loire Valles, southeastern Margaritifer Sinus, Mars. In *Reports of Planetary Geology and Geophysics Program – 1985*. NASA Technical Memorandum 88383; 442–445.
- Grant JA, Parker TJ. 2002. Drainage evolution in the Margaritifer Sinus region, Mars. *Journal of Geophysical Research* **107**(E9): 5066. DOI: 10.1029/2001JE001678.
- Grant JA, Schultz PH. 1990. Gradational epochs on Mars: Evidence from west-northwest of Isidis Basin and Electris. *Icarus* **84**: 166–195.
- Grant JA, Schultz PH. 1993. Degradation of selected terrestrial and Martian impact craters. *Journal of Geophysical Research* **98**: 11 025–11 042.
- Gulick VC. 1998. Magmatic intrusions and a hydrothermal origin for fluvial valleys on Mars. *Journal of Geophysical Research* **103**: 19 365–19 388.
- Gulick VC. 2001. Origin of the valley networks on Mars: A hydrological perspective. *Geomorphology* **37**: 241–268.

- Gulick VC, Baker VR. 1989. Fluvial valleys and Martian paleoclimates. *Nature* **341**: 514–516.
- Gulick VC, Baker VR. 1990. Origin and evolution of valleys on Martian volcanoes. *Journal of Geophysical Research* **95**: 14 325–14 344.
- Gulick VC, Tyler D, McKay CP, Haberle RM. 1997. Episodic ocean-induced CO<sub>2</sub> pulses on Mars: Implications for fluvial valley formation. *Icarus* **130**: 68–86.
- Haberle RM. 1998. Early Mars climate models. *Journal of Geophysical Research* **103**: 28 467–28 479.
- Hack JT. 1957. Studies of longitudinal stream profiles in Virginia and Maryland. *U. S. Geological Survey Professional Paper* 294-B.
- Harrison KP, Grimm RE. 2002. Controls on Martian hydrothermal systems: Application to valley network and magnetic anomaly formation. *Journal of Geophysical Research* **107**(E5): DOI: 10.1029/2001JE001616.
- Harrison KP, Grimm RE. 2005. Groundwater-controlled valley networks and the decline of surface runoff on early Mars. *Journal of Geophysical Research* **110**: E12S16. DOI: 10.1029/2005JE002455.
- Hartmann WK. 1966. Martian cratering. *Icarus* **5**: 565–576.
- Hartmann WK. 1974. Geological observations of Martian arroyos. *Journal of Geophysical Research* **79**: 3951–3957.
- Hartmann WK, Neukum G. 2001. Cratering chronology and the evolution of Mars. *Space Science Reviews*, **96**: 165–194.
- Horton RE. 1932. Drainage-basin characteristics. *Transactions of the American Geophysical Union* **13**: 351–361.
- Horton RE. 1945. Erosional development of streams and their drainage basins: Hydrophysical approach to quantitative morphology. *Geological Society of America Bulletin* **56**: 275–370.
- Howard AD. 1971. Optimal angles of stream junction: Geometric, stability to capture and minimum power criteria. *Water Resources Research* **7**: 863–873.
- Howard AD. 1988. Introduction: Groundwater sapping on Mars and Earth. In *Sapping Features of the Colorado Plateau: A Comparative Planetary Geology Field Guide*, Howard AD, Kochel RC, Holt HE (eds). NASA Special Publication 491;1–5.
- Howard AD. 1990. Theoretical model of optimal drainage networks. *Water Resources Research* **26**: 2107–2117.
- Howard AD, Kochel RC, Holt HE (eds). 1988. *Sapping Features of the Colorado Plateau: A Comparative Planetary Geology Field Guide*. NASA Special Publication 491.
- Howard AD, Moore JM, Irwin III RP. 2005. An intense terminal epoch of widespread fluvial activity on early Mars: 1. valley network incision and associated deposits. *Journal of Geophysical Research* **110**: D12S14. DOI: 10.1029/2005JE002459.
- Hynek BM, Phillips RJ. 2003. New data reveal mature, integrated drainage systems on Mars indicative of past precipitation. *Geology* **31**: 757–760.
- Irwin III RP, Howard AD. 2002. Drainage basin evolution in Noachian Terra Cimmeria, Mars. *Journal of Geophysical Research* **107**(E7). DOI: 10.1029/2001JE001818.
- Irwin III RP, Howard AD, Maxwell TA. 2004. Geomorphology of Ma'adim Vallis, Mars, and associated paleolake basins. *Journal of Geophysical Research* **109**: E12009. DOI: 10.1029/2004JE002287.
- Irwin III RP, Craddock RA, Howard AD. 2005a. Interior channels in Martian valley networks: Discharge and runoff production. *Geology* **336**: 489–492.

- Irwin III RP, Howard AD, Craddock RA, Moore JM. 2005b. An intense terminal epoch of widespread fluvial activity on early Mars: 2. increased runoff and paleolake development. *Journal of Geophysical Research* **110**: E12S15. DOI: 10.1029/2005JE002460.
- Jaumann R, Reiss D, Frei S, Neukum G, Scholten F, Gwinner K, Roatsch T, Matz K-D, Mertens V, Hauber E, Hoffman H, Köhler U, Head III JW, Hiesinger H, Carr MH. 2005. Interior channels in Martian valleys: Constraints on fluvial erosion by measurements of the Mars Express High Resolution Stereo Camera. *Geophysical Research Letters* **32**: L16203. DOI: 10.1029/2005GL023415.
- Jerolmack DJ, Mohrig D, Zuber MT, Byrne S. 2004. A minimum time for the formation of Holden Northeast fan, Mars. *Geophysical Research Letters* **31**: L21701. DOI: 10.1029/2004GL021326.
- Kasting JF. 1991. CO<sub>2</sub> condensation and the climate of early Mars. *Icarus* **94**: 1–13.
- Kereszturi A. 2005. Cross-sectional and longitudinal profiles of valleys and channels in Xanthe Terra on Mars. *Journal of Geophysical Research* **110**: E12S17. DOI: 10.1029/2005JE002454.
- Kieffer HH, Martin TZ, Peterfreund AR, Jakosky BM, Miner ED, Don Palluconi F. 1976. Thermal and albedo mapping of Mars during the Viking Primary mission. *Journal of Geophysical Research* **82**: 4249–4291.
- Kieffer HH, Jakosky BM, Snyder CW. 1992. The planet Mars: From antiquity to the present. In *Mars*, Kieffer HH, Jakosky BM, Snyder CW, Matthews M (eds). University of Arizona Press: Tucson; 1–33.
- Kliore AJ, Fjeldbo G, Seidel BL, Sykes MJ, Woiceshyn PM. 1973. S band radio occultation measurements of the atmosphere and topography of Mars with Mariner 9: Extended mission coverage of polar and intermediate latitudes. *Journal of Geophysical Research* **78**: 4331–4351.
- Knighton, D. 1998. *Fluvial forms and processes: A new perspective*. Oxford University Press: New York.
- Kochel RC, Piper JF. 1986. Morphology of large valleys on Hawaii: Evidence for groundwater sapping and comparisons with Martian valleys. *Journal of Geophysical Research* **91**: E175–E192.
- Komar PD. 1979. Comparisons of the hydraulics of water flows in Martian outflow channels with flows of similar scale on Earth. *Icarus* **37**: 156–181.
- Komar PD. 1980a. Modes of sediment transport in channelized water flows with ramifications to the erosion of the Martian outflow channels. *Icarus* **42**: 317–329.
- Komar PD. 1980b. Channel meandering and braiding: Are empirical equations based on terrestrial rivers applicable to Mars? In *Reports of Planetary Geology Program 1980*. NASA Technical Memorandum 82385; 361–363.
- Kramer MG, Potter CS, Des Marais D, Peterson D. 2003. New insight on Mars: A network of ancient lakes and discontinuous river segments. *Eos, Transactions of the American Geophysical Union* **84**: 1.
- Kuiper GP. 1952. *The atmosphere of the Earth and planets*. University of Chicago Press: Chicago.
- Laity JE, Malin MC. 1985. Sapping processes and the development of theater-headed valley networks on the Colorado Plateau. *Geological Society of America Bulletin* **96**: 203–217.
- Leighton RB, Murray BC, Sharp RP, Allen JD, Sloan RK. 1965. Mariner IV photography of Mars: Initial results. *Science* **149**: 627–630.
- Lowell P. 1895. *Mars*. Houghton-Mifflin: New York.
- Lowell P. 1906. *Mars and Its Canals*. Macmillan: New York.
- Lowell P. 1908. *Mars as the Abode of Life*. Macmillan: New York.
- Lucchita BK, Dembosky J. 1994. Scarp heights of Martian channels from shadow measurements. *Lunar and Planetary Science Conference 25*, 811–812.

- Luo W. 2000. Quantifying groundwater-sapping landforms with a hypsometric technique. *Journal of Geophysical Research* **105**: 1685–1694. DOI: 10.1029/1999JE001096.
- Luo W. 2002. Hypsometric analysis of Margaritifer Sinus and origin of valley networks. *Journal of Geophysical Research* **107**(E10): 5071. DOI: 10.1029/2001JE001500.
- Luo W, Howard AD. 2005. Analysis of Martian valley network basins using a circularity function. *Journal of Geophysical Research* **110**: E12S13. DOI: 10.1029/2005JE002506.
- Luo W, Stepinski TF. 2006. Topographically derived maps of valley networks and drainage density in the Mare Tyrrhenum quadrangle of Mars. *Geophysical Research Letters* **33**: L18202. DOI: 10.1029/2006GL027346.
- Malin MC. 1976a. Nature and origin of intercrater plains on Mars. In *Studies of the surface morphology of Mars*, Ph.D. dissertation, California Institute of Technology: Pasadena, California.
- Malin MC. 1976b. Age of Martian channels. *Journal of Geophysical Research* **81**: 4825–4845.
- Malin MC, Edgett KS. 2000a. Evidence for recent groundwater seepage and surface runoff on Mars. *Science* **288**: 2330–2335.
- Malin MC, Edgett KS. 2000b. Sedimentary rocks of early Mars. *Science* **290**: 1927–1937.
- Malin MC, Edgett KS. 2001. Mars Global Surveyor Mars Orbiter Camera: Interplanetary cruise through primary mission. *Journal of Geophysical Research* **106**: 23 429–23 570.
- Malin MC, Edgett KS. 2003. Evidence for persistent flow and aqueous sedimentation on early Mars. *Science* **302**: 1931–1934. DOI: 10.1126/science.1090544.
- Mangold N, Quantin C, Ansan V, Delacourt C, Allemand P. 2004. Evidence for precipitation on Mars from dendritic valleys in the Valles Marineris area. *Science* **305**: 78–81.
- Mars Channel Working Group. 1983. Channels and valleys on Mars. *Geological Society of America Bulletin* **94**: 1035–1054.
- Masursky H. 1973. An overview of geologic results from Mariner 9. *Journal of Geophysical Research* **78**: 4009–4038.
- Masursky H, Boyce JM, Dial AL, Schaber GG, Strobell ME. 1977. Classification and time of formation of Martian channels based on Viking data. *Journal of Geophysical Research* **82**: 4016–4038.
- Maxwell TA, Craddock RA. 1995. Age relations of Martian highland drainage basins. *Journal of Geophysical Research* **100**: 11 765–11 780.
- Maxwell TA, Otto EP, Picard MD, Wilson RC. 1973. Meteorite impact: A suggestion for the origin of some stream channels on Mars. *Geology* **1**: 9–10.
- McCauley JF, Carr MH, Cutts JA, Hartmann WK, Masursky H, Milton DJ, Sharp RP, Wilhelms DE. 1972. Preliminary Mariner 9 report on the geology of Mars. *Icarus* **17**: 289–327.
- McEwen AS, Belton MJS, Breneman HH, Fagents SA, Geessler P, Greeley R, Head III JW, Hoppa G, Jaeger WL, Johnson TV, Keszthelyi L, Klaasen KP, Lopes-Gantier R, Magee KP, Milazzo MP, Moore JM, Pappalardo RJ, Phillips CB, Radebaugh J, Schubert G, Schuster P, Simonelli DP, Sullivan R, Thomas PC, Turtle EP, Williams DA. 2000. Galileo at Io: Results from high-resolution imaging. *Science* **288**: 1193–1198.
- Milton DJ. 1973. Water and processes of degradation in the Martian landscape. *Journal of Geophysical Research* **78**: 4037–4047.
- Moore JM, Howard AD. 2005. Large alluvial fans on Mars. *Journal of Geophysical Research* **110**: E04005. DOI: 10.1029/2004JE002352.
- Moore JM, Howard AD, Dietrich WE, Schenk PM. 2003. Martian layered fluvial deposits: Implications for Noachian climate scenarios. *Geophysical Research Letters* **30**: 2292. DOI: 10.1029/2003GL019002.

- Mouginis-Mark PJ. 1990. Recent melt water release in the Tharsis region of Mars. *Icarus* **84**: 362–373.
- Murray BC, Soderblom LA, Sharp RP, Cutts JA. 1971. The surface of Mars 1. cratered terrains. *Journal of Geophysical Research* **76**: 313–330.
- Nummedal D. 1977. Entrainment of sediment by fluid flow on Mars. In *Reports of the Planetary Geology Program 1976-1977*. NASA Technical Memorandum X-3511;162–164.
- Öpik EJ. 1966. The Martian surface. *Science* **153**: 255–265.
- Osterkamp WR, Hedman ER. 1982. Perennial-streamflow characteristics related to channel geometry and sediment in Missouri River basin. *US Geological Survey Professional Paper* 1242.
- Parker TJ. 1985. *Geomorphology and geology of the southwestern Margaritifer Sinus-Northern Argyre region of Mars*, Master's thesis, California State University: Los Angeles.
- Patton PC, Baker VR. 1976. Morphometry and floods in small drainage basins subject to diverse hydrologic controls. *Water Resources Research* **12**: 941–952.
- Pieri DC. 1976. Distribution of small channels on the Martian surface. *Icarus* **27**: 25–50.
- Pieri DC. 1980. Geomorphology of Martian valleys. In *Advances in Planetary Geology*. NASA Technical Memorandum 81979; 1–160.
- Pollack JB, Kasting JF, Richardson SM, Poliakov K. 1987. The case for a wet, warm climate on early Mars. *Icarus* **71**: 203–224.
- Quantin C, Allemand P, Mangold N, Dromart G, Delacourt C. 2005. Fluvial and lacustrine activity on layered deposits in Melas Chasma, Valles Marineris, Mars. *Journal of Geophysical Research* **110**: E12S19. DOI: 10.1029/2005JE002440.
- Sagan C, Chyba C. 1997. The early faint sun paradox: Organic shielding of ultraviolet-labile greenhouse gases. *Science* **276**: 1217–1221.
- Sagan C, Fox P. 1975. The canals on Mars: An assessment after Mariner 9. *Icarus* **25**: 602–612.
- Sagan C, Toon OB, Gierasch PJ. 1973. Climate change on Mars. *Science* **181**: 1045–1049.
- Scott DH, Dohm JM, Rice Jr JW. 1995. Map of Mars showing channels and possible paleolake basins. US Geological Survey Map I-2461.
- Segura TL, Toon OB, Colaprete A, Zahnle K. 2002. Environmental impacts of large impacts on Mars. *Science* **298**: 1977–1980.
- Sharp RP. 1968. Surface processes modifying Martian craters. *Icarus* **8**: 472–480.
- Sharp RP, Malin MC. 1975. Channels on Mars. *Geological Society of America Bulletin* **86**: 593–609.
- Shreve RL. 1966. Statistical law of stream numbers. *Journal of Geology* **74**: 17–34.
- Shreve RL. 1967. Infinite topologically random channel networks. *Journal of Geology* **75**: 178–186.
- Sinton WM, Strong J. 1960. Radiometric observations of Mars. *Astrophysical Journal* **131**: 459–469.
- Smith DE, Zuber MT, Frey HV, Garvin JB, Head III JW, Muhleman DO, Pettengill GH, Phillips RJ, Solomon SC, Zwally HJ, Banerdt WB, Duxbury TC, Golombek MP, Lemoine FG, Neumann GA, Rowlands DD, Aharonson O, Ford PG, Ivanov AB, Johnson CL, McGovern PJ, Abshire JB, Afzal RS, Sun X. 2001. Mars Orbiter Laser Altimeter: Experiment summary after the first year of global mapping of Mars. *Journal of Geophysical Research* **106**: 23 689–23 722.
- Soderblom LA, Condit CD, West RA, Herman BM, Kreidler TJ. 1974. Martian planetwide crater distributions: Implications for geologic history and surface processes. *Icarus* **22**: 239–263.
- Squyres SW, Kasting JF. 1994. Early Mars: How warm and how wet? *Science* **265**: 744–749.
- Squyres SW, Grotzinger JP, Arvidson RE, Bell III JF, Calvin W, Christensen PR, Clark BC, Crisp JA, Farrand WH, Herkenhoff KE, Johnson JR, Klingelhöfer G, Knoll AH, McLennan SM, McSween Jr. HY, Morris RV, Rice Jr. JW, Rieder R, Soderblom LA. 2004. In situ

- evidence for an ancient aqueous environment at Meridiani Planum, Mars. *Science* **306**: 1709–1714.
- Stepinski TF, Collier ML. 2004. Extraction of Martian valley networks from digital topography. *Journal of Geophysical Research* **109**: E11005. DOI: 10.1029/2004JE002269.
- Stepinski TF, Coradetti S. 2004. Comparing morphologies of drainage basins on Mars and Earth using integral-geometry and neural maps. *Geophysical Research Letters* **31**: L15604. DOI: 10.1029/2004GL020359.
- Stepinski TF, Stepinski AP. 2005. Morphology of drainage basins as an indicator of climate on early Mars. *Journal of Geophysical Research* **110**: E12S12. DOI: 10.1029/2005JE002448.
- Stepinski TF, Marinova MM, McGovern PJ, Clifford SM. 2002. Fractal analysis of drainage basins on Mars. *Geophysical Research Letters* **29**: DOI: 10.1029/2002GL014666.
- Stepinski TF, Collier ML, McGovern PJ, Clifford SM. 2004. Martian geomorphology from fractal analysis of drainage networks. *Journal of Geophysical Research* **109**: E02005. DOI: 10.1029/2003JE002098.
- Stoney GJ. 1898. Of atmospheres upon planets and satellites. *Transactions of the Royal Dublin Society* **6**: series 2, part 13.
- Strahler AN. 1952. Hypsometric (area-altitude) analysis of erosional topography. *Geological Society of America Bulletin* **63**: 1117–1142.
- Strom RG, Malhotra R, Ito T, Yoshida F, Kring DA. 2005. The origin of planetary impactors in the inner Solar System. *Science* **309**: 1847–1850.
- Sun T, Meakin P, Jossang T. 1994. The topography of optimal drainage basins. *Water Resources Research* **30**: 2599–2610.
- Tanaka KL. 1986. The stratigraphy of Mars. *Journal of Geophysical Research* **91**: E139–E158.
- Tanaka KL. 1997. Sedimentary history and mass flow structures of Chryse and Acidalia Planitiae, Mars. *Journal of Geophysical Research* **102**: 4131–4149.
- Tanaka KL, Dohm JM, Lias JH, Hare TM. 1998. Erosional valleys in the Thaumasia region of Mars: Hydrothermal and seismic origins. *Journal of Geophysical Research* **103**: 31 407–31 420. DOI: 10.1029/98JE01599.
- Tarboton DG, Bras RL, Rodríguez-Iturbe I. 1991. On the extraction of channel networks from digital elevation data. *Hydrological Processes* **51**: 81–100.
- Thornhill GD, Rothery DA, Murray JB, Cook AC, Day T, Muller JP, Iliffe JC. 1993. Topography of Apollinaris Patera and Ma'adim Vallis: Automated extraction of digital elevation models. *Journal of Geophysical Research* **98**: 23 581–23 587.
- Tomasko MG, Archinal B, Becker T, Bézard B, Bushroo M, Combes M, Cook D, Coustenis A, de Bergh C, Dafoe LE, Doose L, Douté S, Eibl A, Engel S, Gliem F, Grieger B, Holso K, Howington-Krans E, Karkoschka E, Keller HU, Kirk R, Kramm R, Küppers M, Lanagan P, Lellouch E, Lemmon M, Lunine J, McFarlane E, Moores J, Pront GM, Rizk B, Rosiek M, Rueffer P, Schröder SE, Schmitt B, See C, Smith P, Soderblom L, Thomas N, West R. 2005. Rain, winds and haze during the Huygens probe's descent to Titan's surface. *Nature* **438**: 765–778. DOI: 10.1038/nature04126.
- Travis BJ, Rosenberg ND, Cuzzi JN. 2003. On the role of widespread subsurface convection in bringing liquid water close to Mars' surface. *Journal of Geophysical Research* **108**: 8040. DOI: 10.1029/2002JE001877.
- Wallace AR. 1907. *Is Mars Habitable?* Macmillan: London.
- Wallace D, Sagan C. 1979. Evaporation of ice in planetary atmospheres: Ice-covered rivers on Mars. *Icarus* **39**: 385–400.

- Ward AW. 1979. Yardangs on Mars: Evidence of recent wind erosion. *Journal of Geophysical Research* **84**: 8147–8166.
- Weihaupt JG. 1974. Possible origin and probable discharges of meandering channels on the planet Mars. *Journal of Geophysical Research* **79**: 2073–2076.
- Weitz C, Irwin III RP, Chuang F, Bourke M, Crown D. 2006. Formation of a terraced fan deposit in Coprates Catena, Mars. *Icarus* **184**: 436–451.
- Whitmire DP, Doyle LR, Reynolds RT, Matese JJ. 1995. A slightly more massive young Sun as an explanation for warm temperatures on early Mars. *Journal of Geophysical Research* **100**: 5457–5464.
- Wilhelms DE. 1987. The geologic history of the Moon. *US Geological Survey Professional Paper* 1348.
- Wilhelms DE, Baldwin RJ. 1989. The role of igneous sills in shaping the martian uplands. *Proceedings of the Nineteenth Lunar and Planetary Science Conference*. Lunar and Planetary Institute: Houston; 355–365.
- Williams GP. 1988. Paleofluvial estimates from dimensions of former channels and meanders. In *Flood Geomorphology*, Baker VR, Kochel RC, Patton PC (eds). John Wiley & Sons: Chichester; 321–334.
- Williams RME, Phillips RJ. 2001. Morphometric measurements of Martian valley networks from Mars Orbiter Laser Altimeter (MOLA) data. *Journal of Geophysical Research* **106**: 23 737–23 751.
- Wilson L, Ghatan GJ, Head III JW, Mitchell KL. 2004. Mars outflow channels: A reappraisal of water flow velocities from water depths, regional slopes, and channel floor properties. *Journal of Geophysical Research* **109**: E09003. DOI: 10.1029/2004JE002281.
- Zimbelman JR, Craddock RA, Greeley R, Kuzmin RO. 1992. Volatile history of Mangala Valles, Mars. *Journal of Geophysical Research* **97**: 18 309–18 317.



# Subject Index

- 1D model, 17
- 2D model, 25, 27–29, 203, 205, 370
- 3D model, 15, 25–29, 33, 36
- Abrasion, 151, 202, 244, 249, 259, 332–333, 440, 442
- Aerial photography, 161, 166
- Aggradation, 152, 186–187, 190, 195, 198–200, 203, 205, 213, 217, 244–246, 251–256, 343, 345–347, 368, 387, 437
- Algae, 401
- ANOVA, 168, 172
- Aquatic biota, 160, 163, 235
- Armouring, 96, 108, 110, 186, 262, 357, 387
  
- Bank erosion, 49, 53, 95–96, 246, 257, 259, 264–265, 337, 348, 350–353, 355, 358–359, 361
- Basin shape, 274, 280–284, 295, 332
- Basin size, 272, 276, 281, 283, 287, 295
- Bedload supply, 154, 256–258
- Bedload supply potential, 259–260
- Bedload transport, 23, 29–30, 37, 55–60, 75, 123, 132–135, 142, 187, 197, 202, 204, 245, 256–257, 259–262, 264, 266, 340, 373–374
- Bedrock, 185, 204–205, 284–285, 372, 388, 406–408, 419, 440–441
- Bifurcation, 3, 53, 67, 96, 119–121, 129–132, 134, 347, 433
- Biological diversity / biodiversity, 3, 153, 175, 209, 213, 215–216, 218, 236, 244
- Biomass, 165, 211, 213, 221–222, 235
- Birds, 223, 231, 234–235
  
- Channel bank, 57, 81, 98, 104, 113, 189, 438–441
- Channel depth, 76, 123, 125, 188, 375–376
- Channel narrowing, 217, 248–249, 252, 259
- Channel slope, 95, 185–186, 194, 196–197, 210, 213, 290, 305, 347, 369–371, 375–379, 381–384, 386–388, 401
- Channel width, 14–15, 19, 21, 30, 74, 83–87, 97, 104, 112, 115, 135, 163–164, 185–186, 191, 201–203, 205, 221, 247–248, 273, 291, 368, 374, 376–377, 405, 437–441
- Check-dam, 252–253
- Chemistry, 2, 163–164, 210–211, 216, 233, 421
- Chlorophyll, 165, 222, 228
- Clearwater tributary, 186, 195, 199
- Conductivity, 165, 401, 410, 412
- Confluence angle, 18, 46, 48–49, 123, 125, 127–128, 284
- Confluence density, 215, 273–274, 284–286
- Confluence environment, 154–155, 215, 271–297
- Coupling, 37, 187, 204, 218, 264, 338–339, 370
  
- Dam, 51, 186, 195, 210, 216–217, 221, 252–253, 256, 388, 408
- Debris flow, 172, 184, 190, 195, 204–205, 245, 275–276, 278, 284, 289, 291, 294, 358, 408, 437
- Deforestation, 245, 247, 260, 265
- Degradation, 154, 186, 198–201, 215, 244, 246, 251, 253, 256, 259, 343, 345, 357, 368, 434
- Dendritic ecological network, 214

- Diffluence, 53, 83, 130, 142
- Digital elevation data/model, 160
- Discharge, 14–15, 18–19, 24–25, 28, 33, 36, 46–52, 56, 67, 74–75, 98, 113–115, 119–120, 125–131, 134, 151–152, 165, 183, 185–188, 191, 194, 197–198, 200–205, 213, 216, 224, 231–232, 261–264, 272–273, 309, 316–317, 329–331, 339, 343, 349, 369, 371, 375–377, 380, 386, 395, 398–410, 422, 427–430, 438–441
- Discontinuity / -ies, 205, 211, 233
- Dolphin, 212, 215
- Downstream fining, 151, 190, 198, 200, 203, 213, 244
- Drainage density, 271, 284–285, 287, 295, 368–370, 432, 434–435
- Ecosystem services, 154, 209, 215, 235, 237
- Ecosystem structure, 217
- Environmental gradient, 167
- Equilibrium, 37, 49, 56, 126, 134, 184, 186, 191, 193–194, 198–199, 205–206, 244, 317, 339, 341, 346, 357, 387, 432, 441
- Erosion-control, 244, 251, 255, 264, 266, 359–360
- EU Water Framework Directive, 265
- Fans, 3, 152, 187, 204, 224, 260, 272–273, 278, 284, 287, 291, 294, 342, 346, 429, 436–438, 441
- Fire, 272–273, 291, 293–295, 369
- Fish, 152, 163–167, 169–174, 210–212, 214–216, 219–220, 223–224, 227, 231–232, 234–235, 244, 246
- Fishless tributary, 172
- Fluvial landscape ecology, 214
- Food web, 214, 235
- Geographical Information System, 169, 358
- Geomorphological adjustment, 152, 213, 217, 236, 246–249
- Geostatistical / geostatistics, 153, 160, 174, 218
- Grain size, 3, 61, 121, 123, 137–142, 151–152, 166–167, 184–188, 190–204, 213–214, 244, 248–249, 262, 266, 273, 276, 278, 280, 290, 305, 367–388
- Gravel-bed, 23, 30, 36, 62, 65, 121–123, 125–127, 135–136, 139, 184–186, 190–191, 194–198, 251
- Groundwater, 64, 165, 169, 232, 256, 397–399, 404, 409–411, 419, 422, 427–430, 432–433, 436
- Habitat, 3, 17, 163, 166–167, 169, 171, 201, 210, 212–217, 219, 221–223, 225, 233, 244, 246, 296–297
- Headwater catchments, 163, 172
- Heterogeneity, 64, 153, 160, 165, 168–169, 175, 201, 212–213, 215, 218–219, 236, 283, 285, 287, 293–297, 315, 319, 329, 331, 338, 347, 397
- Hotspot, 3, 153, 213–214, 218, 236, 297, 360, 408
- Human impact, 245
- Humid, 275–276, 278, 280, 284–285, 387, 404–405, 438
- Hydraulic geometry, 24, 81, 126–128, 184–186, 188–189, 192, 195–197, 201, 273, 316–318, 321, 323–324, 329, 331–332, 388
- Hyporheic, 210, 219, 224, 232–233, 304, 397, 401–404, 406–412
- Incision, 129, 152, 154, 204, 244–246, 248–249, 251–256, 261, 264, 266, 345–346, 351, 362, 423, 432–435, 440
- Insect, 152, 221–222, 225, 227, 230, 234–235
- Invertebrates/macroinvertebrates, 163, 165
- Junction bars, 81, 183
- Knick-point, 152, 276, 291, 388, 408
- Landslide, 184, 195, 205, 254–256, 294, 340, 358, 371
- Lentic, 214, 216, 233
- LiDAR, 161, 166, 295
- Link Discontinuity Concept, 211
- Lithology, 151, 205, 249, 259, 296, 406
- Logistic regression, 276, 279
- Long profile, 141, 184, 190, 194, 198, 200, 205, 254–255
- Longitudinal patterns, 151, 161, 163, 165, 169, 172, 219, 282
- Lotic, 159, 214, 216

- Lotic ecology, 4, 164, 236  
 LOWESS, 169–173  
 Low-order catchments, 233, 244–245, 253, 289, 369, 403, 406  
 Management, 4–5, 14–15, 93–116, 154, 202, 210, 215–217, 243–265, 296–297, 332, 338–340, 346–347, 358  
 Manning, 193, 198, 375, 400, 438  
 Manning-Strickler, 194  
 Meyer-Peter and Müller, 185, 194, 261  
 Mining, 152, 184, 191, 246–247, 251, 256, 259  
 Morphology, 13–16, 18, 23, 30, 45–55, 75–80, 93, 95, 103, 119–127, 129–131, 134, 136–137, 139, 142, 154, 156, 160, 165, 169, 202, 205, 212, 236, 246, 256, 272, 278, 290, 294–296, 304, 338, 370, 401, 405–406, 408, 410, 431–432  
 Network architecture / structure, 214, 236, 245  
 Network dynamics hypothesis, 218  
 Network pattern / geometry, 271–272, 280–281, 283–284, 329  
 Nitrate / nitrogen, 165, 216, 221, 224, 227, 234, 403, 419  
 Numerical modelling, 4, 13, 18, 26–27, 33, 88, 139, 154, 184, 202  
 Nutrient, 31, 165, 210–211, 213, 215–216, 218–219, 222, 224–225, 234, 307, 347, 409  
 Oligotrophic, 234  
 Parker-Bray, 195  
 Patchiness, 165, 292  
 pH, 164  
 Phosphorus, 165, 221, 224, 226–227, 234, 396  
 Power law of stream sizes, 273–274, 289  
 Primary producer / productivity, 225, 227, 234  
 Progressive erosion, 245  
 Punctuated downstream fining, 190, 201, 203  
 Red alder, 234  
 Redd, 215, 219, 223–224, 231–233  
 Reforestation, 248, 251–252, 254, 256, 266  
 Refugia, 3, 212, 215, 236, 297  
 Regressive erosion, 246  
 Regulated river, 2, 152, 217, 278  
 Remote sensing, 137, 166–169  
 Restauration des Terrains en Montagne, 252  
 Riparian, 161, 166–167, 217–219, 233–234, 245, 271–273, 278, 294, 296, 398, 411  
 River continuum, 161, 211, 296, 396  
 River corridor, 237, 264  
 Roundness, 249  
 Salmon / salmonid, 6, 166, 211–213, 216, 219, 223–224, 232, 235, 275  
 Sampling, 20, 154, 160–166, 170, 205, 224, 227, 234, 341, 344, 355, 357, 396, 404  
 Sand-bed, 29, 79, 123, 125, 128, 139, 186, 191, 193–198, 202, 374, 401, 439  
 Sandy tributary, 123, 135, 186, 201, 401  
 Scour hole, 24, 27, 47, 49, 55–57, 60, 75, 110, 124, 132–135, 139, 141, 212  
 Sedimentology, 1–2, 5, 60–66, 121, 142  
 Sediment load, 48, 56, 66, 186, 192, 197, 204–205, 358, 369, 373, 376, 379, 381, 386–388  
 Sediment replenishment, 256, 259, 264–265  
 Sediment routing, 67, 78, 153–154, 175, 202, 213–214, 244, 259, 266–267, 338–339, 345–346, 357  
 Sediment source, 154, 211, 213, 249, 259–260, 264–265, 283, 293, 338, 350, 358  
 Sedimentary link, 190–191, 199, 201, 280  
 Semi-arid, 275–276, 285  
 Sensitivity analyses, 199  
 Shear stress, 20, 29–30, 37, 112, 132, 134, 185, 189–190, 193, 196–197, 199, 205, 331, 339, 368, 371–372, 374–378, 386, 440  
 Sorting, 121, 124, 126, 135–139, 152, 213  
 Spatial autocorrelation, 172–173  
 Spatial pattern, 56, 132, 134, 137, 159, 164–167, 175, 254, 273, 280, 283, 286, 359, 389  
 Spawning, 166, 219, 223–224, 229–233  
 Steep tributary, 101, 190  
 Stochastic, 154, 204, 271, 273, 279, 287, 291, 293, 295, 361–362  
 Substrate, 164, 166, 210, 213, 219, 221, 233, 235, 272–273, 275, 291, 373–374, 377–379  
 Suspended load / sediment, 31–34, 36, 441  
 Symmetry ratio, 273–279, 283, 287

- Temperature, 3, 96, 112, 153, 160–161, 163–165, 168–169, 210, 215–216, 219, 222, 224–225, 233, 235, 419, 422
- Topology, 119, 159–160, 187, 214, 236, 303, 311, 404
- Torrent-control, 251–256
- TRIB, 198–200, 204–205, 213
- Tributary impact / effect, 153, 245–246, 254
- Trophic level, 234–235
- Trout, 153, 160, 169–174
- Turbidity, 164, 166, 212
- Variogram/semivariogram, 160, 172–173, 175
- Wavelet analysis, 175
- Wetland, 233, 237, 401
- Width-averaged, 153, 185, 198, 202
- Wood, 168, 213, 235, 252, 272, 287, 290, 402
- Woody / Organic debris, 244, 290
- Zoogeographic barriers, 215

# Place Index

- Ain River, 249–250  
Archiane Torrent, 253  
Arkansas River, 191
- Bacon Creek, 221, 225–228, 234  
Barnavette Torrent, 257, 262  
Béoux torrent, 257, 264–265  
Bez River, 253–256, 265
- Camp Creek, 160, 169–174  
Canning River, 216  
Cascade Mountains, 210, 219  
Catskills, 215  
Cedar River, 103, 219–221, 224–229,  
233–234  
Colorado River, 216, 275
- Drôme River, 255
- Eel River, 212  
Esconavette torrent, 257, 262  
Eygues River, 248, 257
- Finney Creek, 221, 223, 225–227, 230–231,  
234–235  
Fulda River, 211
- Glen Canyon Dam, 216
- Hunter Creek, 247, 285–286
- John Day River, 160, 168
- Mahakam River, 212  
Mississippi River, 93–94, 101, 106–108, 111,  
115, 395
- Oregon Coast Range, 280, 282, 285, 291,  
293, 372  
Osage River, 214  
Ouvèze River, 249–251
- Pacific Northwest, 219  
Paria River, 216  
Pine Creek, 246–247  
Pine River, 187, 211, 213, 275
- River Rheidol, 217  
Roubion River, 252, 257
- Siuslaw River, 280, 289  
Skagit River, 220–221, 225  
Snake River, 211, 275  
Snowy River, 217  
Solimões-Amazon River, 24, 31, 33–34, 36,  
87, 211  
Stillaguamish River, 219–220, 235  
Sukunka River, 187, 211, 213, 275
- Umpqua River, 160
- Valcroissant torrent, 262
- Wenaha River, 275, 291
- Yzeron Catchment, 245–246



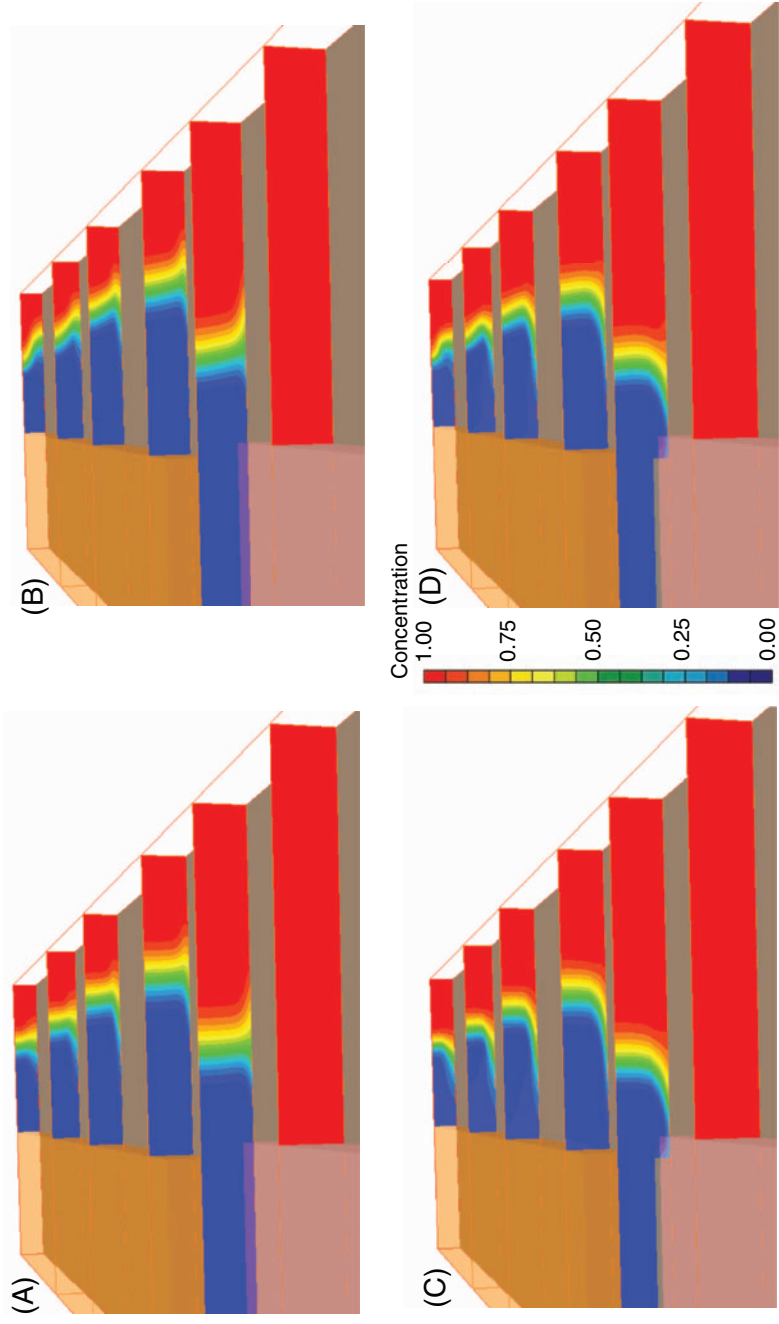


**Figure 3.5** Simulated numerical tracer downstream of the confluence where blue corresponds to a value of 0 and red to a value of 1 for (A) concordant beds with equal density, (B) concordant beds where the tributary density is increased to  $998.32 \text{ kg m}^{-3}$ , with the density of the main channel set at  $996.57 \text{ kg m}^{-3}$  (following the density difference of the Paraguay and Paraná Rivers, Lane *et al.*, in press), (C) discordant beds (shallower tributary) with equal density and (D) discordant beds with a higher density in the tributary (same as in B). Flow is towards the top.

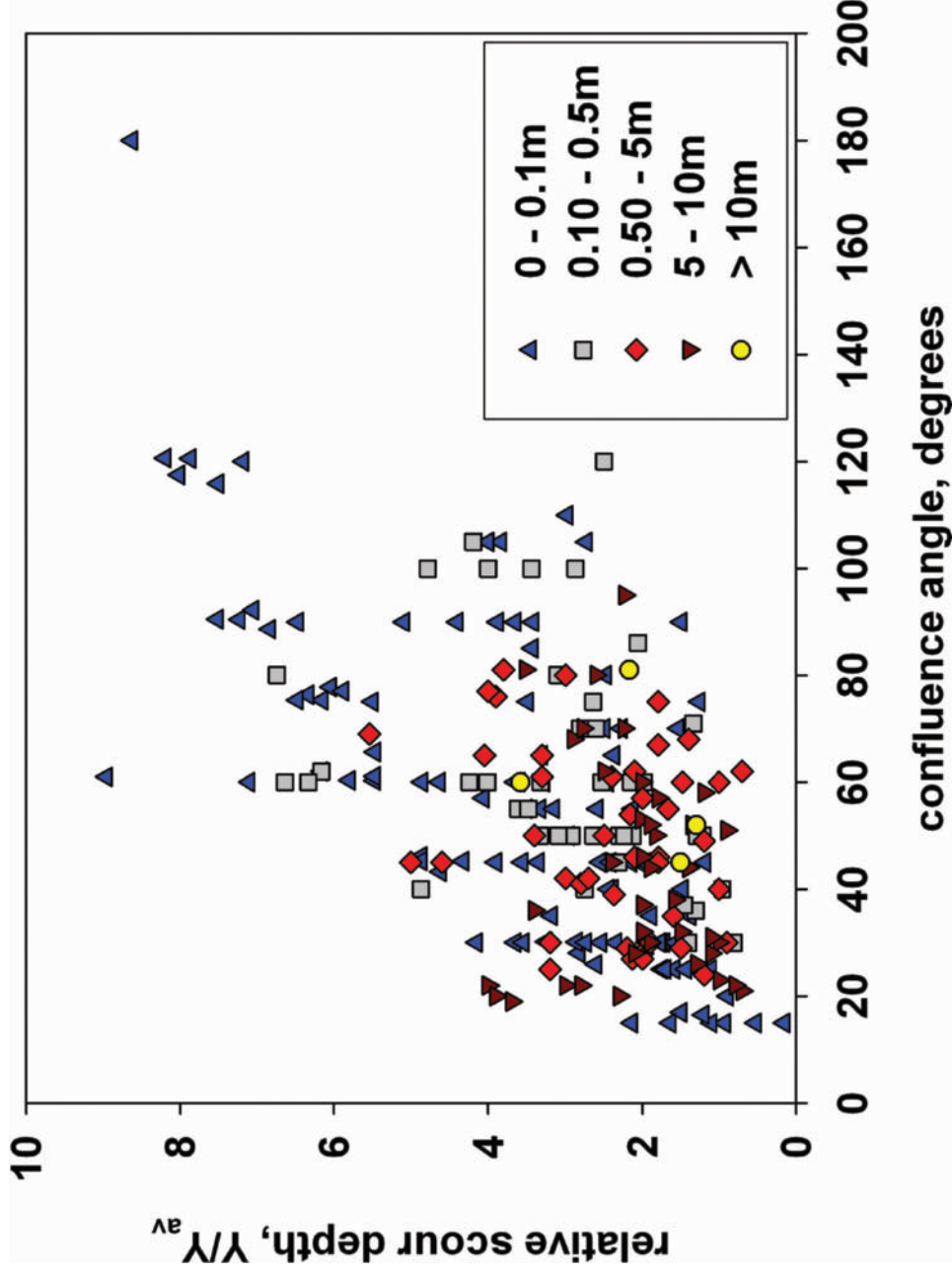


**Figure 4.2** A summary of scour depth data from channel confluences (see Sambrook Smith *et al.*, 2005). Data sources are from experimental studies of channel junctions and a range of field studies. Data from Mosley (1975, 1976, 1982), Ashmore and Parker (1983), Best (1985, 1988), Klaassen and Vermeer (1988), Roy and De Serres (1989), Orfeo (1995), Best and Ashworth (1997), Roy *et al.* (1988), McLeland *et al.* (1996), Rhoads and Sukhodolov (2001) and from research in Bangladesh (see Sarker, 1996; Delft Hydraulics and Danish Hydraulics Institute, 1996).

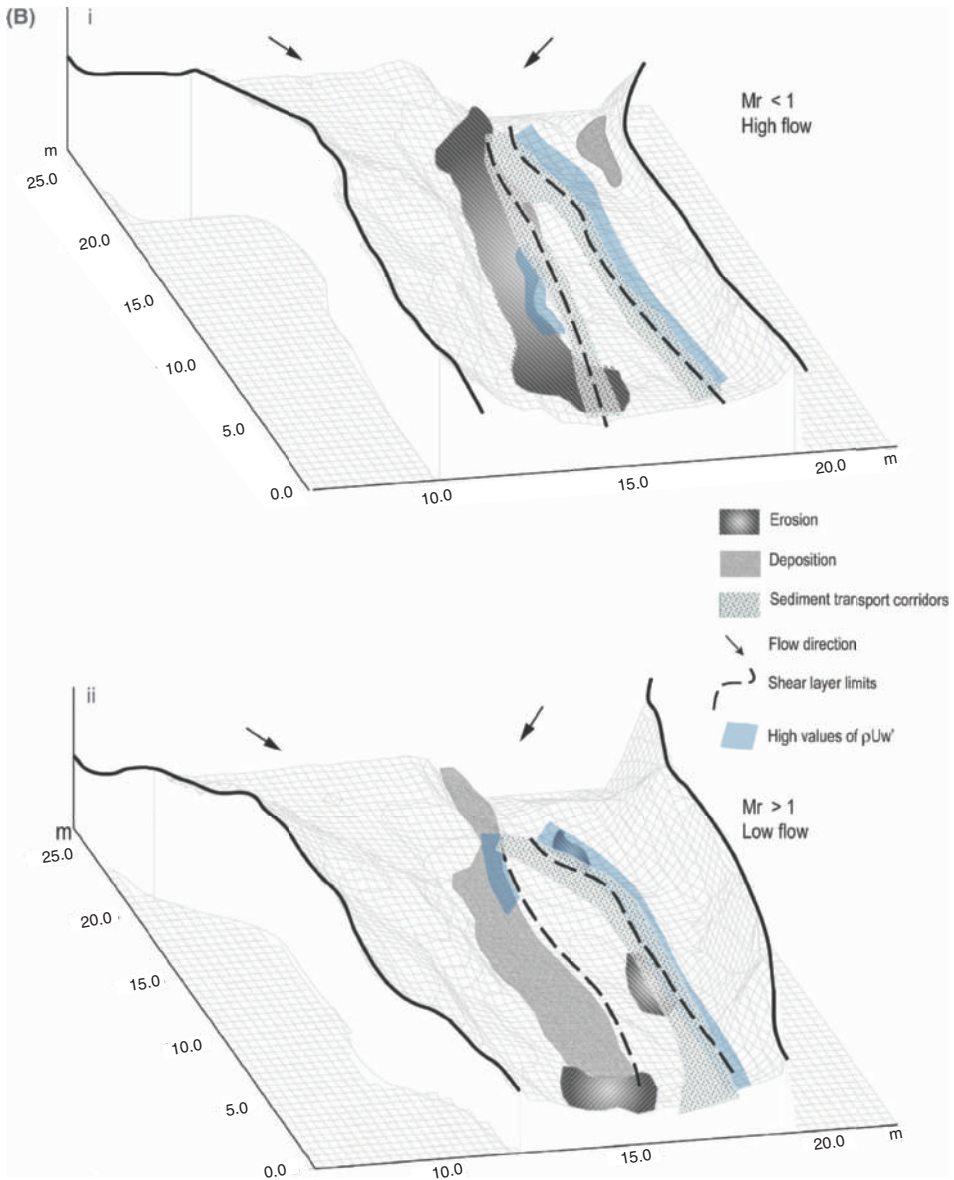


**Figure 4.5b** (B) A conceptual model of sediment transport and morphological change at the Bayonne–Berthier bed confluence (from Boyer *et al.*, 2006), at different flow stages and momentum ratios: (i)  $M_r < 1$  and high flow; (ii)  $M_r > 1$  and low flow. The background grids show the bathymetry of the bed. In the confluence, high values of turbulent stresses ( $Uw'$ ; where  $U$  is the mean downstream velocity,  $w$  is the vertical component of flow and the prime denotes the deviatoric value) were observed along the edges of the shear layer, with the center of the shear layer being dominated by normal turbulent stress in  $w$  ( $w'^2$ ). Bedload transport measurements were used to define transport corridors, whilst regions of erosion and deposition were assessed from the measured changes in bed morphology and bedload transport patterns.

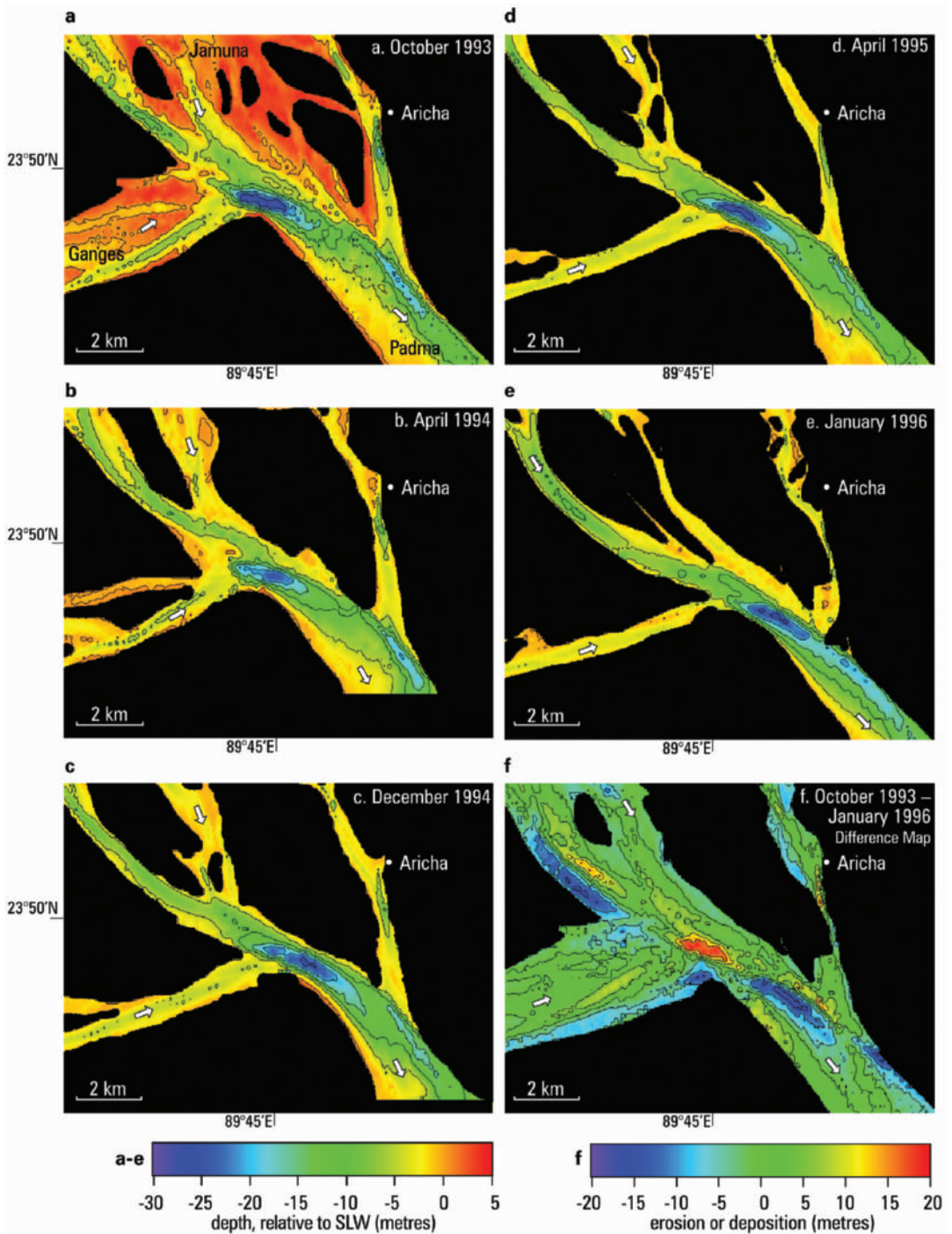


**Figure 5.1** Bed morphology at the confluence of the Jamuna and Ganges rivers, Bangladesh. Plots show morphology of confluence at various times (a–e) and a difference map of bed elevation (f). Reproduced from *Nature*, **387**: 275–277 (1997).

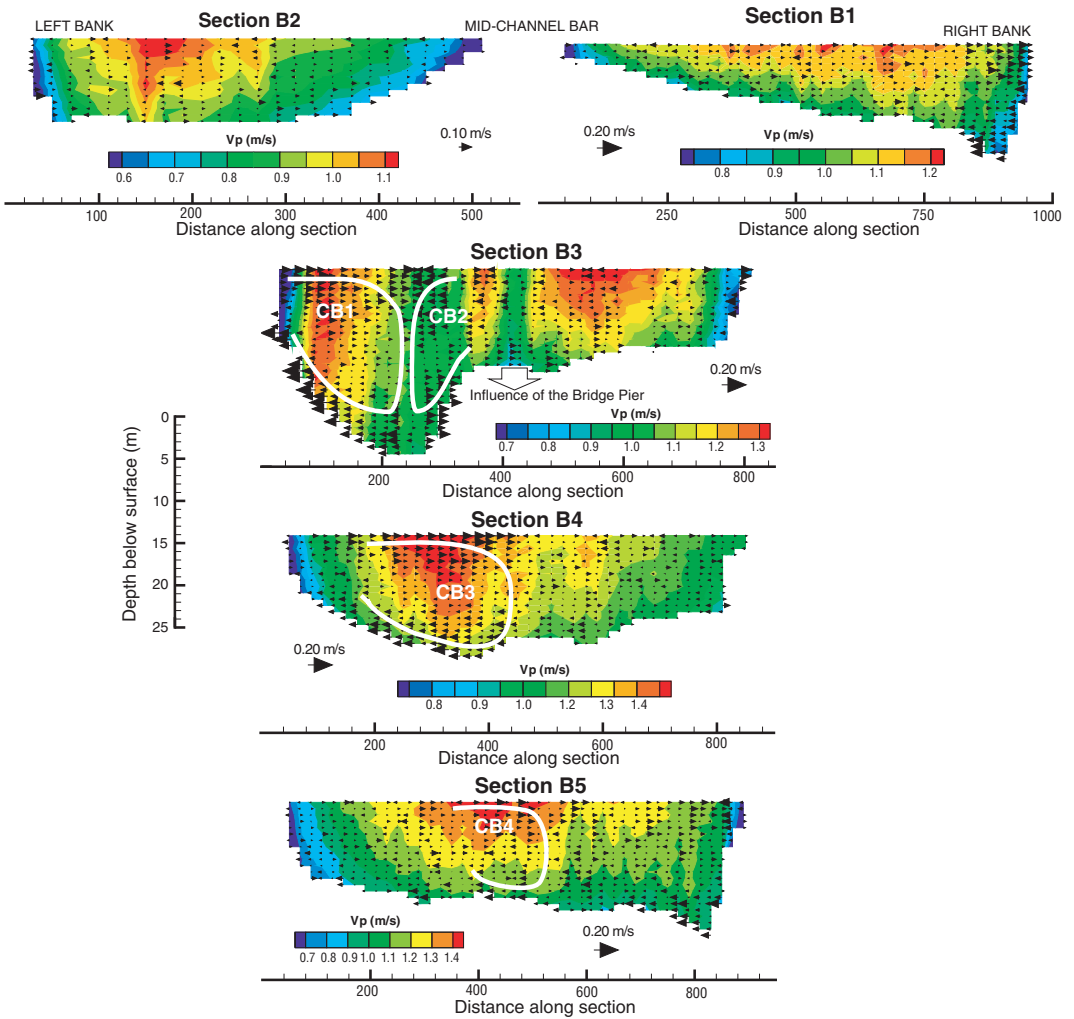


**Figure 5.5** Primary and secondary flow velocity fields at sections through a braid bar confluence on the Rio Paraná (Confluence B in Figure 5.4). Reproduced from proceedings of the 5th International Conference on River, Coastal and Estuarine Morphodynamics, Twente, The Netherlands (2007).



**Figure 5.6** Oblique aerial photograph of the junction of the Río Paraná and Río Paraguay. Note the contrast produced by the higher suspended sediment concentrations of the Río Paraguay and the vorticity present along the mixing interface.

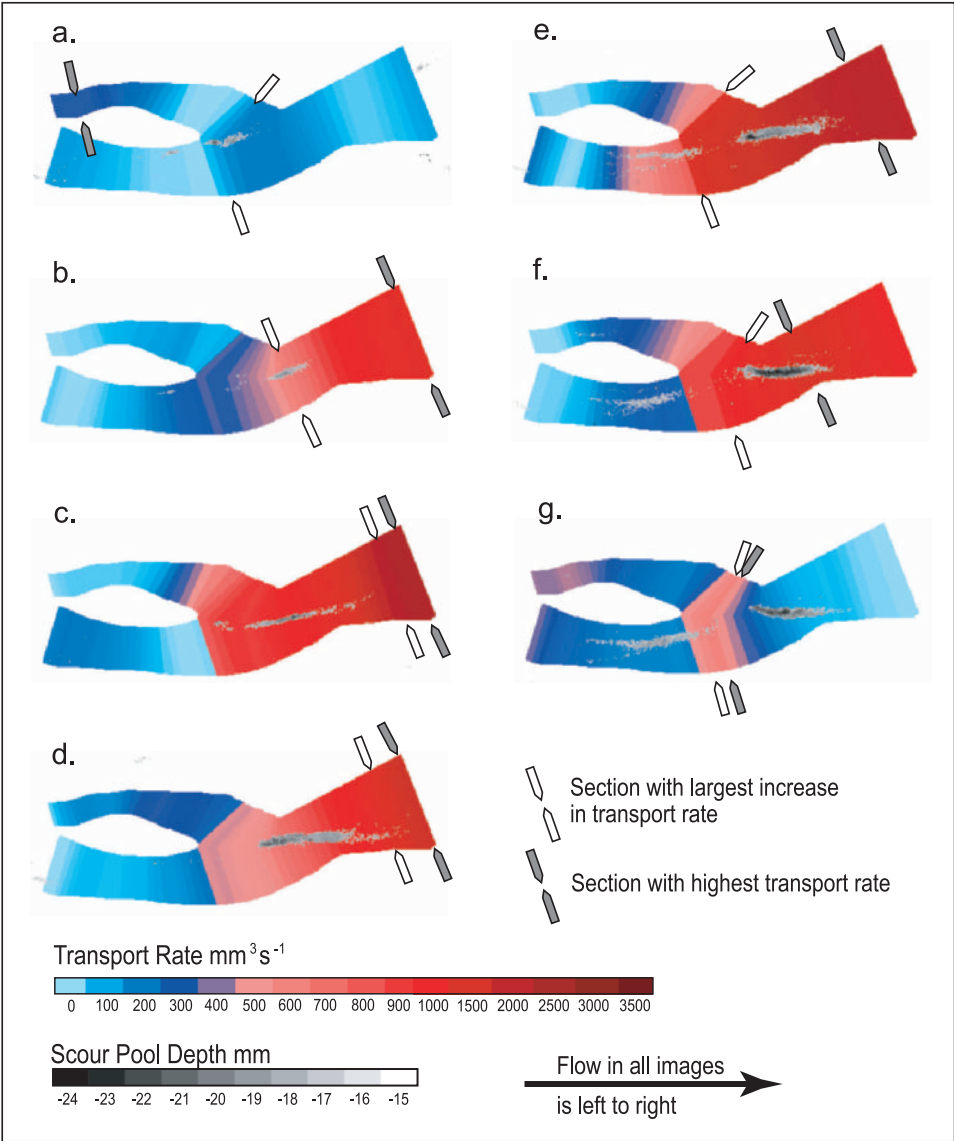


**Figure 7.5** Maps of a sequence (a–g) of changes in the downstream pattern of bedload transport rate in two confluent anabranches and the downstream confluence in a physical model of a braided river over a period of approximately one hour. The plots are approximately 10 minutes apart in time. Colour transition from blue to red indicates increasing transport rate and the location and bed elevation in the scour hole is shown in grey tones superimposed on the transport pattern. Cross-section average transport rates were calculated by morphological methods (Ashmore and Church, 1998) at a series of closely spaced cross-sections based on high-resolution, photogrammetric DEMs (Stojic *et al.*, 1998). Flow is left to right.

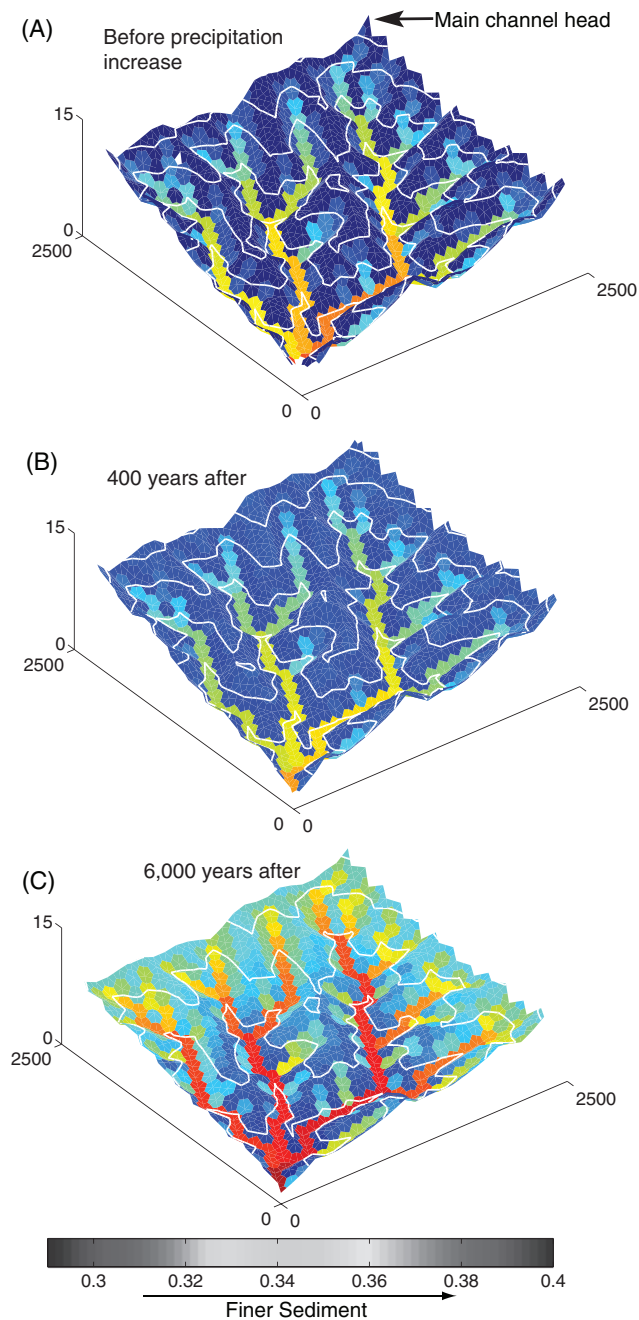


**Figure 17.5** Topography of the drainage network shaded by the proportion of sand in the surface layer, as indicated by the colour bar. The same scale applies to all three figures. The white lines are two-metre contour lines, and the axes scales are in metres. (A) illustrates the initial steady-state network; (B) and (C) illustrate changes in the surface texture at two different times following the change in precipitation. The network configuration does not change between the figures.